Development of Sustainable and Low Carbon Concretes for the Gulf Environment

Abu Saleh, Saleh

Award date:
2014

Awarding institution:
University of Bath

Development of Sustainable and Low Carbon Concretes for the Gulf Environment

Abu Saleh Mohammod Akhter uz Zaman

A thesis submitted for the degree of Doctor of Philosophy

University of Bath

Department of Architecture and Civil Engineering

April 2014

[ ]

Table of Contents

List of Figures

List of Tables

Acknowledgements

Beside hard work and dedication, it is not possible to accomplish a mammoth task of writing a PhD thesis without constant inspiration, advice and moral supports from a group of people who are closely associated with me. This is the time to appreciate those invaluable supports.

Firstly, it is my late father, who would have been immensely proud to see the completion of this great task of my life. His deep moral support encouraged me to embark upon this massive task as I knew how happy he would be to see me succeed. It is my utmost regret that he was not able to see the end. However, I take great satisfaction by knowing how happy he would be should he around in this world now.

The two great ladies who inspired in every success of my life and encouraged in any difficulties I might have faced, must be honoured and appreciated during this great moment of my life. They are my beloved and cherished mother and wife. Both of them at their own capacity have greatly influenced, encouraged and contributed to successfully complete this thesis by means of moral support, compassions and perseverance.

It would not be possible to complete this work without the great help, guidance and support of my principal supervisor Dr Kevin Paine. It was a challenging task for him undertaking the supervision of a PhD work which was in a different time zone of +4 hours GMT. Often he needed to work beyond his working hours and weekend to suite my working hours in the UAE. He had to fly over to Abu Dhabi several times for this purpose.

I must also acknowledge the great support provided by my second supervisor Prof. Pete Walker, especially for his kind advice to improve the quality of this thesis. Along the last four years I received great deal of help directly or indirectly from people close to me to accomplish my work. I must acknowledge the extraordinary assistance provided by my ex-colleagues and good friends Mr Ekramul Haque, Mr Mohiuddin, Mr Abul Kashem and many others from Xtramix, UAE and the University of Bath, UK. It would be very difficult for me to complete this work without their sincere support and help.

Abstract

Massive construction activities in the countries of Arabian Peninsula have raised legitimate concerns about the associated impact on the environment in terms of emission of greenhouse gas and other environmental factors. As concrete is the most commonly used building materials, reduction of eCO_2 and other impacts are a necessity.

Use of high volume of Supplementary Cementitious Materials (SCMs) such as GGBS, fly ash, microsilica and rice husk ash together with Portland cement in different combinations could reduce the eCO_2 substantially. Use of specific sustainable practices such as utilizing finer particles of unwashed crushed limestone fine aggregates, recycled concrete aggregate (RCA), additionally entrained air and utilizing higher ambient temperature to design concrete strength and durability parameters could be the key strategies to reduce the impact of the environmental factors.

The effect of different type of cementitious combinations together with finer particles of unwashed sand, RCA, entrained additional air and elevated curing temperature were tested on concretes and validated against a commonly used concrete mix proportion and a set of specific performance criteria based in the Arabian Gulf. The microstructure of the cement pastes and mortars made of similar cementitious combinations were analysed using techniques like TGA, SEM and MIP.

The engineering and durability properties of the selected concrete mixes were validated against the environmental performance and corresponding cost effectiveness based on the regional implications of Arabian Peninsula. To evaluate the environmental performance of the concrete a concept of strength/eCO_2 index and a set of sustainability environmental factors (ESF) are introduced.

It was found that concrete mix proportion containing 15% Portland cement, 70% GGBS and 15% rice husk ash of total cementitious materials combining with other associated sustainable practices such as RCA, additional finer particles of ‘unwashed’ crushed limestone fine aggregates and entrained air met the overall performance of engineering, durability and environmental parameters compared to the control mix and conditions. A concrete with 85% GGBS could be another alternative with the most cost effective scenarios.

Chapter 1

Introduction and Background

1.1 Introduction

Oil and power industries in the Gulf region are driving economic growth by supporting a population boom and diversification into new business sectors. This rapid growth also means that the region is amongst the world's worst polluters per capita, although moves to address CO_2 emissions in the region are developing at an extraordinary pace.

Since the majority of construction within the Gulf region utilizes concrete as the core building material it is imperative that CO_2 emissions related to its use are controlled. For example, Portland cements which act as the principal binding material in almost all concrete used in ordinary construction produces over 1.6 billion tonnes of CO_2 per annum globally (Wilson, A., 1993).

The cement industry has sought to improve energy efficiency and reduce CO_2 emissions through incremental process improvements and the use of cement replacement materials, although much of this research is focusing on use of alternative forms of concrete that can be used in low to medium performance concretes, where requirements for strength and durability are less severe.

However, the Gulf environment is particularly severe with regard to: temperature and aggressive environment such as chloride and sulfate exposure. Therefore, options to improve the sustainability of concrete for this environment will need to be more robust and technologically sound, leading to significant new research problems.

1.2 Background

Gulf countries particularly UAE, KSA and Qatar have set ambitious goals to reduce the impact due to fast growing development in the region. The Masdar Initiative (Masdar, 2014) in Abu Dhabi is the most ambitious sustainability program ever launched by a government – an initial investment of US$15 billion in projects targeting solar, wind and hydrogen power; carbon reduction and management; sustainable development; education; manufacturing; and research and development.

WWF and the government of Abu Dhabi (Emirates Wildlife Society in association with WWF, 2010) have launched a sustainability strategy to deliver the Masdar city programme by embracing ten principles of 'One Planet Living' i.e. zero Carbon, zero Waste, sustainable transport, local and sustainable material, local and sustainable food, sustainable water, natural habitats and wildlife, culture and heritage, equity and fair trade and health and happiness.

A green building code was introduced in Abu Dhabi as part of a major new sustainability programme. The Pearl Building Rating System (PBRS) initiative is designed to cut the use of water by 30 percent and energy by 20 percent. It is part of the Estidama (sustainability in English) programme intended to earn Abu Dhabi the title of the Middle East's green capital within 15 to 20 years. The code would be applied first to upcoming buildings and then to existing ones in phases (Estidama, 2010).

The PBRS code has five ratings – from one pearl to five pearls – and the more effort that a developer puts into achieving sustainability the higher the ranking the building will be given. Buildings with a sustainability level of 35 percent will receive one pearl, 45 percent will earn two pearls, 55 percent will get three pearls, 65 percent will receive four pearls and 75 percent will earn five pearls. Since September 2010, it has been mandatory to achieve at least one pearl in all villa, buildings and community projects in the Emirate of Abu Dhabi.

According to the Environmental Master Plan of the Emirates of Dubai (Government of Dubai, n.d.), the government is committed to the concept of "green buildings", which take into account the durability of a site's design, efficiency of water and energy consumption, and the quality of the internal environment and the materials and resources employed. This comes as part of the government's commitment to environmental rules and concepts as in line with international standards which aim to reduce pollution and consumption of natural resources, as well as reduce operational costs, enhance performance of buildings and create a healthy working and living environment. Accordingly, the Dubai Government will apply the concept of "green buildings" in the government's future projects, facilities and buildings to preserve the environment in line with international environmental standards.

Accordingly, Dubai issued a new resolution on the implementation of green building specifications and standards in the Emirate of Dubai. Under the new resolution, all owners of residential and commercial buildings and properties in Dubai must comply with internationally recognized environmentally-friendly specifications. The resolution was effective from January 2008.

Similarly, the Gulf organization for research and development (GORD) based in Qatar has developed Global sustainability assessment system (GSAS) to promote environmentally sustainable building and construction process. GSAS is being promoted as a unique building rating system suitable for entire gulf region (Al Horr, Y., 2013).

1.3 Concrete in the Arabian Peninsula

Concrete is the most common construction material in the Arabian Peninsula due to the ready availability of limestone, the most common raw materials needed to produce cement and aggregate. Severe summer heat and high humidity along the coastal region also makes concrete buildings or buildings made of stone and mud ideal dwelling structure for locals due to their unique characteristics of thermal insulation, durability and strength.

It is a challenge to use reinforced concrete to under such extreme climatic and severe exposure conditions of Arabian Peninsula. Both plastic and hardened properties of concrete need to be at their optimum level to satisfy demanding parameters set by the local industry to ensure ultimate durability and serviceability of structures during their service lives.

The tremendous boom in the construction industry, the region has been experiencing since the mid of last decade due to higher demand of oil and petrochemical products, has attracted attention from across the world. This resulted in an unprecedented rush of activities from wide range of organizations related to concrete and construction industries from the more developed world with rich in technology and expertise coming over to the Middle East, particularly in the gulf region. Each organizations has brought in their own sets of standards, specifications, design criteria, guide-lines and code of practices from their country of origin to influence local standards and practices, resulting in a confluence of conflicting sets of standards and specifications.

Often these specifications do not satisfy the harsh demand of local climatic and exposure conditions. It is also common to observe conflicting specifications for same set of exposure conditions within a project or within projects at the same environmental exposure conditions due to the engagement of different designers who use their own set of design parameters. Lack of unified guidance to harmonize existing code of practices has created an acute situation resulting in overdesign and waste of resources. Though this is beyond the scope of this work, however, it is important to mention that to achieve an environmentally sustainable construction practice, a harmonized code of practices for the Arabian Gulf region is essential.

Beside costs and availability of raw materials, the main factors affecting the concrete design are concrete strengths and its durability requirements. Chloride and sulfate exposures are the main concern. As most of the development is along the coastal region, the concrete structures are often subject to high concentration of chloride exposure. Underground waters are often found to be very high in both chloride and sulfate concentration. Air borne chloride and chloride directly from sea water for marine structures are the main sources of chloride. Rich deposit of underground gypsum contributes to the sulfates in the underground water. Higher temperature and permeable underground soil have made the underground condition very conducive to the sulfate attack to the underground concrete structures.

1.4 Aims and Objectives

In order to address the above environmental and durability concern, a series of options to produce a new set of concretes are proposed. The **aim of this study** is to achieve that these new concretes are low in embodied CO_2, environmentally sustainable in terms of reduced impact on different environmental factors as well as with adequate mechanical and durability and permeation properties to provide a new alternative to current practices of concrete production and use.

Methods to achieve these low carbon and sustainable concretes that will be investigated as part of this research include:

i. Concrete with very low Portland cement content by using high volume supplementary cementitious materials
ii. Use of specific sustainable practices such as
    - unwashed sand
    - recycled concrete aggregate
    - increased volume of air content
    - utilizing higher ambient temperature of the Arabian Peninsula

It is probable that the development of performance-based standards may be critical to the acceptance of these materials. To this end research is required to investigate low carbon concretes with the performance requirements for the range of industry significant applications in the Gulf region, specifically those in the UAE, and compare these with the current blended cement alternative.

Clearly, if any low carbon concrete is to have a real impact on embodied CO_2 and other sustainability factors then it will need to have a performance and durability characteristics at least as good as the current generation of blended cements based on Portland cement. Therefore a set of programme or objectives have been designed to assess whether the proposed concrete mix proportions would achieve the required performance. It is anticipated that **this set of objectives would consist of following five phases** in order to:

1. Identify the environment, exposure conditions and limitations on concrete materials that are specific to the Gulf region, and ascertain appropriate, representative types of concrete and associated requirements.

2. Ascertain and design appropriate forms of new and developing concretes that may be used to reduce sustainability and carbon impacts in the Gulf region.

3. Understand of the fundamental cement science and concrete technology that underpins the behaviour of these novel concretes.

4. Normalise (standardize) the performance of new-sustainable concretes with former blended cement concretes with respect to performance-based specifications, and demonstrate the equivalence in performance.

5. Identify the most-appropriate forms of sustainable concrete for use in the gulf region with regard to the balance between strength, durability, and CO_2 emissions and other sustainability measures.

The total illustration of above five phases has been made into seven main chapters excluding the chapter of introduction and conclusions. A comprehensive review of the state of the art of concrete in the Arabian Peninsula was undertaken. It covered the climate and exposure conditions, concrete practices and standards to address these conditions using locally available raw materials to mitigate chloride and sulfate and other associated attacks and the properties and chemistry behind these attacks.

The literature review also explored the associated eCO_2 of supplementary cementitious materials (SCMs) including GGBS, fly ash, microsilica and rice husk ash to partially replace the Portland cement from concrete at high volume and other sustainable practice such as use of recycled concrete aggregate to reduce the environmental impact of concrete and its production. The chemistry behind the hydration process of these SCMs together with Portland cement was also reviewed. Fundamental theories of particle packing were reviewed to understand the basic science behind this phenomenon. As part of the sustainable practice, an unwashed crushed limestone fine aggregate containing excessive finer particles was used.

The programme and methodology of the work are explained in the following chapter where the work method of different type of tests on concrete, mortar and paste to analyse their mechanical, durability and microstructure are explained. In subsequent chapters the results of these tests in terms of their plastic properties, compressive strengths, durability and permeation properties are presented and discussed.

Among the durability parameters, resistance to chloride and sulfate ions to these new concretes has been investigated. Carbonation is not considered as part of the work programme as it was assumed that carbonation resistance to these novel concretes would be good.

The analytical properties of the microstructure of cement paste to evaluate their hydration products and pore structures are presented and discussed using techniques like thermogravimetry analysis, scanning electron microscopy and mercury intrusion porosimetry tests. The effects of different types of cement and sand on the microstructure of paste and mortar are observed and verified with the compressive strength and durability performance of concrete made with equivalent cement and sand combinations.

The eCO_2 of concrete comprising cradle to gate of concrete ingredients using local data available for Abu Dhabi, UAE was computed and compared. The relationship between the eCO_2 and their corresponding compressive strengths were established to determine the effective concrete mixes with optimum performance of eCO_2 and compressive strengths as these two parameters are linearly proportional. The effects of other environmental factors designed on the basis of the environmental factors described by the local 'Pearl building rating system' of Estidama were also analysed.

Finally, an analysis of the performance of engineering, durability and permeation properties of different type of concrete has been performed with their corresponding development of microstructures. Thereafter, the regional implications of the new novel concretes in terms of the acceptance by the industry, cost implication and validation of the performance were made. The validation works compared the performance of their compressive strength, durability, permeation properties and environmental performance with a set of selected targets based on a performance based specification and the performance of the control concrete.

1.5 Summary

Concrete is the main construction materials used to meet the massive construction demand in the Arabian Peninsula. The harsh environmental condition with severe exposure to chloride and sulfate, concrete in the Middle East needs to be with high performance and durable. Environmental sustainability is the key concern to the local governments and set of environmental standards have already been legislated and enforced. As concrete is a major contributor to the CO_2 emission due to its heavy dependency on the Portland cement, finding a low carbon concrete is the main goal of this research work. A methodology and work programme have been designed and validated to achieve this goal which include reduced Portland cement, use of SCMs, use of recycled aggregate and follow specific sustainable practices.

Chapter 2

Literature Review

2.1 Introduction

Extremely high summer temperature and chloride laden environment makes the Arabian Peninsula the most extreme region in the world to produce concrete with quality and maintain the durability of concrete structure. Massive construction activities which started during 1960s after the discovery of oil have now been moved into a modern and dynamic phase. Cities like Dubai, Abu Dhabi, Doha, Riyadh, and Jeddah are witnessing massive investment in infrastructure, real estate, transportation, utilities, tourism and other sectors.

Concrete structures in such aggressive environment requires very high level of standards of construction practice, raw material selection, design method to achieve similar level of service life expectancy of structures from the other part of the world (Concrete Society, 2002).

As the main focus of the designer is how to achieve the required level of durability and serviceability of the structure, the notion of sustainable construction activities and its impact on the environment is paramount. To establish a low carbon concrete ideally suitable to meet these necessary durability requirements of the region is the basis of this research work.

Therefore, an extensive literature review has been undertaken to establish the current knowledge in the area of research. The main sections of this literature review are:

i. Climate and geology of the Arabian Peninsula
ii. Availability of raw materials in the gulf region
iii. Standards and practices of concrete mixes in the Gulf region
iv. Durability assessment of concrete
v. Low carbon and environmentally sustainable concrete
vi. Review of the fundamental cement science and concrete technology
vii. Review of particle packing

Based on the findings from the literature review, a comprehensive test programme has been designed comprising of different possible concrete mixes containing low embodied CO_2 and environmentally sustainable methods and practices. These concrete mixes then tested for their structural and durability properties to ascertain their acceptability as legitimate concrete mix for regular use in the Arabian Peninsula.

2.2 Climate and geology of the Arabian Peninsula

The Arabian Peninsula can be divided into five predominant geographical zones:

1. The narrow and flat western coastal plain
2. Western mountain zone
3. The hilly central plateau
4. The flat terrain of the eastern coastal plain next to the Arabian Gulf
5. A variable width southern coastal plain bordering the Oman mountains

The climate of Arabian Peninsula is hot-desert environment with very low level of rainfall. Most of the region consists of a rolling plateau with low to medium elevation. It has higher mountainous rim at the west and low plain coastal region at the eastern gulf.

The temperature is at the highest level in between May and September over much of the region except at higher mountainous level. The temperature could rise above 48 degree centigrade during summer. Beside high temperature, high humidity makes it unbearable to work outside during summer, especially at the coastal region. The inner region is normally having lower humidity and lower temperature at night. During winter the inner region and at the north-western mountains of Saudi Arabia often encounter frost and snow. Winter nights at the desert are also very cold. (CIRIA and Concrete Society, 2002)

The macro climate of the Arabian Peninsula is hot and arid with higher rate of evaporation of moisture than the rainfall. This imbalance is made up by the evaporation of water from the surface of the sea or the ground-water which is often fed by the sea especially at the coastal region, increasing the higher level of relative humidity. Typical data of average daily temperature and relative humidity of the emirates of Dubai of UAE have been plotted in Figure 2.1 and Figure 2.2. (WeatherSpark, 2014)

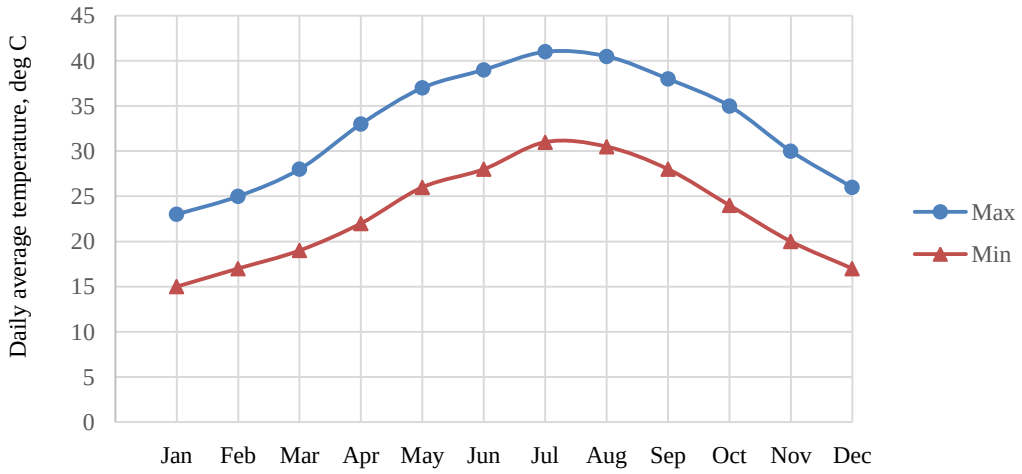

Figure 2.1: Typical data of daily average temperature of the emirates of Dubai, UAE (WeatherSpark, 2014)

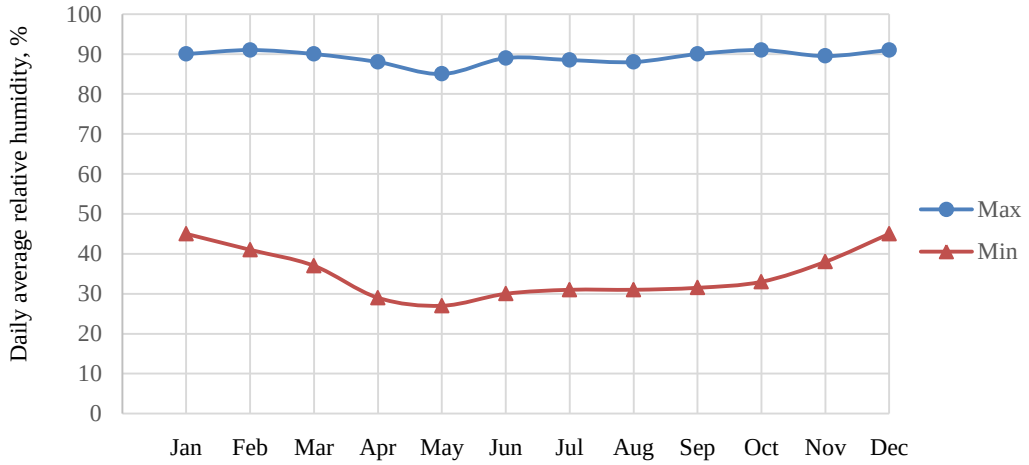

Figure 2.2: Typical data of daily average relative humidity of the emirates of Dubai, UAE (WeatherSpark, 2014)

The level of salt at the two water bodies at the east and west of the region, the Red Sea and the Arabian Gulf are very high due to lower level of tidal activities between them and the open sea (Arabian Sea) due to their semi-enclosed geographical nature. It has been reported that the salt concentration of chloride and sulfate is almost 20% higher than the open sea at the shallower water near the Gulf. This figure near the Red Sea is 10% (CIRIA and The Concrete Society, 2002). A map of the Arabian Peninsula has been shown in Figure 2.3.

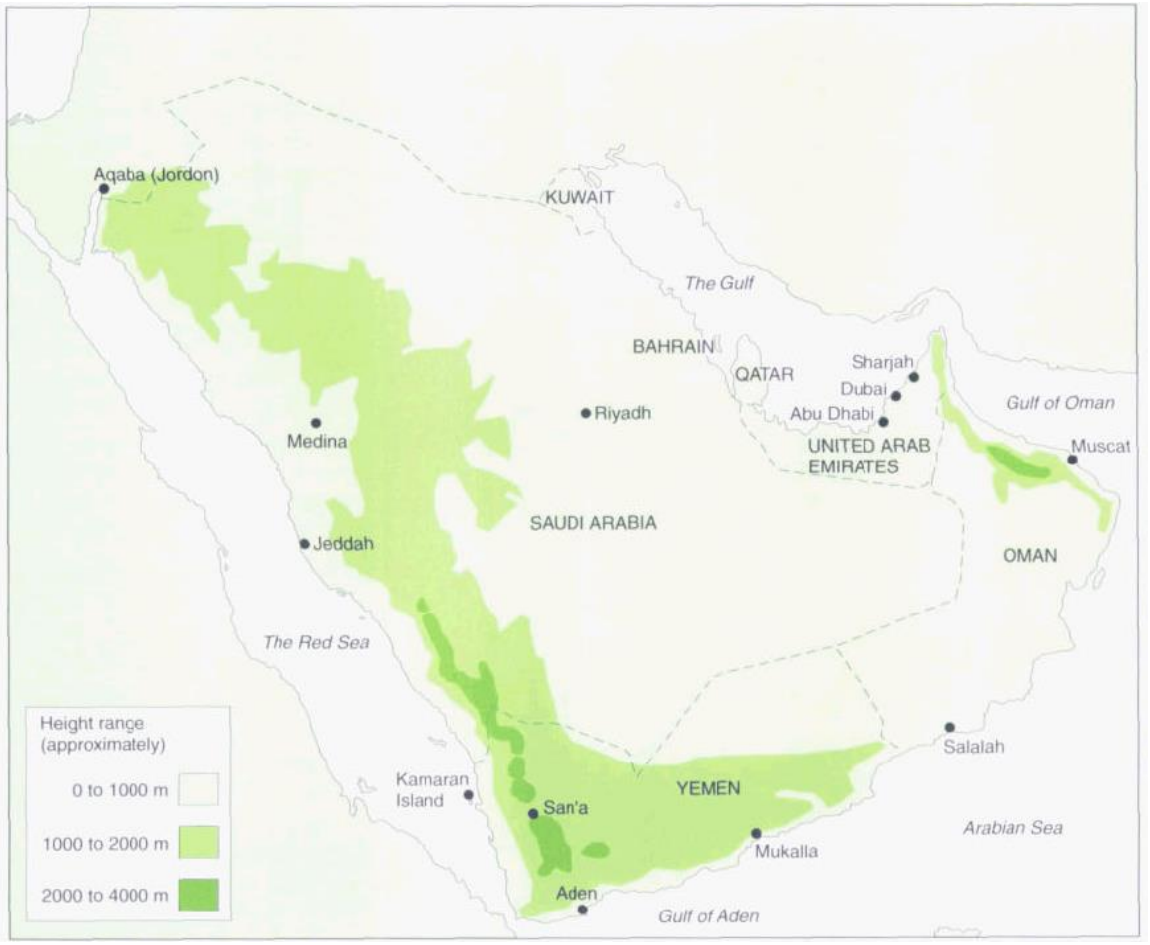

Figure 2.3: Map of the Arabian Peninsula (from Concrete Society, 2002)

The level of salt at the two water bodies at the east and west of the region, the Red Sea and the Arabian Gulf are very high due to lower level of tidal activities between them and the open sea (Arabian Sea) due to their semi-enclosed geographical nature. It has been reported that the salt concentration of chloride and sulfate is almost 20% higher than the open sea at the shallower water near the Gulf. This figure near the Red Sea is 10% (CIRIA and The Concrete Society, 2002).

In the coastal region the sea water is the only source of the ground-water (see Figure 2.4). This makes the ground water with very high concentration of salt. As the level of the ground water is very high, the salty water rise up to the surface by capillary through the granular soils and being evaporated, leaving behind deposits of salt on the ground. This makes the construction at the ground very difficult as the soils are contaminated with salt (CIRIA and The Concrete Society, 2002).

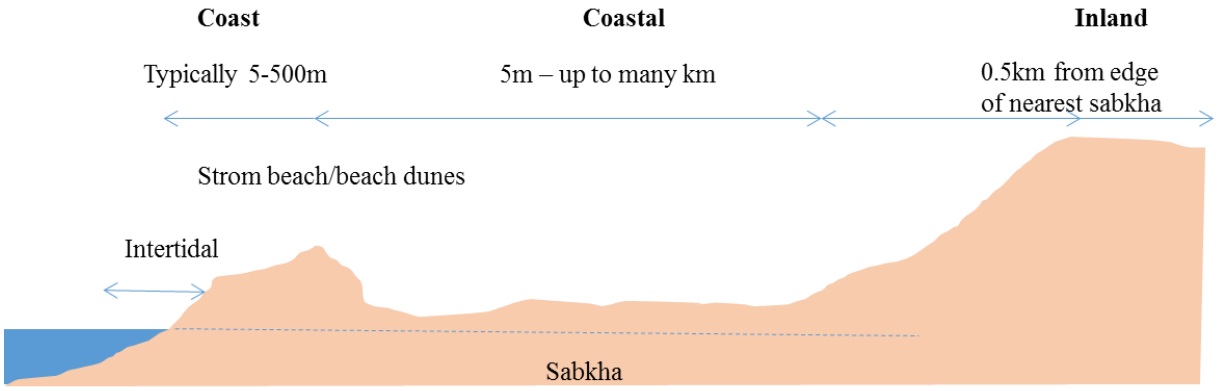

Figure 2.4: Sea water at the coastal region forms the main source of ground water (after CIRIA and The Concrete Society, 2002)

Sabkha along the coastal plain where most of the development is concentrated, have developed from the infilling of coastal lagoons. High groundwater level maintained by the seawater percolating through beach and sand bars has made the Sabkha as a natural evaporating pan saturated with brine, precipitating chloride, sulfate and carbonate minerals. The concentration of ions such as Ca^{2+}, K^{+}, Mg^{2+}, Na^{+}, Cl^{-}, $CO_3^{2-}$and SO_4^{2-} in the Sabkhas are reportedly as high as 50% of the volume (Fookes, French and Rice, 1985 as cited in CIRIA and The Concrete Society, 2002, p.25). Table 2.1 shows a typical chemical analysis of Sabkha and seawater (Al Amoudi, B., et al., 1994).

Table 2.1: Typical chemical analysis of Sabkha brine and seawater in Arabian Peninsula as per Al Amoudi, B., et al. (1994)

Ions (g/l)	**Sabkha brine**	**Seawater**
Na^{+}	78.8	20.7
Mg^{2+}	10.32	2.3
K^{+}	3.06	0.73
Ca^{2+}	1.45	0.76
Fe^{2+}	Trace	–
Sr^{2+}	0.029	0.013
Cl^{-}	157.2	36.9
Br^{-}	0.49	0.121
SO_4^{2-}	5.45	5.12
HCO_3	0.087	0.128
pH	6.9	8.3

The salt deposit from the ground surface can also be taken up by wind and can be deposited on concrete structures. This salt in combination with moisture from condensation, leaks or discharge from the air conditioning units can permeate into the concrete to attack steel reinforcement (Concrete Society, 2002).

The solar radiation in Arabian Peninsula is very high due to the presence of clear sky for most of the year due to its hot-arid micro climate created by the high atmospheric pressure along the tropic of cancer. This makes rapid rise of temperature of objects subjects to direct sunlight. Rate of cement hydration and rapid loss of water by evaporation from the plastic concrete makes producing and placing of concrete very challenging. The rate of deterioration of any chemical process within concrete such as corrosion could be very rapid due to this phenomenon (CIRIA and The Concrete Society, 2002).

Moreover, very high temperature differential between day and night time should be considered into the structural design of the concrete structure to avoid any thermal cracking. The relative humidity of the region in both summer and winter can vary from as low as 5% to as high as 90% or more. The average humidity is around 50% in summer and 70% in winter.

The wind speed in the coastal region often exceeds 17km/hour. This occasional higher wind compounded with higher temperature creates a permanent problem of plastic shrinkage of freshly placed concrete in this region. The wind also carries salt laden dust depositing them on constituent materials of concrete especially aggregates, increasing the level of chloride content in concrete. Typical data of daily average sunshine, daily average wind speed and probability of rain at some of point of the day of the emirates of Dubai of UAE have been plotted in Figure 2.5, Figure 2.6 and Figure 2.7 respectively. (WeatherSpark, 2014)

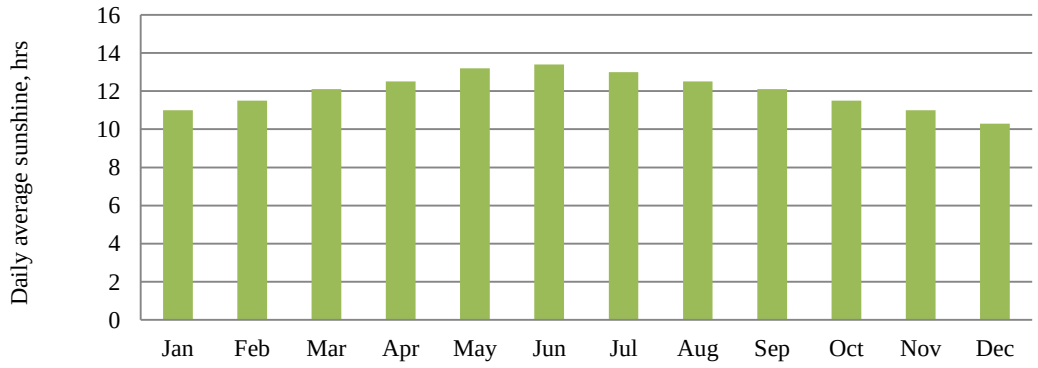

Figure 2.5: Typical data of daily average sunshine of the emirates of Dubai, UAE (WeatherSpark, 2014)

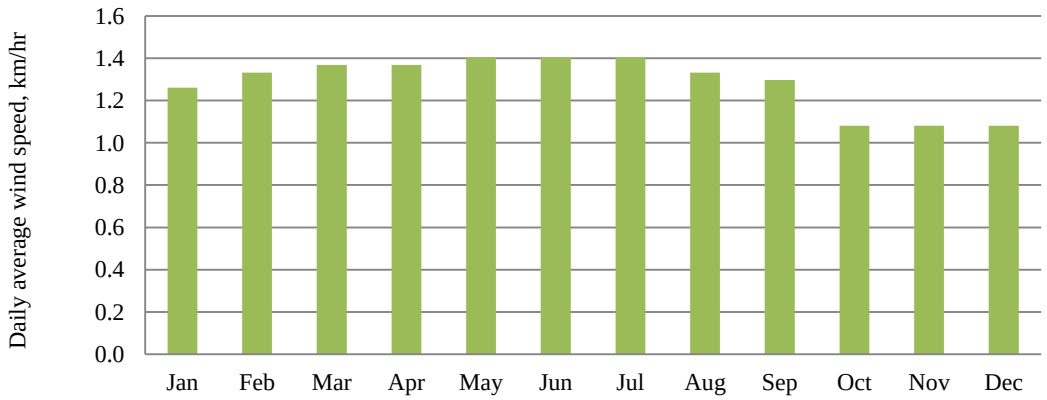

Figure 2.6: Typical data of daily average wind speed of the emirates of Dubai, UAE (WeatherSpark, 2014)

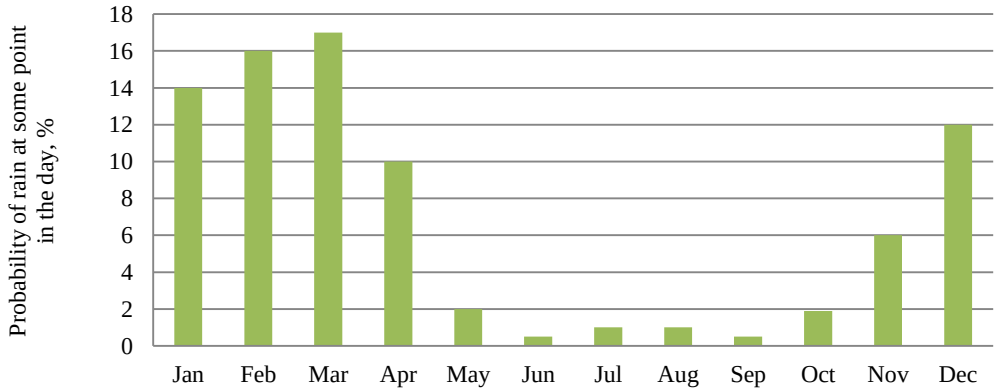

Figure 2.7: Typical data of the probability of rain at some point in the day of the emirates of Dubai, UAE (WeatherSpark, 2014)

2.3 Availability of raw materials in the gulf region

Availability of raw materials with acceptable quality to produce concrete with higher degree of durability to withstand the severe climatic conditions of the region is a pre-requirement. The degree of sustainability and the level of embodied CO_2 in the concrete mixes are also affected by the availability of raw materials within the region. In this chapter the local availability of concrete constituents to be discussed.

2.3.1 Aggregates

Wide range of rock types and source of aggregates are available in the region of Arabian Peninsula. Approximately one third of Saudi Arabia is underlain by Precambrian age metamorphic and igneous rocks. The remaining areas are underlain by the sedimentary rocks of various ages between Cambrian to Quaternary (CIRIA and The Concrete Society, 2002).

Limestone is the most common type of sedimentary rock available in the eastern part of the Arabian Peninsula. Ras Al Khaimah in the UAE at the northern tip of the Oman mountains (Al Hajar mountain) is a good source of Jurassic age limestone. Crushed rock of such limestone meets both coarse and fine aggregate demand of the local concrete industry. Lower thermal expansion property of limestone has also made it ideal for concrete in this region where thermal expansion of concrete is a major factor for designer. Approximately 12 billion tonnes of limestone deposits in the Burami region at the border of Oman and UAE is another good source of limestone (Kamoonpuri, H., 2010). Limestone deposit also found in Quriyat, Musandam, Sur and Salalah of Oman.

Although most of the limestone found in the region are chemically stable, some of the limestone deposit may contain cherts. These types of aggregates need to be carefully verified for potential risk of alkali silica reaction. Limestone in the region can be rich in magnesium or magnesium carbonate mix dolomites which could be a concern of long term alkali-carbonate reaction in the concrete.

Predominantly dolomitic limestone is the main source of aggregate in the eastern province of the Saudi Arabia along Arabian Gulf (Maslehuddin, M. et al., n.d). Though some of the limestone found in the eastern part of Saudi Arabia could be porous with higher water absorption. Denser limestone could be found in the central region while more igneous and metamorphic rock such as Basalt are common in the western part of the Saudi Arabia (Zein A1-Abidien, H. M., 1987).

Although Alkali-aggregate reaction has not been extensively reported in this region, expansive alkali-silica reaction has been noted by Fearson (1996) in concrete in southern Oman with potentially reactive aggregate material noted by French and Poole (1976) and Sims and Poole (1977) as cited by the CIRIA and The Concrete Society, (2002).

Igneous and metamorphic rocks such as gabbro or granite are harder and ideal for concrete application. Gabbro can be found in the Oman Mountain especially in Fujairah. Granite can be found in the western part of the Saudi Arabia and Yemen (CIRIA and The Concrete Society, 2002). Crushed limestone is the main source of coarse aggregate beside some proportion of gabbro is being used. The most common maximum size of aggregates for concrete is 20mm and 10mm. The quality of the aggregates is often good with higher aggregate crushing value and lower in absorption.

The crushed rock fine of limestone aggregate (fine aggregate) is the main source of fine aggregates, derived often from the same quarries as the coarse aggregates. The average maximum size of the sand is 5mm. The fine aggregate often contains a high percentage of fine limestone particles of less than 75μm in size which could be as high as 10-15% of particles by mass. To comply with local practice which is maximum 5% by mass (ADNOC, n.d.), the fine aggregate would often been washed to remove the finer particles. Washing fine aggregate by water is very wasteful as it needs huge amount of water which is very scarce in this arid part of the world. The sludge derived from the washing also needs to be disposed, creating another source of waste. However, it is the author's opinion that the finer filler particles of the limestone dust could contribute to the strength and durability of the concrete as it is a good source of filling materials and should not wash off in the first place.

Natural well graded sand and gravel as a source of aggregate can be found in the wadi channels in Oman, Saudi Arabia and UAE. The types of minerals could be gabbro, limestone, serpentinites or granite. These wadi aggregates are relatively free from salt contaminations. Extraction of many such wadi materials have now been discontinued due to environmental concerns (CIRIA and The Concrete Society, 2002).

Dune sand is windblown, single sized, well rounded sand. Since wind can only blow dry sand, contamination of mobile dune from the capillary risen ground water is low. This makes dune sands often low with sulfate and chloride content (Ismael, N.F., 1997).

Dune sand is a major ingredient in the concrete mixes in the Arabian Peninsula due to its abundance in the dune. Being natural aggregate, it is rounded and provides vital contribution to the flow and rheology of the concrete mix. It can be blended with the crashed rock fine aggregates to increase the workability, reduce bleeding and optimize cohesiveness. The size of dune sand is normally between 75μm and 300μm - it typically contributes approximately 15% of the total aggregate volume of concrete mixes. (Chapter 3, Table 3.4, Particle size distribution of aggregates).

2.3.2 Cement

The abundant availability of limestone in the region has made cement and concrete the main construction materials and has contributed tremendously to the ongoing construction boom in the Arabian Peninsula. Cement is produced in every country in the gulf though only Saudi Arabia, UAE and Oman have the limestone deposits. The cement producing capacity of the Gulf Cooperation Council (GCC) countries in year 2010 was 110 million tonne per annum, which is approximately 2.8% of total global capacity. GCC has the highest per capita cement production capacity in the world (Karmani, 2011).

The quality of cement produced in the Arabian Peninsula is considered to be good and generally widely available throughout the region (Annex M: Cement Test Certificate: National Cement Company, UAE). Occasional shortfalls generally be met by importing cement and clinkers in some parts of the region from various sources may cause variations in characteristics and quality of cement (Concrete Society, 2002).

2.3.3 GGBS, fly ash and microsilica

Ground granulated blast-furnace slag (GGBS), fly ash and microsilica are the main supplementary cementitious materials (SCM) to partially replace Portland cement are used in this region (CIRIA and The Concrete Society, 2002). The fly ash and microsilica used in this region are imported from various sources. Fly ash predominantly comes from India and South Africa. The main source of microsilica is China. Granulated blast-furnace slags are normally imported from China or Japan and are ground in the ball mill in the Arabian region. Therefore GGBS, the final product, can be considered as locally produced material.

In Saudi Arabia microsilica is the most common SCM used while GGBS and microsilica either in combination or separately with Portland cement are widely used in the UAE. The author has experienced that the reason of using of SCM in this region is mainly for durability requirements of concrete structures. Harsh climatic condition of Arabian Peninsula compounded with severe exposure of sea borne chloride and underground sulfate rich environment has made almost all new concrete constructions with very stringent requirements of protection against corrosion and sulfate attacks.

2.3.4 Admixtures

Sulphonated naphthalene formaldehyde (SNF) based admixture with good set retarding and slump retention effect is the most common admixture to cater for harsh summer temperature of the gulf region (CIRIA and The Concrete Society, 2002). However, polycarboxylate ether (PCE) based superplasticizer has become popular due to its superior water reduction and requirement for high performance concrete. Low-end PCE admixture is becoming more cost effective compared to traditional SNF based admixture (Sika, 2011).

Beside high range water reducing and plasticizing admixtures special admixtures such as waterproofing/ water resisting, corrosion inhibiting, lightweight foam admixtures are widely used (CIRIA and The Concrete Society, 2002/ADCO, 2007). Use of polypropylene fibre to resist plastic shrinkage crack is common in the petrochemical industry in the UAE (GASCO, 2007).

2.4 Standards and practices of concrete mixes in the gulf region

Specification, design and production of concrete in the gulf region are greatly influenced by the British and American codes, practices, and standards. Former British standards together with harmonized European standards under BSEN suffix are the most common standards being specified. Parallel standards from ASTM and codes and practices from American Concrete Institute (ACI) are often specified together with the British and European standards. Specific standards for testing are often specified from former German (DIN), Norwegian (NORDIC) and RILEM standards (ADCO, 2007/ ADNOC, n.d. / GASCO 2007).

To provide a snapshot of the current standards and practices of concrete mixes in the region, three project specifications from the UAE are discussed here. Specifications from three major petro-chemical organizations namely i) GASCO ii) ADCO and iii) ADNOC operating at the western part of the Abu Dhabi emirate of the UAE are considered. They are currently investing multi-billion dollars to increase the capacity of the oil and gas production. Table 2.2 provides the name of the specifiers/clients and the projects (GASCO, 2007/ADCO, 2007/ADNOC, n.d.).

Table 2.2: Details of three petro-chemical projects in Abu Dhabi

	Specifier	Project
1	Abu Dhabi gas industries Ltd (GASCO)	General specification for concrete supply
2	Abu Dhabi company for onshore oil operations (ADCO)	Project no. P14333 - FEED service for SAS full fields development
3	Abu Dhabi national oil company (ADNOC)	Ruwais housing complex expansion project – phase III

All these three projects are located almost at the similar environmental exposure. The sources of raw materials of all these projects are also very similar if not the same. However, the project requirements for concrete properties are varied and often contradicting. Table 2.3 provides a summary of the applicable standards for concrete and its constituents for these three projects.

As it can be seen from Table 2.3 the specification requirements of the constituent materials of concrete in GASCO projects are including almost all major standards. Former British standards, its equivalent new European and American standards are referred to the specification of concrete and its constituents. This approach creates contradictions and confusion instead of complementing each other. For example allowing both former BS 5328 and current BS 8500/BSEN 206 for concrete production, creates confusion and requires more clarification from the specifiers by the producers which is often a time consuming process.

Table 2.3: Applicable standards for concrete for GASCO, ADCO and ADNOC projects

Materials	Specifier	Standards
Cement	GASCO	BS 12 / BSEN 197-1 / ASTM C150
	ADCO	ASTM C150
	ADNOC	BSEN 197-1
Aggregates	GASCO	BS 882 / BSEN 12620 / ASTM C33
	ADCO	BS 882
	ADNOC	BSEN 12620
Admixture	GASCO	BS 5075 / BSEN 934-2 / ASTM C494
	ADCO	ASTM C494
	ADNOC	BSEN 934-2
Water	GASCO	BS 3148 / BSEN 1008
	ADCO	BS 3148
	ADNOC	None
Concrete	GASCO	BS 5328 / BS 8500-1&2/ BSEN 206-1 / ASTM C94/C94M
	ADCO	None
	ADNOC	ASTM C 94 / BS EN 206-1
Durability testing of concrete		
Chloride permeability	GASCO	ASTM C1202, Rapid chloride permeability test (RCPT) <1500 Coulomb
	ADCO	None
	ADNOC	AASHTO- T-277/ ASTM C 1202, 1,500 – 3,000 coulomb
Water permeation	GASCO	BS EN 12390-8, <10mm
	ADCO	None
	ADNOC	DIN 1048, 8-15mm
Water absorption	GASCO	BS 1881, Part 122, < 2.0%
	ADCO	None
	ADNOC	30 Minute Absorption (BS 1881, Part 122) 2.5% - 3.5%
Porosity	GASCO	RILEM CPC 11.1, < 10.0%
	ADCO	None
	ADNOC	RILEM CPC 11.3, <12% @ 28 days

The ADCO specification is a mix of both the former versions of British specification and ASTM standards. For example, in ADCO specification ASTM C150 has been referred for cement, but for aggregate the referred specification is the withdrawn BS882. Similarly for admixture, it is ASTM C494 and for water it is the former BS 3148. There is no specific standard has been referred for the concrete as a material in ADCO specification.

ADNOC specification adopts the new BSEN standards for all categories except the specification for concrete where both ASTM C94 and BSEN 206-1 have been referred. There is no reference of the former British standards in ADNOC specification can be found.

GASCO specification is a typical example of the project specifications of the region where different international standards have been adopted into one project specification. Often these specifications are old and obsolete elsewhere, but locally practiced. To meet the demand and requirements, the raw material producers such as cement and aggregate producers continued with the older version of the standards (Annex M: Cement Test Certificate: National Cement Company, UAE).

However, there is a shift to move from this trend to adopt the new standards, such as ADNOC's approach. The practical problem is that the industry is still not ready to move entirely to the new standards. Perhaps that is the reason a specification like the one from GASCO is being adopted which refer to all available standards. However, a new addendum to GASCO's Shah Gas Development project moved away from former British standards and accepted only BSEN and ASTM standards (GASCO, 2010).

Special requirements such as durability parameters draw other international standards into the specifications of local projects. Chloride permeation resistance in terms of 'Rapid Chloride Permeability Testing (RCPT) as per ASTM C1202-97, water permeation as per former German standard DIN1048 or new BSEN 12390-8 and half hour water absorption as per BS 1881: Part 122 are the most common durability testing procedures have been adopted by the industry to measure the durability of concrete structure subject to chloride and sulfate exposures.

Initial surface absorption test (ISAT) as per BS 1881: Part 208 is another common durability test often specified. There is no testing requirements can be seen for other durability issues such as carbonations, delayed ettringite formation or salt weathering. Both GASCO and ADNOC specified these tests in addition to the porosity test as per RILEM CPC 11.1 &11.3. ADCO did not specify any durability test at all.

To satisfy the durability requirement as well as the compressive strength requirement of GASCO and ADNOC project specification, the most common concrete mix design adopted by the concrete industry is a concrete with a double blend of 30% Portland cement and 70% GGBS of total cement content by mass. The w/c ratio would also need to reduce to around 0.40 w/c ratio for better water permeation and chloride resistivity values. In fact in GASCO specification it has been clearly specify to use a double blend of 30% Portland cement and 70% GGBS content cementitious blend (GASCO, 2007).

2.5 Durability assessment of the concrete

Harsh climatic condition of the Arabian Peninsula with aggressive salt in ground and ground water and extremely high temperature and variation of relative humidity have made durability requirement of the concrete as an absolute necessity. To address this concern Concrete Society together with CIRIA and the Bahrain Society of Engineers published dedicated guidance on design, construction and repair concrete structures with reinforcement in the Arabian Peninsula (CIRIA and The Concrete Society, 2002/ Concrete Society, 2008/ Concrete Society, 2002).

The Concrete Society Technical Report CS 163 (Concrete Society, 2008) adopted a 'deemed to satisfy' approach with a general principle of designing structures for a given exposure class and design life with necessary related factors such as the cement type, maximum water/cement ratio and minimum cement content.

However, it is author's view that a balanced approach between performance and prescription based specification is the best suitable approach for the Arabian Peninsula as that would provide some degree of flexibility and ownership of the concrete design to the concrete producers. This promotes innovation and novelty which is the core idea of this research.

Based on the similar principle of BS EN 206-1 and BS 8500-1, the CS163 has advised durability parameter of concrete mix designs for concrete structures exposed to chloride and sulfate exposures in the Arabian Peninsula.

There are four main reasons identified by the CS 163 which would have detrimental effect to the concrete structures in this region. They are: i) reinforcement corrosion induced by chloride and carbonation, ii) sulfate attack iii) delayed ettringite formation and iv) physical salt weathering. In the following sections the mechanisms of these attacks have been briefly discussed to understand their local implications in the Arabian Peninsula.

2.5.1 Reinforcement corrosion

In Arabian Peninsula the main cause of the deterioration of the reinforced concrete structure is due to the corrosion of the reinforcement. (CIRIA and the Concrete Society, 2002). Corrosion of steel is an electro-chemical process. It is divided into two processes: i) anodic process and ii) cathodic process. A schematic diagram of these two processes is shown in Figure 2.8.

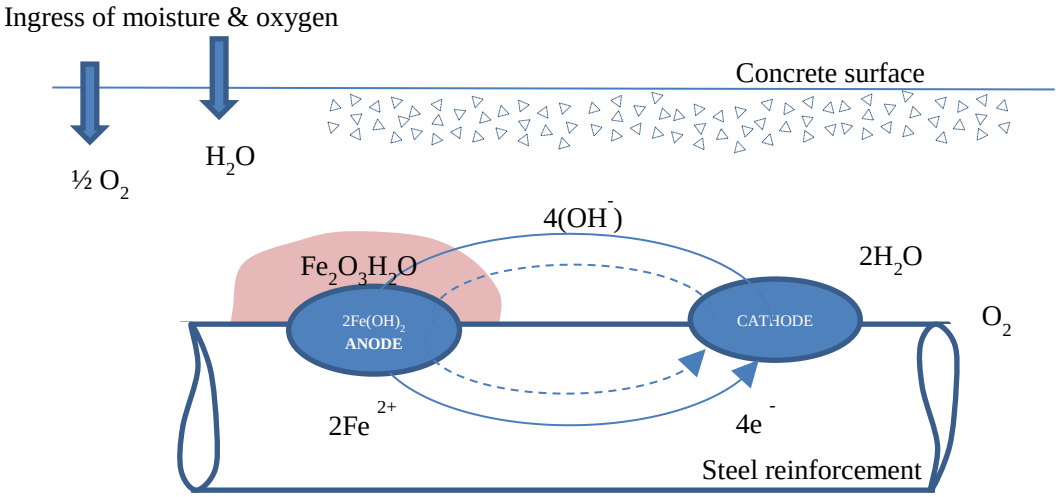

$$\text{Anode} \qquad Fe \rightarrow Fe^{2+} + 2e^{-}$$

$$\text{Cathode} \qquad O_2 + 2H_2O + 4e^{-} \rightarrow 4OH^{-}$$

$$\text{Overall} = Fe^{2+} + 2OH^{-} \rightarrow Fe(OH)_2 \xrightarrow{O_2} Fe_2O_3 \times H_2O$$

Figure 2.8: Schematic diagram of corrosion process (Neville, A.M. 2006)

2.5.1.1 Anodic process

Reinforcement steel embedded into concrete has a passivating oxide layer due to alkaline rich solution of concrete pore water which protects steel from corrosion. However, this passivating layer can be broken down if the pH of the area comes down due to the presence of chloride ions or carbonic acid as a result of carbonation. At the anode, once the protective passivating oxide layer is gone, the dissolution of steel is taken place producing positive iron ions and negative electrons into the solution. (Neville, A.M. 2006)

2.5.1.2 Cathodic process

At the cathode, the liberated negative electrons combine with water and oxygen to form negative hydroxyl ion. These hydroxyl ions then travel to the anode to add with positive iron ions to form ferric oxide $Fe_2O_3.H_2O$ or rust. The volume of the corrosion product or rust is three to six times more than the original volume of steel. Thus the formation of rust resulting into an expansive pressure to the concrete. When this pressure exceeds the tensile strength capacity of concrete, it cracks.

Presence of oxygen and water are two most important factors necessary for corrosion to take place. Oxygen is required because it helps to form hydroxyl ions which eventually combined with iron ions to form ferric oxide or rust. Water acts as an electrolyte, facilitating the travel of the ions through anode and cathode. (Neville, A.M. 2006)

Two major type of corrosions are i) chloride induced corrosion and ii) corrosion due to carbonation. The following sections will discuss briefly about the mechanism and their effect in the concrete structures in Arabian Peninsula.

Chloride induced corrosion:

Chloride induced corrosion is the most common form of corrosion in the Arabian Peninsula (CIRIA and The Concrete Society, 2002). Chloride ions diffuse through the concrete pore water towards the steel reinforcement increasing the level of concentration. Once the level reached the threshold level, the passivating layer of the steel reinforcement are destroyed and creates corrosion cells by establishing cathodic and anodic sites within the different sections of the steel reinforcement bar.

Surface concentration level of chloride C_s, diffusion coefficient of the concrete D, and the critical chloride threshold level C_{cr} are important parameters to determine the initiation of corrosion process (CIRIA and The Concrete Society, 2002). A typical scenario of chloride ingress has been depicted in Figure 2.9.

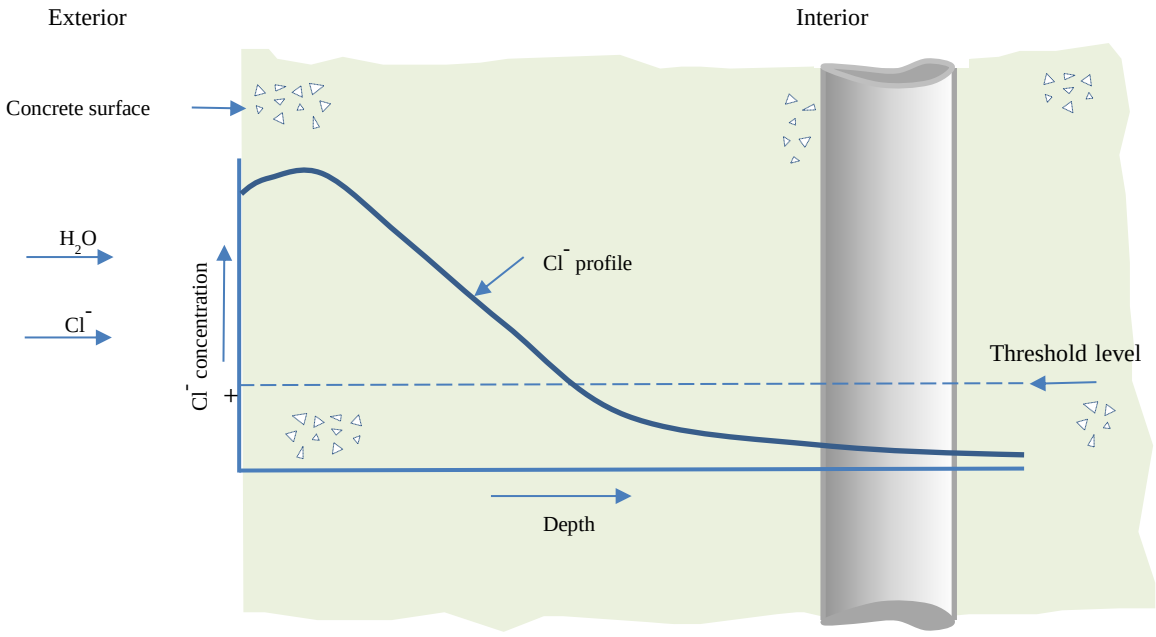

Figure 2.9: Typical scenario of chloride ingress. Chloride profile changes with the depth which is depending on the surface chloride concentration, concrete composition, pore structure and microclimate. Once the threshold level breached at the reinforcement steel depth, the corrosion will initiate. (after CIRIA and Concrete Society, 2002)

Adopting a probabilistic approach ZHANG, X., et.al. (2011) concluded that the probability of the depassivation of the reinforcement bar increases with the increase of exposure time. The extent of the probability of the depassivation depends more on the critical threshold level of chloride concentration at the surface of the reinforcement steel. The next critical factors are the chloride concentration at the surface of the concrete and the diffusion coefficient of the concrete matrix. However, there is a wide opinion on the critical threshold level of chloride to initiate corrosion of the embedded steel reinforcement bar. One of the reasons is the large number of variables that influence the chloride number in the pore solution. Another reason is the lack of agreement to the very definition of the chloride threshold itself (Alonso, C. et al., 2000).

Arabian Gulf region is exposed to very high concentration of chloride. The splash zone of the marine structure and just above the ground level for bridge and buildings where the water is taken in by the concrete and the salt adhere to the surface due to the evaporation of the water have the highest surface concentration of chloride Cs. Table 2.4 shows that both chloride concentrations in the nature and at the concrete surface are the highest in the Gulf region (Smith, BG. 2001). This makes the concrete structures in the Arabian Peninsula most vulnerable from the chloride induced corrosion.

Table 2.4: Cl^- concentration and Cs range in the region as per Brouce, G.S. (2001)

Exposure	**Typical condition**	**Cl^- concentration (%)**	**Cs range (% concrete)**
Extreme	Sea water in tropical climate	2.9 in the Gulf	0.6–0.9
Severe	Sea water in temperate climate, ground water in a hot climate	2.5 in Atlantic Ocean 0.45 in Saudi Arabia	0.3–0.6 0.3–0.6
Moderate	Foundation and superstructure to first floor in hot climates	<0.1	0–0.3

Carbonation:

Carbonation of concrete occurs when carbon dioxide from the atmosphere diffuses into the concrete and reacts with the alkaline properties of pore fluid of the concrete. The reaction causes the neutralization of the pore fluid and conversion of $Ca(OH)_2$ into $CaCO_3$ which eventually destroy the alkaline passivating layer of the reinforcing steel. With the presence of moisture and oxygen the corrosion of the reinforcing steel initiates causing cracks and spalling of concrete though the whole process could take several years to happen (Neville, A.M. 2006).

It has been reported that there is a direct relation between the environmental sustainability and the carbonation of concrete. Typical concentration of carbon dioxide in the atmosphere is 350 ppm, though it could reach up to 1000 ppm in city or industrial areas. However, the rise in the emission of carbon dioxide associated with global warming has been expected to be between 600 ppm to 1000 ppm by next 100 years. This could have a significant effect on the carbonation of concrete (Dhir, 2004).

Mechanism of carbonation:

Carbonation is a diffusion controlled chemical reaction. It can be divided into three stages. In the first state the ingress of CO_2 happens through the process of diffusion into the concrete pores due to a concentration difference between the external and internal pore atmosphere. In the second stage the CO_2 reacts with the pore fluid which is mainly water to form carbonic acid.

$$CO_2 + H_2O = H_2CO_3$$

In the third and last stage the carbonic acid reacts with the calcium hydroxide, the alkaline hydration product of cement hydration to form calcium carbonate. With the presence of continuous carbon dioxide, the carbonic acid will further convert calcium carbonate into calcium bicarbonate. Calcium bicarbonate can further reduce the calcium hydroxide to calcium carbonate and water.

$$H_2CO_3 + Ca(OH)_2 = CaCO_3$$

$$H_2CO_3 + CaCO_3 = Ca(HCO_3)_2$$

$$Ca(HCO_3)_2 + Ca(OH)_2 = CaCO_3 + 2H_2O$$

A schematic diagram of carbonation process is shown in Figure 2.10.

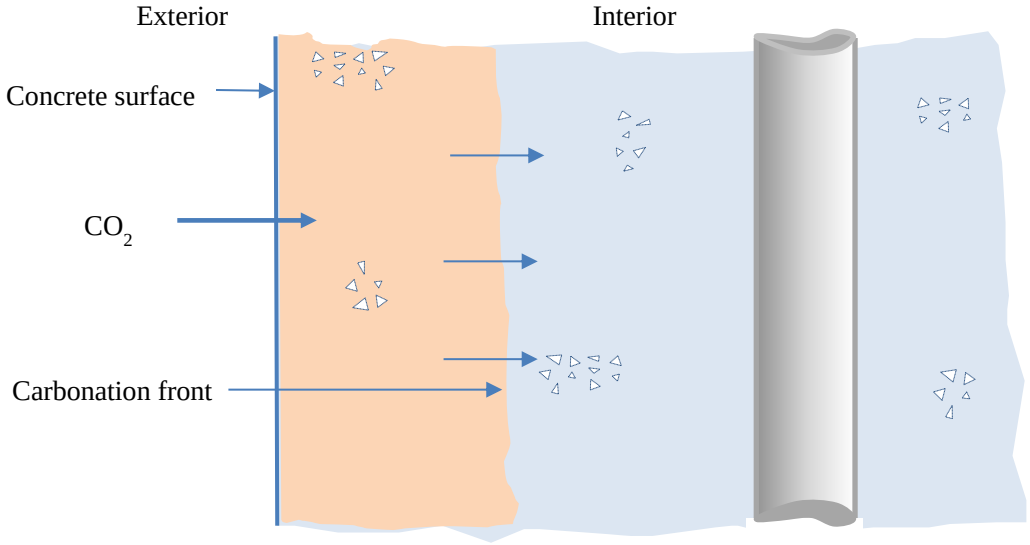

Figure 2.10: Development of carbonation (after CIRIA and Concrete Society, 2002)

This consumption and further consumption of calcium hydroxide reduce the alkalinity of the pore structure until it neutralizes, triggering the depassivation of the alkaline passivating hydroxide layer of the reinforcement steel, initiating corrosion process (Dhir 2004).

Factors influencing carbonation:

As carbonation is a chemical process, therefore, environmental as well as physical and chemical properties of concrete play vital roles of the carbonation of concrete. Among the environmental factors, humidity, ambient temperature and concentration of CO_2 in the atmosphere are important factors (Dhir 2004).

Environmental factors:

Humidity: An optimum level of 55% of relative humidity is said to have the maximum impact. Relative humidity of less than 30% is too dry and more than 70% is too saturated for carbon dioxide to react with water.

Temperature: Higher temperature will increase the rate of the increase of the diffusion of the carbon dioxide and the rate of the reaction. However, too high temperature i.e. above 55°C will drive off the moisture and reduce the carbonation process.

Carbon dioxide concentration: By theory, higher the carbon dioxide concentration, higher the carbonation, but it is not clear about the optimum level of concentration.

Physical properties:

Denser microstructure and increased tortuosity due to the reduction of water/cement ratio reduce the ingress of carbon dioxide, thus reduce the carbonation. Improvement of permeation properties would improve the resistance to the carbonation process.

Chemical properties:

Though supplementary cementitious materials (SCM) such as GGBS, fly ash and microsilica improve the permeation properties, they also consume the alkaline calcium hydroxide, the hydration product of the cement hydration. Carbonation process will accelerate with reduced alkalinity in the pore water.

However use of SCM often enhance the microstructure of concrete paste by reducing the porosity and increasing the tortuosity of concrete pore structure, therefore increasing the carbonation resistance of concrete (Dhir, 2004).

Carbonation in the Arabian Peninsula:

Several research works mainly conducted in Kuwait on the carbonation of concrete along Arabian Gulf show that concrete structures along the coastal region of the Arabian Gulf are prone to the carbonation attack perhaps due to high ambient temperature and high humidity.

A survey of 50 buildings in Kuwait suggests attack of carbonation of concrete structures (Haque and Al Khaiat, 1997). The average depth of carbonation of structures of average age of 8.5 years is 9.6mm. In hot dry climate the rate of carbonation is around 1mm per year depending on the microstructure (Fookes, 1995 as cited in Haque, M.N. and Al Khaiat, H., 1997). This is due to perhaps higher humidity in the coastal region aggravates the carbonation process.

This is also supported by the findings in the Kuwait survey that structures located near the coast (0-2 km) is having significantly higher carbonation depth than the structures situated further inland (6-10 km). Another study also in Kuwait also suggest the similar phenomenon of higher carbonation of cement mortar close to the coast of Arabian Gulf (Al-Khaiat and Fattuhi, 2002).

Though there are some concern about carbonation in the Arabian Peninsula raised from the above studies, overall carbonation is not considered to be a major concern by the local industry, perhaps because the concrete structures are generally designed to withstand chloride and sulfate attack with very low permeation properties often using high volume SCMs and low w/c ratio, which made concrete virtually water-tight. Therefore harmful chemical reaction which needs water including carbonation cannot take place.

2.5.2 Sulfate attack

The geology along the Arabian gulf coast such as UAE and other neighbouring countries is mainly consist of Sabkha, a gypsum rich deposit created inland by the evaporation of tidal sea water. The ground water of Sabkha consists of gypsum ($CaSO_4.2H_2O$) and anhydrite ($CaSO_4$) which may have a concentration over 50% of the solution. Other common chemicals are calcium carbonate and sodium chloride. These makes concrete structures build in Sabkha subject to very aggressive sulfate and chloride attack as loose sandy and silty underground soil composition makes the ground water to be mobile to increase the risk of sulfate attack more acute (Atkins 2010).

2.5.2.1 Mechanism of sulfate attack

A porous concrete with saturated mobile ground water with concentration of sulfate anions SO_4^{2-} together with cations of calcium, sodium or magnesium can experience expansive sulfate attack. Generally two types of sulfate attacks are common on concrete structures, i) conventional form of sulfate attack and ii) thaumasite form of sulfate attack. Thaumasite form of sulfate attack will generally appear in low temperature of 15°C. For Arabian Peninsula this type of sulfate attack can be disregarded as the ambient temperature of the Arabian Peninsula is more than 15°C for most of the year (BRE, 2005).

In a highly alkaline environment with pH>10 due to the liberation of sodium, potassium and calcium hydroxide during the cement hydration, the diffused sulfate ions from the nature react with calcium aluminate hydrate to form calcium sulfo-aluminate hydrate or ettringite ($3CaO.Al_2O_3.3CaSO_4.31H_2O$). The volume of ettringite is greater than original compounds, thus it produces expansive stress, causing cracks.

The sulfate ions may also react with calcium hydroxide to produce gypsum ($CaSO_4.2H_2O$). Volume of gypsum is also higher than the original ingredients, thus causing destructive expansion. Presence of magnesium ions together with sulfate may produce brucite, $Mg(OH)_2$ by reacting with calcium hydroxide, producing more volume than original volume resulting cracking. Magnesium ions may also attack calcium silicate hydrate, the principal hydration product of cement hydration.

2.5.2.2 Sulfate attack reactions

The chemical reactions of the sulfate attacks on three different hydration products of cement pastes namely $CaO.Al_2O_3.H_2O$, $Ca(OH)_2$ and $CaO.SiO_2.H_2O$ are given below.

Attack on calcium aluminate hydrate ($CaO.Al_2O_3.H_2O$) components:

Sulfate generally sodium sulfate attack the calcium aluminate hydrate component, producing calcium sulfoaluminate (ettringite), and expansive product and soluble hydroxides

$2(3CaO.Al_2O_3.12H_2O) + 3(Na_2SO_4.10H_2O) = 3CaO.Al_2O_3.3CaSO_4.31H_2O + 2Al(OH)_3 + 6NaOH + 17H_2O$

Attack on $Ca(OH)_2$ components:

Sulfate ions such as sodium sulfate attacks the calcium hydroxide component in an 'acid' type attack, producing crystalline calcium sulfate (gypsum) and soluble hydroxide.

$Ca(OH)_2 + Na_2SO_4.10H_2O = CaSO_4.2H_2O + 2NaOH + 8H_2O$

Attack on calcium silicate hydrate ($CaO.SiO_2.H_2O$) components:

Certain sulfate ions such as magnesium sulfate can attack the calcium silicate hydrate as well as the calcium aluminate hydrate and calcium hydroxide, producing very severe sulfate attack and expansive product and soluble hydroxides.

$3CaO.2SiO_2.aq + MgSO_4.7H_2O = CaSO_4.2H_2O + Mg(OH)_2 + SiO_2.aq$ (Neville, A.M. 2006)

2.5.2.3 Minimizing the effect of sulfate attack

In general to minimize the effect of sulfate attack at least one of the three following factors needs to be ensured:

1. No sulfate ion can penetrate into the concrete matrix
2. Reduce the amount of tri-calcium aluminate from the cement to reduce the calcium aluminate hydrate product to react with the sulfate ions
3. Water-tightness of the concrete matrix as presence of moisture is a requirement of sulfate attack

To stop the permeation of sulfate ions and moisture movement within the concrete, the concrete matrix needs to be densified. Appropriate mix design with the addition of SCMs such as GGBS, fly ash or microsilica will enhance the microstructure of concrete by producing more calcium silicate hydrate, reducing calcium hydroxide and increasing the tortuosity of the capillary pores.

However, it has been reported that though materials like GGBS and microsilica enhance the sulfate resistance against sodium sulfate environment by enhancing permeation properties, densification and consumption of calcium hydroxide, however the performance of GGBS and microsilica in magnesium sulfate solution is different. This is due to the conversion of calcium silicate hydrate by magnesium sulfate into non cementing fibrous magnesium silicate hydrate product, resulting loss of weight and strength reduction of cement paste (Al-Amoudi, 2002).

Using of sulfate resisting Portland cement (SRPC) with lower C_3A content is a popular option to resist sulfate attack. To address this BS 5027:1996 the specification for sulfate-resisting Portland cement has restricted the C_3A content by 3.5% by volume (Dhir, 2004).

Beside the above providing physical barrier by means of bituminous or other polymeric membrane can produce an effective barrier to prevent sulfate rich solution to penetrate into the concrete micro-structures.

2.5.2.4 Sulfate attack in the Arabian Peninsula

High concentration of sulfate and chloride ions are very common in Sabkha area of Arabian Peninsula. Al-Amoudi (2002) reported that the presence of chloride and sulfate ions together in the ground water changes the dynamic of the sulfate attack under different types of sulfate ions. Under sodium sulfate situation the influence of chloride tends to reduce the intensity of sulfate attack due to dissolution of gypsum and ettringite. However, chloride ions seem not to have similar effect on magnesium sulfate ions (Al-Amoudi, 2002).

The geotechnical interpretive report of Yas Island Water project, Abu Dhabi, prepared by Atkins (2010) suggested that the ground water chemical tests had shown existence of aggressive chemical environment due to the presence of layers of gypsum underneath. The percentage of SO_3 in the $CaSO_4.H_2O$ is approximately 49% of the oxide element. Yas Island Water project can be considered as a typical projects representing most of the projects in the Arabian Peninsula subject to sever exposure of sulfate and chloride laden environment as it is built on a Sabkha region.

The borehole analysis of the soil reveals the presence of silty sand up to 9.0m deep underground followed by mudstone from -11.5m, a layer of gypsum from 11.5 - 17.0m and again presence of mudstone thereafter. Presence of a 3.0 m thick layer of 'Sabkha clay – local term for sandy silt' has also been found sandwiched at the upper layer of silty sand layers of the soil. The ground water level has also been reported to be very high.

The sulfate content in the rock strata and the ground water is also very high. The report suggested adopting a design concrete class of DC-4 and an Aggressive Chemical Environment for Concrete (ACEC) classification of AC-4 as per BRE SD-1:2005 to design concrete for foundation structures (Atkins 2010). The proposed concrete mix design to satisfy DC-4 class could be a minimum 380kg/m^3 cement content with maximum w/c ratio at 0.35. The type of cement could be CEMII/B-V+SR or CEMIII/A+SR which is either fly ash or GGBS blend cement with appropriate sulfate resistance requirement as per BRE SD-1:2005 (BRE, 2005).

With very higher ground water level with the presence of silty sand soil type ground condition and very sever concentration of sulfate ions have made the foundation structures of Yas Island projects susceptible to sever sulfate attack. The recommended DC and AC class for appropriate concrete design reflects the harsh reality of the ground conditions of Arabian Peninsula.

2.5.3 Delayed Ettringite Formation

Delayed Ettringite Formation (DEF) which is associated with high concrete temperature could be a cause of concern in the Arab Peninsula due to the high ambient temperature during summer.

As a part of the hydration process, ettringite, $C_6AS_3H_{32}$ is normal to produce at the early stage due to the reaction of C_3A with gypsum. However, if the concrete temperature exceeds 70°C, the early formation of ettringite does not occur. The formation of ettringite could be delayed, generally after hardening in the prolonged presence of water when the temperature cooled down. As the volume of ettringite is larger than its original hydration product, it would produce internal stress, and induce cracks (BRE, 2001).

The most common factors of DEF in Portland cement are elevated temperature and prolonged exposure to water. However, the expansion and cracking may need few more factors to occur, such as, i) composition of concrete ii) aggregate type iii) aggregate paste bond iv) cement type and chemical composition of cement and v) the exposure condition. Presence of high sulfate and alkali content in the original mix is also contributed to the DEF (Concrete Society, 2008).

The aggregate paste bond is an important factor as one of the theories of the expansion of DEF as the ettringite re-crystallises at the aggregate paste interface or any other such defects. The other theory suggests that ettringite forms within the paste and exerted expansion, thus opening up space between paste and aggregate. Ettringite then re-crystallise in that space and exert more pressure until cracks. Nevertheless, the quality of bond between aggregate and paste is important to resist DEF (BRE, 2001).

Use of fly ash, GGBS or silica fume or reduced C_3A content cement may have good resistance against the formation of DEF. Fly ash, GGBS and microsilica can densify the cement paste thus enhancing the permeation properties of the concrete. As water is a requirement to DEF, the exposure condition of the structure is one of the important factors.

Though DEF is not widely reported in the Arabian Peninsula but it is susceptible in the mass concretes such as raft slab or deep foundations in the Arabian Peninsula due to its high ambient temperature during summer. The ambient temperature and temperature of raw materials can increase the core temperature in the mass concrete if appropriate actions are not taken. Micro-cracks formed due to thermal differentials can lead underground water readily available in the microstructure of concrete to feed the formation of delayed ettringite. The ettringite can be developed within the microcracks and generate expansive stress to open up more cracking.

2.5.4 Salt weathering

In the Arabian Peninsula, salt weathering is a common phenomenon. Salts, particularly sulfate, from the underground water can rise up through the concrete structure by capillary or by diffusion. In the surface the moisture will dry up depositing salts in the concrete pore near the surface. The deposition of salt crystal will exert pressure on the concrete pore wall due to expansive volume of crystalline salts, creating tensile stress, causing cracks and erosion (Concrete Society, 2002 / CIRIA and The Concrete Society, 2002).

Liu Z. et. al. (2010), however, concluded that the deterioration in the interfacial transition zone of concrete partially submerged in sulfate solution is due to the formation of gypsum and subsequent sulfate attack, not salt crystallization. However, the salt crystallization does aggravate the deterioration process, but it is not the main cause of cracking. It would be a combined effect of sulfate attack and salt weathering. Nevertheless, appropriate precautions must be considered against sulfate attack as well as salt weathering in the Arabian Peninsula due to the sever exposure to sulfate rich environment and exceptionally high summer ambient temperature.

2.6 Low carbon and environmentally sustainable concrete

As concrete is one of the main construction materials used in the Arabian Peninsula, the environmental impact associated with concrete is also substantial. Local regulatory authorities and construction industry have embarked upon different strategies to mitigate this global issue. Awarding environmental building credit ratings is one of the approaches has been taken by different authorities across the region.

Leadership in Energy and Environmental Design – LEED (U.S.GBC, 2009) is a popular standards in the region especially in Dubai to measure the environmental credit ratings of new buildings. The Change Initiative Building in Dubai has achieved 107 credit points of total available 110 credit points to achieve LEED Platinum rating the highest in the World, making it the most sustainable building in the world according to LEED rating system (Economic Times, 2013).

Local authorities like Estidama of Abu Dhabi have introduced Pearl Building Rating System – PBRS to suite the local environmental conditions of the Arabian Peninsula in the credit rating requirements (Estidama, 2010). Another similar environmental credit rating system in the region is Global Sustainability Assessment System – GSAS, developed by the Gulf Organization for Research and Development of Qatar (Al Horr, Y., 2013).

All of these standards have provided certain credits for sustainable use of concrete and its raw materials in terms of low greenhouse gas emission, use of recycled aggregates and use of locally sourced materials to reduce environmental impact. However, the weightings dedicated for concrete as a material have been found to be not robust enough to encourage the industry to prioritize the use of environmentally sustainable low carbon concrete. Detailed discussions on this issue have been made in Chapter 7 and Chapter 8 of this thesis.

Though concrete is one of the most common building materials in the world, a substantial amount of embodied carbon dioxide is associated with concrete and its raw materials. Concrete made of cement, aggregate, water and chemical admixtures are not only carbon dependent but also consume huge amount of non-renewable resources such as limestone and other virgin rocks. In the following section a review of strategies to reduce the environmental impact by the concrete as a material is discussed.

There are two main approaches to address this issue to reduce this carbon dependency from the concrete and its constituents.

1. Reduction of embodied CO_2 from the concrete
2. Reduction of the use of non-renewable resources as concrete ingredients

In the following sections reviews of the literatures on how to reduce eCO_2 from concrete have been presented followed by the discussion on the use of recycled concrete aggregate as one of way to reduce the use of non-renewable resources as concrete ingredients.

2.6.1 Reduction of embodied CO_2 from concrete

The embodied CO_2 (eCO_2) from concrete can be reduced in two ways:

1. Reduction of eCO_2 from the concrete constituents i.e. cement, aggregate, water and admixtures
2. Use of low eCO_2 binder such as novel cements and geopolymer. There will not be any review on the novel cement and geopolymer as these cements have been chosen not to include in the scope of this study.

2.6.1.1 Embodied CO_2 in cement

Cement, which is 12% - 15% of total concrete by weight, is responsible for the most embodied CO_2 per m^3 of concrete. In 2001 approximately 1.6 billion tonne cement was produced worldwide, which accounts for almost 7% of world's total CO_2 emission (Mehta, P.K., 2001). WBCSD and IEA estimate this to be around 5% of global anthropogenic CO_2 emission (WBCSD and IEA, 2009). The yearly cement production in 2009 has increased to 2.5 billion tonne and expected to rise up to 3.2 billion tonne by 2020 (Agarwal, A., 2011). Therefore, the emission of CO_2 has increased overtime with increased production of cement.

Portland cement or CEMI is the most common cementitious materials needed to make concrete. The embodied CO_2 of one tonne of Portland cement is 930 kg (BCA, CSMA, UKQAA Fact sheet 18 [P1], 2009). This high amount of eCO_2 is attributed to the energy intensive process to produce clinker by calcinations of limestone and grinding the clinker to powder.

To produce clinker, limestone or chalk together with clay or shale at a precise blend needs to be heated at 1450 ºC temperature. The calcium carbonate of the limestone calcinate to form clinker. The clinker with the addition of approximately 5% of gypsum to control setting time of cement ground in ball or vertical mill to get the final product (BCA Fact sheet 12, 2009).

Therefore the emission of CO_2 in cement making process are contributed by two separate processes i) burning of fossil fuel to generate the huge energy required to raise the kiln temperature to 1450°C, energy required to preheat the constituent materials and grind the clinker & constituents to make the final products and ii) the calcination of limestone ($CaCO_3$). Therefore, to reduce the eCO_2 of cement, attempts need to be taken to reduce the emission of CO_2 from these two stages.

Reduction of CO_2 during production process:

World Business Council for Sustainable Development (WBCSD) and International Energy Agency (IEA) have suggested in the 'Cement Technology Roadmap 2009' that there are four key levers to reduce eCO_2 of cement during the production process (WBCSD and IEA, 2009): i) thermal and electric efficiency ii) alternative fuel use iii) clinker substitution and iv) carbon capture and storage. Other factors affecting the eCO_2 in cement during manufacturing process include (Gartner, E., 2004):

1. *Energy efficient plant*: The thermal energy required in clinkering process may vary among plants depending on its efficiency level. For a modern efficient coal fired pre-heater plant or dry process plant, the fuel energy required for clinkering can be as low as 3.06 GJ/ton of clinker, whereas for a wet process plant the energy requirement could be double of that.
2. *Kiln shell insulation properties*: Better insulation properties reduce the heat loss more effectively, thus reducing the energy requirements.
3. *Reduction of clinkering time and temperature*: It will reduce the kiln shell losses as shorter period of clinkering process will reduce the exposure time.
4. *Reduction of the volume of exhaust gases*: 60% of the kiln exhaust gasses is nitrogen and it is not practically possible to reduce the temperature of the exhaust gas below 120ºC due to condensation of water in the gas duct. Therefore, reduction in volume of the exhaust gas would reduce energy loss.
5. *Reduction of the lime saturation factor (L.S.F) of the kiln feed*: Lower L.S.F means lower requirement of limestone as the quantity of belite increase while quantity of alite decreases. Effectively around 10% of the total CO_2 can be reduced by using less limestone. However factors related to higher belite i.e. slower strength gain and higher grinding energy due to harder clinker to grind need to be considered.

6. *Energy efficient grinding process*: Grindability of clinker and use of grinding aid to reduce the energy demand. Grinding aid is a surface active polar chemical which neutralize the charges on the agglomerating particles during the grinding process. Grinding aids promote the development of fineness, boosting significantly the output of the mill and reduce the unit power consumption (Cemnet GM01, 2006).

2.6.1.2 Embodied CO_2 of constituent materials of concrete in the UAE

The eCO_2 of concrete ingredients per metric tonne of each material from three different sources (UK, Masdar UAE and Estidama UAE) can be compared from Table 2.5. It is interesting to observe that the value of eCO_2 can vary significantly from source to source which can be misleading and confusing. The eCO_2 of same material in UK and the UAE may not be the same as factors like transportation, and distance from the sources are not same. However, the eCO_2 values for Masdar (UAE) and Estidama (UAE) should be similar if not the same. Care should be taken before adopting any eCO_2 value to obtain accurate data.

Table 2.5: eCO_2 (kg CO_2/tonne) of concrete constituents

Materials	UK[a]	Masdar, UAE[b]	Estidama, UAE[c]	Others
Portland cement	930	959	797	-
GGBS	52	155	170	-
Fly Ash	4	93	6	-
Microsilica	-	150	170	10[f]
Rice husk ash	-	-	-	0[g]
Aggregate	4	7[e]	3	-
Dune sand	-	5	-	-
Water	0.3	1	-	-
Admixture, Polycarboxylate	720[d]	508	-	-
Admixture, retarding type	76[d]	-	-	-
Admixture, air entraining	86[d]	-	-	-

a = BCA, CSMA, UKQAA Fact sheet 18 [P1]
b = Masdar 2011
c = Estidama 2011
d = EFCA EPD
e = Limestone crushed agg.
f = Elkem
g = N.K. Enterprize

The value of eCO_2 for Portland cement given by Estidama (UAE) is relatively low. Caution should be exercised prior to using this value as it is lower than the UK data given by the BCA and Concrete Centre. The eCO_2 value for fly ash given by Estidama is 6, which may not be correct as UAE do not produce any fly ash and import from elsewhere. The eCO_2 of aggregate is even lower than the UK. The UAE embodied CO_2 values of different ingredients of concrete given by Masdar are more rational than those given by Estidama.

The embodied CO_2 of concrete constituents can be affected by the following factors:

1. Process of extraction of raw materials
2. Manufacturing process and its efficiency
3. Energy used
4. Chemical process during the manufacturing
5. Transportation type used
6. Distance from the source of the raw materials and distance to the final destination
7. Type of raw material used
8. Packaging

Due to the above factors the same material can have different eCO_2 in different locations. For example, the eCO_2 of GGBS in UK is 52 kg-CO_2/tonne compared to 155 kg-CO_2/tonne used by the Masdar, UAE. The reason behind this difference is that the construction industry in the UAE need to import granulated blast-furnace slag either from Japan or China and grind it in the UAE. The emission of CO_2 due to the transportations has increased the eCO_2 of GGBS in the UAE. The large difference of the eCO_2 of fly ash between UK and Masdar (UAE) is also for the same reason. The eCO_2 value of Portland cement of the UK and Masdar (UAE) is very close. This is because both UK and UAE are producing cement from their local sources.

The microsilica and the rice husk ash also are not native to the Middle East. Microsilica is mainly sourced from China. Sources from Elkem claimed that the eCO_2 of microsilica is approximately 10 kg-CO_2/MT. However, the ultimate eCO_2 due to the transportation and shipment could increase to a much higher level.

Rice husk ash is not being used by the construction industry in the Middle East. However India could be a good source of rice husk ash. The eCO_2 of rice husk ash has been considered as zero as it has an organic source (N. Singania / Rice Husk Ash, 2008). However, the eCO_2 associated with shipment and transportation will increase its eCO_2 in the UAE and the region.

2.6.1.3 Embodied CO_2 in blended cement

To reduce the eCO_2 of the concrete, Portland cement or clinker can be substituted by supplementary cementitious materials (SCMs) such as ground granulated blast furnace slag (GGBS), fly ash, microsilica, rice husk ash, or inert materials such as limestone powder. These materials in a certain combination can substitute the Portland cement. As all these cementitious materials are byproducts of other materials/industry, the eCO_2 of these materials are extremely low. So substitution of the Portland cement by any of these materials is a very effective way to reduce the eCO_2 of concrete.

The eCO_2 of cement can be reduced further by pre-blending the SCMs at the cement plant to produce cement as listed in the British Standard for 'Concrete – Complementary British Standard to BS EN 206-1' BS 8500:2006'. The embodied CO_2 of such cements are listed in the Table 2.6. It can be seen that there is a direct relationship between the lower eCO_2 values and the proportion of replacement materials.

Table 2.6: Embodied CO_2 of factory made cements and combinations (BCA, CSMA, UKQAA Fact sheet 18 [P2], 2009)

Cement	Proportion, %	eCO_2 (kg-CO_2/tonne)
CEMI	-	930
CEM II/A-LL or L Portland limestone cement	6 – 20 Limestone	880 - 750
CEM II /A-V Portland fly-ash cement	6 – 20 Fly ash	870 - 750
CEM II/B-V Portland fly ash cement	21 – 35 Fly ash	730 - 610
CEM II/B-S Portland slag cement	21 – 35 GGBS	740 - 620
CEM III/A Blastfurnace cement	36 – 65 GGBS	610 – 360
CEM III/B Blastfurnace cement	66 – 80 GGBS	340 – 230
CEM IV/B-V Pozzolanic (siliceous fly ash) cement	36 – 55 Fly ash	590 - 420

2.6.1.4 Embodied CO_2 in aggregates

Aggregate comprises the bulk of the concrete which is approximately 70-80% by weight per m^3 of concrete. Hence, reduction in the eCO_2 of aggregate should have significant reduction of the eCO_2 in concrete. However, the eCO_2 of aggregate compared to Portland cement is very low, therefore, though the volume of aggregate is much higher, but overall impact by the aggregate on the eCO_2 of concrete is not significant.

Globally the total consumption of sand, gravel and crushed rock is approximately 10-11 billion tonne a year. The mining, processing and transportation of such amount of materials required huge amount of energy. The adverse impact on the ecology of the forested area and riverbeds are hugely significant (Mehta, P.K., 2001).

In the UAE all coarse and fine aggregate source are from crushed rock limestone aggregate, beside smaller addition of dune sand. Perhaps that is the reason the eCO_2 of aggregate between UK and Masdar UAE differs (Table 2.5).

2.6.1.5 Embodied CO_2 in water

International construction codes and practices require using potable water to produce and cure concrete. The mixing water requirement to produce concrete alone is 1 trillion liter every year (Mehta, P.K., 2001). Although there is a plenty of water in the earth, but only 3% of its total reserve is freshwater.

In Arabian Peninsula especially Gulf Cooperation Council (GCC) countries in particular, water is the most precious item, as it is situated in one of the most water-stressed region in the world. Water demands are largely met by the water processed by the desalination plants. The GCC countries alone having total 44 desalination plants which is about 50% of world's total number of desalination plants (Al Rukaibi, D., 2010).

Desalination of sea water requires huge amount of energy for large amount of water to be extracted from the source, evaporate or force it though filters or membrane and eventually discarding huge amount of liquid waste or brine back to the sea. The carbon dioxide emission of desalination by thermal desalination technologies and multiple effect distillation are 23.41 and 18.05 kg CO_2/m^3 of water respectively. However, the reverse osmosis process is having much lower eCO_2 of 1.78 kg CO_2/m^3 (Dickie, P., 2007).

However, thermal desalination plant is the bulk of desalination facilities in the region. In year 2002, 77% of total desalination capacity in the GCC countries were thermal desalination plant (Hamed. O.A., 2004). Other climatic impact of the desalination process such as intake of water, disposal of brine, impact of chemical use to maintain the filters and membranes have far reaching detrimental effect on the environment (Dickie, P., 2007). The eCO_2 of water for Masdar UAE is much higher than UK (as shown in Table 2.5) due to these energy intensive desalination process.

2.6.1.6 Embodied CO_2 in admixtures

Beside the three primary ingredient of concrete i.e. cement, aggregate and water, all mineral and chemical admixtures added to concrete also contain significant amount of carbon footprint due to the requirement of energy to process and transportation (Metha, P.K., 2001). However, their impact to the concrete is small due to relatively lower dosage of admixture to the concrete.

The eCO_2 for superplasticizer for UK/Europe is 720 kg CO_2/tonne compared to 508 kg CO_2/tonne as cited by Masdar (UAE). This is perhaps due to the reason that most of the raw materials of superplasticizing admixtures are deriving from the petro-chemical industries which is UAE's main industry. However, the main solid materials of these admixtures may not be processed in the Middle East therefore increasing their respective eCO_2 values.

2.6.2 Reduction of the use of non-renewable resources as concrete ingredients

2.6.2.1 Types of resource

One of the strategies to reduce the environmental impact of concrete would be using recycled materials as concrete constituents. As aggregate in concrete consist of approximately 70-80% of total volume, substituting the natural aggregate with a more sustainable source like waste products would reduce the environmental impact of concrete production significantly. Numerous researches have been conducted to find alternatives to virgin aggregate by using locally available waste materials. Based on sources, the wastes materials which has potential to use in concrete as aggregates can be categorized as: i) industrial waste aggregates and ii) construction and demolition waste (CDW) aggregates.

Industrial wastes aggregates could be derived from i) plastics wastes such as PET bottle, PVC pipes and shredded plastics ii) coal bottom ash and boiler slag from coal fired power industry iii) rubber tyre iv) air cooled slags from metal industry such as ferrous and non-ferrous slag / copper slag v) waste from food and agricultural industries such as meat and bone mill bottom ash vi) pulp and paper mill waste vii) leather waste viii) industrial sludge and ix) mining industry waste (Brito, J., and Saikia, N., 2013). However, in this study aggregates derived from CDW is of interest due to their relative availability in the Middle East.

2.6.2.2 Recycled concrete aggregate

CDW has the huge potential to effectively, at least partially, replace the natural aggregate as the properties of CDW are somewhat similar to natural aggregate but poorer in quality. BS8500-1:2006 (BSI, 2006) has categorized CDW as RCA and RA where RCA stands for recycled concrete aggregate i.e. demolition waste of concrete structures where minor presence of masonry (maximum 5%), asphalt (5%) and other minor impurities included. Recycled aggregates (RA) mainly comprise of masonry demolition waste with some asphalt (maximum 10%) and other minor impurities included (BSI, 2006).

Due to relatively inferior quality of RCA compared to natural aggregate, BS8500-1:2006 has allowed maximum 20% replacement of total aggregate proportion in the structural concrete design. However, Paine, K.A. and Dhir, R.K., (2010) have argued that use of RCA in structural concrete should be based on the performance of individual RCA as many RCA which are perfectly suitable to produce good quality structural concrete would not be permitted under current BS8500 specification.

Though RCA is not widely used in concrete industry in the Middle East, they are fairly available within the region. The CDW mostly goes to landfill or as sub-base to the road constructions which are normally larger in size and not suitable for concrete use. This is mainly due to lack of local guidance of using such materials in concrete.

In the UAE the author found only one aggregate crushing company which produce RCA at 10mm and 20mm size suitable for concrete use. The properties of this aggregate found to be suitable for concrete use except for higher absorption and higher chloride content which creates a practical problem of the use of such RCA in structural concrete, unless the salt can be washed off. The detail properties of this aggregate are presented in Chapter 3.

2.6.2.3 Plastic properties of RCA concrete

Concrete with RCA tends to have lower slump compared to concrete with natural aggregate due to the higher water absorption of RCA and its physical propeties such as surface texture and angularity. Pre-wetting has been recommended to minimize the slump loss using RCA in concrete (Brito, J., and Saikia, N., 2013).

Polishing off the old cement paste adhered to RCA to reduce the water absorption could be another alternative. Through a single rubbing process, using a vertical mill of eccentric rotor type, high quality RCA was produced in Japan with acceptable qualities of plastic and hardened properties of concrete (Yanagibashi. K et.al., 2002).

There is a concern of losing the angularity of the aggregate due to excessive mechanical rubbing process. An alternative to that process could be heating up the concrete rubble at 300ºC to disintegrate the paste from the aggregate. However, CO_2 emission for heating is high. A low carbon heating system is using microwave. (Noguchi, T., 2010). Any attempt to reprocess the RCA would certainly increase its cost and increase its eCO_2 which are two important parameter required to be minimum to produce a low carbon and environmentally sustainable concrete.

Beside the concern of lower slump, density of concrete using RCA is appeared to be lower than the density of concrete made of natural aggregate due to lower density of RCA because of its adhered cement paste. Other plastic properties of RCA concrete are quite similar to concrete with natural aggregates (Brito, J., and Saikia, N., 2013).

2.6.2.4 Hardened properties of RCA concrete

The mechanical properties of concrete with RCA have been reported to be relatively lower in performance than the concrete with natural aggregate perhaps due to lower mechanical strength, lower density and higher absorption of RCA compared to natural aggregates.

Katz, A., (2003) reported approximately 22% loss of compressive strength of concrete at the age of 28 day containing 100% RCA and Portland cement (at 0.55 w/c ratio). The reduction in tensile and flexural strength and modulus of elasticity are 11.4%, 6% and 50% respectively. Shrinkage, carbonation and water absorption of RCA concretes are also significantly higher than concrete made with natural aggregate.

However with addition of fly ash and with reduced w/c ratio Kou, S.C. et al., (2008) have shown that concrete with RCA could compensate the reduction in the mechanical properties including compressive strength, tensile and flexural strength, modulus of elasticity and drying shrinkage properties. Beside that the chloride penetration resistance as per ASTM C1202 has also been significantly improved by using fly ash with different proportion of RCA in concretes. Similar results have been obtained by Ann, K.Y., et al. (2008) by improving the durability properties such as chloride ion permeation resistance and rate of corrosion of RCA concrete by using fly ash and GGBS with RCA concrete.

2.7 Review of the fundamental cement science and concrete technology

In order to understand the behaviour of low carbon concrete, it is important to look into the fundamental cement science and the concrete technology that underpins the behaviour of these concretes. The basic chemical and physical properties and hydration products of Portland cement, ground granulated blast-furnace slag and pozzolanic materials including fly ash, microsilica and rice husk ash have been discussed in the following sections.

2.7.1 Portland cement

Portland cement consists of finely ground clinker to an optimum fineness with added gypsum during grinding process to control the setting characteristics. During anhydrous state mainly four types of minerals could be found, namely alite, belite, tricalcium aluminate and tetra calcium aluminoferrite. Beside these four major constituents also present small amount of clinker sulfate: sulfate of sodium, potassium and calcium (Lawrence, C.D., 2003). Among minor additional constituents magnesium oxide, alkalis, phosphate, borate, titanium oxide, fluorides and fluorosilicates can be present (Macphee, D.E and Lachowski, E.E., 2003). Table 2.7 describes the mineral composition of Portland cement.

Table 2.7: Portland cement compound composition (Lawrence, C.D., 2003)

Name	Oxide Compound	Cement Notation	Remarks
Alite	$3CaO.SiO_2$	C_3S	Also contains minor constituents such as MgO and Al_2O_3 in solid solution
Belite	$2CaO.SiO_2$	C_2S	Exists in a number of forms but most common as bC_2S
Tricalcium aluminate	$3CaO.Al_2O_3$	C_3A	Seldom present in quantities >15%, but has a large influence on cement properties
Tetracalcium aluminoferrite	$4CaO.Al_2O_3.Fe_2O_3$	C_4AF	Provides Portland cement with its characteristic colour
Gypsum	$CaSO_4.2H_20$		Added separately

2.7.1.1 Cement hydration

Cement hydration is a combination of complex mainly exothermic reactions between water and the mineral compounds of cements occurring at different stages as the hydration progress. These stages have been explained in the following sections by illustrating a cement hydration heat evolution curve in Figure 2.11.

At the first stage, which is immediately after addition of water the clinker sulfate and gypsum dissolved into the water producing an alkaline sulfate rich solution. At the same time, C_3A, the most reactive clinker mineral, reacts with water to form an aluminate rich gel. This reaction is strongly exothermic lasting few minutes creating the first peak at I as shown in Figure 2.11. Ettringite like small rod like crystals forms when the aluminate gel reacts with the sulfate in the solution. This period is termed as pre-induction period. (Odler, I., 2003)

The second stage of the hydration process is called dormant or induction period (at II in Figure 2.11) as the amount of heat evolution becomes low. The dormant period normally last couple of hours. At the beginning of this time normally concrete can be placed and compacted because after this period the concrete becomes too stiff to properly place.

The concrete stats getting stiffer as the dormant period progress to the next stage when the alite and belite start reacting producing calcium silicate hydrate and calcium hydroxide. This is the third phase when concrete starts getting strengths as it hardens indicated as location III in Figure 2.11.

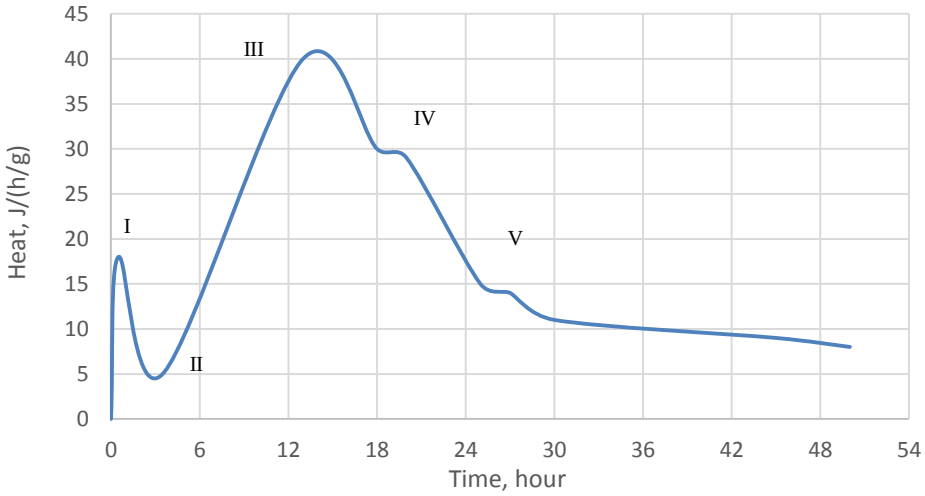

Figure 2.11: Cement hydration heat evolution curve (after Odler, I., 2003)

The formation of ettringite ($C_3A.3CaSO_4.32H_2O$) continues on the surface of C_3A particles with the presence of sulfate rich solution creating layers of ettringite on top of the particles creating a 'shoulder' at the location of IV in Figure 2.11. As the layer thickens, the formation of ettringite on the surface exerts expansive pressure, resulting bursting of ettringite layers. This leads to more sulfate solution coming in contact with C_3A and produce more ettringite. Eventually the gypsum in the solution totally consumed. (Odler, I., 2003)

However, due to ever presence of C_3A, the ettringite starts losing its $CaSO_4$ and converting into single $CaSO_4$ compound containing monosulfate ($C_3A.CaSO_4.12H_2O$). The replacement of ettringite to monosulfate could be either fully or partially. Normally monosulfate starts appearing in the system after few days of the hydration as indicated by the location V in Figure 2.11.

Ferrite phase also reacts quickly after the addition of water, but it slowed down possibly due to the formation of iron hydroxide gel on the ferrite. This coating of iron hydroxide gel works as barrier for ferrite to get in touch of water and reaction slows down. (Odler, I., 2003)

Figure 2.12 by SEM images give a chronological visual confirmation of the stages of hydration of Portland cement at different ages. At the 1 hour image (Figure 2.12a) after the mixing with water the anhydrous cement particles are still visible. Thereafter at the age of 1 day needle like ettringite on top of cement particles are formed (Figure 2.12b).

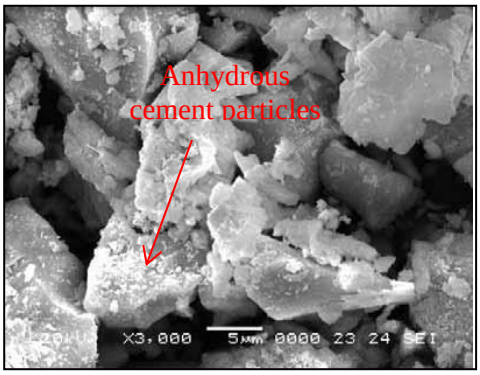

Figure 2.12a: Hydration at 1 hour

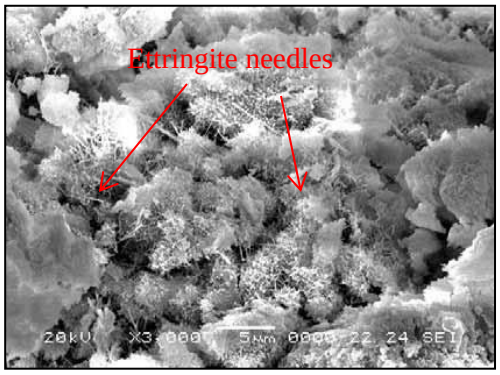

Figure 2.12b: Hydration at 1 day

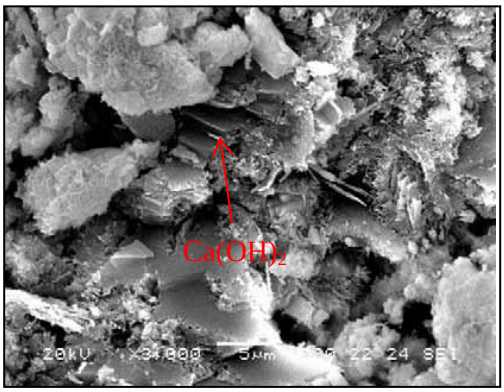

Figure 2.12c: Hydration at 7 days

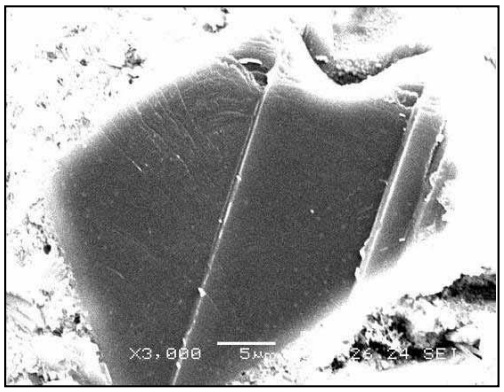

Figure 2.12d: Hydration at 28 days

Figure 2.12 (a-d):Progress of hydration of Portland cement at different age (Sivakumar, G. and Ravibaskar, R., 2009)

At the age of 7 day the ettringite was disappeared, and hexagonal shaped $Ca(OH)_2$ crystals together with honeycombed structures of C-S-H was created. Finally at the age of 28 days a solid structure of C-S-H occupied the spaces of dark pores almost completing the hydration process (Sivakumar, G. and Ravibaskar, R., 2009).

2.7.2 Ground granulated Blastfurnace slag (GGBS)

Blastfurnace slag is a byproduct of pig iron manufacturing process. During the process, to remove the impurities from the iron ore, slagging agents such as iron ore, coke ash and limestone are added. The slagging agent removes the impurities from the iron ore as a form of slag floating on top of molten iron. The slag is basically consisting of silicates and aluminosilicates of calcium and other bases.

The molten slag is quenched quickly with water to form granulated slag. After grinding to an optimum fineness to increase its reactivity ground granulated blast-furnace slag (GGBS) derived. If the slag is not quickly quenched, rather air cooled, the slag lost its reactivity and generally used as aggregates (Li, C., et. al. 2010). GGBS is latent hydraulic material i.e. it has both hydraulic and pozzolanic properties.

2.7.2.1 Composition of GGBS

The chemical composition of slag is mainly consisting of four phases i. lime (CaO) ii. silica (SiO_2) iii. alumina (Al_2O_3) and iv. magnesia (MgO) and some minor components of sulfur in the form of sulfide and ferrous and manganese oxides. This proportion of the component may vary depending on the nature of the ore, the composition of the limestone flux, the coke consumption and the kind of iron being made (Moranville-Regourd, M., 2003).

This $CaO\text{-}SiO_2\text{-}MgO\text{-}Al_2O_3$ system can be described as a mixture of phases with compositions resembling gehlenite ($2CaO.Al_2O_3.SiO_2$) and akermanite ($2CaO.MgO.2SiO_2$) and depolymerized calcium aluminosilicate glass (Li, C., et. al. 2010).

The chemical composition of slag can be considered as super-cooled liquid silicate glass. The Si-O-Si of vitreous silica is broken and neutralized by metal cations to isolate or polymerized into silica tetrahedral with bridging oxygen atoms. These condensed groups are negative charged anionic and can be again neutralized by cations such as Ca^{2+} or Mg^{2+}. Calcium atoms are octahedrally coordinated to the oxygen atoms, whereas magnesium atoms are either octahedral or both octahedral and tetrahedral. Alumina also appears in the system as Al^{3+}, AlO^{6+} or AlO_4^{5-} (Moranville-Regourd, M., 2003). Figure 2.13 illustrate a schematic molecular structure of a glassy slag.

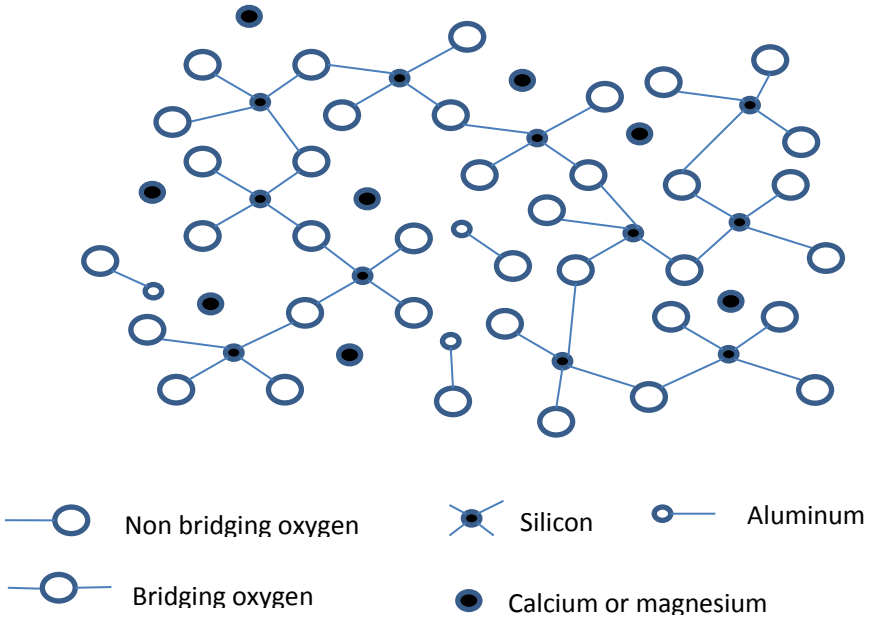

Figure 2.13: Schematic structure of a glassy slag (Moranville-Regourd, M., 2003)

The slag also contains crystalline phases such as merwinite $Ca_3Mg(SiO_4)_2$, melilite $(CaNa)_2(AlMgFe^{2+})[(AlSi)SiO_7]$, calcite $CaCO_3$ and quartz SiO_2. Often the crystalline phase of merwinite and melilite is dendritic.

It has been reported that the degree of reactivity of slag is depending on its glass content at varying proportion (Li, C., et. al. 2010) as linear relationship between strength and glass content has been established while increasing content of crystalline components reduce the cementing properties with some exception (Schweite and Dolbor, 1963 cited in Moranville-Regourd, M., 2003, p. 643).

2.7.2.2 Hydration of GGBS

GGBS is a latent hydraulic materials meaning it reacts with water. Therefore hydration of GGBS with Portland cement is more complex than that of Portland cement alone. The hydration of slag is influenced by the calcium hydroxide liberated from the Portland cement. Without the presence of C_2S, any hydration products suppose not to be observed when GGBS is placed in water.

Tanaka has provided interesting insights of the chemical reactions between Portland cement and slag by observing the cross-section of a hydrated slag/Portland cement interface using SEM techniques. He described the formation of outer hydrated layer, inner hydrated layer and skeletal hydrated layer forming on top of unhydrated slag base as illustrated by Figure 2.14.

The outer hydrated layer is the pure hydration products of Portland cement however, the inner hydrated layer is the result of the attack of Ca^{2+} and appeared to be crystalized and dense. The more porous solid of C-S-H skeletal hydrated layer has been produced as a result of the dissolution of Ca^{2+} from the supersaturated solution of cement paste and Al^{3+} contributed by the slag. It has been suggested that the skeletal hydrated layer slowly transformed into the inner hydrated layer by the continuous supply of Ca^{2+} from Portland cement solution. Therefore, the porous CSH of porous skeletal layer will become more densified overtime and converted into inner hydrated layer.

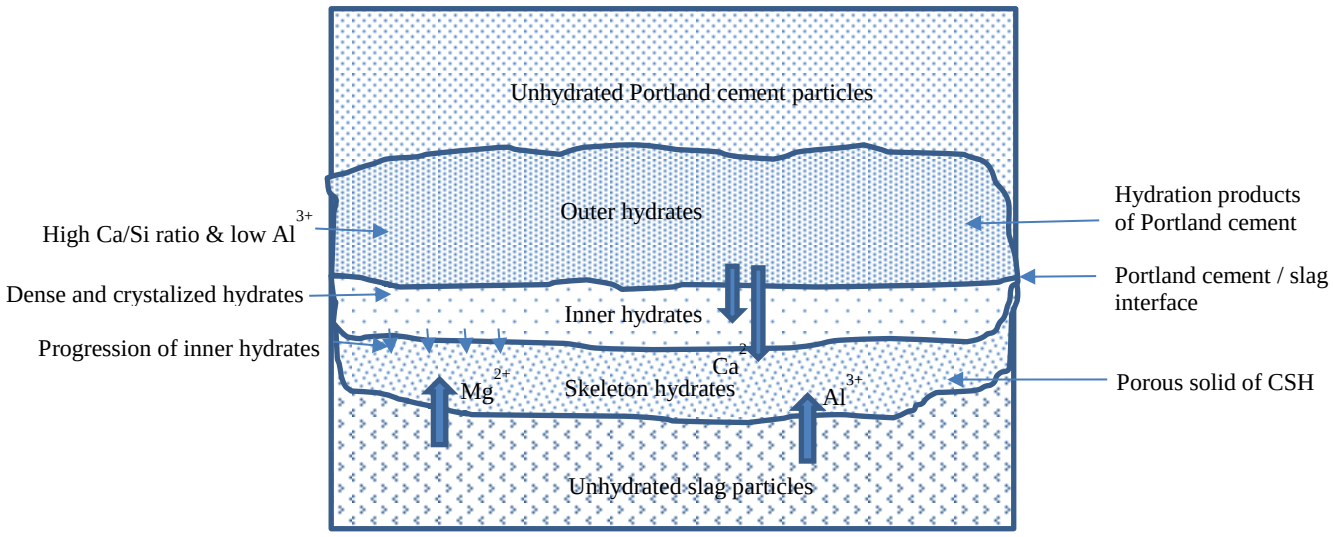

Figure 2.14: Schematic diagram of hydration process of Portland cement / slag interface (Tanaka H, et.al., 1983)

The elemental distribution suggested higher Ca/Si ratio and lower Al^{3+} at the outer hydrate compared to the skeleton hydrates validate the influence of relative proximity of Portland cement and slag grains and the chemical composition of the hydrates. However, the mobility of Mg^{2+} has been found to be restricted within skeleton hydrates. (Tanaka H, et.al., 1983)

Beside Portland cement, GGSB can be activated either by alkaline activators such as sodium hydroxide, lime, sodium carbonate and sodium silicate or sulfate activators like calcium sulfates or phosphogypsum. However, the hydration products of GGBS will depends on the type of activator. Table 2.8 describes the hydration products of slag activation under the influence of different kind of activators. In this study Portland cement is the sole activator of interest, therefore no further discussion have been made on the activation of GGBS with other activator except Portland cement.

Table 2.8: Slag reaction products in the presence of different activators (Glasser, FP., 1991, cited in Moranville-Regourd, M., 2003, p. 658)

Nature of activator	Crystalline phases
Portland cement	C-S-H, AFt, AFm, Hydrogarnet C_3AH_6, hydrotalcite $Mg_6Al_2(CO_3)(OH)_{16}\cdot 4(H_2O)$ like phase, and vicatite ($C_3S_2H_3$)
NaOH, Na_2CO_3, Na silicate	C-S-H, C_4AH_{13}, C_2AH_8, $Mg(OH)_2$
$Ca(OH)_2$	C-S-H, C_4AH_{13}
Sulfate eg. gypsum, hemihydrates, phosphogypsum	C-S-H, AFt, $Al(OH)_3$

Due to the slow reaction of GGBS the heat of hydration of GGBS concrete is exceptionally low compared to concrete containing 100% Portland cement (52.5N). Kolani, B., et. al., (2012) have shown that cement paste containing 30% Portland cement and 70% GGBS has almost 50% reduction in total heat of hydration compared to paste containing 100% Portland cement as shown in Figure 2.15. Due to this reason use of high volume GGBS in mass concrete is a common practice to reduce the temperature differentials in concrete to minimize the risk of thermal cracks.

Paine, K. et al. (2005) have shown the relationship of the heat evolution between Portland cement, high volume GGBS and fly ash pastes at different test temperatures. A mathematical model has been proposed to predict the heat of hydration of blended cement by considering three stage of reactions i) the initial hydration of Portland cement ii) the combined reaction between Portland cement and the blend and iii) the latent hydraulic/pozzolanic reaction of the blend.

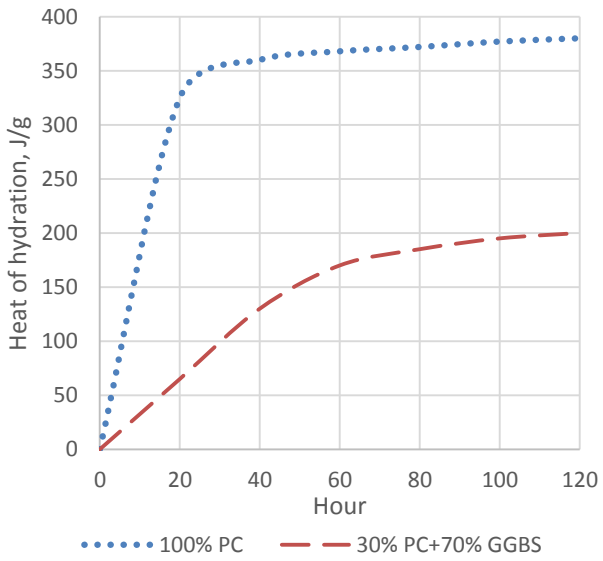

Figure 2.15: Heat of hydration of cement paste made of 100% Portland cement and 30% Portland cement + 70% GGBS (Kolani, B., et. al., 2012)

However, the hydration of GGBS can be increased with increased curing temperature and increased w/c ratio due to the accesses of more water as Escalante, J.I., et al., (2001) have demonstrated. It has been reported that mortar with 0.35 w/c ratio at 28days and 50% GGBS content can have at least 5% more slag hydrated if the curing temperature can be increased from 30°C to 50°C. At 0.50 w/c ratio, at least 6% more slag could be hydrated for the same scenario. This could have a significant effect for Arabian Peninsula where the ambient temperature during summer can reach up to 50°C.

2.7.2.3 Durability properties

GGBS have been widely used either as a part of blended cement as specified in BSEN 197-1 or mixed together with Portland cement in the concrete batching plant for its excellent durability properties against chloride and sulfate environment. In an extensive research on the durability properties of concrete containing different proportion of GGBS content, Osborne, J.G., (1999) has concluded that concrete with GGBS as much as 70% of total cementitious content would have excellent durability properties in terms of chemical resistance to chloride, sulfate and sea-water ingress. He recommended to reduce the GGBS content to 50% if the risk of carbonation is high. However, it is the Author's view that the risk of carbonation can be reduced by enhancing the permeation properties of concrete by reducing the w/c using high range water reducing admixture.

The corrosion resistance of concrete with GGBS concrete has also been shown to be increased with the increased proportion of GGBS content in terms of chloride ion penetration resistance, chloride diffusion coefficient and surface area of corroded steel bar embedded in concrete (Yeau, K. Y. and Kim, E.K., 2005).

GGBS have been proven to be equally effective with limestone Portland cement (8% limestone powder). O'Connell, M. et. al., (2012) have shown that mortars made with limestone cement + 70% GGBS and Portland cement + 70% GGBS (at 0.50 w/c ratio) exposed in 5% sulfate rich solution for 1 year had little or no expansion compared to mortars made with plain limestone cement /Portland cement or sulfate resisting cement.

Cheng, A., et. al., (2005) have shown that although the durability of mortar made with 40% to 60% GGBS replacement at 0.55 w/c ratio enhance the durability parameters such as water permeation, chloride ion penetration resistance and chloride induced corrosion of reinforcement bar, however, under sustained loading when visible crack (crack width 0.02mm) formed, the rate of corrosion of reinforcement steel embedded in mortars made with Portland cement and GGBS do not perform any better than mortar made with 100% Portland cement.

2.7.3 Pozzolanic materials (Fly ash, microsilica and rice husk ash)

Pozzolanic materials are natural or artificial materials contain silica (SiO_2) in a reactive form (Neville, A.M. 2006). Fly ash, microsilica and rice husk ash are considered to be pozzolanic materials because of the relatively higher presence of reactive silica in them. In this study these three pozzolanic materials have been studied and the discussion will be limited only to these pozzolanic materials.

ASTM C125 define the term pozzolan as a siliceous or siliceous and aluminous material, which in itself possesses little or no cementitious value but will, in finely divided form and in the presence of moisture, chemically react with calcium hydroxide at ordinary temperatures to form compounds possessing cementitious properties.

Portland cement after reacting with water produce hydration products which are mainly calcium-silicate-hydrate and calcium hydroxide. In pozzolanic reaction, the reactive silica reacts with the calcium hydroxide to produce more C-S-H and water. All pozzolanic materials like fly ash, microsilica and rice husk ash behave the similar way.

$$PC + H_2O = C\text{-}S\text{-}H + Ca(OH)_2$$

$$SiO_2 + Ca(OH)_2 = C\text{-}S\text{-}H + H_2O$$

The ternary diagram in the Figure 2.16 shows the relative position of Portland cement, GGBS, fly ash, microsilica and rice husk ash in terms of the combination of silica (SiO_2), alumina (Al_2O_3) and lime (CaO).

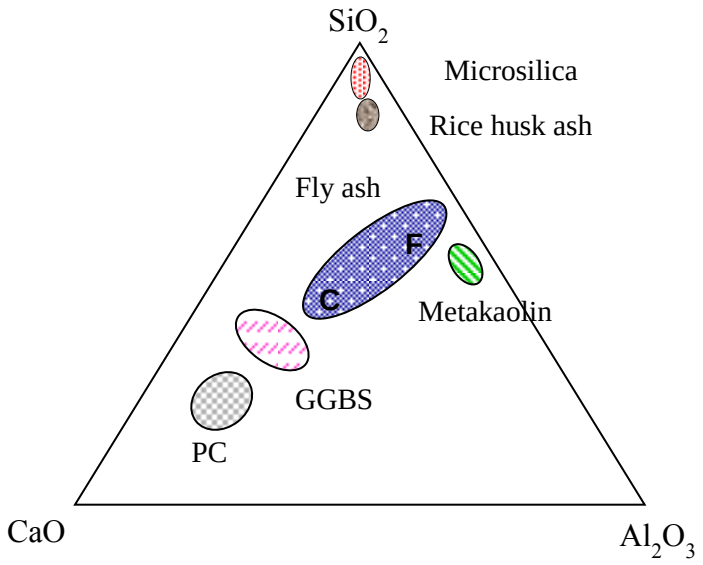

Figure 2.16: Ternary diagram of Portland cement, GGBS, fly ash, microsilica and rice husk ash (after Elkem, n.d.)

2.7.3.1 Fly ash

Physical and chemical properties:

Fly ash consist of finely divided ash produced by burning pulverised coal in power stations. They are removed from the combustion gases and collected by special mechanical devices and electrostatic precipitators. It consists of spherical glass particles, which formed due to rapid cooling of melted minerals from combusted pulverized coal.

Fly ash particles are typically spherical and glassy cenosphere, but they also show other topologies. The finest glassy particles are generally thick but many are hollow. Sometimes the biggest ones look like empty spheres filled with other smaller, spherical particles. Other types of particles are irregular and sometimes contain a variable amount of bubbles, which makes them take on a spongy aspect, or a high content of crystalline minerals. The morphology and behaviour of fly ash depend on the burning process of the pulverized coal (Massazza, F., 2003). Figure 2.17 shows a SEM image of fly ash particles (Xu, Aimin., 1997).

Fly ash can be categorized into two types based on the lime content. Type F with lower lime content and type C with relatively higher lime content. In this study low lime fly ash is of interest which is pure pozzolanic material. High lime fly ash would have some hydraulic properties.

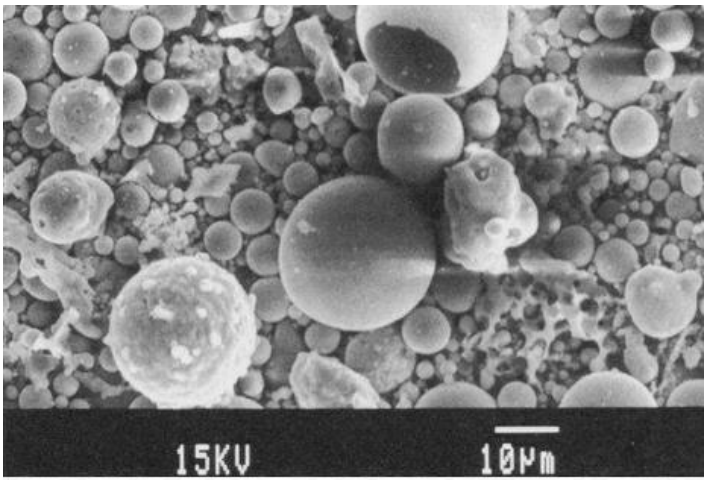

Figure 2.17: SEM image of fly ash particles (Xu, Aimin., 1997)

According to BS EN 450-1 fly ash is a fine powder of mainly spherical, glassy particles, derived from burning of pulverized coal, which has pozzolanic properties and consists of SiO_2, Al_2O_3 and Fe_2O_3. The minimum content of SiO_2 should be at least 25% of the total mineral content (BS EN 450-1, 2007). Generally, chemical composition of bituminous fly ash (class F) varies rather within wide limits. SiO_2 usually varies from 40% to 60%, Al_2O_3 from 20% to 30%, Fe_2O_3 content also varies quite widely. CaO content of class F fly ash is low, ranging between 2% and 5% of total oxides.

Due to spherical morphology of fly ash particles, it has a natural ability to reduce the water demand in concrete primarily due to the 'ball bearing' effect. However, the linear relationship of fineness in terms of mass of % retained in 45µm sieve and LOI on the consistence of fly ash concrete have also been recognized (Dhir, R.K., et al. 1988).

Hydration products:

When combined with Portland cement, SiO_2 and Al_2O_3 originating from the glass phase of the fly ash will partly dissolve due to the high pH of the pore solution and will react with $Ca(OH)_2$ to form hydration products similar to the ones formed by ordinary Portland cement. The main hydrates found in the hardened pastes containing Portland cement with fly ash are: C-S-H, $Ca(OH)_2$, Ettringite, Tetracalcium aluminate hydrate (often carbonated), Monosulfoaluminate, C_2ASH_8 (gehlenite hydrate), and $CaCO_3$ (Massazza, F., 2003).

Figure 2.18 show the reaction of class F fly ash particles with $Ca(OH)_2$ over time on a cement paste containing 30% fly ash content of total cement. Even at 90 days age not all fly ash particles have been reacted, though they are embedded on a solid microstructures of hydrates (Figure 2.18a). However, over time (Figure 2.18b) fly ash particles can be seen more consumed by $Ca(OH)_2$ as pozzolanic reaction continues with the presence of water (Xu, Aimin., 1997). Studies have shown that at 7 days only 10% of fly ash particles can be reacted and it could take up to 2 years to get around 80% of the particles to get reacted (Dhir, R.K., et al. 1988).

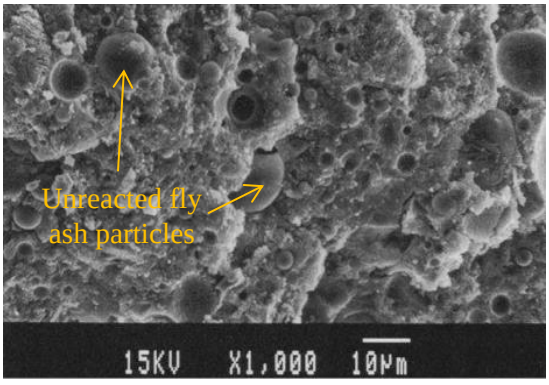

Figure 2.18a: 90 days age

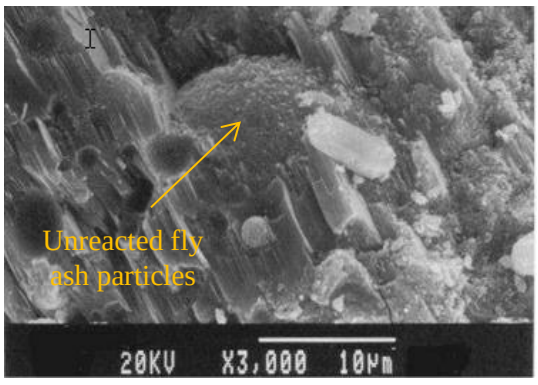

Figure 2.18b: 180 days age

Figure 2.18: Hydrated cement paste with 30% fly ash (class F) (Xu, Aimin., 1997)

Durability properties:

Fly ash has been widely used for it excellent durability parameters against different chemical attacks including chloride, sulfate, ASR and other attacks from the environment. Dhir, R.K. et al. (1997) has shown that fly ash up to 33% replacement of Portland cement has excellent properties of chloride diffusion resistance and its capability to bind chloride ions. However, from 50% the resistance to chloride diffusion of concretes starts reducing (Figure 2.19).

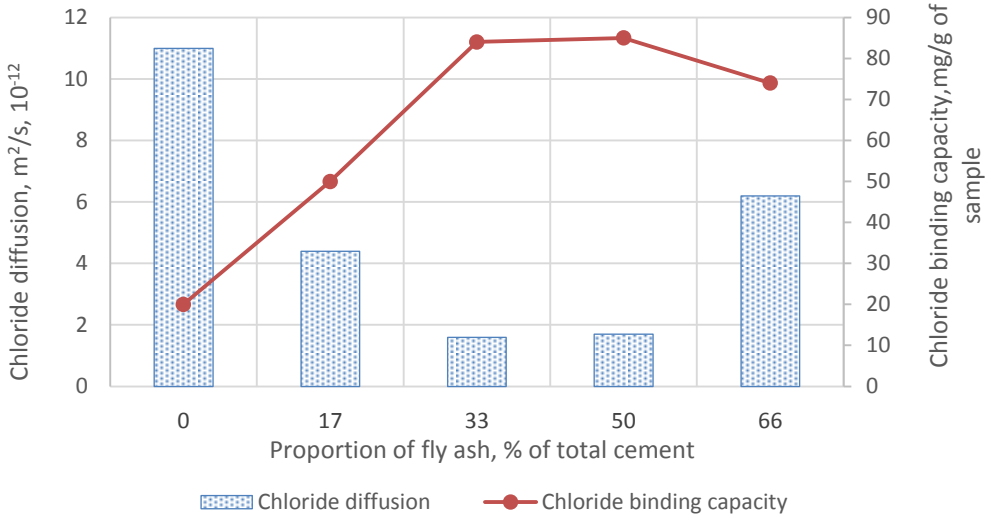

Figure 2.19: Chloride resisting and binding capacity of fly ash (from Dhir, R.K., et al. 1997)

One of the main reasons of the enhanced durability properties of fly ash concrete is its ability to enhance the permeation properties of concrete. Studies have shown that the water absorption and air permeability of concrete at the reinforcement steel cover area, which is most important area of concrete structure to protect the steel reinforcement, can be enhanced significantly by replacing 15% to 30% of Portland cement by fly ash (Dhir, R.K. and Byars, E. A. 1993).

The durability of concrete in terms of chloride penetration and permeation properties have been reported to be significantly better in ternary blend concretes comprising different combinations of fly ash, GGBS or microsilica with Portland cement compared with concrete containing double blend of Portland cement and fly ash (Jones, M.R., et al., 1997). This improvement has been attributed to the enhanced microstructure of cement paste of ternary blends. However, the carbonation resistance of concrete containing ternary blend has been reported to be poorer than concrete with only Portland cement or Portland cement and fly ash blend. This could be due to reduced alkalinity of pore solutions as suggested by Page, C. L. and Vennesland, O., (1983).

In recent studies with fly ash to produce high strength concrete it has been seen that the durability properties including sorptivity and chloride ion penetration resistance are enhanced using 30% and 40% fly ash content of total cementitious materials (Nath, P. and Sarker, P. 2011). The chloride ion penetration resistance of self-compacting concrete containing fly ash ranging from 15% to 35% has been reported to be below 700 coulomb at 90 days age (Siddique, R. 2011). Fly ash has also been equally effective to enhance the chloride ion permeation resistance of concrete containing recycled concrete aggregates (Kou, SC and Poon, CS, 2013).

2.7.3.2 Microsilica

Physical and chemical properties:

Microsilica is a very fine non-crystalline amorphous silica (SiO_2), produced in electric arc furnaces as a byproduct of the production of elemental silicon or alloys containing silicon (ACI 116R). Most of the particles of microsilica are at submicron level with average particle diameter of 0.15 microns, about 100 times smaller than cement grains. The shapes of the particles are smooth, spherical with approximate specific gravity of 2.2. The specific surface area of microsilica particles are ranging from 15,000 to 30,000 m^2/kg, measured by nitrogen absorption or BET method (Holland, T.C., 2005).

Figure 2.20 show a Transmission Electron Microscopy (TEM) image of microsilica particles depicting a very clear spherical submicron size of microsilica (Fidjestol, P. and Lewis, R., 2003).

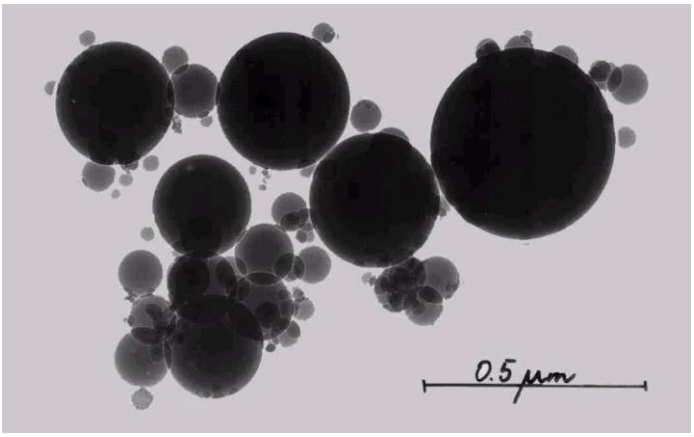

Figure 2.20: TEM image of microsilica particles (Fidjestol, P. and Lewis, R., 2003)

The SiO_2 content of microsilica is ranging from 85% – 97% depending upon the requirement of the application. The comparative oxide composition of different cementitious materials have been discussed in Chapter 3 of section 3.2.1 Characterization of concrete constituent materials.

Pozzolanic reaction and microstructure:

Microsilica is a pozzolanic material i.e. it does not hydrate with water. However, the SiO_2 of microsilica reacts with the $Ca(OH)_2$ liberated during the hydration of Portland cement producing more CSH in addition of CSH and other hydration products produced by the hydration of Portland cement. This additional production of CSH together with the physical void filling effect by the minute spherical microsilica particles between cement grains produced a densified microstructure of hardened cement paste (Fidjestol, P. and Lewis, R., 2003).

Mechanical properties of concrete:

Due to enhanced microstructure of paste by the production of additional CSH and void filling by microsilica particles the mechanical strengths and durability properties of concrete including permeation properties improved significantly with microsilica added concrete. Microsilica has been widely used to produce high strength concrete. It does not only increase the compressive strength but also increase the tensile and flexural strength of concrete. Though the brittleness of concrete increased with the compressive strength, however, ductility of concrete structure can be designed using appropriate design criteria using reinforcement steel (Fidjestol, P. and Lewis, R., 2003).

Due to higher surface area of microsilica particles, microsilica concrete tends to have higher bond with paste-aggregate and paste- reinforcement bar interfaces. The shrinkage and creep of concrete containing microsilica have been studied to be similar to concretes without microsilica. However fire resistance is a concern like any other high strength concrete, due to the possibility of building up of steam pressure due to inability of steam to escape through extremely impermeable pastes containing microsilica. This can be minimized, among other measures, by introducing plastic fibre in the concrete. Due to higher compressive strength and superior bond strength microsilica concrete exhibits greater abrasion and erosion resistance than concrete without microsilica (Fidjestol, P. and Lewis, R., 2003).

Durability properties:

Microsilica is an ideal addition to concrete to enhance its durability properties because it enhances the permeation properties of hardened concrete. This effectively reduce the permeability, absorption and diffusion of water and other deleterious substances such as chloride and sulfate ions to attack reinforcement steel or hydrates of concrete paste.

With appropriate mix design and proper mixing and consolidation, microsilica added concrete is virtually water tight. Therefore deleterious chemical reaction which require the presence of water such as sulfate attack, alkali-silica reaction, multi aggressive sea water attack can be reduced significantly using microsilica added concrete.

As microsilica reduce the porosity and increase the tortuosity of capillary pores, thus reduce the rate of ionic and gaseous diffusion, therefore corrosion induced by chloride and carbonation can be significantly reduced and the service life of structure will be increased (Fidjestol, P. and Lewis, R., 2003).

It has been established that concrete with ternary blend using Portland cement, GGBS / fly ash and microsilica provide better performance in durability than the double blends of Portland cement and microsilica. Fidjestol, P., and Frearson, J., (1994) have shown that concrete with a ternary blend of Portland cement, GGBS and microsilica performed better than concrete with double blends with Portland cement and GGBS or microsilica alone (Figure 2.21). This enhancement of performance is due to the additional contribution of hydration products by the GGBS, as it has been discussed before that GGBS, being latent hydraulic it produce more hydration products.

Similar work done by Alexander, M.G. and Magee, B.J., (1999) suggested the electrical resistance to chloride conductivity significantly reduced with concrete containing a ternary blend of Portland cement (50%), GGBS (40%) and microsilica (10%).

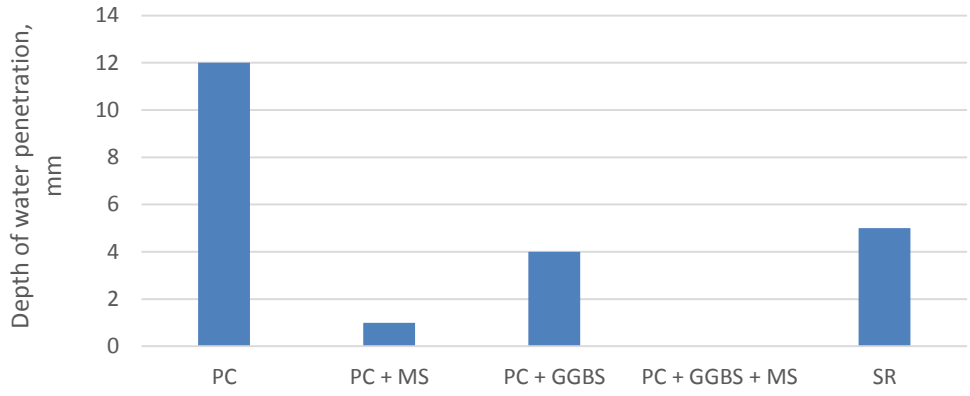

Figure 2.21: Effect of different type of cement combination on the water permeability of concrete, 0.42 w/c ratio (from Fidjestol, P. and Frearson, J., 1994)

However, concerns have been raised by the reduced chloride binding capacity of cement pastes containing SiO_2 of 10% or more of total cement mass due to reduced alkalinity of pore solutions. The concern is the acidic environment may alter the passivity of embedded steel reinforcement to initiate corrosion (Page, C. L. and Vennesland, O., 1983). However extremely impermeable paste microstructure using microsilica as seen in Figure 2.21 would virtually eliminate the possibility of water ingress to facilitate the corrosion process. The significantly reduced rate of chloride ion diffusion due to enhanced microstructure of microsilica added paste would increase the time to initiation of corrosion process as discussed earlier.

Problem with agglomeration:

Microsilica can be found as undensified, densified and slurry form. An undensified microsilica is the true form of microsilica as it is collected from the bag house of microsilica production process. Due to very low bulk density of undensified microsilica (200 – 300 kg/m^3) it is not logistically economical. Therefore, undensified microsilica are densified by a densification process where the microsilica particles loosely agglomerate together to give a higher bulk density of 500-700 kg/m^3. A high shear concrete mixing plants equipped with centralized batching system using twin shaft or planetary mixer would be required to effectively disperse the agglomerated microsilica particles (Fidjestol, P. and Lewis, R., 2003).

However, it has been reported that concrete made in the laboratory with undensified microsilica has higher compressive and tensile strength than concrete made with densified microsilica (Deshinia, A. and Ioannides, A. M., 2012). This could be due to the lack of shear force exerted by the laboratory mixer to effectively disperse the agglomerated microsilica particles during mixing of concrete. By acknowledging this problem Silica Fume Association (2003) provided a detailed guidance on the mixing procedure of concrete using densified microsilica (silica fume) using laboratory mixer by doubling the total mixing operation to 16 minutes instead of 8 minutes as described by ASTM C192.

2.7.3.3 Rice Husk Ash

Rice husk is a harsh, woody elliptical shell composed of cellulose fibres. The cellulose fibres are embedded in lignin and polymerized silicic acid. The average composition of dry rice husk corresponds to 50% cellulose, 30% lignin and 20% silica. After burning at a controlled temperature the cellulose and lignin are removed from the ash leaving rice husk ash with high content of amorphous silica and some unburnt carbon. To enhance its reactivity rice husk ash need to be ground to increase its specific surface area to approximately 35,000 m^2/kg. Under scanning electron microscope as shown in Figure 2.22, the particle of rice husk ash appeared to be irregular in shape with visible porosity which increase its water demand (Elkem, n.d.).

The physical and chemical composition of rice husk ash depends on many factors such as soil types, paddy types, fertilizer used, type of combustion process and combustion temperature and duration of combustion.

Production process:

Depending on combustion type rice husk ash can be collected as fly ash from the flue gas and bottom ash. Often the fly ash (of rice husk) are 100% amorphous, while the bottom ash contains some portion of crystalline products. However, the combustion temperature is a deciding factor to control the crystalline content in the rice husk ash. It has been reported that 800°C is the optimum combustion temperature to obtain amorphous rice husk ash (Department of Trade and Industry, 2003). Other works suggest much lower temperature of 650°C burning for 60 minutes as the optimum temperature indicating optimum burning temperature may not be fixed for all types of rice husk ash production (Ramezanianpour, A. A., et. al. 2009).

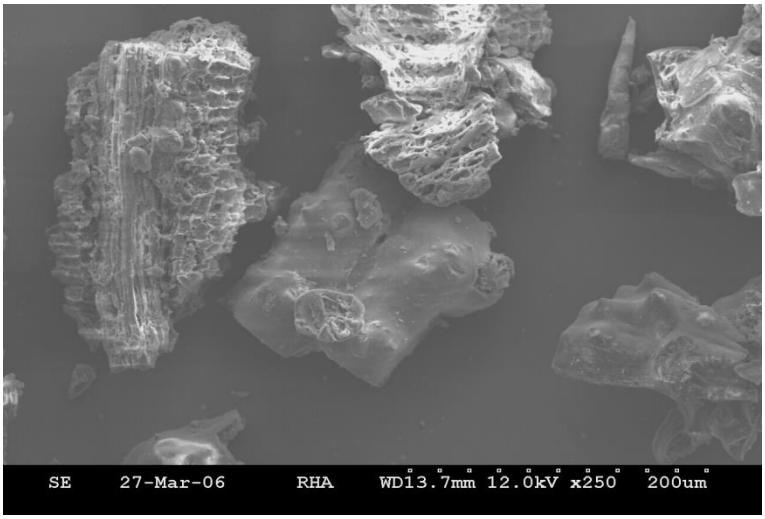

Figure 2.22: Microscopic image of rice husk ash grain with visible porosity (Elkem, n.d.)

In the 'Rice husk ash market study' commissioned by the Department of Trade and Industry (2003) it has been discussed about a process of the production of highly amorphous rice husk ash patented by P.K. Mehta, produced through a low temperature, but relatively longer burning time process. The rice husk ash produced by this method was collected as fly ash by the multi cyclone separator from the flue gas. The quality of this rice husk ash has been reported to be very high for the use in cement and concrete industry.

Mechanical and durability properties:

Due to higher presence of amorphous silica rice husk ash reacts with $Ca(OH)_2$ of the cement hydration and produce CSH as pozzolanic reaction. Therefore, rice husk ash can be effectively replaced microsilica or can be combined with other supplementary cementitious materials such as fly ash and GGBS to enhance durability and mechanical strength of concrete.

Ganesan, K. et. al., (2008) suggest up to 30% replacement of Portland cement with rice husk ash without any detrimental effect on strength and substantial improvement in water and chloride permeation properties. Enhanced durability have also been reported on a ternary blends mortar comprising Portland cement, fly ash and rice husk ash with up to total 30% replacement by fly ash and rice husk ash combination (Chindaprasirt, P. and Rukzon, S., 2008).

More works by Ramezanianpour, A. A., et. al. (2009) suggest that concrete with lower level of replacement (7% - 15%) by rice husk ash can effectively enhance the mechanical strengths of concrete including compressive and tensile strengths. Durability properties such as water permeability and chloride penetration resistance values of concrete have also been enhanced by the rice husk ash.

Tangchirapat, W. et. al., (2008) have shown that reduction in compressive strength due to the use of 100% recycled concrete aggregate replacing natural limestone coarse aggregate can be compensated by the use of rice husk ash of 20% and 35% of total cement content, though unfavourable slump loss and higher dosage of superplasticizer was reported due to high specific surface area and higher porosity within the rice husk ash particles.

Hydration products:

The visual presentation of the enhancement of the microstructure of paste using 80% Portland cement and 20% rice husk ash at 0.40 w/c ratio have been presented in Figure 2.23. In the 1^{st} hour the surface of the rice husk ash particles are covered by hydration products and unreacted rice husk ash particles are seen within cement grains (Figure 2.23a).

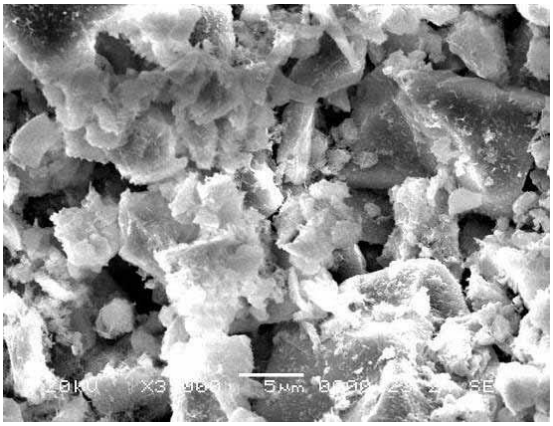

Figure 2.23a: Hydration at 1 hour

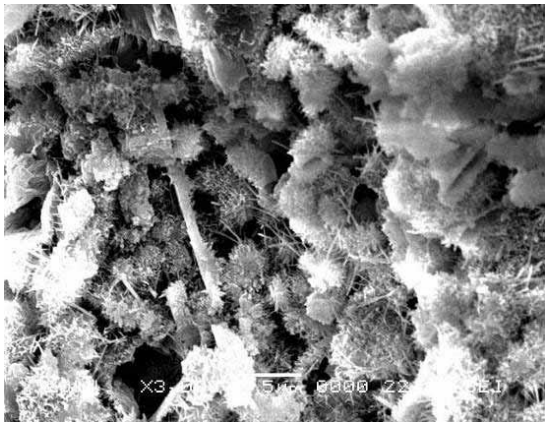

Figure 2.23b: Hydration at 1 day

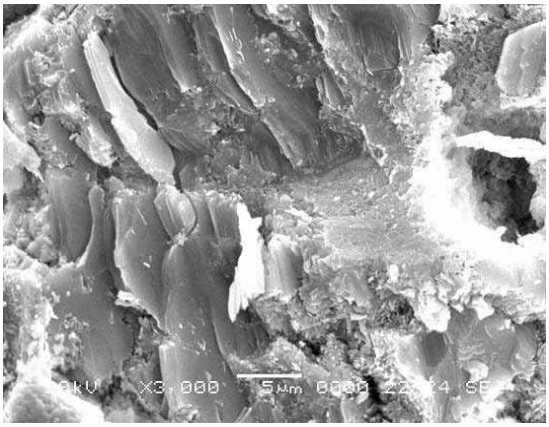

Figure 2.23c: Hydration at 7 day

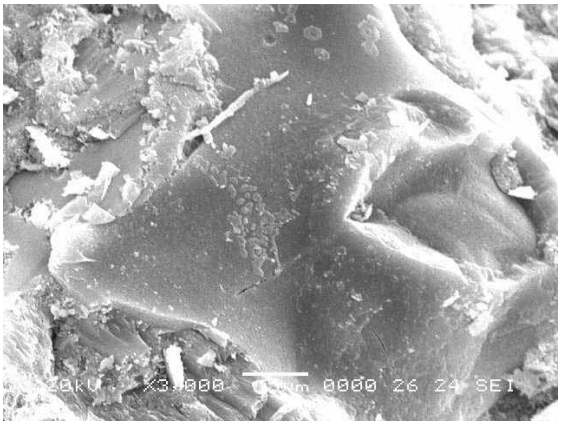

Figure 2.23d: Hydration at 28 day

Figure 2.23: Chronological SEM images of development of microstructure of Portland cement (80%) and rice husk ash (20%) paste (Sivakumar, G. and Ravibaskar, R., 2009)

After 1 day the presence of AFt, AFm phases, $Ca(OH)_2$ and CSH products can be identified. The pores are still visible at this age (Figure 2.23b). However by the age of 7 days the pores are filled with CSH and other hydration products such as plate like AFm phases (Figure 2.23c). At the age of 28 days the microstructure becomes totally dense with CSH microstructure as shown in Figure 2.23d (Sivakumar, G. and Ravibaskar, R., 2009).

2.8 Particle Packing

Particle packing is an important factor to obtain optimum packing density of concrete ingredients to enhance its ultimate mechanical strengths and durability properties as well as rheology of plastic concrete. It has a great relevance to the development of low carbon and environmentally sustainable concrete as the optimum usage of raw materials such as the possible void filling ability of the excess finer particles of 'unwashed' crushed limestone fine aggregates used in the region of Arabian Peninsula could yield higher mechanical and durability parameters of concrete. Exploring these effects of the 'unwashed sand' to the concrete properties is one of the major objectives of this study.

Therefore, in the following sections a brief review of the different theories behind the particle packing of grains have been presented to understand the science behind the particle packing of concrete constituents. Particle packing is usually described by the packing density or void ratio of particles in a unit volume and can be expressed as:

Packing density, $\varphi = \frac{\boldsymbol{Vs}}{\boldsymbol{Vt}} = \frac{\boldsymbol{Vs}}{\boldsymbol{Vs+Vv}}$

Where, $\boldsymbol{Vs}$ = Volume of solid

$\boldsymbol{Vt}$ = Total volume = $\boldsymbol{Vs + Vv}$

$\boldsymbol{Vv}$ = Volume of voids

Particle packing can be described by a set of perfect spheres as illustrated in Figure 2.24 where, the packing volume of perfect mono-size sphere is approximately two thirds of the unit volume of the total packing (Figure 2.24a). However, the interstitials space between larger particles can be filled in by the smaller sized perfect spheres creating another sets of interstitial space for next smaller size spheres to fill in and so on as shown in Figure 2.24b.

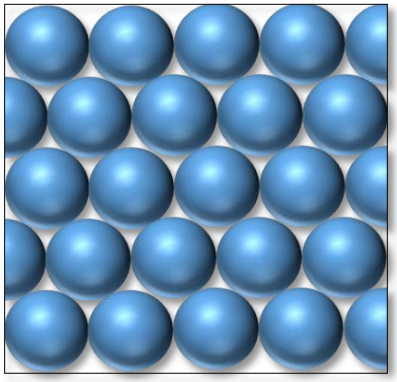

Figure 2.24a

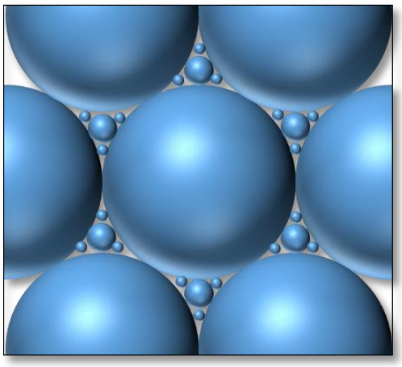

Figure 2.24b

Figure 2.24: Particle packing of perfect spheres

However, for a compacted mixture of grains of different sizes like concrete, the larger grains are generally surrounded by smaller grains by filling in the interstitial voids between them as shown in Figure 2.25. The relative stability between the different sizes of grains is perturbed by each of the grains because of the physical interactions among them. The larger grains surrounded by the smaller grain exert an effect on the smaller grains, termed as 'wall effect' to destabilize the smaller grains. As shown in Figure 2.25, the larger grains marked as 1 is exerting wall effect on smaller grains marked as 2 to destabilize them. Therefore, the mean packing density along the walls of larger grains is lower than the rest of the packing (de Larrard, F. 2009).

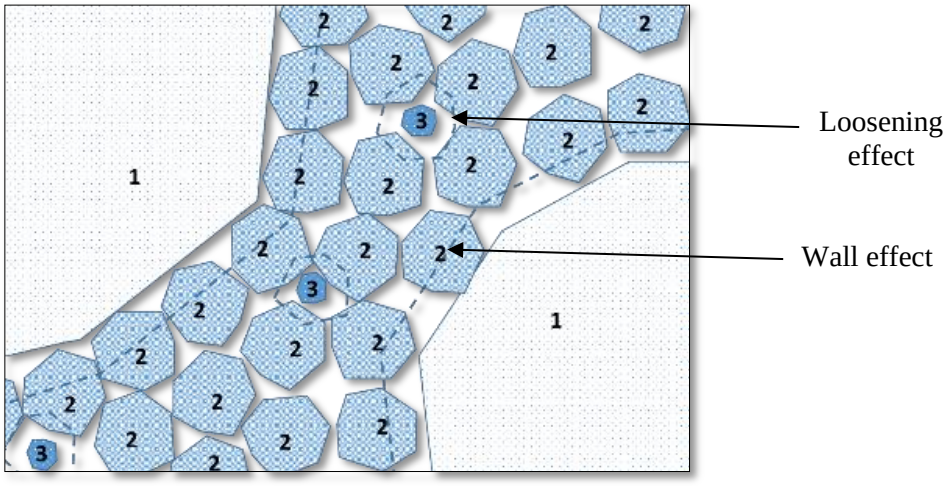

Figure 2.25: Ternary packing of particles (de Larrard, F. and Sedran, T., 2002)

Similarly if a smaller grain is surrounded by a cluster of larger grains and the size of the smaller grain is larger than the interstitial space between the larger grains, the stability of the larger grains could also be compromised by the 'loosening effect' exerted by the smaller grain over the surrounding larger grains. In an ideal particle packing scenario, these effects of grains over others need to be stabilized (de Larrard, F, and Sedran, T., 2002). In Figure 2.25, the relatively smaller grain 3 is exerting loosening effect on the surrounding larger grains 2 to destabilize them.

For a ternary packing of particles as shown in Figure 2.25, de Larrard and Sedran, T. (2002) have proposed 'Compressive packing model' to predict optimum packing of concrete to produce high performance concrete with predicted compressive strength and other plastic and hardened properties. A concept of virtual packing density has been introduced by considering the residual density of a dominant cluster of uniformly sized grains (grain 2, in Figure 2.25) in a scenario when only those dominant sized grains are compacted alone.

The packing density of overall mixer can be computed by considering the scenario as illustrated in Figure 2.25, where the dominant grains surround the larger grains, and smaller grains fill in the space between the dominant grains. If there is an 'n' number of grain size have been determined by a particle size distribution analysis, then subsequent 'n' number of virtual packing densities for each particle size can be computed, considering the immediate smaller grain is the dominant size for that relative interstitial location. Therefore, the virtual density of the last grain of 'n' number of grains would be the densest packing density.

In order to compute the actual packing density of overall mixer, a compaction index have been introduced which determines how close the actual packing could be relative to its corresponding virtual one (as described above). The compaction index is practically an index of compaction process such as consolidation of concrete, however, mathematically it can be expressed as the summation of the compaction index of all individual cluster of grains.

The compaction index of each individual cluster of grains would determine how much is the actual volume of that particular grain size have been compacted compared to possible maximum volume which could be compacted (de Larrard, F. and Sedran, T., 2002). A corresponding computer software have been proposed based on this method for users to determine the actual proportion of concrete mix constituents based on the predicted mix proportions given by the software.

Prior to the compressive packing model, Larrard proposed a linear packing model (LPM) to predict the maximum packing density. In LPM de Larrard has used eigen-packing density of each individual grain instead of virtual packing density. From the particle size distribution, the grains have been divided into few clusters, based on the ratio of maximum and minimum size of the diameter of grains. The eigen-packing density of grains of each cluster have been calculated and the total packing density have been summed up after establishing the fraction of grains retained per cluster as the percentage of the total volume.

The modified Toufar model as illustrated by Jones, M.R. et al., (2002), use the packing density φ and characteristics diameter of each ingredients to calculate the total packing density of a multi component mix. In this model the packing densities of first two ingredients need to be computed, then the third ingredient would be added up using the model and the process would be repeated to combine all remaining components. Jones, M.R. et al., (2002) also used Dewar model which use void ratio, instead of packing density and log mean diameter of particles to calculate the packing density of the mixture. Another difference from the modified Toufar model is in Dewar model, the finest two materials are computed first, and then the next larger ingredient added on to the model.

Jones, M.R. et al., (2002) have applied above four models to predict the packing density of a given concrete mix using laboratory tests and published data. They have found that all four models predicted similar output with optimized particle packing mainly at aggregate phase. However, little differences have been made for paste fraction, perhaps due to close particle size distribution pattern among cementitious materials.

2.9 Conclusion and discussion

In order to establish the current knowledge of the low carbon and sustainable concrete suitable for the extreme environment of the Arabian Peninsula a systematic but comprehensive review of literatures has been undertaken. The main sections of the literature reviews are:

1. Climate and geology of the Arabian Peninsula
2. Availability of raw materials in the gulf region
3. Standards and practices of concrete mixes in the Gulf region
4. Durability assessment of concrete
5. Low carbon and environmentally sustainable concrete
6. Review of the fundamental cement science and concrete technology
7. Review of particle packing

It is vital to discuss the geology and climatic conditions of the Arabian Peninsula as the plastic and hardened properties of concrete are greatly influenced by the local climatic conditions and the macro and micro environment the concrete structures are exposed to. Harsh arid conditions of the Arabian Peninsula specially along the coast of the Gulf in the east where the salt concentration is 20% higher than the open sea has made the production, placing and use of concrete with relevant plastic, mechanical and durability properties a challenge. The main concern of the concrete structures in the Arabian Peninsula is its long term durability against chloride and sulfate attack due to very high concentration of chloride and sulfate ions in the ground water especially along the Sabkha region where most of the major cities in the Arabian Peninsula are situated.

Availability of locally sourced materials to produce concrete to mitigate these challenging environmental conditions as well as with low embodied CO_2 is a prerequisite objectives of this study. Aggregate the main bulk constituents of concrete which is almost 70% to 80% to total concrete volume is in general abundant across the region mainly in the form of precambrian age metamorphic, igneous and sedimentary rocks. Therefore, crushed rocks mainly limestone and gabbro are the common source of coarse and fine aggregates in the region.

Generally crushed limestone fine aggregate contains high amount of finer particles passing below 75µm sieve, which could be good filler in the concrete. However, the practice of the local industry is to literally wash off these fine materials from the sand to meet project specifications which often restrict the maximum fine content to 5% by mass. From Author's view this tends to an absolute waste of resources from two angles. Firstly, the fine limestone filler can be utilized in the mix proportion to enhance the much needed mechanical and durability properties of concrete and secondly, huge amount of water and other energy and resources can be saved if the washing of sand can be avoided.

To enhance the rheology of the concrete mix, the rounded natural fine dune sand is widely used in the region. Dune sand is often single sized and rounded in shape due to being blown by winds. Provided it is free from chloride and other impurities, dune sand is a good and important constituents of concrete produced in the Arabian Peninsula.

The most important binding materials, Portland cement is widely available in the region and mostly produced locally due to the presence of huge deposits of limestone across the region. Imported blastfurnace slags are normally ground in the local mills of cement factories in the region to produce GGBS. It is the most widely used supplementary cementitious materials (SCM) beside microsilica due to its availability, logistic advantage and relatively low cost compared to other SCMs.

SCMs are widely used in the region mainly to produce high performance concrete to increase the durability of concrete structure to mitigate the extreme exposure conditions as mentioned earlier. Microsilica is also widely used in the region either with Portland cement or as ternary blend with GGBS/fly ash to enhance mechanical strength as well as durability of concrete structures. Microsilica is an imported material generally from China; therefore, its embodied CO_2 is not very favourable compared to GGBS. Similarly fly ash also needs to be imported, mainly from India. Fly ash, though it enhances durability and rheological properties, is not very widely used materials in the region, perhaps due to its cost and logistic disadvantages over GGBS.

Use of high performance admixtures such as polycarboxylate ether (PCE) is common in this region due to higher demand of improved concrete properties in terms of consistency, compressive strength and durability of concrete. Use of SNF based superplasticizer is also popular due to its cost advantage over PCE. Cement and concrete admixtures are generally produced locally. Beside chemical admixtures, other additions such as PPE fibre to mitigate plastic shrinkage cracking are also widely used, especially in the petrochemical industries in the region.

To understand the local practices in the concrete industry to address the durability and exposure conditions, a review of concrete specifications of three petrochemical organizations of Abu Dhabi have been conducted. It has been found that the project specifications are largely following a combination of former British and American standards with a trend to move towards current BSEN standards.

To address the durability issues of concrete the most common measure to test the chloride resistivity of concrete is Rapid Chloride Permeability test as per ASTM C1202-97. The permeation properties of concrete are measured using BSEN12390-8 and BS 1881: Part 122 to measure water permeation and water absorption respectively. To achieve the satisfactory durability performance with relevant mechanical strength the local industry often use a common concrete mix using 30% Portland cement and 70% GGBS as total cement content with a relatively low w/c ratio. A direct recommendation to use this cement combination has been given by the GASCO specification (GASCO 2007).

It has been found to have a lack of holistic approach in the concrete specifications by often allowing different international standards to measure the same parameter of concrete or raw materials in any given project. Therefore, a review of the durability parameters of the concrete structures in the Arabian Peninsula have been undertaken to see whether the current specification regime is sufficient.

Detailed discussions on the mechanism and process of different chemical attack on concrete in the Arabian Peninsula have been made in a series of documents jointly collaborated by Concrete Society with Bahrain Society of Engineers and CIRIA where specific guidance is given to design, construct and subsequent repair of concrete structure subject to the harsh climatic condition of Arabian Peninsula (Concrete Society, 2008/ CIRIA and The Concrete Society, 2002/ Concrete Society, 2002). Though the reports are holistic in nature but no guidance is given in terms of the environmental sustainability and low carbon concrete. Beside that very limited references of this guidance are found in the concrete specifications of projects across the region.

Among the chemical attacks, chloride induced corrosion is found to be the most profound type of attacks the concrete structures in the region are subjected to due to very high chloride concentration in the sea water of the Gulf. Corrosion due to carbonation could be a major concern in the gulf cities where relative humidity is high during certain period of time as works in Kuwait suggested higher rate of carbonations in concrete structures close to the coastal areas (Haque and Al Khaiat, 1997/ Fookes, 1995/ Al-Khaiat and Fattuhi, 2002).

Beside chloride attack, sulfate attack is perhaps the next most concerns for durability of concrete structures situated in the Sabkha region of the Arabian Peninsula as Sabkha regions are predominantly enriched with sulfate ions combined with higher ground water level and permeable granular sandy soil type ideal for sulfate attacks (Atkins, 2010). Al Amoudi (2002) reported that a combine presence of chloride and magnesium sulfate ions could change the dynamics of the sulfate attacks on the concrete foundations.

Delayed ettringite formation and salt weathering are other two concerns related to high ambient temperature of the Arabian Peninsula. Use of SCMs with reduced w/c ratio and appropriate protections of concrete during production, transportation, placement and in-service are the key element to provide a comprehensive protection against the harsh environmental conditions of the region. Most of the concrete specifications in the region generally address these issues by enhancing the chloride permeation resistance and permeation properties. Enhancement of the water permeation properties is one of the key strategy against these chemical attacks and the presence of water is the key factor for the chemical reactions to activate beside other requirements for each individual type of attacks.

As concretes in the Arabian Peninsula generally designed for its mechanical and durability properties, the local authorities like Estidama and GORD are increasingly leading the industry for sustainable buildings and construction. Therefore strategies like using concrete with low eCO_2 and recycled concrete aggregates are increasingly encouraged by the credit rating schemes like LEED, PBRS and GSAS (U.S.GBC, 2009/ Estidama, 2011/ Al Horr, Y., 2013).

Reduction of eCO_2 of cementitious materials is the most important factor to reduce the overall eCO_2 of concrete as Portland cement has the maximum contribution of eCO_2 per m^3 compared to any other constituent materials of concrete. The eCO_2 in Portland cement can either be reduced by optimizing its manufacturing process by adopting low energy, low CO_2 emitting process or by replacing the clinker by supplementary cementitious materials (SCMs) such as GGBS, fly ash, microsilica, rice husk ash or similar materials. The inherent eCO_2 of these SCMs are very low and most of these materials are already being used in the Arabian Peninsula to enhance durability and permeation properties of concrete.

The eCO_2 data of concrete ingredients to calculate the eCO_2 of concrete for Abu Dhabi from its 'cradle to gate' have been taken from a comparative study between three sources namely BCA fact sheets, Estidama and Masdar. Beside low eCO_2 concrete, use of recycled materials as aggregates such as RCA is an important strategy to reduce the environmental impact. A partial replacement of natural aggregate with RCA together with SCMs have been proven to be an ideal alternatives to produce a low carbon sustainable concrete with similar plastic and hardened properties of concrete containing natural aggregate and Portland cement (Kou, S.C. et al., 2008/ Ann, K.Y., et al. 2008).

As it has been discussed that use of SCMs is one of the smart way to reduce the eCO_2 of concrete, it is imperative to review the fundamental science of these cementitious materials. Therefore, a brief discussion of the basic physical and chemical properties, chemical compositions, hydration products and the ability to resist deleterious chemicals to enter into the cement matrix of these materials have been made. Beside Portland cement, the cementitious materials discussed are GGBS, fly ash, microsilica and rice husk ash.

The microstructure of cement paste made of GGBS and other pozzolanic materials are enhanced due to the production of additional hydration products. However, it can further be enhanced by appropriate designing of concrete ingredients by applying suitable particle packing models such as compressive packing model and linear packing model of de Larrard, modified Toufar and Dewar models (Jones, M.R. et al., 2002). Using suitable computer software based on these models plastic and mechanical properties of concrete can be predicted.

From the above discussion it can be concluded that a comprehensive set of study and related information are already available on concrete properties especially on durability parameters suitable for the harsh environment of the Arabian Peninsula. However, there was little evidence found on the research and state-of-the-art works related to low carbon and sustainable concrete for the region, even though there is a regulatory framework from authorities around the regions to implement low carbon concrete such as initiatives by Estidama in Abu Dhabi and GORD in Qatar are in place.

Therefore, to address this fundamental problem, a wide range of works involving different SCMs to replace Portland cement up to a certain extent and various sustainable techniques using local resources to produce concrete to reduce the environmental impacts have been undertaken, discussed and proposed under this programme.

Chapter 3

Programmes and Methods

3.1 Introduction

In the previous chapter a comprehensive literature review has been undertaken to identify and define the environment, exposure conditions and limitations on concrete materials that are specific to the Gulf region, and ascertain appropriate, representative types of concrete and associated requirements. In this chapter in order to establish the most sustainable concrete for the gulf region a suitable programme of works which has to be methodical and scientific have been considered.

Characterization of constituent materials have also been established by a comprehensive testing programme of raw materials including Portland cement, GGBS, fly ash, microsilica, rice husk ash, aggregates, water and admixtures.

In this chapter development of proportioning and design techniques have been discussed. This is to enable achievement of satisfactory levels of performance when using new and developing concretes in a range of products and exposure conditions specific to the Gulf environment. In order to achieve this level of performance a series of concrete mixes have been designed and the plastic and hardened properties in terms of strengths and durability properties are tested.

Advanced analytical technique such as thermogravimetry (TG) and scanning electron microscopy (SEM) have been used to understand the fundamental cement science and concrete technology that underpins the behaviour of these novel concretes. The performance of these new-sustainable concretes has then been normalized with control concretes with respect to performance-based specifications, and the equivalence in performance.

The most-appropriate forms of sustainable concrete for use in the gulf region would be identified by optimizing the compressive strength, durability, CO_2 emissions and other sustainability factors of these concretes.

Therefore, the work methodology of the entire work was divided into the following three segments:

1. Characterization of concrete constituent materials
2. Concrete test programme
3. Analysis of hydration product

Figure 3.1 illustrates the work flow programme for the entire work.

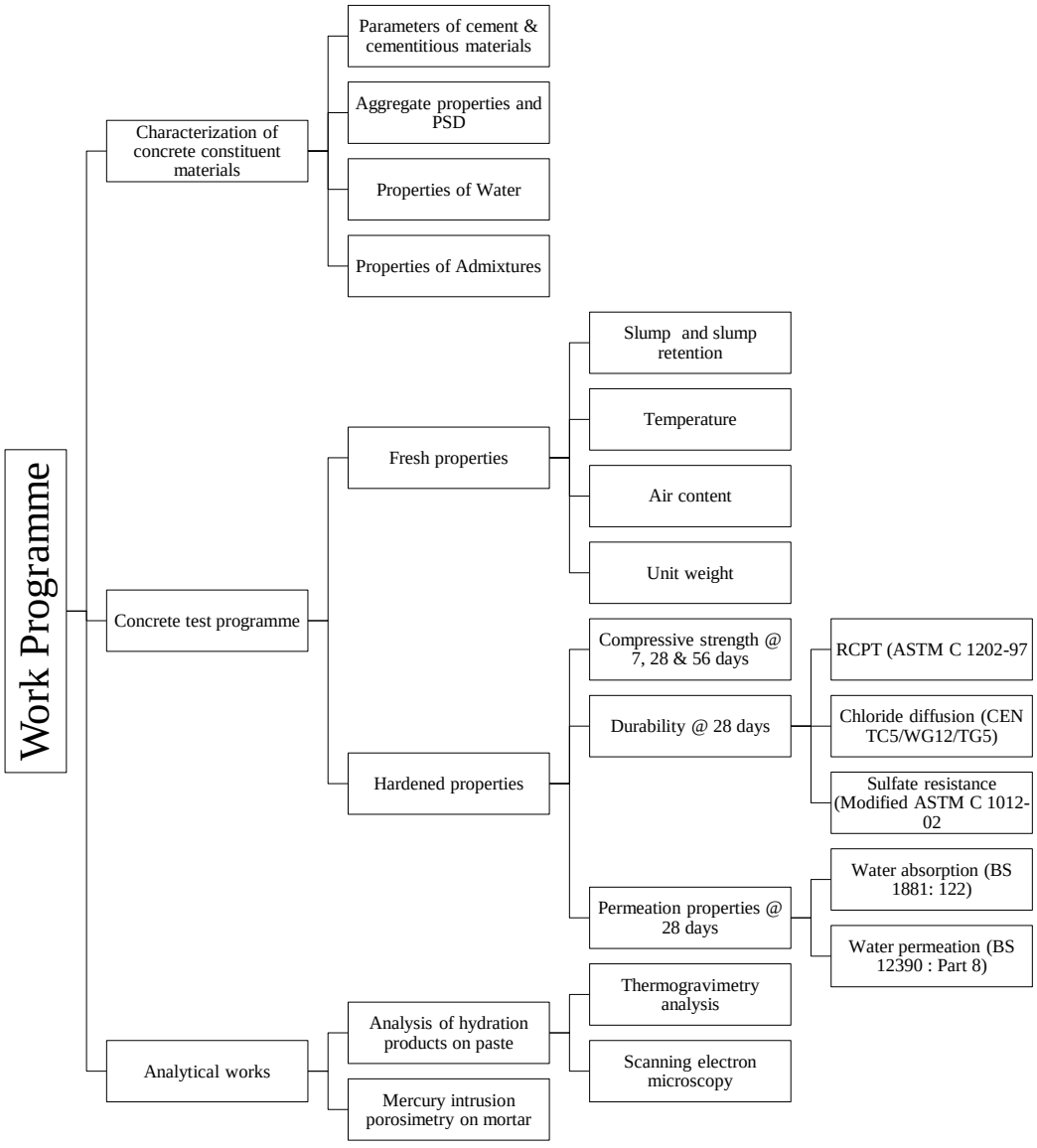

Figure 3.1: Work programme flow diagram

3.2 Characterization of concrete constituent materials

The characteristics of concrete constituent materials were analyzed prior to the work programme to understand and establish the suitability of the materials to the programme. Table 3.1 presents the main concrete constituents and their sources used in this programme.

Table 3.1: Concrete constituents used in this programme

	Constituent materials	Source
1	Portland cement	National cement, Dubai, UAE
2	GGBS	Super cement, Abu Dhabi, UAE
3	Fly ash	Ashtech, UAE
4	Microsilica	Elkem materials, China
5	Rice husk ash	NK Enterprises, India
6	20 mm crushed limestone aggregate	Ras Al Khaima, UAE
7	10 mm crushed limestone aggregate	Ras Al Khaima, UAE
8	5 mm crushed limestone aggregate	Ras Al Khaima, UAE
9	20 mm recycled concrete aggregate	Rostamany, UAE
10	10 mm recycled concrete aggregate	Rostamany, UAE
11	Dune sand	Al Ain, UAE
12	Water	ADWEA, UAE
13	Polycarboxylate admixture	Chryso Fluid Optima 245 EMx, UAE
14	Retarding admixture	Sodamco Admix CR 152, UAE
15	Air entraining admixture	BASF Microair 100, UAE

All constituent materials have been tested to check their physical and chemical properties.

3.2.1 Physical and chemical properties of the cement and cementitious materials

Table 3.2 provides the physical and chemical properties of the Portland cement, GGBS, fly ash, microsilica and rice husk ash. The bulk oxide of Portland cement, GGBS, and microsilica are provided by the manufacturer. The fly ash and rice husk ash bulk oxide are tested in the UAE. The copies of the test certificates of the cementitious materials are given in the Annex M-S.

Table 3.2: Parameters of cement and cementitious materials

Parameters	% by weight					
	Portland cement	**PC UK**	**GGBS**	**Fly ash**	**Microsilica**	**Rice husk ash**
Moisture	-	-	0.32	0.07	0.18	0.88
LOI	2.9	2.68	0.34	2.64	1.35	1.55
SiO_2	21.67	20.36	34.5	61.3	92.2	90.1
Al_2O_3	6.41	5.10	13.8	26.8	-	1.72
Fe_2O_3	3.94	3.60	1.12	3.13	-	1.14
CaO	65.98	64.56	42.4	1.1	-	0.41
MgO	1.24	1.95	6.2	0.8	-	0.94
SO_3	2.68	3.5	0.24	0.23	-	0.03
Mn_2O_3	-	-	-	0.07	-	-
Cl	0.01	0.01	0.008	0.01	-	0.01
Na_2O	-	0.20	0.24	0.43	-	0.59
K_2O	-	0.51	0.30	2.16	-	1.42
Total alkali (Na_2O+0.685)	0.50	0.54	-	-	-	-
Fineness, m^2/kg	330	-	437	370	24,600	35,000
Soundness, Le Chatelier exp.	1.0%	-	0.5%	-	-	-
Initial setting time, Vicat test	160 min	-	205	-	-	-
Final setting time	255 min	-	310	-	-	-
Pozzolanic activity index	-	-	-	-	125	111

3.2.2 Properties of aggregates

The bulk of the work was conducted using crushed limestone aggregates of 20mm and 10mm as coarse aggregates and 5mm as fine aggregates. Depending on the fine contents, the 5mm crushed limestone aggregates are categorized as i) washed and ii) unwashed sand. Figure 3.2 shows the images of crushed limestone coarse aggregate and its preparation of characterization works in the laboratory in Abu Dhabi.

Figure 3.2: Preparation for aggregate testing in the concrete lab and concrete mixer

It is a common practice in the local industry to wash the crushed limestone fine aggregate to remove the finer particles below 75μm 'dust' to below 5% by weight. This is to satisfy local project specifications. Fine aggregate with less than 5% dust was considered to be 'washed' sand and with approximately 10% dust was termed as 'unwashed' sand in this work. Dune sand, fine rounded natural sand in abundance in the desert dunes is very common sand used to add the finer particle size in the mix gradation. Dune sands are mostly single sized.

Beside the natural coarse aggregates, 20mm and 10mm sized recycled concrete aggregates (RCA) used for RCA series works. All coarse aggregates including RCA were tested indirectly for strengths such as aggregate crushing values and 10% fine values. The geometrical properties such as grading, flakiness and elongation index test and their physical properties such as density, absorption and impurities such as clay lumps and friable particles were also tested.

The RCA were also tested to classify the constituents of the coarse recycled aggregate as per BSEN 933-1:2009 Part 11: Classification test for the constituents of coarse recycled aggregate. The test results as shown in the Annex A & B, both 20mm and 10mm RCA contains 100% Rc constituents i.e. concrete, concrete products, mortar and concrete masonry units.

The fine aggregates were tested for grading, density, absorption and impurities including clay lumps, friable particles, and shell contents. The particle size distribution of aggregates tested as per BS 812: Part 103: Sec. 103.1: 7.3: 1985; AMD 6003: 1989 has been given in Table 3.3 and the properties of different type of aggregates are presented in Table 3.4.

Table 3.3: Particle size distribution of aggregates (BS 812: Part 103: Sec. 103.1: 7.3: 1985;AMD 6003 : 1989)

Test Sieve Size	**Cumulative Percent Passing**						
(mm)	**20mm**	**10mm**	**5mm Washed**	**5mm Unwashed**	**Dune sand**	**20mm RCA**	**10mm RCA**
20	95.6	100.0	100.0	100.0	100.0	100.0	100.0
14	41.9	100.0	100.0	100.0	100.0	68.0	100.0
10	4.1	94.8	100.0	100.0	100.0	8.0	98.7
5	0.3	17.1	98.5	95.0	100.0	0.7	5.3
2.36	-	3.1	70.7	59.1	100.0	-	1.1
1.18	-	-	41.4	33.2	100.0	-	-
0.60	-	-	23.7	21.3	100.0	-	-
0.30	-	-	13.0	14.2	94.6	-	-
0.15	-	-	6.8	11.3	38.4	-	-
0.075	0.5	1.0	3.8	9.3	0.1	0.3	0.9

Table 3.4: Aggregate properties and test reports

Test Designation	Test Method	Limiting values as per BS 882:1992	Result						
			20mm	10mm	5mm Washed	5mm Unwashed	Dune	20mm RCA	10mm RCA
Particle Density (Oven Dry) Mg/m^3	BS 812: Part 2: 1995	None	2.80	2.80	2.79	2.73	2.61	2.50	2.40
Particle Density (SSD) Mg/m^3	BS 812: Part 2: 1995	None	2.81	2.81	2.81	2.79	2.63	2.59	2.50
Particle Density (Apparent) Mg/m^3	BS 812: Part 2: 1995	None	2.82	2.83	2.85	2.91	2.67	2.75	2.71
Water Absorption (%)	BS 812: Part 2: 1995	None	0.30	0.40	0.90	2.30	0.70	3.70	5.00
Clay Lumps and Friable Particles (%)	ASTM C 142 : 1997	None	0.30	0.40	0.30	0.50	>0.10	0.20	0.30
Flakiness Index (%)	BS 812: Sec. 105.1: 89	<40.0	11.00	14.0	-	-	-	6.60	4.50
Elongation Index (%)	BS 812: Sec. 105.2: 89	None	17.00	12.0	-	-	-	13.0	5.10
Aggregate Crushing Value (%)	BS 812: Part 110:1990	None	19.00	18.0	-	-	-	21.0	25.5
Mean 10% Fine Value (kN)	BS 812: Part 111:1990	>50	212.00	196.00	-	-	-	-	-
Material Finer than 75µm (%)	BS 812: Part 103:1985	None	0.50	1.00	3.8	9.3	0.1	0.4	0.9
Bulk Density (Compacted) Kg/m^3	BS 812: Part 2:1985	None	1599	1502	1763	1853	1531	1463	1440
Bulk Density (Uncompacted) Kg/m^3	BS 812: Part 2:1985	None	1465	1378	1603	1659	1448	1342	1339
Shell Content (%)	BS 812: Part 106:1985	<20% (5-10mm) <8% (>10mm)	-	-	0.20	0.10	>0.10	-	-
Acid soluble chloride content as Cl^- (%)	BS 812:Part 117:1988	<0.05	0.01	0.01	0.02	0.02	0.01	0.09	0.11
Acid soluble sulfate as SO_3 (%)	BS 812:Part 118:1988	None	0.02	0.02	0.03	0.03	0.02	1.55	0.84

3.2.3 Properties of water

Potable water was used in this work with the properties of following chemical analysis results as shown in Table 3.5. Though according to BSEN 1008:2002 there is no testing required for potable water, however it has been found that the chloride and sulfate contents in the water are well within the maximum allowable range. The content of carbonate and bicarbonate content to affect the setting time of cement is also at very low range in accordance with BS 3148:1980.

Table 3.5: Results of the chemical analysis of water

Parameters	**Test Methods**	**Unit**	**Results**	**Limiting values as per BS 3148:1980**
Total dissolved solids	BS 1377 Part 3 Cls 8:1990	mg/l	196	<2,000
Chloride as Cl^-	ASTM D 512-04	mg/l	47	<500
Sulfate as SO_4^{2-}	ASTM D 516-07	mg/l	<10	<1,000(as SO_3)
Carbonate as CO_3^{2-}	ASTM D 513-06	mg/l	Nil	Combined total <1,000
Bicarbonate HCO_3^-	ASTM D 513-06	mg/l	29	
Total alkalinity as $CaCO_3$	ASTM D 513-06	mg/l	24	-
pH at 20°C	ASTM D 1293-99 (2005)	-	7.6	-

3.2.4 Properties of chemical admixtures

A high range water reducing admixture was used to produce concrete with reduced w/c ratio of 0.25, 0.32 and 0.40, while maintaining a workable consistency. Though the retention of the slump is not a major requirement in this work, nevertheless a retarding type admixture was used to maintain reasonable slump retention to achieve a level of consistency between concrete mixes.

An air entraining admixture was used for concretes in air entrained series. The main purpose to use air was to determine whether air can effectively replace a reasonable proportion of aggregate and paste volume and reduce the impact on environment. Though there was no compatibility tests between these admixtures were carried out, but these

admixtures did not show any sign of incompatibility during the trial works. The technical data sheets of the admixtures have been enclosed in the Annex D, E and F.

Superplasticizing admixture: This polycarboxylate based superplasticizing admixture is made of especial proprietary polymer to boost the hydration of high volume GGBS and fly ash concrete. This is the only high range water reducing and plasticizing admixture was used in the work. The technical properties of the superplasticizing admixture used in the work have been given in Table 3.6.

Table 3.6: Technical properties of superplasticizing admixture

	Properties	**Description / Values**
1	State	Liquid
2	Colour	Brownish yellow
3	Density	1.100 ± 0.020
4	pH	6 ± 2
5	Cl^- content	Nil to EN 934 and BS 5075
6	Na_2O equivalent	≤1.0 %
7	Recommended dosage	0.3 to 3.0 kg per 100 kg cement

Retarding admixture: A retarding admixture was used to maintain the slump retention for more than 1 hour. The dosage of this admixture was depended on the w/c ratio, type and proportion of cement and cementitious materials and type of aggregates. Table 3.7 is giving the technical properties of the retarding admixture.

Table 3.7: Technical properties of retarding admixture

	Properties	**Description / Values**
1	State	Liquid
2	Colour	Light yellowish
3	Specific gravity at 20°C	1.103 - 1.108
4	Chloride content	Nil to BS 5075
5	Recommended dosage	0.15 to 0.35 kg per 100 kg cement

Air entraining admixture: The technical properties given in Table 3.8 is for the air entrain admixture which was used to entrain air into the concrete to increase the air content from design 2% by volume to 5% to 15% to explore the effect of air content on the properties of concrete.

Table 3.8: Technical properties of air entraining admixture

	Properties	Description / Values
1	Specific gravity	0.986 - 1.036
2	pH	10.5 - 12.5
3	Colour	Amber - brown
4	Dry extract (%)	11.6 - 13.5
5	Chloride content	Nil to BS 5075: 1982
6	Flash point	Not applicable
7	Freeze point	-1°C
8	Recommended dosage	No fixed dosage

3.3 Concrete test programme

3.3.1 Introduction

Concrete test programme is one the major work undertaken by this study as it compared the performance of different possible combinations of concrete groups using different type of constituent materials in different conditions. The programme tested the validity of these new concretes with a set of control concrete to verify their strength, durability and environmental sustainability credentials.

The concrete test programme was designed in such a way that total five distinctive areas of interests as described below, can be explored to observe their effects on the concrete properties such as compressive strengths, durability and environmental factors. Total 88 numbers of concrete mixes were prepared across these distinctive areas. These five identified areas are:

1. The effect of different type of cements (cement type series)
2. The effect of unwashed sand (sand type series)
3. The effect of recycled concrete aggregates (RCA series)
4. The effect of air entrainment (Air entrained concrete series)
5. The effect of elevated curing temperature (Higher curing temperature series)

3.3.2 The effect of different type of cement

In this group the effect of different type of cements and their combinations were examined and compared to a controlled set of concrete mixes. The following cement and cementitious materials were used:

i. Portland cement
ii. Ground granulated blastfurnace slag (GGBS)
iii. Fly ash
iv. Microsilica
v. Rice husk ash (RHA)

3.3.2.1 Control concrete

As mentioned in the literature review (Chapter 2) 30% Portland cement and 70% GGBS of total cement combination is the most common combination of total cementitious materials in the UAE/ME due to specific requirements for durability. Due to this reason concrete made with this particular cement combination was chosen to be the control concrete mix to compare the performance with the other type of concretes.

3.3.2.2 Concrete with GGBS

GGBS is a very important component of this work due to two main reasons. Firstly being latent hydraulic, it replaces large portion of the Portland cement compared to any other similar materials. Thus using GGBS as part of the sustainable mix is an advantageous strategy. The excellent durability properties was the another reason to use GGBS in combination with Portland cement and other pozzolanic materials. GGBS has been successfully used in the Arabian Peninsula as it has been discussed in the Literature review for both chloride and sulfate resisting purpose.

Including the control concrete, total five different proportions of Portland cement and GGBS were investigated in this work. The GGBS proportion of all these mixes were very high starting from 100% to 70% of total cement content by mass. The sole objective of using very high proportion of GGBS content is to reduce the eCO_2 of concrete mix. The Portland cement and GGBS proportions were:

i. 0% Portland cement and 100% GGBS
ii. 2.5% Portland cement and 97.5% GGBS
iii. 5% Portland cement and 95% GGBS
iv. 15% Portland cement and 85% GGBS
v. 30% Portland cement and 70% GGBS

3.3.2.3 Concrete with pozzolanic materials

Three more concrete mixes using three specific pozzolanic materials i. fly ash ii. microsilica and iii. rice husk ash with Portland cement were made. The combinations between the Portland cement and the pozzolanic materials were:

i. 20% Portland cement and 80% fly ash
ii. 90% Portland cement and 10% microsilica
iii. 80% Portland cement and 20% rice husk ash

3.3.2.4 Triple blend of Portland cement, GGBS and rice husk ash

It was anticipated that the reduction of strength due to high volume GGBS mixes could be traded off by the addition of certain percentage of rice husk ash. To examine the effect of these triple blends following two mixes were added to the above pozzolanic concrete mixes:

i. 5% Portland cement + 70% GGBS + 25% RHA
ii. 15% Portland cement + 70% GGBS + 15% RHA

3.3.2.5 Water cement ratio

Each type of concrete mixes was made at three different water to cement ratio of 0.25, 0.32 and 0.40 to construct a three point graph to obtain any unknown variables during the data analysis. The selected range of the w/c ratio is relatively lower to reflect the high durability and permeation properties required in the Arabian Peninsula. This three w/c ratio were used in all other concrete mixes tested under this programme for the same reason as mentioned above.

3.3.3 The effect of unwashed sand

In this series the effect of two types of sand were examined on the properties of concrete by using concrete with higher fines content passing 75μm sieve, termed as 'unwashed sand' compared with 'washed sand' concretes used in the previous series. These higher finer particles in unwashed sand which was approximately 10% by weight would normally be reduced by washing to below 5% to satisfy local specifications.

Similar to the Cement type series the concrete with 30% Portland cement and 70% GGBS was considered as the control mix. The performance of other four groups of mixes was compared with this control mix. The four groups of concrete were:

i. 0% Portland cement and 100% GGBS
ii. 20% Portland cement and 80% fly ash
iii. 90% Portland cement and 10% microsilica
iv. 80% Portland cement and 20% rice husk ash

3.3.4 The effect of recycled concrete aggregate (RCA)

The effect of RCA with high volume slag cement was examined with initial work of 100% GGBS for both washed and unwashed sand. The proportions of RCA compared with the natural coarse aggregate were varied to understand the effect of different proportions of RCA.

An additional series of RCA was investigated with different proportion of cementitious materials due to the lower strength obtained by 100% GGBS. In this series 15% Portland cement and 15% Rice husk ash was added to 70% GGBS to provide a boost to the compressive strength gain of GGBS blended concrete. The proportion of RCA was also changed to obtain a wider variation. Each set of concrete mixes was made at three w/c ratio of 0.25, 0.32 and 0.40. Table 3.9 shows the different proportion of RCA content with their corresponding cement and sand type.

Table 3.9: Proportions of RCA and natural aggregates in the series, % of total coarse aggregate

Type of cementitious materials	Sand type	RCA %	Natural aggregate %
100% GGBS	Washed and unwashed	100	0
		80	20
		50	50
		0	100
15% PC+70% GGBS+15% RHA	Only washed	100	0
		50	50
		20	80
		0	100

3.3.5 The effect of air entrainment

This series of the work was designed to investigate the impact of high volume entrained air to the concrete properties. The objective is to reduce the quantity of non-renewable constituents i.e. aggregates by increasing the air volume. As the air content and compressive strength is linearly proportionate, microsilica was added to the mix to compensate the strength loss. The proportion of the air was targeted to 2% (as control), 5%, 10% and 15% by volume. Each set of mixes was designed for 0.25, 0.32 and 0.40 w/c ratio to determine the effect of w/c ratio on the concrete properties with different proportion of air content.

3.3.6 The effect of curing temperatures

The standard practice of curing of concrete cubes according to international standards and specification such as BS EN 12390-2 is to cure concrete specimen at 20±2 ºC in water, however the concrete structures in Arabian Peninsula are subjected to much higher temperature which can rise up to 50ºC during summer days.

It has been discussed in the literature review that the hydration of GGBS can increase by increasing the curing temperature. Escalante, J.I., et al., (2001) have demonstrated an increase of 5% more slag hydration by increasing the curing temperature from 30ºC to 50ºC. Therefore, a properly placed, compacted, protected and cured concrete should achieve higher strength than a cube specimen taken from the same concrete cured at 20±2ºC in the laboratory as cement hydration is higher at higher temperature.

In this group, the curing temperature of triple blend of Portland cement, GGBS and rice husk ash was elevated to 40 ºC. The compressive strength and durability results of these cubes were compared with the results for the same mixes at 20ºC to find a representative performance of actual concrete subject to the high ambient temperature. Table 3.10 presents the proportion of Portland cement, GGBS and rice husk ash which was used to study the effect of elevated curing temperature on the hardened properties of concrete. Only washed sand was used and each set of concrete was made at 0.25, 0.32 and 0.40 w/c ratio.

Table 3.10: Proportions of Portland cement, GGBS and rice husk ash to study the effect of elevated curing temperature

No	Reference	w/c ratio	%		
			Portland Cement	GGBS	RHA
1	1P5S70R25W	0.25	5	70	25
2	2P5S70R25W	0.32	5	70	25
3	3P5S70R25W	0.40	5	70	25
4	1P15S70R15W	0.25	15	70	15
5	2P15S70R15W	0.32	15	70	15
6	3P15S70R15W	0.40	15	70	15

3.3.7 Concrete mixes referencing system

A comprehensive concrete mix referencing system was designed by giving each concrete mix a unique reference number for the purpose of easy identification of concrete mixes. The referencing system was based on a common sequence by which the reader could be able to distinguish one concrete mix from another by understanding the meaning of the particular concrete mix reference. The reference of cement type and sand type concretes can be explained from Table 3.11 where 1P30S70W, the reference of concrete mix made with 30% Portland cement and 70% GGBS using washed sand at 0.25 w/c ratio has been taken as an example.

Table 3.11: Concrete mix referencing explanation of 1P30S70W concrete

	1	2	3	4	5	6
Description of different items	w/c 0.25 = 1 0.32 = 2 0.40 = 3	Portland cement	% of total cementitious content	SCMs GGBS = S Fly ash = F Microsilica = M RHA = R	% of total cementitious content	Sand type W=Washed U=Unwashed
Reference	1	P	30	S	70	W

In this example column 1 describes the w/c ratio of the concrete where the numbers 1, 2 and 3 denote the w/c ratio of 0.25, 0.32 and 0.40 respectively. Column 2 represents Portland cement and it is denoted by the letter 'P'. Column 3 is the percentage of Portland cement in the concrete compared to total content of cementitious materials. Column 4 describes the type of supplementary cementitious materials and each SCMs has its own designated letter. In this example 'S' stands for GGBS. Column 5 is the percentage of that particular SCM of total cementitious content and lastly column 6 denotes the type of sand, W for washed and U for unwashed sand.

Therefore, the concrete 1P30S70W stands for a concrete with 0.25 w/c ratio, with 30% Portland cement and 70% GGBS as cementitious combinations using washed sand. In the event of the triple blend concrete from 'Higher curing temperature series', where 15% Portland cement, 70% GGBS and 15% rice husk ash was used, the reference should be written as 1P15S70R15W where R15 denotes 15% rice husk ash. Therefore, the referencing system in Table 3.11 can explain the concrete referencing of concretes from the Cement type, Sand type and Higher curing temperature series.

Due to the presence of different variables, the reference of RCA and Air entrained concrete series concretes have to be explained by a different set of referencing sequence as explained by the Table 3.12 and Table 3.13 respectively. In Table 3.12 the concrete mix reference of RCA series have been explained where 2R50N50W stands for a concrete with 0.32 w/c ratio and 50% RCA and 50% natural crushed limestone coarse aggregate with triple blend of Portland cement, GGBS and rice husk ash cement combinations.

Table 3.12: Concrete mix referencing explanation of 1R50N50W concrete

	1	2	3	4	5	6
Descriptions of different items	w/c 0.25 = 1 0.32 = 2 0.40 = 3	Recycled concrete aggregate	% of total coarse aggregate content	Natural aggregate	% of total coarse aggregate content	Cement type W= 100% GGBS TB= 15%PC+70%GGBS+15%RHA
Reference	2	R	50	N	50	TB

Similarly in Table 3.13, the concrete mix reference of 3P90M10A2 represents a concrete from the Air entrained concrete series where the concrete is made at 0.40 w/c ratio with 90% Portland cement and 10% microsilica with designed air content of 2% by volume of the concrete.

Table 3.13: Concrete mix referencing explanation of 3P90M10A2 concrete

	1	2	3	4	5	6
Descriptions of different items	w/c 0.25 = 1 0.32 = 2 0.40 = 3	Portland cement	% of total cementitious content	Microsilica	% of total cementitious content	% of air content A2=2% A5=5% A10=10% A15=15%
Reference	3	P	90	M	10	A2

3.3.8 Mix designs and mixing of concrete

The mix designs of different concrete mixes of different series have been presented in Annex G-L. In the following section following aspects of the mix design have been briefly discussed.

i. Mix design procedure
ii. Water to cement ratio
iii. Aggregate grading and proportions
iv. Admixture dosage
v. Mixing of concrete and test specimen

3.3.8.1 Mix design procedure

Concrete were designed using a volumetric method for 1000ml of total concrete volume. Using this method the volume of paste fraction which comprises of cement and cementitious materials, water and entrapped air were computed. The volume of Portland cement and other cementitious materials such as GGBS, fly ash, microsilica and rice husk ash were computed by dividing the known weight of each material by their respective specific gravity. The individual weight of each cementitious material was predetermined. The w/c ratio for each individual mix was also predetermined whether it was 0.25, 0.32 or 0.40. Therefore, the volume of water was also known. The volume of entrapped air except for Air entrained concrete series was assumed to be 2%.

The volume of total aggregate was computed by subtracting the volume of the paste fraction from total volume of 1000 ml. The volume of each type of aggregate could be computed by the known proportion of each aggregate which was predetermined to satisfy the combined aggregate grading chart as per BS 882:1992 as shown in Table 3.15. The weight of each type of aggregate then could be computed by multiplying the volume of each aggregate by the specific gravity of respective type of aggregates.

The weight of superplasticizing admixture was determined during the trials to achieve the initial slumps of approximately 200 - 250 mm and after 90 minutes 150 – 200 mm. The retarding admixture was used between 0.5 to 1.0 kg/m^3 depending on the requirement of slump retention.

Table 3.14 illustrates a typical design calculation of concrete mix design using 30% Portland cement and 70% GGBS content with 0.25 w/c ratio. During concrete mixing works in the laboratory the water absorption and moisture contents of aggregates were taken into consideration to compute actual water to be added. This effectively made small variation on the aggregate content which was considered to be negligible.

Table 3.14: Typical design calculation of 1P30S70 concrete mix

	Constituents	Proportion	Content, kg	Specific Gravity	Volume, ml
Paste	Portland Cement	30%	120	3.15	38
	GGBS	70%	280	2.90	97
	w/c	0.25			
	Water		100	1	100
	Air	2%			20
	Paste volume				255
Aggregate	Aggregate volume				745
	20 mm limestone	32%	670	2.81	239
	10 mm limestone	21%	440	2.81	157
	5 mm limestone	32%	665	2.79	239
	Dune Sand	15%	294	2.63	112
	Total volume				1000

3.3.8.2 Water / cement ratio

All concrete mixes were designed with a fixed total cementitious content of 400 kg with varied water to cement ratio of 0.25, 0.32 and 0.40. In this study water to cementitious ratio written as w/c ratio meant for all combinations of cementitious materials. The reason for selecting w/c ratio of 0.40 and less is that in the Arabian Peninsula most of the structural concrete grade w/c ratio is 0.40 or less due to the requirements of strengths and durability.

Another reason of choosing very low w/c ratio is to gain sufficient compressive strength as most of mixes are containing high volume replacement of Portland cement. A three point graphs can be drawn from the data provided by three w/c ratio which would eventually help to determine the data for any specific w/c ratio of choice or vice versa.

3.3.8.3 Aggregate grading and proportions

As discussed before total 7 types of coarse and fine aggregates were used in this work which include 20mm and 10mm coarse aggregate made of natural crushed limestone and RCA, 5mm fine aggregates made of crushed limestone with or without excessive finer particles passing 75 μm sieve termed as ‘unwashed and washed sand’ and dune sand as part of the fine aggregate fraction.

An average proportion of each type of aggregate in terms of percentage of the total mass of aggregate is given in Table 3.15. A combined aggregate grading as per BS882:1992 of natural crushed limestone coarse aggregates, washed fine aggregates and dune sand based on the proportions given in Table 3.15 have been given in Table 3.16 and corresponding graph in Figure 3.3.

Table 3.15: The average proportions of the aggregates used in the mix designs

Type of aggregate	**Conditions**	**% of total mass of aggregate**
20 mm crushed Limestone	Natural or RCA	32%
10 mm crushed Limestone	Natural or RCA	21%
5 mm crushed Limestone	Washed or unwashed	32%
Dune sand	-	15%

Table 3.16: The combined grading of the aggregates using natural crushed limestone coarse aggregate and washed fine aggregate conforming BS 882:1992

B.S. Sieves	**20 mm**	**10 mm**	**0-5 mm**	**Dune Sand**	**Comb. Grading**	**B.S. 882 Limits**
37.5 mm	100.0	100.0	100.0	100.0	100.0	100
20.0 mm	95.6	100.0	100.0	100.0	98.6	95-100
5.0 mm	0.3	17.1	98.5	100.0	50.2	35-55
0.60 mm	0.0	0.0	23.7	100.0	22.6	10-35
0.15 mm	0.0	0.0	6.8	38.4	7.9	0-10

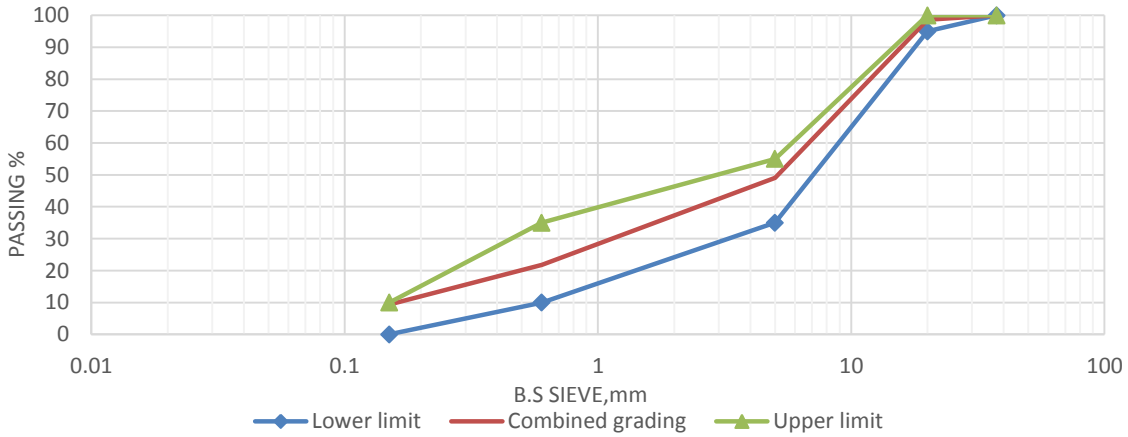

Figure 3.3: Combined aggregate grading chart as per BS882:1992 using natural crushed limestone coarse aggregate and washed fine aggregate

3.3.8.4 Admixture dosage

Superplasticizer:

Chryso Fluid Optima 245EMx, the polycarboxylate based admixture is the only superplasticizer used throughout the work. This particular admixture was chosen due to its ability to enhance the hydration of high volume GGBS or fly ash mixes as claimed by the manufacturer. Beside enhancing hydration, the superplasticizer also helped to reduce the water demand and providing a workable level of consistency. The initial slumps of all concrete mixes were kept between 200 – 250 mm and the slump retention was measured up to 90 minutes to maintain a final slump between 150 – 200mm.

The dosage rate of Chryso admixture is wide, depending on the water demand of any particular mix, type of aggregates or cementitious materials. The typical dosage rate in Cement type series was 0.5% to 2% by weight of total cementitious content. Typically concrete with 0.25 w/c required 2% admixtures. The requirement of admixture reduced with the increase of w/c ratio due to the availability of water in the mix. For Sand type series where the filter content in the 5mm sand was higher, the dosage requirement increased slightly.

For better rheology properties, the admixture dosage requirement for fly ash concretes reduced to 0.3% to 1.5% by weight of cementitious content. For Sand type series it was between 0.45% – 1.25% by weight of cementitious content. Superplasticizer demand for microsilica concrete is always higher due to its very high specific surface area compared to Portland cement, GGBS and fly ash. For Cement type series the dosage range was 1.75% to 1.25% by weight of cementitious content. For Sand type series it slightly increased to 2.13% to 1.25% by weight of cementitious materials.

Rice husk ash required excessively higher amount of admixture perhaps due to two reasons i) its very high specific surface area which is similar to microsilica and ii) its very high surface absorption as it has very porous morphology as seen in Chapter 2. The admixture demand for concrete at 0.40 w/c ratio with rice husk ash was similar to concrete with microsilica which was 1% for Cement type and 1.25% for Sand type series. However, the demand for admixture increased significantly with the reduction of w/c ratio which was as high as 5.0% by weight of the cementitious content. This huge demand of admixture increased the actual w/c ratio due to the water content in the admixture itself as shown in Table 3.17. It affected the strength gain of concrete containing rice husk ash.

The solid content of the superplasticizing admixture Considering Chryso Fluid Optima 245EMx was 34% by mass. Therefore, the remaining 66% of the admixture was water. For ordinary dosage rate this additional water content was considered negligible. However, for rice husk ash concrete, the water content from the admixture should be considered as part of the mixing water due to its huge requirement for admixture, especially for concrete with lower w/c ratio.

Table 3.17: The actual and designed w/c of P80R20 containing mix

Series	**Mix reference**	**Admixture dosage, kg/m^3**	**Additional water due to admixture, kg/m^3**	**Designed w/c**	**Actual w/c**
Cement type	1P80R20W	17.5	11.5	0.25	0.28
	2P80R20W	9.5	6.3	0.32	0.34
	3P80R20W	4	2.6	0.40	0.41
Sand type	1P80R20U	20	13.2	0.25	0.28
	2P80R20U	10	6.6	0.32	0.34
	3P80R20U	4.5	2.97	0.40	0.41

Retarder:

The dosage of Admix CR152 was kept at minimal to 0.125% to 0.25% of total cementitious content throughout the work. The main task of this admixture was to provide adequate slump retention to maintain a consistency of slump for entire work. The intended slump retention in room temperature was 90 minutes. In few occasions it was extended to 120 minutes if the concrete mix appears to maintaining the slump.

Air entraining admixture:

Micro-air 100, an air entraining admixture (AEA) was used to entrain the air content ranging from 5 to 15%. The dosages of Micro-air 100 were 0.1% to 0.13% for 5% air, 0.3% – 0.45% for 10% air and 1.0% - 1.13% for 12% air. Though the design target was to achieve maximum 15%, but it was practically not achievable. The concrete became 'fluffy' and lost workability without gaining any entrainment of air for any further addition of dosage beyond 1.0% of total cementitious content. Therefore, 12% air entrainment was considered to be the optimum air for this double blend concrete with 10% microsilica. This limitation could be due to factors of fine materials like microsilica as mentioned in the product datasheet of BASF Micro-Air100 or the lab scale mixer which was not producing enough shear force to entrain air into the paste. The relationship between the dosage of AEA and the entrained volume of air is given in Figure 3.4.

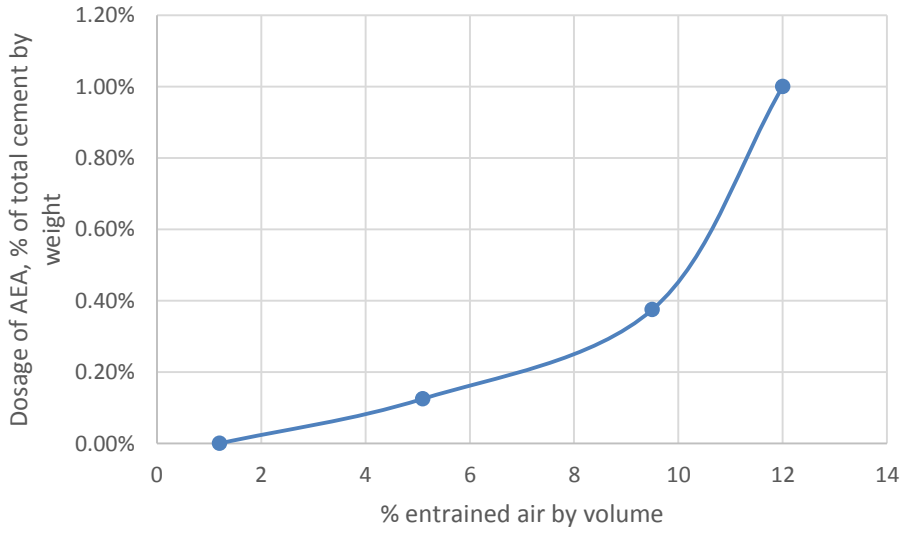

Figure 3.4: Relationship between the dosage of AEA and the entrained air

Figure 3.4 explains the optimum level of the dosage of the Air Entraining Admixture used to achieve the maximum air content of 12% by volume of concrete. The rate of air entrainment was almost linear up to the dosage of AEA of 0.40% of the total cementitious weight. However, after that the curve went straight vertical up indicating the optimum level of the dosage.

3.3.8.5 Mixing of concrete and preparation of test specimen

All concretes were mixed in a temperature controlled laboratory using a 60 liter capacity Matest C166-01 pan mixer (Figure 3.2). Constituent materials i.e. cements and aggregates were kept in a controlled laboratory environment prior to weighing for each batch (Figure 3.5) The size of the each batch was 0.050 m^3 of concrete. Prior to the weighing of each ingredients, the water absorption and moisture content of aggregate were taken into consideration to determine the free water. Based on this calculation the actual mass of aggregates was also adjusted.

Figure 3.5: Storage of cementitious materials and admixtures

Mixing sequence:

i. Coarse aggregates, fine aggregates and cement/cementitious materials were mixed without water for 30 seconds.
ii. Water was added for next 30 seconds while the mixing was continued. Once the concrete ingredients were fully coated with water, admixture was added until

desired consistency had been reached. The whole mixing process was completed by 4 minutes time.

iii. The initial slump (BSEN 12350-2:2000), concrete temperature (using a calibrated digital thermometer), air content (BSEN 12350-7:2009) and fresh density (BSEN 12350-6:2000) were measured and recorded.

iv. The consistency of concrete was measured by slump tests at 30 minutes interval at T_0, T_{30}, T_{60} and T_{90} minutes. Concrete was rested with a cover over the mixer during the interval. A 30 sec. re-mix was done prior to each slump measurement.

Concrete specimen for compressive strength and durability tests:

150mm x 150mm x 150mm size cubes were taken as per BS 1881-108:1983 for compressive strengths and durability tests. Compressive strength tests were conducted as per BSEN 12390-3:2009 at the age of 7, 28 and 56 days. 3 cubes were taken for each test and an average of 3 cubes was considered as the compressive strength of that particular concrete.

Concrete cubes were taken for four types of durability tests, i) rapid chloride permeability as per ASTM C1202-97, ii) water absorption as per BS1881:Part122 iii) water permeation as per BS EN 12390: Part 8 and iv) chloride diffusion test as per CEN TC51/WG12/TG5, (Draft 4 Version 2 Date: 20 April 2008) . For sulfate resistance test (as per a modified method of ASTM C 1012 – 02) concrete prisms of 75mm x 75mm x 280mm size were taken from each concrete mix.

Curing of concrete specimen:

All concrete specimen including cubes for compressive strength and durability testing and concrete prisms for sulfate resisting tests were cured in water in a temperature controlled curing tank as shown in Figure 3.6. All specimens were properly marked and labelled prior to placing into the curing tank. The curing temperature was kept at 20±2°C as per BSEN 12390-2. Concrete specimens for higher curing temperature concrete series were kept in a separate tank with elevated temperature of 40±2°C.

3.3.9 Compressive strength and durability testing

3.3.9.1 Compressive strength

As one of the main objectives of this work was to replace Portland cement using SCMs, achieving reasonable level of compressive strength was a challenge. Strength enhancing techniques, such as use of special type superplasticizer to enhance hydration of GGBS and fly ash, particle packing using additional finer particles in the unwashed sand and higher temperature curing to demonstrate higher in-situ strength, were adopted.

As mentioned previously compressive strength test of 150x150x150 mm cube specimen were conducted as per BS EN 12390-3:2009 for 7, 28 and 56 days. For each age an average of the results of three specimens have been taken as the compressive strength results of that concrete mix. Figure 3.6 shows the compressive strength machine and curing tank used for this work.

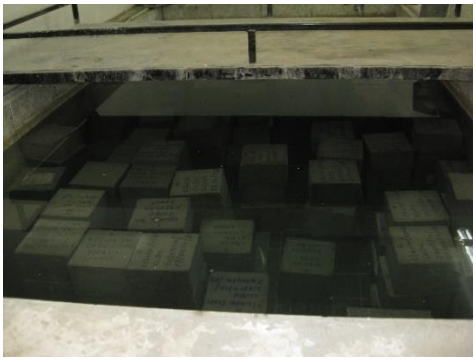

Figure 3.6 : Compressive strength testing machine and curing of cube specimen

3.3.9.2 Durability properties

In the previous Chapter 2 of literature review, it has been discussed that the concrete structures in the Arabian Peninsula are exposed to most severe environmental conditions and subjected to chloride and sulfate attack and in certain extent other chemical attacks such as carbonation, delayed ettringite formation (DEF), salt weathering, and alkali silica reactions. However, chloride and sulfate are the two most common concerns exist in the local construction industry.

It has also been reflected in the local specifications and soil reports as discussed in the literature review that stringent durability and permeation parameters related to chloride, water permeation, and water absorption tests are the only properties tested and concerned about. These measures have inadvertently made the concrete structures watertight, a key factor to achieve resistance against most of the chemical attack including carbonation, DEF and salt weathering.

Therefore, the permeation properties of concrete such as water permeation and water absorption need to be enhanced and investigated. Accordingly, concrete specimens in this work were tested for their permeation properties in term of i) water permeation test as per BSEN 12390: Part 8 and ii) water absorption test as per BS1881: Part 122.

Beside permeation tests three durability tests were undertaken to test the chloride and sulfate ion resistivity of concrete. These test are i) Rapid chloride permeation test as per ASTM C1202-97 ii) Chloride diffusion test as per CEN TC51/WG12/TG5, (Draft 4 Version 2) and iii) sulfate resistance test as per a modified method of ASTM C 1012 – 02. A brief description of each tests have been given below.

As concretes have been designed to make highly water-tight by reducing the w/c ratio and using high volume of SCMs at different proportions, other durability parameter mentioned in the literature review such as carbonation, DEF and salt weathering were not tested under this work programme.

Water penetration test:

Water permeation is a permeability property of concrete where the flow of water under a pressure differential is measured. It is a function of the pressure gradient, capillary size and their interconnectivities and the hydrate structure of cement paste. The microstructure of paste depends on the w/c ratio and the cement type. Type of aggregate also affects the permeation of concrete.

Permeation can be described by the Darcy's law for laminar flow through a porous medium such as a concrete structure where the rate of flow of water over a cross sectional area is equal to the 'coefficient of permeability' of the concrete for a given hydraulic pressure difference over the thickness of the concrete structure (Concrete Society, 1988).

The water permeation test was conducted as per BSEN 12390:2009 - Part 8 where the concrete cubes were subjected to water pressure at 5 bar for 72 hours. The depth of water penetration was measured after splitting the cube into two halves along the same axis to the water penetration. Visible water profile could be measured using a measuring scale.

The age of the concrete cubes subjected to the water penetration tests was 28 days. The cubes were fitted in the triangular metal frame with rubber gasket as shown in Figure 3.7 where the water pressure was applied by the compressed air generating pump controlled by pressure valves. The concrete face of the applied pressure should not be the trowel face. A 500±50 kPa (5 bar) water pressure was applied for 72 hours by making sure that there was no drop in the pressure and no leaking of water through the interface of concrete and the rubber gasket.

Figure 3.7 : Equipment of water permeation test according to BS EN 12390: Part 8

At the end of 72 hours, the concrete specimen was removed from the metal frame, wiped off the excess water and spilt into two halves along the perpendicular direction of the applied water pressure. The visible water penetration profile along the spilt face of the cube was marked and the depth of the water penetration from the applied face was measured to its nearest millimeter. For each type of concrete three cubes were tested and the result of the average of three was considered as the water penetration results of that particular type of concrete.

Water absorption test:

Water absorption is a process by which concrete takes in water by capillary action. It is the function of the moisture gradient, capillary pore size, inter-connectivity of concrete pores and the microstructure of the hydrates. The moisture gradient can be influenced by the environmental factors such as cyclic wetting and drying of the marine structures in the tidal zone, but the capillary size, the pore connectivity and the hydrate micro-structure would be influenced by the aggregate type, water/cement ratio and cement type of concrete. Another factor which would affect the water absorption is the pore fluid content which is depended on the degree of saturation of the concrete structure (Concrete Society, 1988).

Water absorption of concrete was measured according to BS 1881: Part 122 test method, where the concrete was immersed in water for half an hour and expressed as the percentage of the initial mass of concrete prior to the immersion.

Samples of 75mm diameter core were taken from the full depth of 150 mm cube specimen of 28 days age. The height of the core was then trimmed to 75mm by sawing 37.5mm from the two ends. The specimen were then dried in an oven at 105°C for 72 hours and cooled down for next 24 hours at room temperature. Prior to the immersion in the water, the initial mass of the specimen was measured. The specimens were immersed in the water for 30 minutes with their longitudinal axis kept horizontal. A depth of 25mm water from the top of each specimen was maintained. Immediately after 30 minutes each of the specimen was removed from the water, wiped with a dry towel and mass of the specimen after immersion was measured.

The measured water absorption was calculated by obtaining the increase in mass due to the immersion and expressed as a percentage of the dried initial mass of the specimen. The average of three specimens was taken as the water absorption of that concrete type.

Rapid chloride permeability test:

Rapid chloride permeability test (RCPT) according to ASTM1202-97 is a widely accepted test in the region of Arabian Peninsula to determine the ability of concrete to resist chloride ion permeability. Though the variability and precision and bias between technicians and laboratories of this test is very high, RCPT was chosen as one of the durability test of this work, mainly due to the widely acceptance of this test in this region with established data range.

This is an indirect test, where a 60v dc electric charge was applied for a period of 6 hours to get a total charge passed in terms of coulombs. The charge was passed through a concrete disk test specimen whose two ends were immersed into sodium chloride (3% by mass in distilled water) and sodium hydroxide solutions (0.3N in distilled water) respectively. The total charge passed through the concrete specimen was found to be related to the resistance of the concrete to the chloride ion penetration. Figure 3.8 shows the set of equipment used for RCPT test for this work.

Figure 3.8: RCPT equipment set used for this study

ASTM C1202-97 has provided a guideline of the performance of concrete's chloride ion penetrability based on the total charged passed in coulombs as illustrated in Table 3.18.

Table 3.18: Chloride ion permeability of concrete in terms of coulomb value

Charge passed (coulombs)	Chloride ion permeability
>4000	High
2000 – 4000	Moderate
2000 – 1000	Low
100 – 1000	Very low
<100	Negligible

Principle of RCPT:

The result of RCPT is influenced by the conductivity of the pore solutions, degree of hydration of the paste and the concrete temperature. The principle of RCPT test (ASTM 1202-97) of electric charge passing through the concrete specimen is based on Ohm's law of,

$$V = i\,R$$

$$\text{or, } i = V/R$$

Where,

V = applied voltage (60V)

i = applied charge in ampere

R = resistance of the specimen in Ohm

As the RCPT test measure the total charge passed (ampere) for 6 hours (21,600 sec), the result is calculated as ampere-sec or coulomb.

The applied charge i can also be written as, $i = V\,G$

Where, G is the conductance of the specimen = 1/R, with the unit of Siemens (S)

The conductivity of the specimen, $\sigma_{specimen}$ is equal to the conductance of the specimen (G) for a given length (L) over the cross sectional area (A) of the concrete specimen and is a function of the conductivity of the pore solution of the concrete. Hence, the RCPT value is the function of the conductivity of the pore solutions and the quality and type of hydrate structure of the paste (Bentz, D. P., 2007).

Chloride diffusion test:

Chloride diffusion test as per CEN TC51/WG12/TG5, (Draft 4 Version 2 Date: 20 April 2008) is a more direct test compared to the RCPT and was considered to obtain a chloride profile at different depth of concrete specimen. The concrete specimens were exposed to a 3% NaCl solution for 90 days before dust was collected at different layers of the concrete specimen. This method determines the acid soluble chloride in concrete which is approximately total of free chloride and bound chloride in the concrete.

Preparation of sample:

Concrete specimen subject to the chloride diffusion tests was cored from concrete cubes cured at 20°C for at least 28 days. The dimension of the core was 100mm in diameter and 150mm in depth. The top 10mm of the as cast surface was cutoff and discarded and another 20mm thick layer was sliced off to establish initial chloride content as shown in Figure 3.9. The core samples subject to chloride exposure were completely coated by epoxy except the sawn surface to make sure a unidirectional diffusion of chloride ion through the concrete specimen could happen.

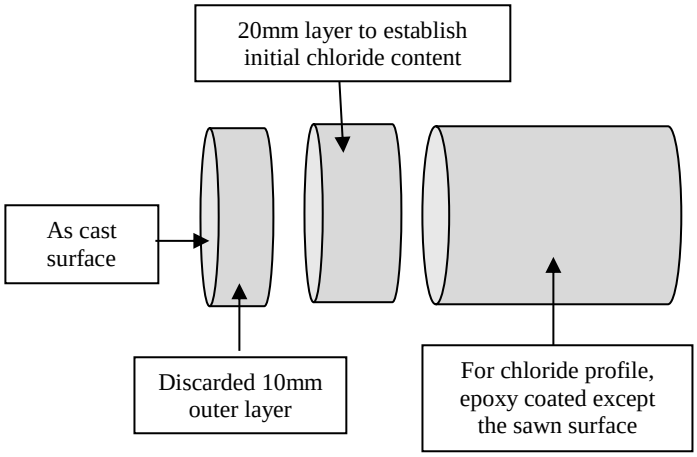

Figure 3.9: Preparation of core specimen for chloride diffusion test

The specimen, duly marked was immersed in a 3.0% NaCl solution for 90 days as shown in Figure 3.10. The 3.0% NaCl solution was prepared by dissolving 50g NaCl salt in distilled water to make a 1000ml solution. This solution had the same concentration of NaCl of sea water.

After 90 days of exposure to the chloride solution samples of concrete powder was collected by grinding off from the exposed surface at 8 equal layers at an average depth of 1 to 2mm distance. This depth was kept equal for all concretes by anticipating very low rate of diffusion due to the use of very high replacement of Portland cement by GGBS and other pozzolanic materials.

Special care was taken to minimize the contaminations while collecting samples at different layers. A drill machine with larger diameter bit was used for first layer and the diameter of bits was subsequently reduced to collect further deeper layers to avoid any contamination from the wall of the hole being drilled. A digital slide calipers was used to measure the thickness of each layer by measuring the total depth of the hole from the surface.

Figure 3.10: Immersion of concrete specimen in 3.0% NaCl solution for 90 days

Chemical analysis to determine the chloride content:

The acid soluble chloride concrete of concrete was determined in accordance with the following procedure of BS EN14629:2007:

A 5.0g of sample was wetted using 50ml of distilled water followed by an addition of 10ml of 5mol/l nitric acid and further addition of 50ml of hot water. The mix was then boiled for 3 minutes followed by cooling it down to the room temperature. The addition of nitric acid dissolved the hydrated cement paste and separated the chloride. A blank solution was then prepared following the above steps except the addition of the concrete powder sample.

A measured volume of (4ml) of silver nitrate was then added to the solution to precipitate the chloride as silver chloride. To coagulate the precipitation, 2-3ml of trimethylhexanol was added to the solution and was shaken it vigorously.

To determine the volume of additional silver nitrate which did not react with the chloride, the solution was titrated by adding 5 drops of iron III indicator solution and ammonium thiocyanate drop by drop until the faint reddish brown coloration did not disappear. The volume of the ammonium thiocyanate was recorded as $V1$.

The same titration procedure was followed for blank solution to get the total volume of ammonium thiocyanate $V2$ required to consume the entire silver nitrate. The difference of this two volume gave the volume of the chloride.

The following formula has given the chloride content as percent of chloride ion by mass of sample of concrete:

Chloride content = $3.545 \times f \times (V2 - V1)/m$

Where, f = molarity of silver nitrate solution, 0.1

m= Mass of concrete powder

Chloride content of the concrete sample not exposed to chloride solution was also determined using the above procedure. Chloride diffusion test was conducted on all concrete type with 0.32 w/c ratio.

Determination of the chloride diffusion coefficient:

The non-steady state chloride diffusion coefficient together with the chloride content at the surface can be obtained by fitting the following equations by measured chloride content at different depth as above procedure by means of a non-linear regression analysis using *Solver* data analysis pack of MS Excel. Annex Z shows a typical calculation of 2P30S70W concrete.

$$C_x = C_i + (C_S - C_i)\left(1 - erf\left[\frac{x}{2\sqrt{D_{nss}.t}}\right]\right)$$

Where,

C_x = Chloride content measured at average depth x, % by mass of concrete

C_i = Initial chloride content, % by mass of concrete

C_s = Surface chloride content, % by mass of concrete

x = Depth of the specimen, mm

D_{nss} = The apparent chloride diffusion coefficient, m^2/s

t = Time, second

erf = The error function

Sulfate resistance test:

The sulfate resistance of the concrete was measured by a direct test of length change of concrete prism immersed in Na_2SO_4 solution for at 12 months period. The test procedure is a modified method of ASTM C 1012 – 02, where 75mm x 75mm x 280mm size concrete prism was used instead of mortar bar. The test method was modified to make it a more direct measurement of the performance of concrete instead of mortar being extracted out of the concrete. The test was applied on cement type, sand type and RCA series concrete.

Concrete prisms as illustrated in Figure 3.11 was cast in 75x75x280 mm moulds and cured in water at 20°C temperature for 28 days. Prior to placing in Na_2SO_4 solution for the test, the initial measurement of the longitudinal length (Li) of the cured sample was taken using a digital slide calipers. The measurement was taken from stud to stud which were embedded at the two end faces of the prism. An average of three measurements was considered as the initial length of the specimen.

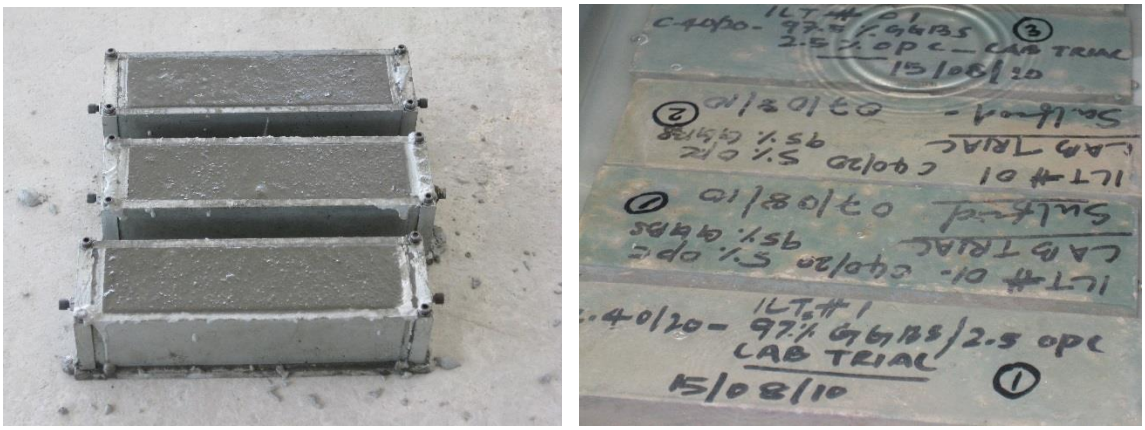

Figure 3.11: Concrete specimen for sulfate resistance test (immersed in Sodium sulfate solution)

A 352 moles of Na_2SO_4 solution per m^3 was prepared by diluting 50g of laboratory grade Na_2SO_4 powder into 900ml of distilled water. Once the powder was totally dissolved, additional distilled water was topped up to make the total volume of the solution to 1 litre. The concrete specimen was submerged in Na_2SO_4 solution bath in an air tight plastic container to minimize the moisture loss from the solution due to evaporation. The temperature and the pH of the solution was kept at 23±2 °C and 6-8 respectively throughout the testing period.

The measure of length change was made at short term at 1, 2, 3, 4, 8, 13 and 15 weeks of the ponding in sulfate solution. A long term measure was also been made at 4, 6, 9 and 12 months after the immersion.

The change of length was measured as a % of initial length and expressed as follows:

$$\Delta L = \frac{Lx - Li}{Li} \times 100$$

Where, $\Delta L =$ Length change in % of the initial length

$Lx =$ Length of the specimen at a specific time

$Li =$ Initial length of the specimen prior to the immersion

Durability test acceptance limit:

The acceptance limit of the durability properties of concrete tested by different durability tests described above are considered to be as per Table 3.19. These acceptance limits have been considered based on the literature review of the local acceptance limits of similar tests in the Arabian Peninsula as described in Chapter 2.

Table 3.19: Acceptance limit of durability and permeation properties of concrete

	Durability tests	**Standard**	**Year**	**Acceptance limit**	**Unit**	**Precision**
1	Water permeation test	BSEN 12390: Part 8	2009	10	mm	Not available
2	Water absorption test	BS 1881: Part 122	1983	2.0	%	Not available
3	Rapid chloride permeability test	ASTM C1202-97	1997	1500	coulomb	42% max
4	Chloride diffusion test	CEN TC51/WG12/TG5, (Draft 4 Version 2)	2008	5×10^{-12}	m^2/s	Not available
5	Sulfate resistance test	ASTM C 1012 – 02 (Modified)	2002	None	%	Varies depending on cement type

3.4 Analysis of hydration products

In order to understand the development of microstructure and the hydration products of the different combinations of cementitious materials, cement pastes made with these materials were analysed using techniques like thermogravimetry (TG) analysis and scanning electron microscopy (SEM). Beside the analysis of hydration products, mercury intrusion porosimetry (MIP) technique was used to analysis the effect of the excess finer particles of the unwashed fine aggregates on the void filling properties to change the microstructure of porosity of cement paste.

3.4.1 Preparation of sample for TGA and SEM

The analysis of hydration using TGA and SEM techniques was conducted on the same set of prepared sample. A brief discussion of the sample preparation for these two tests is given below. Total seven sets of cement pastes using 0.32 w/c ratio were prepared with the different combination of Portland cement and SCMs as shown in Table 3.20. The Portland cement used in these tests are sourced from UK and termed as UKPC. All other cementitious materials are from the same source as mentioned in Table 3.1.

Table 3.20: Proportion of cementitious combination in the paste for TGA and SEM tests

	Reference	% of total cementitious materials				
		Portland cement	GGBS	Fly ash	Microsilica	Rice husk ash
1	UKPC	100	-	-	-	-
2	P30S70	30	70	-	-	-
3	P15S85	15	85	-	-	-
4	P20F80	20	-	80	-	-
5	P90M10	90	-	-	10	-
6	P80R20	80	-	-	-	20
7	P15S70R15	15	70	-	-	15

The following laboratory procedure was employed to obtain the powder sample for TG and fragmental sample for SEM testing. Each sample was tested for 1, 7, 56 and 365 days for TGA. However, for SEM 1day sample was not considered.

3.4.1.1 Preparation of paste

a. The paste was prepared using total 100g of cementitious materials of each cement combination as shown in Table 3.20. 32g of distilled water was used to obtain the 0.32 w/c ratio. A superplasticizer with fixed dosage of 0.9g was added on every paste.

b. Mixing

   i. The measured water and admixture was carefully added to the cement powder contained in zipped plastic pouch. The powder and water was mixed in a uniform manner by holding the plastic bag by both hand and squeezing it by thumbs and fingers.

   ii. Upon satisfactory mixing, the paste was tapped by gently dropping the bag on the working table while holding the top two corners of the bag. This was done for 10 times. This helped to consolidate the paste at the bottom of the plastic bag. At the end of this process, the bag was zipped after squeezing out the air and rolls the paste to wrap it with the excess portion of the bag.

c. The paste was cured in air in a controlled humidity room. After hardening, it formed like a hardened flat bar of cement paste.

3.4.1.2 Preparation of sample for TG

a. To arrest the hydration, small fragments of the hardened paste was broken off the paste bar using chisel and hammer at the appropriate test age. A thoroughly cleaned mortar and pestle was used to grind the hardened paste into fine powder. The powder was made finer than 125μm using a 125μm sieve.

b. The powder was transferred from the sieve to a thoroughly cleaned metal container. Sufficient amount of acetone was added to the dry powder such that it was totally immersed with the acetone.

c. The acetone was removed after 1 hour of immersion, using a vacuum fitted filtering process and the filtered powder sample was dried off using oven. The dried sample was kept in a properly labeled air-tight glass bottle.

3.4.1.3 Preparation of sample for SEM

a. For SEM a 5-10mm long fragment of sample from the hardened paste was removed using chisel and hammer, making sure of obtaining broken face with flat surface for appropriate projection of electron beam on the surface.

b. The fragment sample was then placed in acetone bath for at least one hour prior to placing in oven at 65˚C for 1 hour for drying.

c. The sample was then kept in a properly labeled airtight glass bottles for further preparation to mount on the metal disk and to be vacuumed as described in section 3.4.3.

3.4.2 Thermogravimetry Analysis

Thermogravimetry or TG analysis was adopted to understand the development of hydration product of different cement combination. TGA is a technique where the mass loss of a compound can be measured while heating up the material at a constant rate of incremental temperature in a controlled environment. In this study a SETARAM 92 TG machine as shown in Figure 3.12 was used where nitrogen was used as a carrier gas to provide a controlled environment.

A 75µl Al_2O_3 crucible was used to contain a pre weighed (15mg-20mg) powdered sample. The crucible was hanging by a balance to insert into the furnace chamber. The furnace temperature was increased at a rate of 10°C per minute for maximum 900°C - 1,000°C. As the temperature increased, the mass of sample reduced due to the decomposition of different compound at different temperature range. From cement thermal analysis database obtained from published literatures, different type of hydration products could be identified based on the temperature they had decomposed.

Crucible containing sample powder is hanging by the balance prior to entering into the furnace chamber

Figure 3.12: Thermogravimetry analyser – TGA 92

In this study three graphs were obtained i) a TG graph with total loss of mass expressed in mg, ii) a dTG graph indicating the individual decomposition of compounds expressed either as %/min of mass or mg/min and iii) a Heat flow graph as mW. A Heat flow in TG is a phenomena when the thermal difference between the crucible with sample and the empty crucible (which was placed at the balance together with the crucible with sample) changes. The temperature of the crucible with sample changes when the state of the compounds changes from solid to gas. Heat flow gives an indication of changes of mass and could be used to verify with dTG to confirm the mass loss.

3.4.3 Scanning Electron Microscopy

In scanning electron microscopy (SEM) an electron beam with very high kinetic energy is accelerated onto a solid sample to produce verities of signals. These signals can be captured and analysed to produce information about the sample such as i) surface morphology ii) chemical composition iii) crystalline structure and iv) orientation of materials. Study of the surface morphology is the interest of this study which allows us to understand the development of hydration of different cement combination at different age.

The surface morphology and topography or SEM 'image' can be obtained as two-dimensional pictures by capturing the secondary electron. When electron accelerated onto a material, it results a number of interaction with the atom of the materials. Production of secondary electron is one of these interactive results. A JEOL JSM 6480LV Scanning Electron Microscopy machine as shown in Figure 3.13 was used in this study.

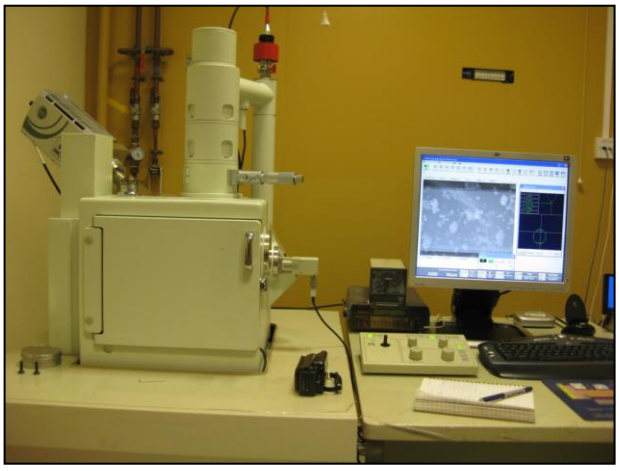

Figure 3.13: Scanning Electron Microscope - JEOL JSM 6480LV

The main component of an SEM instrument to produce electron and capture the signals are i) electron source or gun ii) electron lenses iii) sample stage iv) detectors for all signals of interest and v) display / data output devices.

3.4.3.1 Sample preparation for SEM imaging

1. For SEM imaging a small (approximately 10 mm long) fragment of hardened paste with relatively flat surface need to mount on the sample holder. The sample holder was eventually placed on the sample stage of the SEM machine.
2. To improve the electric conductivity the sample was placed on sticky carbon tape as shown in Figure 3.14a. Silver paint was used to connect the sample with the metal disk the sample was mounted on.
3. SEM is not capable to analyse wet samples as the projection of electron has to be in vacuum state, all samples prepared for SEM must go through outgassing by placing the sample assembly overnight in a high vacuum system. Edward Coating System E306A equipment was used to outgas the samples as shown in Figure 3.14b.
4. As the hardened cement pastes are electrically insulated materials, a thin layer of gold coating was required to enhance the production of secondary electron by providing a conductive coat over the sample assembly. Edward Sputter Coater S150B equipment was used for this purpose as shown in Figure 3.14c.

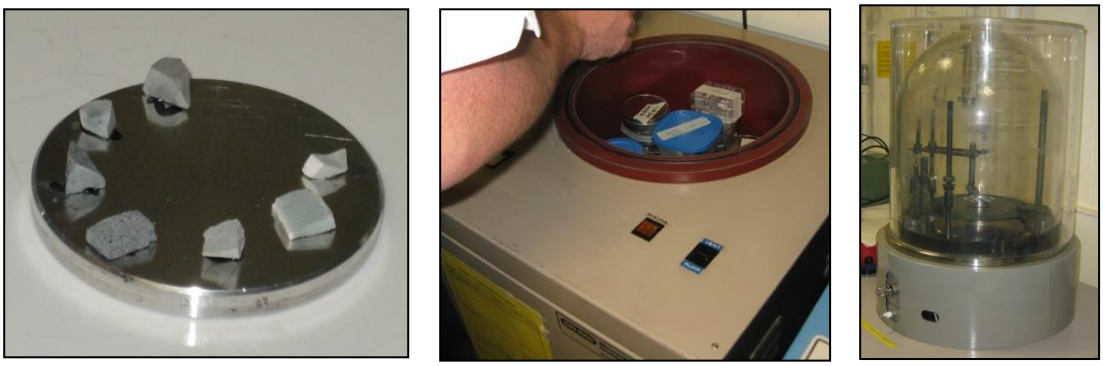

a) Paste fragments b) Vacuum chamber c) Gold coating

Figure 3.14: Sample preparation for SEM imaging

3.4.4 Mercury Intrusion Porosimetry

3.4.4.1 Introduction

Mercury intrusion porosimetry is one of the most common methods to characterize pore structures of the cement paste of concrete and other porous materials. The principle of this test is based on the following Washburn's equation where, ΔP is the pressure required to cause mercury intrusion, r is the radius of the pore (assumed as cylindrical), $\boldsymbol{\sigma_{l/v}}$ is the surface tension of mercury and θ is the contact angle between mercury and pore wall.

$$\Delta \boldsymbol{P} = \frac{-\boldsymbol{2} \times \boldsymbol{\sigma_{l/v}} \times \boldsymbol{cos\theta}}{\boldsymbol{r}}$$

Mercury need to force into the pores of the concrete through a stringently controlled pressure as it does not wet concrete and would not penetrate into the concrete pores through capillary actions. As the Washburn equation suggests, the pressure required to penetrate mercury into the pores are inversely proportional to the size of the pores (Beaudoin., J.J. and Marchand., J. 2001).

Through mercury intrusion porosimetry the characteristics of concrete pore structures such as pore size distributions, total pore volume, total pore surface area, median / average pore diameter, and bulk / skeletal densities can be analysed.

3.4.4.2 Sample preparation

In this study the mercury intrusion porosimetry techniques have been applied to understand the effect of the finer particles of the unwashed sand on the pore structure of hardened cement paste. It has been anticipated that concrete with unwashed sand would have higher compressive strength and enhanced durability parameter due to enhanced microstructure by the void filling of the finer particles of unwashed sand. The pore structure of the hardened cement pastes by different cementitious combinations can also be analysed by MIP techniques. To achieve these objectives mortars of following three cementitious combinations were made together with washed and unwashed sand:

i) 30% Portland cement and 70% GGBS
ii) 20% Portland cement and 80% fly ash
iii) 15% Portland cement, 70% GGBS and 15% rice husk ash

The proportion of the ingredients of mortars is given in Table 3.21. Each mortar was made with 0.32 w/c ratio and cast into 40mm cubes. They were cured in immersed water for 28 days and subsequently air cured for 365 days prior to prepare the sample for MIP testing.

Table 3.21: Proportion of mortars for MIP tests

Reference	Sand type	Total cementitious gm	Portland cement gm	GGBS gm	Fly ash gm	Rice husk ash gm	Sand gm	Water gm
P30S70U	Unwashed	450	135	315	-	-	1350	144
P30S70W	Washed	450	135	315	-	-	1350	144
P20F80U	Unwashed	450	90	-	360	-	1350	144
P20F80W	Washed	450	90	-	360	-	1350	144
P15S70R15U	Unwashed	450	67.5	315	-	67.5	1350	144
P15S70R15W	Washed	450	67.5	315	-	67.5	1350	144

The mortar cubes were broken into small pieces of approximately 10mm in size so that it can be easily placed into the sample cup or bulb of the penetrometer. To get true porosity of internal structure and avoid any side effect of the cube walls, the outer surface of the cube was avoided from the broken pieces. The prepared samples were than kept in oven at 60°C for at least 24 hours to remove absorbed moisture. The dried sample was then kept into duly marked small air-tight bottles as shown in Figure 3.15.

Figure 3.15: Prepared sample for MIP testing

3.4.4.3 Testing process

To conduct the MIP testing a Micromeritics Autopore III equipment was used. In this equipment there are 4 ports for low pressure analysis and 2 ports for high pressure analysis allowing consecutive testing of multiple samples as shown in Figure 3.16. The equipment is connected to a set of computer to analyze the data by WIN9400 Vol.2.0 software.

The mortar samples were housed in the bulb of a penetrometer which was mounted on top a glass capillary stem. The volume of the penetrometer bulb used for this work was 5cc and the volume of the stem was 0.392cc.

At low pressure analysis the samples are subjected to vacuum pressure (50µmHg) to evacuate any adsorbed moisture from the pore walls prior to the application of low pressure. After the evacuation, the stem and the sample were flooded by mercury at low pressure to determine the upper limit of the pore size, which was normally 1 mm.

After the initial filling by mercury, the supply of mercury was separated and the pressure was progressively raised to force the mercury to penetrate into the pores. At high pressure port, the mercury intrusion pressure went up to 60,000 psia. The rate of pressure build up was progressive with an equilibrium time of 10sec for each progression to allow the mercury to penetrate into the porous network of the microstructure of mortar.

Figure 3.16: Micromeritics Autopore III porosimeter

As per Washburn's equation at a certain pressure, mercury would enter into a given diameter of the pores as the size of the pore is related to the intruded pressure and the volume of the pores is the volume of the intruded mercury (Beaudoin., J.J. and Marchand., J. 2001).

Obtained data was transferred to Microsoft excel to plot pore size distribution for cumulative and incremental pore volumes expressed in ml/g of sample. Information of the porosity, total pore volume, total pore area and median and average diameter of pores were obtained and analysed to demonstrate the effect of excess finer particles in the unwashed sand and the pore microstructure of pastes containing different cementitious combinations. Appropriate precautions were needed to handle and disposal of mercury and related contaminated wastes.

3.5 Conclusion

A comprehensive and methodical work programme has been designed to explore the effect of different combinations of alternative cementitious materials and concrete constituents on the plastic and hardened properties of concrete. Total work was divided into three segments i) characterization of constituent materials ii) concrete test programme and iii) analytical works.

The physical and chemical properties of cementitious materials, aggregates, water and admixture have been described. Beside Portland cement, other cementitious materials used are GGBS, fly ash, microsilica and rice husk ash. There are total 7 types of coarse and fine aggregates were used including 20mm and 10mm natural crushed limestone and RCA coarse aggregate. Among 5mm fine aggregates, there were washed and unwashed sand of crushed limestone depending on the fine content passing 75 µm sieve. Dune sand was also used with all concrete.

A PCE based superplasticizer was used to achieve required initial slump of 200mm. Appropriate dosage of a retarding admixture was used to retain the consistency up to 150mm at 90 minutes. An AEA was used to increase the entrained air content for Air entrained concrete series.

To understand the effect of different type of cement and aggregates and other factors like higher curing temperature and air content on the properties of concrete, the total concrete programme was divided into five series namely i) cement type ii) sand type iii) RCA iv) Air entrained concrete and v) Higher curing temperature. Each series was consist of different sets of concrete with varied proportion of cementitious combinations, washed or unwashed sand, RCA proportion, and different volume of air content.

Each sets of concrete were made at three w/c ratio of 0.25, 0.32 and 0.40. Total 88 concrete mixes were prepared in this work and tested for plastic properties such as slump, air content, densities and hardened & durability properties. Compressive strength of each set of concrete was tested as an average of three cube specimen at 7, 28 and 56 days age. Permeation and durability tests such as water permeation, water absorption and RCPT were conducted on each set of concrete. The chloride diffusion and sulfate resistance test were conducted on selected sets of concrete groups.

A set of analytical tests comprising TGA, SEM and MIP were conducted on cement pastes and mortars to understand the microstructure of cement paste and pore structure of hydration products. The process and principles of these tests have been discussed in this chapter.

Chapter 4

Plastic Properties & Compressive Strength of Concrete

4.1 Introduction

In this chapter the results of the plastic properties and compressive strengths of concrete are presented and discussed. Measurement of concrete consistence in terms of slump, slump retention, concrete temperature, plastic density and air content are among the plastic properties of concrete which were tested. The measured hardened properties are the compressive strengths and durability and permeation properties of concrete. The durability and permeation properties are separately discussed in the Chapter 5. The test methods according to their corresponding international standards used to measure the hardened properties of concrete including compressive strength, durability and permeation properties are tabulated in Table 4.1.

Table 4.1: Type of tests and associated standards of hardened properties of concrete

	Test types	Standards
1	Compressive strength	BS EN 12390-3:2009
2	Rapid chloride permeability	ASTM C1202:97
3	Water absorption	BS 1881: Part 122
4	Water penetration	BS EN 12390: Part 8
5	Chloride diffusion	CEN TC51/WG12/TG5, (Draft 4 Version 2 Date: 20 April 2008)
6	Sulfate resistance tests	ASTM C 1012 – 02 (modified -75mm x 75mm x 280mm size concrete prism has been used instead of mortar bar)

4.2 Plastic properties of concrete

4.2.1 General descriptions of tests

4.2.1.1 Slump and slump retention

The results of the plastic properties of concrete including slump, slump retention, unit weight and air content are presented in Table 4.2 – 4.9. These tables also provide the state of the rheology of different type of concretes in terms of harshness, stickiness and presence of bleed water.

All concretes were designed to have an initial slump between 200-250 mm in order to retain the slump between 150 – 200 mm after 90 minutes period. This is a reasonable time for concrete to be produced, transported and placed by pumps on site with maximum 50km distance from the batching plants. Beside initial and final slump, slump at 30 and 60 minutes intervals were measured to understand the slump retention behaviour of each type of concrete.

In order to achieve this level of consistency and slump retention a polycarboxylate based superplasticizer (Chryso Fluid Optima 245EMX, conforming ASTM C494 Type E & F) and a retarding admixture (Admix CR152 conforming ASTM C949 Type B & BS EN 934 Part 2) were used. The dosage of the superplasticizer and the retarding admixture was varied depending on the water demand and chemical and physical composition of each type of cement and aggregate combinations.

4.2.1.2 Unit weight

The unit weight was measured to ensure that the concrete was designed and produced to its yield. The percentage difference between the designed and actual unit weight was controlled to ±2.5% of the designed unit weight. On average the unit weight of all plastic concretes were at the higher end due to relatively higher specific gravity of limestone aggregates used in this work (Table 3.4, Chapter 3).

4.2.1.3 Air content

The designed entrapped air content was considered to be 2% of concrete volume except the concretes from Air entrainment series. A 2% air or even lower is an acceptable value in practice in the Arabian peninsula where higher air content is not required as there is no requirement of durability related to freeze and thaw conditions (ADNOC, n.d.). The target air contents for Air entrained concrete series were 2, 5, 10 and 15 percent of the total volume of concrete. To achieve this level of air volume, an air entrainment admixture (Micro-Air 100 conforming to ASTM C260-86 & BS 5075:1982 Part 2) was used at appropriate dosage rates.

4.2.1.4 Visual appearance

Visual appearance of freshly mixed concretes was observed and their subsequent changes, if any, was monitored. Visual appearance of fresh concrete can be defined as the characteristics appearance of concrete at its plastic stage to demonstrate its physical behaviour. These appearances were noted down to compare between the mixes to figure out whether there were any significant changes in behaviour of plastic properties in terms of bleeding, segregation, harshness, stickiness or cohesiveness of the plastic concrete. The appearance and any other abnormal behaviour of concrete was also noted and reported.

Harshness is the visual appearance of concrete where lack of paste coating the coarse aggregates are obvious resulting into lower in consistency. Stickiness can be defined when concrete behave more thixotropic due to lack of free water due to higher specific surface area of cementitious materials mainly contributed by microsilica or rice husk ash.

4.2.2 Cement type series

As the consistency of concretes was controlled by the superplasticizer, the dosage of superplasticizer was directly affected by the w/c ratio of each concrete mix. In Cement type series the dosage of superplasticizer for 0.25 w/c ratio GGBS concrete ranged from 7 to 8 kg/m^3 (1.75 to 2.0% of total cementitious content) to give an initial slump of 220 to 250mm and a final slump of 145 - 200mm at 90 minutes. However, 1.0 kg/m^3 of retarding admixture was needed to keep the slump retention within the acceptable range.

The dosage requirement of superplasticizer for 0.32 and 0.40 w/c ratio GGBS concretes was much lower at 1.7 to 5.0 kg/m^3 (0.425 to 1.25%) with higher dosage for 0.32 w/c ratio with higher proportion of GGBS content due to higher specific surface area of GGBS particles. The slump and slump retention over 90 minute time was well acceptable.

Slump range for fly ash, microsilica and rice husk ash concretes were also within the acceptable range which was controlled by varied dosage rate of the combination of superplasticizer and retarder. The dosage of superplasticizer was dependent on the factors like w/c ratio, specific surface area and morphology of cementitious materials. This has been discussed further in Chapter 3. The unit weight and air content of all concretes at their plastic stage were within the acceptable range as shown in Table 4.2.

Table 4.2: Plastic properties of concrete of Cement type series

No	Reference	w/c	Admixture dosage, kg/m^3		Slump, mm				Unit weight	Air	Rheology / Observation
			Superplasticizer	Retarder	T_0	T_{30}	T_{60}	T_{90}	kg/m^3	%	
1	1P30S70W	0.25	7.0	1.0	250	250	220	200	2525	1.9	No bleeding, slightly harsh, not workable
2	2P30S70W	0.32	2.3	1.0	235	225	185	160	2470	1.7	Initial slight bleeding
3	3P30S70W	0.40	2.2	0.9	235	215	200	170	2448	1.1	Initial slight bleeding
4	1P0S100W	0.25	8.0	1.0	240	220	200	150	2502	2.1	Initial slight bleeding, sticky, slightly higher air
5	1P2.5S97.5W	0.25	8.0	1.0	250	240	190	150	2498	1.3	Initial slight bleeding, sticky
6	1P5S95W	0.25	7.5	1.0	230	220	190	145	2510	2.2	Initial slight bleeding, sticky, final slump is low, slightly higher air
7	1P15S85W	0.25	7.5	1.0	220	210	210	190	2541	1.8	Initial bleeding, workable
8	2P0S100W	0.32	5.0	1.0	240	230	220	180	2456	2.5	Initial slight bleeding, sticky, higher air content
9	2P2.5S97.5W	0.32	3.5	1.0	250	240	190	140	2498	1.3	Initial slight bleeding, sticky, lower final slump
10	2P5S95W	0.32	2.0	0.0	250	240	190	160	2480	0.8	Initial slight bleeding, sticky and harsh
11	2P15S85W	0.32	2.5	1.0	220	200	180	150	2510	2.0	Initial bleeding, workable
12	3P0S100W	0.40	2.5	1.0	240	235	200	180	2467	1.4	Initial bleeding, workable
13	3P2.5S97.5W	0.40	2.5	0	240	220	200	160	2448	1.4	Initial bleeding, workable
14	3P5S95W	0.40	2.0	0	240	220	190	155	2449	0.8	Initial bleeding, workable
15	3P15S85W	0.40	1.7	1.0	235	220	180	150	2450	1.7	Initial bleeding, workable
16	1P20F80W	0.25	1.6	1.0	240	240	230	220	2495	1.8	Initial bleeding, workable
17	2P20F80W	0.32	1.6	0.5	230	210	180	150	2445	1.3	Workable
18	3P20F80W	0.40	1.2	0.5	230	220	200	180	2387	1.1	Workable
19	1P90M10W	0.25	7.0	1.0	200	190	160	140	2593	1.1	Workable, lower final slump
20	2P90M10W	0.32	6.5	1.0	210	190	175	145	2543	1.2	Workable, lower final slump
21	3P90M10W	0.40	5.0	1.0	220	210	180	150	2484	1.0	Workable
22	1P80R20W	0.25	17.5	1.0	240	220	200	150	2600	1.9	Lack of paste but workable
23	2P80R20W	0.32	9.5	1.0	240	220	210	155	2542	1.6	Harsh but workable
24	3P80R20W	0.40	4.0	0.5	220	215	170	140	2479	1.8	Workable, lower final slump

It was observed that most of the concrete with high GGBS replacement were too sticky, especially with 0.25 w/c ratio due to relatively higher water demand of GGBS. Most of the GGBS concrete showed initial signs of bleeding, but it receded within 30 minutes without creating any major concern.

Fly ash concretes were the most workable mixes due to comparatively lower water demand and spherical morphology of fly ash particles. Very high water demand of rice husk ash concrete due to the porous and irregular morphology and very high specific surface area of rice husk ash particles removed the available water from the paste, making it 'harsh' looking with lesser paste volume. However all three rice husk ash concretes would have been reasonably workable and pumpable.

4.2.3 Sand type series

The initial slump of concretes in the Sand type series was moderate ranging from 200 to 240 mm suggesting higher water demand due to higher finer particles in the sand. Nevertheless the overall slump retention and the final slump after 90 minutes were well within the acceptable range including the unit weight and air contents of all concretes.

Similar to the Cement type series, the rheology of GGBS concretes was sticky and harsh with better workability for the fly ash concretes. Both 0.25 w/c ratio concretes of microsilica and rice husk ash were sticky but the 0.32 and 0.40 w/c ratio concretes were acceptable. The plastic properties of the Sand type concretes are presented in Table 4.3.

In the Sand type series the water demand of concrete was expected to be increased due to higher finer particles in the unwashed sand. However for GGBS concrete the results were not conclusive as for 100% GGBS mixes the dosage of superplasticizer was more for concrete with washed sands compared with concrete with unwashed sands (Table 4.4). It must be noted that the initial slumps for concretes with washed sand were higher compared to the concretes with unwashed sand.

Nevertheless the fly ash concretes showed that concretes with unwashed sand had much higher water demand (especially for 0.25 w/c ratio) than the washed counterpart. The higher water demand by unwashed sand for microsilica and rice husk ash was only moderately higher.

Table 4.3: Plastic properties of sand type series

No	Reference	w/c	Slump				Unit weight	Air	Rheology / Observation
			T_0	T_{30}	T_{60}	T_{90}	Kg/m^3	%	
1	1P30S70U	0.25	240	230	210	200	2511	0.9	Initial bleeding, lack of paste
2	2P30S70U	0.32	230	220	210	180	2456	1.1	Initial bleeding, harsh
3	3P30S70U	0.40	220	210	190	150	2460	1.2	Workable
4	1P0S100U	0.25	230	210	200	200	2490	2.2	Bleeding after 35 min, lack of paste, sticky
5	2P0S100U	0.32	220	210	180	150	2493	1.8	Harsh but workable
6	3P0S100U	0.40	220	210	200	190	2463	1.6	Workable
7	1P20F80U	0.25	230	220	210	190	2510	1.9	Initial bleeding, sticky
8	2P20F80U	0.32	220	210	190	160	2445	1.7	Workable
9	3P20F80U	0.40	220	210	200	160	2441	1.6	Workable
10	1P90M10U	0.25	200	180	170	140	2598	1.2	Harsh but workable
11	2P90M10U	0.32	210	200	170	140	2542	1.3	Normal Setting
12	3P90M10U	0.40	205	180	165	130	2506	1.3	Normal Setting
13	1P80R20U	0.25	210	190	170	150	2534	1.6	Lack of paste but workable
14	2P80R20U	0.32	230	220	200	190	2497	1.4	Harsh but workable
15	3P80R20U	0.40	230	220	200	190	2463	1.6	Workable

Table 4.4: Change in water demand due to additional finer particles in the unwashed sand

Reference	Superplasticizer, kg/m^3		% change
	Unwashed	Washed	
1P30S70	9.0	7.0	29%
2P30S70	3.5	2.3	56%
3P30S70	2.0	2.2	-7%
1P0S100	6.5	8.0	-19%
2P0S100	2.5	5.0	-50%
3P0S100	1.7	2.5	-32%
1P20F80	5.0	1.6	213%
2P20F80	2.0	1.6	25%
3P20F80	1.8	1.2	50%
1P90M10	8.5	7.0	21%
2P90M10	7.0	6.5	8%
3P90M10	5.0	5.0	0%
1P80R20	20.0	17.5	14%
2P80R20	10.0	9.5	5%
3P80R20	4.5	4.0	13%

4.2.4 Recycled Concrete Aggregate (RCA) Series

Table 4.5 provides the test results of the plastic properties of the RCA series. In the RCA series 100% GGBS was used to compare the performance of different proportion of RCA content at three different w/c ratios of 0.25, 0.32 and 0.40. The effect of the excess finer particles contributed by the unwashed sand was also tested. No retarding admixture was used in order to observe whether the existing impurities in the RCA had any negative effects on the properties of concrete.

Table 4.5: Plastic properties of concrete of RCA series

No	Reference	RCA	w/c	Slump				Unit weight	Air	Rheology / Observation
				T_0	T_{30}	T_{60}	T_{90}	Kg/m^3	%	
1	1R100N0W	100R	0.25	190	230	220	210	2473	1.4	Initially no bleeding, it starts after 25 min, cohesive, Harsh
2	2R100N0W	100R	0.32	200	220	210	-	2412	1.1	Initial little bleeding, workable, hardening delayed
3	3R100N0W	100R	0.40	200	190	170	-	2383	1.3	Workable, hardening delayed
4	1R80N20W	80R+20N	0.25	180	220	210	200	2492	1.3	Initially no bleeding, it starts after 25 min, cohesive, Harsh, hardening delayed
5	2R80N20W	80R+20N	0.32	190	220	210	-	2472	1.4	Workable, hardening delayed
6	3R80N20W	80R+20N	0.40	210	200	190	-	2407	1.3	Soft, Workable, hardening delayed
7	1R50N50W	50R+50N	0.25	170	220	210	200	2522	1.3	Initially no bleeding, it starts after 35 min, Cohesive, Harsh, hardening delayed
8	2R50N50W	50R+50N	0.32	200	210	190	-	2486	1.4	Workable, hardening delayed
9	3R50N50W	50R+50N	0.40	220	210	200	-	2428	1.1	Soft, Workable, hardening delayed
10	1R100N0U	100R	0.25	190	220	230	210	2438	1.3	No initial bleeding, starts after 35 min, cohesive, harsh, workable, normal hardening
11	2R100N0U	100R	0.32	235	135	-	-	2414	1.3	Initial bleeding, harsh, workable, rapid slump loss
12	3R100N0U	100R	0.40	240	120	-	-	2370	1.2	Initial bleeding, workable, soft, rapid slump loss
13	1R80N20U	80R+20N	0.25	180	200	230	210	2468	1.5	No initial bleeding, starts after 35 min, cohesive, harsh ,workable, normal hardening
14	2R80N20U	80R+20N	0.32	230	220	160	-	2436	1.3	Cohesive, harsh, workable, normal hardening
15	3R80N20U	80R+20N	0.40	230	220	160	-	2372	1.2	Cohesive, harsh, workable, normal hardening
16	1R50N50U	50R+50N	0.25	180	220	220	210	2493	1.2	No initial bleeding, starts after 25 min, cohesive, harsh, workable, normal hardening
17	2R50N50U	50R+50N	0.32	210	200	170	-	2456	1.4	Cohesive, harsh, workable, normal hardening
18	3R50N50U	50R+50N	0.40	210	200	180	-	2398	1.2	Cohesive, harsh, workable, normal hardening

A common behaviour among 0.25 w/c ratio concrete for both washed and unwashed sand can be observed from Table 4.5 where initial slumps were lower than the slump at 30 minutes. This is perhaps due to a slower rate of adsorption of the super plasticizer polycarboxylate ether molecules on the surface of cement particles. This phenomenon seems to be more acute with higher dosage of admixture and low w/c ratio.

The same trend can also be observed for washed sand and 0.32 w/c ratio concretes, however, for concretes with unwashed sand this behaviour did not occur. For all 0.25 w/c ratio concretes (both washed and unwashed sand) the slump retained up to 90 minutes without any significant drop indicating slight overdose of admixture. They behaved also the same way by not having any bleeding at the initial but bleeding started after 30 minutes and eventually disappeared.

In terms of hardening characteristics there was a significant difference observed between washed and unwashed sand concretes. For washed sand, concretes tended to have a delayed hardening in the cube moulds. This could have negative effects on strength gain and durability parameters possibly due to the formation of weak microstructure of the hydrates. The delayed hardening could be due to the presence of impurities in the RCA such as salts, since some salts act as retarders.

There was no such delayed hardening problem for unwashed sand concretes. These contradictory results could be due to the procedural error and contaminations where all RCA were soaked for 16 hours and washed thoroughly to create the saturated surface dry (SSD) condition.

Another significant difference observed between the behaviour of washed and unwashed RCA concretes was rapid slump loss. This occurred only for concretes with unwashed sands and with 0.32 and 0.40 w/c ratio with 100% RCA content. The reason could be the presence of higher finer particles increased the water demand and the dosage of the superplasticizer used was not adequate. This is in conjunction with the observation of relatively faster loss of slump of RCA concrete compared to concrete without RCA.

A common relationship can be seen between proportion of RCA and loss of slump for unwashed sand where the final slumps were lower for concrete with higher RCA content (Table 4.5), except for 0.25 w/c ratio where excessive dosage of admixture obscured this phenomenon. However, for washed sand concretes, this phenomenon was not very obvious. Higher loss of slump due to higher RCA content could be related to higher water absorption of RCA concretes even though all RCA were made in a SSD condition with a prolong soaking in water.

The overall plastic consistency of RCA concretes was harsh, due to the lack of paste in the system as higher water demand from both GGBS and RCA reduced the effective paste volume. Otherwise the concretes were workable except certain cases where rapid loss of slump was experienced. Concretes with 0.40 w/c ratio were more workable and pumpable compared to the concretes with 0.32 and 0.25 w/c ratio due to the presence of higher available water as part of the paste fraction.

The water demand for unwashed sand concretes are relatively higher than concrete with washed sand as shown in Table 4.6 due to the higher surface area contributed by the additional finer particles smaller than 75μm in diameter.

Table 4.6: Change in water demand due to the finer particles in the unwashed sand (RCA series)

Reference	**Superplasticizer, kg/m^3**		**% difference**
	Unwashed	**Washed**	
1R100N0	7.2	6.0	20%
2R100N0	3.0	2.5	20%
3R100N0	2.4	2.0	20%
1R80N20	7.2	7.0	3%
2R80N20	2.5	2.5	0%
3R80N20	2.1	1.8	17%
1R50N50	7.0	6.5	8%
2R50N50	2.0	2.5	-20%
3R50N50	1.7	1.1	55%

4.2.5 RCA Triple blend concrete series

In this series instead of 100% GGBS, a triple blend of Portland cement (15%), GGBS (70%) and rice husk ash (15%) was used to eliminate the unpredictable characteristics related to 100% GGBS concrete. The proportion of RCA content of this series was considered as 100, 50 and 20% of total coarse aggregate by weight. The w/c ratio was varied to 0.25, 0.32 and 0.40 for each type of RCA concrete. Table 4.7 presents the results of the plastic properties of RCA triple blend concretes.

The slump retention in RCA triple blend concrete was maintained by using higher level of superplasticizing and retarding admixtures. The admixture demand for the lower w/c ratio of 0.25 was high due to the presence of rice husk ash. The retarding admixture was introduced to eliminate the rapid slump loss experienced in the previous RCA series.

Table 4.7: The plastic properties of concretes of RCA triple blend series

No	Reference	RCA	w/c	Admixture, kg/m^3		Slump				Unit weight	Air	Rheology / Observation
				Superplast.	Retard.	T_0	T_{30}	T_{60}	T_{90}	Kg/m^3	%	
1	1R100N0TB	100%	0.25	17.1	1.0	220	230	210	180	2482	2.1	Initial bleeding, sticky, lack of paste
2	2R100N0TB	100%	0.32	7.0	1.0	230	225	220	190	2428	2.4	Initial bleeding, harsh but workable
3	3R100N0TB	100%	0.40	3.7	0.5	230	210	160	-	2370	1.6	Initial bleeding and workable
4	1R50N50TB	50%	0.25	17.5	1.0	170	220	210	200	2497	1.6	Initial slight bleeding, sticky and harsh
5	2R50N50TB	50%	0.32	7.0	1.0	235	230	225	180	2475	2.1	Initial bleeding, harsh but workable
6	3R50N50TB	50%	0.40	3.5	1.0	230	230	120	-	2425	1.9	Initial Bleeding and workable
7	1R20N80TB	20%	0.25	18.0	1.0	210	220	200	170	2492	1.4	Initial slight bleeding, sticky and harsh
8	2R20N80TB	20%	0.32	7.8	1.0	230	220	210	190	2448	2.1	Initial slight bleeding, sticky and harsh
9	3R20N80TB	20%	0.40	3.5	1.0	230	225	140	-	2492	1.4	Initial Bleeding and workable

The water demand for both 0.25 and 0.32 w/c ratio concretes for all RCA proportions were very high due to the presence of 15% rice husk ash which has very high water demand as explained in Chapter 3. The phenomena of lower initial slumps compared to slumps at 30 minute could be observed at 0.25 w/c ratio concretes similar to the previous RCA series. Rapid loss of slump at 0.40 w/c ratio shows inadequate dosage of superplasticizing admixtures at 0.40 w/c ratio concretes.

There was no relationship between RCA content and slump retention observed in this series. Initial bleeding was observed for almost all concrete mixes where sticky and harsh mixes were produced for lower w/c ratio concretes due to the lack of available water from the paste fraction. At 0.40 w/c ratio, concretes were more workable and pumpable. The unit weight and air content results were also within the acceptable range.

4.2.6 Air Entrained Concrete Series

In general the air content of concrete, except for the Air entrained concrete series (where the air is nominally entrained including entrapped), was below 2%, which is an acceptable range in the construction industry in Arabian Peninsula. However, the air content for the concretes in the Air entrained concrete series were targeted as 2%, 5%, 10% and 15% by volume of concrete to determine whether concrete with higher air content could provide acceptable level of performance.

Practically it was not possible to achieve the maximum targeted 15% air, which has been explained in Chapter 3. Therefore, the maximum air entrainment was taken as 12%, instead of 15% of the concrete volume. Table 4.8 presents the plastic properties of concrete in the Air entrained concrete series.

In this series 10% microsilica and 90% Portland cement was used by anticipating loss of strength due to higher air content. Concrete for each category of air content was also designed for 0.25, 0.32 and 0.40 w/c ratio to evaluate the effect of w/c ratio on the concretes with different air content.

Table 4.8: Plastic properties of concretes in the Air entrained concrete series

No	Reference	Entrained air, %		AEA		SP	Retard	Slump, mm				Unit weight	Rheology / Observation
		Design	Actual	Kg	%	Kg	kg	T_0	T_{30}	T_{60}	T_{90}	Kg/m^3	
1	1P90M10A2	2	1.1	0.0	0.00	7.0	1.0	200	190	150	110	2547	Workable
2	2P90M10A2	2	1.2	0.0	0.00	6.5	1.0	210	190	140	120	2515	Workable
3	3P90M10A2	2	1.0	0.0	0.00	5.0	1.0	220	210	180	150	2502	Workable
4	1P90M10A5	5	4.8	0.7	0.18	7.5	1.0	180	160	130	-	2468	Bouncy and soft consistency
5	2P90M10A5	5	5.1	0.5	0.13	6.0	1.0	190	160	140	-	2399	Bouncy and soft consistency
6	3P90M10A5	5	5.3	0.4	0.10	3.5	1.0	210	200	160	120	2363	Soft and workable
7	1P90M10A10	10	9.8	1.8	0.45	7.5	1.0	160	150	120	-	2321	Bouncy, soft and foamy
8	2P90M10A10	10	9.5	1.5	0.38	6.0	1.0	210	180	170	140	2284	Bouncy, soft and foamy
9	3P90M10A10	10	9.5	1.2	0.30	3.3	1.0	200	170	160	130	2249	Bouncy, soft and foamy
10	1P90M10A15	15	12.0	4.5	1.13	7.5	1.0	200	160	140	-	2224	Bouncy, very soft and foamy
11	2P90M10A15	15	12.0	4.0	1.00	5.0	1.0	210	180	150	130	2149	Bouncy, soft and foamy
12	3P90M10A15	15	11.8	4.0	1.00	2.1	1.0	190	170	150	140	2134	Bouncy, soft and foamy

As can be seen in Table 4.8, dosage of air entraining admixture (AEA) was affected by the w/c ratio with lower w/c ratio required higher dosage of AEA to achieve similar level of air entrainment. The rheology was also directly affected by the volume of air entrained. Concrete became ‘fluffy’ and ‘foam like’ and was less flowable when the air was increased from 5% to 10% and subsequently to 12% of total concrete volume.

The water demand of concrete with 10% microsilica was higher due to its very high specific surface area especially for concrete with lower w/c ratio of 0.25 and 0.32. However, there was a trend of reduced water demand with increased air content for the w/c ratio of 0.32 and 0.40 as the air bubbles acted as ‘ball-bearing’ at the plastic stage, reducing the water demand for equal level of consistency.

The slump retention was within the acceptable range except for 0.25 w/c ratio with 5% air content and above due to rapid slump loss after 60 minute of mixing of concrete ingredient. Addition of retarding admixture could not stop this slump loss. Concrete without AEA did not have this problem. Therefore, it was considered to be an issue of compatibility between the AEA and the superplasticizer / retarding admixture combinations. Concretes with higher water content (0.40 w/c ratio) did not encounter this problem as well. The unit weight of all concretes of this series was kept within acceptable rang of ±2.5% of the design unit weight.

4.2.7 Higher curing temperature series

In this series two sets of concretes were made using two combinations of cementitious materials of triple blends of Portland cement, GGBS and rice husk ash. The proportions of these triple blends are i) 5% Portland cement, 70% GGBS, 25% rice husk ash and ii) 15% Portland cement, 70% GGBS and 15% rice husk ash. Each set of concrete was also designed for three w/c ratio of 0.25, 0.32 and 0.40.

The main objective of this series was to evaluate the performance of concrete cured at an elevated temperature of 40°C to simulate an average ambient temperature of the Arabian Peninsula. The plastic properties of concrete made of triple blend intend to cure at 40°C have been tabulated in Table 4.9.

Similar to other rice husk ash concrete, the triple blend concrete of this series had very high water demand especially for 0.25 and 0.32 w/c ratio concretes. However, the consistency level in terms of slump and slump retention was within the acceptable range. The unit weight and air contents were also within the acceptable range.

The rheology of 0.25 w/c ratio concretes for both mixes was very sticky and harsh due to the lack of available water in the paste of concrete. This condition improved with increased w/c ratio of the concrete. Initial bleeding was observed in concrete with 0.32 and 0.40 w/c ratio mixes.

Table 4.9: Plastic properties of temperature effects on triple blend series

No	Reference	w/c	Admixtures, kg		Slump, mm				Unit weight	Air	Rheology / Observation
			Superplast	Retard	T_0	T_{30}	T_{60}	T_{90}	Kg/m^3	%	
1	1P5S70R25W	0.25	22.0	0.5	190	200	180	140	2530	2.1	Sticky, lack of paste
2	2P5S70R25W	0.32	10.0	0.5	230	220	210	190	2516	1.5	Initial slight bleeding, harsh but workable
3	3P5S70R25W	0.40	5.0	0.5	230	220	180	150	2465	1.7	Initial slight bleeding, cohesive and workable
4	1P15S70R15W	0.25	18.0	0.5	220	190	170	140	2532	2.2	Sticky, lack of paste
5	2P15S70R15W	0.32	7.5	0.5	220	210	190	150	2502	2.0	Harsh but workable
6	3P15S70R15W	0.40	3.8	0.5	230	210	160	130	2462	1.8	Initial slight bleeding, workable

4.2.8 Summary

Most of the concrete mixes have shown reasonable level of consistency in terms of slump, slump retention, unit weight and air content. Concretes with 0.25 w/c ratio with higher content of GGBS, microsilica or rice husk ash were very sticky and often would have not been pumpable due to the lack of water in the paste fraction. Higher water demand due to higher specific surface area of these cementitious materials is the reason. Concretes with fly ash provided better performance in this regard.

Use of unwashed sand did not adversely affect the water demand, though it was higher compared to concretes using washed sand. This was also observed for both natural aggregate and RCA concretes. RCA concretes with 100% GGBS and lower w/c ratio were often harsh and less workable due to higher water demand. Erratic behaviour or delayed hardening of RCA concretes with washed sand and rapid loss of slump for RCA concrete with unwashed sand could be attributed to the impurities within the RCA and the contamination during the testing procedure. Higher loss of slump with higher RCA content was also other properties to highlight associated with RCA concretes.

Most of the problems associated with RCA concretes were eliminated by using the triple blend of cementitious materials consisting Portland cement, GGBS and rice husk ash. However, very high water demand observed at 0.25 w/c ratio RCA concretes with triple blend of cementitious materials resulted into sticky concretes. This characteristic was also observed with triple blend concrete with normal aggregates.

In the Air entrained concrete series, high volume entrained air in the concretes acted as 'ball bearing' reducing the water demand, though overall water demand was higher due to the presence of 10% microsilica. The optimum dosage of AEA to achieve maximum 12% air was 1.0% by the mass of total cementitious content. However the fresh concrete with higher air content became fluffy and soft which affected their flowing ability.

4.3 Compressive strengths

In this section the results of the compressive strength of concrete tested as per BSEN 12390-3:2009 have been presented and discussed. The compressive strength results of the all type of concretes including the compressive strength of individual cubes and average of three cubes are tabulated in Annex AA to AF.

4.3.1 Cement type series

The effects of different combinations of cementitious materials on the compressive strength of concrete are discussed in this section. Based on the type of cementitious materials the discussions have been presented into two subsections:

i) Concrete only with the combinations of different proportion of GGBS and Portland cement
ii) Concrete with other cementitious materials including GGBS, fly ash, microsilica, and rice husk ash with Portland cement

In the first section the compressive strength of concretes made with different proportions of GGBS including 100%, 97.5%, 95%, 85% and 70% of total cementitious content are discussed. The second section will discuss the compressive strength results of concrete made with GGBS of 100% and 70%, fly ash of 80%, microsilica of 10% and rice husk ash of 20% of total cementitious materials.

All these concretes are made at three w/c ratios of 0.25, 0.32 and 0.40 to demonstrate the effect of w/c ratio on the compressive strengths of different combinations of cementitious materials.

4.3.1.1 Concrete with GGBS

Effect of GGBS content:

The effects of GGBS content on the compressive strength at 7, 28 and 56 days are discussed in the following sections by considering 70% GGBS concrete as the control concrete. The rate of strength reduction due to the increased content of GGBS compared to 70% GGBS of total cementitious materials are examined. The rate of strength loss due to increased w/c ratio for different proportion of GGBS content is also analysed by comparing with the compressive strengths at 0.25 w/c ratio.

In general the compressive strengths of concrete containing high volume GGBS (95% or more) are high which could be due the effect of the superplasticizer used in this study. As the chemical composition of the superplasticizer is the trade secret of the manufacturer of the admixture, it is not possible to conclude whether there is any active constituent material in the admixture is responsible for such higher strength, especially at 7 days age of concretes.

At the age of 7 day:

As the curves in Figure 4.1 are demonstrating decreased compressive strength at the age of 7 day with increased GGBS content, Figure 4.2 explains further the relationship between the strength reduction and the content of GGBS comparing with concrete with 70% GGBS content.

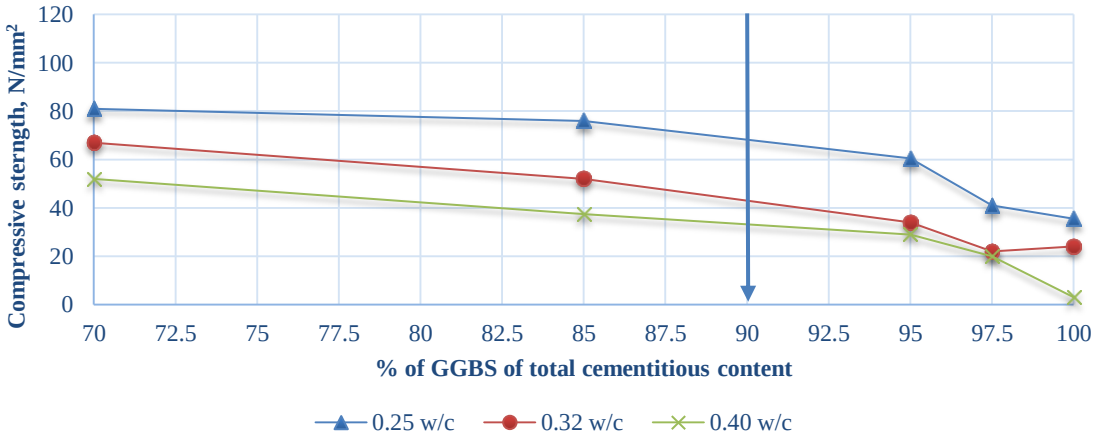

Figure 4.1: Effect of GGBS content on the development of compressive strength at 7 day age

The line graphs (Figure 4.2) at primary axis suggest that concretes with 0.25 w/c ratio had the least reduction in strength comparing with 0.32 and 0.40 w/c ratio concretes. The performance of 0.32 and 0.40 w/c ratio concretes are similar. For example concrete with 85% GGBS content and 0.25 w/c ratio can expect to have a 6% reduction in strength comparing with 70% GGBS and 0.25 w/c ratio.

However, this reduction rate went up to 22% and 28% for the same concrete with 0.32 and 0.40 w/c ratio respectively. Therefore, to produce concrete with lower eCO_2 using higher GGBS would require to reduce the w/c ratio to compensate the strength loss.

The secondary axis of Figure 4.2 (column graph) also illustrates the percentage reduction of strength due to increased w/c ratio with respect to 0.25 w/c ratio. For example concrete with 70% GGBS has reduced 17% of its compressive strength due to increased w/c ratio from 0.25 to 0.32. This reduction was more than double to 36% at 0.40 w/c ratio. The results of concretes with 100% GGBS at 0.32 and 0.40 w/c ratio appeared to be not proportionate comparing to the 97.5% GGBS concretes.

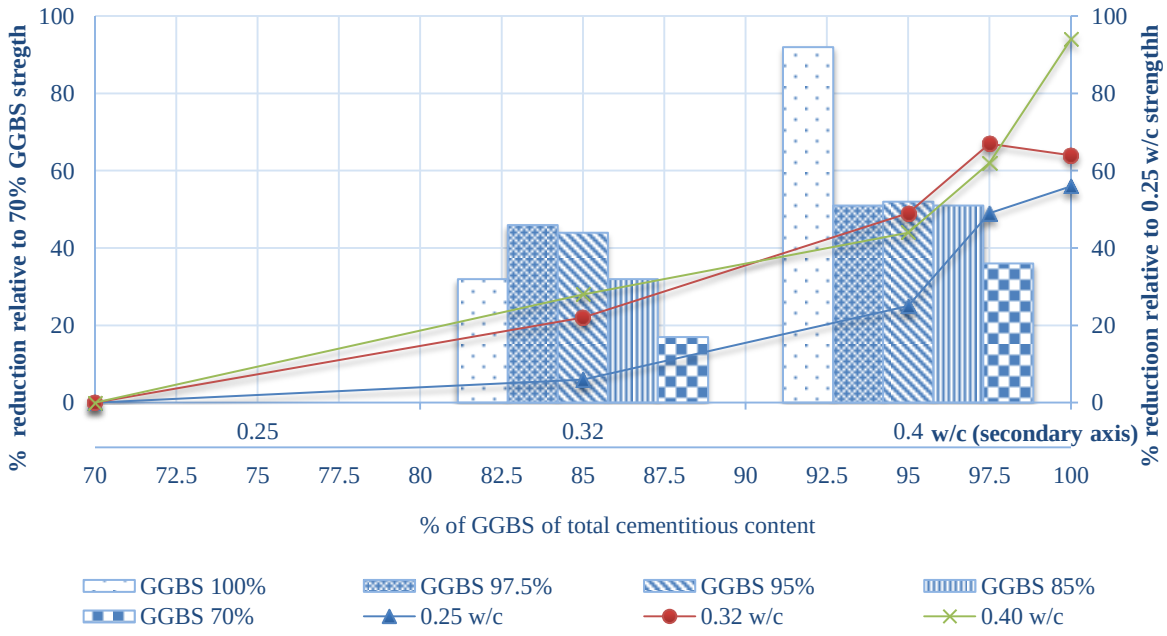

Figure 4.2: Percentage reduction of compressive strength at 7 day due to i) increased proportion of GGBS comparing with 70% GGBS (line graph at primary axis) and ii) increased w/c ratio comparing with 0.25 w/c ratio (column graph at secondary axis)

If this apparent anomaly of 100% GGBS concretes can be ignored, it can be seen that the effect of increased w/c ratio on the strength reduction was affected by the GGBS content. At the 0.32 w/c ratio of the column graph, it is clear that the rate of reduction in strength due to increased w/c ratio was reduced with reduced GGBS content.

This relationship also exists at 0.40 w/c ratio (at least with 70% GGBS concrete) where the rate of reduction is significantly reduced (36% of 0.25 w/c strength). This rate of reduction for 97.5%, 95% and 85% GGBS concrete were almost similar and as discussed before the 100% GGBS concrete was abnormally high.

At the age of 28 day:

At 28 days (Figure 4.3) the relationship between the GGBS content and compressive strength became more linear especially at 0.32 and 0.40 w/c ratio. This linear relationship is also largely maintained in Figure 4.4 where the rate of strength reduction of concrete with increased proportion of GGBS with respect to the compressive strength of 70% GGBS is linear mainly up to 95% GGBS level.

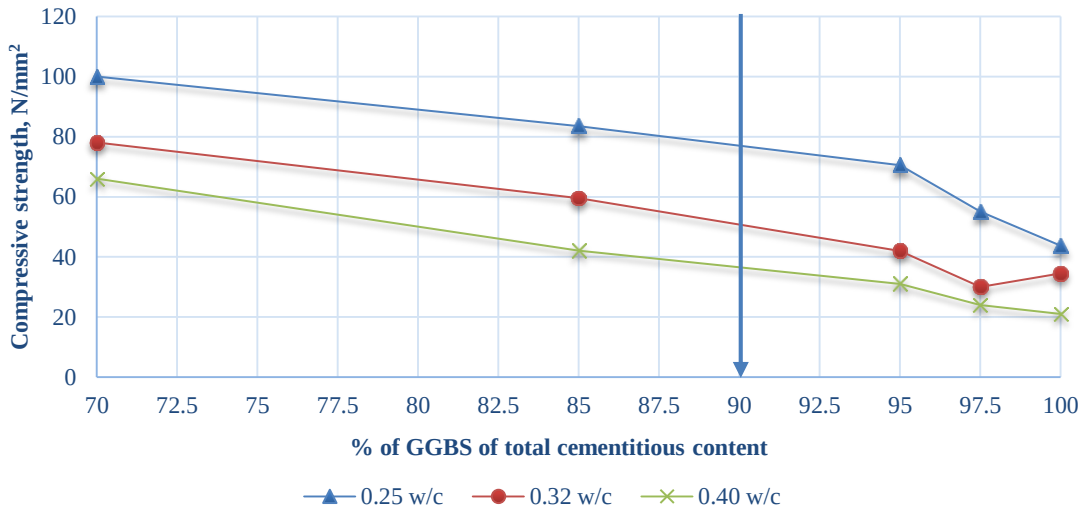

Figure 4.3: Effect of GGBS content on the development of compressive strength at 28 day age

The reduction of compressive strength increased at a higher rate when the GGBS content increased from 95% to 97.5% and 100%, perhaps due to the lack of pozzolanic reaction due to severe limitations of $Ca(OH)_2$ due to minimal or no presence of Portland cement. This is applicable for all three w/c ratios except a sudden drop of 0.32 w/c ratio at 100% GGBS concrete.

The effect of increased w/c ratio on the reduction of compressive strength was also affected by the GGBS proportion as found in 7 day results. Except 100% GGBS concretes, the percentage reduction of compressive strength due to increased w/c ratio with respect to 0.25 w/c ratio was reduced with reduced proportion of GGBS content. This was demonstrated for both 0.32 and 0.40 w/c ratio with respect to 0.25 w/c ratio (Figure 4.4, secondary axis).

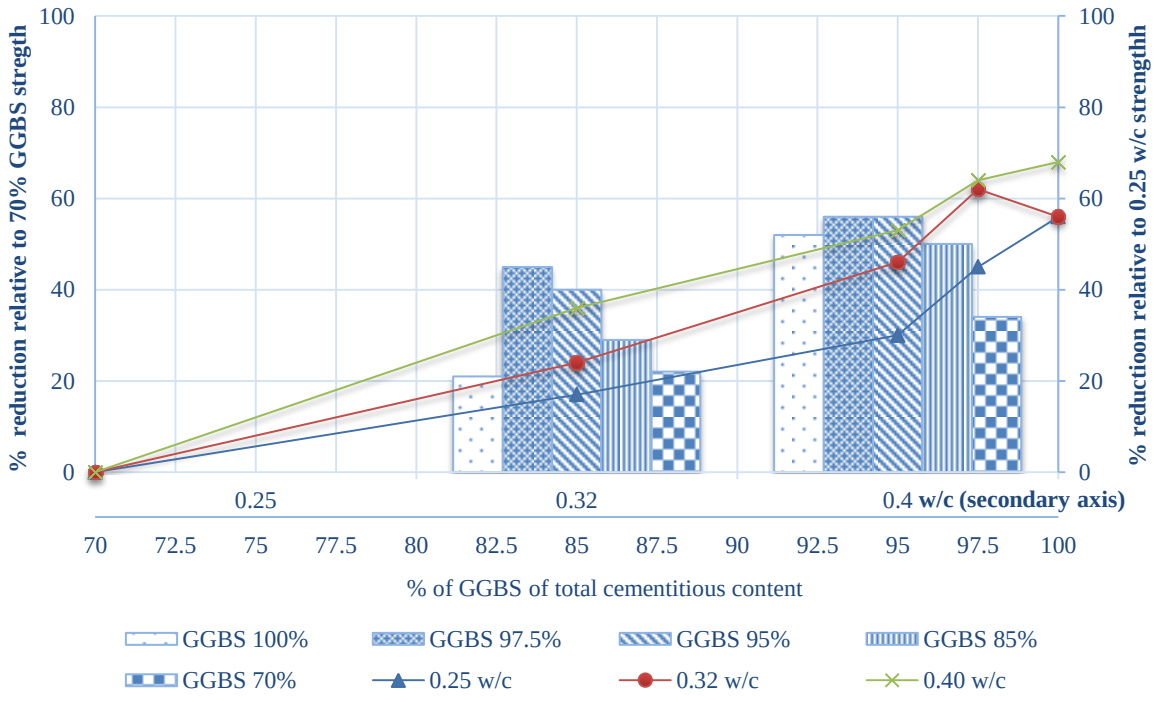

Figure 4.4: Percentage reduction of compressive strength at 28 day due to i) increased proportion of GGBS comparing with 70% GGBS (primary axis) and ii) increased w/c ratio comparing with 0.25 w/c ratio (secondary axis)

At the age of 56 day:

A linear reduction of strength with the increased proportion of GGBS content can be seen in Figure 4.5 where the curve fitting polygonal trend lines are almost linear especially for 0.32 and 0.40 w/c ratio concretes. Similar to 7 days and 28 days age, the linear relationship between the compressive strength and the GGBS content seemed to be discontinued at the higher GGBS concretes (95% and above).

In Figure 4.5, the slopes of the trend lines indicate the rate of reduction of compressive strength from 70% to 85% for all three w/c ratio are seem to be equal. This is also demonstrated in Figure 4.6 (secondary axis) where the strength reduction rate for 70% GGBS concrete at 0.40 w/c ratio (35%) is almost double than at 0.32 w/c ratio (18%). For 85% this behaviour has been similarly repeated by having 47% reduction at 0.40 w/c ratio and 27% reduction at 0.32 w/c ratio.

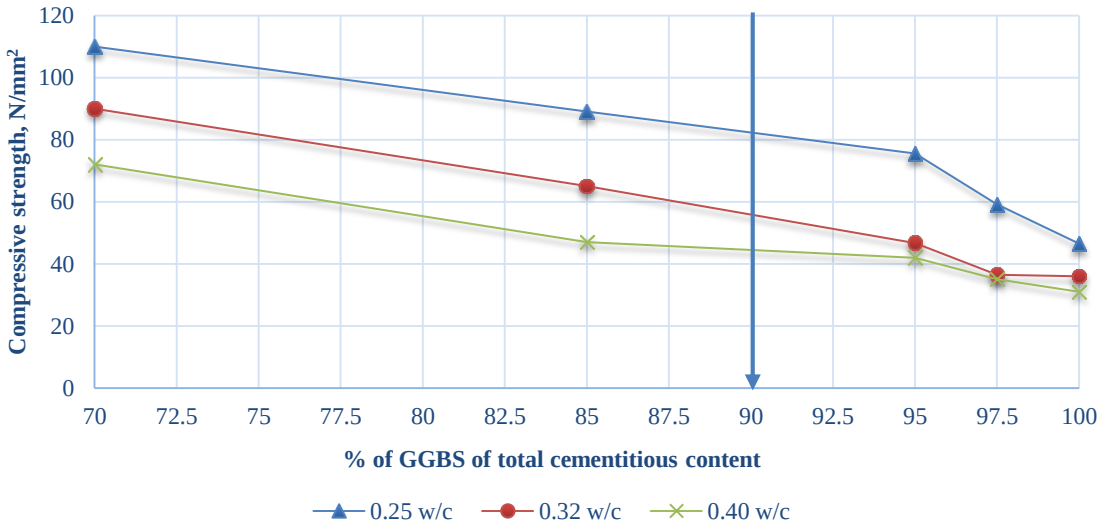

Figure 4.5: Effect of GGBS content on the development of compressive strength at 56 day age

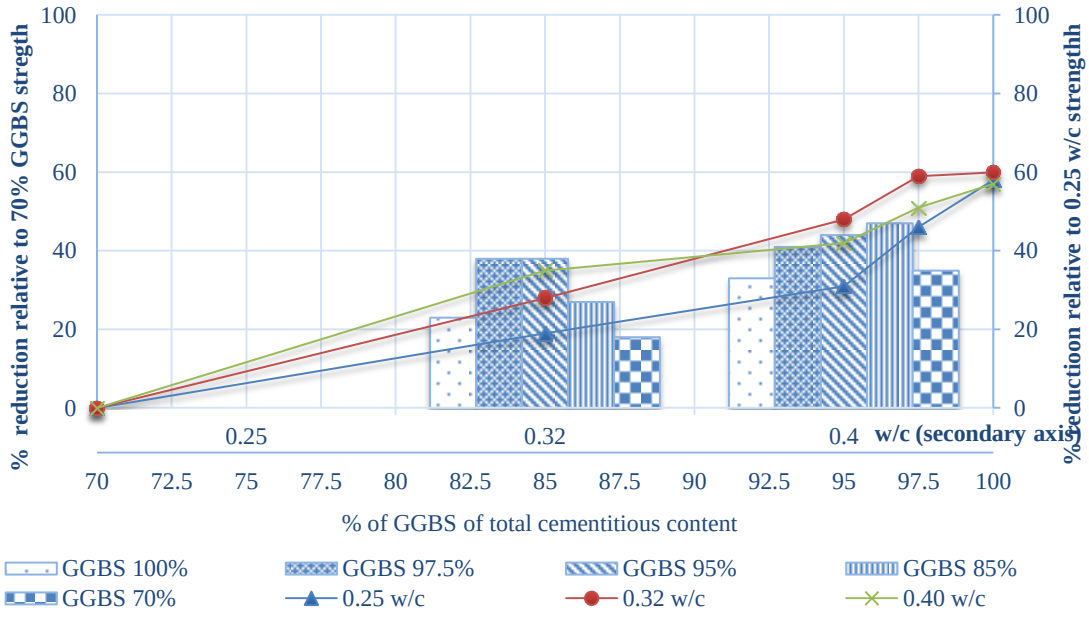

Figure 4.6: Percentage reduction of compressive strength at 56 day due to i) increased proportion of GGBS comparing with 70% GGBS (primary axis) and ii) increased w/c ratio comparing with 0.25 w/c (secondary axis)

As it can be seen from the above discussion that the compressive strength of concretes with 95% and above GGBS contents did not produce a linear relationship with the proportion of GGBS. Therefore, GGBS content with 95% or below would be the target proportion where concrete with stable results of compressive strength can be achieved. By considering these findings a target of 90% GGBS of total cementitious content can be considered to produce concrete with acceptable compressive strength with higher replacement of Portland cement.

Therefore, it is important to understand the possible strength gain of concrete with 90% GGBS concretes. This can be interpolated from the trend line equations of Figure 4.1, 4.3 and 4.5, and tabulated in Table 4.10 where concrete with 90% GGBS at 28 days could have achieve at least 64% to 77% of the compressive strength of 70% GGBS concrete at w/c ratio of 0.32 and 0.25 respectively.

Table 4.10: Equivalent compressive strength of concrete with 90% GGBS content

Age	% of the compressive strength of 70% GGBS concrete		
	0.25 w/c	0.32 w/c	0.40 w/c
7day	85	64	65
28day	77	64	55
56day	75	62	60

Rate of strength gain:

In the following sections the rate of strength development of different type of GGBS concrete over time for different w/c ratios are discussed. Figure 4.7 a, b and c present the compressive strength of GGBS concretes of 0.25, 0.32 and 0.40 w/c ratio respectively to demonstrate incremental gain of compressive strength of GGBS concrete over time. The effect of age, w/c ratio and proportion of GGBS on the compressive strength of concretes are clearly visible from these three figures.

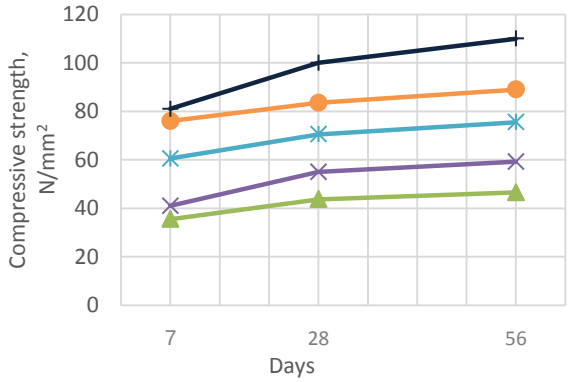

Figure 4.7a: 0.25 w/c ratio

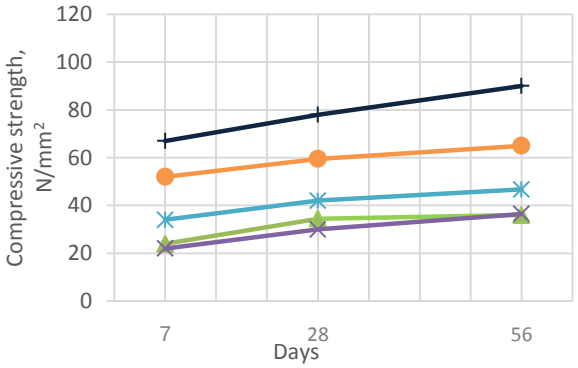

Figure 4.7b: 0.32 w/c ratio

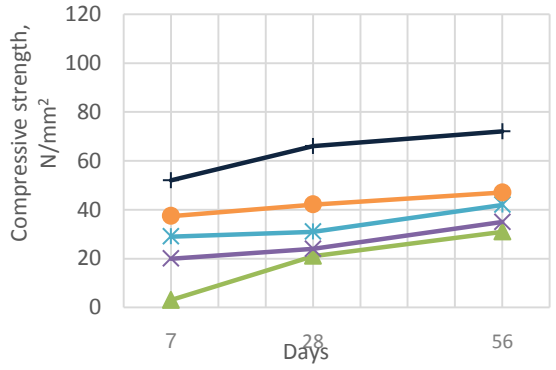

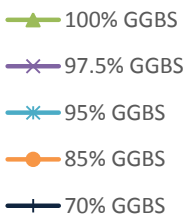

Figure 4.7c: 0.40 w/c ratio

Figure 4.7: Development of compressive strength over time – GGBS concrete

However, in Figure 4.8 these results have been collated together and expressed them in percentage of the maximum strength of 56 day age, assuming that concretes would have achieved the maximum strength at 56 days. It is interesting to observe that at the age of 28 day all 0.25 w/c ratio concrete achieved more than 90% of their maximum strength (56 days strength). All 0.32 w/c ratio concretes achieved almost similar level of maturity at 28 days, but 0.40 w/c ratio concretes with higher GGBS content the rate of strength gain was much slower than concrete with 70% and 85% GGBS content.

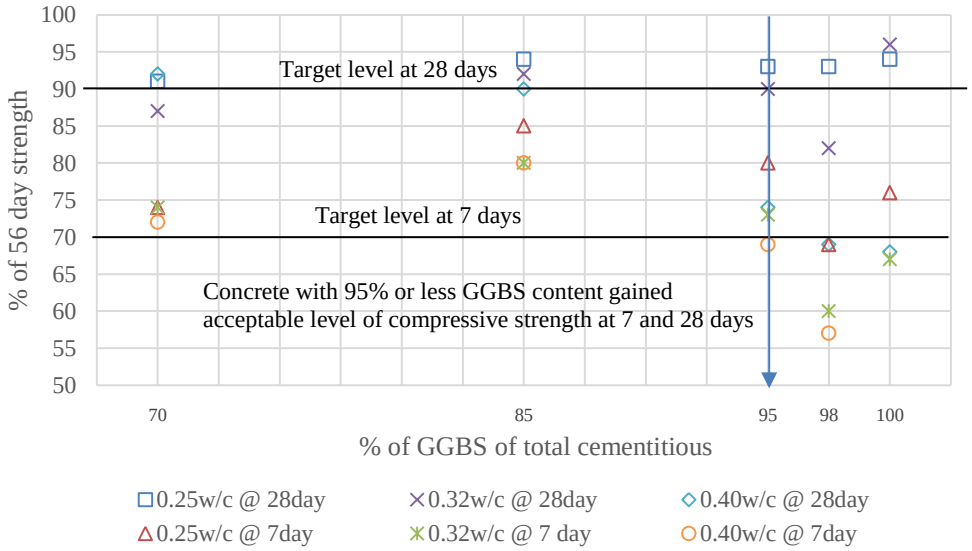

Figure 4.8: Development of compressive strength at different w/c ratio at 7 and 28 day compared with 56 day strength

It is a general quality control practice in the ready-mix concrete industry to assess the 7 day strength of concrete to predict the maximum strengths, however, the strength gain of concretes at 7 days were not consistent, though with 70% GGBS it achieved around 74% of the maximum strength, which could be considered as quite acceptable value. Concrete with higher GGBS content could not show a consistent maturity at 7 days. With higher w/c ratio, this inconsistency was more profound.

On the other hand, achieving 85% of the maximum strength at 28 days by 85% GGBS concrete is considered to be high as the rate of hydration of GGBS is slower compared to Portland cement. With 95% GGBS concrete at 0.25 w/c ratio this achievement was 80% of the maximum strength, which is also very remarkable.

If 70% is considered to be an acceptable level of early maturity at 7day, then it could be seen from Figure 4.8 that almost all concrete at all w/c ratio with GGBS content 95% or less had achieved that (except 95% GGBS at 0.40 w/c ratio which had 69%). If only 0.25 w/c ratio to consider, than all GGBS concrete (except 97.5% GGBS which had 69%) achieved the required 70% maturity at 7 days. Early strength gain is an important parameter in the construction industry for early striking off formworks. Therefore from the above analysis it could be concluded that any concrete with total GGBS content less than 95% will be a safer selection.

Summary:

Compressive strength of concrete with different proportion of GGBS is related to the GGBS content and w/c ratio. This relationship was observed as linear from 70% to 95% GGBS content of total cementitious materials. At 90% GGBS replacement, 64% to 77% of the compressive strength of 70% GGBS concrete could be achieved at the age of 28 days with lower w/c ratios.

Slower hydration process of GGBS is another practical issue to be dealt with for higher GGBS content concrete. However the above discussions suggest that earlier strength gain can be achievable for equivalent GGBS content but with reduced w/c ratio, concretes with maximum 95% GGBS of total cementitious content would achieve the required early and ultimate strength.

4.3.1.2 Concrete with different pozzolanic materials

In this section the compressive strength of concrete containing different proportion of GGBS and pozzolanic materials including fly ash, microsilica and rice husk ash have been discussed to demonstrate the effect of these materials on the compressive strength of concrete.

Five sets of concrete containing i) 70% GGBS (P30S70), ii) 100% GGBS (P0S100) iii) 80% fly ash (P20F80) vi) 10% microsilica (P90M10) and v) 20% rice husk ash (P80R20) with corresponding proportion of Portland cement was used. In addition, another two sets of triple blend of cementitious materials comprising i) 5% Portland cement, 70% GGBS, 25% rice husk ash (P5S70R25) and ii) 15% Portland cement, 70% GGBS, 15% rice husk ash (P15S70R15) concretes compared together with the other five sets of double blend concretes.

Effect of pozzolanic materials:

The concrete with 70% GGBS was considered to be the control concrete to compare the effect of these cementitious materials. The effect of three different w/c ratios of 0.25, 0.32 and 0.40 was discussed together with the effect of age of each type of concrete. Figure 4.9 illustrate the percentage of the compressive strength gains of all concretes compared to the compressive strength of 70% GGBS concrete. Figure 4.9a, 4.9b and 4.9c are the results at the age of 7, 28 and 56 days respectively.

Considering the results of 70% GGBS concrete as the control, the results of 100% GGBS, fly ash and triple blend with 25% rice husk ash had the lowest compressive strength. At 7 day age all of them were below 50% of the equivalent strength of 70% GGBS concrete. At 28 and 56 days, though there was some improvement, but the results of these three sets of concrete remained below 60% of the control.

On the other hand, concrete with microsilica and rice husk ash (except 0.25 w/c ratio) gained strength more than the control at all three ages. This was expected from these two groups of high silica based pozzolanic materials with higher Portland cement content concretes. However, the eCO_2 credential of these two sets of concrete would be far worse than the control considering the use of much higher quantity of Portland cement. The quantitative comparison with eCO_2 and compressive strengths are discussed in Chapter 7.

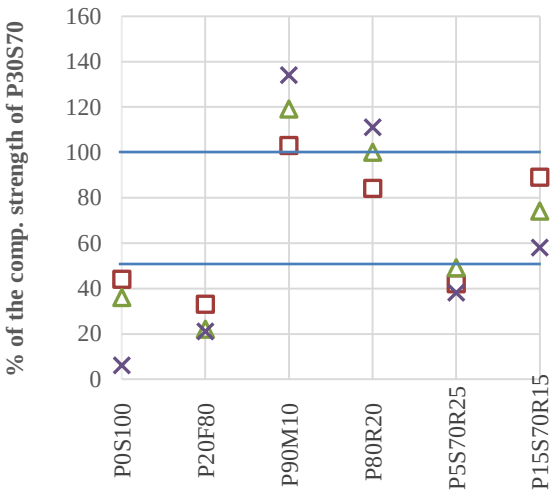

Figure 4.9a: 7 day age

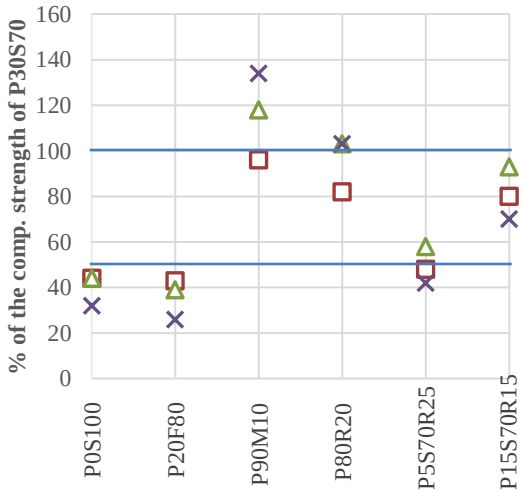

Figure 4.9b: 28 day age

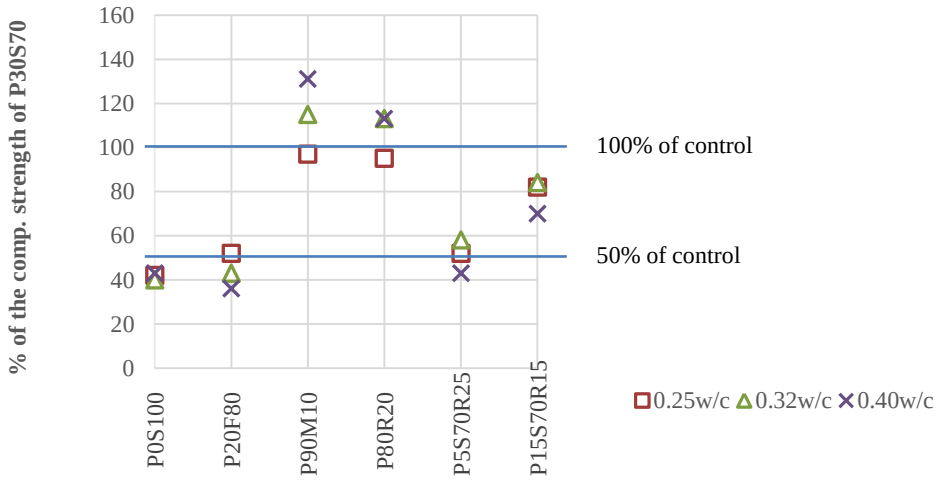

Figure 4.9c: 56 day age

Figure 4.9: Comparison of the compressive strengths of concrete with different cementitious combinations with the control concrete made of 70% GGBS

Comparatively lower compressive strength at 0.25 w/c for microsilica and rice husk ash are mainly due to two reasons. Firstly for microsilica at 0.25 w/c, the available water perhaps, was not adequate enough for effective dispersion of microsilica particles (though high volume superplasticizing admixture was used), resulting into unreacted microsilica particles left behind in the microstructure of the paste.

Secondly for rice husk ash, excessive water demand increases the requirement of superplasticizing admixtures resulting into higher w/c ratio than designed 0.25 w/c ratio which has been discussed previously in Chapter 3, Table 3.16. Therefore, the compressive strength was affected compared with P30S70 concrete where the w/c ratio was maintained as 0.25.

The triple blend concretes with 15% Portland cement, 70% GGBS and 15% rice husk ash which has one of the lowest quantities of Portland cement content posted a moderate strength gain. At the age of 7 day the 0.25 w/c ratio concrete achieved 89% of the compressive strength of the control concrete. At 28 days the 0.32 w/c ratio concrete reached up to the 93% of the compressive strength of the control concrete. At 56 days it remained at 86%. Therefore from the strength gain point of view, triple blend concrete with 15% rice husk ash could be a viable alternative of the control concrete with low eCO_2 content.

Figure 4.10 also shows another picture of the relative position of the triple blend concrete compared with concrete with 70% GGBS where the development of compressive strengths of all concretes have been presented over time. The triple blend concrete with 15% rice husk ash demonstrated comparable trend of strength development similar to the control mix (P30S70) and the double blend 20% rice husk ash concretes (P80R20) particularly at 0.25 and 0.32 w/c ratio. As expected concretes with microsilica posted higher results. At the lower level are the concrete with 100% GGBS, 80% fly ash and the triple blend concrete with 25% rice husk ash. All three of them had similar results.

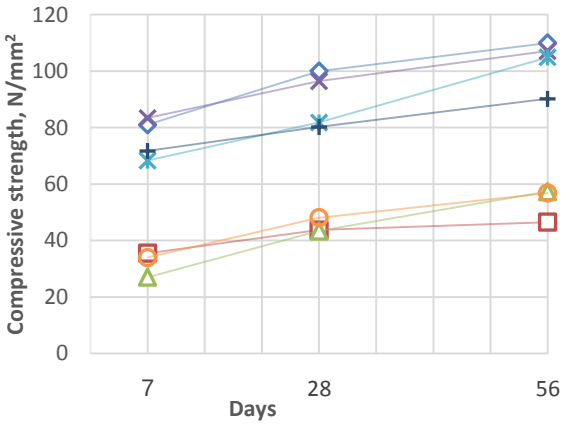

Figure 4.10a: 0.25 w/c ratio

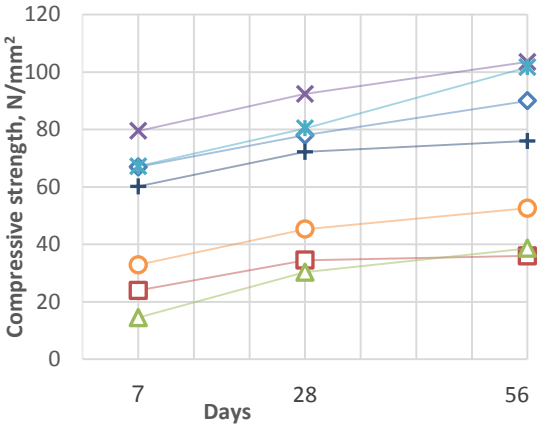

Figure 4.10b: 0.32 w/c ratio

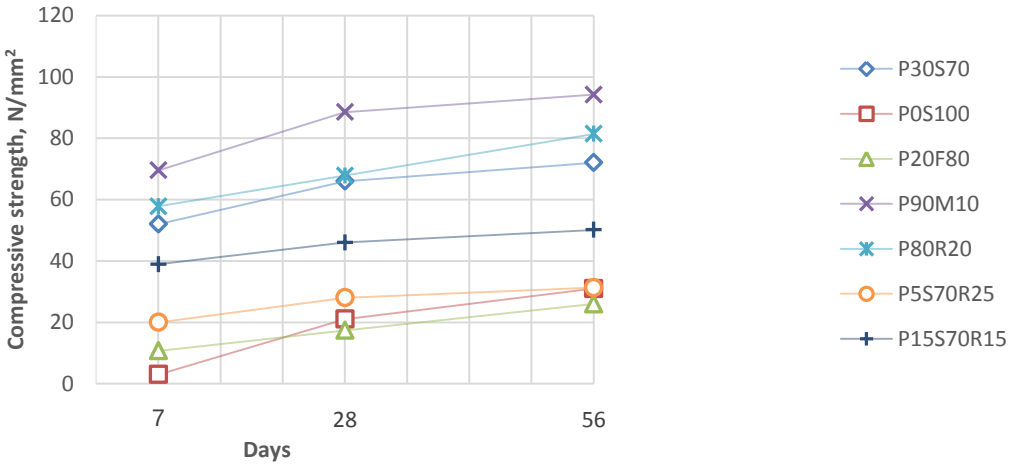

Figure 4.10c: 0.40 w/c ratio

Figure 4.10: Compressive strength development of concrete over time with different combinations of cementitious materials

Rate of strength gain:

The rate of strength development can be clearly illustrated by Figure 4.11 where the 7 and 28 days compressive strengths of all concretes are expressed in percentage of the compressive strength of 56 day age. Assuming that concrete will gain their final strength at 56 days age, it can be seen from Figure 4.11b that triple blend concrete containing 15% rice husk ash (P15S70R15) achieved almost 90% of its final strength at 28 days. This was achieved for all three w/c ratio of this concrete. At the age of 7 days (Figure 4.11a) the results were close to the 80% of the final strength which was more improved results than the control concrete, P30S70.

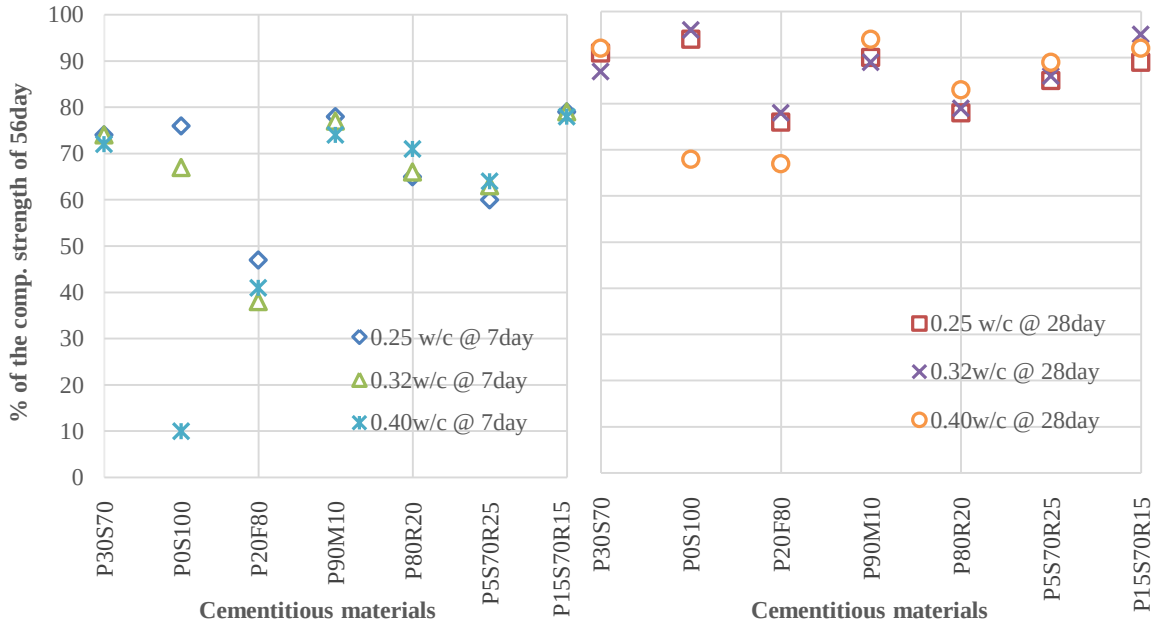

Figure 4.11a: 7 day age

Figure 4.11b: 28 day age

Figure 4.11: Percentage of 56 days compressive strength of concrete with different cementitious combinations at 7 and 28 day

Microsilica (P90M10) and rice husk ash with double blend (P80R20) concretes also showed early maturity at 7 days age. For the triple blend concrete with 25% rice husk ash (P5S70R25), though the 28 days result was almost 90% of its final strength, the 7 days result was around 60-64%. The compressive strength of this blend was also not very encouraging. The strength gain rate for 100% GGBS and 80% fly ash concrete were also lower compared to the control concrete.

Effect of w/c ratio:

Figure 4.12 illustrates the percentage increment of the compressive strength at the age of 28 days due to the reduction in w/c ratio from 0.40 to 0.32 and from 0.32 to 0.25 w/c ratio. There was a very little improvement in strength for concrete with microsilica, rice husk ash and two triple blend concretes when the w/c ratio was reduced further from 0.32 to 0.25, demonstrating that after 0.32 w/c ratio, the concrete is reaching towards its optimum w/c ratio for any further strength improvement. However, for triple blend concretes (P5S70R25 and P15S70R15) the improvement in strength from 0.40 to 0.32 w/c ratio was very significant which was 62% and 57% respectively.

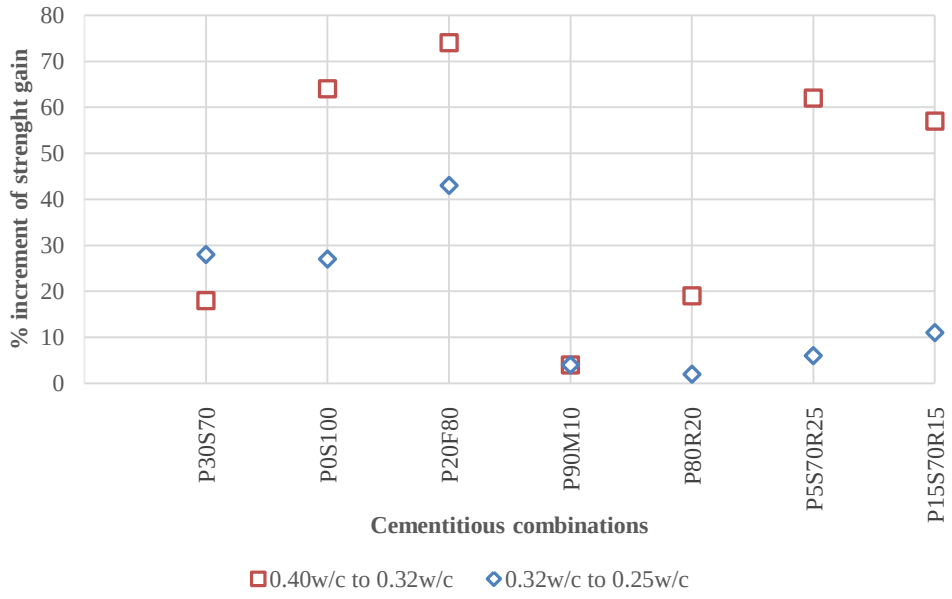

Figure 4.12: Increment in compressive strength due to reduced w/c ratio at the age of 28days

It is interesting to note that only the control concrete (P30S70) had higher rate of strength increment of 28% at 0.32 to 0.25 w/c ratio, than from 0.40 to 0.32 w/c ratio which was 18%. All other concretes had the opposite trend i.e. higher increment in strength at 0.40 to 0.32 w/c ratio and lower at 0.32 to 0.25 w/c ratio. For microsilica concrete it was 4% increment for both reductions in w/c ratios.

Summary:

Concrete with P15S70R15 showed good potential to achieve compressive strength which is close to the control concrete of P30S70 concrete. Concrete with very high replacement of Portland cement such as P0S100 and P20F80 concrete did not achieve reasonable strength gain. Concretes with microsilica and rice husk ash (P90M10 and P80R20) had satisfactory strength gain, but their very high Portland cement content would have increased their carbon footprint.

The early strength gain and effect of w/c ratio on the triple blend concrete with 15% rice husk ash were at acceptable range. With having only 15% Portland cement content P15S70R15 should be considered one of the low carbon concrete with acceptable compressive strength characteristics.

4.3.2 Sand type series

In the Sand type series similar to the Cement type series a group of pozzolanic cementitious materials was used. They were i) 70% GGBS (control), ii) 80% fly ash, iii) 10% microsilica and iv) 20% rice husk ash with corresponding amount of Portland cement. The main difference between these two types was in the Sand type 'unwashed' crushed rock (limestone) sand with higher finer particle (almost 10%) passing 75µm was used.

The objective of the Sand type series was to evaluate the effect of the unwashed sand on different parameters of concrete to evaluate their performance comparing with concrete using washed sand. In the following sections comparisons would be made between concrete with washed and unwashed sands to evaluate the effectiveness of the unwashed sand in terms of compressive strength gain. This performance will also be validated with the washed sand concrete in terms of different w/c ratio of 0.25, 0.32 and 0.40. The rate of strength gain at the age of 7, 28 and 56 days would also be verified.

4.3.2.1 Effects of unwashed sand

The effects of the unwashed sand have been demonstrated in the Figure 4.13 where the improvement of compressive strength due to the use of unwashed sand over the washed sand concrete is presented in percentage of the compressive strength of washed sand concrete. This improvement has been reflected for all three w/c ratios of each cementitious material at the age of 7, 28 and 56 days.

The significant improvement of compressive strength of 42% demonstrated by 0.25 w/c ratio, fly ash concrete (at 28 days age) explains the effect of unwashed sand containing higher fines on the porous microstructure of fly ash concrete. Even at 56 days age, the room for improvement was 27% which is quite significant relative to other concretes.

This effect was largely demonstrated in all other concretes, but it was predominantly more effective at lower w/c ratio of 0.25 and 0.32 w/c ratio and at 28 days age. This could be due to the reason of reaching the required fractional volume contributed by the additional finer particles of the unwashed sand at lower w/c ratios to achieve an enhanced particle packing of the ingredients of concrete.

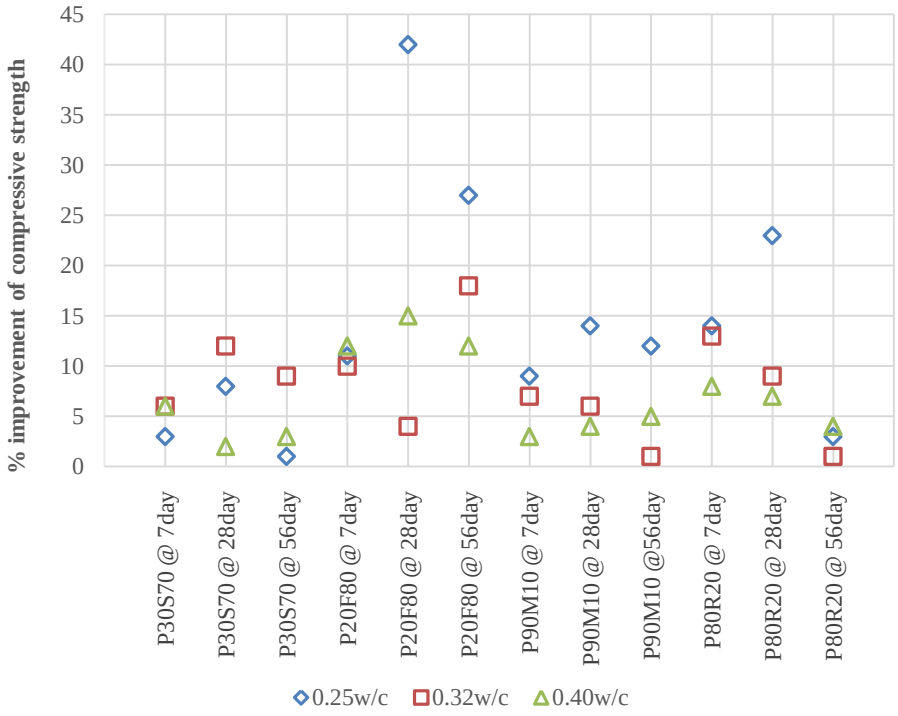

Figure 4.13: Improvement of compressive strength due to the effect of unwashed sand

The degree of hydration of different cementitious materials at different ages also affected this improvement. However, there was no distinctive relationship could be established between the w/c ratios, type of cementitious materials and age of the concrete with the improvement of the compressive strength due to this effect.

4.3.2.2 Effects on the cementitious materials

The additional fines in the unwashed sand did not adversely affect the compressive strength gain behaviour of different cementitious materials comparing with the control concrete of 70% GGBS. Figure 4.14 shows that at the age of 28 days the percentage of the compressive strengths of concretes made with different pozzolanic materials comparing with the 70% GGBS concrete were very similar for both washed and unwashed sand concretes.

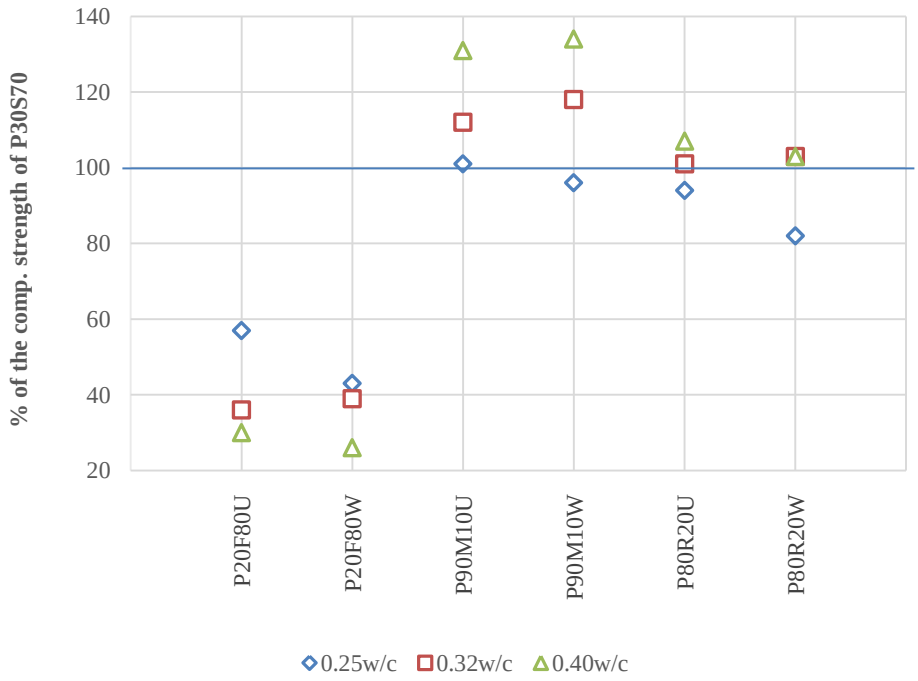

Figure 4.14: Compressive strength gain of concrete comparing with P30S70 – effect of unwashed sand

However, the effect of the unwashed sand is relatively higher in fly ash and rice husk ash concretes than the microsilica concretes, perhaps the effect of unwashed sand was obscured by the void filling characteristics of microsilica particles. For example, the fly ash concrete with unwashed sand at 0.25 w/c achieved 57% strength of the equivalent concrete with 70% GGBS. The same fly ash concrete with washed sand, this achievement is 43% of 70% GGBS concrete strength. This positive effect is more pronounced on 0.25w/c ratio concretes. For 0.32 and 0.40 w/c ratio it is more inconclusive.

4.3.2.3 Rate of strength gain

In order to understand the rate of strength gain of concrete with unwashed sand, the compressive strength at the age of 7 and 28 days have been compared with the strength at the age of 56 day assuming that the 56 day strength would be the final ultimate strength. Figure 4.15 has plotted the compressive strength of concrete at the age of 7 and 28 days in percentage of the compressive strength of concrete at the age of 56 days.

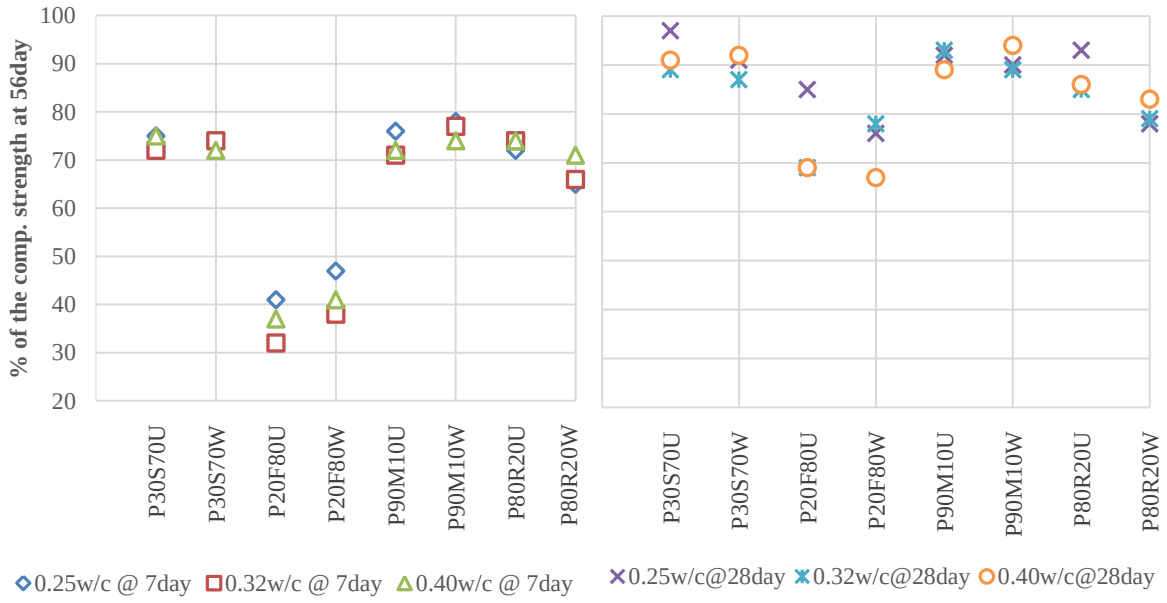

Figure 4.15a: 7 day age

Figure 4.15b: 28 day age

Figure 4.15: Percentage of 56 days strength gain at 7 and 28 days of concrete made of different cementitious materials with washed and unwashed sands

The effect of the unwashed sand to enhance the strength gain was very clearly demonstrated in Figure 4.15b, where the 70% GGBS concrete with unwashed sand at 0.25 w/c ratio gained 97% of the final strength at 28 days age. The same concrete with washed sand gained 92%. This improvement was repeated in almost all concrete especially at 28 day age. In terms of early strength development at 7 days, the improvement is inconclusive, though except the fly ash concrete all other concretes with unwashed sand achieved 70% of the ultimate strength (Figure 4.15a).

This improvement would suggest that the unwashed sand would not only increase the corresponding compressive strength, it would also help to gain its ultimate strength faster than the concrete made with washed sand.

4.3.2.4 Effect on the w/c ratio

The unwashed sand did not have any significant effect on the rate of strength increment due to reduced w/c ratio. Figure 4.16 shows that concrete with or without unwashed sand posted similar rate of increment in compressive strength. There is no particular relationship can be drawn between the increment of 0.40w/c to 0.32w/c and 0.32w/c to 0.25w/c for both washed and unwashed sand concretes.

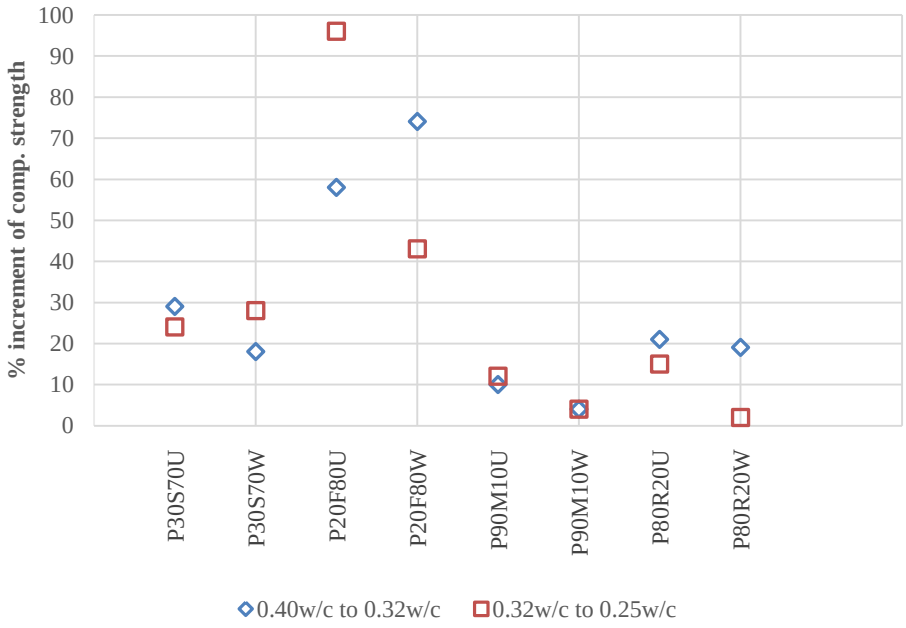

Figure 4.16: Comparison between the washed and unwashed sand concretes of the increment of compressive strength due to the increase in w/c ratios

Except concretes containing fly ash, these increments remained within 30% which seem to be moderate for all concretes. The increment in compressive strength for fly ash concretes was significantly high. It is especially prominent for fly ash concrete with unwashed sand (P20F80U). This signifies that the paste microstructure of 80% fly ash concrete had much larger room to accommodate finer particles to increase its mechanical strength. Reduction in w/c ratio enhanced these phenomena further demonstrating the positive effect of the unwashed sand.

4.3.2.5 Summary

It can be summarized from the above discussions that the unwashed sand have positively enhanced the compressive strength of concrete with different cementitious combinations. Enhanced compressive strength with lower w/c ratio at 28 days age perhaps suggest the positive effect of the finer volume fraction to reaching to an optimum particle packing of the ingredients in the concrete paste. This improvement was also observed on the cementitious materials which produced relatively porous microstructure such as fly ash due to its low hydration with very high replacement of Portland cement. The effect of unwashed sand also enhanced the rate of strength gain at 7 and 28 days compared with concrete made with washed sand.

4.3.3 Recycled concrete aggregate series

In the following sections the effect of different proportions for coarse recycled concrete aggregates (RCA) on the compressive strength of concretes has been discussed. The effect of RCA was examined in two different combinations of cementitious materials. In the first series 100% GGBS was used with RCA in a proportion of 100%, 80%, 50% and 0% of total coarse aggregate content. In this series both washed and unwashed sands were used to explore the effect of the unwashed sand on the compressive strength of RCA concretes.

In the second series a triple blend of cementitious materials consist of 15% Portland cement, 70% GGBS and 15% rice husk ash was used. In this series the RCA content was modified to 100%, 50%, 20% and 0% of total coarse aggregate content. The reason of this modification was to have a uniform distribution of RCA to understand the effect of RCA at its lower range. Replacing coarse aggregate by RCA at a lower proportion is more practical due to the relative shortage of RCA in the Middle East. Only washed sand was used for this series.

In both series the effect on the changes of w/c ratios by the RCA content was explored by considering three w/c ratios of 0.25, 0.32 and 0.40. Therefore in the following sections the effect of RCA on i) the compressive strengths of concrete, ii) different w/c ratio and iii) effect of the unwashed sand would be discussed.

4.3.3.1 Effect on the compressive strength

100% GGBS with washed sand:

The compressive strength of RCA concrete with 100% GGBS and washed sand have been presented in Figure 4.17 in terms of percentage of the compressive strength of 0% RCA concrete. The Figure 4.17a, b and c are presenting the compressive strengths of concrete at the age of 7, 28 and 56 days respectively.

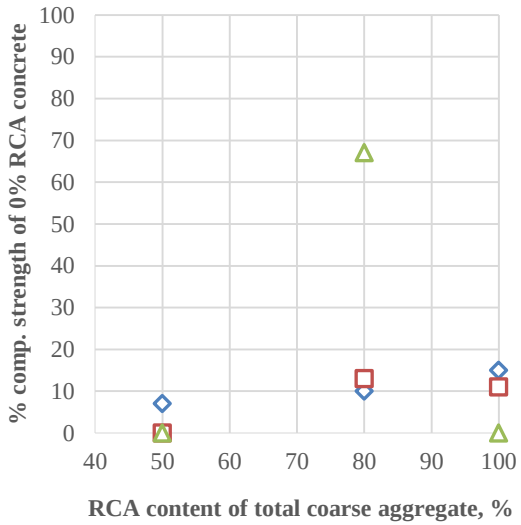

Figure 4.17a: 7 day age

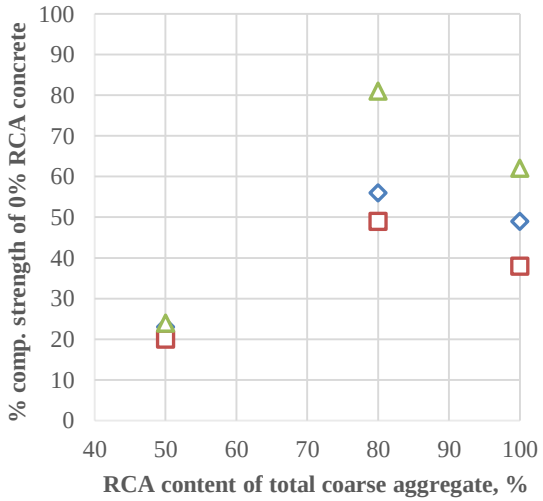

Figure 4.17b: 28 day age

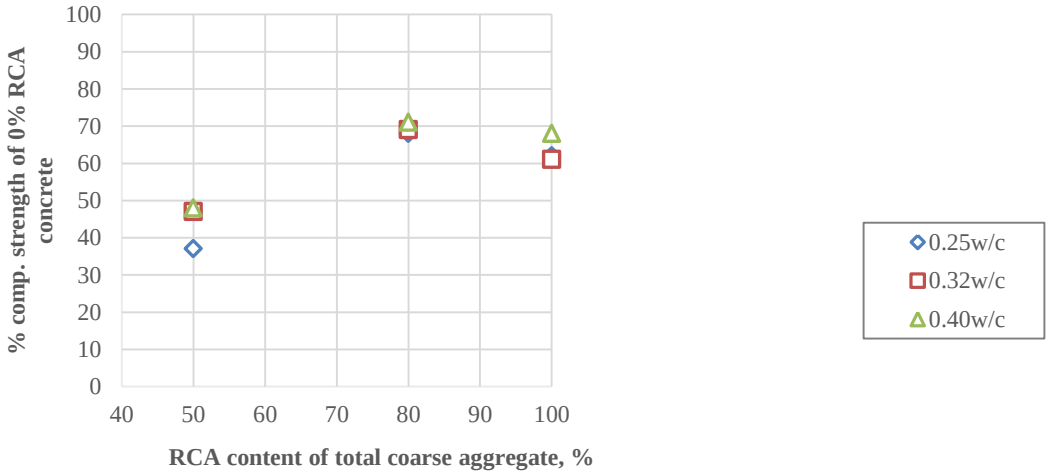

Figure 4.17c: 56 day age

Figure 4.17: Effect of RCA content on the compressive strengths of concrete with 100% GGBS and washed sand

It was anticipated that the compressive strength should be reduced with increased RCA proportions as the inherent characteristics of RCA is inferior to natural coarse aggregate as shown in Chapter 3 at Table 3.4. That is the reason in Figure 4.17, the results of the compressive strengths of RCA concretes have been presented in terms of the compressive strength of concrete with no RCA. However, there is no relationship between the proportion of RCA and percentage of compressive strength of concrete without RCA could be established from Figure 4.17. This could be attributed to the erratic hardening behaviour of 100% GGBS concretes experienced in this study.

At the age of 7 days, the strength gains remained below 20% for concretes with different proportion of RCA content. This had occurred for all three w/c ratio. The only exception was the concrete with 80% RCA content at 0.40 w/c ratio. This particular result seems to be an anomaly as it was abnormally higher than the other results. At 28 and 56 days though the compressive strengths increased significantly but there was no proportional effect of RCA could be established. In addition, the compressive strengths of 50% RCA concrete remained abnormally low which was not expected as well.

100% GGBS with unwashed sand:

The effect of RCA content on the compressive strength of concretes made with unwashed sand and 100% GGBS have been presented in Figure 4.18. Though there is a major improvement of compressive strength compared with the concrete with washed sand demonstrating the effect of unwashed sand however, the effect of RCA was not demonstrated. In fact the opposite relationship between the development of compressive strength and the RCA content raised questions on the reliability of 100% GGBS concrete.

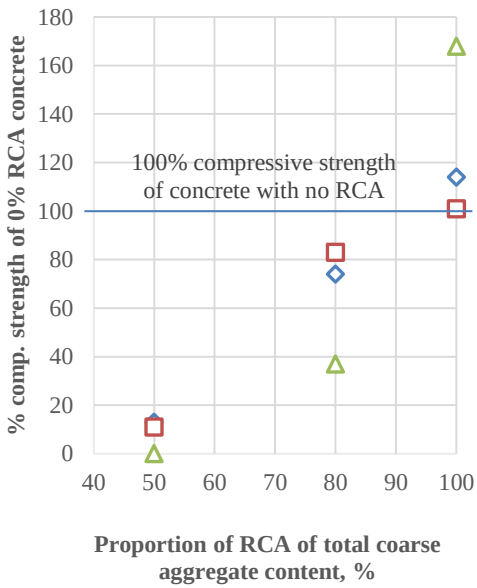

Figure 4.18a: 7 day age

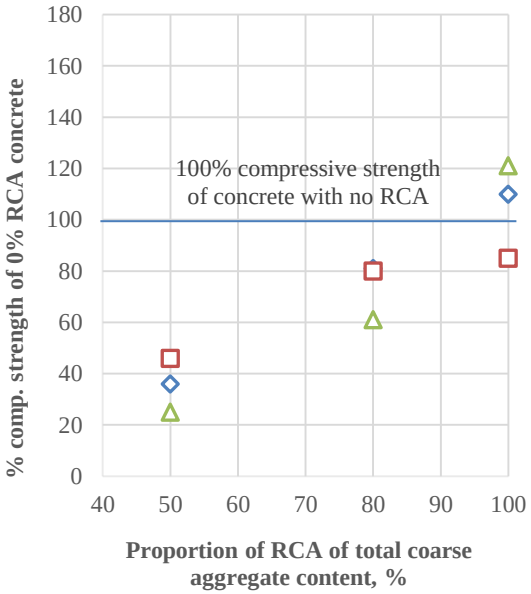

Figure 4.18b: 28 day age

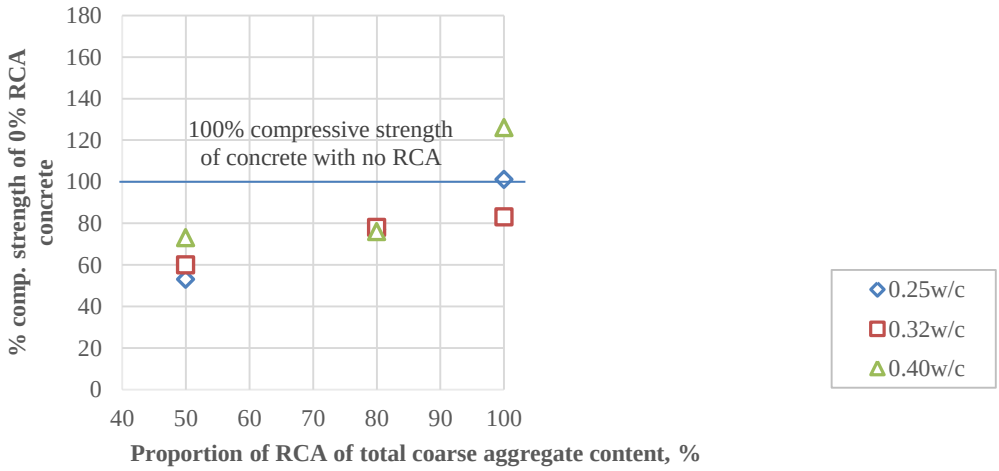

Figure 4.18c: 56 day age

Figure 4.18: Effect of RCA content on the compressive strength of concrete with GGBS and unwashed sand

Concrete with triple blend cementitious materials:

Due to the erratic behaviour of 100% GGBS concrete, the effect of RCA on the compressive strength of concretes was explored in concrete made with a triple blend of cementitious materials consist of P15S70R15.

Figure 4.19 is showing the direct results of compressive strengths of triple blend RCA concretes. The compressive strengths of concretes with no RCA seem to be little lower than the 20% RCA especially at 0.32 and 0.40 w/c ratios. Otherwise there was a good trend of reduction in compressive strength with the increase in the RCA content of concrete could be observed.

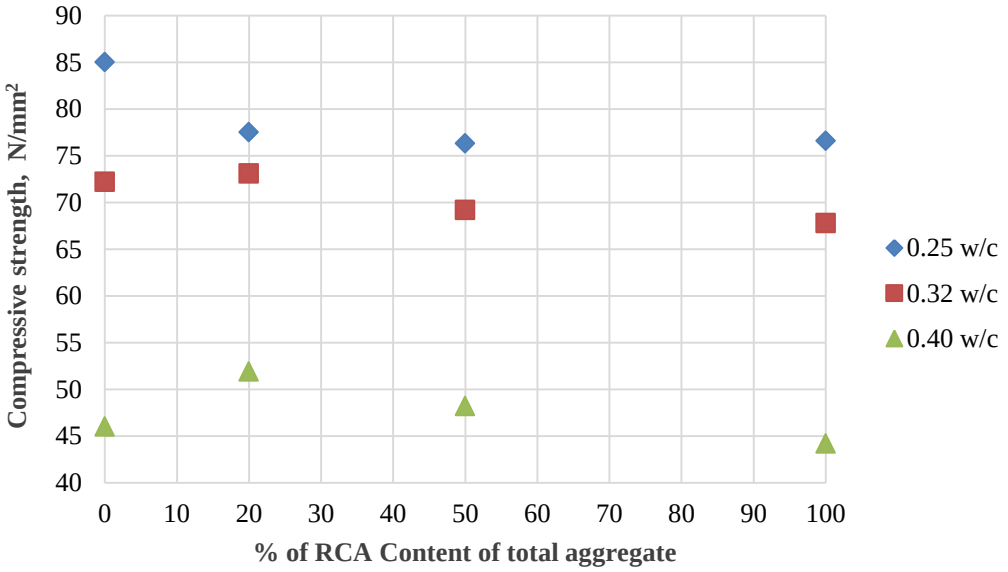

Figure 4.19: Compressive strengths of concrete made with RCA and triple blend of cementitious materials at the age of 28 day

There is also a clear effect of the RCA proportions on the compressive strength of concrete with triple blend cementitious materials can be seen in Figure 4.20 where the development of compressive strength expressed as the percentage of the compressive strength of 0% RCA concrete followed a downward trend with the increased proportion of RCA in the concrete.

At the age of 7 day the 20% RCA concrete achieved little more than 100% of the compressive strength of concrete without any RCA at 0.40 and 0.32 w/c ratio. The compressive strength of subsequent RCA proportions i.e. at 50% and 100% reduced accordingly. Though no clear relationship could be established between the reduction of compressive strength and the RCA proportion from these three point graphs, however the trend of reduced compressive strength with increased RCA content could be observed.

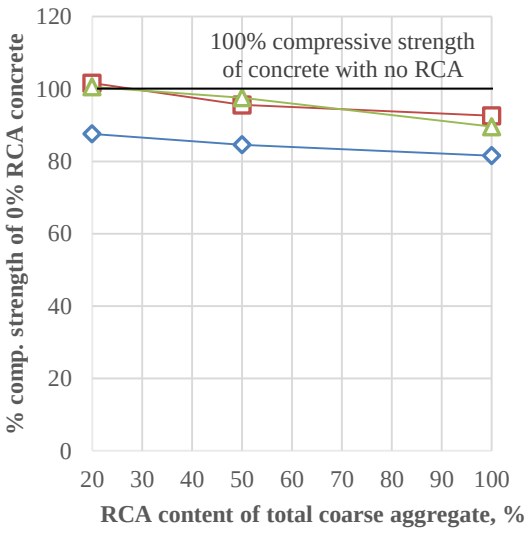

Figure 4.20a: 7 day age

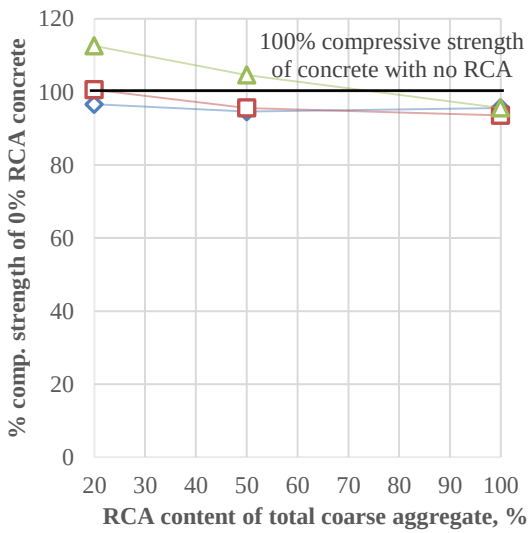

Figure 4.20b: 28 day age

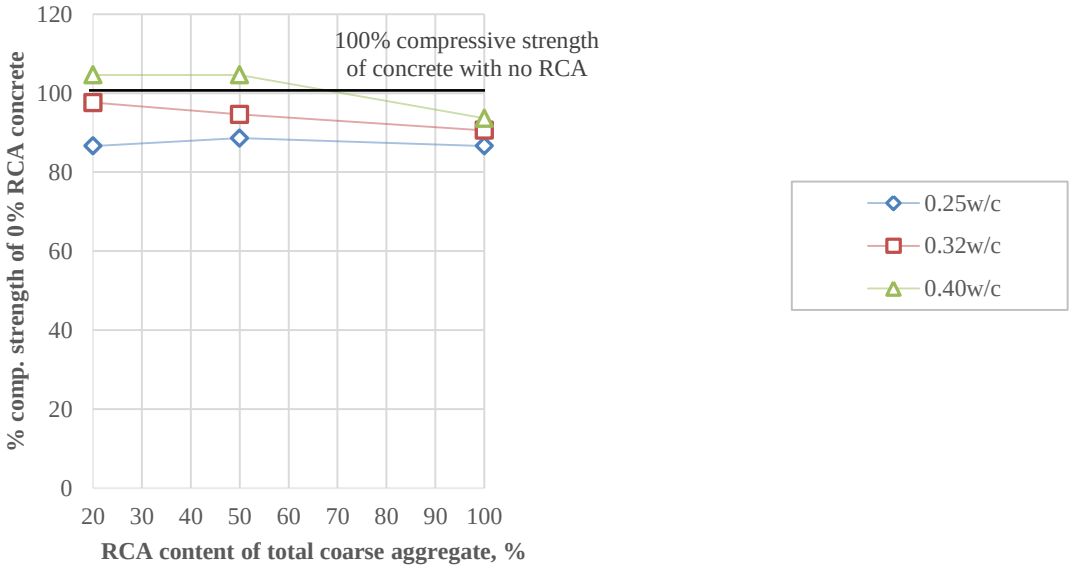

Figure 4.20c: 56 day age

Figure 4.20: Effect of RCA content on the compressive strength of concrete with triple blend of cementitious materials

At 28 days the strength gain of RCA concrete at all three w/c ratio compared to 0% RCA concrete improved further especially 0.40 and 0.25 w/c concretes. It is to note that the effect of RCA on the compressive strength gain is more pronounced at lower w/c ratio and at early ages. At 7 day the strength gain declined for all 3 w/c ratio especially at 0.40 w/c. At 28 and 56 days age there is no effect of RCA can be seen on 0.25 w/c concretes. It is because at lower w/c ratio and at later age the improved mechanical strength of paste had offset the weakness of the RCA.

The overall performance of RCA concrete is at satisfactory level which is about 94 - 96% for 100% RCA concrete at 28 days age which is much better than 78% achieved by Katz, A., (2003) using Portland cement at 0.55 w/c as discussed in the literature review.

Effect on early strength gain behaviour:

Figure 4.21 illustrates the achievement of compressive strengths at the age of 7 and 28 days expressed as the percentage of the compressive strength of 56 day age. The compressive strength at the age of 56 days has been considered to be the maximum strength of concretes studied in this work.

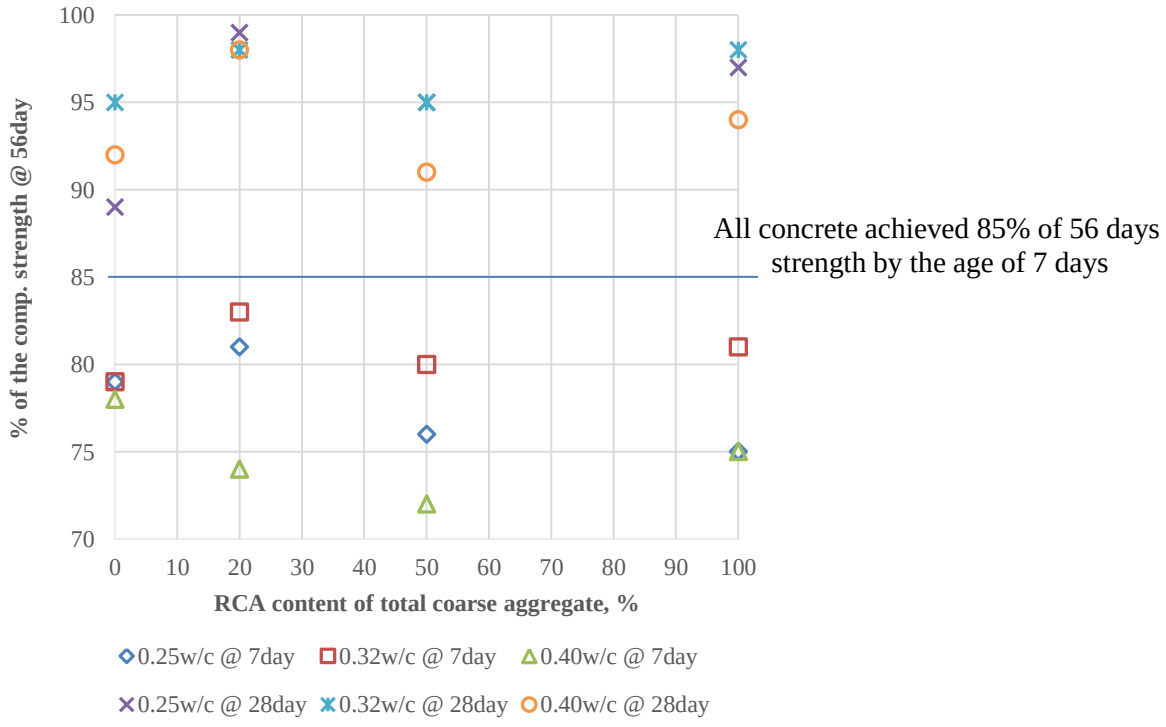

Figure 4.21: Effect of RCA content on the strength development on 7 and 28 day

As shown in Figure 4.21, concretes made with different proportion of RCA content and triple blend of cementitious materials gained 70% to 85% of their maximum strength at the age of 7 days. At the age 28 days this achievement reached from a minimum of 89% to maximum of 98% of 56 days compressive strength. These achievements are considered to be at the satisfactory level as the strength gains at 28 days were equal if not higher than the strength gain of similar concrete without any RCA.

Concretes with lower w/c ratio had higher gain to achieve the ultimate strength with few exceptions. At the age of 7 days concrete with 0.40 w/c ratio with different RCA content posted lower strength gain compared to concrete without any RCA. Therefore, lower w/c ratio concrete with RCA would be more desirable to achieve early maturity in compressive strength.

4.3.3.2 Effect of RCA on the compressive strength increment due to reduced w/c ratio

Figure 4.22 shows that the increment in compressive strength due to the reduced w/c ratio can be positively affected by the proportion of RCA in the concrete. The vertical axis in Figure 4.22 plotted the increment in compressive strength due to the decrease of w/c ratio from 0.40 to 0.32 and from 0.32 to 0.25. This increment has been expressed as the percentage of the compressive strength of the concrete with the higher w/c ratio. A trend of higher increment with higher RCA content can be observed from Figure 4.22. This trend was observed for both sets of w/c ratios validating this particular relationship.

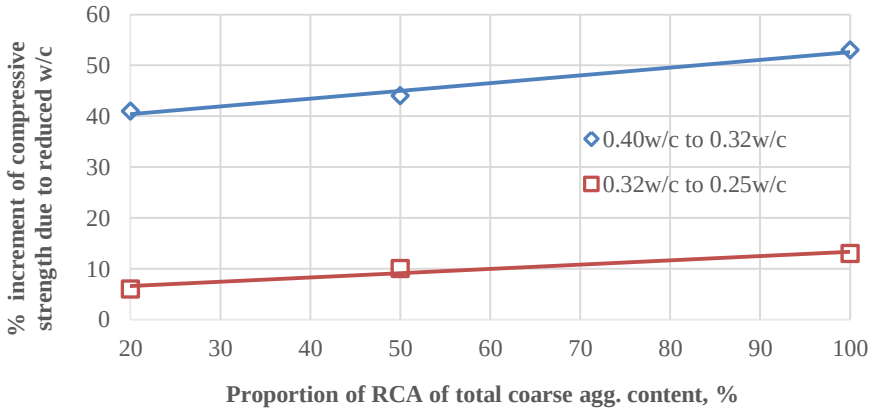

Figure 4.22: Effect of RCA on the increment of compressive strength due to reduced w/c ratio of triple blend concrete at the age of 28 days

It is interesting to figure out that the difference in compressive strength between two decreasing w/c ratios were higher with higher RCA content concretes. It was seen that the compressive strength of RCA concrete with triple blend cementitious materials reduced with increased proportion of RCA, but this rate of reduction is reduced if the w/c ratio is reduced. One of the reasons, as mentioned earlier, could be with reduced w/c ratio the strength of paste and the bond strength between paste and aggregate interface increased.

The scope of strength increment is much higher if the w/c ratio could be reduced from 0.40 to 0.32, than 0.32 to 0.25. It indicates that at 0.25, concretes were reaching towards their optimum w/c ratio for any further strength gain.

Figure 4.22 is only showing the effect of RCA on the w/c ratios of concrete made with triple blend at the age of 28days. At the age of 7and 56 days this effect was also very similar (not shown here). However, concretes made with 100% GGBS for both washed and unwashed sand did not show any specific relationship between the increment in compressive strength due to the change in w/c ratios and the proportion of RCA. This could be due to the erratic hardening behaviour of 100% GGBS concretes as discussed earlier. Therefore, those results are not presented here.

4.3.3.3 Effect of unwashed sand

The effect of unwashed sand on RCA concrete (with 100% GGBS) was largely demonstrated at 56 days strength as shown in Figure 4.23. Except concrete with 0% and 80% RCA at 0.40 w/c ratio all other concretes showed positive improvement of compressive strength at the age of 56 day. The erratic hardening behaviour of 100% GGBS concrete should be the reasons of having negative results at 0% and 80% RCA concretes at 0.40 w/c ratio. There was no relationship between the improvement in compressive strength and the RCA proportion could be established, perhaps also due to the same reasons.

Though the relationship between the effect of unwashed sand and the proportion of RCA is inconclusive, it can be concluded that the unwashed sand was able to enhance the compressive strength of concrete made with RCA.

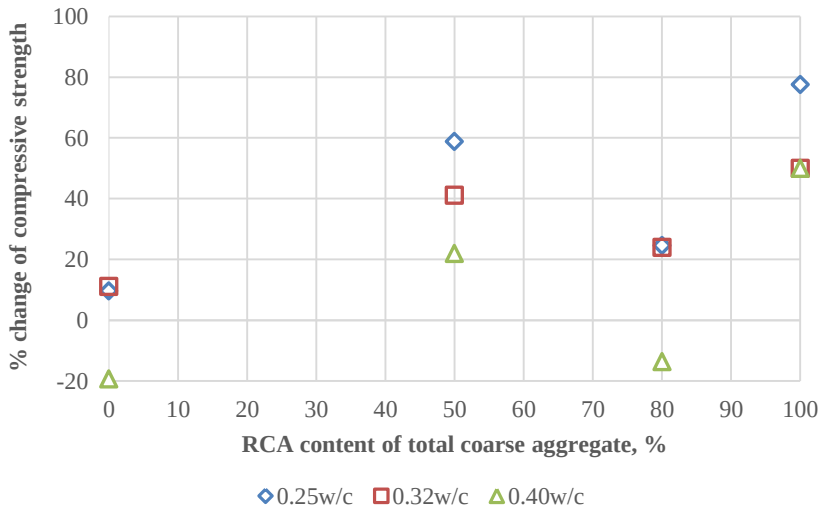

Figure 4.23: Improvement in compressive strength due to unwashed sand at the age of 56 days

4.3.3.4 Summary

It can be summarized from the above discussion that the effect of RCA content on the compressive strength of concrete can be effectively demonstrated by the triple blend concretes made with P15S70R15. This effect was not conclusive for concretes made with P0S100 due to the erratic hardening characteristics of 100% GGBS concretes was experienced in this study. However, gain in compressive strength of RCA concrete using unwashed sand was observed.

In triple blend concrete, the compressive strengths was reduced with increased RCA content, however, this reduction could be offset by reducing w/c ratio. It was recorded that at the age of 28 day concrete with 100% RCA at 0.25 w/c ratio achieved 96% of the compressive strength of same concrete without any RCA content.

It was observed that RCA did not have any negative effect on the rate of compressive strength gain, it behave the same way as concrete without RCA. The RCA content had a positive effect on the compressive strength gain if the w/c ratio was reduced. It was observed that concrete with higher RCA content tended to have higher rate of strength gain when the w/c ratio reduced compared with lower RCA content concretes for the same w/c ratio range.

4.3.4 Higher curing temperature series

In this section the compressive strengths of concretes made of triple blend of Portland cement, GGBS and rice husk ash and cured at 20°C and 40°C in immersed water for 7, 28 and 56 days have been presented to explore the effect of elevated curing temperature on the compressive strength of concrete.

There are two combinations of triple blends comprising of i) 5% Portland cement, 70% GGBS, 25% rice husk ash and (P5S70R25) ii) 15% Portland cement, 70% GGBS, 15% rice husk ash (P15S70R15) were used. Each sets of concrete was made at 0.25, 0.32 and 0.40 w/c ratio to explore the effect on the compressive strength due to the change of the w/c ratio at elevated curing temperature.

In Figure 4.24, the effect of the elevated curing temperature on the compressive strength of concretes is presented. The effect has been illustrated in terms of the percentage increase in compressive strength of concrete cured at 40°C relative to the concretes cured at 20°C temperature.

It is interesting to observe from Figure 4.24 that concrete with higher (25%) rice husk ash proportion reacted more positively on higher curing temperature over concrete with lower (15%) rice husk proportions. At the age of 28 days the compressive strength of 0.25 w/c ratio concrete made with 25% of rice husk ash increased 10% more than the concrete with 15% rice husk ash due to the elevated curing temperature. The reason behind this increased performance could be due to higher pozzolanic reactions at higher temperature producing more CSH gel contributing higher compressive strength. At 7 days this difference was 13%.

At 56 day age, this difference of improvement, however, reduced to 4% perhaps due to reduced pozzolanic activities due to reduced content of $Ca(OH)_2$ available at the later age of the concrete. Though the content of $Ca(OH)_2$ at 56 day by TG analysis was inconclusive, at the age of 365 it was significantly low (Figure 6.7, Chapter 6). The effect of time should also be recognized as the difference in improvement reduced from 13% to 10% from 7 day to 28 day and eventually to 4% at 56 day.

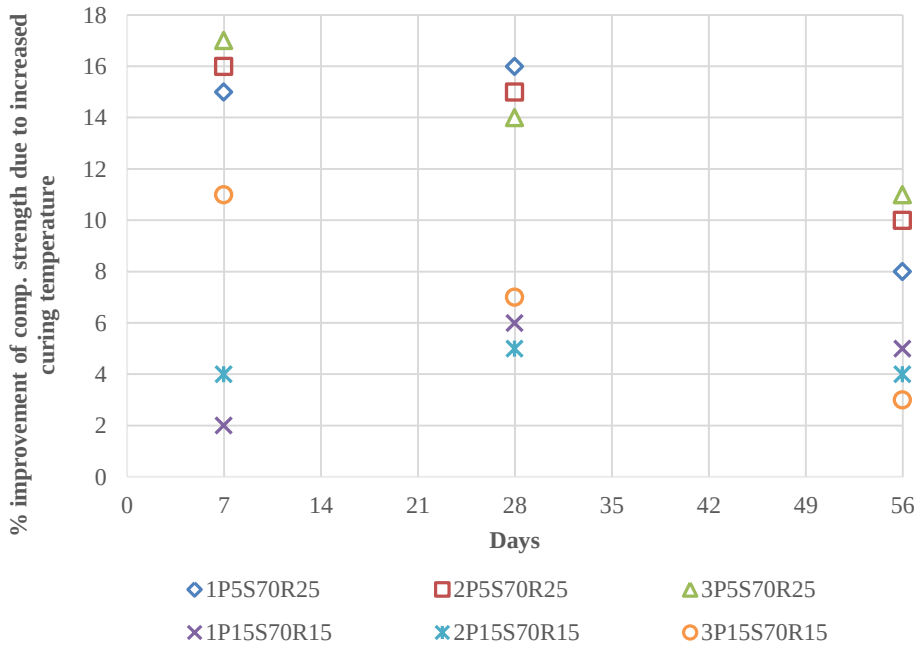

Figure 4.24: Effect of elevated curing temperature on the compressive strengths of concrete made of triple blend of cementitious materials

There is no significant effect of the w/c can be seen as mostly all three w/c ratio concretes of each set are grouped together without showing any specific relationships. The only exception is P15S70R15 concrete of 0.40 w/c at 7 days age, which can be considered as an anomaly.

Though the effect of elevated curing temperature was more pronounced on concrete with higher rice husk ash content, a 5% to 7% increment at the age of 28 day on concrete with 15% rice husk ash based triple blend concrete is considered to be a good improvement in compressive strengths. This finding would certainly add values to the use of rice husk ash based triple blend concrete in a hot climate like Arabian Peninsula.

4.3.4.1 Summary

The compressive strength of concrete containing triple blend of cementitious materials of Portland cement, GGBS and rice husk ash have positively reacted with elevated curing temperature with increased compressive strength. However, this improvement is more pronounced with concrete containing higher rice husk ash proportion (25%) perhaps due to the higher pozzolanic reactions at higher curing temperature. This improvement is also time dependent as over the time the effect was reduced due to reduced pozzolanic activities at the later age of concretes.

4.3.5 Air entrained concrete series

In this series the effects of specific proportions of entrained air in the concrete have been examined to observe the effect of the entrained air on the compressive strengths of concretes. Four specific volume of air content of 2%, 5%, 10% and 15% of total concrete volume designed to entrain to a set of concrete made of 90% Portland cement and 10% microsilica of total cementitious content.

Though the maximum design air content was 15%, the maximum air content achieved during the test was 12% of total concrete volume. An air entraining admixture was used to entrain the required volume of the air into the concrete. Each concrete was again dived into 0.25, 0.32 and 0.40 w/c ratios to observe the effect of the air on varied w/c ratios.

Figure 4.25 plotted the compressive strengths of concrete with different air contents with three different w/c ratios. The trend lines drawn on the plotted data indicate that concrete at 0.40 and 0.32 w/c ratio had similar rate of loss of strength as the trend lines are almost parallel for all three ages.

However, at 0.25 w/c ratio this reduction was more moderate. Compressive strength results at 0.25 w/c ratio with 10% air content seemed to be relatively higher at all three ages, making the slope of the 0.25 w/c ratio trend line to be higher than the other two w/c ratio concretes. If this relatively higher result of 0.25 w/c @ 10% air content can be ignored, the slopes of all three w/c would be similar, giving a same trend of reduction of compressive strength over increased air content regardless of w/c ratio of concrete.

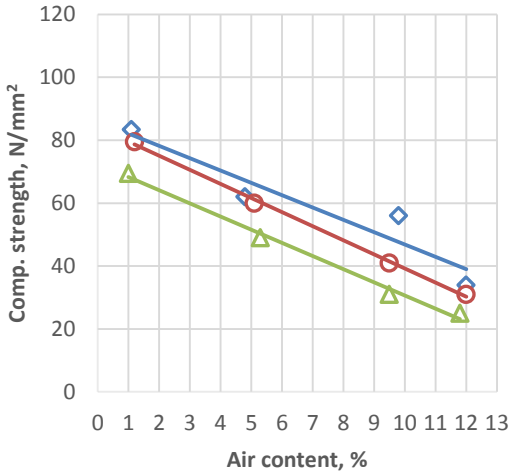

Figure 4.25a: 7 day age

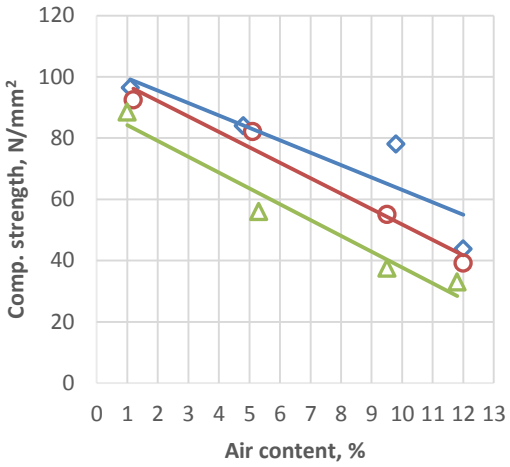

Figure 4.25b: 28 day age

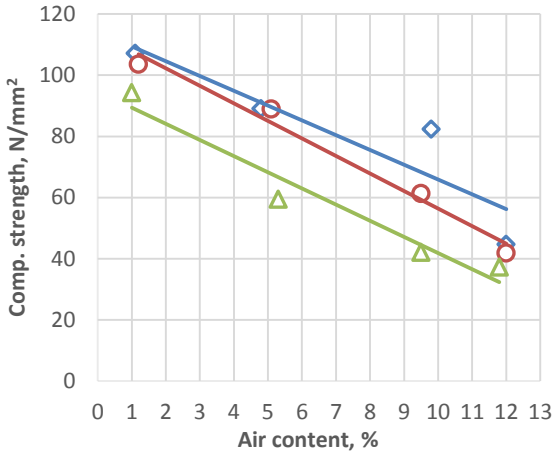

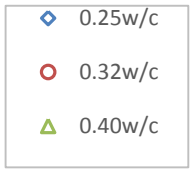

Figure 4.25c: 56 day age

Figure 4.25: Compressive strength of concrete with different air content at the age of 7, 28 and 56 day

The relative positions of the reduction in compressive strengths at the age of 28 days of concretes with different air contents have been plotted in Figure 4.26 where the reduction of compressive strength due to the increased air was calculated by comparing with the compressive strength gain of concrete with designed 2% air content. The actual achieved air content during the work is used to plot the horizontal axis of Figure 4.26.

As shown in Figure 4.26, the percentage reduction in compressive strength comparing with the same concrete with 2% air is substantially higher especially at 10% and 12% air content level. However, concrete with 5% air content at 0.25 and 0.32 w/c ratios posted a reduction of 13% and 11% which can be considered to be relatively low. This level of strength reduction could be addressed up to a certain extent possibly by using the excess finer particles of unwashed sand. Unwashed sand was not used for the concrete mixes with RCA in this series.

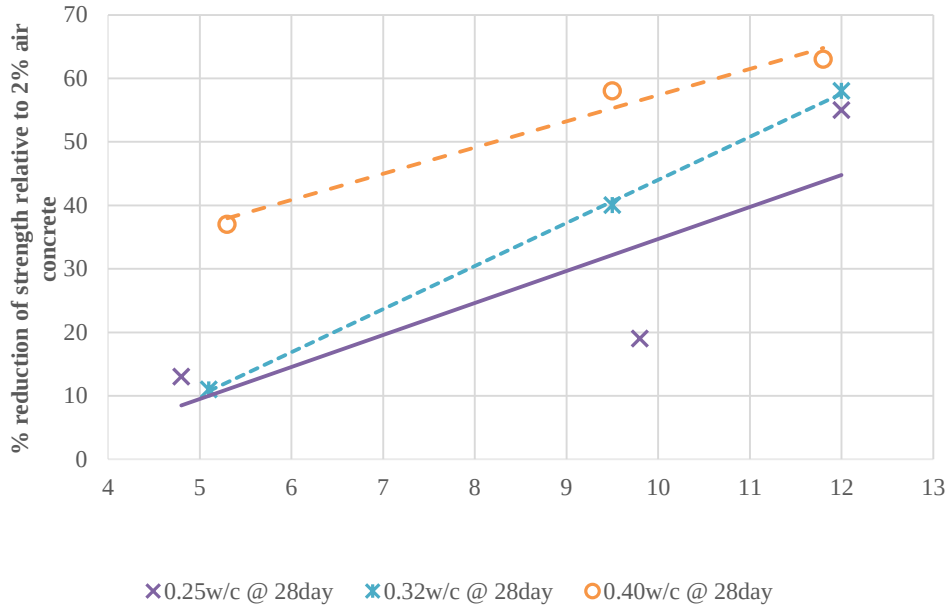

Figure 4.26: Percentage reduction of the compressive strengths of concretes with different air content relative to the concrete with 2% air content at 28 day age

A 37% reduction in strength between 2% and 5% air content with 0.40 w/c concrete seems to be excessively higher than normally expected comparing with 14% drop experience by Pinto, R.C.A., and Hover, K.C. (2001) at 90 days with 0.40 w/c ratio. Cordon, W. A., (1946) reported a drop of 12.5% at 28days with total cement content of 364 kg/m^3. This drop was lower for lower cement content concretes.

4.3.5.1 Summary

A linear relationship between the loss of compressive strength and increase in air content of concrete can be seen at all w/c ratio concretes. Concretes containing higher air content had huge reduction of compressive strengths especially at 10% and 12% air. This reduction was uniform for all three w/c ratio concretes. However concrete with lower w/c ratio and lower air content at 5% shown relatively better and more manageable reduction of strength.

4.4 Conclusion

In this chapter beside the plastic properties, compressive strength of concretes with different type of cementitious materials, aggregates, air content and curing temperatures have been presented and discussed.

It has been seen though the compressive strengths of concrete was reduced with increased GGBS content, this reduction could be offset by reducing the w/c ratio to any specific value. Concrete with 90% GGBS content at 0.25 to 0.32 w/c ratio would be able to achieve at least 64% to 77% of the compressive strength of equivalent concrete with 70% GGBS content. The rate of strength gain of high GGBS content concrete could also be enhanced by reducing the w/c ratio of the concrete.

Though use of microsilica and rice husk ash enhanced the compressive strength significantly, the eCO_2 credential of these two sets of pozzolanic materials are in question due to the requirement of very high content of Portland cement in the concrete. As the use of P20F80 and P0S100 concretes could not provide a consistent compressive strength result, a triple blend of P15S70R15 concrete appeared to be both consistent in good compressive strength and high replacement of Portland cement.

The effect of the unwashed sand adequately enhanced the compressive strengths of concrete, especially concrete at lower w/c ratio and at the age of 28 days, this perhaps indicates the effect of the finer particles contributed by the unwashed sand by achieving an optimum volume fraction for a possible particle packing of concrete. The enhancement of compressive strength of fly ash concrete with porous microstructures also validated its effectiveness.

The effect of unwashed sand to enhance the compressive strength was also demonstrated in RCA concretes, though the erratic hardening behaviour of 100% GGBS made it difficult to comprehend this output. For that reason, the triple blend (P15S70R15) of cementitious materials could be the ideal cementitious combination to demonstrate the effect of RCA on the compressive strength of concrete. It was seen that the reduction of compressive strength due to the increased proportion of RCA could be offset by reducing the w/c ratio of P15S70R15 concrete.

The compressive strength of the triple blend concrete could be further enhanced by elevating the curing temperature from 20°C to 40°C by emulating the high summer temperature of the Arabian Peninsula. Though the effect was more pronounced on higher rice husk ash concrete (P5S70R25), the concrete with 15% rice husk ash (P15S70R15) would be the appropriate choice of cement combination due to its relatively higher gain in compressive strength.

The approach to use higher air content to reduce the raw materials usage to produce a more sustainable concrete mix could be limited to 5% air as the reduction of compressive strength with the increment in air content was significantly high, even with 10% microsilica addition. However, a strength reduction of 11% by using 5% air could be more acceptable target. The loss of strength perhaps could be minimized further by using the higher finer fraction of unwashed sand.

However, one needs to be aware of issues related to plastic properties of higher air content concrete as concretes tend to become soft and foamy and lose its flowablity especially at low w/c concretes as described in Table 4.8 of Chapter 4. The actual air content on hardened concrete would also be another important issue, as the stability of air bubble during production, pumping and placement are important factors, which are not discussed in this study.

Chapter 5

Durability & Permeation Properties of Concrete

5.1 Introduction

In the previous chapter the plastic properties and compressive strengths of concrete have been presented and in this chapter the durability results and the permeation properties of concrete will be discussed. There are five types of durability tests have been performed on concrete samples to understand and validate their performance in chloride and sulfate environment which are the predominant risk factors for concrete structures in the Arabian Peninsula.

The durability tests were rapid chloride permeability test (RCPT) as per ASTM C1202-97, chloride diffusion (CEN TC51/WG12/TG5 - Draft 4 Version 2) and sulfate resistance test (modified version of ASTM C 1012 – 02). The test on the permeation properties were water absorption (BS1881:122) and water permeation (BS EN 12390:8) tests.

Table 5.1 – 5.7 show durability results including RCPT, water absorption and water permeation of concretes. No numerical results from the sulfate resistance test can be presented as all concrete samples immersed in rich sulfate solutions did not show any visual changes on volume expansion, distortion, length changes or any sign of sulfate attack. Only photographical evidences of the concrete bar have been presented.

Table 5.1: Durability properties of concrete at 28 days - Cement type series (washed sand)

No	Reference	Proportion of cementitious materials over total	W/C	RCPT	Water Absorption	Water Penetration
				Coulomb	%	mm
1	1P0S100W	100% GGBS	0.25	450	0.6	3
2	1P2.5S97.5W	97.5% GGBS	0.32	735	0.5	0
3	1P5S95W	95% GGBS	0.40	478	0.6	0
4	1P15S85W	85% GGBS	0.25	648.9	1.2	6
5	1P30S70W	70% GGBS	0.32	380	0.8	0
6	2P0S100W	100% GGBS	0.40	535	0.6	3
7	2P2.5S97.5W	97.5% GGBS	0.25	360	1.4	4
8	2P5S95W	95% GGBS	0.32	389	1.5	5.3
9	2P15S85W	85% GGBS	0.40	692.1	1.4	7
10	2P30S70W	70% GGBS	0.25	254	0.7	0
11	3P0S100W	100% GGBS	0.32	585	1.8	0
12	3P2.5S97.5W	97.5% GGBS	0.40	538	1.9	5
13	3P5S95W	95% GGBS	0.25	181	0.7	0
14	3P15S85W	85% GGBS	0.32	744.3	1.2	7
15	3P30S70W	70% GGBS	0.40	306	1.6	0
16	1P20F80W	80% Fly ash	0.25	253	0.5	2.8
17	2P20F80W	80% Fly ash	0.32	162.3	1.2	0
18	3P20F80W	80% Fly ash	0.40	274.8	1.4	0
19	1P90M10W	10% Microsilica	0.25	231.6	1.2	0
20	2P90M10W	10% Microsilica	0.32	185.1	1.2	0
21	3P90M10W	10% Microsilica	0.40	253.8	1.2	0
22	1P80R20W	20% RHA	0.25	287.1	0.7	0
23	2P80R20W	20% RHA	0.32	175.5	0.9	0
24	3P80R20W	20% RHA	0.40	198.9	1.3	0
25	1P15S70R15W	70% GGBS & 15% RHA	0.25	326.7	0.9	6
26	2P15S70R15W	70% GGBS & 15% RHA	0.32	430.2	0.9	3
27	3P15S70R15W	70% GGBS & 15% RHA	0.40	488.7	1.3	8

Table 5.2: Durability properties of concrete at 28 days - Sand type series (unwashed sand)

No	Reference	Proportion of cementitious materials over total	W/C	RCPT	Water Absorption	Water Penetration
				Coulomb	%	mm
1	1P30S70U	70% GGBS	0.25	475.2	0.7	0
2	2P30S70U		0.32	375.3	0.5	0
3	3P30S70U		0.40	342	0.7	0
4	1P0S100U	100% GGBS	0.25	491.1	1.4	0
5	2P0S100U		0.32	508.4	1.8	0
6	3P0S100U		0.40	701.1	1.8	1
7	1P20F80U	80% Fly ash	0.25	318.6	0.8	5
8	2P20F80U		0.32	612	0.9	5
9	3P20F80U		0.40	675.4	0.8	3
10	1P90M10U	10% Microsilica	0.25	324	0.7	2
11	2P90M10U		0.32	339.2	0.6	0
12	3P90M10U		0.40	541.8	0.8	0
13	1P80R20U	20% Rice husk ash	0.25	195.3	0.5	0
14	2P80R20U		0.32	272.7	0.6	0
15	3P80R20U		0.40	379.8	1.6	0

Table 5.3: Durability properties of concrete at 28 days - RCA series (washed sand / 100% GGBS)

No	Reference	Proportion of RCA over total	W/C	RCPT	Water absorption	Water Penetration
				Coulomb	%	mm
1	1R100N0W	100% Recycled	0.25	1400	1.2	W/P*
2	2R100N0W		0.32	1243	0.9	W/P
3	3R100N0W		0.40	1993	1.3	W/P
4	1R80N20W	80% Recycled + 20% Normal	0.25	1549	1	W/P
5	2R80N20W		0.32	1562	0.9	W/P
6	3R80N20W		0.40	1179	1.3	W/P
7	1R50N50W	50% Recycled + 50% Normal	0.25	1593	2.2	25
8	2R50N50W		0.32	1583	1.8	22
9	3R50N50W		0.40	1655	1.7	17
10	1R0N100W	100% Normal	0.25	450	0.6	3
11	2R0N100W		0.32	535	0.6	3
12	3R0N100W		0.40	585	1.8	0

*W/P: Water penetrated through the entire length of the 150mm concrete cube under testing.

Table 5.4: Durability properties of concrete at 28 days - RCA series (unwashed sand / 100% GGBS)

No	Reference	Proportion of RCA over total	W/C	RCPT	Water absorption	Water Penetration
				Coulomb	%	mm
1	1R100N0U	100% recycled	0.25	531	0.5	7
2	2R100N0U		0.32	511	1.5	8
3	3R100N0U		0.40	517.5	0.8	5
4	1R80N20U	80% recycled + 20% normal	0.25	623.7	0.8	7
5	2R80N20U		0.32	566.1	0.6	5
6	3R80N20U		0.40	602.1	0.5	5
7	1R50N50U	50% recycled + 50% normal	0.25	651.6	0.6	2
8	2R50N50U		0.32	1118.7	0.8	16
9	3R50N50U		0.40	801.9	1.1	20
10	1R0N100U	100% normal	0.25	491.1	1.4	0
11	2R0N100U		0.32	508.4	1.8	0
12	3R0N100U		0.40	701.1	1.8	1

Table 5.5: Durability properties of concrete at 28 days - the RCA series (P15S70R15)

No	Reference	Proportion of Recycle aggregate over total	W/C	RCPT	Water absorption	Water Penetration
				Coulomb	%	mm
1	1R100N0TB	100% recycled	0.25	1895.4	0.8	12
2	2R100N0TB		0.32	1906.2	1.0	7
3	3R100N0TB		0.40	2145.6	0.6	5
4	1R50N50TB	80% recycled + 20% normal	0.25	1344.6	1.0	3
5	2R50N50TB		0.32	552.6	0.7	0
6	3R50N50TB		0.40	1512.9	0.6	5
7	1R20N80TB	50% recycled + 50% normal	0.25	778.5	0.7	2
8	2R20N80TB		0.32	1077.3	0.9	0
9	3R20N80TB		0.40	1094.4	1.0	0
10	1R0N100TB	100% normal	0.25	638.1	0.9	0
11	2R0N100TB		0.32	647.1	0.7	3
12	3R0N100TB		0.40	701.1	0.6	5

Table 5.6: Durability properties of concrete at 28 days - the higher curing temperature series

No	Reference	Proportion of cementitious materials over total	W/C	RCPT	Water absorption	Water Penetration
				Coulomb	%	mm
1	1P5S70R25W	5%PC+70%GGBS+25%RHA	0.25	326.7	1.3	4
2	2P5S70R25W		0.32	450.9	1.5	0
3	3P5S70R25W		0.40	592.2	1.3	4
4	1P15S70R15W	15%PC+70%GGBS+15%RHA	0.25	326.7	0.9	6
5	2P15S70R15W		0.32	430.2	0.9	3
6	3P15S70R15W		0.40	488.7	1.3	8

Table 5.7: Durability properties of concrete at 28 days - the air entrained concrete series

No	Reference	W/C	Air content		RCPT	Water absorption	Water Penetration
			Design %	Actual %	Coulomb	%	mm
1	1P90M10A2	0.25	2	1.1	231.6	1.2	0
2	2P90M10A2	0.32	2	1.2	185.1	1.2	0
3	3P90M10A2	0.40	2	1.0	253.8	1.2	0
4	1P90M10A5	0.25	5	4.8	32.4	1.3	0
5	2P90M10A5	0.32	5	5.1	27.3	1.3	0
6	3P90M10A5	0.40	5	5.3	27.3	1.1	0
7	1P90M10A10	0.25	10	9.8	245.7	1.2	12
8	2P90M10A10	0.32	10	9.5	141	1.5	9
9	3P90M10A10	0.40	10	9.5	55.8	1.6	11
10	1P90M10A15	0.25	15	12	46.8	1.3	11
11	2P90M10A15	0.32	15	12	237.6	1.3	11
12	3P90M10A15	0.40	15	11.8	293.4	1.3	8

5.2 Rapid Chloride Permeability Test (RCPT)

Rapid chloride permeability test as discussed in Chapter 3 is an indirect test of chloride permeability by passing electric charge (ampere) over 6 hours period of time to get total charge passed in coulomb. This is a function of the type and quality of hydration products of cement paste and the conductivity of pore solutions. In this section the results of concrete specimen tested for RCPT have been discussed.

As discussed in Chapter 3 (Table 3.18), ASTM C1202-97 classified the chloride ion permeability of concrete according to the coulomb values ranging from high, moderate, low, very low and negligible category. Concretes with RCPT values between 100 – 1000 coulomb have been classified as concrete with very low chloride permeability. In this work the acceptable range of the RCPT value was targeted at maximum 1500 coulomb as in the Arabian peninsula RCPT value of below 1500 coulombs is considered to be an acceptable value for concrete structure subject to severe chloride exposure (GASCO, 2007 / ADNOC).

5.2.1 RCPT of cement type series

In the Cement type series concretes were made with different types of cementitious materials to look into the effect of these materials on the performance of concrete. Different proportions of GGBS, fly ash, microsilica and rice husk ash were used to replace the Portland cement to reduce the embodied CO_2 of the concretes.

5.2.1.1 RCPT of concrete with GGBS

The chloride permeability of all concretes containing GGBS was very low, according to ASTM C1202-97 criteria, as the coulomb values ranged from 181 – 744 coulombs (Figure 5.1). The lines at 2000 coulombs and 1000 coulombs read ‘Low’ and ‘Very low’ of chloride ion penetrability of concrete as per ASTM C1202-97. As discussed earlier in Chapter 3, the coulomb values depend on the concrete paste quality and the conductivity of pore solution, different proportion of GGBS and w/c ratio would affect the RCPT values. The following sections will examine these effects.

Effect of different proportion of GGBS:

The RCPT values of concrete containing GGBS ranging from 70% to 100% of total cementitious content are illustrated in Figure 5.1. Though the overall individual results are outstanding giving RCPT values of below 1000 coulombs, there is no specific relationship with the proportion of GGBS can be seen. Concretes containing 70% GGBS had the least coulomb values indicating optimum hydration of the paste compared with higher GGBS replaced concretes. Inadequate hydration at higher replacement of GGBS could result into variable coulomb values.

The varied results could also be attributed to the fact that RCPT test results as per ASTM C1202 are highly variable. A maximum variation of 42% has been acknowledged in the standard.

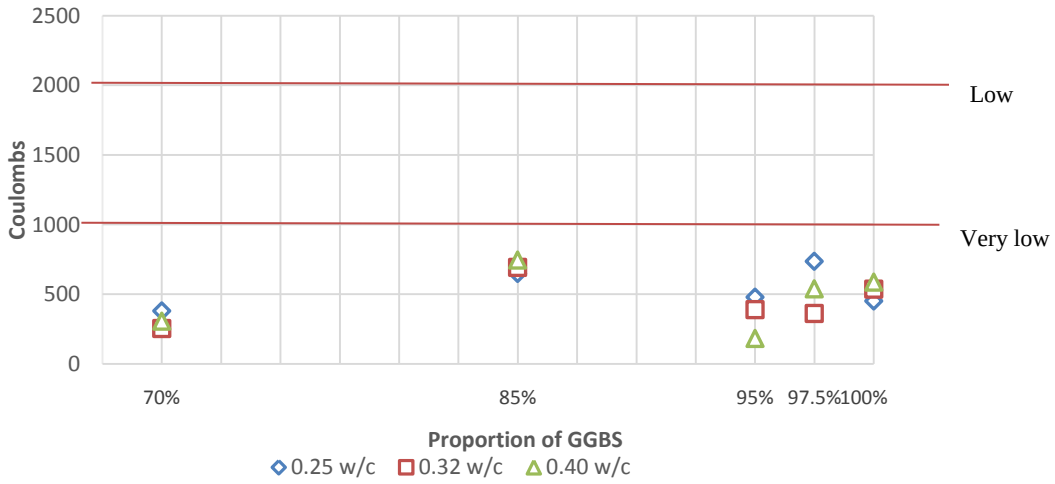

Figure 5.1: RCPT results of Cement type concrete – concrete with GGBS

Effect of w/c:

The RCPT values would normally be expected to reduce with w/c ratio as the concrete microstructure improved with reduced w/c ratio; but this is not demonstrated in Figure 5.1. This is perhaps due to the fact that, concretes with very high replacement level of supplementary cementitious materials which already reduced the RCPT values drastically below 1000 coulombs could not be affected further by the reduction of w/c ratio. Moreover, the range of w/c ratio investigated itself was very low (0.25 to 0.40). The high variability of the test results as recognized by the ASTM C1202 could also be the reason.

5.2.1.2 RCPT of concrete with other cement combinations

The chloride ion permeation resistance of concrete made with high volume fly ash (P20F80), microsilica (P90M10) and rice husk ash (P80R20) further enhanced compared with the GGBS concrete (Figure 5.2) with coulomb values ranging from 162-287 coulombs. However, concrete made with triple blend of Portland cement, GGBS and rice husk ash (P5S70R15) posted around 650 - 700 coulombs, well below the 'very low' level as specified by ASTM C1202. To compare the performance of GGBS with these three set of concretes two concretes made of 70% (P30S70) and 100% (P0S100) GGBS of total cementitious content were considered in the Figure 5.2.

Effect of different pozzolanic materials:

The coulomb values of concrete made with pozzolanic materials with high silica content (Fly ash, microsilica and rice husk ash) were extremely low falling below 300 coulombs. This could be due to the fact that the pozzolanic materials reduced the alkalinity of the pore solution of the hydrated cement paste and effectively reduced the conductivity of the concrete (Bentz, 2007) providing lower RCPT values.

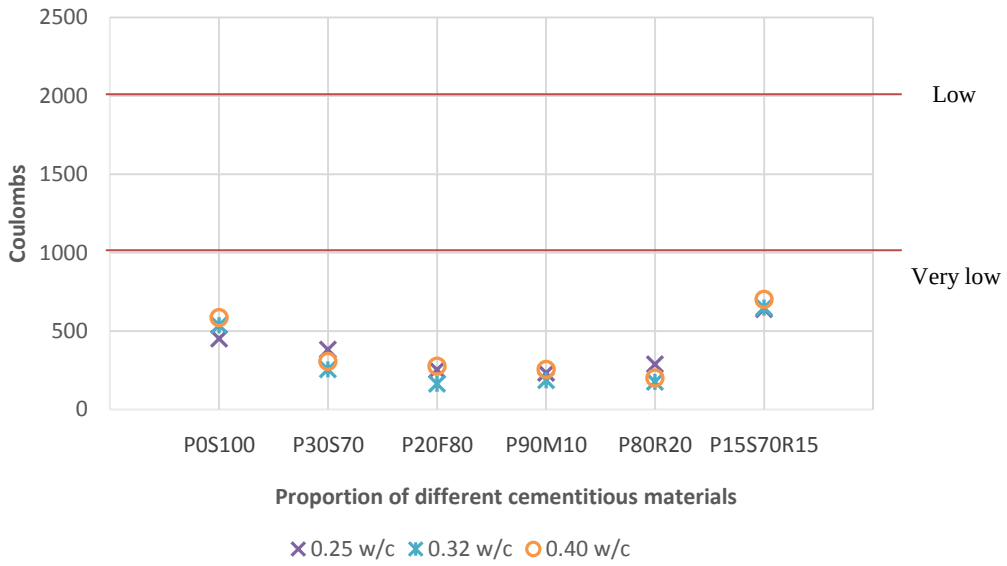

Figure 5.2: RCPT results of cement type concrete – including others

80% fly ash effectively performed very similarly to 10% microsilica and 20% rice husk ash concrete. The SiO_2 content of fly ash, microsilica and rice husk ash used in this work were 61.3%, 92.2% and 87.6% by weight respectively providing a net contribution of SiO_2 of 49.0%, 9.2% and 17.5% by each of these three materials. The contribution of SiO_2 by 100% and 70% GGBS concrete were 34.5% and 24.1% respectively. Though the degree of reduction on RCPT values was not proportionate to the SiO_2 contribution by each materials (perhaps due to other electro-chemical properties of those materials), it could be concluded that concretes with very high volume replacement of fly ash has equal or better RCPT values compared with GGBS (70%), Microsilica (10%) and 20% rice husk ash concrete.

Effect of w/c:

Similar to Figure 5.1 with different proportion of GGBS, the RCPT values of concretes with different cementitious materials (Figure 5.2) were not affected by their w/c ratios. As mentioned before the effect of w/c could not be visualized due to i) the effect of using very high replacement of supplementary cementitious materials which already brought down the coulomb value to a very low level, ii) testing variability and iii) low range of w/c ratio.

5.2.2 RCPT of sand type series

Figure 5.3 shows the chloride ion permeability values of concretes containing unwashed sand with higher fine contents. In general the RCPT results of all concrete posted a very good coulomb values ranging from 195 to 701 coulomb demonstrating that concrete made with different proportion of supplementary cementitious materials with unwashed sand (containing 10% of finer particles passing 75µm) could produce very durable concrete to sustain chloride laden environment.

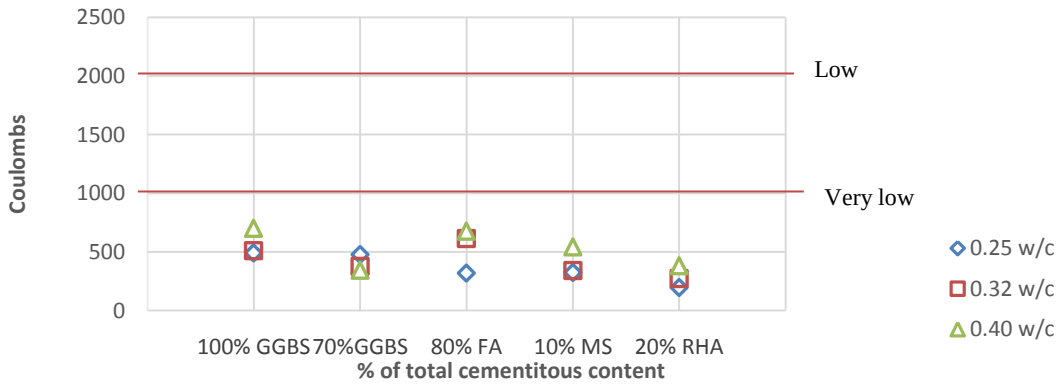

Figure 5.3: RCPT results of concrete with unwashed sand

5.2.2.1 Effect of unwashed sand

Though the RCPT results were within the acceptable range, the effect of unwashed sand in the concrete is not visible. In Figure 5.4 chloride ion permeation results for both washed and unwashed sand concretes are plotted together to visualize the direct comparison between them. In fact the chloride ion permeability values of almost all concrete made with unwashed sand tends to be greater than concrete made with washed sand. This shows that the washed sand failed to post any positive effect to lower the chloride ion permeability.

This could be due to the fact that the expected void filling with an additional 10% filler (of total 5mm aggregate content) of a size of below 75µ could not have substantial effects on the electrochemical properties of concrete to post a positive improvement on the RCPT results as RCPT is a test to measure the electro-chemical properties of concrete. Nevertheless, the very low coulomb values of all concrete made with unwashed sand showed that these concretes were extremely durable against any ingress of chloride ions.

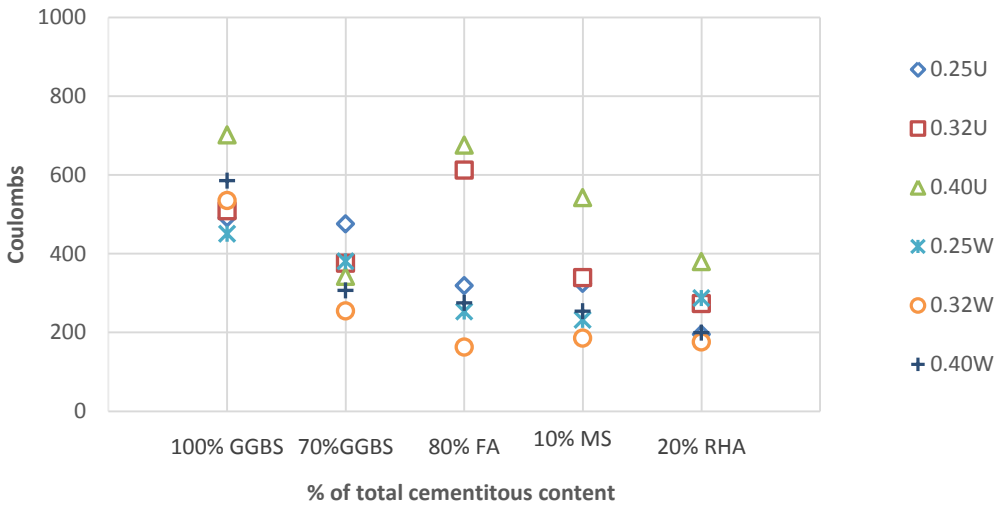

Figure 5.4: RCPT results of concretes made with washed and unwashed sand

5.2.2.2 Effect of different cement combination

Figure 5.4 shows that concrete made with microsilica and rice husk ash had the lowest chloride penetration values compared with the GGBS and fly ash concrete. This is in consistent with the concrete made with washed sand, though with unwashed sand concrete the results were little higher. The results of 70% GGBS concrete are comparable with the results of microsilica and rice husk ash concretes with chloride penetration results were around 500 coulombs and below. The performance of 100% GGBS and fly ash concretes was quite close ranging between 500-700 coulomb.

Similar to concrete with washed sand, the effect of w/c ratio on the chloride penetration resistance is not clearly demonstrated, especially between 0.32 and 0.25 w/c concrete. Most of unwashed sand concrete with 0.40 w/c ratio had the maximum coulomb values, demonstrating some effect of w/c ratio on the chloride ion penetration resistance values.

5.2.2.3 Comparing with published data

The RCPT results of concrete with GGBS and other pozzolanic materials are seem to be well below the published data of similar cementitious content and w/c ratio. Ahmed, M.S., et. al. (2009) published 28 days RCPT results of 0.38 w/c ratio concretes containing 10% microsilica, 70% GGBS and 70% fly ash were 1100, 1,500 and 6,000 coulomb respectively. Guneyisi, E. and Gesoglu, M. (2008) published 1,600 and 1580 coulombs for 70% and 80% GGBS concretes. The w/c ratio of these two concretes was 0.40 w/c and the test age was 28 days. At 90 days the results were 960 and 880 coulombs respectively.

However, Nikam, V.S. and Tambvekar, V.Y. (2003) reported much improved RCPT results for concrete with triple blend made with 37% PC, 60% GGBS, 3% microsilica and 55.5% PC, 37% fly ash, 7.5% microsilica. At 28 days the RCPT results of these two sets of concretes were 726 and 885 coulomb respectively. These very low coulomb values were achieved using total 320 kg cementitious materials with 0.45 w/c ratio.

5.2.3 RCPT of recycled concrete aggregate series

In the RCA series 100% GGBS concrete was tested with various combinations of coarse recycled concrete aggregates and natural aggregates proportions. In this section the RCPT results of RCA concretes are analysed to examine the effect of i) the RCA proportion ii) the unwashed sand and iii) the various w/c ratio on coulomb values to determine their respective ability to resist chloride ion penetration.

5.2.3.1 Effect of RCA content

Figure 5.5 and Figure 5.6 represents RCPT test results of RCA series concrete made with washed and unwashed sand. The chloride penetration values for concretes with RCA and washed sand are very high ranging between 1000 to 2000 coulombs compared to other results obtained in this study. However, chloride penetration values between 1000 - 2000 coulomb is still considered to be 'Low' as per ASTM C1202-97. There is no any significant effect of the RCA contents can be observed in Figure 5.5 where all 3 sets of concrete with different proportion of RCA contents posted almost similar results which is approximately 1500 coulombs in average. However, compared with concretes without any RCA, these results were very high which was almost 3 times higher.

Wee, T.H., et. al., (1999) found out that due to higher conductivity of cement paste compared to coarse aggregate, concrete containing higher cement paste and lower coarse aggregate tends to have higher RCPT values, though this could be misleading as the actual chloride penetration of higher cement paste fraction concrete is lower. Therefore, the higher RCPT of RCA concrete could be contributed by the hardened paste fraction of RCA.

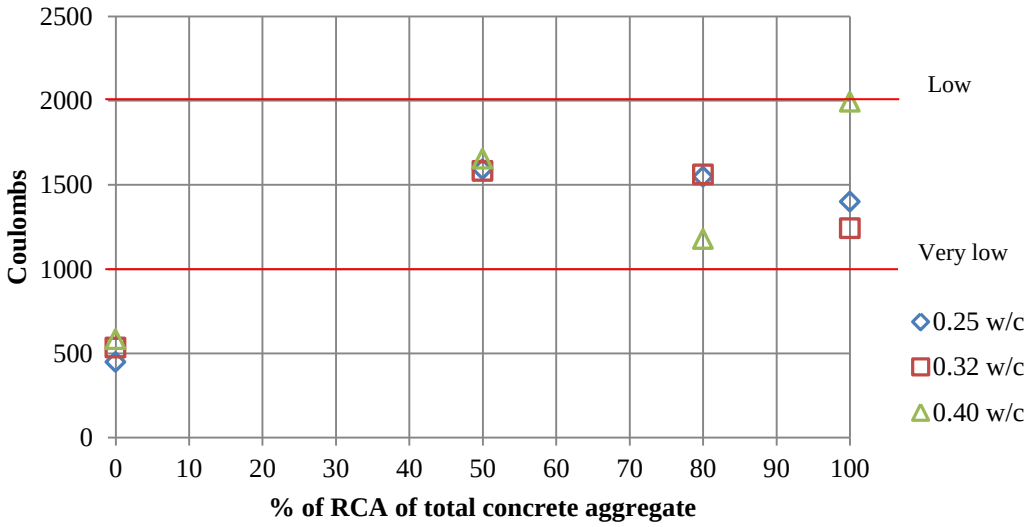

Figure 5.5: RCPT results of coarse RCA with washed sand

Similarly for concretes with RCA and unwashed sand, though the results were much improved, but the effect of RCA content was not demonstrated. Except for 50% RCA concrete, all concrete including without RCA had very similar chloride ion penetration results of around 500 - 600 coulombs which is similar to concrete without any RCA.

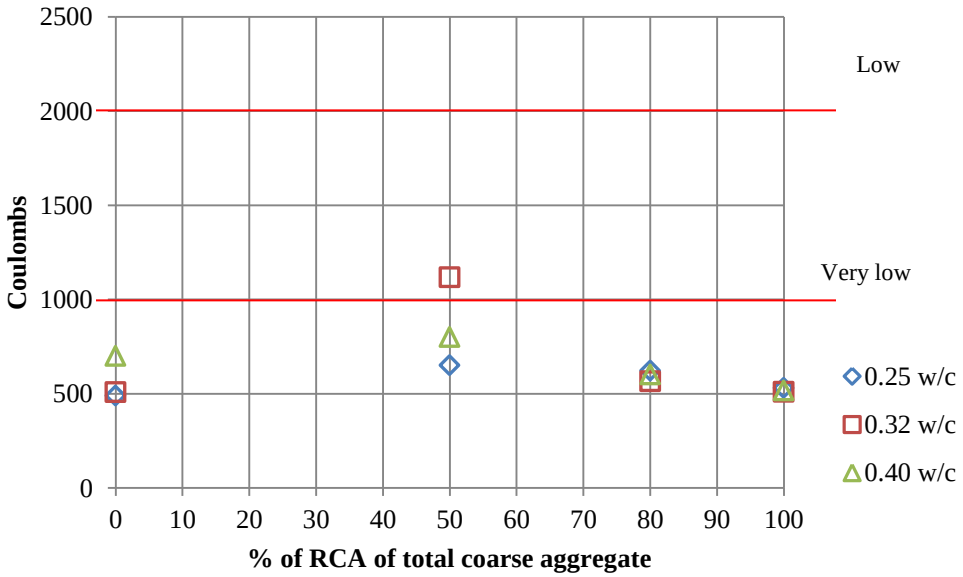

Figure 5.6: RCPT results of coarse RCA with unwashed sand

5.2.3.2 Effect of unwashed sand

The recycled aggregate series showed a very clear reduction in chloride ion penetration due to the effect of the unwashed sand. In the previous series with normal aggregate, the unwashed sand concrete could not demonstrate any improvement on chloride penetration values, though the overall results were very impressive. In RCA series however, as Figure 5.7 illustrates concrete with all RCA proportions at all three w/c ratio had significant improvement on the resistance of chloride ion penetration.

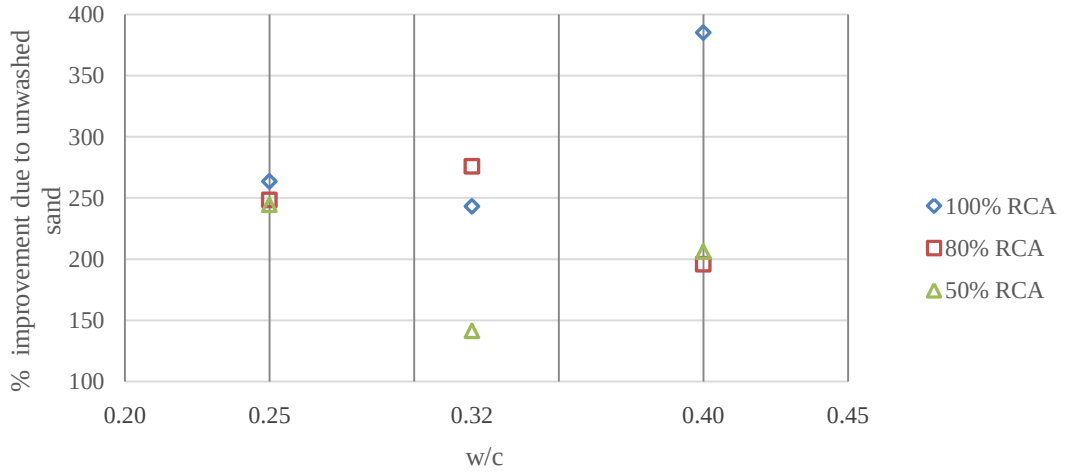

Figure 5.7: Improvement of the resistance of chloride ion penetration due to the effect of unwashed sand in RCA concrete

Figure 5.5 and Figure 5.6 are also clearly demonstrating the effect of unwashed sand in terms of chloride ion penetration resistance. Most of the results of unwashed sand concrete are below 1000 coulombs mark indicating very low penetration of chloride ion and on the other hand for washed sand concrete most of them are between 1000 - 2000 coulombs marks positioning in between low and very low region.

A possible answer to the question as why the effect of unwashed sand was not demonstrated for normal aggregate concrete could be that the chloride ion penetration results of washed sand concrete with normal aggregate was already very low, below 500 coulombs, which was already close to their optimum level and any further addition of finer particles contributed by the unwashed sand could not improve it further. But for the RCA concretes with washed sand, the chloride ion penetration values were higher with average values of 1500 coulombs, and thus the impact due to the finer particles was demonstrable.

5.2.3.3 Effect of w/c

Figure 5.5 and 5.6 for both washed and unwashed sand RCA concrete do not show any relationship between the chloride ion penetration resistance and w/c ratio. Furthermore Figure 5.7, shows no influence of w/c ratio on the performance improvement due to the effect of unwashed sand. It has been seen from the literature that concrete with Portland cement and higher w/c ratio of 0.40, 0.50 and 0.60 the RCPT results increased with increased w/c ratio (Chang, J.J. et. al., 2004), however, in this study the effect of w/c on RCPT was largely not visible, perhaps due to very low water cement ratio and use of high volume supplementary cementitious materials.

5.2.4 RCPT of RCA with triple blend

In this concrete a triple blend of 15% Portland cement, 70% GGBS and 15% rice husk ash was used together with washed sand. The objective of the series was to observe whether the RCA with this triple blend of cementitious materials could provide better performance compared with concrete with RCA and 100% GGBS. Figure 5.8 presents the RCPT results of this series. The RCA proportion of the triple blend series was modified with a 20% RCA instead of 80% RCA of total coarse aggregate content used in 100% GGBS RCA series.

5.2.4.1 Effect of RCA content

Figure 5.8 shows a clear trend of higher chloride ion penetration with higher RCA content for same w/c ratio concretes. Concrete with 100% RCA had the highest chloride ion penetration at an average value of around 2000 coulombs followed by concrete with 50%, 20% and 0% RCA concrete. The sudden drop at 0.32 w/c for 50% RCA concrete could be considered as an anomaly due to high variability in results recognized by ASTM C1202-97.

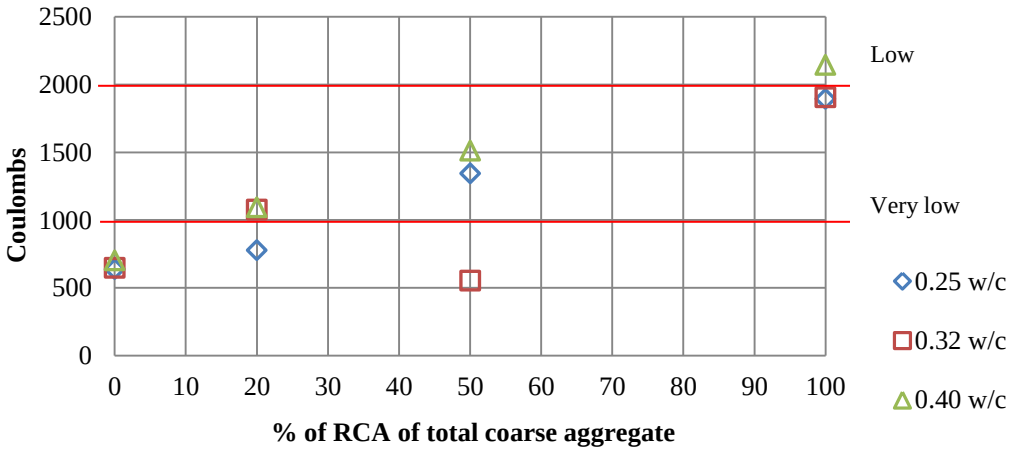

Figure 5.8: RCPT results of concrete with RCA and P15S70R15

Though the chloride ion penetration for 100% RCA was at higher end of 'Low' range of chloride ion penetrability index as suggested by ASTM C1202-97, the results of 50% and 20% RCA concrete concretes were well within the acceptable range of the local industries of the Arabian peninsula (ADNOC, GASCO 2007) at below 1500 coulombs. It is to be noted that in this series only washed sand was used. Use of unwashed sand using additional filler would have reduced the chloride ion penetration further as demonstrated by the previous RCA series.

5.2.4.2 Effect of w/c

No significant effect of the w/c can be observed in Figure 5.8, though there was an increase in chloride ion penetration at 0.40 w/c could be seen for all types of concrete compared with 0.25 and 0.32 w/c results. Similar trend has also been noticed with concrete with natural aggregate made with unwashed sand as discussed earlier.

5.2.5 RCPT of higher curing temperature series concretes

In this series, two sets of triple blend concrete containing different proportion of Portland cement, GGBS and rice husk ash P5S30R25 (5% Portland cement + 70% GGBS + 25% rice husk ash) and P15S70R15 (15% Portland cement + 70% GGBS + 15% rice husk ash) were made to study the effect of elevated curing temperature on the performance and properties of the concrete. The concrete was cured at 20°C and 40°C and each set of concrete was made of 0.25, 0.32 and 0.40 w/c to examine whether there was any effect of the w/c at this condition. The sand used was washed sand.

In this section the results of the RCPT values have been discussed to evaluate the effect of i) temperature ii) different cementitious proportion and iii) w/c ratio on the chloride ion penetration resistance of concrete.

5.2.5.1 Effect of temperature

Figure 5.9 illustrates the chloride ion penetration values of concrete made with different proportion of three cementitious materials and cured at 40°C temperature. In general the results are extremely low ranging from 327 to 592 coulombs. To study whether there is any improvement on the properties due to higher curing temperature, another set of concretes made of P15S70R15 was cured at 20°C beside the 40°C curing regime.

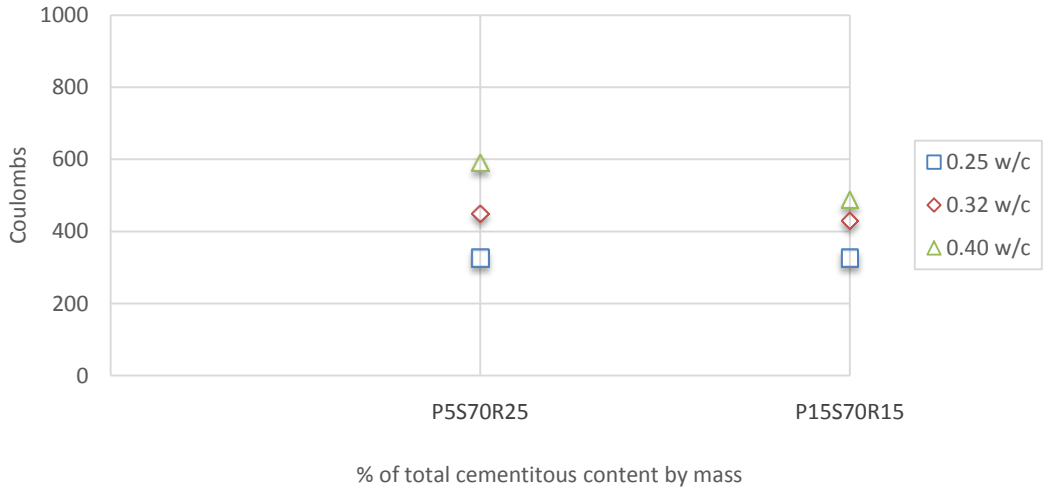

Figure 5.9: RCPT results of Portland cement, GGBS and rice husk ash blend concrete cured at 40°C

Figure 5.10 compares the RCPT values of these two sets of concrete. The improved resistance to the chloride ion penetration in terms of coulomb values of all 3 sets of concrete at different w/c ratio were very significant ranging from 30% to 50% reduction from concrete cured at 20°C temperature. This shows that the elevated curing improved the microstructure of concrete resulting better resistance to electric charge passed.

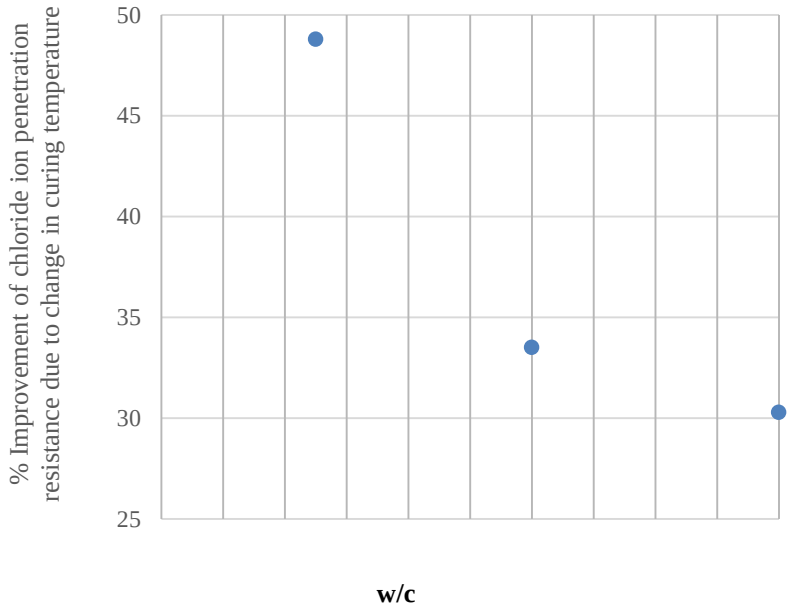

Figure 5.10: Improvement of chloride ion penetration resistance due to higher curing temperature from 20°C to 40°C of P15S70R15 concrete

5.2.5.2 Effect of different cementitious proportions

In this series there were two proportion of Portland cement, GGBS and rice husk ash used where Portland cement and rice husk ash proportions was varied as 5/25 and 15/15 respectively while keeping the GGBS at 70% for both. Figure 5.9 shows that the results of chloride ion penetration resistance were affected slightly due to this variation of Portland cement and rice husk ash. Concretes with lower Portland cement and higher rice husk ash had slightly higher coulombs than the concretes with higher Portland cement and lower rice husk ash. Though this slight higher results could be insignificant due to very high variability recognized by ASTM C1202, nevertheless presence of higher Portland cement contributed to better hydration products may have provided some positive effect to the lower coulomb values.

5.2.5.3 Effect of w/c

The triple blend concretes cured at 40°C temperature demonstrated a very clear trend of positive improvement of rapid chloride penetrability resistance when the w/c ratio was reduced further. Figure 5.11 shows that the improvement can be ranged from 12% to 45% depending on the proportion of cementitious materials. The most significant improvement was observed for 25% rice husk ash concretes where a substantial 45% improvement of chloride ion penetration resistance was recorded between concrete made of 0.40 w/c and 0.25 w/c ratio. Concretes with 15% rice husk ash also demonstrated significant improvement of chloride ion penetration resistance by reducing the w/c ratio, though at a reduced rate than the 25% rice husk ash concretes. This demonstrates that at higher curing temperature, the effects of reduced w/c ratio on the chloride ion penetration resistance are very significant.

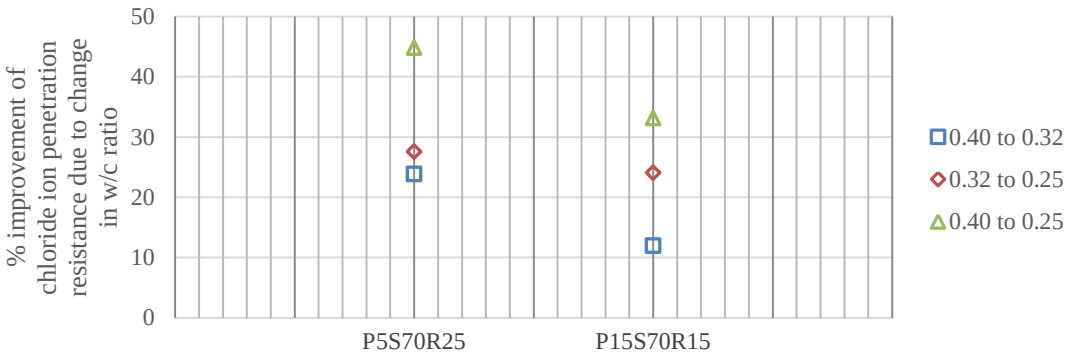

Figure 5.11: Effects of w/c ratio on the chloride ion penetration resistance for concrete cured at 40°C temperature

5.2.5.4 Combined effect of increased curing temperature and reduced w/c

The higher chloride ion penetration resistance observed due to increased curing temperature was positively affected by the reduced w/c ratio as demonstrated by Figure 5.10. There was a net 19% improvement of chloride ion penetration resistance between concrete with w/c ratio of 0.40 cured at 20°C and concrete with w/c ratio of 0.25 cured at 40°C temperature. The improvement of chloride ion penetration resistance between 0.40 to 0.32 w/c ratio and 0.32 to 0.25 w/c ratio concretes are 4% and 15% respectively (Figure 5.10). This demonstrates an improved chloride ion penetration resistance with the combined effect of reduced w/c ratio and increased curing temperature.

5.2.6 RCPT of air entrained concrete series

In the Air entrained concrete series the effect of increased air content on the properties of concrete was studied. Concretes made with 10% microsilica and washed sand were entrained with 2, 5, 10 and 12% air and tested for strength and durability performances. In this section beside the effect of the air, effect of the w/c ratio of the air entrained concrete on the chloride ion penetration resistance have been examined.

5.2.6.1 Effect of the air content

The chloride ion penetration resistance of the concretes of this series are extremely low (Figure 5.12). All three results at 5% air are below 100 coulombs registering 'negligible' chloride ion penetrability status as per ASTM C1202-97. The similar results can also be seen for 10% and 12% air concrete for 0.40 w/c ratio and 0.25 w/c ratio respectively. All Other results are below 300 coulombs registering the lowest results of chloride ion penetration resistance in this work.

These extremely low results could be attributed to the presence of 10% microsilica as well as higher air content which created a physical barrier for electric charges to pass through the concrete matrix during the testing process. It is interesting to observe that the RCPT values remains very low even the compressive strength of concrete due to higher air content have been significantly low.

From the literature it can be seen that RCPT values increased with reduced compressive strength due to increased w/c ratio for concrete with 100% Portland cement but in the presence of supplementary cementitious materials the increment of RCPT due to reduced compressive strength becomes negligible. The same study also suggests that the RCPT values of concrete with 5% air and 15% metakaolin (96.88% SiO_2, very similar to the microsilica used in this study) at 0.32 w/c ratio are at negligible level, similar to the results shown in Figure 5.12 (Dhinakaran, G. et. al., 2012).

No correlation between air content and the chloride ion penetration resistance of concrete could be established perhaps due to the fact that chloride ion penetration resistance was very low and was already at an optimum level.

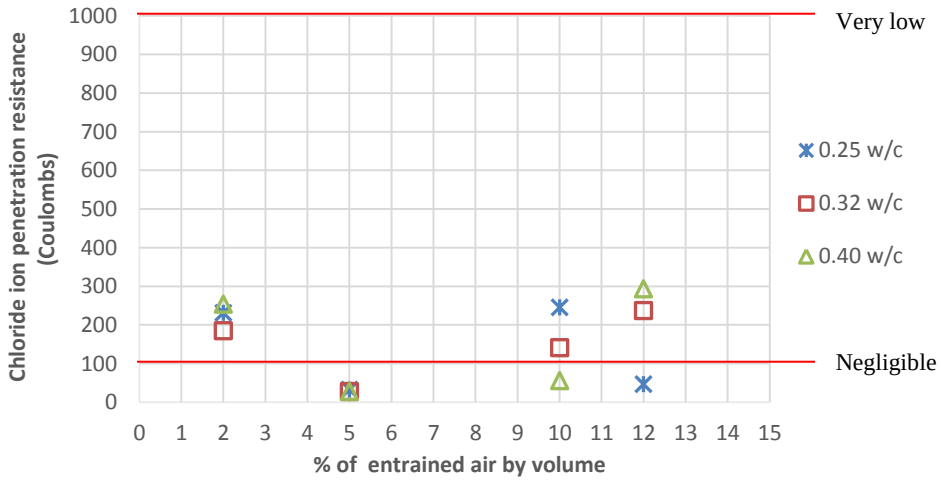

Figure 5.12: Results of chloride ion penetration resistance of concrete of air entrainment series

5.2.6.2 Effect of the w/c ratio

There is no any consistent relationship with the w/c ratio and chloride ion penetration resistance can be established from the Figure 5.12. This could be attributed to the extremely low results due to the factors of air and microsilica diminished the effects of w/c ratio.

5.3 Water Absorption

In this section the water absorption of different types of concretes have been analysed to determine the effect of different combinations of constituents of concrete on the water absorption. The effect of different w/c ratio on water absorption has also been examined.

5.3.1 Water absorption of cement type series

Figure 5.13 and 5.14 present the water absorption values of concrete containing washed sand. Figure 5.13 presents concretes containing only GGBS at different proportions and Figure 5.14 shows concrete containing other cementitious materials (fly ash, microsilica and rice husk ash) including 70% and 100% GGBS mixes.

It was interesting to investigate whether the proportion of GGBS content at very high level would have any positive impact on the permeation properties of concrete. However, Figure 5.13 does not give any clear correlation between the GGBS content and water absorption. This is perhaps due to the fact that at this very high level of replacement there was no significant additional improvement on the microstructure of concrete had happened to provide any positive impact on the water absorption properties.

The effect of w/c ratio on the water absorption values of concrete made with different proportion of GGBS are demonstrated in the Figure 5.13 with 0.40 w/c ratio is largely with higher water absorption except for 95% and 85% GGBS mixes. The variation of water absorption values could be attributed to the variations due to the testing precision between each tests conducted in the laboratory.

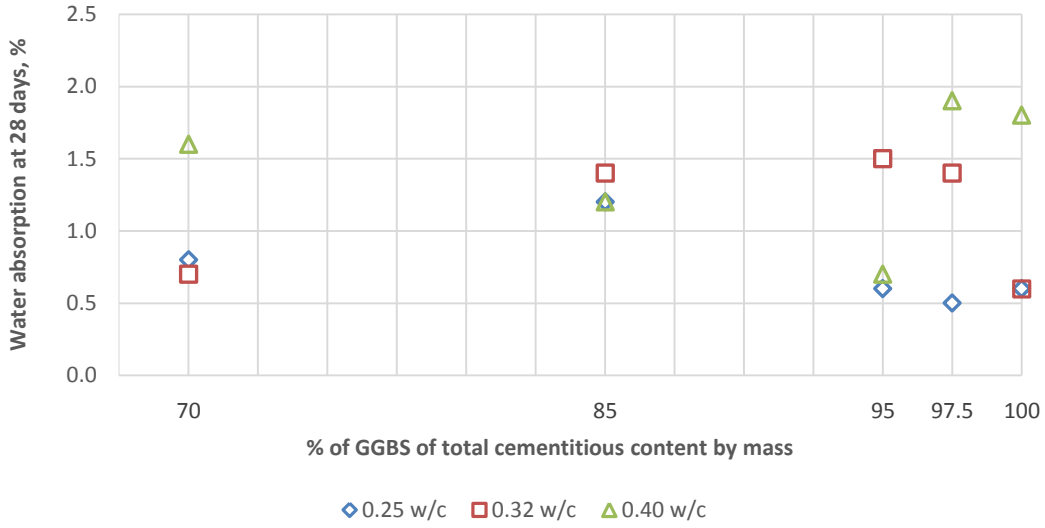

Figure 5.13: Water absorption – Cement type / washed sand (GGBS only)

Figure 5.14 is however, more consistent on the effect at 0.40 w/c ratio on the water absorption values of concrete made with different type of cementitious materials. The water absorption values of 0.40 w/c ratio concretes are consistently higher than the lower w/c ratio concretes (except P15S70R15), though there was no any significant relationship between 0.25 & 0.32 w/c ratio and water absorption values can be obtained. This is perhaps due to the fact that both w/c ratio were too low for any significant differences to demonstrate.

The results are also getting better toward triple blend concrete with P15S70R15 cementitious combination.

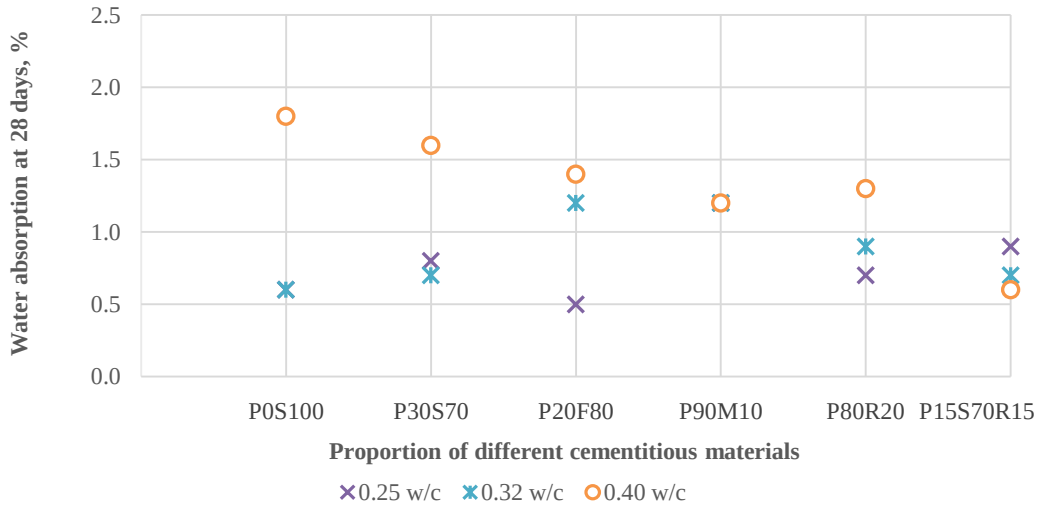

Figure 5.14: Water absorption – Cement type / washed sand

The difference on the effect of different cementitious materials on the water absorption properties is also non-significant though all results were below 2.0%, which is within the accepted level of this study as mentioned in Chapter 3 (Table 3.19). The results in Figure 3.13 and Figure 3.14 are found to be similar to water absorption results reported by a similar study by Elchalakani, M. et. al., (2014) where concrete containing high volume GGBS and fly ash blend achieved below 2% water absorption without any significant effect of the proportion of GGBS content.

There is no relationship between the water absorption values of concrete made with 0.25 and 0.32 w/c ratio concretes could be due to variability due to human and testing factors as reported by Pocock, D. and Corrans, J. (2007). The coefficient of variation of water absorption tests was found to be around 5.6%.

5.3.2 Water absorption of sand type series

Figure 5.15 presents the water absorption values of concrete containing unwashed sand. There was an overall improvement of water absorption values for concrete with unwashed sand compared with concrete with washed sand (Figure 5.14) demonstrating the effect of the excess filler of unwashed sand on the water absorption properties of concrete.

To analyse further on the effect of the unwashed sand on the water absorption properties, Figure 5.16 has shown a direct comparison of water absorption values for each type of concrete with its respective w/c ratio. As the void filling at unwashed sand is presumed to be enhanced compared with the washed sand due to the presence of additional limestone powder at the lower range of particle size distribution, the water absorption values for unwashed sand concretes should be better than the concretes made of washed sand.

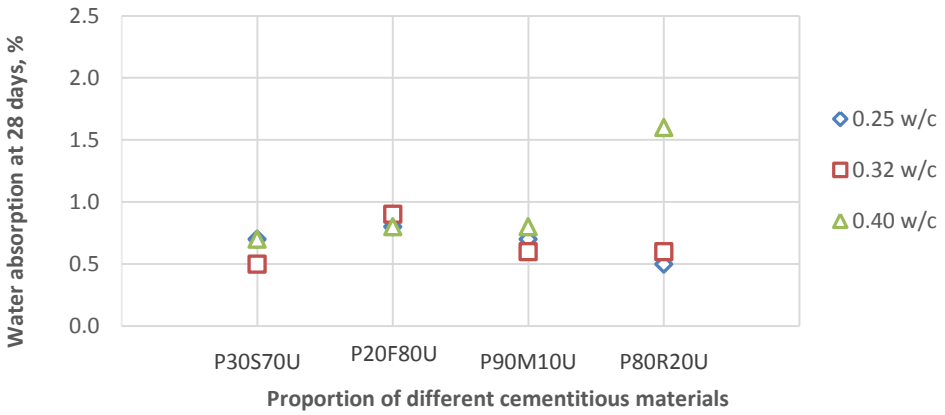

Figure 5.15: Water absorption – Sand type / unwashed sand

However, Figure 5.16, did not reflect that all the time. Concretes made with unwashed sand at 80% fly ash (0.25 w/c) and 20% rice husk ash (0.40 w/c) had higher water absorption values compared to the same concretes with washed sand. Nevertheless, in general concretes with additional filler produced better absorption properties compared to concretes with no additional filler. Higher water absorption of 1P20F80U and 3P80R20U can be attributed to human factors.

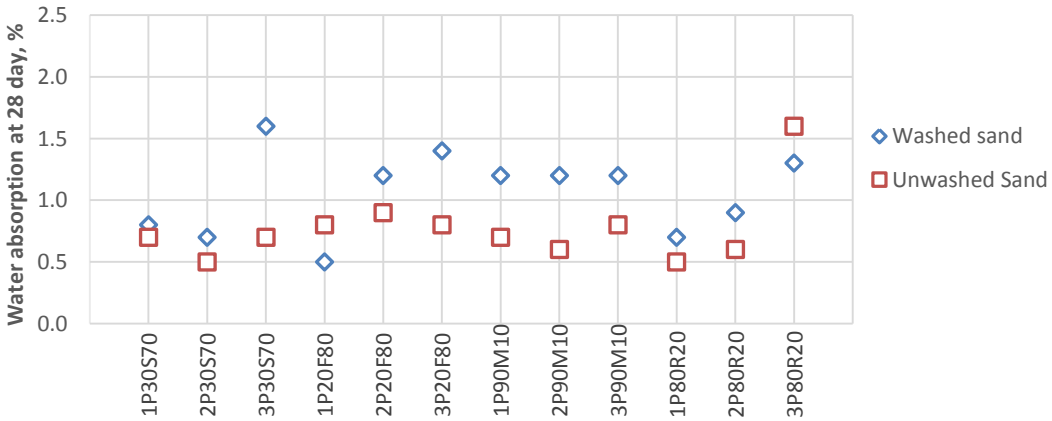

Figure 5.16: Water absorption – washed sand vs. unwashed sand concrete (Cement type vs. Sand type)

To understand the positive effect of using unwashed sand on different w/c ratio, Figure 5.17 is drawn. It illustrates the percentage of the improvement of water absorption values due to the effect of the additional filler of unwashed sand comparing with washed sand concrete.

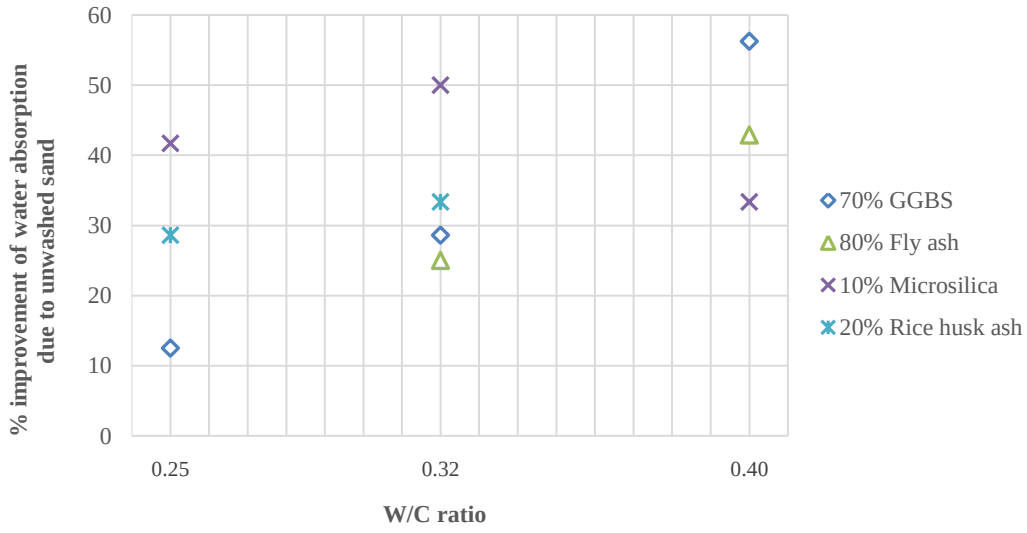

Figure 5.17: Improvement of water absorption properties due to unwashed sand compared to concrete made with washed sand

It has been observed that the effect of the unwashed sand to reduce the water absorption was more pronounced for concrete with higher w/c ratio compared to the concrete with lower w/c ratio. With lower w/c ratio, the additional limestone powder with lower particle size had little room to further improve the already reduced porosity and pore structure. This was observed for all cement type except microsilica concrete. For microsilica concrete at 0.40 w/c ratio the improvement due to the finer particles of unwashed sand did not follow the trend of other cement types. This could be attributed to the test variability.

However, excluding 0.40 w/c ratio, microsilica concretes had the best effect of the additional finer particles to enhance the water absorption properties compared to other cement combinations, followed by the rice husk ash and the GGBS concretes.

The percentage improvement, though seems to be quite significant, however, they are based on very low water absorption values due to low w/c ratio and high volume of supplementary cementitious material content. Therefore the effect of precision of testing variability need to be acknowledged while interpreting this positive effect.

5.3.3 Water absorption of recycled concrete aggregate series

In this section the effect of varied proportion (100%, 80%, 50% and 0% of coarse aggregate) of recycled concrete aggregate (RCA) on the water absorption properties of concrete have been discussed. Each proportion was tested for three different water/cement ratios (0.25, 0.32 and 0.40) using washed and unwashed sand. Following sections have analysed the effect of i) RCA content, ii) w/c ratio and iii) finer particles of unwashed sand, on the absorption properties of concrete.

5.3.3.1 The effect of RCA content

The water absorption of RCA was much higher than the crushed limestone aggregate. Table 3.4 from Chapter 3 has provided the information on aggregate properties and test reports. The water absorption tested as per BS 812: Part 2: 1995 of 20mm and 10mm limestone aggregate are 0.3% and 0.4% compared with 3.7% and 5.0% for RCA with 20mm and 10mm respectively.

This significant increase in water absorption is due to the fact that the RCA contain old hardened cement paste, which is highly absorptive than the original natural limestone aggregate. Therefore, water absorption of concrete containing different proportion of RCA should be affected by the presence of RCA. This section will discuss about this effect.

Figure 5.18 and Figure 5.19 show the water absorption of different proportion of RCA concrete at different w/c ratio made of washed and unwashed sand. The effect of RCA content on the water absorption should be proportional, i.e. higher the RCA content higher the water absorption. This should be irrespective of the w/c ratio of the concrete. Both washed and unwashed (Figure 5.18 & Figure 5.19) concretes did not conform to this fact except that for concrete with washed sand the water absorption of 100% natural aggregate was the lowest at 0.25 and 0.32 w/c ratio. For unwashed sand, none of the concretes showed any uniform trend towards higher water absorption due to higher RCA content.

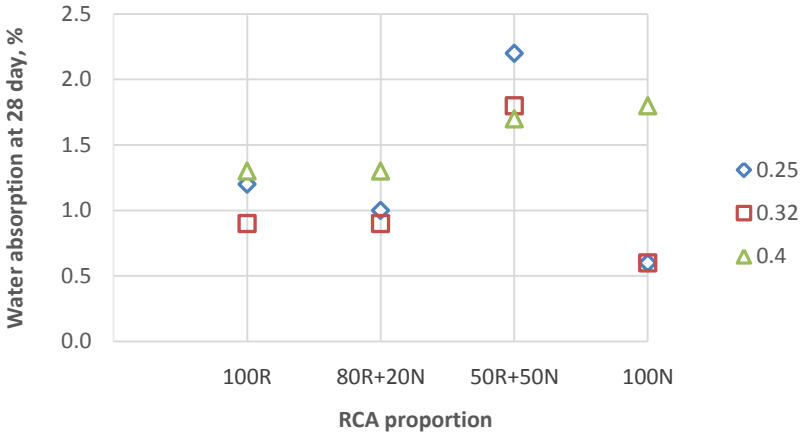

Figure 5.18: Effect of RCA and w/c ratio on water absorption of washed sand concrete with P0S100

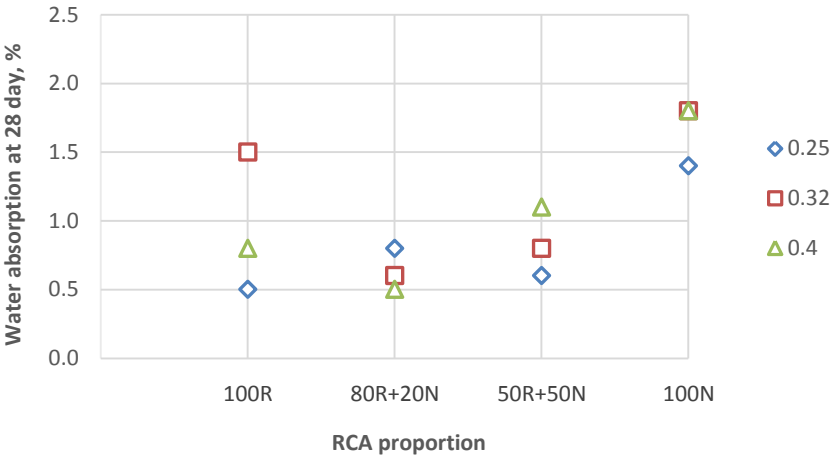

Figure 5.19: Effect of RCA and w/c on water absorption for unwashed sand concrete with P0S100

5.3.3.2 The effect of w/c ratio

Lower w/c ratio should provide lower water absorption due to lower porosity in the cement paste matrix. In Figure 5.18, the 0.40 w/c ratio has the maximum water absorption except for 50% RCA concrete. Otherwise 0.32 has better water absorption properties than 0.25 w/c ratio, contradicting the expectation. In Figure 5.19 with unwashed sand, all concrete with 0.25 w/c ratio has the lowest water absorption except at 80% RCA concrete. Water absorption results at 0.32 and 0.40 w/c ratio concretes also did not follow the expected norm with lower absorption with lower w/c ratio showing the variability in the testing process.

5.3.3.3 Effect of unwashed sand

Similar to natural aggregate concrete in Figure 5.16, for RCA concrete the comparison of the performance on water absorption between concretes made with washed and unwashed sand has been shown in Figure 5.20. This should be able to demonstrate the filler effect of unwashed sand on RCA concretes. Ideally the water absorption of unwashed sand concrete should be lower than that of washed sand concrete due to dense matrix contributed by the finer particles in the mix. In general that is what demonstrated by this figure, except only in one incident of 100% RCA with 0.32 w/c concrete. The possible reasons for having opposite results for concrete with 0% RCA and 100% GGBS have been discussed earlier.

Figure 5.20: Water absorption of RCA concretes made with washed and unwashed sand

Figure 5.21 shows that there is a positive effect of the finer particles of unwashed sand to the water absorption performance of RCA concretes, as the difference between almost all concretes made with washed and unwashed were positives. However, the impact of the effect of unwashed sand was more pronounced at lower w/c ratio with 100% and 50% RCA concrete than at the higher w/c ratio. This trend is almost reversed for natural aggregate concrete as shown in Figure 5.17. However, 80% RCA concrete is conforming the trends of natural aggregate. This contradiction perhaps again highlights the high variability on concrete water absorption tests conducted as per BS 1881:122.

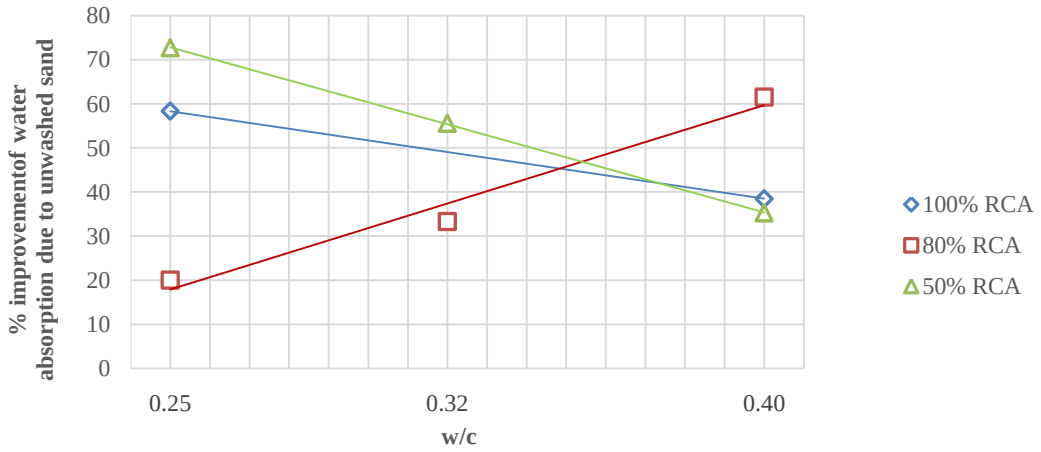

Figure 5.21: Improvement of the performance of water absorption by the unwashed sand in RCA concretes

5.3.3.4 Reasons for variable water absorption results

In RCA series the water absorption values did not always conform to the expected norm with respect to the water to cementitious ratio, RCA content and the effect of unwashed sand. The reasons of this anomaly could be attributed to the following:

1. Variable compressive strength development
2. Plastic properties of RCA concrete
3. Variability of testing

Water absorption and variable development of compressive strength:

Use of 100% GGBS with RCA resulted into very low initial strength at the age of 7 days, especially for concretes made with washed sand. However, the strength gain at 28 days was significantly higher (Section 4.3.3, Figure 4.17).

Figure 5.22 shows the relationship between the compressive strength at the age of 28 days and water absorption of RCA concretes made with washed and unwashed sand. Ideally the water absorption should be reduced with higher compressive strengths as both compressive strength and water absorption are related to the quality of microstructure of cement paste. The compressive strength is also related to the w/c ratio as concretes gain higher compressive strength with reduced w/c ratio. Though, these relationships in Figure 5.22 have largely been maintained, the compressive strength/water absorption relationship has not been always observed.

For unwashed sand this relationship has been maintained except for 50% RCA concrete category (Figure 5.22c). As it can be seen from Figure 5.22d, only concrete without any RCA show the right relationship between compressive strength and water absorption for both washed and unwashed sand categories indicating variability in water absorption values due to the presence of RCA. This could be due to higher water absorption values of RCA compared to natural aggregates.

Plastic properties of RCA concrete:

It has been observed from Table 4.5 (Chapter 4) that the plastic properties of RCA concrete for both washed and unwashed sand were not consistent. It was noted of occasional delayed bleeding, delayed setting for washed sand concretes and rapid slump loss for unwashed sand concretes. These inconsistent plastic properties could influence the pore structure of the cement paste resulting into inconsistent water absorption results. The reasons of the inconsistent plastic properties of RCA concrete could be attributed to the impurities which might have been present in the recycled concrete aggregates.

Testing variability:

The water absorption test was conducted as per BS1881: Part 122. Though the standard itself did not provide any information on the variability of the test results in terms of precision and bias due to operator and equipment used, variability in the test results should be recognized. This is because the water absorption test procedures require the actions of concrete sampling, cube making, curing, coring, drying in oven, immersing in water and weighing. Every single process of the testing procedure would be subjected to the variability due to human and equipment factors.

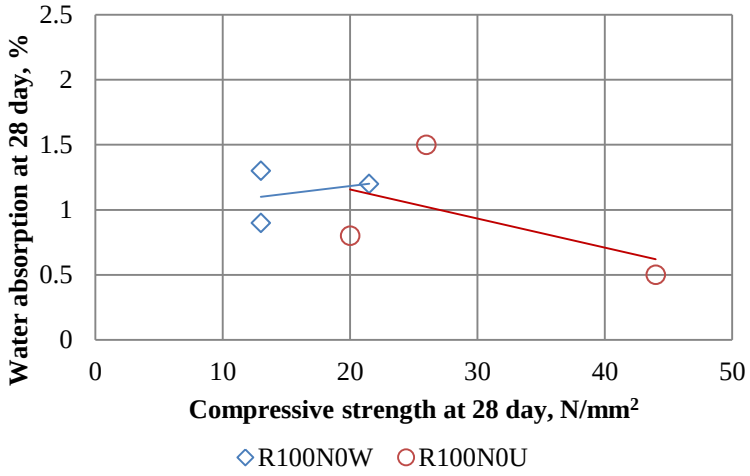

Figure 5.22a: 100% RCA (Washed and unwashed sand)

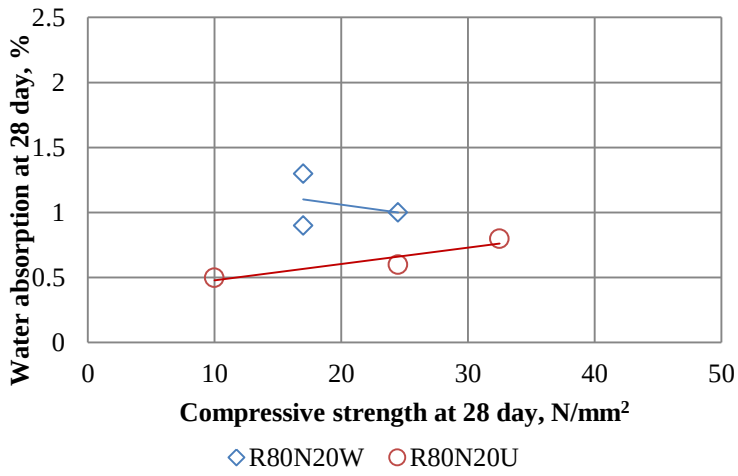

Figure 5.22b: 80% RCA (Washed and unwashed sand)

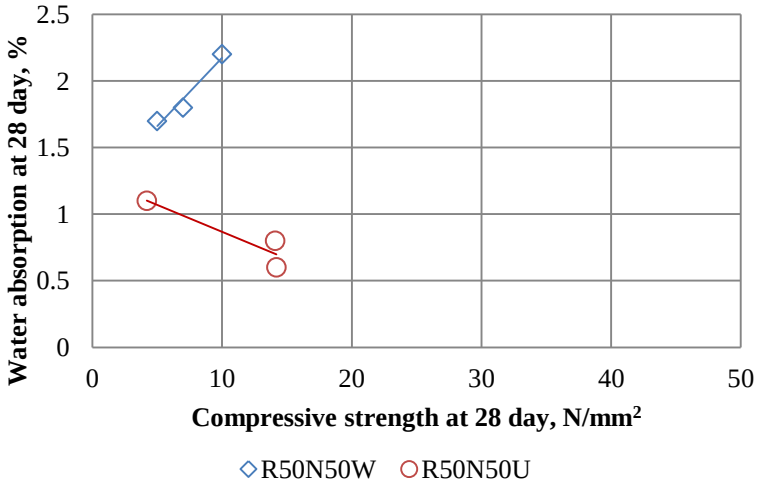

Figure 5.22c: 50% RCA (Washed and unwashed sand)

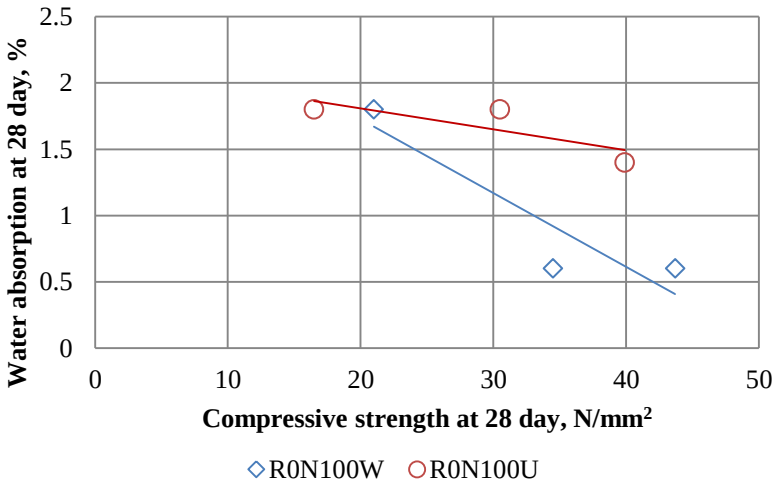

Figure 5.22d: 0% RCA (Washed and unwashed sand)

Figure 5.22: Relationship between compressive strength and water absorption of concrete made with washed and unwashed sand (RCA with 100% GGBS)

5.3.3.5 Summary

In RCA series the overall results of water absorption for both washed and unwashed sand concrete were below 2.0%. This can be concluded as satisfactory results given the very high water absorption of recycled aggregates compared to natural aggregates.

Use of 100% GGBS which contributes to variable development of compressive strength could be one of the reasons for variable results and not conforming to the expected results related to w/c ratio, RCA content and the effect of unwashed sand. Other reasons of having inconsistent results could be attributed to the variable plastic properties of RCA concretes and testing variability of water absorption test itself.

5.3.4 Water absorption of RCA with triple blend

In this series a triple blend with 15% of Portland cement, 70% of GGBS and 15% of rice husk ash, P15S70R15 was used with RCA instead of 100% GGBS to get a more consistent hydration and strength gain. The sand type was also fixed to only washed sand. Therefore, the effect of two variables, i) proportion of RCA and ii) w/c ratios of concrete on the water absorption properties have been discussed in this section. Figure 5.23 presents the water absorption results of the triple blend concrete with RCA.

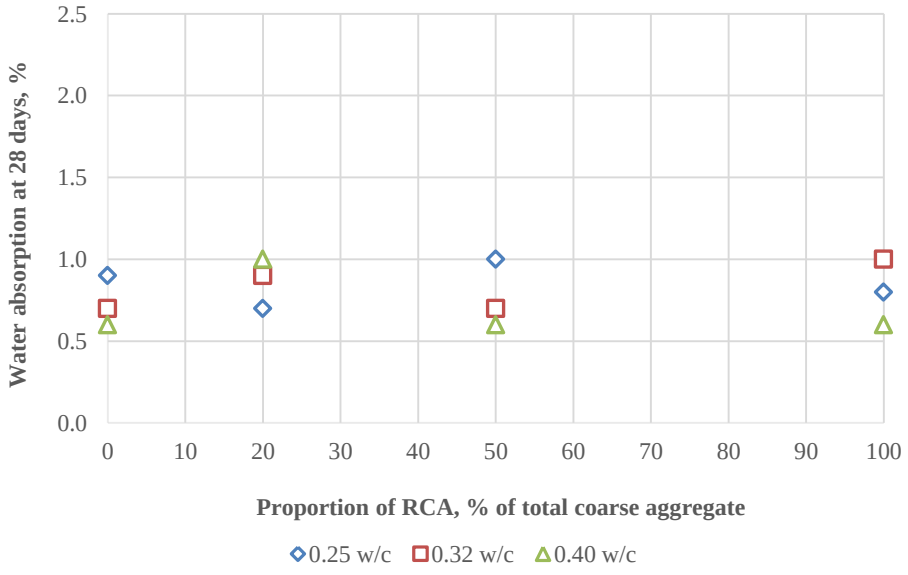

Figure 5.23: Water absorption of concrete with RCA and P15S70R15

Though the overall results of each concrete mixes were very impressive with water absorption equal to or below 1.0%, there was no direct relationship between water absorption and the proportion of RCA content or the w/c ratio of concrete could be established. There is only 0.40% water absorption value difference between the maximum and minimum values among the concretes. This signifies the fact that the microstructure of the triple blend concrete even at a w/c ratio of 0.40 is so well developed that other variability such as aggregate types did not affect or improve the performance any further, suggesting 0.40 w/c ratio could be the optimum w/c ratio to achieve the best performance. No further improvement of water absorption for 0.32 and 0.25 w/c ratio confirmed that.

The very robust microstructure of the triple blend paste could be confirmed by the SEM images at Chapter 6. Though the paste prepared for SEM testing was with 0.32 w/c ratio, nevertheless, the improvement of microstructure at 0.40 w/c ratio would also be significant. The almost similar water absorption results between all three w/c ratios shown in Figure 5.23 prove that argument.

5.3.4.1 RCA 100% GGBS vs P15S70R15

To understand the effect of triple blend of P15S70R15 instead of 100% GGBS on the water absorption properties of concrete, Figure 5.24 has been drawn. It has plotted normal distribution curves of water absorption values of 100% GGBS and P15S70R15 blend RCA concretes using Data Analysis Tool of Microsoft Excel.

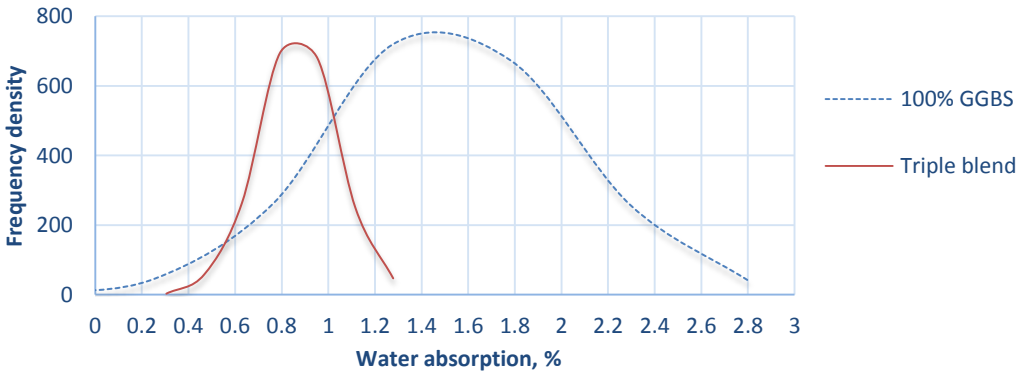

Figure 5.24: Normal distribution of water absorption of 100% GGBS and triple blend RCA concrete

The normal distribution curves have been plotted using MS Excel by randomly generated data but within the parameter of actual water absorption values of concrete made with RCA. The randomly generated data was used to form the basis for the normal distribution curve. This helped to obtain smooth normal distribution curves of the water absorption values of both type of concrete for clearer comparison and provide a comparison of the relative positions of both set of data.

The graph for the triple blend, though slightly skewed to the right, is narrow and positioning at the left side of the chart, giving a very narrow range of water absorption values. In comparison, the graph of 100% GGBS is very wide demonstrating very high variability in the data. The reason for this very high variability of water absorption values for RCA with 100% GGBS has been discussed earlier.

The standard deviation of the water absorption values of RCA concretes with 100% GGBS and triple blend are 0.510 and 0.162 respectively, which are significantly apart. This also signifies the effect of variability in water absorption results in RCA concretes with 100% GGBS compared to triple blend. Therefore it can be concluded that, the triple blend of P15S70R15 concrete would provide more controlled performance of water absorption compared with 100% GGBS concrete using RCA.

5.3.5 Water absorption of higher curing temperature series concretes

In this series two sets of concrete were made of P5S70R25 & P15S70R15 and cured at an elevated temperature of 40°C to simulate the actual site temperature of Arabian Peninsula. Each sets had three w/c ratio of 0.25, 0.32 and 0.40 making it total 6 concrete mixes. The water absorption tests were conducted on samples taken from all 6 concrete mixes. The water absorption values as shown in Figure 5.25 are well within the acceptable range of 2.0% and below.

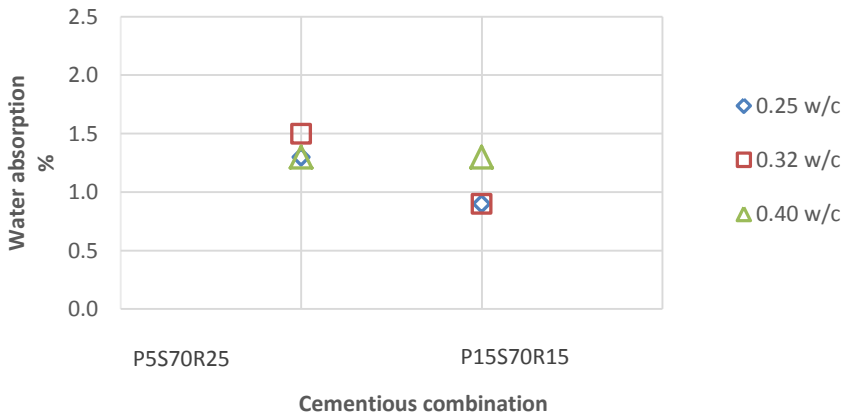

Figure 5.25: Water absorption of concrete with triple blend cured at 40°C temperature

It is intriguing to observe that concrete with higher rice husk ash, P5S70R25 was with higher water absorption compared with lower content (P15S70R15) of rice husk ash. This is perhaps due to higher inherent porosity of rich husk ash particles. The water demand of rice husk ash concrete was also higher due to this reason. This has been discussed in Chapter 3, Table 3.16. There is no significant impact of the w/c ratio was observed on the water absorption properties of concrete. This is similar to the previous series confirming reaching the optimum performance at 0.40 w/c ratio and beyond.

The relationship between compressive strength and water absorption of the triple blend concrete is presented in Figure 5.26 and Figure 5.27. In Figure 5.26, the compressive strength and water absorption of concretes made with P5S70R25 cured at 40°C temperature is presented. As the compressive strength increased with the reduced w/c ratio, the water absorption results remain same at 0.25 and 0.40 w/c ratio of 0.9% and at 0.32 w/c ratio it increased to 1.5%, showing no variation in the water absorption values.

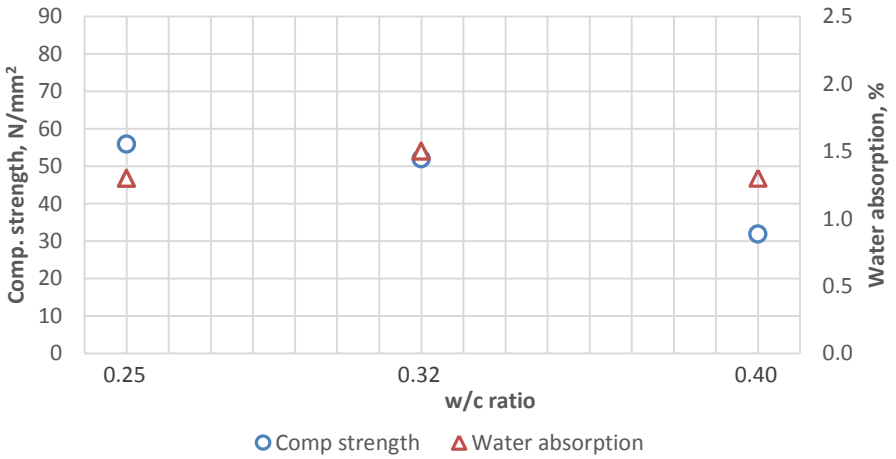

Figure 5.26: Relationship between compressive strength and water absorption of P5S70R25 cured at 40°C temperature

In Figure 5.27, P15S70R5 concrete cured at 20°C is compared with the same concrete cured at 40°C temperature. The compressive strength posted better results with 5-7% improvement but the water absorption results did not show any improvement. At both temperature the water absorption values of P15S70R15 concretes did not show any relationship with the w/c ratio, similar to the concretes made with P5S70R25 as mentioned in previous paragraph.

In summary, water absorption of concrete made with Portland cement, GGBS and rice husk ash seemed to be not affected by the increase in curing temperature. Nevertheless the overall results remained low (1.5% or below). The water absorption of concrete with higher rice husk ash proportion was higher due to its inherent porosity of rice husk ash particles.

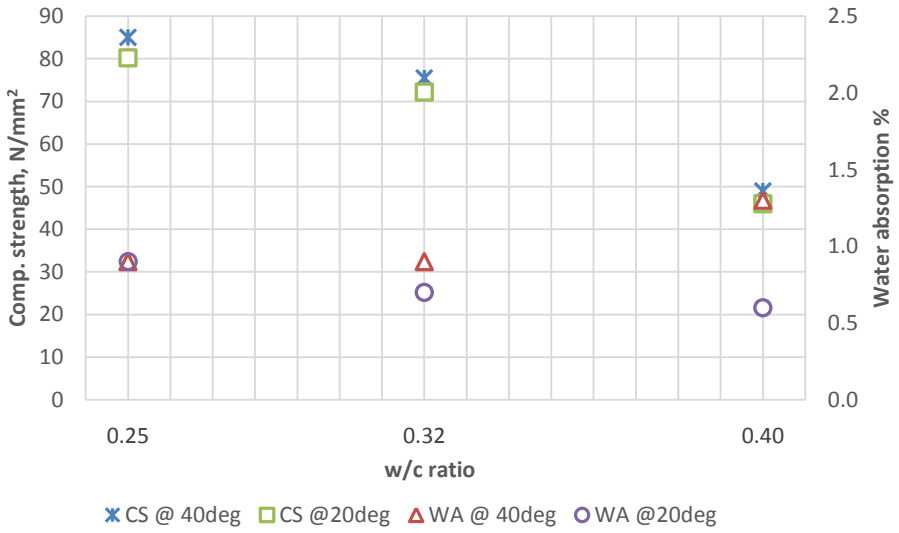

Figure 5.27: Relationship between compressive strength and water absorption of P15S70R15 cured at 20 & 40°C temperature

5.3.6 Water absorption of air entrained concrete series

Concretes in this series are with air entrained at different level to explore the effect of entrained air on their plastic and hardened properties. Water absorption tests on concrete mixes containing 4 different air content (2, 5, 10 and 12%) were tested. The w/c ratio of each type of concrete was 0.25, 0.32 and 0.40 creating total 12 concrete mixes. 90% Portland cement and 10% microsilica, P90M10 and washed sand were used for all mixes in this series.

Figure 5.28 shows that there is no significant effect of different air contents on the water absorption of concretes. The water absorption of all concretes varied between 1.1 to 1.6% which was considered to be extremely low for concrete with very high level of air entrainment. This demonstrates that though the cement pastes were highly porous, it was likely that the pores were not interconnected. This is due to the use of high level of microsilica (10% of total cementitious content) and low w/c ratio which improved the microstructure of cement paste.

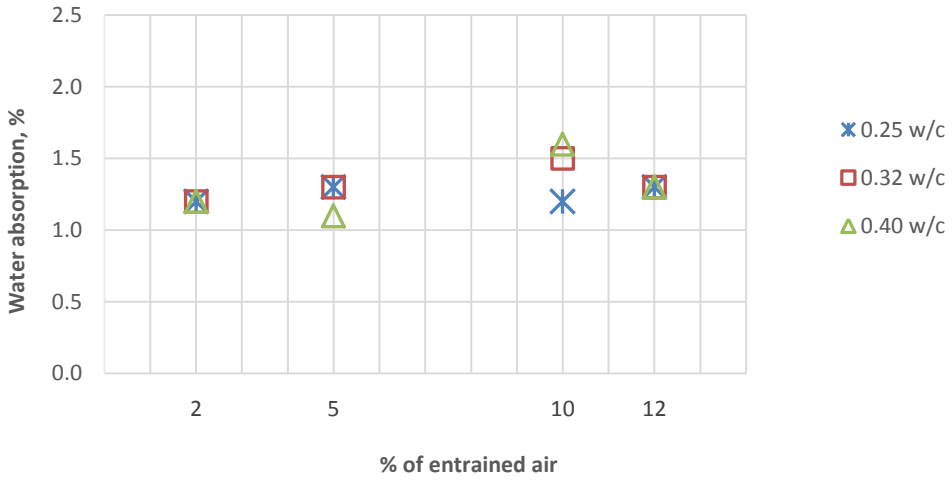

Figure 5.28: Water absorption of air entrainment series

Relationships between the compressive strengths and water absorption of air entrained concretes can be seen from Figure 5.29. The water absorption values of all four groups of concretes remained very similar without showing any significant relationship with w/c ratio or compressive strengths, though as expected the compressive strengths were higher with lower w/c ratio and in certain cases there was a clear trend of having lower water absorption with higher strength such as concretes with 10% air content in Figure 5.30c. Otherwise, there was little change in the water absorption values across three w/c ratios for individual air content concretes. This insignificant difference in water absorption between concretes with different w/c ratio could be attributed to the improved microstructure due to the addition of microsilica.

It is interesting to observe that though the compressive strength of concrete due to increased air reduced significantly (37% due to 5% air compared to 2% air as shown in Figure 4.26), but there is no significant difference in water absorption between 2% and 5% air concrete. This is could be due to the discontinued air voids as Fagerlund, G (1982) confirmed that water absorption does not depend on the air void.

In summary the water absorption results of concrete with higher entrained air content remained low though there is no any significant relationship between air content and water absorption could be established.

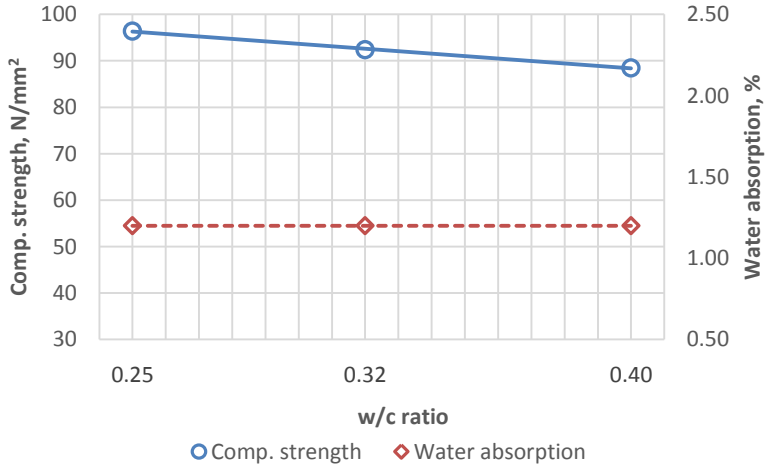

Figure 5.29a: 2% Air

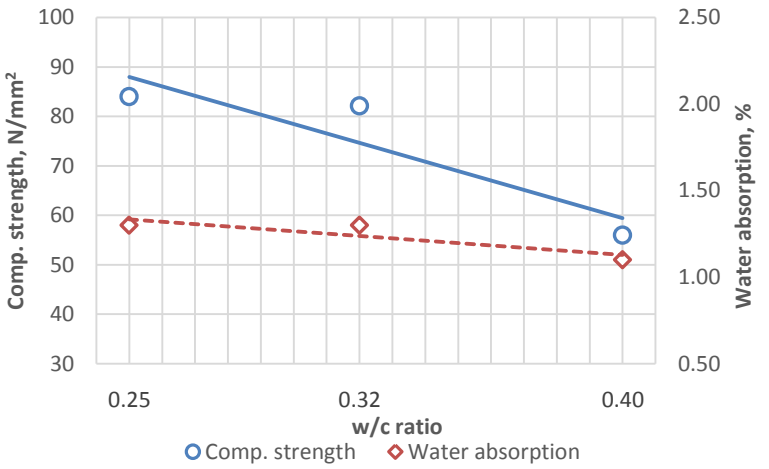

Figue 5.29b: 5% Air

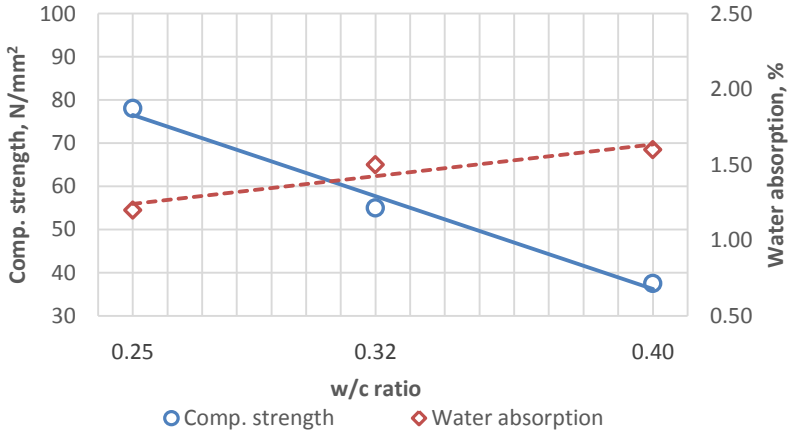

Figure 5.29c: 10% Air

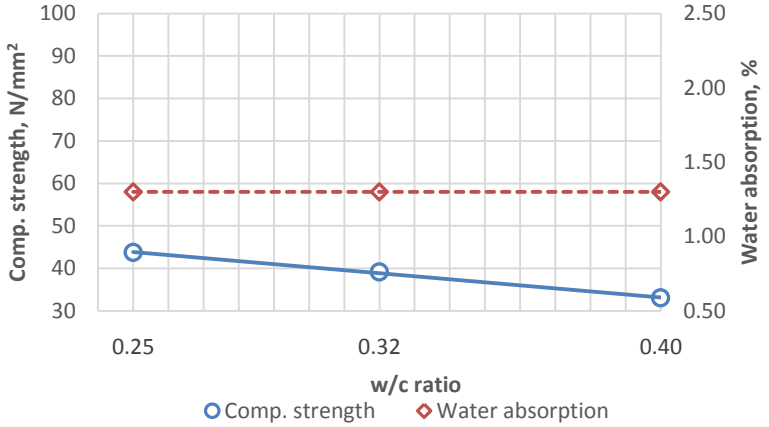

Figure 5.29d: 12% Air

Figure 5.29: Relationships between compressive strengths and water absorption (air entrained concrete series)

5.4 Water permeation

In this study, water permeation of concrete was tested according to BS EN 12390: Part 8, where direct water penetration for a static hydraulic pressure (500 kPa for 72 hours) was measured. The water penetration value of below 10mm was considered to be the accepted result as this is the normal acceptable limit in the Gulf region.

5.4.1 Water permeation of cement type series

Figure 5.30 and Figure 5.31 present the water permeation results of the concretes from cement type series where only washed sand was used. Figure 5.30 shows the water permeation results of concrete containing only GGBS and Figure 5.31 contains concrete with 70% GGBS as control and 100% GGBS and other type of cementitious materials i.e. fly ash (80%), microsilica (10%) and rice husk ash (20%). Each group of concrete mixes contained w/c of 0.25, 0.32 and 0.40 w/c ratio.

In Figure 5.30 the water penetration values are ranging from 0 to 7mm. Six concrete mixes from total 15 concrete mixes did not have any penetration of water at all. It was only for the concretes with 85% GGBS content had water penetration results.

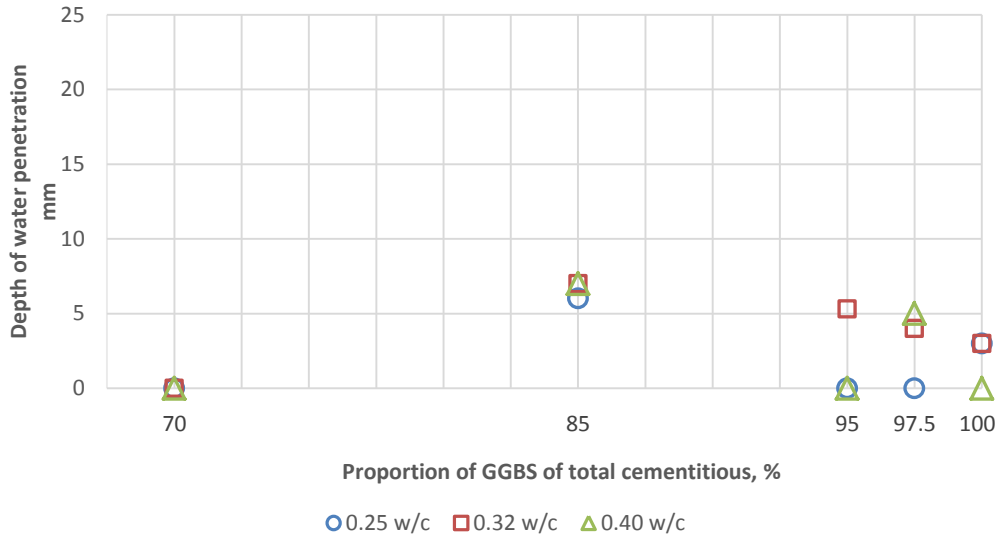

Figure 5.30: Water permeation of cement type series – GGBS only

The results in Figure 5.31 are ranging from 0 to 5mm. It is interesting to observe that only those concrete contain very low Portland cement had some penetration of water, though they are very small. The maximum water penetration recorded was only 7mm, compared to target 10mm. Therefore, it can be concluded that the water penetration properties of these concrete are well within the satisfactory limit.

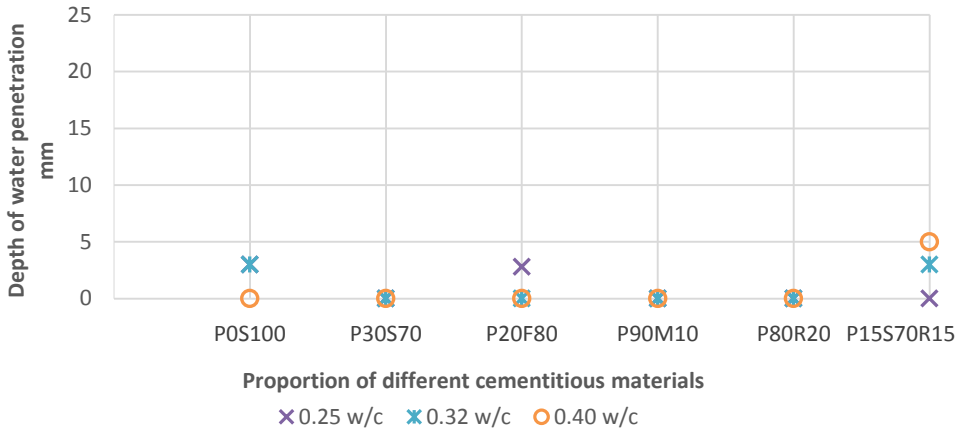

Figure 5.31: Water permeation of cement type series including other cementitious materials

5.4.2 Water permeation of sand type series

The water penetration results for concretes with unwashed sand (Figure 5.32) are very similar to that of concrete with washed sand. The depth of water penetration is ranging from 0 to 5 mm. Most of the concrete matrixes were so dense that only concrete mixes with fly ash (all three w/c ratio) and 10% microsilica (0.25 w/c ratio) had water penetrations. All other mixes had no penetration of water at all.

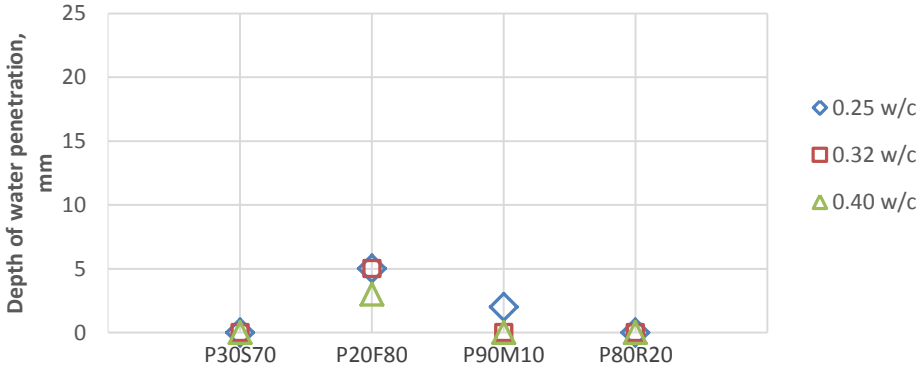

Figure 5.32: Water permeation test – Sand type series

There is no sign of any effect of additional finer particles available in the unwashed sand concrete on the water penetration properties. This is due to the fact that the microstructure of the cement paste blended with pozzolanic materials already produced too dense microstructure for water molecules to penetrate through. Consequently there was no other room left for further improvement by the additional finer particles.

5.4.3 Water permeation of recycled concrete aggregate series

Table 5.8 presented the water permeation results of RCA concrete for both washed and unwashed sand type. The water permeation tests for100% and 80% RCA concrete with washed sand was inconclusive as during the testing process, the water penetrated through the full depth of the concrete specimen before the completion of the test and the test procedures had to abandon. This phenomenon could be linked to the delayed setting of cement paste in the concrete during the production in the lab as reported in Chapter 4 (Section 4.2.4, Table 4.5). The test was completed for the rest of the concretes.

Table 5.8: Water permeation results of concrete made with RCA

No	REF	Proportion of RCA over total weight of coarse aggregate	w/c	Water Permeation, mm	
				Washed	Unwashed
1	100R	100% RCA + 0% Normal	0.25	W/P*	7
2	100R		0.32	W/P	8
3	100R		0.40	W/P	5
4	80R+20N	80% RCA + 20% Normal	0.25	W/P	7
5	80R+20N		0.32	W/P	5
6	80R+20N		0.40	W/P	5
7	50R+50N	50% RCA + 50% Normal	0.25	25	2
8	50R+50N		0.32	22	16
9	50R+50N		0.40	17	20
10	100N	0% RCA + 100% Normal	0.25	3	0
11	100N		0.32	3	0
12	100N		0.40	0	1

*W/P: Water penetrated through the entire length of the 150mm concrete cube under testing

RCA: Coarse recycled concrete aggregate

Normal: Coarse natural crushed limestone aggregate

Excluding the abandoned test results of 80% and 100% RCA concretes Figure 5.33 is drawn showing the water permeation results of 0% and 50% RCA concrete results. The water penetration results for 50% RCA concretes were fairly high ranging from 17-25 mm, where 10 mm penetration was considered to be the acceptable limit.

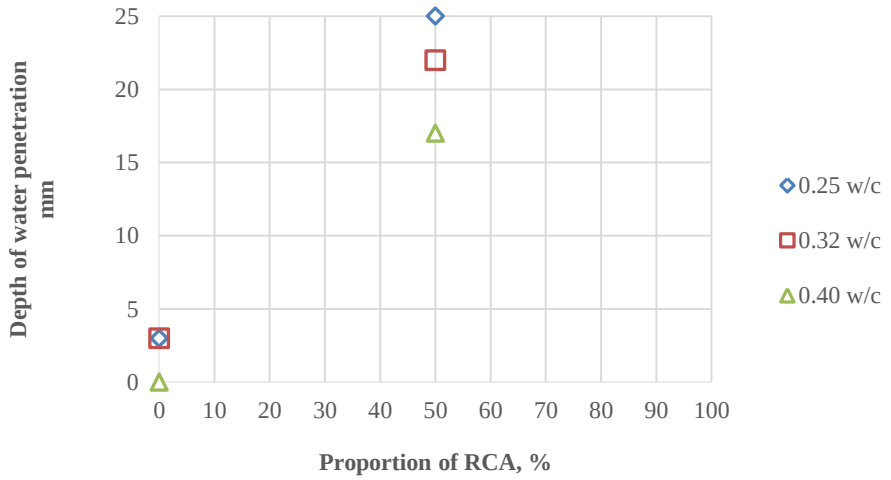

Figure 5.33: Water permeation results – RCA (washed sand)

However, the same concrete using unwashed sand posted much improved results with below 10mm for 100% RCA and 80% RCA concretes (Figure 5.34). The results of 50% RCA were higher except at 0.25 w/c ratio concrete. The 0% RCA which is effectively 100% GGBS mix from the Sand type series is drawn together to compare the effect of RCA against the natural aggregates. It is obvious that the RCA concrete had much higher water permeation properties compared to the concrete with natural aggregates.

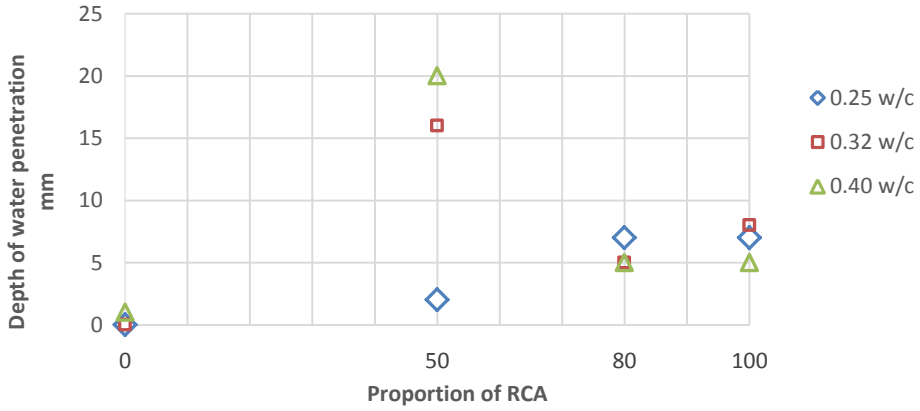

Figure 5.34: Water permeation results – RCA (unwashed sand)

5.4.3.1 Effect of RCA content on water permeation

Type and quality of aggregates is one of the factors affecting the permeation of concrete. RCA which is inherently porous due to the presence of old cement paste is susceptible for higher water penetration under hydraulic pressure provided the 'new' cement paste is also porous and interconnected. Though certain concrete mixes with RCA showed very high water penetration, concrete made with unwashed sand and with 100%, 80% and 50% RCA (0.25 w/c ratio) showed extremely low water penetration (Figure 5.34), perhaps proving that the new pastes with unwashed sand concrete was well hydrated and the concrete specimen was made with proper compaction.

There is no distinctive relationship between the RCA content and the water penetration value could be observed. This effectively established that the quality of the surrounding cement paste of the concrete became the dominating factors on the permeability properties of RCA concretes.

5.4.3.2 Effect of w/c ratio

As the paste quality could be the dominating factors affecting the water permeability, the w/c ratio of the pastes should be one of the determining factors on the quality of paste with lower w/c ratio providing better results. Both Figure 5.33 and 5.34 do not show any superior performance of water permeation results of lower w/c ratio over higher w/c ratio. Ignoring the very high results of above 10mm (as the abnormally high results could be due to improper hydration due to delayed setting), the 2-8 mm variation between different type of concrete with varied w/c ratio was due to the variability of testing and human factors. At this very low level of water penetration, influence associated with w/c ratio became less dominant.

5.4.3.3 Effect of finer particles of unwashed sand

Results posted in Figure 5.34 are better than Figure 5.33, showing signs of improvement in the hydrated cement paste. Presence of additional finer particles below 75μm would provide additional volume fraction to the paste. The only exception is the 50% RCA with 0.40 w/c ratio where the water penetration results of concretes with unwashed sand were higher than the equivalent concrete with washed sand. However, as the results of both mixes were above 10mm, they should not be taken into consideration.

5.4.4 Water permeation of RCA with triple blend

In this section the effect of RCA and w/c ratio to the water permeation of concrete made with RCA and P15S70R15 is analysed. The water permeation results as shown in Figure 5.35 are very good except only 100% RCA (0.25 w/c ratio) concrete which has more than 10mm water penetration. Otherwise the results are ranging from 0 to 7mm.

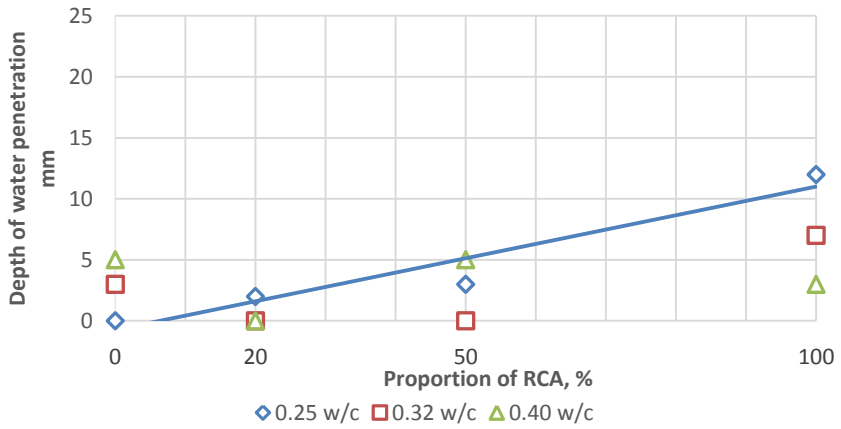

Figure 5.35: Water permeation results – RCA with P15S70R15

5.4.4.1 Effect of RCA content

The effect of RCA content on the water penetration can be observed in Figure 5.35 where the overall water penetration of higher RCA concrete is higher than the lower proportions of RCA. Though there is no significant relationship can be established at these low level figures, at 0.25 w/c ratio the reduction of the water permeation with the reduction of RCA content is noticeable as shown by the trend line. As the quality of paste considered to be similar to all concretes, the only factor which could vary the results is related to testing and human factors.

5.4.4.2 Effect of w/c ratio

Similar to the RCA with GGBS concrete, the w/c ratio is not the determining factor to influence the water penetration as no relationship could be observed between the w/c ratio and the water penetration results.

5.4.5 Water permeation of higher curing temperature series concretes

In this section the effects of elevated curing temperature of 40°C on the water permeation of concrete made with triple blends of P5S70R25 and P15S70R15 are analysed. The effect of two different sets of triple blended cementitious materials on the water penetration of concrete will also be described.

5.4.5.1 Effect of curing temperature

The performance comparison of water permeation performance of P15S70R15 concrete cured at 20°C and 40°C temperature can be seen in Figure 5.36. Though there is no effect of higher curing temperature could be observed on the water penetration values, all concretes demonstrated very high resistance to water penetration as the water penetration results of all concrete in Figure 5.36 are lower than targeted 10mm. Beside that at 20°C the water penetration results were already very low, therefore further improvement at higher curing temperature could not be detected. The testing variability could also influence the results.

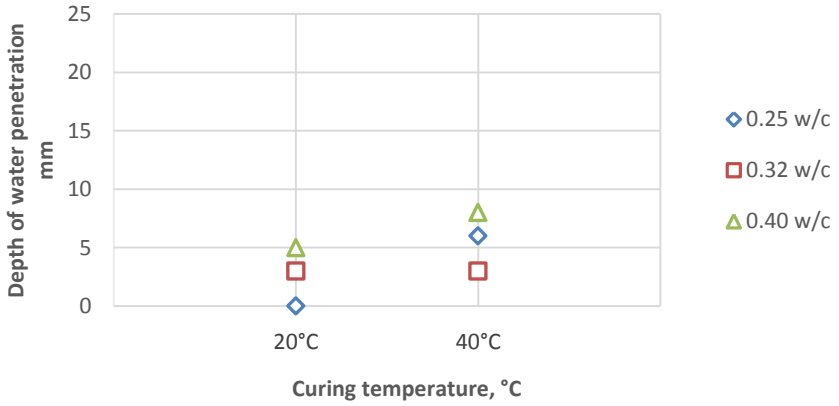

Figure 5.36: Water permeation of concrete made with P15S70R15 cured at 20°C & 40°C temperature

5.4.5.2 Effect of triple blends of cementitious materials

Figure 5.37 presents the water permeation results of P5S70R25 and P15S70R15 concretes. Both concretes were cured at 40°C temperature. The results of water permeation for both sets were well within 10mm demonstrating dense microstructure of cement matrix.

However, it is intriguing to see that the concrete with higher rice husk ash content posted better resistance to water penetration. The reason for this improvement could be attributed to the development of additional CSH gels due to pozzolanic reactions of the additional silica available from the rice husk ash. The additional unreacted rice husk ash perhaps also made the paste denser by its finer particles size by means of particle packing.

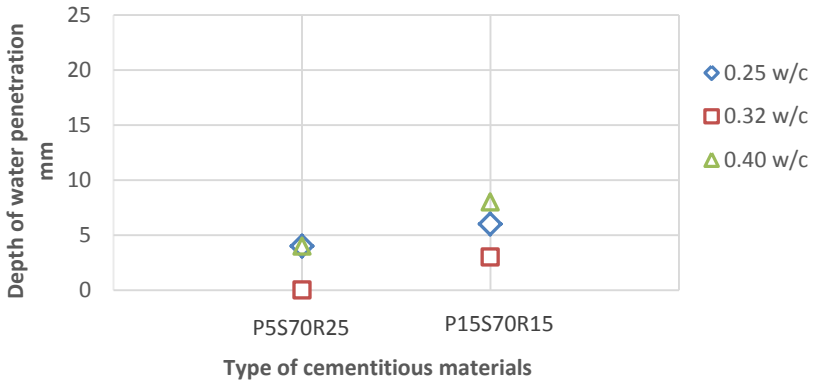

Figure 5.37: Water permeation of triple blend - natural aggregates cured at 40°C temperature

5.4.5.3 Effect of w/c

The effect of w/c ratio on the water permeation properties of concrete cured at higher temperature could not be observed. Though at 20°C with P15S70R15 (Figure 5.36), the water permeation results followed the w/c ratio with reduced permeation with reduced w/c ratio of concrete. At 40°C curing temperature, that trend was not maintained. P5S70R25 concrete cured at 40°C also did not follow the same sequence (Figure 5.37).

5.4.6 Water permeation of air entrained concrete series

In this section the effect of entrained air (2, 5, 10 and 12%) at different w/c ratio (0.25, 0.32 & 0.40) on the water permeation resistance of P90M10 concrete are discussed.

5.4.6.1 Effect of entrained air

The effect of air content on the water penetration resistance of concrete can be seen in Figure 5.38. Both 2% and 5% air concretes were with zero water penetration showing development of extreme dense matrix of cement paste contributed by the addition of microsilica. However concretes containing 10% and 12% air demonstrated water permeation results ranging from 8 – 12 mm slightly exceeding the acceptable range of 10mm. This could be due to the development of inter-connected capillary voids inside concrete pastes due to unstable bubble of micro air at higher air content level. The water permeation results of both 10% and 12% air concretes were close to the accepted limit set by this works.

5.4.6.2 Effect of w/c ratio

There was no effect of w/c ratio can be seen on the water penetration resistance of concretes tested under this series. As discussed above, there was no water penetration at 2% and 5% air for all three w/c ratio concretes and at 10% and 12% air, the water permeation results are also very close to each other. Therefore, finding any effect of different w/c ratio on the water permeation properties of concrete entrained with air was not possible.

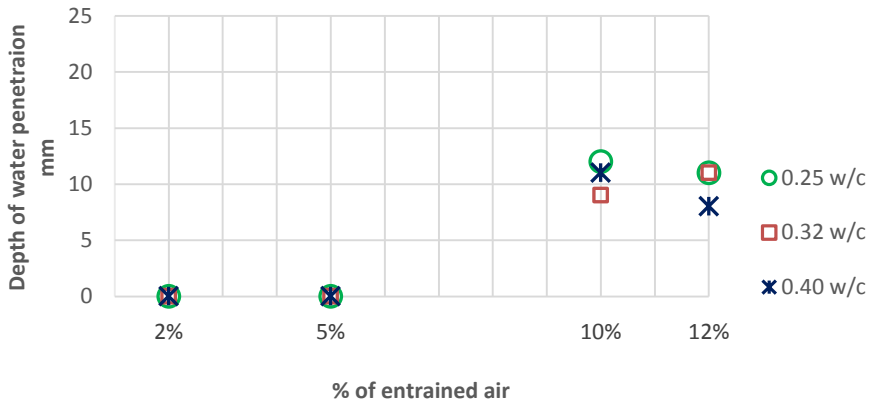

Figure 5.38: Water permeation results of air entrained concrete series

5.5 Chloride diffusion test

As described in Chapter 3, concretes with different combinations of cement and aggregate types were subjected to chloride diffusion test to find out the non-steady chloride diffusion properties of different types of concretes undertaken by this study. The draft European standard CEN TC51/WG12/TG5, (Draft 4 Version 2) was used to test the non-steady chloride diffusion where the diffusion coefficient consider the ability of concrete to bind the chloride ions during its diffusion through the concrete.

The diffusion coefficient has been expressed as m^2/s where the rate of transfer of chloride ions are considered through a unit area of concrete surface due to the concentration difference of chloride ions across the depth of concrete structure. In the following sections the chloride diffusion of different type of concrete are discussed to study the effect of different type of cement, aggregate, air content and curing temperature on the chloride diffusion of concretes. All concretes tested for chloride diffusions were made with 0.32 w/c ratio.

5.5.1 Chloride diffusion test of cement type series

5.5.1.1 Concrete with different proportion of GGBS

The chloride diffusion coefficient of concrete with different proportion of GGBS at 28 days and with 0.32 w/c ratio appeared to be below 5×10^{-12} m^2/s as shown in Figure 5.39. It is interesting to see that increase in GGBS content in concrete from 70% of total cementitious content decreased the diffusion coefficient up to a certain extent. At 85% GGBS content it was a reduction of 29% of P30S70. This reduction reduced to 12% when the GGBS content was further increased to 95%. However, at 97.5 and 100% GGBS content the chloride diffusion coefficient did not improve, rather increased, possibly due to weak microstructure of the paste due to poor hydration of the paste.

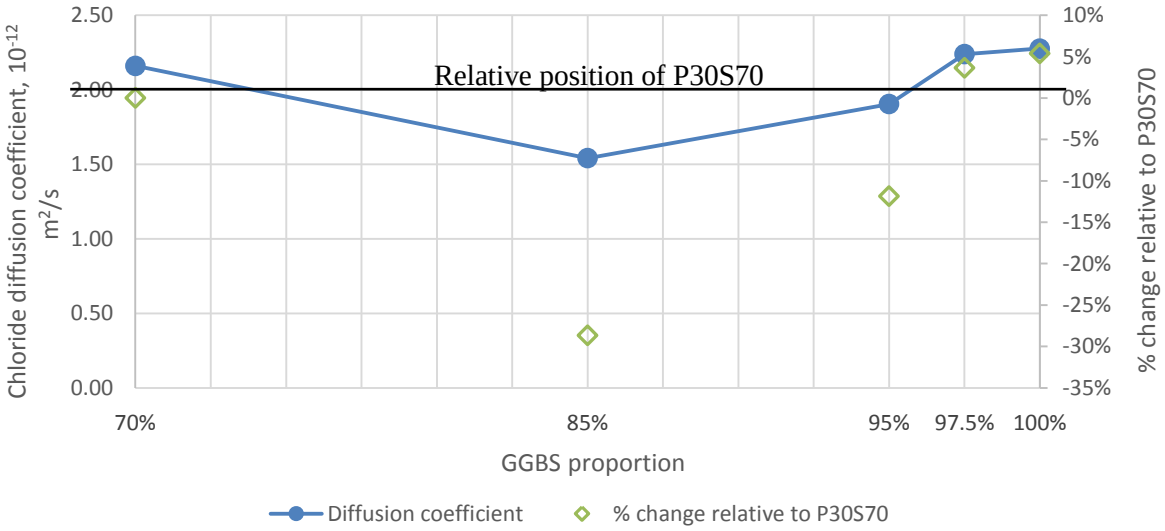

Figure 5.39: Chloride diffusion of concrete with different proportion of GGBS experienced

Chloride diffusion test is a direct test to measure the depth of diffusion of chloride ion compared to the rapid chloride permeability test (RCPT). RCPT is an indirect test providing indication of the concrete's ability to resist chloride ion penetrability. In Figure 5.40 the results of these two tests are plotted together to illustrate their relationship.

Although the chloride diffusion and RCPT results for each individual concrete with a specific proportion of GGBS, did not follow any particular relationship, the overall trend lines of these two tests show a similar trend of higher values with higher GGBS content. The R^2 value for both linear regression line are very poor, suggesting higher variability between results. Combining the findings in Figure 5.39 and Figure 5.40, it can be suggested that concrete with excessive amount of GGBS, perhaps above 95% tends to have reduced chloride resistance due to poorer formation of paste microstructure.

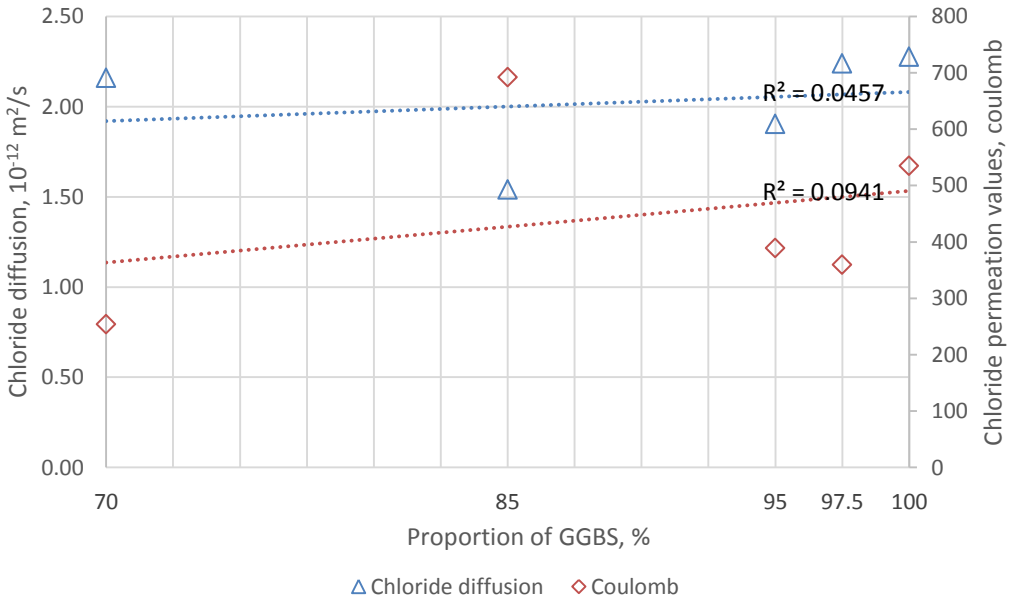

Figure 5.40: Comparison between chloride diffusion coefficient and rapid chloride permeation test results

5.5.1.2 Concrete with different combination of SCMs

The chloride diffusion results of concrete containing different proportion of SCMs are plotted in Figure 5.41 where concretes were made with washed sand with 0.32 w/c ratio. It is interesting to observe the significant reduction of 44% in chloride diffusion of P15S70R15 concrete compared to control P30S70.

Concrete with other cementitious materials also had reduced chloride diffusion compared to the control. It is to note that concrete containing fly ash (P20F80) had comparatively lower chloride diffusion (22% reduction) perhaps due to higher chloride binding capabilities of fly ash concrete compared to other cementitious materials. Both microsilica (P90M10) and rice husk ash (P80R20) posted better performance than the control as expected.

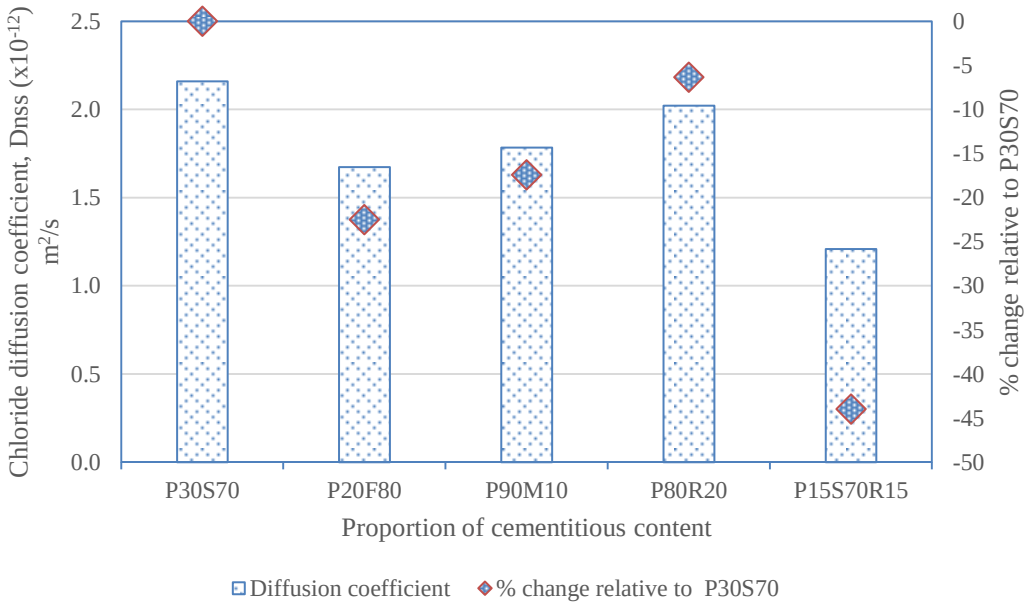

Figure 5.41: Chloride diffusion of concrete with different cementitious type

There is no significant correlation found between the chloride diffusion and rapid chloride permeation resistance properties of concrete with different cementitious combination. For example, though the chloride diffusion coefficient of P15S70R15 concrete is much lower than the control concrete, but the chloride permeation resistance as per ASTM C1202-97 is comparatively higher than the control, though the individual RCPT results of P15S70R15 are very low (Figure 5.2).

As mentioned earlier, very high variability of ASTM C1202-97 test makes it difficult to establish a correlation with chloride diffusion test results. Very low results of both chloride diffusion and RCPT due to the use of high volume pozzolanic materials with very low w/c ratio makes it further difficult to establish any effect of different type of cementitious materials on the relationship between these two properties.

5.5.2 Chloride diffusion test of sand type series

The effect of the additional finer particles in the unwashed sand on the chloride diffusion coefficient can be seen from Figure 5.42 where the percentage improvement of the chloride diffusion of concrete made with different combinations of supplementary cementitious materials and unwashed sand are plotted together with the chloride diffusion coefficient of concretes made with both unwashed and washed sand.

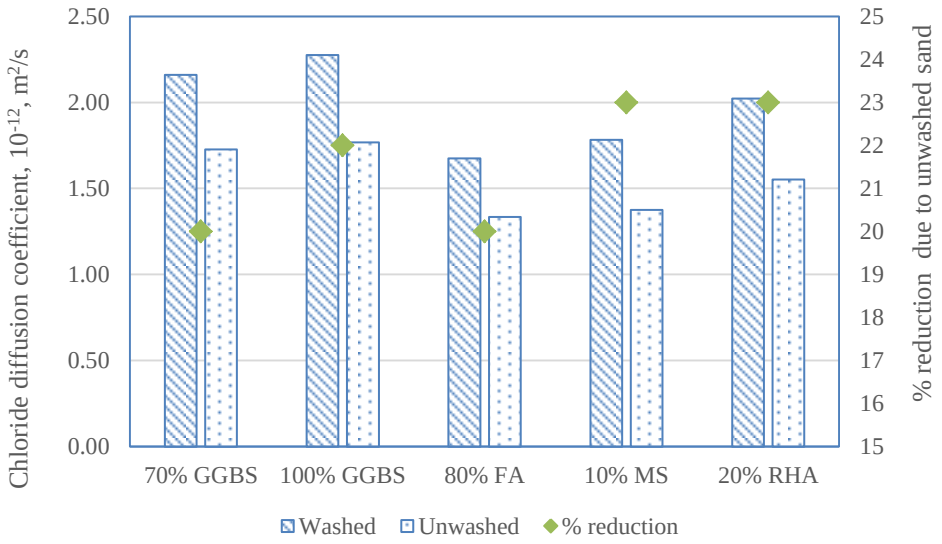

Figure 5.42: Effect on unwashed sand on the chloride diffusion coefficient of concrete with different combinations of cementitious materials made with 0.32 w/c ratio

Similar to the concrete with washed sand, the effect of the different cement combinations on the chloride diffusion coefficient are similar with concrete made with unwashed sand. Concrete with fly ash, microsilica and rice husk ash had lower chloride diffusion compared to the control P30S70.

In addition, the chloride diffusion coefficient reduced further perhaps due to increased tortuosity of the pore structure and improved microstructure due to the presence of the additional finer particles contributed by the unwashed sand. This reduction ranged from 20% to 23% depending on different combinations of cementitious materials relative to the chloride diffusion coefficient of concrete made with washed sand.

5.5.3 Chloride diffusion test of recycled concrete aggregate series

The chloride diffusion coefficient of concrete with RCA is relatively higher than concrete without RCA due to higher chloride content of RCA itself. The acid soluble chloride content tested as per BS 812: Part 117:1988 of 10mm and 20mm RCA aggregates are 0.11% and 0.09% respectively. The chloride content of natural crushed limestone aggregates are 0.01% for both sizes (Chapter 3, Table 3.4).

The higher chloride content of RCA increased the initial chloride content of the concrete, therefore the diffusion co-efficient also increased. The effect of RCA content on the chloride diffusion coefficient are clearly visible in Figure 5.43 where a linear trend line can be established with increased in diffusion coefficient with increased proportion of RCA content in the concrete.

However, as seen in Figure 5.43, the increase in the diffusion coefficient is dependent on other factors such as type of cementitious materials and fine aggregates. The increment in the chloride diffusion is higher in concretes with 100% GGBS content than concretes with P15S70R15 cementitious combination. The weak microstructure development of 100% GGBS compared to P15S70R15 could be the reason. In fact the rise in chloride diffusion with increased RCA content for P15S70R15 concrete was very remarkable compared to the 100% GGBS concrete, demonstrating very robust and dense microstructure of the P15S70R15 paste which 'tightly encapsulated' the RCA aggregates preventing any contribution of chloride ions from the aggregates within.

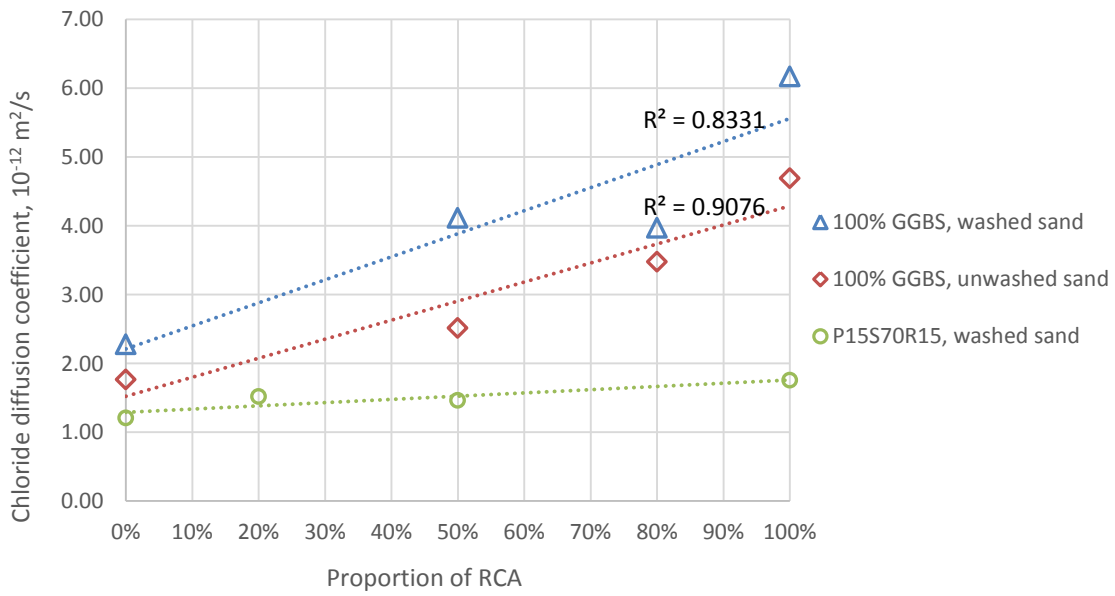

Figure 5.43: Chloride diffusion coefficient of concrete with RCA

The positive effect of the additional finer particles of unwashed sand can also be seen from Figure 5.43 with lower chloride diffusion coefficient in concretes made with unwashed sand compared to the concretes with washed sand, though the effect of RCA content on the chloride diffusion were very similar for both types of concrete.

5.5.4 Chloride diffusion test of air entrained concrete series concretes

In general it can be suggested from Figure 5.44 that the chloride diffusion coefficient increased with the increase in air content. However, there is a 8% reduction in the chloride diffusion coefficient in concrete with 5.1% air relative to the control concrete (1.2% air), suggesting an improved microstructure perhaps due to enhanced consolidation due to the presence of additional air.

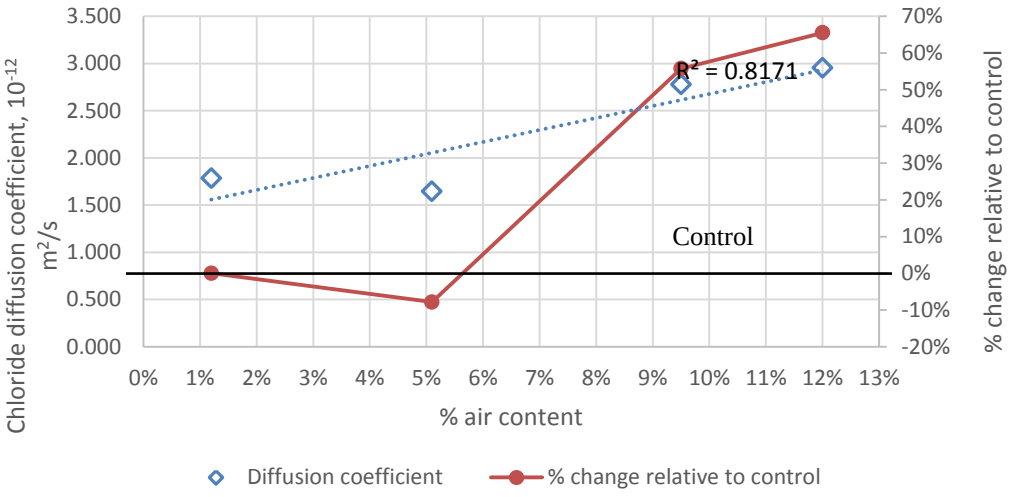

Figure 5.44: Effect of air content on the chloride diffusion of concrete

However at higher air content level (9.5% and 12% air) the chloride diffusion coefficient increased to 56% to 66% of the control concrete. This relatively higher level of chloride diffusion values suggests the weaker microstructure of the paste. Relatively very low gain in compressive strength of these two concrete as seen in Figure 4.26 of Chapter 4 where there was a reduction of compressive strength of 68% and 136% relative to the control concrete at 0.32 w/c ratio validate this high chloride diffusion values.

5.5.5 Summary

It has been seen from the above discussion that the chloride diffusion coefficient of concretes undertaken by this study are relatively low within 10^{-12} m^2/s range. This is due to the fact that all concrete evaluated under this programme were made with high volume supplementary cementitious and pozzolanic materials which enhanced and densified the microstructure of the cement paste. The use of relatively lower w/c ratio of 0.32 also enhanced these characteristics.

However very high volume of SCM such as 100% GGBS produced weaker microstructure resulting into a relatively higher chloride diffusion coefficient values. It has been seen that concrete containing 85% and 95% had better chloride diffusion results than the control P30S70 concrete. The chloride diffusion coefficient improved further on concrete consisting of fly ash, microsilica and rice husk ash. However, concrete containing P15S70R15 had the lowest chloride diffusion coefficient, which was 44% lower than the control P30S70. The effect of the additional finer particles of unwashed sand was clearly demonstrated by having lower chloride diffusion compared to the same concrete made with washed sand.

This effect has also been demonstrated in concrete with RCA, though the overall chloride diffusion coefficient of RCA concretes were relatively higher due to high inherent chloride content of RCA. Therefore, the chloride diffusion coefficient of RCA concrete was proportional with the RCA content. However, the effect of RCA content on the chloride diffusion coefficient was largely addressed by the use of P15S70R15 cementitious combination in concrete.

The effect of air was also demonstrated on the chloride diffusion coefficient where a moderate increase of air up to 5.1% reduced the chloride diffusion due to the development of improved microstructure. However further increment of air increased the chloride diffusion coefficient indicating development of relatively weaker microstructure.

5.6 Sulfate resistance test

Sulfate resistance test of concrete specimen was conducted according to a modified method of ASTM C1012 – 02 where concrete specimen of 75x75x280 mm size of concrete bar was immersed in a 352 moles/m^3 Na_2SO_4 solution for a prolonged period for up to 12 months and a periodical measurement of length was taken to measure the length change due to the sulfate attack. The periodical interval to take the measurement was initially at 1, 2, 3, 4, 5, 8, 13 and 15 weeks and further measurement was taken at a later intervals of 4, 6, 9 and 12 months after the immersion of the specimen in the sulfate solution.

This test was applied for concrete specimen from i) Cement type, ii) Sand type and iii) RCA type series to evaluate the performance of these group of concrete exposed to rich sulfate environment. After 12 months of continuous exposure to the sulfate solutions none

of the concrete specimen showed any sign of sulfate attack in terms of change of length, shape or deterioration of concrete. Pictures of selected specimen after the sulfate exposure are shown in Figure 5.45 and Figure 5.46 to illustrate the physical condition of concretes after 12 months sulfate exposure.

In Figure 5.45, photographs of concrete specimen from Cement type and Sand type series with different type of cementitious materials with different w/c ratios have been presented. As these images show, none of the specimen have any physical distortion or change of length or shape or any signs of sulfate attack. Only colour of the concrete surfaces changed to a greenish colour for concretes with high GGBS mixes.

This is perhaps due small presence of sulphide in the slag which supposed to disappear as sulphide reacts with air to produce hydrogen sulphide (Leung, P.W.C and Wong, H.D., 2011). Due to long term ponding in rich sulfate solution, a deposition of sulphide on the surface of concrete specimen could also be the reason.

Very high level replacement of Portland cement by supplementary cementitious materials including GGBS, fly ash, microsilica and rice husk ash made the concrete very durable against the sulfate attack. As discussed in Chapter 2 section 2.5.2 the Na_2SO_4 would react with calcium aluminate hydrate to form expansive calcium sulfo-aluminate hydrate or ettringite.

The sulfate ions may also react with calcium hydroxide to produce gypsum ($CaSO_4.2H_2O$). In both reactions presence of water is required. All concretes under this study were made with various proportions and different type of SCMs with very low w/c ratio. The water permeation and water absorption properties of almost all concretes were excellent. This is one of the main reasons of having no signs of sulfate attacks on the concrete specimen.

Cement type **Sand type**

Figure 5.45a: 100% GGBS, washed sand, 0.32 w/c

Figure 5.45b: 100% GGBS, unwashed sand, 0.40 w/c

Figure 5.45c: 80% fly ash, washed sand, 0.40 w/c

Figure 5.45d: 80% fly ash, unwashed sand, 0.40 w/c

Figure 5.45e: 10% microsilica, washed sand, 0.32 w/c

Figure 5.45f: 10% microsilica, unwashed sand, 0.32 w/c

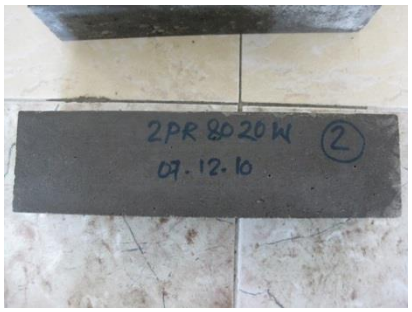

Figure 5.45g: 20% rice husk ash, washed sand, 0.32 w/c

Figure 5.45h: 20% rice husk ash, unwashed sand, 0.32 w/c

Figure 5.45: Sulfate resistance test, concrete specimen of Cement and Sand type series

Figure 5.46 show the images of concrete bars made with RCA and 100% GGBS with washed and unwashed sand exposed in sulfate environment. It is intriguing to observe that concretes made with RCA with 100% GGBS were also totally unaffected by the sulfate exposure even though the water permeation of RCA washed sand concrete were relatively higher.

RCA with washed sand **RCA with unwashed sand**

Figure 5.46a: 100% RCA, 0.25 w/c

Figure 5.46b: 100% RCA, 0.25 w/c

Figure 5.46c: 80% RCA, 0.25 w/c

Figure 5.46d: 80% RCA, 0.25 w/c

Figure 5.46e: 50% RCA, 0.32 w/c

Figure 5.46f: 50% RCA, 0.25 w/c

Figure 5.46: Sulfate resistance test, concrete specimen of RCA type for both washed and unwashed sand

The reason could be due to unavailability of water at the interface of CAH, the hydration product susceptible to be attacked by the Na_2SO_4 ion, though the water permeation of RCA concrete made with washed sand was high. The presence of water is an important factor for the sulfate attack to take place. The higher permeation could be due to porous substructure of the recycle concrete aggregate itself, instead of having higher porosity within the 'new' paste.

5.7 Conclusion

In this chapter the results of the durability and permeation properties of concretes have been presented and discussed. The durability tests considered are i) RCPT as per ASTM C1202-97, ii) Chloride diffusion as per draft European standard CEN TC51/WG12/TG5, (Draft 4 Version 2) and iii) Sulfate resistance test as per modified ASTM C1012 – 02. The permeation tests are i) Water absorption test as per BS1881: Part 122 and ii) Water permeation test as per BSEN 12390: Part 8.

The accepted level of the chloride penetration resistance value in terms of coulomb was considered to be 1500 coulomb. Most of the concrete undertaken by this study achieved this level of performance. All concrete made with different proportion of GGBS, fly ash, microsilica and rice husk ash achieved 'very low' level of coulomb values as per ASTM C1202-97 indicating outstanding chloride ion penetration resistance properties. Same concretes made with unwashed sand also achieved very low level of chloride penetration resistance, though there was little evidence on the effect of the additional finer particles on the RCPT results could be found.

Overall performance of RCA concrete made with 100% GGBS and washed sand was not very satisfactory perhaps due to erratic setting behaviour of 100% GGBS. However, use of unwashed sand improved the coulomb values of RCA concrete quite significantly.

Replacing 100% GGBS to P15S70R15 made the real difference in the performance of RCA concrete where a clear linear relationship between the RCA proportion and coulomb values could be established. With 100% GGBS there was no such relationship between the proportion of RCA and the coulomb values could be seen. The chloride ion penetration resistance could also be enhanced by increased curing temperature and increased air content of concrete. Concrete with higher entrained air showed extremely low level of coulomb values.

The water absorption properties of concrete with different proportion of GGBS and other pozzolanic materials were found to be well within the acceptable level of 2.0%. However the effect of the unwashed sand on the water absorption of concrete made with different proportion of pozzolanic materials was more pronounced. The improvement in the water absorption performance could be as much as 56% for a 3P30S70U concrete.

Though most of the water absorption values of RCA concrete made with GGBS were below 2.0%, but there was no correlation between the water absorption properties and the RCA content could be found. Similar to the natural aggregate, the RCA concrete also showed the effect of finer particles of unwashed sand on the improvement of water absorption values. Use of P15S70R15 cementitious combination instead of 100% GGBS did enhance the water absorption results of RCA concrete. The variability between the water absorption results of RCA concrete was also reduced significantly by P15S70R15 cement combinations. Significant effect of higher curing temperature and higher air content on the properties of water absorption could not be found, though in both cases the water absorption values remained below 2.0%.

Water permeation results of concrete containing different proportion of GGBS and pozzolanic materials showed extremely impermeable concrete matrix with many occasions without having any water penetration at all. This was due to the development of very robust microstructure of cement paste due to the development of additional hydration products contributed by the pozzolanic reactions. The effect of the additional finer particles in the washed sand concrete was more pronounced with maximum 5 mm water penetration recorded with P20F80U concrete, with most of the other concretes did not have any water penetration at all.

The water permeation results of RCA concrete made with washed sand and 100% GGBS were not satisfactory. However, significant improvement was made by the use of unwashed sand, though the results were not consistent. Use of P15S70R15 with RCA not only improved the water permeation results but also provided relatively consistent results proportionate to the RCA content.

Higher curing temperature on triple blend of cementitious materials containing Portland cement, GGBS and rice husk ash could not demonstrate any further improvement on the performance of water permeation, though the overall results were below the targeted value of 10mm. Concrete with higher entrained air up to 5% showed no sign of water penetration. However the properties of water permeation increased with the increase in the air content.

Chloride diffusion of all concrete tested under this work showed well below the targeted value of 5×10^{-12} m^2/s. Concrete with different proportion of GGBS showed that up to 95% replacement of GGBS could have better chloride diffusion results compared to the control P30S70 concretes. Use of other pozzolanic materials such as fly ash, microsilica and rice husk ash reduced the chloride diffusion further, especially P15S70R15 posted a 44% reduction compared to P30S70. The chloride diffusion of concrete made with unwashed sand reduced further depending on their cementitious combinations. Both P30S70 and P20F80 posted 20% reduction in chloride diffusion compared with the same concrete made with washed sand.

The chloride diffusion coefficient of concrete using RCA was relatively higher mainly due to higher inherent chloride content of RCA. The effect of RCA content on the chloride diffusion was linear and the effect of the unwashed sand and use of P15S70R15 were also very pronounced. P15S70R15 cementitious combination improved the chloride diffusion of RCA concrete very effectively perhaps by encapsulating the existing chloride ions within the RCA itself.

Increase in air content to 5% had a positive impact to reduce the chloride diffusion to further 8% of control; however, with further increase in air content increased the chloride diffusion significantly due to the development of porous microstructure.

There was no visual sign of sulfate attack from prolong exposure up to 12 months of concrete prisms in rich 352 moles/m^3 Na_2SO_4 solution tested as per modified ASTM C1012 – 02 method. Concretes made with different type of cementitious materials and aggregates according to the Cement, Sand and RCA types did not show any physical distortion or change of length or shape or any signs of sulfate attack. The main reason of no sulfate attack is due to the use of SCMs such as GGBS, fly ash, microsilica and rice husk ash and use of reduced w/c ratio of 0.25, 0.32 and 0.40. Improved microstructure and reduced permeation properties of paste made it not possible for sulfate ions and water molecules to permeate through the concrete matrix.

Though the overall outcome of the durability and permeation properties of concretes tested under this study conform to the target level of performance, often there were inconsistencies related to w/c ratios, RCA content, effect of finer particles, curing temperature or air content were observed. These inconsistencies are potentially due to the factors related to i) the erratic setting behaviour of 100% GGBS ii) impurities in RCA and iii) testing variability. Wide range of variability related to human and testing factors was reported by Pocock, D. and Corrans, J. (2007) for durability tests including water permeation, water absorption and RCPT. The CoV of water permeation results was reported to be 125% and ASTM C1202-97 recognized a testing variability of 42% between two RCPT of same concrete. By recognizing this variability, it could be concluded that the durability and permeation properties of concretes studied largely conformed to their respective target values and suitable to use in the Arabian Peninsula.

Chapter 6

Analytical Works on cement paste and mortar

6.1 Introduction

The results of the analytical works carried out to determine and analyse the characteristics of the output of different form of cement combinations in terms of hydration products, morphology and the effect of the additional finer particles in the pore structure are presented in this Chapter. The following analytical works were undertaken to conduct this study:

1. Thermogravimetry analysis (TGA): This was to determine the presence and quantity of different hydration phases in hydrated cement pastes. Different combinations of cementitious materials were tested at different ages.
2. Scanning electron microscopy (SEM): To ascertain the development of the different hydration phases.
3. Mercury intrusion porosimetry (MIP): To analyse the characteristics of the pore structure and the effect of the additional finer particles in concrete made with unwashed sand.

The following sections will present and discuss the results of the above experimental works and will be compared to validate the outcome of each technique.

6.2 Thermogravimetry Analysis

6.2.1 Introduction

In thermogravimetry analysis, hardened cement pastes at different cementitious combination were analysed at different ages of 1, 7, 56 and 365 days to understand the formation of different hydration product. The w/c ratio was kept constant at 0.32 for all cement combinations. The proportion of different cement combinations comprising of Portland cement, GGBS, fly ash, microsilica and rice husk ash are described in Chapter 3, Table 3.19 and designated as UKPC, P30S70, P15S85, P20F80, P90M10, P80R20 and P15S70R15.

The procedure of sample preparation for TG work has been described in Chapter 3. All above samples were tested at 1, 7, 56 and 365 days except 1d fly ash sample (P20F80) as the fly ash sample did not set at 24 hours. An attempt to prepare a sample for 100% GGBS was discarded as the paste made with 100% GGBS did not set at all, unlike the 100% GGBS concretes. This could be due to low room temperature as the paste for TGA was prepared in the laboratory of the University of Bath in UK. The concrete was made in Abu Dhabi, in the concrete laboratory of Xtramix Concrete Solutions. The average room temperature of concrete laboratory of the University of Bath and Xtramix in Abu Dhabi were approximately 15 °C and 25°C respectively.

6.2.2 Discussions

The graph of mass loss as derivative TG of all specimen at four different ages have been illustrated in Figure 6.1 to 6.4. In general there are three distinctive dips can be identified from these four figures. They are at i) 100 - 200^{0}C ii) 400 - 500^{0}C and iii) 700 - 800^{0}C. From the literature it can be derived that close to 100 - 200^{0}C temperature the moisture and the water combined as hydrate of hydration products are liberated. At 400-500^{0}C the disintegration of $Ca(OH)_2$ occur and at 700-800^{0}C the calcium carbonate disintegrate (Lawrence, R.M.H., et. al. 2006 / Ramachandran, V.S. and James J. Beaudoin, J.J., 2001 / Ukrainczyk, N. et. al. 2006 / Anastasiou, M. et. al., 2006). The dTG graphs for all cementitious combination at all ages followed similar trends.

As most of the hydrates disintegrated at a temperature of 100 - 200^{0}C, to measure the performance of each cement combination in terms of its ability to produce most hydration product, it is important to look deep into this region. As all specimens went through same preparation process including drying, it was assumed that the quantity of absorbed moisture evaporated for all samples was the same.

A careful observation can reveal that at 100^0C region, pastes containing maximum Portland cement had the biggest decomposition of minerals especially at 1 day age. In Figure 6.1 the UKPC had the maximum loss of mass at 100^0C temperature followed by P90M10, P80R20, and P30S70. P15S85 and P15S70R15 had the least loss of mass. This was due to the fact that at 1 day only the primary hydration process of Portland cement had happened and the pozzolanic reaction was yet to start. Detailed quantified analysis of the formation of the hydration products have been discussed later.

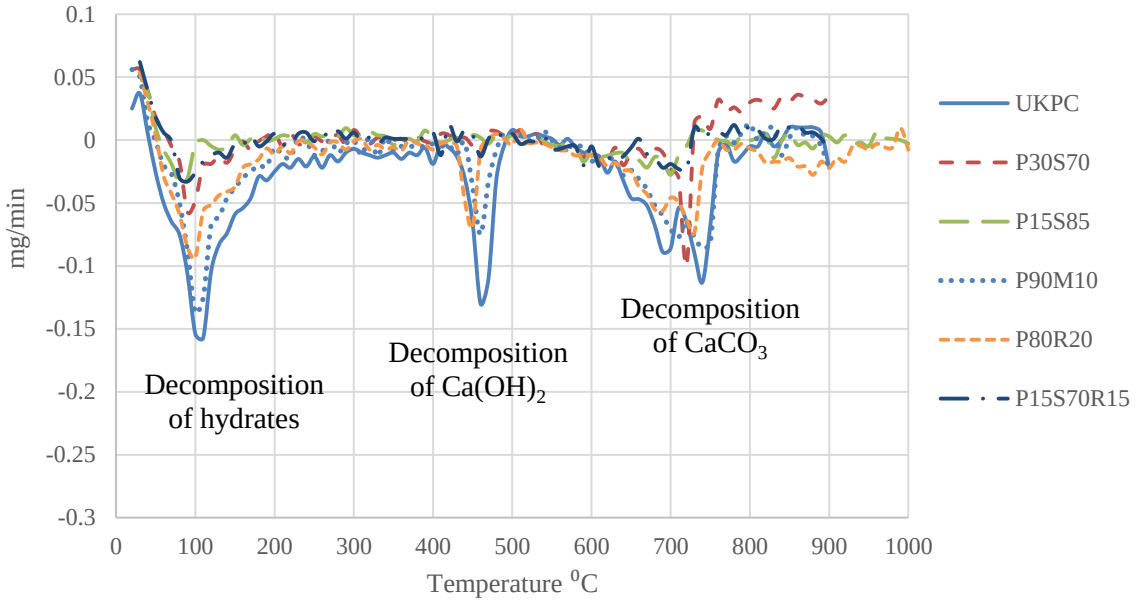

Figure 6.1: dTG graph of cement pastes of 1 day age

However at the age of 7 day (Figure 6.2) the P90M10 with 10% microsilica had almost similar loss of weight as of 100% UKPC paste followed by 20% rice husk ash (P80R20), 70% GGBS (P30S70), triple blend with 15% Portland cement, 70% GGBS, 15% rice husk ash (P15S70R15), 85% GGBS (P15S85) and 80% fly ash (P20F80) pastes. This trend is in harmony with the result of 1 day, except the fact that perhaps the pozzolanic reaction of microsilica mix was more than other cementitious combinations resulting into the production of more hydrates.

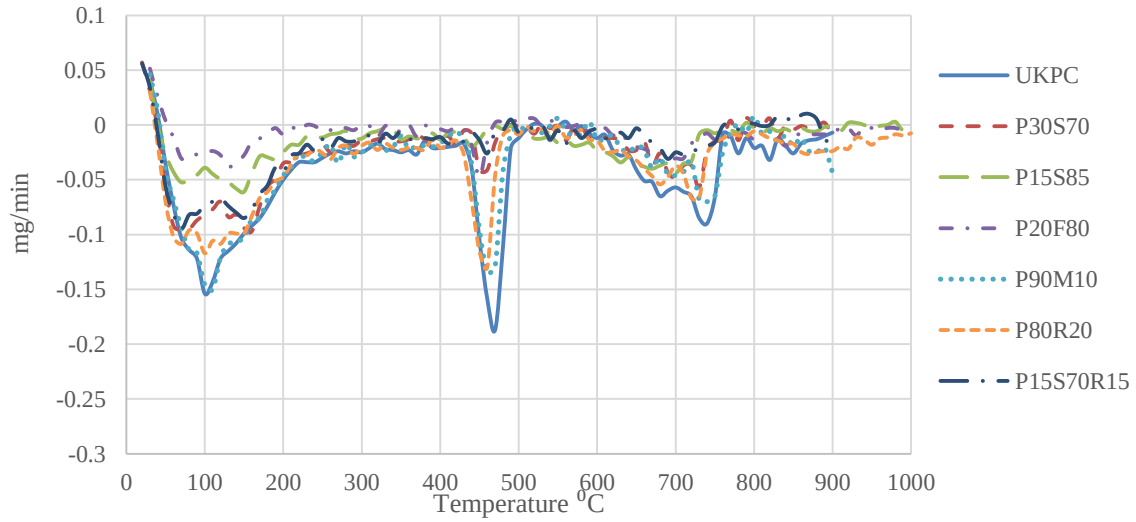

Figure 6.2: dTG graph of cement pastes of 7 day age

At the age of 56 day, the microsilica mix had the most loss of hydrates mass followed by the UKPC, P80R20, P30S70, P15S85, P15S70R15 and P20F80. It is not clear why at 56 day the mass loss was relatively lower than 1 and 7 day, as logically it should be higher as more hydration products were formed over the time.

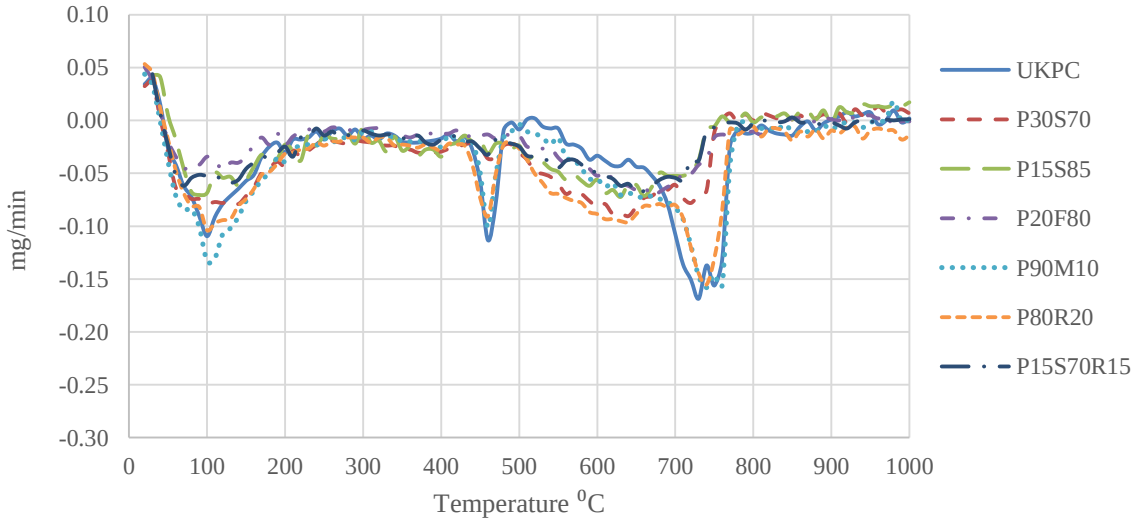

Figure 6.3: dTG graph of cement pastes of 56 day age

The behaviour of the mass loss of all combination at 365 day gives a very interesting insight. Three combinations namely P80R20, P90M10 and UKPC had 2 distinctive dips at 100^{0}C temperature region. The first dip, which was much smaller, occurred before 100^{0}C and the second and larger dip occurred after the 100^{0}C mark. Perhaps the first dip could be attributed to the evaporation of moisture and the second dip is the disintegration of hydrates.

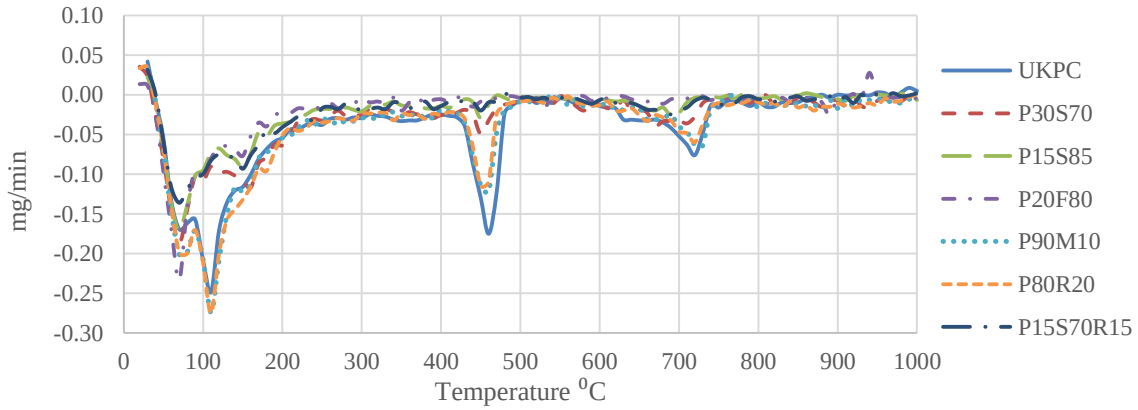

Figure 6.4: dTG graph of cement pastes of 365 day age

Interestingly paste containing P80R20 had the maximum mass loss followed by P90M10 and UKPC. P20F80 had the higher mass loss than P30S70 followed by P15S85 and P15S70R15. The overall mass loss at 365 day was also much larger than other ages confirming the maximum production of hydrates over time, mainly due to the secondary hydration of pozzolanic materials.

6.2.3 Production of $Ca(OH)_2$ and its consumption

Production of $Ca(OH)_2$ is a direct function of the production of hydrates as $Ca(OH)_2$ is liberated during the cement hydration process. This was demonstrated at 400-500^{0}C region at all four ages. Cement pastes mainly UKPC, P90M10 and P80R20 mixes which have higher production of hydrates at 100-200^{0}C had deeper dips of the $Ca(OH)_2$ disintegration.

However, the produced $Ca(OH)_2$ might have reacted again with the amorphous SiO_2 of cement combinations with pozzolanic materials and produced more hydrates as a result of the pozzolanic reactions. This effectively reduced the quantity of $Ca(OH)_2$. This reduction would be able to provide information on the extent of pozzolanic reaction for any particular cement combination. However, at the same time, $Ca(OH)_2$ might be consumed by the atmospheric CO_2 to produce $CaCO_3$ as a process of carbonation. This process would also reduce the quantity of $Ca(OH)_2$.

The mass of $Ca(OH)_2$ in terms of percentage of initial mass of each cement combinations which was disintegrated during the TG analysis experimental works is shown in Figure 6.5. The proportion of $Ca(OH)_2$ is computed by considering the relative atomic mass of

individual components of that particular disintegration process. The calculation and data are presented in Annex AG.

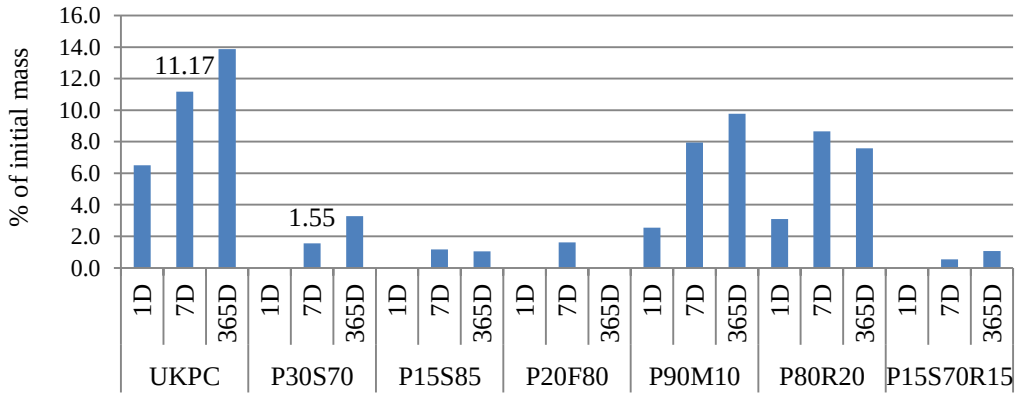

Figure 6.5: Decomposition of $Ca(OH)_2$ at TG analysis

It can be observed from the Figure 6.5 that net content of $Ca(OH)_2$ is high for mixes with higher Portland cement content (UKPC, P90M10 and P80R20) and low to minimal at other mixes where the Portland cement content ranged from 15% - 30% of total cementitious content. This net content of $Ca(OH)_2$ was deduced after part of it had been consumed in two chemical processes. Firstly the pozzolanic reaction with the supplementary cementitious materials (which contains SiO_2) and secondly the carbonation process.

The rate of carbonation i.e. the rate of consumption of $Ca(OH)_2$ to produce $CaCO_3$ can be assumed to be same for all cement combinations due to the fact that all cement combinations were exposed to the environment at equal exposure level. However, the mass of $CaCO_3$ produced in different cement combinations were not same, as available mass of $Ca(OH)_2$ for different cement combination were not same as well. This has been discussed further in the later sections of this chapter.

The lower content (net) of $Ca(OH)_2$ at P30S70, P15S85 and P15S70R15 (Figure 6.5) can be attributed to the pozzolanic reaction and lack of Portland cement content. This can be validated by the SEM images and compressive strength of concrete made of same cement combinations. The SEM images of these three mixes show very robust and rigid formation of mass of hydration product as an evidence of the pozzolanic reaction. (Section 6.32 & 6.33). High compressive strengths of these mixes also validate the pozzolanic reactions (Chapter 4, Section 4.3.1).

Lack of net content of $Ca(OH)_2$ at fly ash mix where it is virtually non-detectable at 1 and 365 days (Figure 6.5), is perhaps due to the fact that most of the produced $Ca(OH)_2$ was consumed by the amorphous SiO_2 as overwhelming amount of unhydrated fly ash particles could be seen in SEM images. The produced mass of $Ca(OH)_2$ by the 20% Portland cement was simply not enough to 'feed' the available SiO_2 contributed by the 80% fly ash. The SEM image with abundant particles of fly ash and lower compressive strength of concrete suggest the same (Section 6.32 & 6.33 and Section 4.3.1 of Chapter 4).

The net content of $Ca(OH)_2$ at microsilica and rice husk ash mixes are relatively higher showing inadequate pozzolanic reaction and relatively higher Portland cement content. The pozzolanic reaction for these two mixes should be more vigorous considering very high content of SiO_2 compared to other cementitious materials used in this study. This was due to incomplete pozzolanic reaction due to lack of adequate water in mix with 0.32 w/c ratio.

It is obvious from the above discussions that only GGBS mixes including P15S70R15 had the maximum pozzolanic reaction in terms of production and consumption of $Ca(OH)_2$. The fly ash mix could not produce enough $Ca(OH)_2$ to contribute to the matrix and both microsilica and rice husk ash mixes had very high content of unused $Ca(OH)_2$ which could not be used due to the lack of water.

6.2.4 Extent of pozzolanic reaction

As different cement combinations with different type and quantity of pozzolanic materials and Portland cement produced different amount of net $Ca(OH)_2$, it will be interesting to understand how much of the produced $Ca(OH)_2$ was consumed by the SiO_2 of each cement type, in another words what was the extent of each pozzolanic reaction.

The extent of pozzolanic reactions by each type of cement pastes relative to their Portland cement content can be seen in Figure 6.6. For example the P30S70 cement paste with 30% Portland cement should achieve total content of $Ca(OH)_2$ equal to the 30% of UKPC's total $Ca(OH)_2$ content for any given age. It is to take note that the proportion of $Ca(OH)_2$ of UKPC shown in Figure 6.5 is the net content after carbonation as certain proportion of the $Ca(OH)_2$ produced by the UKPC had already been consumed by the atmospheric CO_2 to produce $CaCO_3$. For other cement pastes it is the net content after carbonation and pozzolanic reaction.

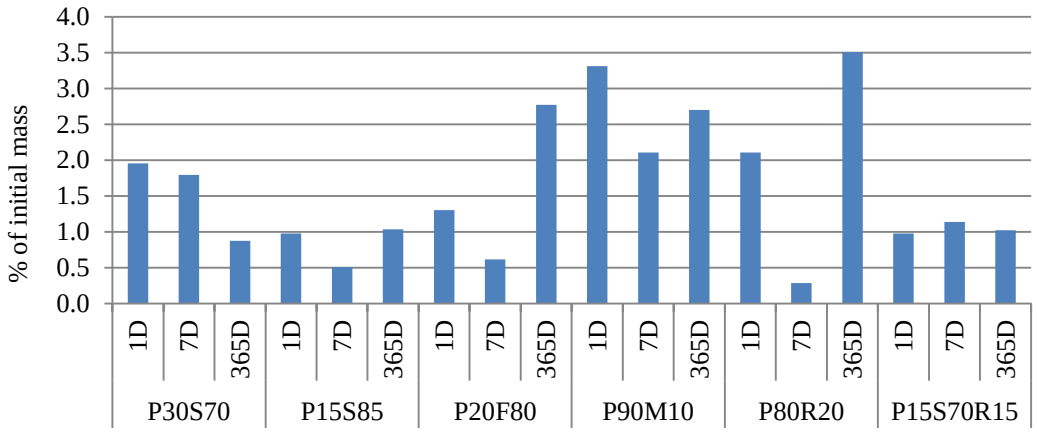

Figure 6.6: Extent of pozzolanic reaction by each type of mixes relative to their Portland cement content

Considering at the age of 7 days (Figure 6.5) 30% of the UKPC's $Ca(OH)_2$ content would be 3.35%. However, Figure 6.5 shows that at 7 days, the P30S70 had $Ca(OH)_2$ content of 1.55%, meaning that the remaining 1.80% perhaps was consumed by the SiO_2 due to the pozzolanic reaction. This 1.80% could be described as the extent of pozzolanic reaction by P30S70 at 7 day. The percentage described here is the percentage of the initial mass of the specimen used in TGA test.

The extent of pozzolanic reaction was most profound in microsilica and rice husk ash mixes due to the presence of highly reactive SiO_2 content and their very high surface area, this is in spite of considerably great proportion of unreacted $Ca(OH)_2$ observed in Figure 6.5. However, at 7 day the pozzolanic reaction of the rice husk ash paste seems to be abnormally low perhaps suggesting testing variability. The same effect can also be observed at 85% GGBS and fly ash mixes.

Content of Portland cement seems to be a positive factor for higher pozzolanic reactivity as suggested by 70% GGBS mix (30% Portland cement) which had better performance than 85% GGBS (15% Portland cement) and the triple blend with 15% Portland cement. The exception to this observation was fly ash mixes which had very high pozzolanic reactivity especially at 365 day age. This could be attributed to its higher reactive SiO_2 content compared to GGBS.

6.2.5 Production of Hydrates

Concrete mixes comprising Portland cement and other SCMs would produce wide range of hydration products with complex chemical compositions. To minutely identify the production of each type of these compounds is beyond the scope of this study. However, by thermogravimetry we can roughly estimate the types of hydration compounds that may have been produced by analyzing the temperature range of the disintegration of compounds. Figure 6.1 to 6.4 show the disintegration of these compounds at different temperature range. From the literature we can summarize this disintegration of different kind of hydration products into the Table 6.1.

In Figures 6.1 to 6.4 the temperature range of the first dip is approximately from 30 – 200^0C. It is shown that the compound which was removed at lower temperature was water. However, as the water evaporating temperature range could overlap with the disintegration of other hydrate, therefore it could be assumed that the water content including the water in the mix (fixed w/c ratio for all paste) and the absorbed moisture from the air were constants for all mixes.

Table 6.1: Temperature range of disintegration of different type of hydration products

	Hydration products	**Temperature range ^{o}C**	**Reference source**
1	CSH	95 - 120	Lawrence, R.M.H, et. al.,2006
2	CAH	110 - 320	
3	Gypsum	160 - 190	
4	Ettringite	125 – 135	
5	Monosulfate	185 – 195	
6	$Ca(OH)_2$	450 – 550	Ramachandran, V.S. and James J. Beaudoin, J.J., 2001
7	$CaCO_3$	750 - 850	

At 1 day (Figure 6.1), the disintegration of hydrates for UKPC, microsilica and rice husk ash mixes had wider temperature range of 40 - 200^0C compared with the GGBS and triple blend mixes which were around 40 – 120 ^{0}C. It shows that at early age, the production of aluminate hydrates of GGBS hydration was yet to materialize as the CAH disintegrates at relatively higher temperature. The mass of the produced hydrates of GGBS pastes including

the triple blend which contained 70% GGBS were lower compared with rest of the mixes, confirming delayed production of CAH phase. In subsequent ages (7, 56 and 365 day, Figure 6.2-6.4) all 6 mixes had similar range of temperature confirming the production of both CSH and CAH products and perhaps other associated hydration products.

At 7 days (Figure 6.2) except for UKPC, P90M10 and P80R20, two distinctive dips can be observed for other mixes. These two peaks occurred roughly before and after 100^0C mark, showing distinctive sign of the production of C-S-H and C-A-H. This pattern vaguely continued at 56d (Figure 6.3), but significantly appeared at 365 day age (Figure 6.4).

Figure 6.7 provides an overall picture of the performance of different type of cementitious combination of the production of hydrates and $Ca(OH)_2$ at different ages. As mentioned earlier due to complicated chemical makeup of the hydration products, Figure 6.7 illustrates the relative production of hydrates in terms of the disintegration of moisture. It is not a direct measurement of the production of hydrates. For comparative reason, the data plotted for $Ca(OH)_2$ are also not the actual proportion of the mass of $Ca(OH)_2$, rather the mass of moisture disintegrated during the TG process.

For obvious reason the highest production of hydrates can be observed at 365 days, followed by 7 day and 1 day. Data obtained at 56 day was for some reason below the expected result perhaps due to the variability of the testing procedure. For this reason the 56 day results are omitted from Figure 6.7.

Considering 365 day as the base, both microsilica and rice husk ash mixes provided the maximum production of hydrates. It is intriguing that the net production of $Ca(OH)_2$ for both of these two mixes were also high and from the SEM images, plenty of unhydrated microsilica particles could be seen, indicating that due to inadequate amount of available water could not complete the pozzolanic reactions. UKPC and P30S70 paste performed almost similar followed by P15S70R15, P15S85 and P20F80 pastes.

Figure 6.7: Relative production of Hydrates and $Ca(OH)_2$ in terms of the disintegration of moisture of different cement paste expressed in percentage of the total mass of specimen tested

The performance of the production of hydrates of different cementitious combinations can be compared with the P30S70 as shown in Table 6.2. The 1 day result is reflecting the fact that GGBS is very slow to produce any reasonable amount of hydrates within 24 hours of mixing with water comparing with 100% or high volume Portland cement mixes. However at 7 day and subsequently at 365 days, the production of hydrates by high volume GGBS mixes considered to be high.

Table 6.2: Proportion of hydrates comparing with P30S70

Pastes	**1day**	**7day**	**365day**
P30S70	-	-	-
UKPC	517%	111%	116%
P15S85	78%	65%	58%
P20F80	0%	25%	70%
P90M10	364%	100%	122%
P80R20	394%	122%	121%
P15S70R15	78%	75%	73%

It is interesting to observe from Table 6.2 that there is little variation of the production of hydrates between 7 day and 365 days among different combinations of cement and pozzolanic materials. Only exceptions are fly ash and microsilica mixes. Especially for fly ash mix, the difference between 7 day and 365 day are significantly high, illustrating substantial amount of pozzolanic reactions had happened over 1 year period of time due to the presence of abundant amount of unreacted fly ash particles which could be seen by SEM images (Figure 6.27). Similar reasons can also be applied for microsilica mixes for the 22% additional proportion of the production of hydrates compared with 70% GGBS paste at the same age.

Production of hydrates of 85% GGBS and the triple blends P15S70R15 can also be considered to be reasonable compared with the 70% GGBS paste. The production of hydrates for 20% rice husk ash (P80R20) between 7 day and 365 day remained unchanged showing that there was little room left for this mix for further hydration after 7 day age.

The compressive strength of concretes made with the similar proportion (90% GGBS with 0.32 w/c) of cementitious materials at 28 days age also demonstrated the similar trend (Table 4.10, Chapter 4), validating the results obtained by the TG analysis.

6.2.6 $Ca(OH)_2$ / Hydrates ratio

A ratio between the produced $Ca(OH)_2$and hydrates (C/H) can be established using the same set of data indirectly obtained from the disintegration of moisture to understand their relationship for different cement type at different ages. Figure 6.8 shows that C/H ratio in UKPC remained similar (40%) at 1 day and 7 days but reduced at 365 days suggesting consumption of $Ca(OH)_2$due to the carbonation process. The ratio is higher with mixes with higher Portland cement content regardless of other cementitious type due to higher production of $Ca(OH)_2$.

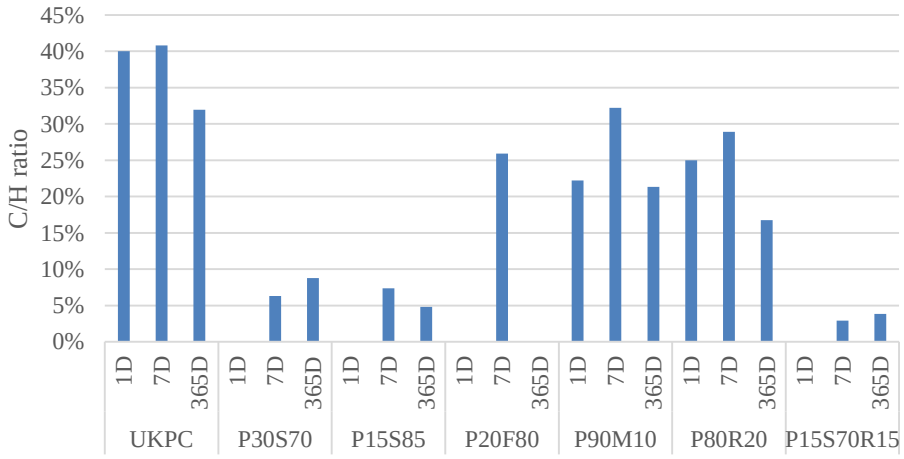

Figure 6.8: Ratio between $Ca(OH)_2$ and hydrates

Higher C/H ratio in P90M10 and P80R20 proved the presence of excessive unconsumed $Ca(OH)_2$ due to incomplete pozzolanic reaction due to unavailability of moisture as explained earlier. Pastes containing GGBS and fly ash mixes including P15S70R15 (fly ash at 7 day is the exception) had the lowest C/H ratio of below 10%. The very low C/H in P20F80 showed low production of $Ca(OH)_2$ as well as low production of hydrates. However low C/H ratio in P30S70, P15S85 and P1S70R15 showed development of excess hydrates due the pozzolanic reaction by reacting with $Ca(OH)_2$. Therefore, concrete containing these cementitious combinations would provide optimum production of hydrates which would have a direct contribution to their mechanical and durability properties of concrete.

6.2.7 Formation of $CaCO_3$

Figure 6.9 shows the disintegration of $CaCO_3$ together with $Ca(OH)_2$ as the percentage of initial mass of different cement pastes in TG analysis. In this analyses the proportion of $CaCO_3$ and $Ca(OH)_2$ has been computed considering the relative atomic mass of individual compounds derived from the TG analysis. Presence of $CaCO_3$ in the mixes could be due to two reasons i) carbonation of $Ca(OH)_2$ ii) grinding of limestone together with clinker as part of the cement making process.

6.2.7.1 $CaCO_3$ contributed by limestone from cement production process

The content of $CaCO_3$ in each cement type could be contributed by the initial presence of ground limestone during the production of Portland cement. Therefore the proportion of $CaCO_3$ from this source should be equal to the proportion of Portland cement content of each type of cement pastes.

Determination of the extent of the mass of $CaCO_3$ produced by TGA gives us an indication of the extent of carbonation different type of cement combination might be subjected to. This gives some insight on the properties of durability of carbonation resistance of the concretes.

6.2.7.2 Carbonation of $Ca(OH)_2$

Carbonation will depend on the availability of $Ca(OH)_2$ and the depth of carbonation of hardened cement paste prior to ground it into a powder sample. The powder samples could also be carbonated further as the specific surface area increased.

Availability of $Ca(OH)_2$ is also dependent on the extent of pozzolanic reaction as both CO_2 and SiO_2 compete to consume $Ca(OH)_2$ for carbonation and pozzolanic reaction respectively. It would be beyond the scope of this study to examine further the extent of this 'competition' and exact share of $Ca(OH)_2$ for each reactant. From Figure 6.9 we can only observe that paste containing higher Portland cement, which formed the highest proportion of $Ca(OH)_2$ led to the highest $CaCO_3$ content.

Theoretically the mass of disintegration of $CaCO_3$ should increase over the time as carbonation is time dependent. A linear trend could be observed at UKPC where no pozzolanic reaction has been taken place confirming the time dependent carbonation, however, other cement paste could not provide the similar trend perhaps due to the effect of pozzolanic reactions. The relationship between the formation of $Ca(OH)_2$ and the content of $CaCO_3$ in UKPC validate the carbonation of $Ca(OH)_2$.

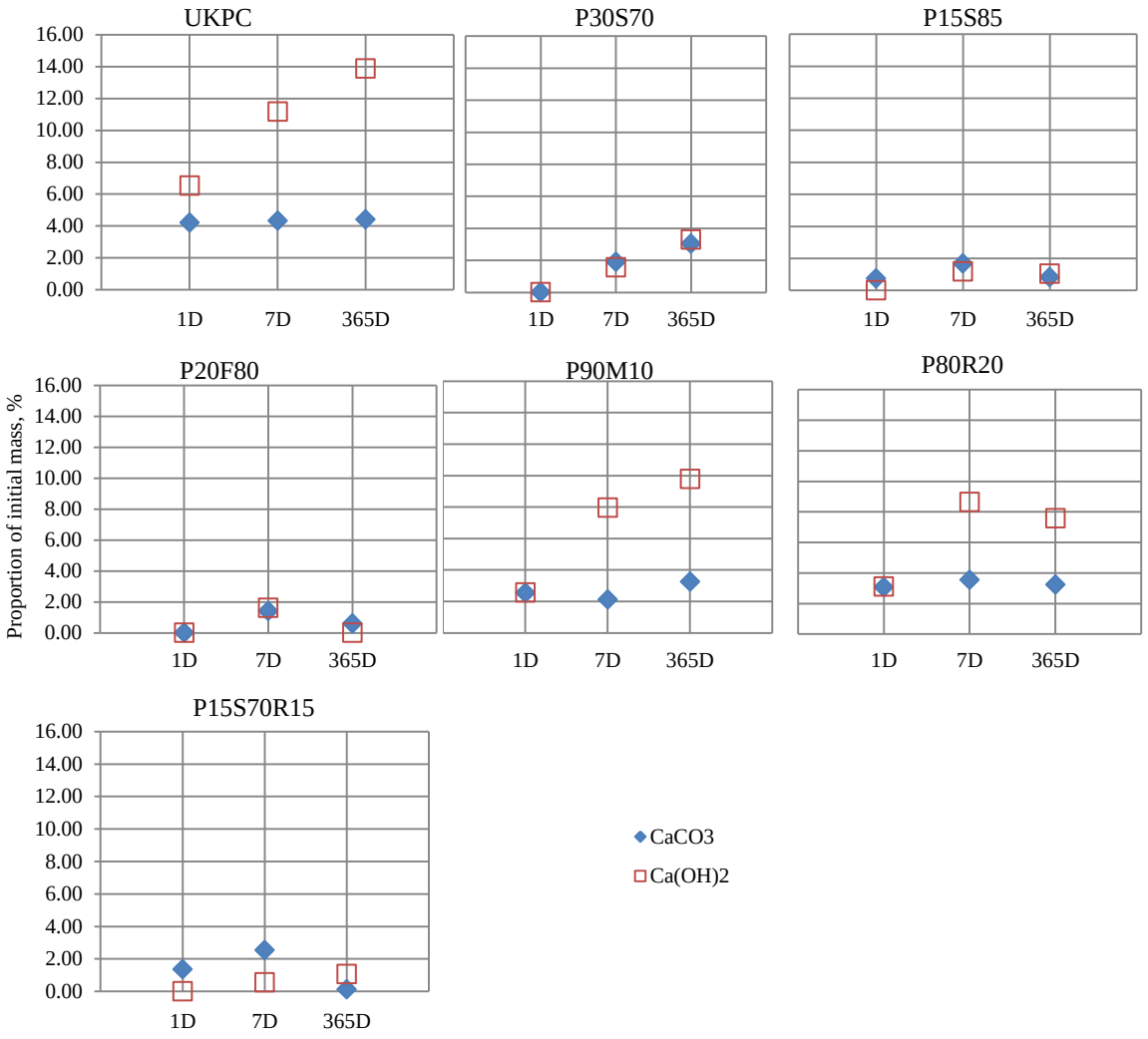

Figure 6.9: Disintegration of $Ca(OH)_2$ and $CaCO_3$ by TGA

It is important to take note that the method of sampling of specimen for TG analysis may not give a representative picture of carbonation as samples were not collected from a fixed depth from the surface of the hardened paste as the extent of carbonation of paste may vary depending on its relative location.

6.2.8 Summary

Thermogravimetry analysis of all 7 cement paste combinations revealed the disintegration of three sets of compounds namely hydrates, $Ca(OH)_2$ and $CaCO_3$ at three distinctive temperature regions. The disintegration of hydrates is mostly profound with paste containing higher Portland cements i.e. UKPC, P90M10 and P80R20 pastes. Two distinctive dips in between 30 - 200°C region separated by 100°C mark clarifies the evaporation of water and the disintegration of hydrates. Formations of CAH for GGBS mixes at later ages are also demonstrated by the dTG graphs.

Production of $Ca(OH)_2$ was higher at pastes containing higher Portland cement content but lower at GGBS and fly ash mixes confirming effective pozzolanic reaction for GGBS mixes but inadequate production in fly ash mix due to low content of Portland cement. Both microsilica and rice husk ash mixes had very high content of unused $Ca(OH)_2$ which could not be used due to the lack of water. Interestingly at the age of 365 days the 'extent of pozzolanic reaction' of microsilica, rice husk ash and fly ash mixes were higher than the GGBS mixes. This proves the pozzolanic reactivity of these materials due to the presence of highly reactive SiO_2 content.

The production of $CaCO_3$ was higher with the paste containing higher Portland cement which produced higher $Ca(OH)_2$ as a direct result of carbonation process.

6.3 Scanning Electron Microscopy

6.3.1 Introduction

As TGA provides the quantitative analysis of the hydration products, scanning electron microscopy (SEM) analysis on the samples have provided the real image of the developed product at different cement combinations at different ages. In this work SEM imaging was taken on the fragments of all 7 types of cement pastes namely UKPC, P30S70, P15S85, P20F80, P90M10, P80R20 and P15S70R15. The specimens were tested at the age of 7, 56 and 365 day. All these images were taken from a single fragment for their specific cement type and age. The work procedure and method of sample preparation were discussed in Chapter 3.

6.3.2 Progression of hydration of cement pastes

Table 6.3 has summarized the analysis of all images to reach a qualitative conclusion of the effective performance of each type of paste. The horizontal row for each type of cement paste provides the progressive improvement of the microstructure starting from 7, 56 and ending at 365 days. The vertical columns of 7, 56 and 365 days compared the relative difference of the quality of the microstructure of different type of cement pastes at any specific age.

Table 6.3: Analysis of SEM images of different types of cementitious pastes over time

Paste	7 days	56 days	365 days
UKPC	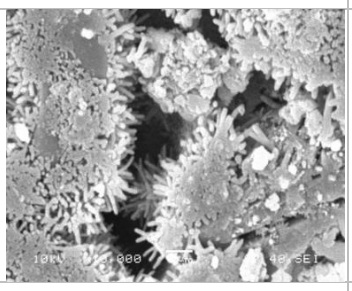	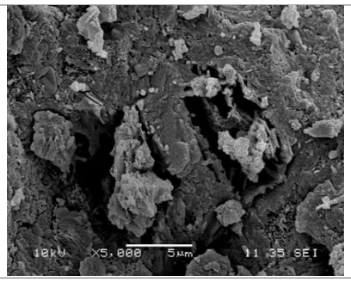	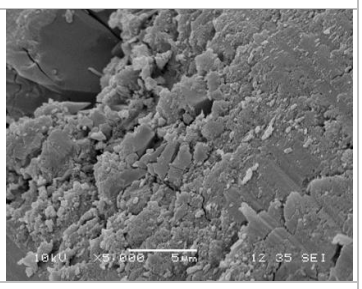
	• Large pores • Presence of ettringite, monosulfate and $Ca(OH)_2$ • Growth of CSH crystals	• Development of solid mass with the presence of large pores	• Improved microstructure with lesser pores
P30S70	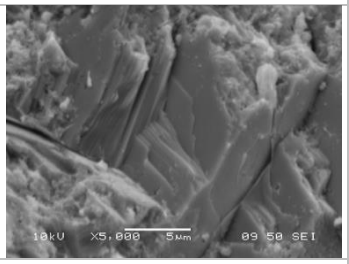	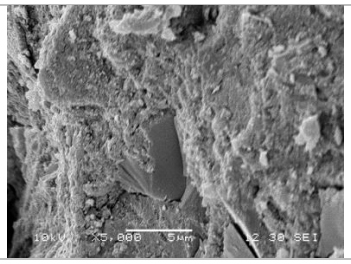	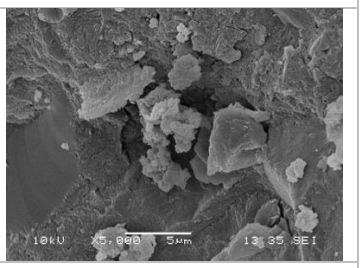
	• Solid microstructure with no visible pores • Unique layered well uniformed hydration product	• Unique morphology, with densely pack of finger like hydration products of slag particles • Presence of large capillary pores, unlike 7day images • Possible autogenous shrinkage cracks	• Perfect solid mass of hydration product with little or no porosity

Table 6.3 (cont.): Analysis of SEM images of different types of cementitious pastes over time

Paste	7 days	56 days	365 days
P15S85	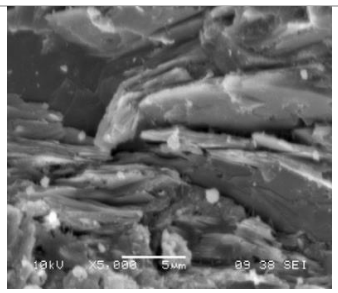	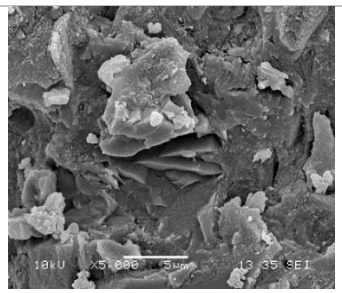	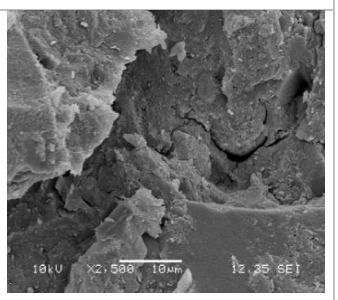
	• Layered hydrated gel similar to P30S70 • The morphology is not as dense as P30S70 • The presence of both dense and porous gel co-exist	• Predominantly solid mass together with flock of wool like microstructure • Larger but fewer number of pores • Autogenous shrinkage cracks	• Similar to P30S70 perfect solid mass with the presence of autogenous shrinkage cracks
P20F80	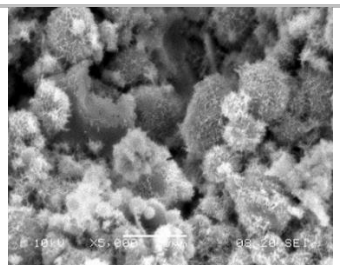	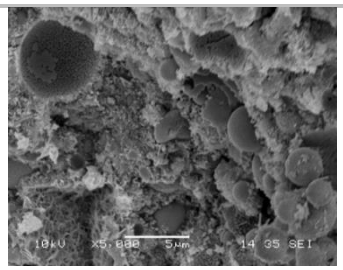	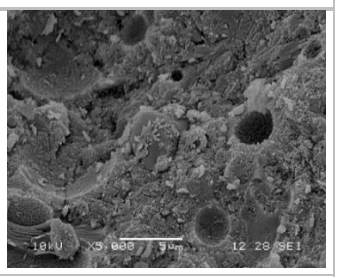
	• Large quantity of unhydrated spheres of fly ash suggesting lack of $Ca(OH)_2$ in the system due to reduced quantity of Portland cement • The morphology is porous, due to the lack of hydration products contributing to the lower compressive strength • Needle like crystals growing over round fly ash particles are CSH, the results of pozzolanic reactions	• Unhydrated and partially hydrated fly ash particles remained in abundance in the system • Porous microstructure	• Porous microstructure with the presence of unhydrated fly ash particles and uncompleted hydration products

Table 6.3 (cont.): Analysis of SEM images of different types of cementitious pastes over time

Paste	7 days	56 days	365 days
P90M10	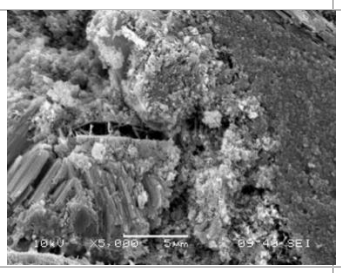	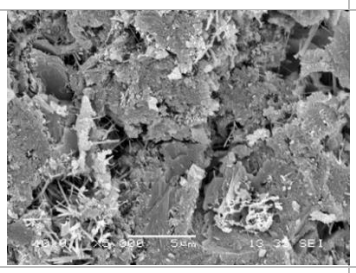	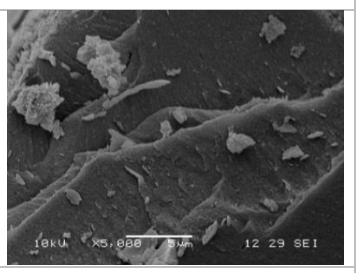
	• Unhydrated larger and conglomerated particles of microsilica particles embedded in relatively dense microstructure. • Presence of ettringite and monosulfate at the cavity of large pores show the hydration activity • Autogenous shrinkage cracks	• Porous microstructure as microsilica concrete with incomplete hydration with the presence of pores, and crystals of hydration products and unhydrated microsilica particles (Figure 6.21a) • Presence of microcracks	• Presence of partially hydrated microsilica particles with rim of secondary hydration product of pozzolanic reaction • Presence of tiny flake like hydration products suggesting the hydration of individual microsilica particles • Overall microstructure is dense with no visible porosity
P80R20	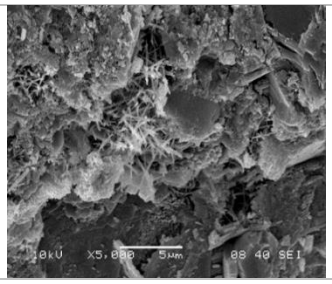	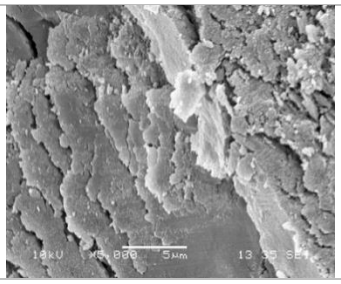	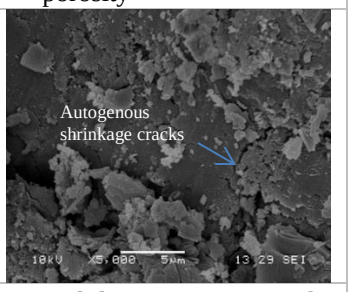
	• Relatively porous, with shrinkage cracks interconnecting the pores • Presence of ettringite and monosulfate (Figure 6.15a)	• Solid mass of hydration product either as layered or loosely packed providing a unique continuous networks of spaces between solid masses • Remarkable improvement in microstructure compared to 7day age	• Solid microstructure with presence of fewer pores • Possible autogenous shrinkage cracks

Table 6.3 (cont.): Analysis of SEM images of different types of cementitious pastes over time

Paste	7 days	56 days	365 days
P15S70 R15	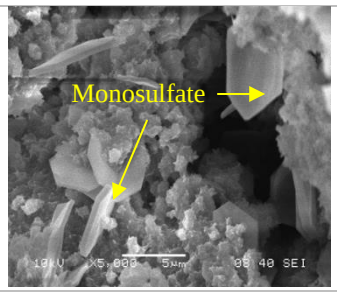	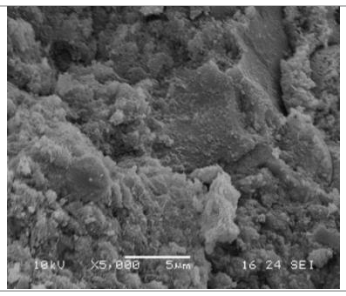	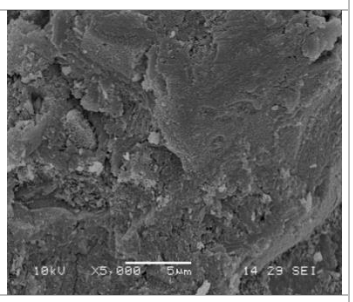
	• Relatively dense microstructure with combination of varied morphologies across the segment, suggesting the production of varied hydration products of triple blends • A large amount of flaky crystals of CSH gel deposited together with monosulfate plates in a cavity of a capillary pore	• Solid mass with virtually no capillary pores of microstructure	• Relatively dense microstructure, though isolated presence of incomplete hydration products due to pozzolanic reaction perhaps on top of rice husk ash particles can be spotted

6.3.3 SEM analysis of the hydration of individual cement pastes

The following sections have analysed the SEM images of hardened cement pastes at the age of 7, 56 and 365 days to observe the development of microstructure and formation and growth of different types of hydration products over the time.

6.3.3.1 Development of microstructure at 7 days

UK PC at 7 day:

At the age of 7 days the paste made with 100% Portland cement showed very porous microstructure with large unoccupied voids of capillary pores (Figure 6.10a and 6.10b). Growth of coral looking CSH crystal (Figure 6.10a) on the surface of anhydrous cement particles is dominantly present with obvious microporosity within themselves showing lack of hydration due to lack of water at 0.32 w/c ratio and relatively early age of 7 days. These voids perhaps were occupied with water prior to the removal of it by acetone during hydration stopping process. The plate like structure of monosulfate can be identified from the Figure 6.10b. Top left corner of Figure 6.10b shows growth of typical hexagonal shaped calcium hydroxide.

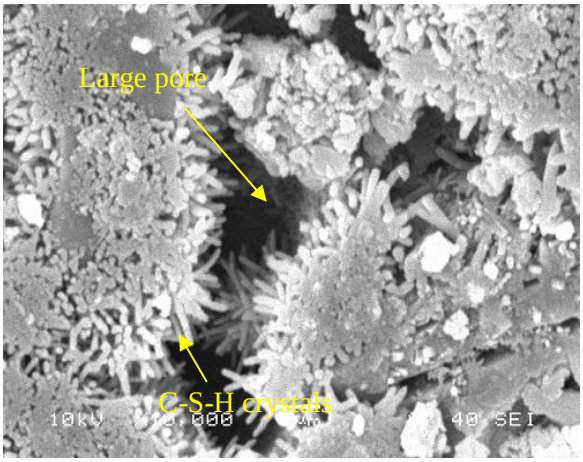

Figure 6.10a (5,000x)

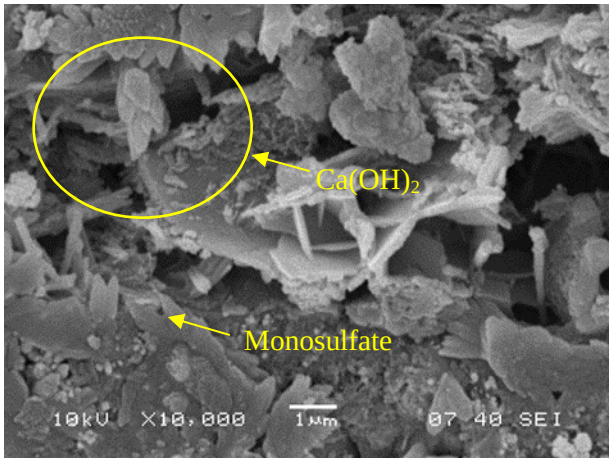

Figure 6.10b (10,000x)

Figure 6.10: SEM images of UKPC paste at the age of 7 days

P30S70 at 7 day:

The morphology of the paste containing 70% GGBS appeared to be with very solid structure of hydration products without having any significant porosity. The huge difference in the morphology from the 100% Portland cement paste is remarkably obvious suggesting the very durable nature of 70% GGBS concrete. A distinctive layered well uniformed CSH product is visible in Figure 6.11a which is unique to GGBS pastes. This layered formation could be due to the transition of Ca^{2+} and Al^{3+} ions from Portland cement and GGBS particles to form the hydration products in the form of 'outer, inner and skeletal hydrates' as described in Chapter 2 (Tanaka H, et.al., 1983). A rounded nodule or particle can be seen in Figure 6.11b which could be an unhydrated slag or cement particle.

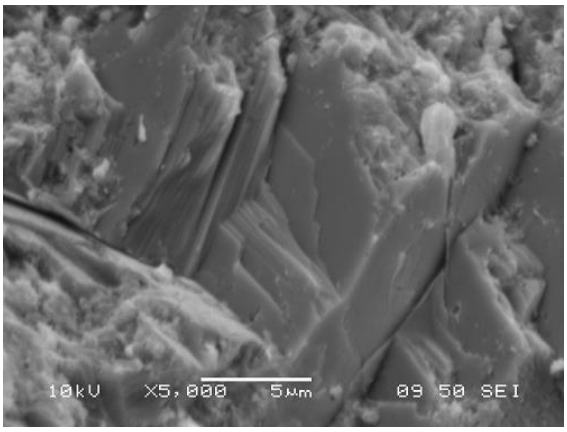

Figure 6.11a (5,000x)

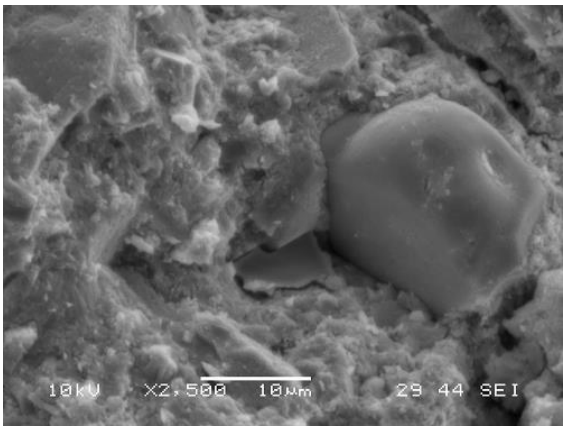

Figure 6.11b (2,500x)

Figure 6.11: SEM images of P30S70 at the age of 7 days

P15S85 at 7 day:

The morphology of paste containing 15% GGBS was not as dense as the 70% GGBS mix. However the presence of both dense and porous gel was in co-existence in Figure 6.12a. The presence of capillary pores in Figure 6.12a suggests that the amount of $Ca(OH)_2$ produced was not sufficient due to the lower content of Portland cement. The lack of $Ca(OH)_2$ has resulted into incomplete pozzolanic reaction leaving unhydrated slag behind. Similar to 70% GGBS layered hydrated gel can be observed in Figure 6.12b.

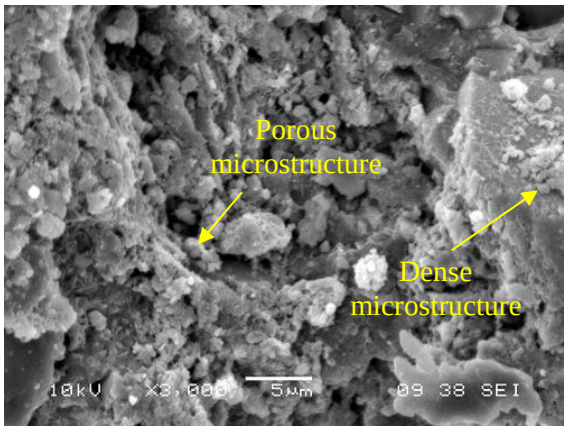

Figure 6.12a (3,000x)

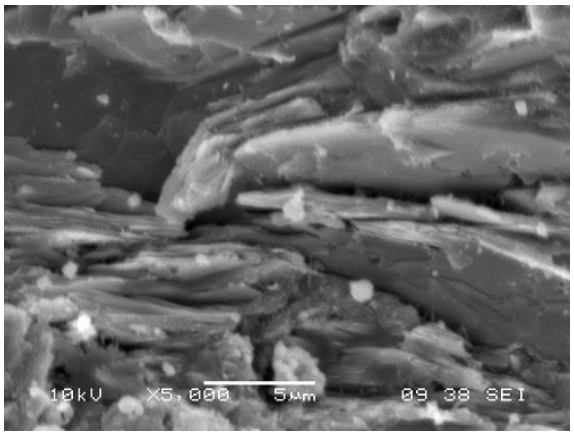

Figure 6.12b (5,000x)

Figure 6.12: SEM images of P15S85 at the age of 7 days

P20F80 at 7 day:

Large quantity of unhydrated spheres of fly ash suggests lack of $Ca(OH)_2$ in the system due to very low content of Portland cement. This was also validated by the TG analysis in previous sections. 80% fly ash of total cementitious content in the paste appeared to be excessive for any positive contribution to the pozzolanic reaction. The morphology was porous, due to the lack of hydration products, this contributed to the lower compressive strengths of concrete as seen in Chapter 4.

Needle like crystals growing over round fly ash particles were most probably CSH, the results of pozzolanic reactions. Figure 6.13b shows solid substrates with embedded fly ash particles. This substrate is appeared to be the CSH gel derived from both primary reaction of Portland cement and subsequent pozzolanic reaction with fly ash particles.

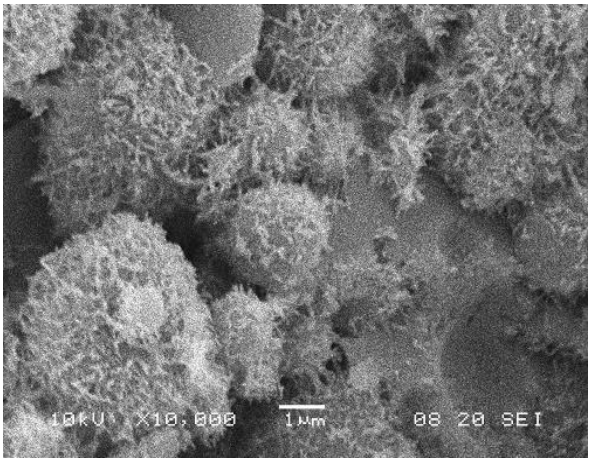

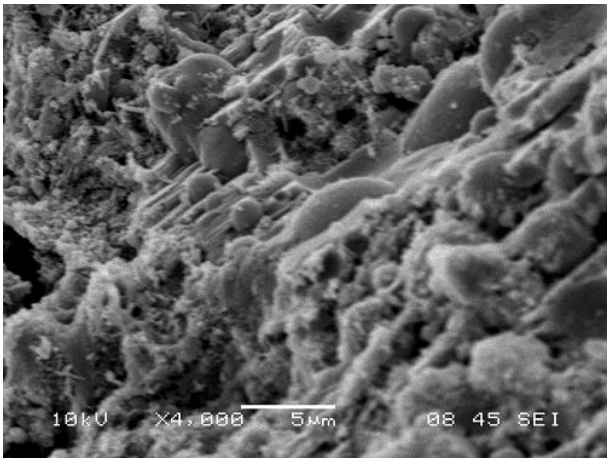

Figure 6.13a (10,000x) Figure 6.13b (4,000x)

Figure 6.13: SEM images of P20F80 paste at the age of 7 days

P90M10 at 7 day:

There are large numbers of unhydrated larger and conglomerated particles of microsilica (approximate diameter of more than 50 µm) are clearly visible even at lower magnification in Figure 6.14a. Higher particle size of microsilica suggests that the densified microsilica particles clearly did not thoroughly breakdown. This shows that hand mixing of paste in the laboratory did not produce enough shear force to disintegrate the densified microsilica particles.

Figure 6.14a shows that a rim of hydration product of CSH due to pozzolanic activities surrounded the conglomerate of two large microsilica particles. Over the time this hydration product of pozzolanic reaction would fill in the large capillary pores which are visible in Figure 6.14b. As an early sign plenty of different hydration phases like needle like ettringite, plate like monosulfate and rigid CSH can be seen growing in large cavities in Figure 6.14b.

Presence of micro-cracks in Table 6.3 suggests early autogenous shrinkage due to the formation of hydration product and lack of water in the system. Growth in between cracks shows that a possible autogenous healing was possible provided that there was enough water and $Ca(OH)_2$ present in the system. No free $Ca(OH)_2$ was detected.

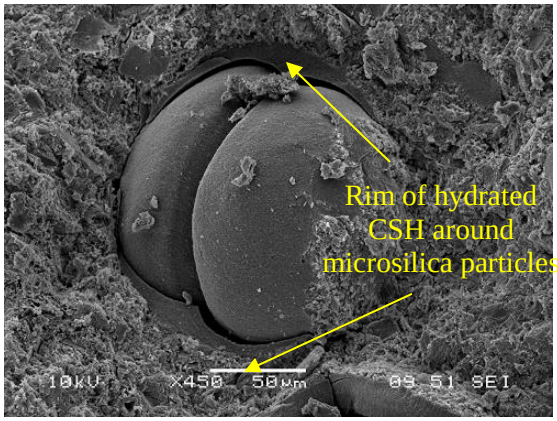

Figure 6.14a (450x)

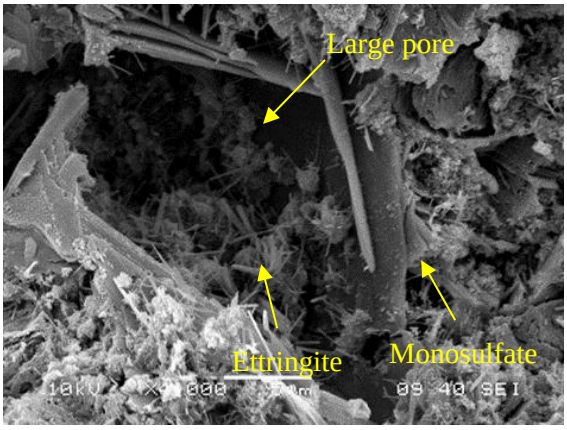

Figure 6.14b (4,000x)

Figure 6.14: SEM images of P90M10 paste at the age of 7 days

P80R20 at 7 day:

The microstructure of the hardened paste of P80R20 at 7 days age is relatively porous. Figure 6.15a show the microstructure with shrinkage cracks interconnecting the pores with the presence of ettringite and monosulfate. In Figure 6.15b a large particles are seen embedded in packed CSH gel which could be unhydrated particles of rice husk ash or Portland cement. The 7 day image of P80R20 in Table 6.3 shows hydrated CSH gel, ettringite growing in capillary pore cavity and unhydrated particles providing a fertile ground for future hydration in the presence of water to produce a denser microstructure at a later age.

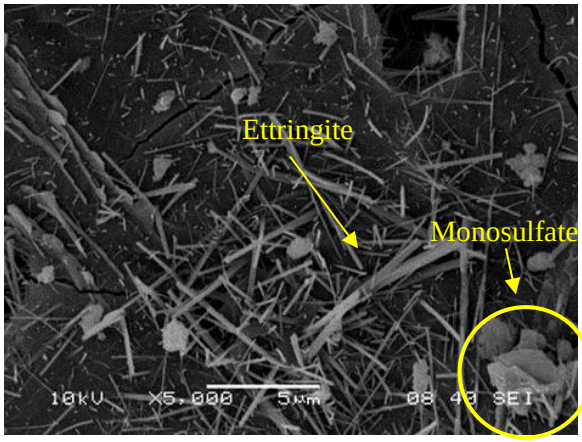

Figure 6.15a

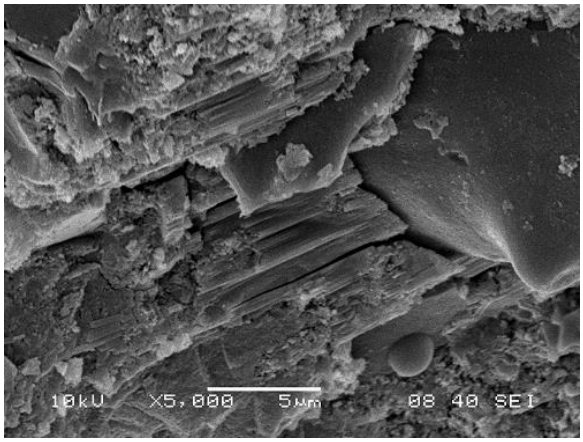

Figure 6.15b

Figure 6.15: SEM images of P80R20 paste at the age of 7 days

P15S70R15 at 7 day:

The 7 days microstructure of the paste of the triple blend of P15S70R15 shows clear presence of the formation of large hexagonal plate of Monosulfate both inside and outside of the capillary pore (7 day image of P5S70R15 in Table 6.3). A large amount of flaky crystals deposited together with the Monosulfate plate believed to be CSH gel. However, most of the other part of the test segments appeared to be with solid mass of microstructure. Relatively dense microstructure with combination of varied morphologies across the segment, suggesting the production of different hydration products due to the presence of three types of cementitious materials.

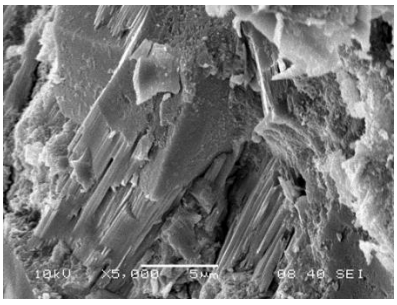

Figure 6.16a (5,000x)

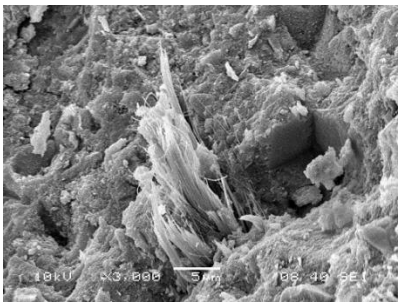

Figure 6.16b (3,000x)

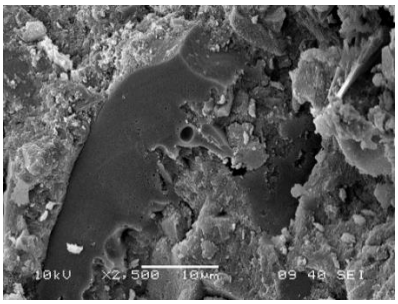

Figure 6.16c (2,500x)

Figure 6.16: SEM images of P15S70R15 paste at the age of 7 days

Solid uniformly layered dense microstructure in Figure 6.16a as seen in other GGBS mixes, unique fibrous material extruding from dense base in Figure 6.16b and clear hydration of perhaps one single particle of rice husk ash in between other phases is giving an 'alien looking' shape in Picture 6.16c illustrate the contribution of Portland cement, GGBS and rice husk ash into the system.

6.3.3.2 Development of microstructure at 56 days

UK PC at 56 day:

Figure 6.17 show that there is a remarkable difference at 56 day images comparing with the 7 day images (Figure 6.10) demonstrating almost complete hydration of cement particles. Though at 56 day the microstructure of UKPC provided rigid mass of hydration product, presences of large capillary pores are very visible.

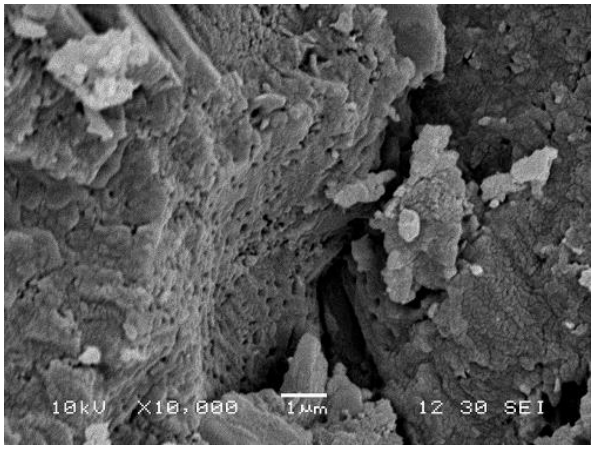

Figure 6.17a (10,000x)

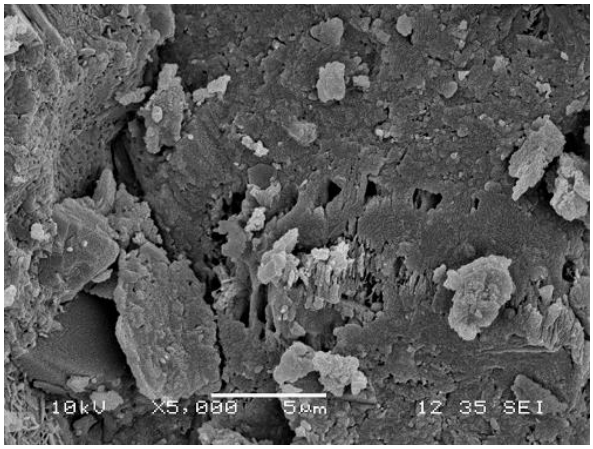

Figure 6.17b (5,000x)

Figure 6.17: SEM images of UKPC paste at the age of 56 days

P30S70 at 56 day:

The microstructure of P30S70 paste at 56 day age can be seen in Figure 6.18. Similar to 7 days images, nodules of unhydrated slag can be seen in Figure 6.18a together with a relatively large capillary pore visible at 10,000 times magnification image of Figure 6.18b. There was no porosity detected at 7 day age segment of P30S70 cement paste. However, the layered microstructure found in 7 day images was not detected at 56 days images.

Figure 6.18a present a very unique morphology, which seems to be a densely pack of sticks of individual hydration products of slag particles. This could resemble to a cross section of a layered microstructure as seen in Figure 6.12b of P15S85 at 7 days and can be described by the layered hydration of GGBS model described by Tanaka H, et.al. (1983) and discussed in Chapter 2.

As slag hydration is more complex than Portland cement, therefore, it is more complicated to predict the type of the hydration products only from the visual shape. However, it can be stated that the slag particles were hydrated at different degree depending on the availability of water and $Ca(OH)_2$ leaving porous microstructure between the interfaces of individual particles. The diameters of the pores are significantly smaller which can only be visible at very high magnification (15,000 to 25,000 times). Formation of clear cracks suggest the autogenous shrinkage of cement paste was taken place due to very low w/c ratio (0.32) and high GGBS content which had relatively higher water demand.

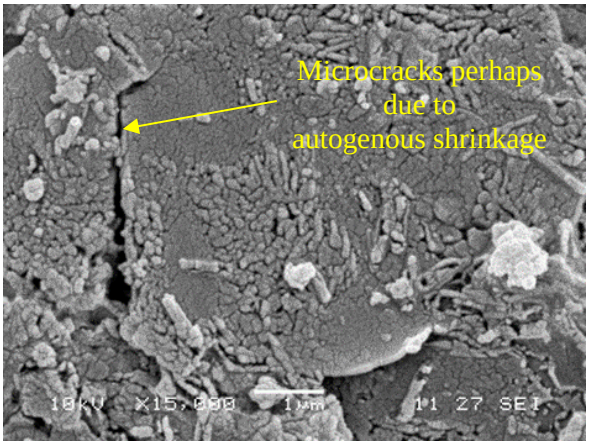

Figure 6.18a (15,000x)

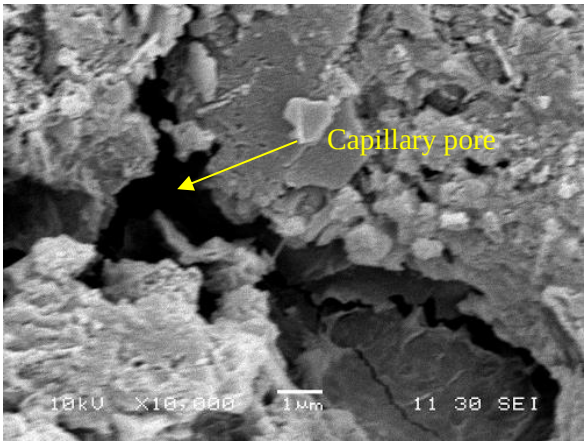

Figure 6.18b (10,000x)

Figure 6.18: SEM images of P30S70 paste at the age of 56 days

P15S85 at 56 day:

At 56 day age the P15S85 paste showed predominantly solid mass of hydration product together with flock of 'wool like' microstructure in Figure 6.19b. Presence of larger but fewer numbers of pores indicates unused water, perhaps due to the lack of $Ca(OH)_2$ in the system due to lower Portland cement content. Presence of layered microstructure similar to 7 day age images can be detected in Figure 6.19a. Presence of microcracks could be due to the autogenous shrinkage as noticed with P30S70 concrete.

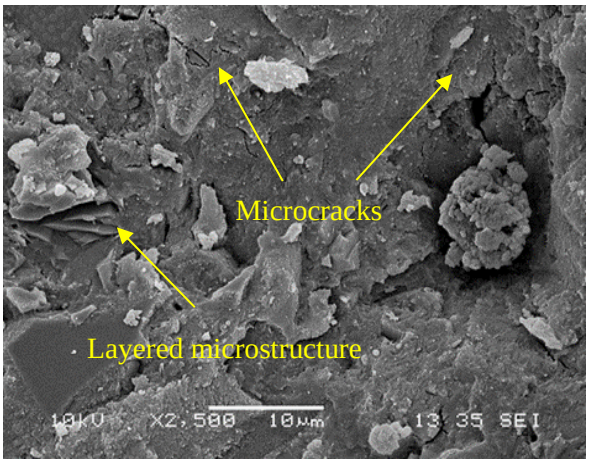

Figure 6.19a (2,500x)

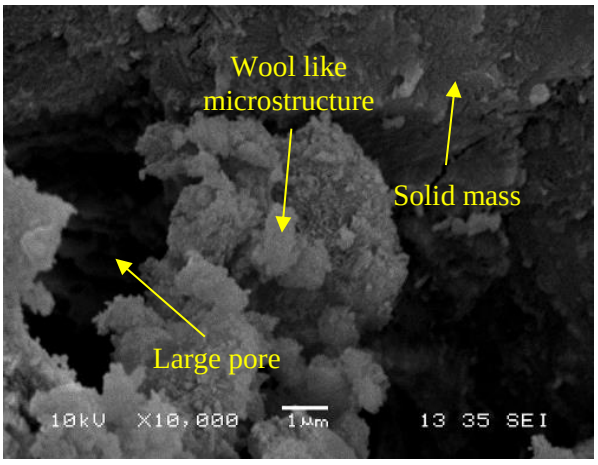

Figure 6.19b (10,000x)

Figure 6.19: SEM images of P15S85 paste at the age of 56 days

P20F80 at 56 day:

Unreacted and partially reacted fly ash particles remained in abundance in the system (Figure 6.20) even after 56 days showing lack of $Ca(OH)_2$ to complete the pozzolanic reaction. Nevertheless, needle like crystals growing on the surface of the fly ash particles were the results of secondary hydration due to the pozzolanic reactions. Presence of unhydrated cement particles in Figure 6.20b shows that available water content at 0.32 w/c ratio was not adequate to all cement particles. As a result the substrate remained porous demonstrating lack of mechanical strength of the microstructure.

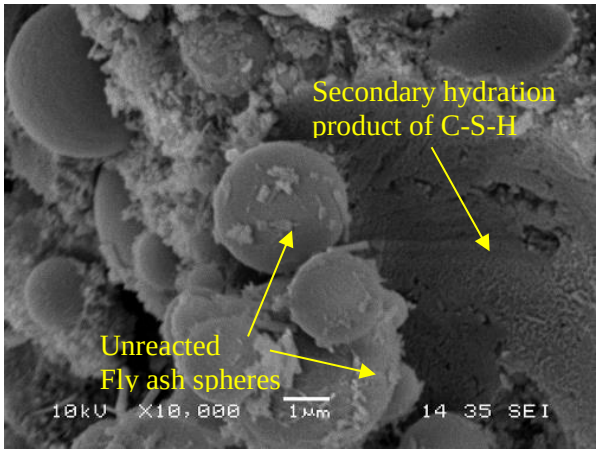

Figure 6.20a (10,000x)

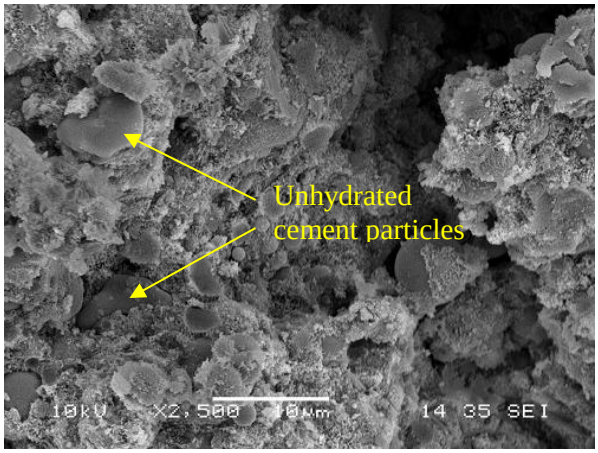

Figure 6.20b (2,500x)

Figure 6.20: SEM images of P20F80 paste at the age of 56 days

P90M10 at 56 day:

Figure 6.21 shows the hydrated microstructure of cement paste of P90M10 at 56 days age. The presence of unreacted microsilica particles in Figure 6.21a which gives an overview of the microstructure at 100x magnification, demonstrates lack of water in the system.

At higher magnification of 2,500x at Figure 6.21b, it shows a thick rim of reacted microsilica particle. There were small needle and plate like crystals protruding out of this rim suggesting the production of additional CSH due to pozzolanic reaction. Large plate like structure similar to monosulfate can also be seen at Figure 6.21b. Abundant presence of needle like CSH is the results of secondary hydration of pozzolanic reaction.

Growth of crystal inside large capillary pore in Figure 6.21c at 10,000x magnification is suggesting further development of hydration product over the time provided adequate availability of $Ca(OH)_2$. Presence of microcracks is suggesting autogenous shrinkage of the paste due to lack of adequate water.

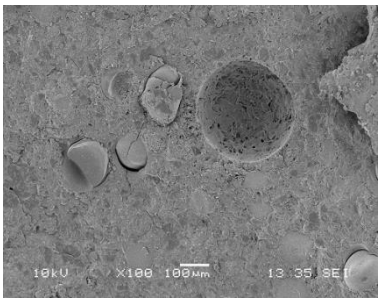

Figure 6.21a (100x)

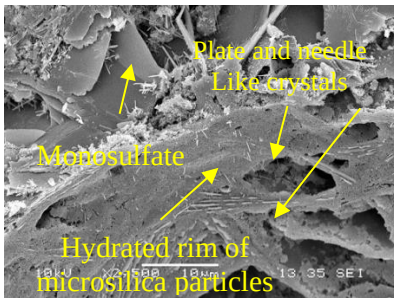

Figure 6.21b (2,500x)

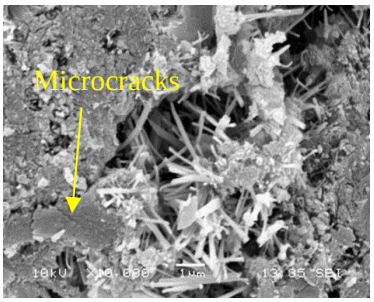

Figure 6.21c (10,000x)

Figure 6.21: SEM images of P90M10 paste at the age of 56 days

It is to note that a porous microstructure of paste containing 10% microsilica at the age of 56 day was not expected. This could be due to the inadequate dispersion of densified microsilica particles and lack of water in the system for further pozzolanic reaction. This is important to note that all specimens were cured at room temperature in a plastic wrap, no water curing was provided. Therefore, there was no additional water was available for long term growth of hydrates by pozzolanic reactions.

P80R20 at 56 day:

There is a remarkable improvement which can be observed at P80R20 paste at the age of 56 day compared to its 7 day age as shown in Figure 6.22. Solid mass of hydration product either as layered or loosely packed was formed over the period. However, the loosely packed hydration products were created continuous networks of interstitial spaces between solid masses.

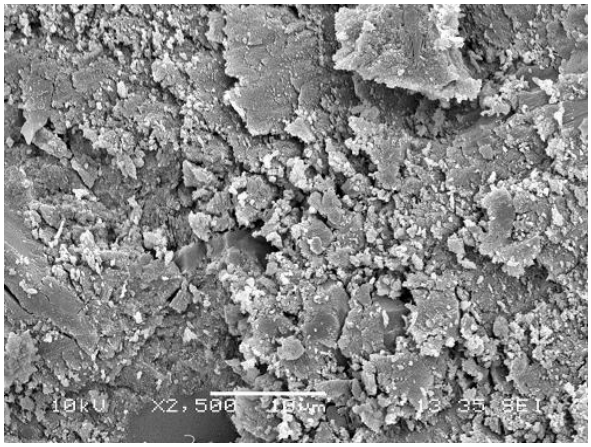

Figure 6.22a (2,500x)

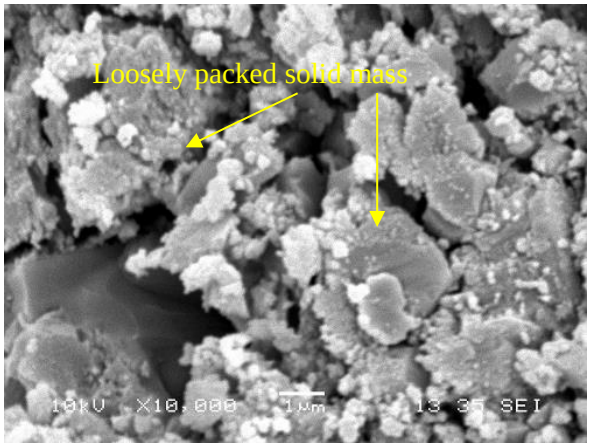

Figure 6.22b (10,000x)

Figure 6.22: SEM images of P80R20 at the age of 56 days

These interstitial spaces between masses are unique as they created a loosely packed non-homogenous mass. Autogenous shrinkage could be the reason for such formation as the water demand for rice husk ash is substantially higher due to its very high specific surface area of the rice husk ash particles and there was no excess water available due to non-water curing process of the paste.

Formation of solid microstructure at the age of 7 and 28 days of a 0.40 w/c paste with 20% rice husk ash are demonstrated in Figure 2.18 in Chapter 2. A proper curing in immersed water would also provide similar formation.

P15S70R15 at 56 day:

At the age of 56 day the triple blend of P15S70R15 produced a solid mass of microstructure with virtually no capillary pores as shown in Figure 6.23. There was a massive improvement over time with no presence of flaky crystals and pores as it was observed at 7 day images (Figure 6.16). Compared with other cement combinations, P15S70R15 produced the soundest microstructure at the age of 56 days.

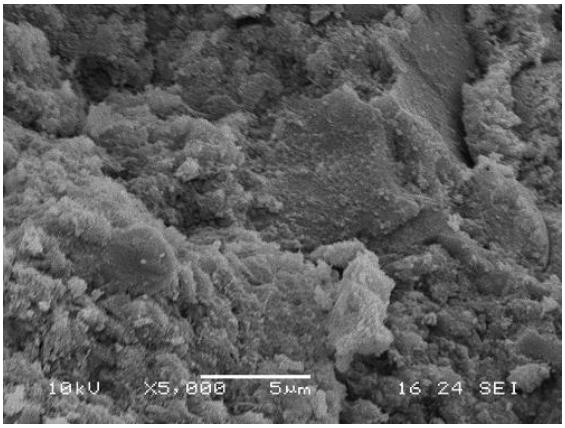

Figure 6.23a (5,000x)

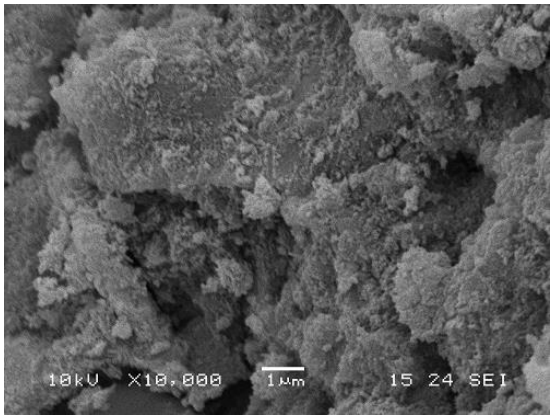

Figure 6.23b (10,000x)

Figure 6.23: SEM images of P15S70R15 paste at the age of 56 days

6.3.3.3 Development of microstructure at 365 days

UK PC at 365 day:

At 365 days the microstructure of UKPC was matured to a solid mass of hydration product with fewer pore structures. However, presence of microcracks and loosely form hydration product are visible in Figure 6.24.

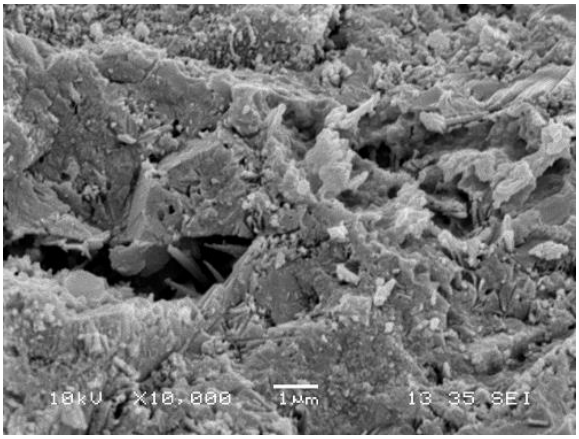

Figure 6.24a (10,000x)

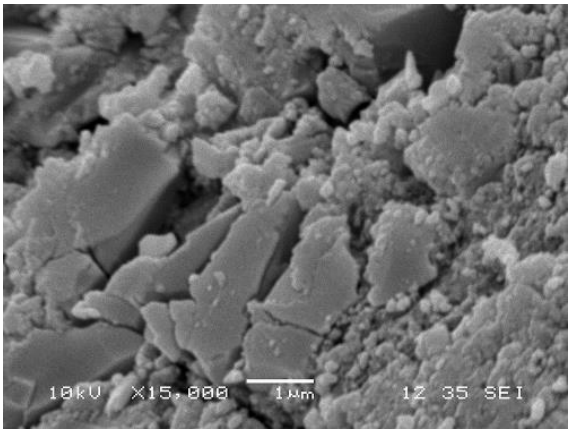

Figure 6.24b (15,000x)

Figure 6.24: SEM images of UK PC paste at the age of 365 days

P30S70 at 365 day:

Absolutely solid mass of hydration product with little or no porosity can be seen in the microstructure of P30S70 paste at 365 days age as shown in Figure 6.25. Distinctive combination of solid plain and solid layered mass can be observed coexisting (Figure 6.25b). The layered mass could be matured and fully hydrated product of loosely packed stick like hydration product appeared at 56 day images (Figure 6.18a). Presence of microcrack is visible at Figure 6.16a due to autogenous shrinkage.

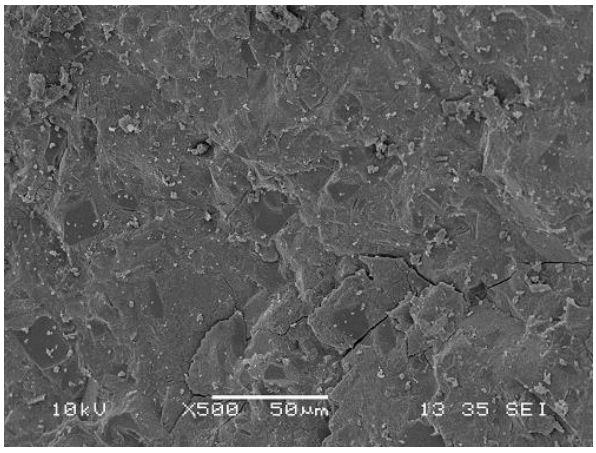

Figure 6.25a

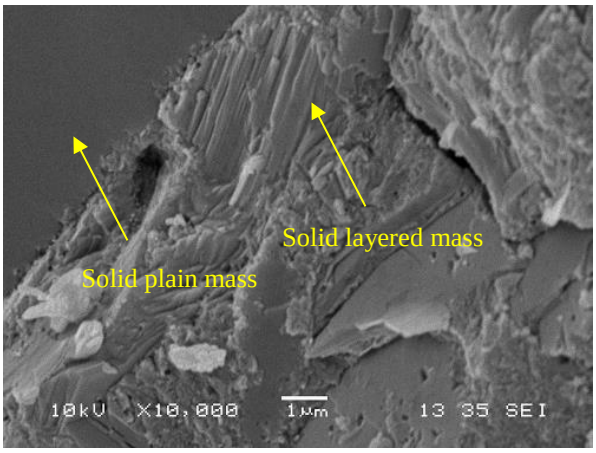

Figure 6.25b

Figure 6.25: SEM images of P30S70 paste at the age of 365 days

P15S85 at 365 day:

Figure 6.26 shows solid microstructure of P15S85 paste at the age of 365 days without any pores which is very similar to the P30S70 paste at the same age (Figure 6.25). Presence of microcracks can be observed most probably due to autogenous shrinkage due to higher GGBS content. Cracks could also appear due to the vacuum process of SEM sample preparation to remove water from the specimen.

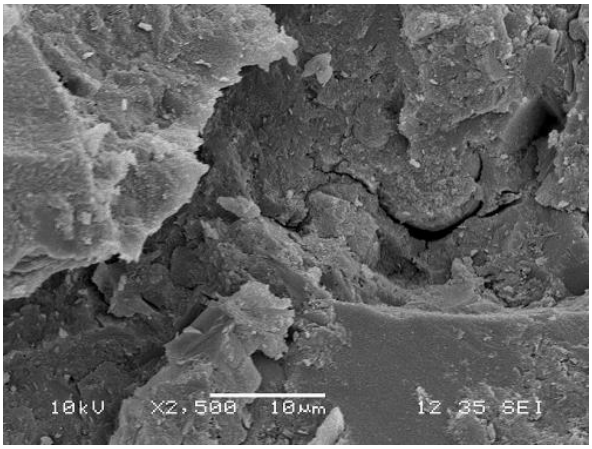

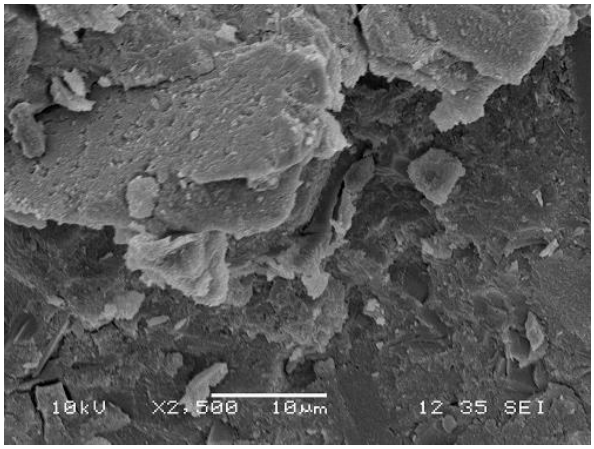

Figure 6.26a Figure 6.26b

Figure 6.26: SEM images of P15S85 paste at the age of 365 days

P20F80 at 365 day:

Figure 6.27 shows that there was a huge quantity of unreacted fly ash particles present even at 365 days of age. This suggests that 80% of fly ash of total cementitious content was more than of an optimum dosage required to have a positive impact to the system. Therefore, the overall microstructure remained porous. The needle like growth of secondary CSH crystals mesh were present but they could not grow further due to the lack of production of $Ca(OH)_2$ due to inadequate Portland cement content and water (Figure 6.27b).

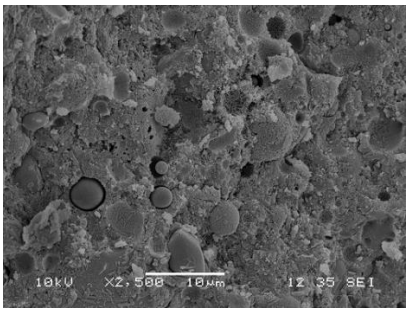

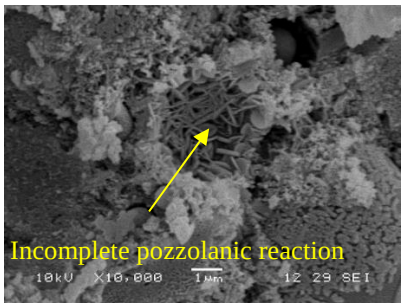

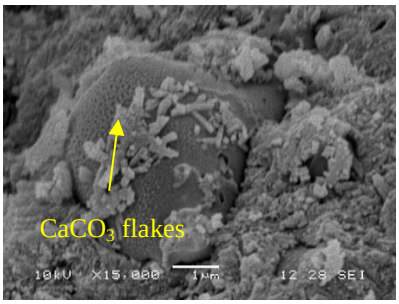

Figure 6.27a (2,500x) Figure 6.27b (10,000x) Figure 6.27c (15,000x)

Figure 6.27: SEM images of P20F80 at the age of 365 days

However, Figure 6.27c shows presence of $CaCO_3$ like flakes on top of an unhydrated cement particle (or a solid hydration product of CSH). This coexistence of incomplete pozzolanic reaction and carbonated cement particles is perhaps due to lack of adequate water during the hydration process with a very low w/c ratio of 0.32.

Unreacted fly ash particles embedded in the paste has been reported in the literature as discussed in the Chapter 2. Dhir, R.K., et al. (1988) reported that it may take around 2 years to get 80% of total fly ash particles reacted. Figure 2.13 of Chapter 2 shows unreacted fly ash particles embedded into solid microstructure of 180 days old.

P90M10 at 365 days:

Figure 6.28 shows the microstructure of cement paste made of P90M10. At 365 days age the microsilica particles were still not totally reacted. Presence of partially reacted microsilica particles with rim of secondary hydration product of pozzolanic reaction can be seen in Figure 6.28a.

Figure 6.28b which is 10 times larger than Figure 6.28a, highlights the presence of flake like hydration products at the edge of the 'crater', the interface between the hydrated rim and unhydrated microsilica particle. The entire surface of the microstructure was scattered with these flaky loose powder like particles. The size of these irregular shaped particles could be estimated from sub-micron to 5 micron, suggesting that they were the hydration products of microsilica particles as the average diameter of a single microsilica particle could be 0.15 micron. However, the overall microstructure was dense as seen in the image of P90M10 at 365 day age in Table 6.3.

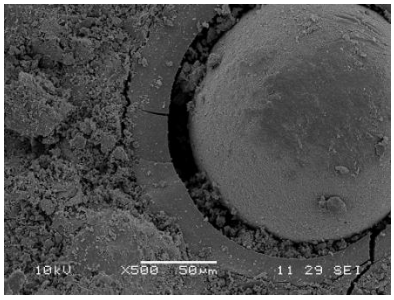

Figure 6.28a (500x)

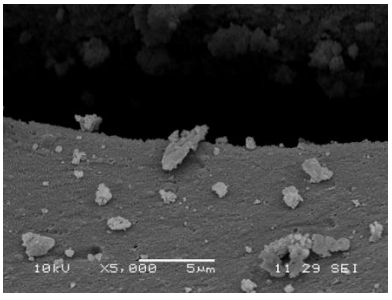

Figure 6.28b (5,000x)

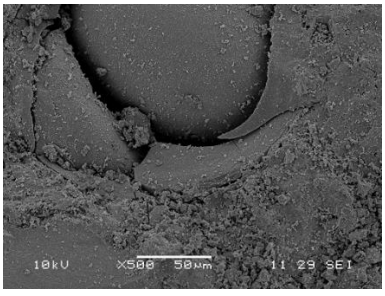

Figure 6.28c (500x)

Figure 6.28: SEM images of P90M10 at the age of 365 days

P80R20 at 365 days:

Comparing with P90M10 paste, at the age of 365 days P80R20 provided a very solid microstructure with the presence of fewer pores as shown in Figure 6.29. However, presence of randomly appeared microcracks shows signs of autogenous shrinkage. Similar to the GGSB mixes presence of layered microstructure can be seen in Figure 6.29b.

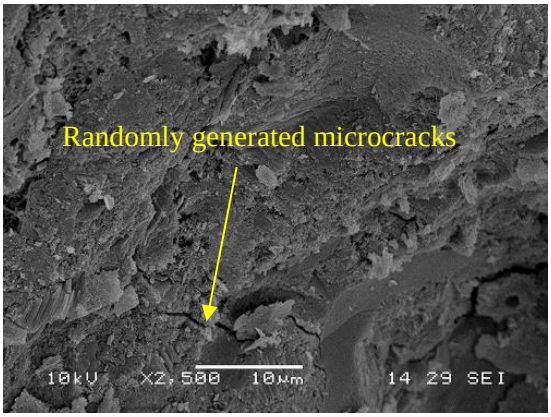

Figure 6.29a (2,500x)

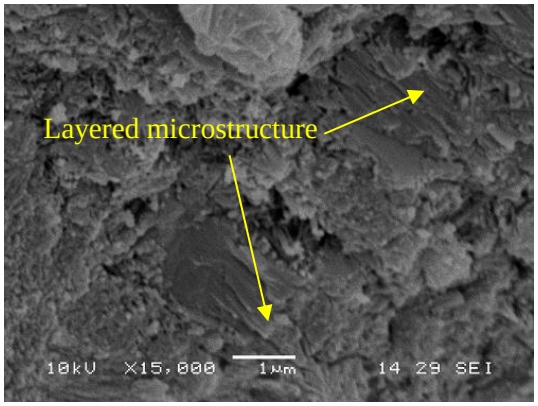

Figure 6.29b (15,000x)

Figure 6.29: SEM image of P80R20 paste at the age of 365 days

P15S70R15 at 365 days

Figure 6.30 illustrates the microstructure of P15S70R15 at the age of 365 days. Presence of hexagonal monosulfate plate (Figure 6.30a) suggests that reaction of alumina phase was taken place. Similar monosulfate plates were detected at 7 day (Table 6.3) with smaller crystal like hydration products. At 365 days these smaller crystals was grown into large fluffy mass suggesting completion of CSH formation, perhaps as a result of pozzolanic reactions or hydration of slag particles.

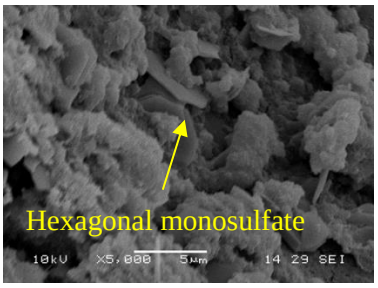

Figure 6.30a

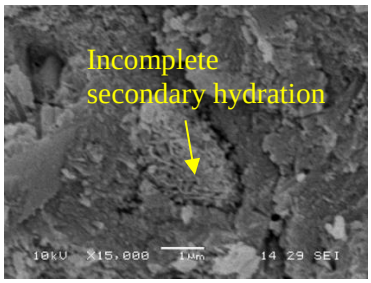

Figure 6.30b

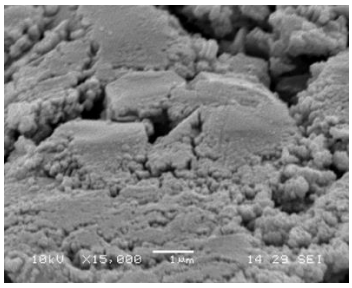

Figure 6.30c

Figure 6.30: SEM images of P15S70R15 paste at the age of 365 days

At 56 day this phase of incomplete hydration process was not detected, suggesting that at a later stage most of the paste was fully hydrated except certain 'pockets of rice husk ash' where the access of water was perhaps limited to complete the hydration process. However, the 365 day image of P15S70R15 in Table 6.3 suggests the production of dense microstructure, though presence of smaller pores is visible at higher magnification at Figure 6.30c. Isolated presence of incomplete secondary hydration product of CSH due to the pozzolanic reaction perhaps on top of a rice husk ash particles can be spotted in Figure 6.30b.

6.3.4 Summary

The SEM images of different combination of hydrated cement pastes at different ages reveal the true formation of their microstructure. From the above analysis it seems that pastes containing GGBS particularly the triple blend mix of P15S70R15 demonstrated dense microstructure with little or no porosity especially at the age of 56 days and beyond.

The microstructure of fly ash and microsilica containing pastes were porous mainly due to unreacted particles of fly ash and microsilica. Microstructure of rice husk ash was relatively denser compared to the microsilica containing pastes for both 56 and 365 days age. Autogenous shrinkage cracks were commonly observed in almost all mixes. Paste with 100% Portland cement contained large capillary pores compared to other pastes containing pozzolanic cementitious materials demonstrating production of additional hydration products due to pozzolanic reaction.

6.4 Mercury Intrusion Porosimetry

6.4.1 Introduction

Concretes made of unwashed sand contains higher amount of finer particles with particle size diameter below 75μm compared to concrete made with washed sand. This excess finer particles was expected to fill the voids and provide a denser matrix of pastes by reducing porosity and pore volume of concrete. A positive effect on the mechanical and durability properties of concrete should be expected due to this reason which has been elaborated in previous chapters. In this section the characteristics of porosity and pore structure of concrete containing washed and unwashed sand have been discussed.

Mercury intrusion porosimetry technique was employed to examine the effect of the excess finer particles of unwashed sand on the porosity and pore structure of concrete. Three sets of mortar with washed and unwashed sand were made using following three different sets of cementitious materials: i) 30% Portland cement and 70% GGBS (P30S70), ii) triple blend of 15% Portland cement, 70% GGBS, 15% rice husk ash (P15S70R15) and iii) 20% Portland cement and 80% fly ash (P20F80). All mortars were made at 0.32 w/c ratio.

Beside the primary objectives to examine the void filling effects of the unwashed sand, three different combinations of cementitious materials would also reveal the characteristics of pore structures of the hydration products derived from them.

As the MIP would be able to detect only within the pore structures of mesopore (diameter ranging from 2nm to 50nm) and macropore (>50nm) ranges, the MIP results presented here would not be able to provide complete pictures of pore structures of mortar samples. The pores at the micropore range which is at the molecular level cannot be accessible by mercury.

6.4.2 Characterization of pore structures

In order to make the comparison between different cement combinations and mortar made with washed and unwashed sand, a summary of all data of the MIP tests of all six mortar specimen is given in Table 6.4. It gives the results of the total pore volumes, specific surface area, pore diameter, density and porosity of individual specimen. The difference of the various characteristics of pores between washed and unwashed sand for each type of cement combinations was given in percentage of the washed sand concrete to illustrate the effect of the excess finer particles in the unwashed sand.

The total intrusion volume of mercury represents the total volume of pores for every gram of sample. It is to note that MIP can only detect the pores with the size of maximum diameter of 2nm and above. The total pore volume for unwashed sand mortar was expected to be reduced as the excess finer particles should be able to fill the macropores between the particles. The particle size diameter of the excess finer particles in the unwashed sand was less than 75μm which could fill the pores mostly in macropore range.

Table 6.4: Summary report of MIP tests

	Unit	P30S70		P15S70R15		P20F80	
		Washed sand	**Unwashed sand**	**Washed sand**	**Unwashed sand**	**Washed sand**	**Unwashed sand**
Total Intrusion Volume	mL/g	0.0236	0.0231	0.0311	0.0325	0.0380	0.0382
			-2.1%		4.5%		0.5%
Total Pore Area	m²/g	6.14	5.62	6.50	7.44	5.38	6.57
			-8.5%		14.3%		22.1%
Median Pore Diameter (Volume)	nm	50.0	67.6	38.3	29.0	115.7	52.9
			35.2%		-24.3%		-54.3%
Median Pore Diameter (Area)	nm	5.1	4.6	7.9	8.1	8.3	9.9
			-9.8%		2.5%		19.3%
Average Pore Diameter (4V/A)	nm	15.4	16.4	19.1	17.5	28.3	23.3
			6.5%		-8.4%		-17.7%
Bulk Density	g/mL	3.46	3.71	3.87	3.53	3.34	3.47
			7.3%		-8.7%		3.9%
Apparent (skeletal) Density	g/mL	3.77	4.06	4.40	3.99	3.83	4.00
			7.8%		-9.3%		4.6%
Porosity	%	8.16	8.57	12.04	11.49	12.71	13.27
			5.0%		-4.6%		4.4%

Total pore area described as m^2/g is the specific surface area of the pore linings. Pore volume, specific surface area and average pore diameter are correlated to each other. The average pore diameter denoted as nm is derived by dividing the median pore diameter of volume (the diameter of the specific pore whose volume is the median among all the volumes of pores) by the median pore diameter of area (the diameter of the specific pore whose surface area is the median among all surface areas of pores) multiplied by 4.

6.4.3 Porosity

Figure 6.31 illustrate the porosity of mortar specimen in terms of the percentage of the pore volume over the total volume of the specimen. Mortars made with P30S70 are the least porous with below 9% porosity compared to P15S70R15 and P20F80. This was validated by the compressive strength and SEM images of P30S70 concretes as discussed in previous chapters.

Relatively higher porosity of P15S70R15 mortars could be attributed to the inherent porosity within rice husk ash particles and development of lesser amount of hydration products due to reduced Portland cement content compared to P30S70. The fly ash mortars are visibly porous with large capillary pores as illustrated by the SEM images in section 6.3 of this chapter and low compressive strength due to inadequate development of hydration products. The highest porosity of P20F80 pastes measured by the MIP tests has validated that fact.

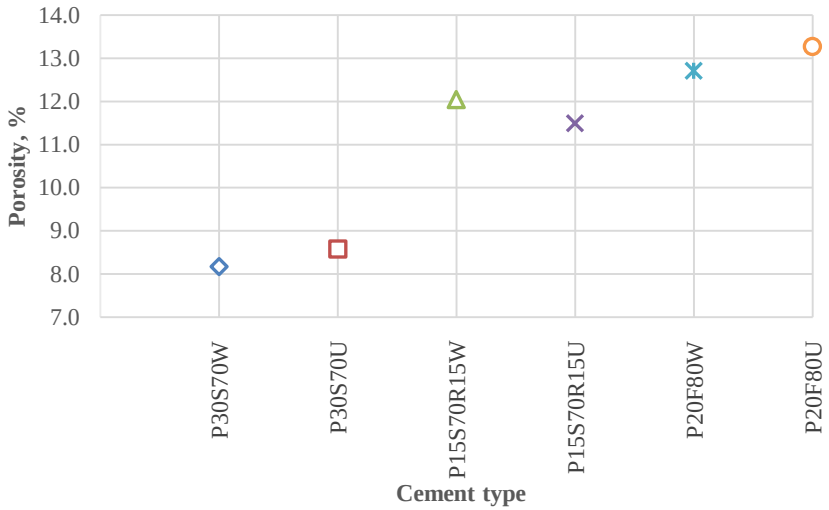

Figure 6.31: Porosity of mortars with washed and unwashed sand

The effect of excess finer particles to reduce porosity of mortar was not demonstrated in Figure 6.31. In fact the porosity for P30S70 and P20F80 mortars with unwashed sand were increased slightly. For P15S70R15 there was a slight reduction of porosity for unwashed sand mortar. The bulk density and skeletal density followed the same trend as shown in Table 6.3 as the density of the mortar are correlated with the porosity of the material.

6.4.4 Pore diameter and specific surface area

As the porosity accounted for the total volume of pores, the pore diameter indicates the size of the pores. Though the porosity of P15S70R15 mortars were almost same as the P20F80 mortars, the average pore diameter were quite similar with the P30S70 mortars as shown in Figure 6.32.

The effect of excess finer particles to reduce the pore diameter was more effective in P15S70R15 and P20F80 mortars. It is especially obvious for P20F80 mortars with a magnitude of 17.7% reduction suggesting wider room for improvement within fly ash mortar matrix due to the presence of very large capillary pores.

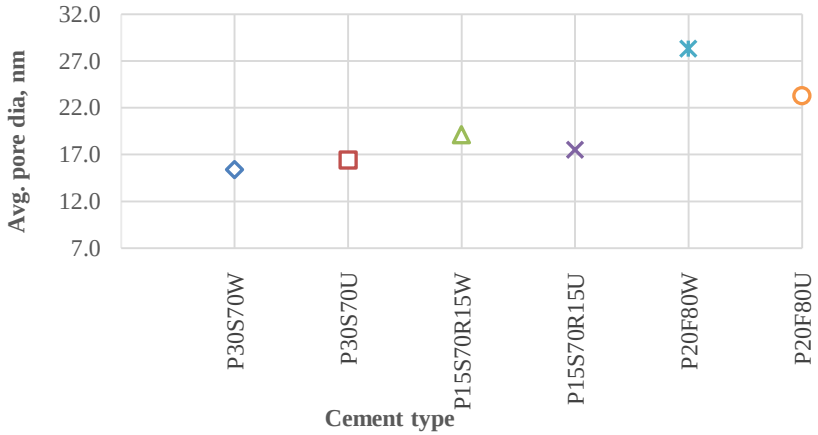

Figure 6.32: Average pore diameter of mortars with washed and unwashed sand

Higher specific surface area (total pore area) for P15S70R15 as shown in Figure 6.33 can be attributed to very high specific surface area of rice husk particles due to its inherent porous characteristics. Higher pore area for unwashed specimen for both P15S70R15 and P20F80 could be attributed to the reduction of pore diameter (Figure 6.32) for a given pore volume. This effect was not demonstrated in P30S70 mortars as the reduction of diameter was not visible in Figure 6.32. An inversely proportional correlation can be observed between pore diameter and specific surface area, as for a given pore volume, reduction of pore diameter would increase the specific surface area of pores.

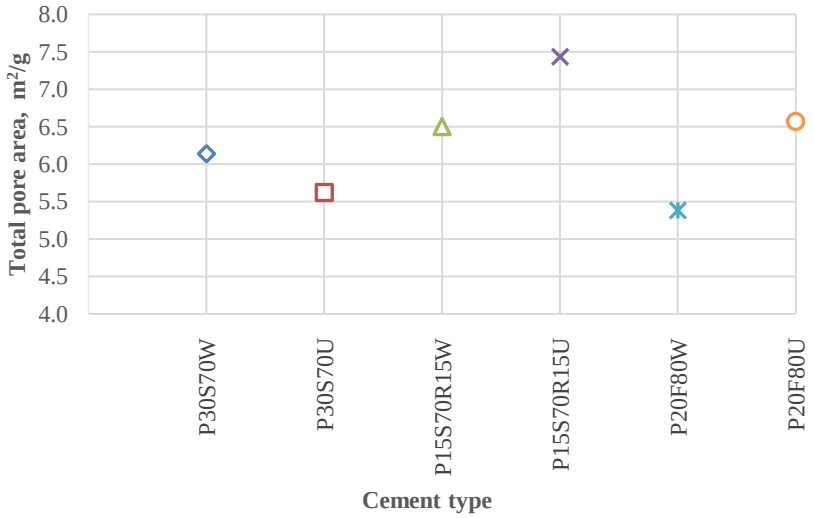

Figure 6.33: Total pore area of mortar made with washed and unwashed sand

From the above discussion, it can be summarized that though there is no effect of the additional filler of unwashed sand on the reduction of porosity of mortars which is a volume parameter, but it has a positive effect to reduce the pore diameter of concrete. The effect is more pronounced on concrete made with P20F80 and P15S70R15 instead of P30S70. Reduction of pore diameter is more important factor than reduction in volume as permeation properties of concrete are more influenced by the pore connectivity, instead of porosity.

6.4.5 Pore size distribution

Pore size distributions in Figure 6.34 to Figure 6.38 illustrate the distribution of the cumulative and incremental pore volumes with respect to its pore diameters. The effect of excess finer particles in the mortar made with P30S70U as shown in Figure 6.34 made little difference in terms of cumulative pore volume distribution and incremental pore volume distribution. In fact the mortar made with washed sand appeared to having reduced volume of pores at macro pore range.

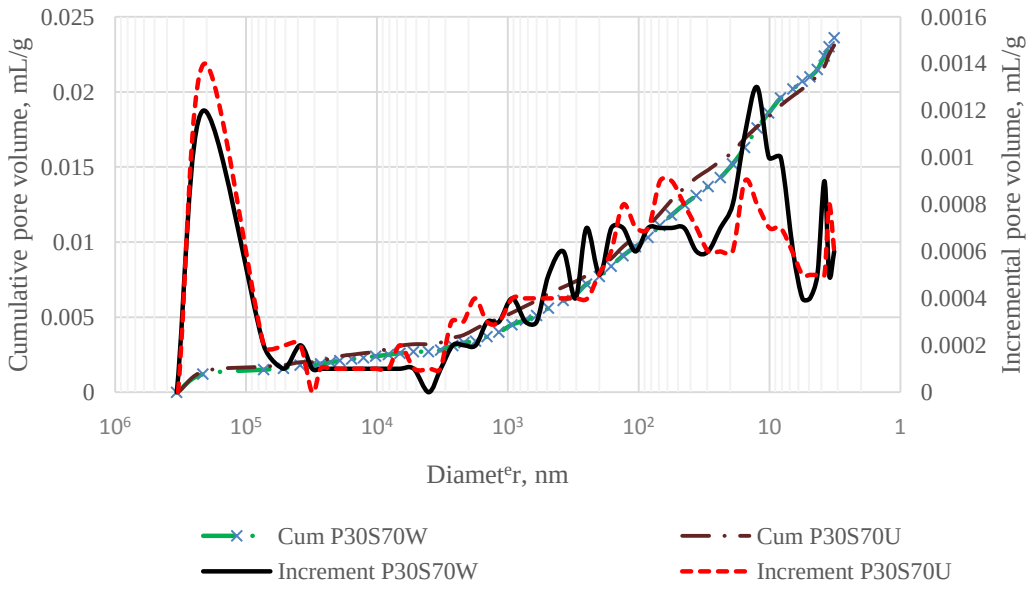

Figure 6.34: Pore size distribution of P30S70 using washed and unwashed sand

However, there is a significant reduction of volume of pores between 5-20 nm size range can be observed due to the use of unwashed sand. It is difficult to conclude whether this reduction of volume was due to the excess finer particles, as for P15S70R15 (Figure 6.35) and P20F80 (Figure 6.36) mortars at this range there was no reduction of pore volume by the unwashed sand.

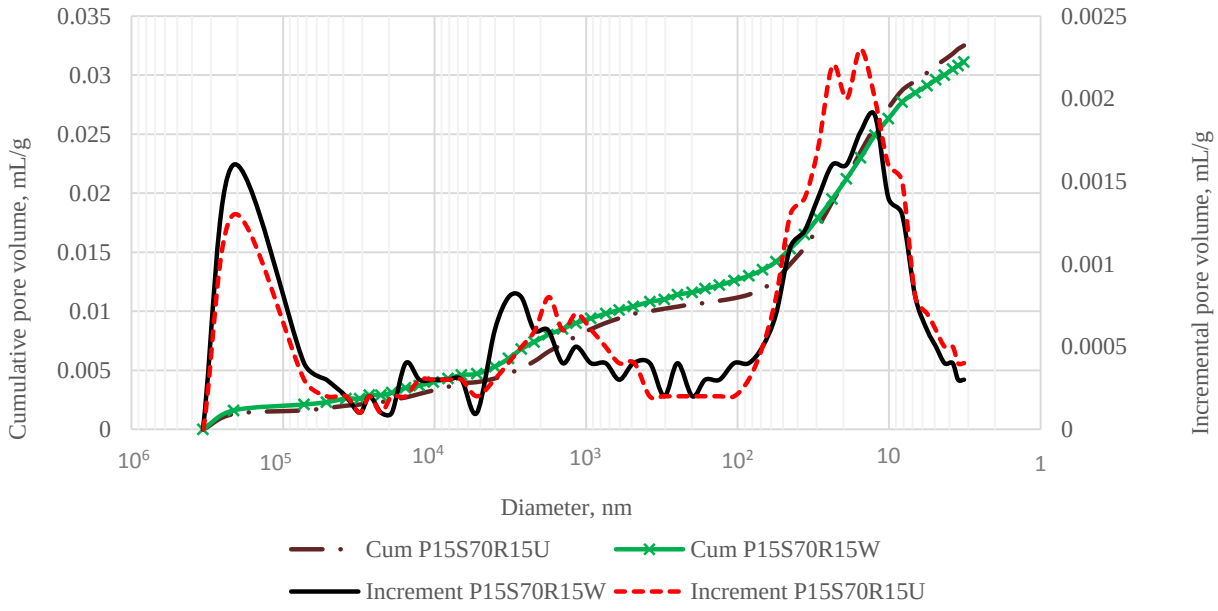

Figure 6.35: Pore size distribution of P15S70R15 with washed and unwashed sand

There is a slight reduction of pore volume can be observed at the macro-pore range between 30,000 – 330,000 nm diameters for P15S70R15 mortars. This reduction was cumulatively consistent from 30 – 330,000 nm range for P15S70R15 mortar as well (Figure 6.35). The cumulative reduction in volume for P20F80U mortar at 10-1000 nm range is very significant demonstrating underlying effect of the excess finer particles of unwashed sand (Figure 6.36).

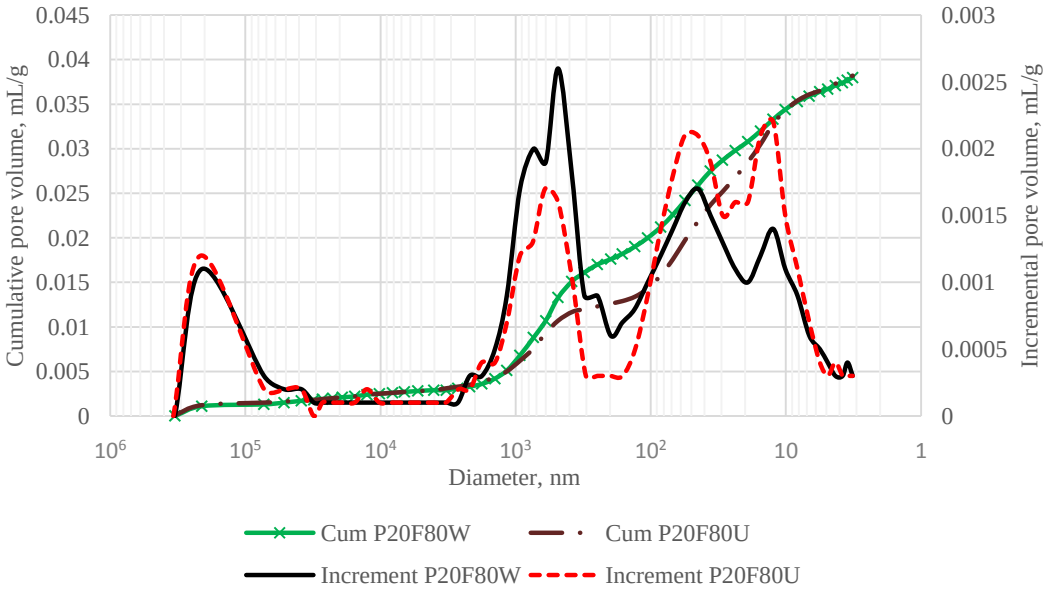

Figure 6.36: Pore size distribution of mortar made with fly ash with washed and unwashed sand

Figure 6.37 provides the overall picture of the pore size distribution of all six specimens. Mortars made with P30S70 were obviously denser with less pore volumes followed by the mortars made with P15S70R15 and P20F80. The effect of the void filling by the excess finer particles of unwashed sand is clearly visible for P20F80 and P15S70R15 mortars. Though at fly ash it was more obvious. There is no effect could be seen in GGBS mortar.

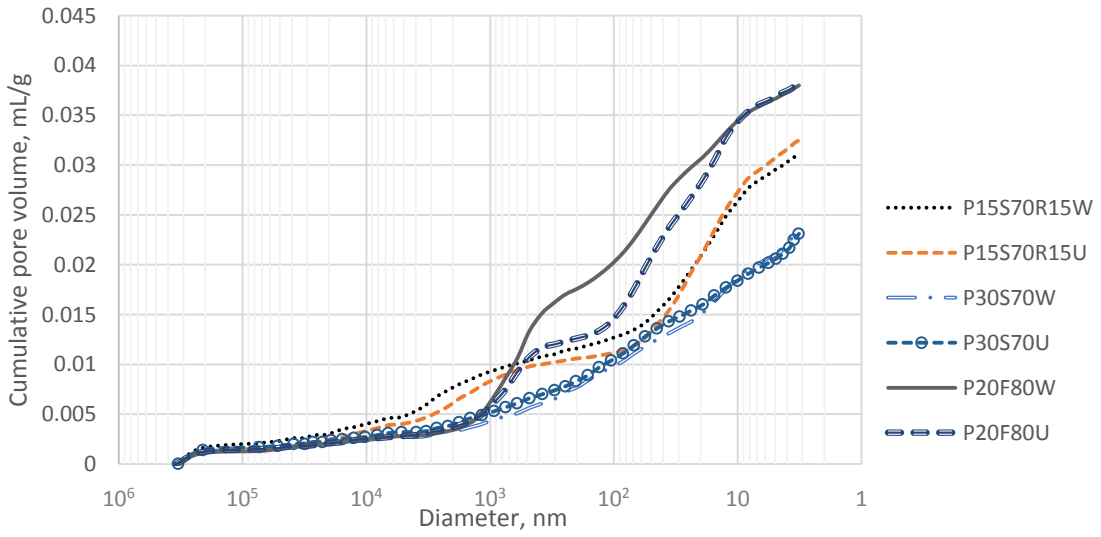

Figure 6.37: Pore size distribution of all specimens in cumulative pore volume

The volumes of the pores in terms of average pore diameter are localized into three main ranges as shown in Figure 6.38. Larger pore diameters are in between 50,000 to 350,000 nm, intermediate size are between 300nm to 50,000 nm and less than 300 nm are the smallest pores as detected by the MIP tests. Interestingly fly ash mortars had the least volume in larger pore size range, though all six specimens had similar volume of pores at this pore diameter size.

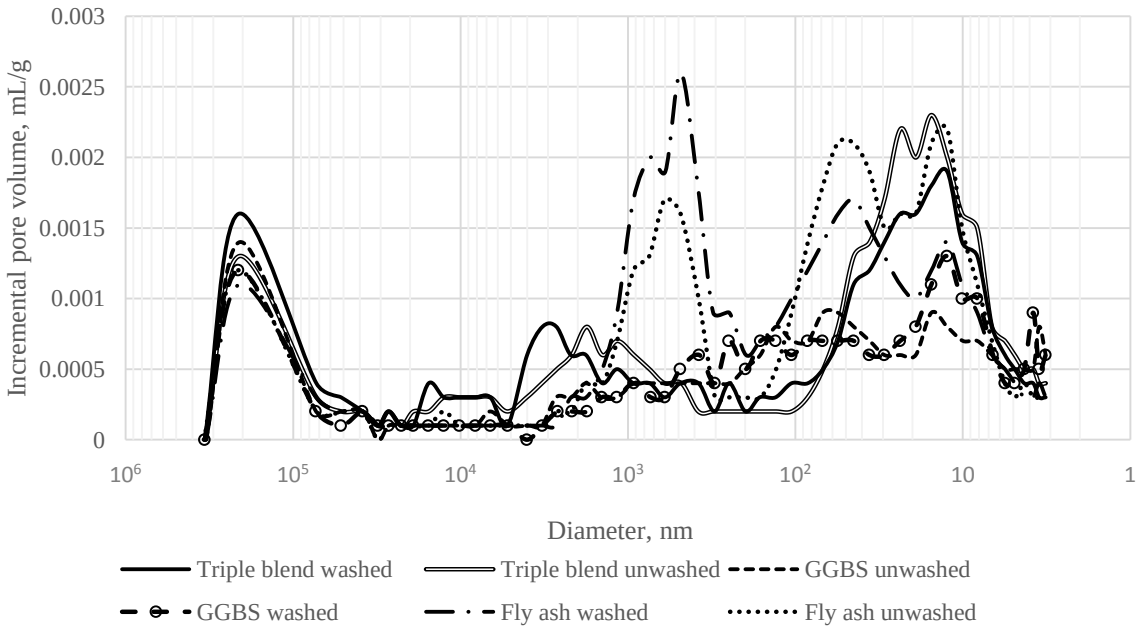

Figure 6.38: Pore size distribution of all specimens in incremental pore volume

However, the pore volumes of fly ash mortars are the largest at the intermediate and smaller pore size range. The P15S70R15 mortars also had large volumes of pores of very small pore diameter size. The volume of pores of P30S70 mortars was distributed more uniformly from the range of 50 – 6500 nm diameter size of pores with a relatively lower volume at the smaller size pores compared to other two groups of cementitious combinations.

6.4.6 Summary

The effect of finer particles filler of unwashed sand was more pronounced to reduce the overall pore diameter than the porosity of mortar and it was mainly effective on P15S70R15 and P20F80 mortars than mortars made of P30S70. This was perhaps due to the fact that microstructure of GGBS paste had little room for further improvement. The pore size distribution and total porosity of GGBS mortars indicate a very dense matrix with least quantity of pore volume compared with other two combinations. There is a cumulative pore volume reduction of P15S70R15 and P20F80 mortars from 30 – 330,000 nm range demonstrating effectiveness of the additional filler of unwashed sand in mortar.

6.5 Conclusion

In this chapter the characteristics of hardened cement pastes have been analysed to understand the hydration products, morphology and pore structure of the matrix of pastes of different cementitious materials and sand combinations.

Thermogravimetry analysis (TGA) provided information of the formation of different hydration products and associated chemical reaction to form and transform the hydration products. Scanning electron microscopy (SEM) provided photographic evidence of the formation of hydration products, pore structure and overall morphology of the hardened cement pastes. Mercury intrusion porosimetry (MIP) provided information of the pore structure of the hydrated pastes of different cement combinations and the effect of the excess finer particles of sand on the paste microstructure.

In TGA and SEM tests total seven different combinations of cement pastes were tested. This includes i) UKPC, ii) P30S70 iii) P15S85 iv) P20F80 v) P90M10 vi) P80R20 and vii) P15S70R15. For MIP tests three combinations of cementitious materials have been tested. This includes i) P30S70, ii) P20F80 and iii) P15S70R15. Each cement combinations for MIP test were made with washed and unwashed sand to demonstrate the effect of excess finer particles in the microstructure of pastes. All pastes and mortars made for TGA, SEM and MIP tests were made with 0.32 w/c. The TGA and SEM samples were tested at 1, 7, 56 and 365days to observe the effect of time. The MIP tests were conducted on 365 days old samples.

TGA tests results validated that pastes containing higher proportion of Portland cement such as UKPC, microsilica and rice husk ash mixes produced the highest amount of hydrates, $Ca(OH)_2$ and $CaCO_3$ at all ages. Effective pozzolanic reactions can be verified in GGBS and P15S70R15 mixes by lower content of net $Ca(OH)_2$ demonstrated by the TGA. Lack of water inhibited the true potential of pozzolanic reaction of P90M10 and P15S70R15 mixes, though both mixes produced higher amount of $Ca(OH)_2$. Among low Portland cement containing mixes, the performance of P15S70R15 past was encouraging in terms of the production of hydrates.

The SEM images produced very dense matrix of hardened cement paste made of GGBS and P15S70R15 mixes validating the findings in the TGA test results. Though the rice husk ash and microsilica pastes produced sound microstructure, particles of unreacted microsilica particles were unused due to lack of adequate water. The porous fly ash matrix with numerous unreacted fly ash particles suggested lack of pozzolanic reaction due to inadequate production of $Ca(OH)_2$ and lack of water.

Higher porosity in fly ash mixes revealed by the MIP tests also validated the findings of TGA and SEM analysis. However, the effect of excess finer particles contributed by the unwashed sand reduced the overall pore size and cumulative pore volume between 30-330,000 nm pore diameter range of mortars made with P20F80 and P15S70R15. There is a little effect of the finer particles on P30S70 mortars could be found by MIP analysis.

As discussed before the effect of the excess finer particles of unwashed sand can be seen on the gain of compressive strength (Figure 4.13), but there is little effect on the water permeability (Figure 5.31 and Figure 5.32) and RCPT values (Figure 5.4) perhaps due to very low w/c ratio of concretes. However, there is a clear improvement can be observed on the water absorption values for both P30S70 and P20F80 concretes (Figure 5.16).

Chapter 7

Environmental Sustainability Factors

7.1 Introduction

In this chapter different factors of environmental sustainability such as embodied carbon dioxide (eCO_2), reduction of waste and reduction of raw materials to produce different type of concrete discussed in the previous chapters have been analysed.

The eCO_2 of different type of concrete with different cement and aggregate combinations have been compared and their effect on the eCO_2 have been analysed. As the content of Portland cement is the common factor of eCO_2 and compressive strength of concrete, the relationship between these two parameters have been discussed for different type of concretes.

Beside the eCO_2 of concrete, the impacts of other environmental sustainability factors (ESF) including waste reduction and reduction of materials contributed by the concrete with different cement and aggregate combinations have been analysed. However, as these factors do not have any direct numerical values, a set of quantitative ratings as a credit is considered to each of the environmental factors depending on their potential impact to the environment.

The Pearl Building Rating System (PBRS) of Estidama, Abu Dhabi has been adopted as a benchmark of this modified credit rating system as PBRS is one of the most established environmental building rating systems of the Arabian Peninsula. Other local and international environmental rating systems such as Gulf sustainability assessment system (GSAS), Leadership in Environment and Engineering Design (LEED) by USGBC and Building Research Establishment Environmental Assessment Method (BREEAM) of BRE UK have also been referred.

7.2 Embodied Carbon dioxide (eCO_2) of concrete mixes

The embodied carbon dioxide (eCO_2) of concrete, given as the mass of CO_2 in kg for every m^3 of concrete, was obtained by calculating the eCO_2 of the constituent materials transporting to Abu Dhabi, UAE. The CO_2 emission related to concrete production and transportation was not considered as it would be very similar for all concrete mixes. Therefore, the eCO_2 of concrete of this study can be considered as the summation of cradle to gate data of the concrete constituents.

The detailed information of the eCO_2 of concrete constituents are given in the Table 7.1 where beside the eCO_2 of individual raw materials, the origin of each raw materials and the source of reference are tabulated. A typical calculation of total eCO_2 of concrete based on the eCO_2 of concrete constituents is given in Appendix AH.

The eCO_2 related to the sea freight was considered for raw materials originated from outside UAE. The eCO_2 related to local transportation was ignored as most of the raw materials such as aggregates and cements travelled by road almost equal distance.

Table 7.1: eCO_2 of concrete constituents

Raw materials	**Origin**	**eCO_2**	**CO_2 emission for sea freight**			**Total eCO_2**	**Reference**
		kg CO_2 /tonne a	Km b	gm CO_2 /tonne -km c	Total Kg CO_2/tonne $d = \frac{bxc}{1000}$	kg CO_2/tonne $e = a + d$	
Portland cement	UAE	930	0	-	0	930	BCA Fact sheet 18 [P1]
GGBS	Japan	52	11,529	13.9	160	212	BCA Fact sheet 18 [P1]
Fly ash	India	4	2,076	13.9	29	33	BCA Fact sheet 18 [P1]
Microsilica	China	10	10,432	13.9	145	155	Elkem
Rice husk ash	India	0	2,076	13.9	29	29	Singhania, NK Enterprise
20mm L/S	UAE	7	-	-	-	7	Masdar, UAE
10mm L/S	UAE	7	-	-	-	7	Masdar, UAE
20mm RCA	UAE	7	-	-	-	7	Assumed to be same as 20mm L/S
10mm RCA	UAE	7	-	-	-	7	Assumed to be same as 10mm L/S
05mm L/S washed	UAE	7	-	-	-	7	Masdar, UAE
05mm L/S unwashed	UAE	6.32	-	-	-	6.32	Attached calculation at Annex C
Dune sand	UAE	5	-	-	-	5	Masdar, UAE
Water	UAE	1	-	-	-	1	Masdar, UAE
Polycarboxylate superplasticizer	UAE	720	-	-	-	720	EFCA, EPD for superplasticizer
Retarder	UAE	76	-	-	-	76	EFCA, EPD for retarder
AEA	UAE	86	-	-	-	86	EFCA, EPD for air entrainer

Note: The reference for CO_2 emission for sea freight is Biomass Energy Centre (2011)

7.2.1 Effect of different type of concrete on eCO_2

7.2.1.1 Concrete with high volume GGBS

The eCO_2 of concrete with different proportion of GGBS content can be seen from Figure 7.1. The eCO_2 of concrete is heavily influenced by the eCO_2 of the cementitious materials, and a linear relationship between the proportion of GGBS and the eCO_2 of concrete can be observed from Figure 7.1.

The rate of decrease of eCO_2 is proportionate to the increase of GGBS content. For 30% increment in GGBS from 70% to 100%, the reduction in eCO_2 is approximately 45%. Therefore a 2:3 relationship can be established between the increase of GGBS in concrete and the decrease in eCO_2 of concrete. However, this relationship has to be within the perimeter of assumptions considered in this study in terms of eCO_2 calculations of raw materials and concrete production process.

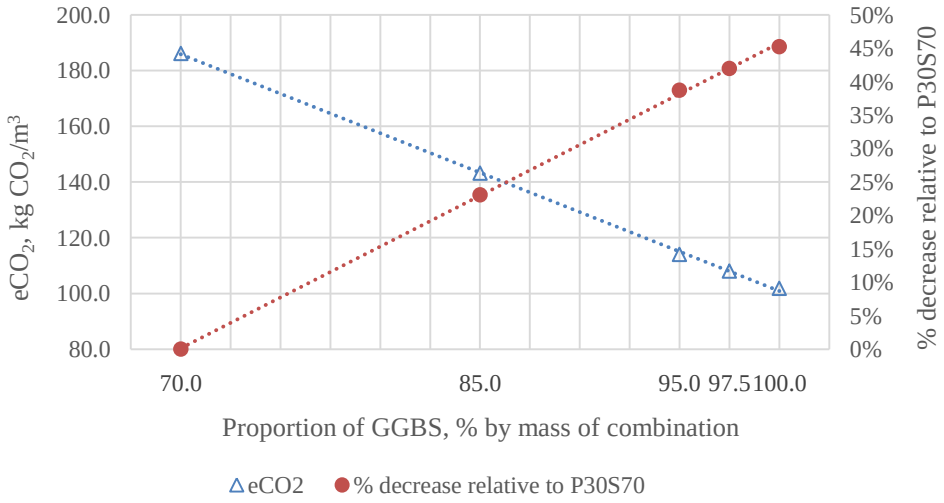

Figure 7.1: eCO_2 of concrete with different proportion of GGBS at 0.32 w/c ratio

The eCO_2 of concrete at three different w/c ratio of 0.25, 0.32 and 0.40 varies due to the requirement of relatively higher dosage of superplasticizer with lower w/c ratio. The eCO_2 of the superplasticizer is relatively higher (0.72 kg-CO_2/kg) compared to other ingredients of the concrete, except Portland cement (0.93 kg-CO_2/kg). However, the influence of the superplasticizer is not very significant due to relatively lower mass of superplasticizer used in the concrete compared to other ingredients.

In this chapter only concrete with 0.32 w/c ratio has been considered to discuss about the eCO_2 of concrete as it can be seen from Chapter 4 that concretes with 0.32 w/c ratio have the acceptable level of plastic and hardened properties.

7.2.1.2 Concrete with different pozzolanic materials

The eCO_2 of concrete with different proportion of pozzolanic materials varies significantly depending on their Portland cement content as seen in Figure 7.2. Comparing with the control P30S70 concrete, the fly ash concrete containing 20% Portland cement has almost 50% reduction in eCO_2. However, the microsilica and rice husk ash concretes which are with higher Portland cement are having 93% and 72% more eCO_2 than the control concrete. Therefore, the microsilica and rice husk ash concretes could not be considered to be a sustainable alternatives due to very high eCO_2 content even both of them had better compressive strength, durability and permeation properties.

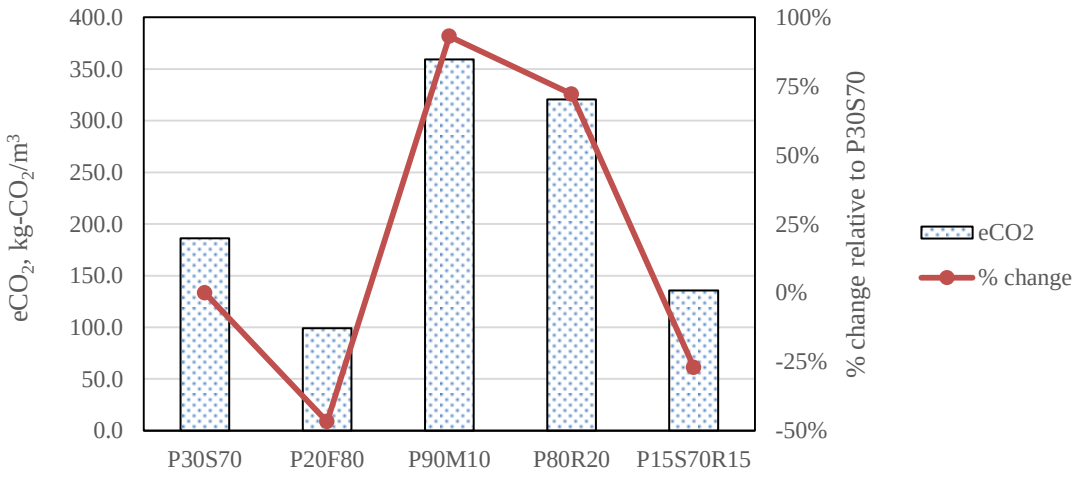

Figure 7.2: eCO_2 of concrete with different proportion of pozzolanic materials

However, the triple blend concrete (P15S70R15) with 15% Portland cement had 27% lower eCO_2 than the control with relatively acceptable level of plastic and durability properties as discussed in previous chapters. Therefore, P15S70R15 can be considered to have the best credential as the low carbon and environmentally sustainable concrete for the Arabian Peninsula.

7.2.1.3 Concrete with unwashed sand

The eCO_2 of concrete made with unwashed sand and different pozzolanic materials have been considered to be almost same as the concrete made with washed sand as the proportion of cementitious content remained the same. There is an insignificant difference in the dosage of superplasticizer between these two sets of concrete, therefore the difference in eCO_2 due to admixture remained negligible.

However, energy spent to wash sand should be considered to calculate the eCO_2 of unwashed sand. It has been estimated that the eCO_2 of unwashed sand (6.3 kg CO_2/tonne) is at least 10% lower than the eCO_2 of washed sand (7.03 kg CO_2/tonne - Annex C). Due to this very low level of eCO_2 value, the impact of reduced eCO_2 of unwashed sand is not significant and therefore, there is very little difference of the eCO_2 between concrete made of washed and unwashed sand.

7.2.1.4 Concrete with RCA

The eCO_2 of recycled concrete aggregates (RCA) and natural limestone aggregates have been considered to be similar as both aggregates were subjected to almost similar crushing and handling process. The initial extraction process of both type of aggregates may not be the same, but the energy input to these process are assumed to be same. Therefore, the eCO_2 values of RCA concretes made with triple blend of cementitious materials (P15S70R15) and 100% GGBS with different proportion of RCA contents are very similar to the similar concrete without any RCA. For the same reason the difference of eCO_2 between concretes with different proportions of RCA is also insignificant.

7.2.1.5 Concrete with entrained air

Additional air entrained into the concrete between 5% to 12% air have made little changes in the eCO_2 of concretes. As all concretes in this series are made of 90% Portland cement and 10% microsilica, the eCO_2 of the control mix was already as high as 359.4 kg/m^3. However, addition of 12% air had only less than 1% change in the eCO_2 compared to the control mix. This is because though almost 10% volume reductions in the raw materials was contributed by the air entrainment, but this reduction was basically the reduction in the volume of aggregates, which has very low inherent eCO_2.

Therefore, there was no positive effect on the reduction of eCO_2 happened due to the air entrainment. For the same reason all concrete mixes in this series with different proportion of air content have very similar eCO_2 content.

7.2.1.6 Concrete with higher curing temperature

The eCO_2 of concrete with two sets of triple blend used in this series to evaluate the effect of the elevated curing temperature on the compressive strength and durability properties of concrete are relatively low because of very low level of Portland cement used. The eCO_2 of the concrete with 5% Portland cement (P5S70R25) is only 101.4 kg/m^3 compared with 135.7 kg/m^3 for the concrete with 15% Portland cement (P15S70R15).

However, as discussed in Chapter 4, comparatively lower compressive strength of P5S70R25 have made it less effective alternative options. Therefore concretes with P15S70R15 cement combinations are considered to be a better alternative and discussed further in the following sections to explore its effects on other environmental factors.

7.2.2 Strength vs. eCO_2 analysis

As the Portland cement is the main contributor to both compressive strength and eCO_2, reduction of Portland cement has a direct effect on the reduction of compressive strength and eCO_2. Therefore, with increased compressive strength due to higher content of Portland cement, the eCO_2 of concretes also increase. However, as it can be seen from the Figure 7.3, with appropriate cement combinations by replacing Portland cement, concrete with lower eCO_2 can achieve higher compressive strength.

The eCO_2 of the group of concretes (P15S85, P15S70R15 and P30S70) encircled in Figure 7.3 have relatively higher compressive strength with lower eCO_2 compared to the other two groups. The Portland cement content of these three concretes P15S85, P15S70R15 and P30S70 are ranging from 15% to 30% of total cementitious materials which is relatively low. That contributed to reduce eCO_2 of below 200 kg-CO_2/m^3 for this group which is well below 250 kg-CO_2/m^3 the maximum cap suggested by the Environment Agency of UK (Black & Veatch, 2001). The triple blend concrete made with P15S70R15 cementitious combination has the lowest eCO_2 with compressive strength of 72.2 N/mm^2.

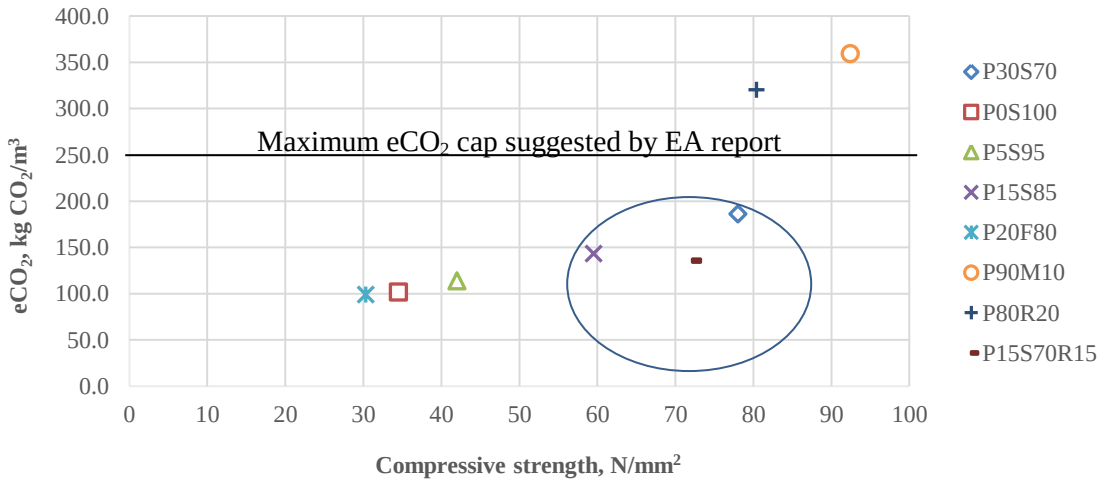

Figure 7.3: eCO_2 vs. compressive strength of concrete at the age of 28 day

Concretes with microsilica (P90M10) and rice husk ash (P80R20) had higher compressive strength, but their higher Portland cement content contributed to their relatively higher eCO_2. Contrarily P20F80, P0S100 and P5S95 had very low compressive strength, as well as lower eCO_2 due to the lower content of Portland cement.

7.2.2.1 Strength / eCO_2 (S/eC) index

The relationship between the compressive strength and the eCO_2 of concrete can be expressed as an index between the compressive strength expressed in N/mm^2 at the age of 28 days and the eCO_2 expressed as kg-CO_2/m^3 of the concrete. It can be denoted as S/eC index where 'S' denotes the compressive strength and 'eC' denotes the eCO_2 of concretes. The S/eC index measures the compressive strength of concrete for one kg embodied CO_2. Figure 7.4 presents the S/eC index of concrete with different proportion of GGBS and other pozzolanic materials.

The S/eC index can be used as an index to measure the ability of any concrete to produce higher compressive strength with lower eCO_2 content. Therefore, concrete with higher S/eC index considered to have better hardened properties (compressive strength) and environmental attributes.

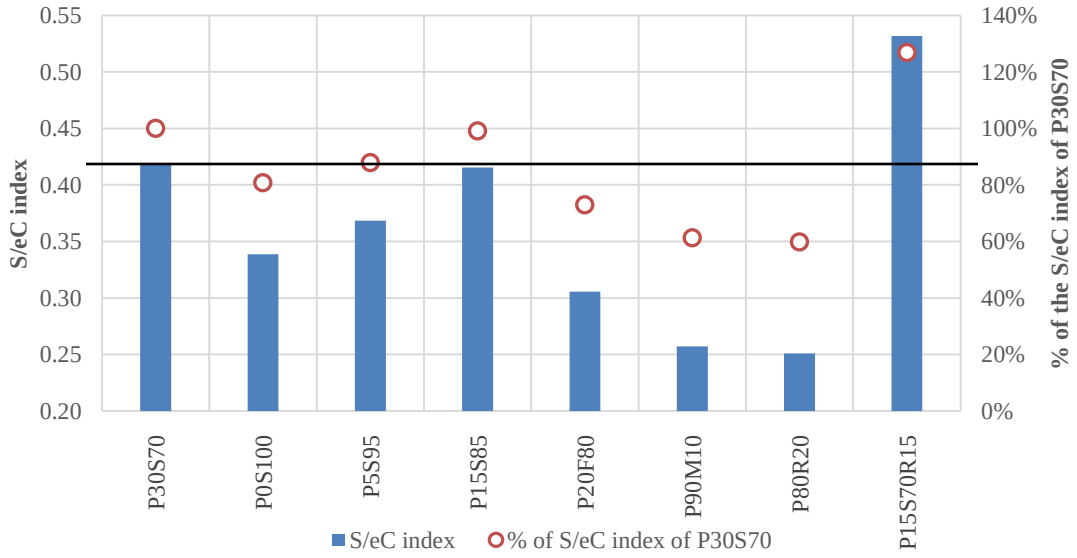

Figure 7.4: S/eC index of different concrete made with washed sand and with different cementitious materials

As seen in Figure 7.4, the S/eC index provides a relative position of each types of concrete in terms of the compressive strength gain and corresponding eCO_2 of each concrete. The triple blend concrete of P15S70R15 has the highest S/eC index of 0.53, followed by P30S70 and P15S85 each with 0.42. Concrete with very high content of Portland cement, the microsilica and rice husk ash have the lowest S/eC index due to their high eCO_2 content.

Relative to the control concrete of P30S70, only P15S70R15 has higher S/eC index, which is 127% of the S/eC index of P30S70. The P15S85 has achieved almost same S/eC index of P30S70. The S/eC index of other concretes is much lower than the control. Therefore, P15S70R15 concrete should be considered to be the appropriate greener alternative to P30S70 as far as eCO_2 is concerned.

7.2.2.2 Effect of unwashed sand on S/eC index

It is to note that the above analysis have been applied to concrete made with washed sand with 0.32 w/c ratio and at the age of 28 days. As it has been established from the Chapter 4 that the compressive strength of concrete with unwashed sand had increased compared to the same concrete made with washed sand, the S/eC index of concrete made with unwashed sand should be better than the same concrete made with washed sand, provided that the eCO_2 of unwashed sand concretes are similar to the concretes made with washed sand. However, as seen in Figure 7.5, the rate of improvement compared to P30S70 is not better than the washed sand concretes.

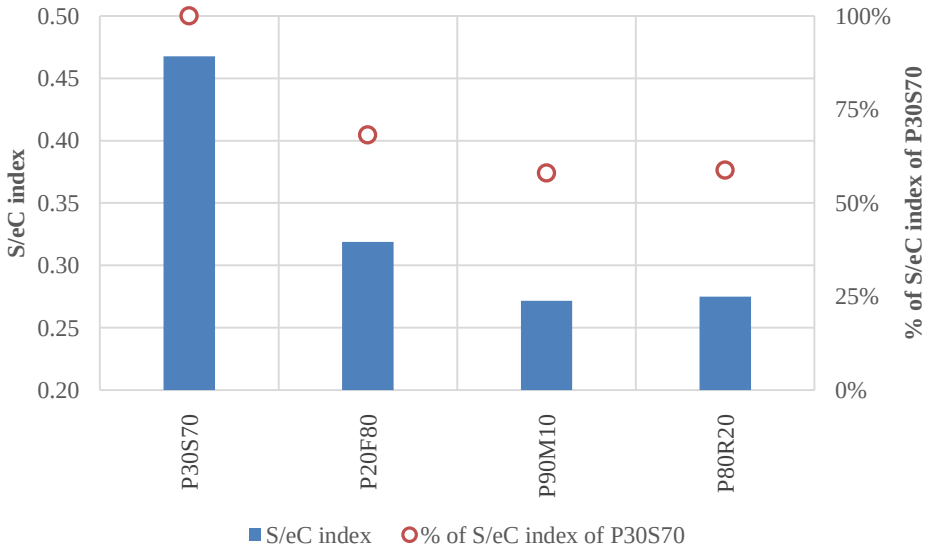

Figure 7.5: S/eC index of different concrete made with unwashed sand and with different cementitious materials

It can be seen from Table 7.2 that the S/eC index of concrete made with unwashed sand are higher than washed sand concrete, due to higher strength gain using unwashed sand. However, relative to P30S70, the percentage of the S/eC index of concretes made with other pozzolanic materials and unwashed sand reduced because the effect of unwashed sand was more pronounced on the S/eC index of P30S70 concrete compared to concretes made with fly ash, microsilica and rice husk ash.

Table 7.2: Comparison of the effect of washed and unwashed sand on S/eC index of concretes made of different cementitious materials

	S/eC Index		% of P30S70	
	Washed sand	**Unwashed sand**	**Washed sand**	**Unwashed sand**
P30S70	0.42	0.47	-	-
P20F80	0.31	0.32	73	68
P90M10	0.26	0.27	61	58
P80R20	0.25	0.27	60	59

However, the difference between these two groups appears to be small and can be considered to be insignificant. No comparison can be made for P15S70R15, as the triple blend concrete was not tested using unwashed sand.

7.2.2.3 Effect of RCA on S/eC index

The S/eC index of concrete with different proportions of RCA are very similar to the concrete without any RCA as shown in Figure 7.6, as the compressive strengths reductions due to the RCA content is not very significant and the eCO_2 of all RCA concrete with P15S70R15 cement combinations are almost similar.

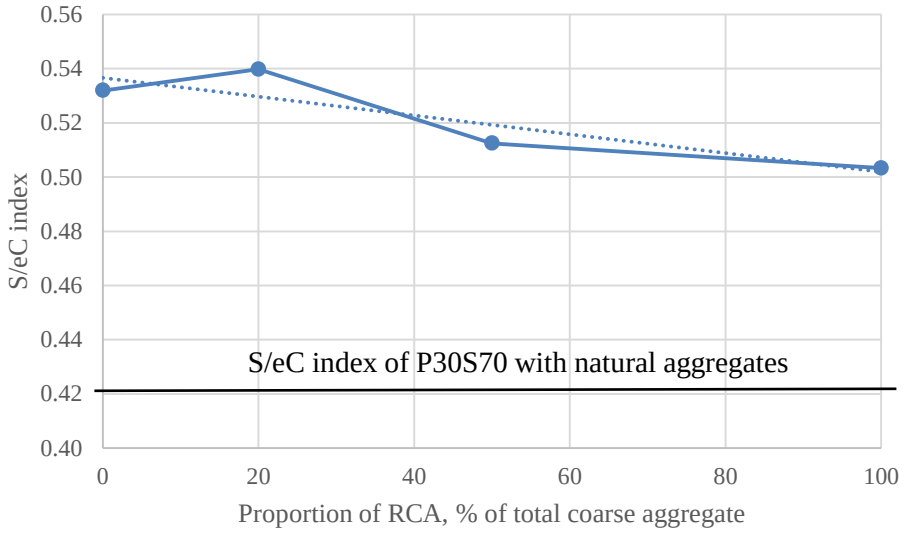

Figure 7.6: S/eC index of concrete made with RCA and P15S70R15 cement combinations

Due to relatively higher compressive strength of concrete made of 20% RCA and P15S70R15 combination compared to concrete without RCA, the S/eC index of 20% RCA is higher than the 0% RCA concrete as shown in Figure 7.6.

The straight line crossing the 0.42 S/eC index at the primary vertical axis representing the S/eC index of concrete made with P30S70 cementitious combinations without any RCA content. The S/eC index of all RCA concrete are much higher than the S/eC index of concrete made of P30S70 with 100% natural limestone aggregates mainly due to relatively higher eCO_2 contributed by the higher content of Portland cement in P30S70 concrete.

7.2.2.4 Effect of higher entrained air on S/eC index

Due to very low S/eC index of P90M10 concrete of 0.26 as shown in Figure 7.4, the S/eC index of all microsilica concrete with higher air content have lower S/eC index. The decrease in compressive strength with increased air content has reduced the S/eC index further. All concrete in this series were made with P90M10 cementitious combinations.

However, concrete made with the triple blend of P15S70R15 cementitious combinations with higher air content would have much higher S/eC index than P90M10 concretes. Though physically there was no concrete made with P15S70R15 and with higher air content, nevertheless, based on the strength development and eCO_2 of these two sets of concrete as discussed in the previous sections, hypothetically it could be concluded that a P15S70R15 concrete with 5% air would have higher S/eC index than the same concrete made with P90M10 combinations.

7.2.2.5 Effect of elevated curing temperature on S/eC index

The increase in compressive strength due to elevated temperature has positive effect on the S/eC index of the two sets of triple blend concrete made with P5S70R25 and P15S70R15 cementitious combinations as shown in Figure 7.7. The significant increase in S/eC index by the triple blend concrete is due to the enhanced pozzolanic reaction activated by the higher curing temperature and relatively lower eCO_2 value due to very low Portland cement content.

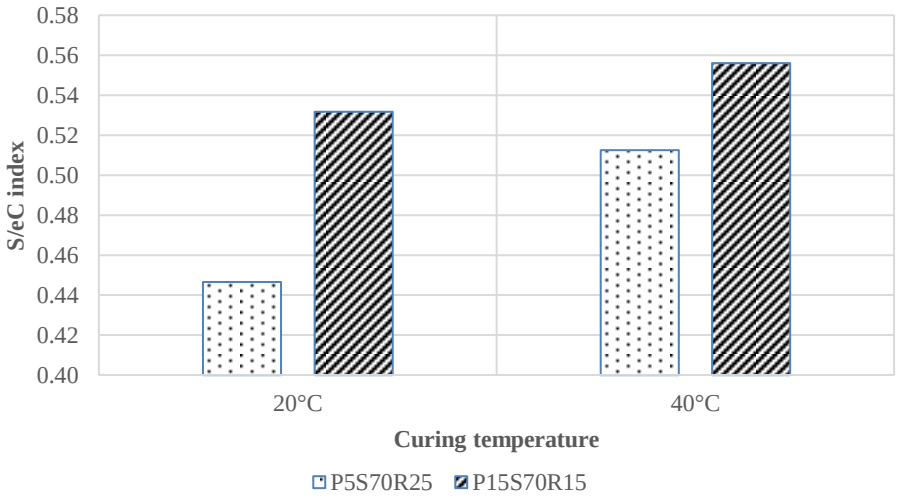

Figure 7.7: Changes in S/eC index due to elevated curing temperature

The percentage increment of the S/eC index of P570R25 due to the change in curing temperature is 15% compared to 5% increment for P15S70R15 concrete, however, relatively lower compressive strength of P5S15R25 compared with P15S70R15 has made P5S70R25 a less attractive alternative.

Though the percentage increment of P15S70R15 due to higher curing temperature is lesser, however, the subsequent increase of the S/eC index to 0.56 is quite significant. The age and w/c ratio considered for this comparison are at 28 days and 0.32 w/c respectively.

7.3 Credit ratings of environmental sustainability factors

7.3.1 The basis of the credit ratings

There are total nine environmental sustainability factors (ESF) are identified and tabulated in Table 7.3 which would have direct impact on environment. The different types of concrete undertaken by this study with different cement combinations, different type of aggregates and air content would have different attributes to mitigate these impacts. To measure the effectiveness of the positive attributes of these concretes, a set of credit rating was designed and attributed to each factors.

The credit rating expressed in percentage of the total sum was designed by benchmarking the Pearl Building Rating System (PBRS) of Estidama, Abu Dhabi as PBRS specifically designed to address the unique environmental requirement of the Arabian Peninsula (Estidama, 2010). The corresponding reference category of PBRS are considered as a guide to decide each credit ratings of this study as not all environmental factors described in Table 7.3 have direct references to PBRS. Nevertheless, the corresponding factors described in PBRS are considered to be similar to those of this study.

Table 7.3: Credit rating of different environmental sustainability factors (ESF)

	Environmental factors	**Application**	**Rating**	**PBRS reference**
1	Waste reduction	Reduction of sludge	9	SM13- Improved construction waste management
2a	Recycled materials	Use of RCA	16	SM10 – Recycled materials
2b	Recycled materials	Use of SCM	16	SM10 – Recycled materials
3	Design for durability	Concrete with durability	4	SM6 – Design for durability
4a	Reduction of raw materials	Increased entrained air	4	SM2 – Design for material reduction
4b	Reduction of raw materials	Use of finer materials of unwashed sand	4	SM2 – Design for material reduction
5	Water	Saving water by using unwashed sand	17	PW2.3 – Exterior water use reduction: water features
6	Energy	Saving resources due to unwashed sand	17	RE5- Peak load reduction
7	Regional materials	Materials sourced from within 500km radius	5	SM9 - Regional materials
8	Rapidly renewable materials	Use of rice husk ash	4	SM11 – Rapidly renewable materials
9	Heat Island effect - High albedo materials	Use of GGBS	4	LBo1 - Improved outdoor thermal comfort
		Total	100	

In PBRS there are total 177 credit points to achieve from 7 distinctive categories namely 1) IDP – Integrated Development Process (13 points), 2) NS – Natural Systems (12 points), 3) LB - Livable Buildings (37 points), 4) PW – Precious Water (43 points), 5) RE – Resourceful Energy (44 points), 6) SM – Stewarding Materials (28 points) and 7) IP – Innovating Practice (3 points). Each of these categories and respective allocated points have been designed based on the urgency of each categories (Estidama, 2010).

The credit ratings of different environmental sustainability factors (ESF) in Table 7.3 have been designed by the author based on similar concept. The allocated points to 9 different categories indicate the assumed gravity of each category in order to achieve the low carbon and environmentally sustainable concrete for the Gulf environment.

7.3.1.1 Effect of unwashed sand

Washing of sand (0-5mm, crushed limestone fine aggregate) is a very wasteful process where beside wasting resources such as raw materials (sand), water, time and energy, a huge amount of sludge is produced at the end of the process which needs to be dumped in the landfill. In the event of using the unwashed sand which contains at least 10% of finer particles passing 75μm sieve instead of washed sand, this waste materials can be saved from being dumped. Besides adding additional eCO_2 to the concrete by the sand washing process, dumping of wet sludge on virgin desert lands leave behind a catastrophic environmental impact on the micro-climate of the area.

Use of unwashed sand would increase the credit rating of concrete by few folds as in Table 7.3 there are four categories where the credit rating would be positively affected due to the use of unwashed sand in the concrete. Reduction or elimination of sludge production due to non-washing of sand would reduce the handling of waste and divert it from being landfill to the use in the concrete production as part of the fine aggregates. Therefore, use of unwashed sand would not only reduce waste but also reduce the volume of raw materials consumptions.

However, the major contribution of using unwashed sand is saving water which is a very precious material in the Arabian Peninsula. Moreover, use of unwashed sand would also save energy and other resources such as manpower, time and lands. Washing of sand required considerably large open area and it is time consuming as well as energy intensive.

7.3.1.2 Effect of RCA and SCM

Use of recycled materials such as recycled concrete aggregate (RCA) and supplementary cementitious materials (SCM) which are the waste product of industrial process such as steel industry and coal fired power stations are a major contributor to earn environmental benefiting credits as they not only being recycled but also replace either virgin aggregates or Portland cement.

7.3.1.3 Design for durability

Durability of concrete enhances the design life of structure, therefore reduce the pressure on the raw material consumption and create a positive effect on the environment. Therefore, design for durability is an important factor to be considered to contribute towards the positive impacts on the environment. However, as almost all concrete studied in this work are highly durable, therefore, all concrete considered here would be benefiting from this credit rating.

7.3.1.4 Effect of air content

Beside enhancement in durability and flow properties of concrete, concrete containing higher air content would contribute towards the environmental sustainability by reducing the quantity of raw materials required per unit volume of concrete. As the additional air in the concrete replaces the concrete ingredients, mainly aggregates, the saving of virgin aggregate should be recognized as an environmental benefit provided by the concrete with higher air content.

7.3.1.5 Effect of regional materials

Use of regional materials within 500 km from the production of concrete has been recognized by most of the major environmental rating systems including Estidama as one of the important environmental factor to be considered. The ingredients of concrete considered in this study are largely from within this range. However pozzolanic materials such as microsilica and rice husk ash are not locally produced in the Arabian Peninsula. Therefore, concrete containing these two materials will not get full credit allocated for this category. However, as the proportion of these pozzolanic materials in the concrete is not very significant, therefore the reduction of credit due to the presence of either microsilica or rice husk ash in the concrete is not substantial.

7.3.1.6 Rapidly renewable materials

Though rice husk ash is not a regional material, but use of rice husk ash would add an additional credit to the concrete due to its rapidly renewable characteristics. Being organic, rice husk ash is the only ingredient used in this study is truly renewable. These characteristics of rice husk ash have been recognized by considering 4 credit ratings in Table 7.3.

7.3.1.7 Heat island effect

Reduction in urban heat island (UHI) effect is another major environmental factor to be considered as light coloured concrete made with high volume GGBS would have higher albedo values, which would lower the negative effect of UHI. The typical albedo values of concrete with 70% GGBS is reported to be around 0.70 compared with grey coloured concrete of 0.30 to 0.40 (Boriboonsomsin and Reza, 2007). Therefore concrete with high volume GGBS content is given a credit rating of 4.

7.3.2 Comparison of the environmental sustainability factors

In order to compare the environmental performance of different type of concretes studied in this work, two sets of cementitious combinations P15S70R15 and P15S85 are selected due to their optimum performance in compressive strength, durability & permeation properties as described in previous chapters. Both of them also have relatively lower eCO_2 values and higher S/eC index shown in previous sections. The environmental performance of these two sets of concretes has been compared with the control P30S70 concrete.

Concrete with other different cementitious combinations are not considered mainly due to two reasons i) lower compressive strengths and ii) higher eCO_2 content. As Section 4.3.1.1 of Chapter 4 discussed most of the concrete above 90% GGBS content did not achieve stable compressive strengths related to their GGBS proportions. Therefore, concrete containing 90% and below GGBS content are not considered.

Concrete with high volume fly ash (P20F80) and triple blend with 5% Portland cement (P5S70R25) have also achieved very low compressive strengths compared to P30S70 concretes as seen in Figure 4.9 in Chapter 4. Therefore, these two sets of concrete are also not considered for further environmental impact analysis.

Concretes which achieved similar or higher S/eC index as per Figure 7.4 are considered for further analysis. As it can be seen from Figure 7.4, all other concretes except P15S70R15 and P15S85 have missed that target. Concretes with P0S100, P5S95 and P20F80 have lower S/eC index due to their lower compressive strength at 28 days. On the other hand concrete with P90M10 and P80R20 have lower S/eC index due to their higher eCO_2 values due to higher Portland cement content in their mixes. Therefore concrete with P15S70R15, P15S85 and P30S70 are considered for further analysis to measure their environmentally sustainable attributes.

These three sets of cementitious combinations are presented in four different scenarios of aggregates combinations and air content, namely i) washed sand ii) unwashed sand iii) 20% RCA with unwashed sand and iv) 5% air content and 20% RCA with unwashed sand to incorporate all positive attributes undertaken by this study.

7.3.2.1 Calculation of weightings

In Table 7.4 the environmental credits points of different combinations of concrete consist of P30S70, P15S85 and P15S70R15 cementitious materials are calculated by using the credit ratings as shown in Table 7.3. In order to obtain an unbiased reflection of the environmental impact, a set of appropriate weightings was used to multiply with the credit ratings of each individual category of the environmental factors.

In Table 7.4 the weighting of the waste reduction by reducing sludge was considered to be 26% by considering the proportion of the mass of fine aggregates (excluding dune sand) over the total mass of concrete, as this impact was limited within the mass of the fine aggregate. For example the total mass of 5mm aggregate of 1P30S70W concrete is 678 kg which is 26.4% of total mass of the concrete which is 2566 kg.

The same weighting was used for all categories impacted by the unwashed sand. Similarly the weightings given to the RCA content and proportion of SCM represents their individual proportion of mass relative to the total mass of concrete.

Concrete containing 5% air by volume received 100% weighting for the reduction of raw materials due to the increase in air content category. At this juncture, a 5% air was considered to be the optimum air in concrete with high volume replacement of Portland cement to produce an equivalent hardened and durability properties of concrete of the control P30S70 concrete.

The weighting for the design for durability category was considered to be 100% considering that each type of concrete met the durability requirements set by this study. Similarly 100% weighting was applied to the rapidly renewable materials and heat island effect categories. Concrete containing rice husk ash was given the 100% weighting for the rapidly renewable materials category by recognizing the unique characteristics of organic renewable source of rice husk ash. As a novel and unique materials, the true potential of rice husk ash to enhance the hardened and durability properties of high volume SCM concrete in the Arabian Peninsula has also been recognized here.

Similarly the unique characteristic of GGBS concrete by increasing the albedo value of concrete to reduce the urban heat island effect has been recognized by awarding 100% weighting for concrete containing GGBS content of 70% and above. In Table 7.4, concretes containing rice husk ash have reduced weighting (97.5%) in regional materials category due to its foreign origin compared to the other ingredients as previously explained. Concretes without rice husk ash received full 100% weighting due to their local source of origin.

It is to take note that it has been hypothetically considered in Table 7.4 that concrete with cementitious combinations of P30S70, P15S85 and P15S70R15 were made with different combinations of 20% RCA, unwashed sand and 5% air. There are no direct tests conducted with these cement types together with the combinations of RCA, unwashed sand and air content for hardened and durability tests. However, it is appropriate to consider that the hardened and durability properties of these combinations would be well within the accepted parameters of this study. This is because as seen in previous chapters concretes made with these types of cement combinations with similar combinations of coarse and fine aggregates posted acceptable results in both plastic and hardened properties of concrete including compressive strength and durability parameters.

Table 7.4: Credit rating of the ESF of P30S70, P15S85 and P15S70R15 concretes

				P30S70								**P15S85**								**P15S70R15**							
				W/ sand		U/ sand		20%RCA, U		5%Air 20%RCA, U		W/ sand		U/ sand		20%RCA, U		5%Air 20%RCA, U		W/ sand		U/ sand		20%RCA, U		5%Air 20%RCA, U	
	Environmental factors	Application	Rating	Wt. %	Pts.	Wt. %	Pts.	Wt. %	Pts.	Wt. %	Pts.	Wt. %	Pts.	Wt. %	Pts.	Wt. %	Pts.	Wt. %	Pts.	Wt. %	Pts.	Wt. %	Pts.	Wt. %	Pts.	Wt. %	Pts.
1	Waste reduction	Reduction of sludge	9	0	0	26	2.34	26	2.34	26	2.34	0	0	26	2.34	26	2.34	26	2.34	0	0	26	2.34	26	2.34	26	2.34
2a	Recycled materials	Use of RCA	16	0	0	0	0	4	0.64	4	0.64	0	0	0	0	4	0.64	4	0.64	0	0	0	0	4	0.64	4	0.64
2b	Recycled materials	Use of SCM	16	11	1.76	11	1.76	11	1.76	11	1.76	13.5	2.16	13.5	2.16	13.5	2.16	13.5	2.16	13.5	2.16	13.5	2.16	13.5	2.16	13.5	2.16
3	Design for durability	Concrete with durability	4	100	4	100	4	100	4	100	4	100	4	100	4	100	4	100	4	100	4	100	4	100	4	100	4
4a	Reduction of raw materials	Increased entrained air	4	0	0	0	0	0	0	100	4	0	0	0	0	0	0	100	4	0	0	0	0	0	0	100	4
4b	Reduction of raw materials	Use of finer materials of u/sand	4	0	0	26	1.04	26	1.04	26	1.04	0	0	26	1.04	26	1.04	26	1.04	0	0	26	1.04	26	1.04	26	1.04
5	Water	Saving water by using u/sand	17	0	0	26	4.42	26	4.42	26	4.42	0	0	26	4.42	26	4.42	26	4.42	0	0	26	4.42	26	4.42	26	4.42
6	Energy	Saving resources due to u/ sand	17	0	0	26	4.42	26	4.42	26	4.42	0	0	26	4.42	26	4.42	26	4.42	0	0	26	4.42	26	4.42	26	4.42
7	Regional materials	Materials within 500km	5	100	5	100	5	100	5	100	5	100	5	100	5	100	5	100	5	97.5	4.87	97.5	4.87	97.5	4.87	97.5	4.87
8	Rapidly renewable materials	Use of rice husk ash	4	0	0	0	0	0	0	0	0	0	0	0	0	0	0	0	0	100	4	100	4	100	4	100	4
9	Heat Island effect - High albedo materials	Use of GGBS	4	100	4	100	4	100	4	100	4	100	4	100	4	100	4	100	4	100	4	100	4	100	4	100	4
		Total		14.76		26.98		27.62		31.62		15.16		27.38		28.02		32.02		19.04		31.26		31.90		35.90	

7.3.2.2 Analysis of ESF performances of the novel concretes

The credit points obtained by the three novel sets of concrete mentioned above are compared in Figure 7.8 where the credit point obtained by P30S70 made with washed sand has been considered to be the benchmark, as P30S70W is the control concrete and widely produced in the Arabian Peninsula for its acceptable durability properties.

It can be seen from Figure 7.8 that concretes with P15S70R15 cementitious combinations have superior environmental credit points over the control P30S70 and P15S85 concretes at all combinations. The two main differences between the control and P15S70R15 can be identified as in P15S70R15, i) there is a higher proportion of SCM as recycled materials and ii) the use of rice husk ash, though there is a reduction in points due to its foreign origin, however, the awarded credits due to be rapidly renewable materials has improved its relative position. The percentage improvement of P15S70R15 is 29% relative to P30S70. This rate of improvement remained fixed for all four scenarios.

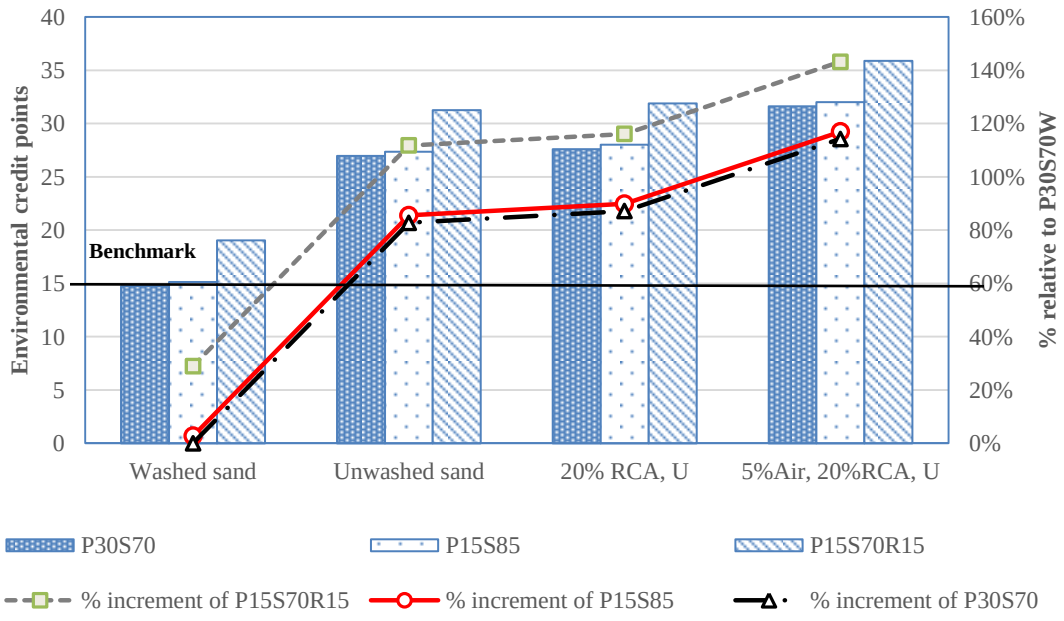

Figure 7.8: Performance of the environmental sustainability factors of concretes made with P15S85 and P15S70R15 compared with P30S70

The credit points of concretes have improved due to the use of unwashed sand, recycled concrete aggregate, and higher air content for both P15S70R15 and P30S70. However, if the credit point of P30S70W can be considered as the benchmark, which is around 15, the subsequent improvement of P15S70R15 due to the addition of rice husk ash, unwashed sand, RCA and higher air content can be as much as 112% to 143% of P30S70W concrete.

It is to acknowledge that without changing the cement type, the potential improvement in environmental credit ration points of P30S70 is also substantially high with a maximum possible improvement of 114% of control P30S70W concrete.

Concretes with P15S85 cement combination could be other viable alternatives to P30S70 which had a relatively smaller advantage of 3% higher credit points at every category as shown in Figure 7.8. The S/eC index of both P30S70 and P15S85 concretes as shown in Figure 7.4, is 0.42, demonstrating that relatively lower compressive strength of P15S85 compared to P30S70 due to lower Portland cement content was compensated by lower eCO_2 values for the same reason.

Though P15S70R15 concretes have superior compressive strength, durability and environmental values over P15S85, P15S85 concretes would be less affected by the practical issues related to local implications, acceptance by the industry and production and handling issues compared to concretes made with P15S70R15 cementitious combinations. These issues will be discussed in detail in the next chapter.

7.4 Conclusion

In this chapter the different types of concrete studied in the entire work have been analysed for their environmental benefits to establish the most sustainable and low carbon concrete for the Arabian Peninsula. In order to achieve this objective, the eCO_2 of concretes have been analysed together with their corresponding 28 days compressive strength by establishing the compressive strength and eCO_2 index (S/eC index) as the eCO_2 and compressive strength are interrelated with the content of Portland cement. However, it has been established that concretes made with P15S70R15 have the best S/eC index due to its lower eCO_2 and higher compressive strength gain. Comparing with control P30S70 concrete with P15S85 has the same S/eC index.

Besides eCO_2, total nine other different type of environmental factors were identified and their environmental impact mitigated by the low carbon concretes of P15S70R15 and P15S85 were measured using a set of environmental credit ratings and appropriate weightings. This environmental performance with different combinations of sand, RCA and air content were compared with the control P30S70 concretes. The comparisons have shown that the concretes with triple blend of P15S70R15 cementitious materials with unwashed sand and 20% RCA would produce the most sustainable concrete suitable for the Arabian Peninsula. Addition of 5% air would enhance its sustainability as well as durability and plastic properties of concrete.

Chapter 8

Analysis of Performance and Regional Implications

8.1 Introduction

In the previous chapter it has been concluded that concretes made with P15S70R15 and P15S85 cement combinations have the best environmental credentials in terms of S/eC index and other environmental sustainability factors. These two sets of cementitious combinations have been used to create different scenarios of concretes with two different types of sand i) washed and ii) unwashed and with RCA (maximum 20% of total mass of coarse aggregates) with and without additional entrained air (5% maximum by volume of concrete). P30S70 made with washed sand has been compared with these two sets of concrete as the control concrete.

In order to validate the engineering and environmental performances of these new concretes, this chapter has been divided into two sections. In the first section an analysis of performance of different type of concretes have been undertaken, where the performance of concretes in terms of compressive strength, durability and permeation properties and associated characteristics of microstructure in terms of TG, SEM and MIP techniques have been analysed and compared with the control concrete.

In the second section factors associated with the regional implications such as specification work, marketing, cost competitiveness, production and placing issues have been critically verified and validated with its engineering, durability and environmental properties.

8.2 Analysis of performance

In the following section the compressive strength and durability and permeation properties and corresponding microstructures of different type of concrete made with different type of cementitious materials, aggregate type with washed and unwashed sand, with and without different proportion of RCA, at different air content and curing temperature have been analysed and discussed together.

8.2.1 Cement type series

8.2.1.1 High volume GGBS

Compressive strength:

The reduction in compressive strength with high volume GGBS concrete compared with the control concrete with P30S70 is the key obstacle to consider high volume GGBS concrete mix as a sustainable alternative. Erratic hardening of concrete with GGBS content above 95% provided inconsistent results in the compressive strengths development. At 28 days the reduction in strength of concrete with 0.40 w/c ratio could be as much as 68% of the control mix (Figure 4.4, Chapter 4). Most importantly the rate of strength reduction between 95% and 100% GGBS concrete were not consistent between different w/c ratios at different ages. Therefore it has been suggested to consider a concrete with maximum 90% GGBS content where a 64% gain in compressive strength of the control mix can be achieved with 0.32 w/c ratio (Table 4.10, Chapter 4).

Though at 0.25 w/c ratio the rate of compressive strength gain would be 77% of the control concrete, but from the point of view of the plastic properties of concrete with high GGBS content and 0.25 w/c ratio, it is advisable to consider concrete with 0.32 w/c ratio. Concrete with 0.25 w/c ratio and high volume GGBS content tend to create a very 'sticky' mix which would not be practical to produce and place (Section 4.2.2, Chapter 4). Relatively higher dosage requirement of superplasticizer with 0.25 w/c ratio would also make it less economical than the concretes with 0.32 w/c ratio.

Hydration products and microstructures:

Analysis from thermogravimetry also sets a close relationship with the development of hydrates and the compressive strength gain of concrete. As shown in Figure 8.1, the proportion of compressive strengths of concrete made with P15S85 and P15S70R15 compared with P30S70 at 28 days posted a similar trend with the proportion of mass of hydrates disintegrated by TG analysis. Though the age of these three sets of data are different, but their similar behaviour should be noted.

Though the same behaviour is not repeated for P90M10 and P80R20 categories, but their higher proportion of the mass of hydrates relates the reasons of the achievement of higher compressive strengths. The result for P20F80 is just reversed that of P90M10 and P80R20. The compressive strength is lower due to the lower production of hydrates due to lack of Portland cement content.

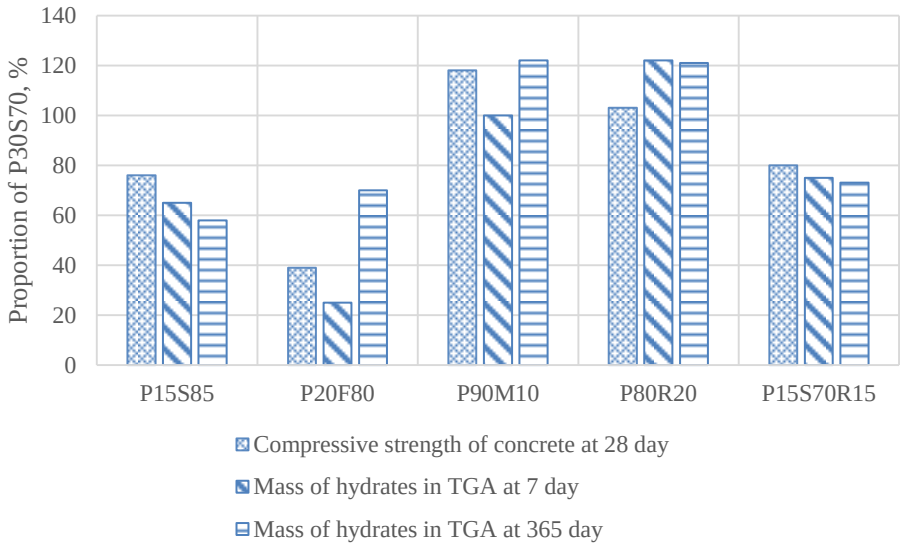

Figure 8.1: Comparative analysis between 28 day compressive strength of 0.32 w/c concrete and mass of hydrates of cement paste made with 0.32 w/c at the age of 7 and 365 days.

The comparative analysis of SEM images between pastes containing P30S70 and P15S85 shows very similar morphology between them. However, at 7 days the microstructure of P15S85 is relatively porous than the microstructure of P30S70 validating the reduced quantity of hydrates as quantified by the TG analysis and confirmed by the reduced compressive strength.

Durability and permeation properties:

The durability and permeation properties of high volume GGBS concrete containing 85% to 100% GGBS is within acceptable range especially the RCPT values to represent the resistance to chloride ion penetrability of concrete. The RCPT values remain below 1000 coulomb for all GGBS concrete irrespective to the proportion of GGBS and w/c ratio which is considered to be very low according to the ASTM C1202 (Figure 5.1, Chapter 5).

However with respect to the P30S70 concrete, the chloride permeation resistance of higher GGBS concrete was not consistent with their respective proportion of GGBS.

The chloride diffusion coefficient of high volume GGBS concrete is also considered to be well within the acceptable range of $5x10^{-12}m^2/s$. The rate of chloride diffusion with the proportion of GGBS also validate the compressive strength, TGA and SEM findings up to a certain extent. Figure 8.2 shows the comparative relationship between chloride diffusion and compressive strength of concrete containing different proportion of GGBS content.

As it can be seen from Figure 8.2, the chloride diffusion reduced with increased GGBS from 70% to 85%, perhaps due to the chloride binding capacity of additional GGBS content. However, the chloride diffusion started increased with increased amount of GGBS content after 85% of total cementitious content, while compressive strength reduced due to the development of poorer microstructure.

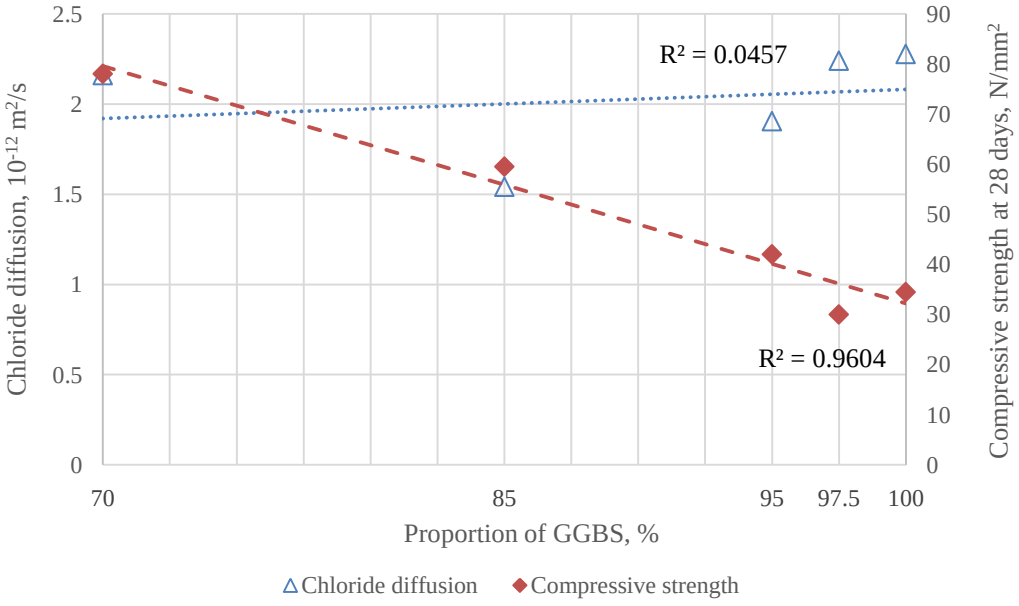

Figure 8.2: Relationship between chloride diffusion and compressive strength of concrete with high volume GGBS content

The properties of sulfate resistance of concrete containing 100% GGBS appeared to be excellent as no visual sign of sulfate attack was observed on concrete bar made of 100% GGBS at three different w/c ratios of 0.25, 0.32 and 0.25.

Among the water permeation properties, the water absorption of concrete with high volume GGBS concrete was found to be relatively higher but well within the acceptable range of 2.0%. Concrete with 97.5% and 100% GGBS with 0.40 w/c ratio have posted water absorption of 1.9% and 1.8% respectively (Figure 5.13, Chapter 5). However the same concrete with 70% GGBS has also achieved relatively higher results of 1.6%. All other concretes in this group are having water absorption results below 1.5%.

The water permeation properties of concrete with high volume GGBS concrete appeared to be well within the acceptable limit with maximum penetration of water of 7mm observed in 85% GGBS concrete (Figure 5.30, Chapter 5). Other results are 5mm or below.

8.2.1.2 Different pozzolanic cementitious materials

Compressive strength:

Beside high volume GGBS, concrete with different combinations of pozzolanic materials have provided interesting solutions to partially replace Portland cement from concretes. Though 80% fly ash (P20F80) produced very similar compressive strength gain of 100% GGBS (Figure 4.9, Chapter 4) comparing with the compressive strength of the control P30S70, the results are well below to be practically implemented. In fact, concrete with P90M10 is the only set of concrete which produced higher compressive strength than the control in almost all cases.

The performance of P80R20 was less than expected especially with 0.25 w/c ratio. The reason of this lower performance of rice husk concrete was due to its very high water demand at low w/c ratio of 0.25. Nevertheless, the compressive strengths of P80R20 concretes were considerably higher. Though the P90M10 and P80R20 concretes presented higher compressive strengths, they are not the attractive options to consider them as the sustainable alternatives due to their relatively higher proportion of Portland cement content.

However, among the two sets of concrete made with triple blends of Portland cement, GGBS and rice husk ash, P15S70R15 concretes posted very encouraging results of compressive strength. At 0.32 w/c ratio it achieved 93% of the control P30S70 concrete at the age of 28 days (Figure 4.9b, chapter 4). The compressive strength of the same concrete at 0.25 w/c ratio was 80% of P30S70. This reduction was due to the reason of very high water demand of this concrete.

The compressive strengths of P5S70R25 are relatively lower than P15S70R15, therefore P5S70R25 could not be considered as an alternative option, though the Portland cement content is only 5% of total cementitious mass which has made it a good option to consider as a sustainable alternative concrete mix.

Hydration products and microstructures:

In terms of the production of the hydration products the TG analysis show that at the age of 7 and 365 days, the paste made of P15S70R15 combination achieved 75% and 73% respectively of the same paste made of 70% GGBS (Table 6.2, Chapter 6 and Figure 8.1). There was very little difference in the hydration production could be observed between the three ages (1, 7 and 365 days) for this particular cement combination. This suggests that the P15S70R15 paste reached almost to the ceiling of the hydration potential at the early ages.

However, the SEM images at different ages suggested that the potential for further growth of hydration products remained open as at the age of 7 days, as shown in Table 6.3, large capillary pore with plate like crystals of monosulphate and growth of CSH gel are visible. The presence of solid microstructure of hydration products with different morphology in Figure 6.16a, 6.16b and 6.16c demonstrate the triple effects of hydration of three types of cementitious materials in a single microstructure.

Though at the age of 56 days, the images (Figure 6.23, Chapter 6) show very solid microstructure and fail to detect any immature hydration, at the age of 365 days signs of unhydrated microstructure reappeared showing that due to the lack of water, the paste did not get opportunity to complete its hydration process. Therefore, the findings by TG of having the hydration products of 73% at the age of 365 days of the equivalent paste made with P30S70 could not show the full potential of the hydration production of P15S70R15 paste.

However, the available $Ca(OH)_2$ of P15S70R15 paste for further pozzolanic reaction to create more hydrates are 0.13% and 0.26% of the initial mass of the TG sample at the age of 7 day and 365 days respectively (Figure 6.5, Chapter 6). This is much lower than other pozzolanic cementitious combinations such as P90M10 and P80R20 pastes. Therefore, the opportunity to gain more hydration products by further pozzolanic reaction is small.

Durability and permeation properties:

The chloride ion permeation values of concrete containing different proportion of pozzolanic materials posted very resilient results with below 300 coulombs for fly ash, microsilica and rice husk ash concretes. The chloride ion permeation resistance level of the triple blend concrete (P15S70R15) also remained at very low level as per ASTM C1202.

The water absorption properties of the concrete made with different pozzolanic materials posted acceptable values between 0.5% to 1.4% (Figure 5.14, Chapter 5). However, the water absorption of the triple blend P15S70R15 concrete was below 1.0%, which is considered to be exceptionally good. The water permeation results of the concrete with pozzolanic materials were also exceptionally good with maximum water penetration of 5mm was observed for 0.40 w/c ratio of P15S70R15 concrete (Figure 5.31, Chapter 5). Most of the other concretes did not have any penetration of water at all.

Figure 8.3 shows a comparative study of the performance of RCPT and water absorption of concrete made with fly ash, microsilica and rice husk ash in double and triple blend compared to concrete made with P30S70 cement combination. There are improved RCPT values, except the triple blend, though the total coulomb value for 2P15S70R15 is well below 1000 coulomb.

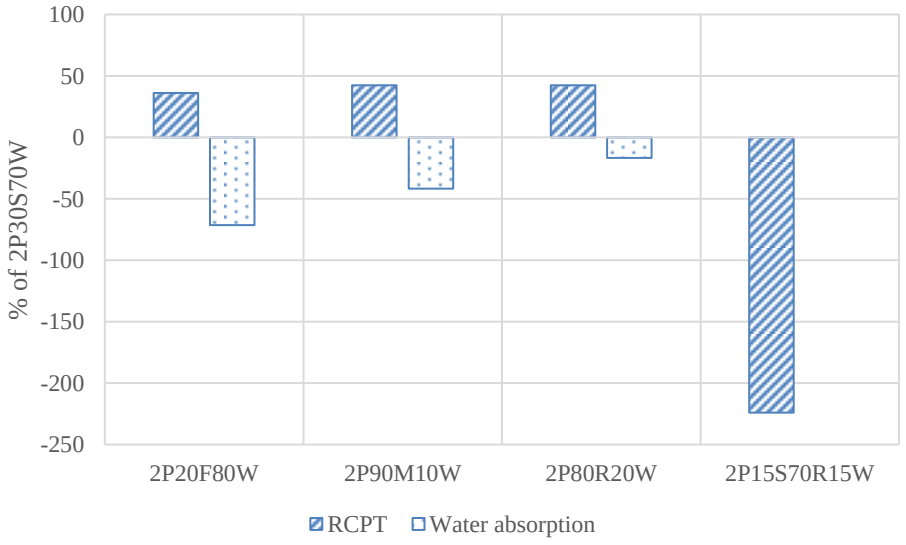

Figure 8.3: Comparative performance of RCPT and water absorption of concretes made with different pozzolanic cementitious materials compared to P30S70

However, P30S70 concrete has better water absorption values than concrete made with other pozzolanic materials. P30S70 and P15S70R15 have same water absorption values. The water permeation values of all double blend concretes including P30S70 are zero while 2P15S70R15 posted 3 mm penetration (not shown in Figure 8.3).

These excellent permeation properties of concrete with pozzolanic materials also made them totally unaffected by the sulfate exposure. The sulfate resistance test applied to the concrete specimen made of P20F80, P90M10 and P80R20 as seen in Figure 5.45 of Chapter 5, did not show any sign of sulfate attack. Though the triple blend concrete (P15S70R15) was not tested for sulfate resistance, the very high water permeation resistance properties would make it also highly resistance to sulfate attack.

The chloride diffusion test also revealed very high level of resistance to the diffusion of chloride ion through the microstructure of concrete made with different proportion of pozzolanic materials compared to control P30S70 concrete as shown in Figure 5.41 of chapter 5. This validates the excellent results on the chloride ion penetration resistance as per ASTM C1202-97.

8.2.2 Sand type series

It has been seen that the excess finer particles of the unwashed sand has a positive effect on the compressive strength and durability and permeation properties of concrete made with different combinations of cementitious materials. It also enhanced the early strength gain of concrete to reach the maximum strength compared to concrete without these excess finer particles.

8.2.2.1 Compressive strength

It can be suggested from Figure 4.13 from Chapter 4 that the effect of unwashed sand to improve the compressive strength is most beneficial to the microstructures which is porous such as concrete with 80% fly ash content (P20F80). However, 8% and 12% improvement of the compressive strength of concrete containing 70% GGBS (P30S70) with 0.25 and 0.32 w/c ratio respectively indicates that the possible particle packing of the volume fraction of the finer particles was reaching towards its ultimate packing density. Improvement of compressive strength due to the effect of additional finer particles of

unwashed sand are observed for all concrete at different rate irrespective of its cementitious content, age or w/c ratio.

The improvement of early strength gain of concrete influenced by the finer particles is an additional benefit of using unwashed sand in the concrete. It has been illustrated by Figure 4.15 of Chapter 4 that in general the compressive strength of concretes containing unwashed sand matured earlier than the same concrete with washed sand. For example for P30S70 with 0.25 w/c ratio, the compressive strength at 28 days achieved 97% of its 56 days strength compared to 92% for the same concrete made with washed sand. Similar improvement was generally maintained for other type of cementitious combination as well.

8.2.2.2 Hydration products and microstructures

The improvement in strength can be explained from the MIP tests conducted on P30S70, P20F80 and P15S70R15 mortars where there was a clear reduction in cumulative pore volume of paste ranging from 30 to 330,000 nm diameter pore size in the P15S70R15 paste due to the finer particles in the unwashed sand (Figure 6.35, Chapter 6). The reduction in fly ash paste ranged from 10 to 1,000 nm pore size diameter (Figure 6.36, Chapter 6). The maximum diameter of the excess finer particles present in the unwashed sand was 75,000 nm. The effect of void filling by theses fines is naturally more pronounced in fly ash paste due to the development of porous microstructure as discussed earlier sections.

With P15S70R15, though this effect is noticeable, but not as pronounced as the fly ash paste, due to its better development of microstructure. MIP test could not detect any influence of the additional finer particles on the microstructure of P30S70 paste, which has had a robust microstructure as seen by SEM analysis. The relative position of the porosity of these three pastes can be seen from Figure 6.37 where the GGBS paste is having the least cumulative pore volume, followed by the triple blend and fly ash pastes.

It is to note that no further reduction of pore size was taken place below 10nm pore size diameter by the additional filler. Therefore, it can be hypothesized that reduction of pore volume above 10nm and enhancement of the compressive strength of concrete are associated with the void filling effect of the excess finer particles contributed by the unwashed sand in the concrete.

8.2.2.3 Durability and permeation properties

The chloride ion permeation resistance of concrete made with unwashed sand with different combination of cementitious materials remained 'very low' with maximum 701 coulomb for P0S100 concrete at 0.40 w/c ratio as shown in Figure 5.3 of Chapter 5. However, there is no effect of the excess finer particles on the chloride ion permeation resistance properties of concrete could be found proving that the additional finer particles did not have any direct impact on the electro-chemical properties of the concrete as the rapid chloride permeability test as per ASTM C1202 is an indirect test method to measure the chloride ion penetrability by measuring the electrochemical properties of concrete.

However, the water permeation properties of concrete were enhanced significantly by the additional finer particles contributed by the unwashed sand of concrete. Figure 5.16 of Chapter 5 suggests that most of the concrete with different cement combinations and made with unwashed sand had lower water absorption values than the same concretes made with washed sand. This enhanced water absorption properties could be as much as 56% for concrete with P30S70 at 0.40 w/c ratio compared to the same concrete with washed sand (Figure 5.17, Chapter 5). Concrete with microsilica, rice husk ash and fly ash had also enhanced properties of water absorption due to the effect of the unwashed sand.

The water permeation of concrete made with unwashed sand and different combinations of cementitious materials also demonstrated very robust water penetration resistance. The performance of water permeation of concretes with or without the additional finer particles are very similar suggesting that the very dense microstructure of concrete had little or no room for further improvement (Figure 5.32, Chapter 5).

The sulfate resistance test conducted on concrete specimen made of different proportion of GGBS, fly ash, microsilica and rice husk ash with washed and unwashed sand produced the same results of no signs of deterioration of concrete due to the sulfate attack (Figure 5.45, Chapter 5). Therefore, the effect of the additional finer particles on the sulfate resistance properties of concrete could not be verified.

There is a direct effect of the unwashed sand on the chloride diffusion coefficient of concrete could be observed where an overall reduction of 20% to 23% was observed compared with concrete made with washed sand. This reduction can be credited to the improved microstructure of the cement paste due to the additional finer particles below 75μm level.

8.2.3 RCA series

Concrete with different proportion of RCA with high volume pozzolanic materials such as P15S70R15 can produce concrete with acceptable range of compressive strength and durability properties compared to concrete without RCA. The effect of the finer particles of unwashed sand on RCA concrete with P0S100 cementitious combination showed good impact on the development of compressive strength. These have raised interesting prospects of creating new concretes not only with reduced Portland cement, but also with reduced natural aggregate and without wasting precious water to wash sand.

8.2.3.1 Compressive strength

It can be seen from chapter 4 that P15S70R15 concretes at the age of 28 days with 20% RCA content at 0.25 and 0.32 w/c ratio achieved 97% and 101% of the compressive strength of the equivalent concretes without any RCA (Figure 4.20, Chapter 4). At 50% RCA this achievement reduced to 96% and remained almost same for 100% RCA concrete. At 0.40 w/c ratio the strength gain was even better. The rate of the maturity of compressive strength of RCA concrete is very similar to concrete without RCA (Figure 4.21, Chapter 4) showing similar hardening characteristics of concrete with or without RCA.

RCA concrete with 100% GGBS with washed sand produced relatively lower compressive strength at early and later ages compared to the concrete without any RCA (Figure 4.17, Chapter 4). The reasons to this lower strength development could be attributed to the delayed hardening of concrete at its plastic stage.

However, RCA concrete with unwashed sand showed tremendous improvement in the compressive strength partially due to normal hardening of concrete and due to the effect of the excess finer particles of the unwashed sand (Figure 4.18, Chapter 4).

8.2.3.2 Durability and permeation properties

The durability properties of RCA concrete with P15S70R15 complied with the satisfactory level similar to the concrete without any RCA. The chloride ion permeation resistance of concretes with RCA proportion of 20% and 50% are within the 'low' range of ASTM C1202-97 (below 2000 coulombs). In fact the RCPT values of these two sets of concretes ranged from 500 to 1500 coulombs depending on their different w/c ratios. Only concretes with 100% RCA had higher values ranging between 1900 – 2150 coulombs (Figure 5.8, Chapter 5).

Interestingly, RCA concretes with P0S100 had better chloride ion permeation resistance properties than the same concretes with P15S70R15 cementitious materials. Especially RCA concretes with P0S100 and with unwashed sand had very low level of chloride ion permeation resistance of below 1000 coulombs which is very similar to the concrete without any RCA (Figure 5.6, Chapter 5). The chloride permeation resistance properties of RCA concrete with P0S100 and with washed sand also had relatively good values with 1000 – 2000 coulombs range (Figure 5.5, Chapter 5). The effect of the unwashed sand perhaps reflected here by achieving higher chloride ion permeation resistance of concrete with unwashed sand.

The water absorption properties of RCA concrete with P15S70R15 were also outstanding. Figure 5.23 from Chapter 5 shows that all concrete with different proportion of RCA contents had equal or less than 1.0% water absorption, which was very close to the water absorption values of concretes without any RCA and well within the acceptable range. However, RCA concrete with P0S100, especially concrete with washed sand showed higher water absorption values ranged from 0.5% to 2.2% (Figure 5.18, Chapter 5), this reveals that the microstructure of concrete with 100% GGBS is relatively porous, perhaps due to the reason of improper and erratic hardening of P0S100 concrete made with washed sand.

Similar to concrete without RCA, the additional finer particles of unwashed sand made positive effect on the water absorption properties of concrete with RCA. The maximum positive improvement of 73% was posted by the 50% RCA concrete with P0S100 and 0.25 w/c ratio (Figure 5.21, Chapter 5).

The water permeation results of RCA concrete with P15S70R15 is considered to be good, especially for 20% and 50% RCA concrete where the maximum water penetration values have been found to be only 5mm (Figure 5.35, Chapter 5). The maximum water penetration for 100% RCA concrete is 12mm.

However, the RCA concrete with P0S100 and washed sand demonstrated a very high water penetration values. The water penetration values of 50% RCA ranged from 17mm to 25mm (Figure 5.33, Chapter 5). The water penetration tests with concrete with 80% and 100% RCA concrete could not complete due to the leakage of water from the opposite face of the concrete cube due to the penetration of water throughout the full depth of the concrete cubes. This was due to the development of porous microstructure of concrete due to erratic hardening as mentioned earlier.

Interestingly, the permeation properties of RCA concrete with P0S100 was dramatically improved by the addition of the unwashed sand. The excess finer particles of unwashed sand reduced the water penetration values of 80% and 100% RCA concrete to below 10mm, though for 50% RCA it went up to 20mm (Figure 5.34, Chapter 5).

The sulfate resistance test conducted on the RCA concrete with P0S100 made with washed and unwashed sand show that after 12 months of prolong ponding in $NaSO_4$ solution, there is no visual effect of sulfate attack on concrete specimen (Figure 5.46, Chapter 5).

Figure 5.43 of Chapter 5 has shown an interesting insight of the effect of chloride diffusion in concretes containing RCA. In general the rate of chloride diffusion followed a linear trend with the proportion of RCA with highest diffusion coefficient with 100% RCA. However, the RCA concrete containing P0S100 cementitious materials had very steep slope compared with RCA concrete containing P15S70R15 cementitious combinations, demonstrating the effect of good microstructure of paste on the chloride diffusion. The positive effect of the finer particles of the unwashed sand on the chloride diffusion of RCA concrete was also demonstrated.

8.2.4 Air entrained concrete series

8.2.4.1 Compressive strength

P90M10 concretes with 10% air content, the minimum reduction of compressive strength was 19% of the equivalent compressive strength of concrete with 2% air at 0.25 w/c ratio and at the age of 28 days (Figure 4.26, Chapter 4). This rate of reduction of compressive strength has gone up to a massive 58% for the same concrete with 12% air.

However, concretes at the age of 28 days with 5% air have a reduction of 13% and 11% at 0.25 and 0.32 w/c ratio respectively. This level of reduction perhaps could be minimized by using unwashed sand instead of washed sand to exploit the effect of the excess finer particles. It has been seen in Chapter 4, Figure 4.13 that an improvement of 14% in compressive strength could be achieved by using unwashed sand with P90M10 at 0.25w/c ratio at the age of 28 days.

8.2.4.2 Durability and permeation properties

Higher air content made the concrete highly durable in terms of the chloride ion permeation resistance and water permeation properties. Figure 5.12, of Chapter 5 shows that concretes containing 5% air are having coulomb values at a negligible level (below 100 coulomb). The maximum chloride ion permeation resistance values of less than 300 coulombs was registered with concrete with 12% air content which is considered to be very low.

Though at 10% and 12% air, the concretes are highly porous, however, the low water absorption and water permeation results of these concretes prove that the pores were not interconnected. Figure 5.28 of Chapter 5 shows that concrete with all 5%, 10% and 12% air are having very good water absorption values similar to the concrete with 2% air content.

The water permeation result of concrete with 5% air (as per Figure 5.38 of Chapter 5) is equivalent to the concrete with 2% air with no sign of water penetration. At 10% and 12% the water penetration values are between 8mm to 12mm which is similar to the acceptable range of 10mm.

Chloride diffusion of concrete has been reduced at 5% air compared to the control of 2%, however it has been increased at higher rate at 10% and 12% air suggesting poor development of microstructure at very higher air (Figure 5.44, Chapter 5). There was no sulfate resistance tests conducted on air entrained concrete.

8.2.5 Summary

It can be summarized from the above analysis that most of the concrete tested under these programme achieved adequate compressive strength, durability and permeation properties required to withstand the microclimate of the Arabian Peninsula. However, comparing with the control concrete made with P30S70 cementitious combination, the performance of the concretes made with triple blend of P15S70R15 appeared to be at acceptable level. The performance of this new concrete can be enhanced further by adopting other sustainable parameters such as use of unwashed sand, replacing at least 20% of the coarse aggregate by RCA, entraining additional 5% air and considering higher curing temperature. Concrete with P15S85 cementitious combination could be another viable alternative to P30S70 as well.

8.3 Regional implication

The regional implications of new concretes made with P15S70R15 and P15S85 cementitious combinations with different scenarios of washed or unwashed sand, RCA or additional entrained air have been discussed based on the following three categories:

1. Acceptance by the construction industry
2. Cost competitiveness
3. Engineering, durability and environmental properties

8.3.1 Acceptance by the industry

Acceptance of any new products into an existing market always faces barriers due to numerous factors. The same can be anticipated for these new sets of concrete which would need novel materials and processes differing from conventional practice to produce concrete in the Arabian Peninsula. Therefore, the following identified factors need to be addressed and discussed to figure out whether these new sets of concrete could be successfully implemented in the industry:

i. Availability of raw materials
ii. Issues related to production and placement
iii. Specification works
iv. Conforming to local environmental standards

8.3.1.1 Availability of raw materials

Most of the concrete constituents used in this study are readily available from local origin. However, as mentioned earlier, rice husk ash, as a novel material is not available in the Arabian Peninsula. Nevertheless, India would be a good source of rice husk ash as India has been a source of fly ash supply to the Middle East. Beside India and countries within Indian sub-continent, other major rice producing region close to the Arabian Peninsula would be South East Asian countries such as Thailand, Vietnam and Indonesia. Therefore, should there be a demand, the availability of rice husk ash would not be a major concern.

Production of recycled concrete aggregates (RCA) suitable for using in concrete production is still at its infancy in the Middle East. As discussed in Chapter 2, most of the construction and demolition waste are not processed for concrete use. However, a 20% replacement of coarse aggregate would be more practical approach given the current short supply of RCA.

GGBS, though an imported materials as granulated slag mainly from Japan but ground in the region, is readily available and widely used mainly due to the durability requirements. Therefore, availability of GGBS is not a major issue. One of the major advantage of using GGBS is that it is supplied by large bulk tanker like the cement, therefore it can be easily pumped into the silos of concrete plants unlike fly ash or microsilica which are supplied by bulk bags which need more manual handling process. Therefore, from the availability of raw materials point of view producing concrete with P15S85 cementitious combination is more convenient than concrete containing P15S70R15 cementitious materials.

8.3.1.2 Production and placement

There are few practical implications related to the production and handling of concrete made with multiple cementitious materials and recycled concrete aggregate which need to be acknowledged so that appropriate actions can be taken. These issues are before, during and after production of concrete and related to i) storage and handling of raw materials and ii) issues related to the plastic properties of concrete.

Storage and handling of raw materials:

Storage and handling of additional raw materials to produce concretes such as P15S70R15 with RCA required additional resources because this concrete needs rice husk ash which is a new cementitious materials and RCA, a new type of aggregate. These requirements may put additional strain on the available resource, manpower and equipment on the existing concrete production system.

Additional cement silos:

Typically concrete batching plants in the Arabian Peninsula are equipped with additional cement silos to handle maximum two additional cementitious materials beside Portland cement based materials namely Portland cement, sulfate resisting cement (SRC) and moderate sulfate resisting cement (MSRC).

The additional silos are generally dedicated for GGBS or fly ash and microsilica. Therefore introduction of rice husk ash would need a separate storage silo. Similar to fly ash and microsilica, rice husk ash would also need a separate shaded and dry stockyard to store the bulk bags prior to discharging them into the silos.

Additional stockyard for RCA:

In a typical concrete batching plants in the UAE and other part of the region aggregate stockpiles would need at least 4 separate compartments to store different type and size of aggregates. The typical types of aggregates are 20mm and 10mm coarse aggregate either crushed limestone or gabbro or both, 0-5mm crushed limestone fine aggregate and dune sand.

These aggregate shades need to be properly shaded against sun and separated by concrete walls to eliminate any cross-contaminations among different type of aggregates. Therefore, introduction of RCA of 20mm and 10mm size would need two additional storage spaces.

Modification of aggregate feeding system:

The concrete batching plants may also need to be modified to cater for two new types of aggregates as the number of prefabricated aggregate hoppers to discharge the aggregates onto the weighing belt would not be sufficient enough to handle six different types of aggregates (RCA, normal coarse aggregates and fine aggregates, two hoppers for two different size of each type of aggregates). This would require additional investment in equipment, manpower and other resources. The additional workload on the manual handling of RCA using 'wheel loader' to transfer aggregates from the storage shade to the weighing hopper would also need to be acknowledged.

Pre-wetting of RCA:

Another practical issue with RCA is its high porosity, requires it to pre-wet by water prior to mixing to prepare it into the SSD condition to avoid variability in concrete properties both in plastic and hardened state. In Arabian Peninsula the pre-wetting of RCA may not be a practical approach given the scarcity of the water.

However, the positive aspect of the pre-wetting of aggregate perhaps by a sprinkler system would enhance the cooling of aggregate to reduce the concrete temperature which is a major factor of concrete production in the Arabian Peninsula due to very high ambient temperature. However, appropriate system need to be designed to drain off and recycle the water to minimize any additional environmental impact due to this process.

Plastic properties:

As discussed in Chapter 4, the rheology of concrete with high volume GGBS and rice husk ash is appeared to be 'sticky' with reduced fluidity especially with low w/c ratio due to very high water demand of rice husk ash and at a lesser extent of GGBS particles. Relatively higher dosage of superplasticizer was required to meet this requirement, however, that made concrete 'stickier' and reduced paste volume by making into a 'harsher' mix.

These two conditions would make concrete difficult to produce and pump, resulting into higher energy consumptions and frequent breakdown of equipment, and increasing cost of production. Problems associated with the similar plastic properties of concrete can be solved by adjusting the aggregate proportions by increasing the paste fraction of the mix.

Entrainment of air or addition of fly ash up to a certain proportion can increase the fluidity of the concrete. Appropriate trials both at laboratory and production scale would be required prior to finalizing the right proportion of the concrete mix.

8.3.1.3 Specification works

Rice husk ash:

Beside the issues related to the production and handling of novel concretes, one of the major obstacle is to get the confidence of the specifiers and the owners to use novel materials like rice husk ash as there is no established performance track records and internationally acceptable standards of production and quality control of this material. Therefore, large scale trials involving local concrete industry and authorities may require to validate the performance of these new constituent materials of concrete.

RCA:

Use of RCA to replace natural coarse aggregate have similar issues as most of the project specifications in the Arabian Peninsula do not have any options to use RCA in structural grade concrete. The project specifications of ADCO, ADNOC and GASCO, the three major organizations of Petrochemical industry in Abu Dhabi have been discussed in Chapter 2. There is no scope of using RCA can be found in these project specifications. However, there is a detailed guidance on the use of RCA on structural grade concrete is given in BSEN 8500-2 which can be followed as BSEN 8500 is widely accepted in Arabian Peninsula.

Unwashed sand with higher fines:

Use of unwashed sand would also need to be accepted into the project specifications in Arabian Peninsula. As discussed in Chapter 2, all major project specification in the petrochemical industry in Abu Dhabi specified maximum fines content for fine aggregate (from crushed limestone) as 5% by mass. However, in this study, 10% maximum finer particles passing 75μm sieve was considered in concrete made with unwashed sand. Therefore, substantial amount of specification work backed by large scale plant trials and test reports would require making changes in the project specifications.

8.3.1.4 Local environmental regulations on construction process

The possible concerns by the local concrete and construction industry to implement environmentally sustainable concrete could be effectively addressed by the local environmental regulations such as Pearl Building Rating Systems (PBRS) of Estidama in Abu Dhabi (Estidama, 2010). Estidama, an environmental agency mandated to implement a sustainable living in Abu Dhabi award numbers of 'Pearls' to the new construction of buildings, villa and community projects in Abu Dhabi. It is mandatory for all new building projects in Abu Dhabi to achieve at least 1 Pearl which is equivalent to achieving all mandatory credits as per Pearl rating system and 2 Pearls for all government funded projects.

As mentioned in Table 7.3 of Chapter 7 the stewarding materials category of PBRS reward credits for the use of supplementary cementitious materials to reduce the greenhouse gas, use of recycled aggregate and use of regional materials beside other measures. This directly encourages the industry to use the SCM and RCA in concretes. The requirement of high solar reflective index to reduce the heat island effect would also encourage to use GGBS concrete which eventually produce lighter coloured concrete compared to grey coloured concrete with 100% Portland cement.

However, in order to encourage the industry to use other novel materials proposed in this study such as unwashed sand, authorities like Estidama need to incorporate the environmental credit factors and corresponding weightings as used in Table 7.3 and Table 7.4 in Chapter 7 into their environmental rating systems.

Other regional and international green building rating systems like 'Global Sustainability Assessment System (GSAS) of GORD, Qatar (Al Horr, Y., 2013) and Leadership in Energy and Environmental Design - LEED, (USGBC, 2009) which are providing guidance of the environmentally sustainable construction system to the region have similar emphasis on the use of 'greener' materials in concrete to reduce the environmental impact.

8.3.2 Cost competitiveness

8.3.2.1 Basis of cost analysis

The financial competitiveness is imperative for any new environmentally sustainable concrete to be successfully accepted by the industry. Therefore, a cost analysis of concrete containing P15S70R15 and P15S85 cementitious combination with different scenarios together with the control P30S70 need to be performed to establish their competitiveness. As described earlier, the different scenarios would be concrete made with i) washed sand ii) unwashed sand iii) 20% RCA using unwashed sand and iv) 5% entrained air with 20% RCA and unwashed sand. There are three ways this cost analysis can be performed i) cost per m^3 of concrete ii) cost per unit area of a structural element and iii) cost of concrete at equal strength.

8.3.2.2 Cost per m^3 of concrete

The costs of individual constituents of concrete delivered to Abu Dhabi are given in Table 8.1. These data were obtained by the author from his personal sources and are used to calculate the total cost of concrete per m^3 (excluding production and other related costs).

Table 8.1: Cost of constituent materials delivered to Abu Dhabi

	Constituents	**Source**	**AED/Kg**
1	Portland cement	UAE	0.20
2	GGBS	UAE	0.20
3	Fly ash	India	0.35
4	Microsilica	China	1.00
5	Rice husk ash	India	0.35
6	20mm crushed limestone aggregate	UAE	0.04
7	10mm crushed limestone aggregate	UAE	0.04
8	20mm RCA	UAE	0.04
9	10mm RCA	UAE	0.04
10	0-5mm sand washed or unwashed	UAE	0.04
11	Dune Sand	UAE	0.015
12	Water	UAE	0.02
13	Superplasticizer	UAE	8.00
14	Retarding admixture	UAE	1.50
15	Air entraining admixture	UAE	1.50

Among the constituents only rice husk ash is not commercially available in the Middle East. Therefore, the cost of rice husk ash has been assumed to be same as fly ash as the source of origin of rice husk ash would be the same source of origin of fly ash which is mainly India for the concrete industry of the Middle East. The cost of concrete and the raw materials are expressed in dirham (AED), the local currency of the UAE.

Comparison of costs per m^3 between concretes made of P30S70, P15S85 and P15S70R15 cementitious materials at four different scenarios are presented in Figure 8.4 together with the cost increment of each type of concrete relative to concrete using P30S70 cementitious materials using washed sand. As shown in Figure 8.4, there is a cost increment of 28.5% by P15S70R15 concrete compared with P30S70 concrete using washed sand. Relatively higher cost of rice husk ash and higher dosage requirement of superplasticizer have increased the cost of P15S70R15 concrete.

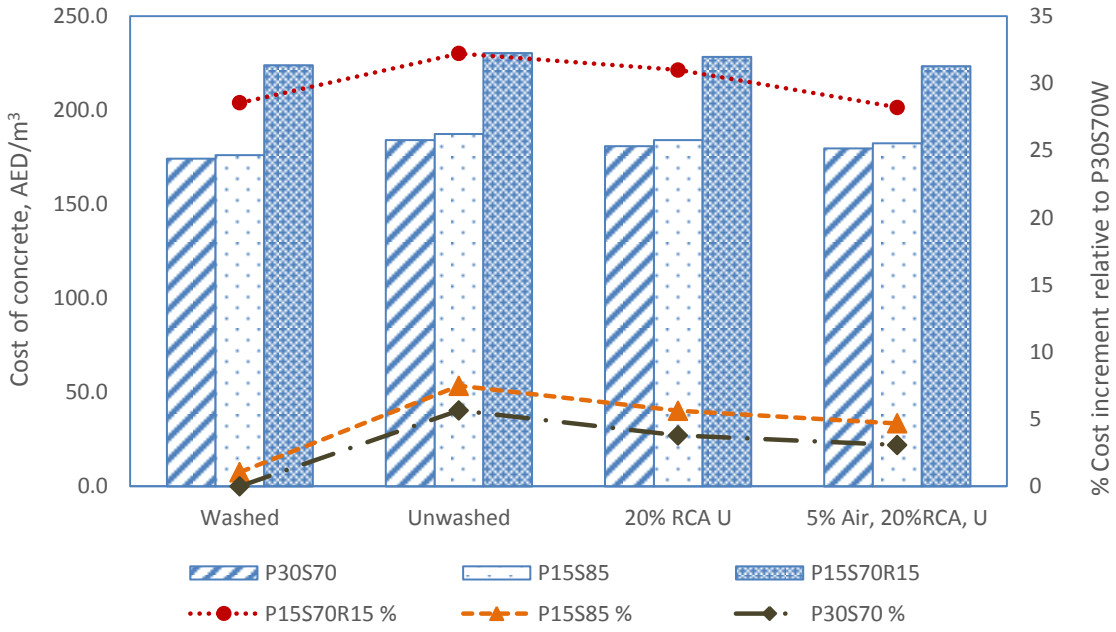

Figure 8.4: Cost comparison per m^3 between concretes made of P30S70, P15S85 and P15S70R15 cementitious combinations

Cost of P15S70R15 concrete with unwashed sand has been increased further to 32.2% due to higher dosage of superplasticizer to satisfy the higher water demand due to the additional finer particles contributed by the unwashed sand. However, this cost has been reduced when 20% of the coarse aggregate is replaced by RCA. The reason of this cost reduction is the requirement of relatively lower mass of total coarse aggregate due to lower combined particle density of RCA and natural limestone aggregate compared to the particle density of natural limestone aggregates alone. The cost has been reduced further with 5% air content due to the reduced requirement of superplasticizer. The additional cost of AEA was lower than the savings due to reduced use of the superplasticizer.

The cost of concretes made with P15S85 and P30S70 at these four different scenarios followed the same trend as P15S70R15, however at much lower level. There is a minor increase in cost of P15S85 concretes compared to P30S70, mainly due to higher requirements of superplasticizer due to higher surface area contributed by the additional GGBS particles.

It is to note from Figure 8.4 that the cost of concrete is increased with increased attributes of environmental measures. The cost difference between P15S70R15 and P30S70 concretes made with 5% entrained air, 20% RCA and unwashed sand is 24.4% of the cost of P30S70 which is around AED43.8 / m^3.

Though this figure could be significant in real business terms, but should there be a requirements in project specifications where achieving sustainability factors as described in previous chapter was mandatory, additional cost of AED43.8/m^3 would not be significantly high. Infrastructure projects such as petrochemicals, railways and highways projects where total cost of concrete compared to the project cost is significantly smaller and the stake on the national interest on the impact on the environment and ecology are much higher, this additional cost would be justifiable.

8.3.2.3 Cost per unit structural element

In Arabian Peninsula concretes are designed mainly to satisfy two main requirements i) characteristics design strength (compressive strength, f_c') and ii) the durability parameters. The requirement of durability often dictates the quantity and type of cementitious materials and the w/c ratio instead of the requirement of compressive strength.

Therefore, often concretes are produced with much higher compressive strength than required due to stringent requirements of durability and permeation properties. The construction industry often do not utilize this additional strength by redesigning the structural element into a more slender size to reduce cost and saving resources due to lack of proper coordination and value engineering works prior to the commencement of projects. Any reduction in element size would also reduce the eCO_2 of unit structural elements.

However, instead of increased strength, if new concretes meeting durability and environmental sustainability criteria produce lower compressive strength, the design engineers then need to consider this restriction into the structural design calculation. To accommodate fixed design loads, concrete sections of elements need to be larger with concrete with lower compressive strength. However, this may lead to higher eCO_2 for a unit element due to higher volume requirement. The section size of foundation elements may also need to be larger to cater for additional dead loads.

However, studies in the Concrete Centre showed that it might not necessarily true. Table 8.2 (reproduced from the publication of the Concrete Centre – Specifying sustainable concrete) illustrates the variations in eCO_2 of concrete of building elements between three different options comparing with a control option. The design calculations and corresponding eCO_2 values are taken from the publications of Concrete Centre - Concrete structures 09 and Specifying Sustainable Concrete (Concrete Centre, 2009 and 2011).

It can be seen from Table 8.2 that perhaps a slender design of structural elements using higher strength concrete can reduce the volume of concrete, but it does not always translate into lower eCO_2 for the element. The savings in cost reduction due to reduced requirement of resources is also not very significant compared to the total cost of the project though the net increase of lettable area may have a long term effect on the economic benefit to the building owners.

Table 8.2: Comparison of eCO_2 of different construction options with varied element size (after Concrete Centre, 2009 and 2011)

	Control	**Option 1**	**Option 2**	**Option 3**
Concrete class, slab	C32/40	C32/40	C50/60	C50/60
Concrete class, columns	C32/40	C50/60	C50/60	C60/75
Concrete volume, slab m^3	2,110	2,110	1841	1841
Concrete volume, columns m^3	1,112	956	956	885
Change in net lettable area	0.0%	1.2%	1.2%	1.8%
Cost reduction, % relative to the control	0.0%	0.03%	0.20%	0.14%
eCO_2, tonne	1,369	1,346	1,492	1,477
Variation from control	100%	98%	109%	108%

The same exercise can be applied using the characteristics cube strength of P3070, P15S70R15 and P15S85 concretes as given in Table 8.3 to figure out whether P15S70R15 or P15S85 can effectively replace P30S70 without increasing total eCO_2 of individual structural elements with a cost competitive manner. Decisions on the suitable concrete type should be made based on the outcome of the structural analysis by incorporating eCO_2 values as one of the design parameters.

Table 8.3: Equivalent characteristic cube strength of concretes

Concrete type	**Compressive strength, N/mm^2**	**Equivalent characteristics cube strength, N/mm^2**
P30S70	78.0	70
P15S70R15	72.2	65
P15S85	59.5	50

The equivalent characteristics cube strengths of concretes made of P30S70, P15S70R15 and P15S85 cementitious combinations are given in Table 8.3 where a target margin of 8 N/mm^2 has been assumed. The w/c ratio and the age of concrete have been taken as 0.32 and 28 days respectively. Washed sand and 100% natural limestone aggregate are considered without any additional air entrainment. However, as the structural analysis is beyond the scope of this study, no further comments can be made on the outcome of the above proposition, except to highlight that it is necessary for structural engineers to incorporate eCO_2 as part of the design parameters to design for structures using low carbon concrete.

8.3.2.4 Cost at equal strength

Concrete made with P15S70R15 and P15S85 can achieve same compressive strength of P30S70 either by reducing corresponding w/c ratio or increasing total cementitious content or both. As in this study a fixed total cement content of 400 kg was used, therefore any analysis of data using higher cement content is beyond the scope of the work. However, it can be demonstrated from Figure 8.5 that by reducing w/c ratio of P15S70R15 and P15S85, the compressive strength of these concretes can equal to the compressive strength of concrete made with P30S70. A compressive strength of 70 N/mm^2 is chosen to demonstrate the following exercise.

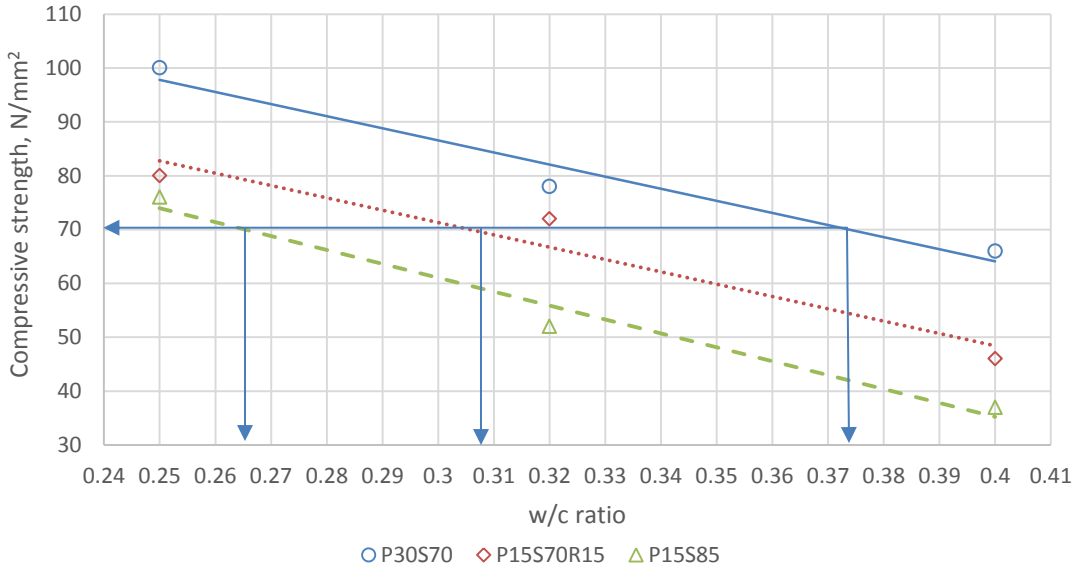

Figure 8.5: Equivalent w/c ratio for fixed compressive strength of different cement combination at 28 days age

Figure 8.5 shows that concrete made with P15S70R15 and P15S85 can achieve the same compressive strength 70 N/mm^2 of P30S70 by a reduced w/c ratio of approximately 0.308 and 0.266 respectively. The w/c ratio of P30S70 would be approximately 0.374. Though the compressive strength could be same by reducing the w/c ratio, however, the impact on cost and eCO_2 and plastic properties should be considered. Durability should not be a concern as reduced w/c ratio had increased the durability and permeation properties of concretes as shown in Chapter 5.

From Figure 8.6, the cost of concrete per m^3 for any given w/c ratio made of the above three cementitious combination can be obtained. Using same w/c ratios which give 70 N/mm^2 compressive strength from Figure 8.5, the cost of concrete made with P30S70, P15S70R15 and P15S85 cementitious combination can be found out.

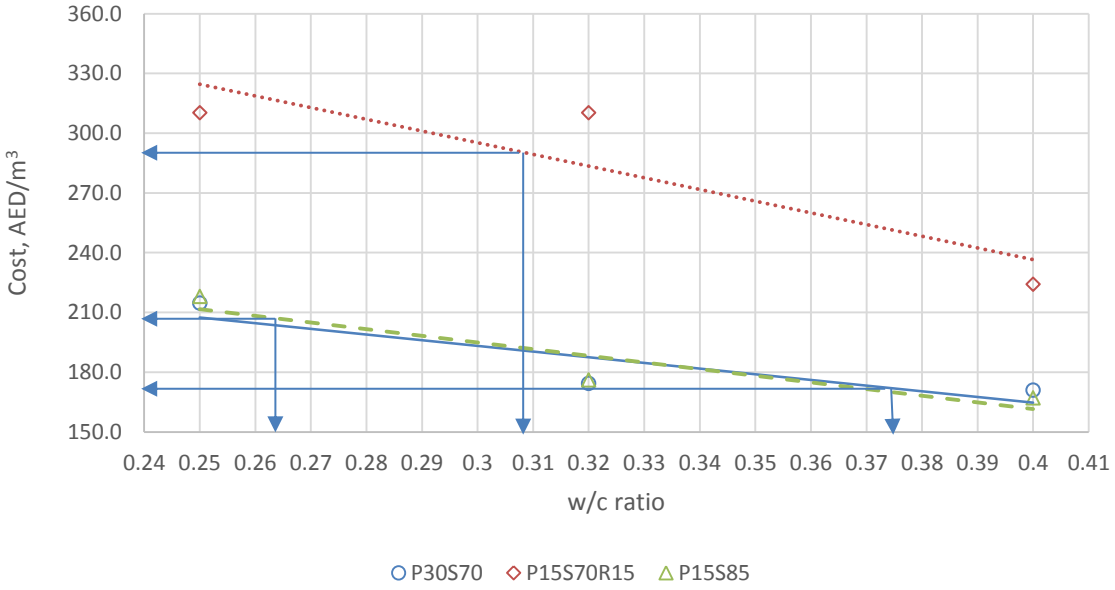

Figure 8.6: Cost of concretes of at equivalent strength of 70 N/mm^2 at 28 days

Similarly, from Figure 8.7, the eCO_2 values of concrete made of P30S70, P15S70R15 and P15S85 cementitious combinations with equal compressive strength of 70 N/mm^2 can be obtained. Combining the outcome of these three figures a comparison of cost and eCO_2 of concrete made of P30S70, P15S70R15 and P15S85 can be given in Table 8.4 where the percentage change of cost and eCO_2 comparing with P30S70 are given in the bracket.

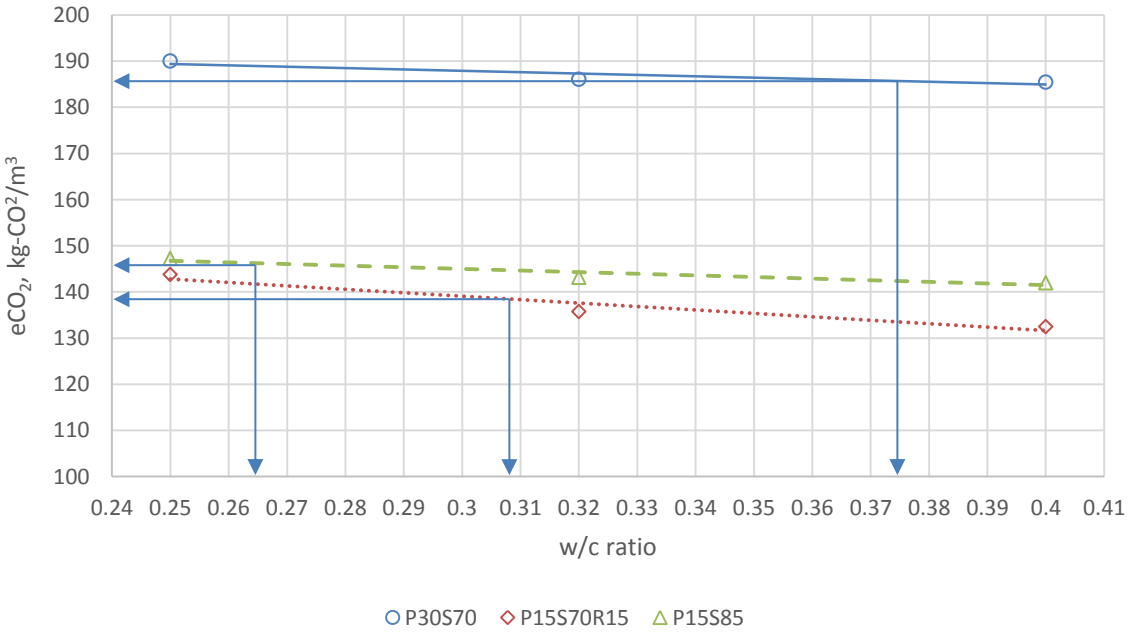

Figure 8.7: Embodied CO_2 of concretes with equivalent compressive strength

It is shown in Table 8.4 that with equivalent compressive strength of 70 N/mm^2 the cost of P15S70R15 per m^3 of concrete can be around 70.6% higher than the equivalent concrete of P30S70. At equal w/c ratio of 0.32 this difference was 28.5% as shown in Figure 8.4. Concrete made with P15S85 is 20.6% more expensive than P30S70 concrete at equivalent strength. However, the eCO_2 of P15S70R15 concrete is 25.3% lower than the P30S70 concrete. The eCO_2 reduction by P15S85 is 21.5% which is quite close to P15S70R15. Comparing with P15S70R15 the performance of P15S85 should be considered as good as its cost increment is not as high as P15S70R15 for equal strength scenario.

Table 8.4: Comparison of cost and eCO_2 of concrete of equivalent compressive strength

Concrete	**Compressive strength, N/mm^2**	**w/c ratio**	**Cost, AED/m^3**	**eCO_2, kg-CO_2/m^3**
P30S70	70	0.374	170	186
P15S70R15	70	0.308	290 (70.6%)	139 (25.3%)
P15S85	70	0.266	205 (20.6%)	146 (21.5%)

At the same cost scenario of P30S70 concrete, i.e. 170 AED/m^3, only P15S85 concrete would be able to produce concrete at a compressive strength of around 42 N/mm^2 (obtained from Figure 8.6 and Figure 8.5), though it is much lower than 70 N/mm^2 achieved by P30S70, however, it is still a reasonable structural grade strength for different structural applications. The eCO_2 value of this concrete would be 21.5% lower than the control P30S70 concrete.

8.3.3 Engineering, durability and environmental properties

8.3.3.1 General discussion

While analysis of cost effectiveness of P15S70R15 and P15S85 concrete are important factors to evaluate their successful acceptance by the industry, it is also imperative to highlight that these concretes using other sustainable practice would enhance their plastic and hardened properties which could outweighed their economic disadvantage, if there is any, compared to P30S70 concretes.

Therefore, in the following sections the engineering and durability properties of concretes which include the compressive strength, durability & permeation properties of P30S70, P15S70R15 and P15S85 concrete with different scenarios of aggregate type/sand type/air content have been analysed. The environmental parameters including eCO_2, S/eC index and environmental sustainability factors (ESF) have been analysed together with the engineering and durability parameters of concretes.

As discussed in Chapter 2, P30S70W concrete made with 70% GGBS and washed sand considered as the control mix of this work, is a widely accepted concrete mix in the Arabian Peninsula due to its acceptable performance of compressive strength and durability and permeation properties. Therefore a comparative analysis of the performance of P15S70R15 and P15S85 with P30S70 would provide the legitimacy of these two new sets of concrete in the construction industry of Arabian Peninsula.

These new concretes would also need to be validated whether they could conform to the stringent requirements of the durability and permeation properties of concrete of the local construction industry. As discussed in the Chapter 2, the requirement of durability and permeation properties of concrete in the Arabian Peninsula is very stringent due to the sever exposure to chloride and sulfate laden environment. Therefore, an equally stringent design target was set up for each durability and permeation properties to measure the performance of each concrete type studied under this work. In the following sections, the durability and permeation properties of each concrete mentioned above have been compared with these target values.

There is no target values are considered for the compressive strengths and the two parameters related to environmental performance i) S/EC index and ii) environmental sustainability factors (ESF). Satisfactory performance compared to P30S70W would be their key performance criteria. However, 250 kg-CO_2/m^3 is considered to be the targeted eCO_2 values for concretes (cradle to gate) following the guideline of UK Environmental Agency for the concrete structures for flood control.

Table 8.5 illustrates the comparison of compressive strength and the environmental performance of the concretes. Table 8.6 tabulated the actual and their corresponding performance related to the control and target values of permeation and durability properties of concretes.

As the plastic and sulfate resistance properties of concretes with these three cementitious combinations are appeared to be within acceptable level, it is not necessary to analyse and compare their performance further. The plastic properties of all these four sets of concretes are also considered to be at the acceptable level. It is also to acknowledge that not all data tabulated in Table 8.5 and Table 8.6 are the results of the direct tests. Some of the data have been predicted from the results of similar type of concrete as explained earlier in Chapter 7 at section 7.3.2.1.

For example there is no work was done using P30S70 cement combinations with RCA and with 5% air. However, as it was seen that there was virtually very little change in compressive strength between concrete (at 0.32 w/c ratio at 28 day using P15S70R15) without any RCA and concrete with 20% RCA (Figure 4.19, Chapter 4), therefore, the compressive strength of concrete with P30S70 and 20% RCA with unwashed sand is considered to be same as the compressive strength of P30S70U.

Similarly there was a 11% reduction in compressive strength due to increased air content of 5% relative to concrete with designed air content of 2% (Chapter 4, Figure 4.26). Therefore, by applying this 11% reduction from the compressive strength of P30S70U, 20%RCA concrete, the compressive strength of P30S70U, 5% air, 20% RCA concrete can be predicted. Similarly other unknown data have been predicted for other concrete types in Table 8.5 and Table 8.6.

For ease of understanding the individual performance relative to the control/target, each performance is expressed in percentage of the control / target data. However, the significance of the numbers of different categories are different. In some categories, such as compressive strength, higher values are better and for rapid chloride permeability test, lower values are better. Therefore in Table 8.5 and Table 8.6, the relative positions of each data have been presented in such that if any specific data is more than 100% of control or target, it means that the performance of that category is positive. All data equal or above 100% are highlighted for easy identification purpose. If the relative performance is less than 100%, it means that the performance of that category is not up to the required level of the control or target values.

8.3.3.2 Compressive strength

Compressive strength is one of the most challenging parameters for these new novel concretes to equal the performance of the control P30S70W due to the reduction of Portland cement content. As shown in Table 8.5 concrete with P15S70R15 cementitious materials and with washed sand achieved 93% of the control.

However it has been predicted that the compressive strength of P15S70R15 would be able to achieve 103% of the control if unwashed sand are used due to the effect of the additional finer particles available in the unwashed sand. With RCA replacing 20% of the coarse aggregate by mass, the same concrete has been predicted to achieve the same 103% of the compressive strength of the control. All concretes considered here are at 0.32 w/c ratio and at 28 days age. No other concrete beside the P15S70R15 and P30S70 with same unwashed sand and coarse aggregate combinations are predicted to match the compressive strength of P30S70W.

8.3.3.3 Environmental performance

As discussed in the Chapter 7, the P15S70R15 concretes have the best environmental performance in terms of eCO_2, S/eC index and other environmental factors. As shown in Table 8.5, the eCO_2 of P15S70R15 is 137% of the control. Concretes made with P15S85 are 130% better than the control. There is no difference found between the P30S70 concretes with different aggregates and air combinations. Comparing with the target eCO_2 values, all concrete including P30S70W have exceeded the required performance of the targeted 250 kg-CO_2/m^3 eCO_2 values. However, the extent of this performance is much higher for P15S70R15 than the control concrete with P30S70 cementitious materials.

Table 8.5: Validation of P15S70R15 and P15S85 concretes (0.32w/c at 28days) – compressive strengths and environmental performances (Highlighted data are equal or above to the control or target values)

		Compressive Strength, N/mm^2		**eCO$_2$, kg-CO$_2$/m^3 Cradle to gate**			**S/eC index**		**Environmental Sustainability Factors**	
		Actual, N/mm^2	**Relative to P30S70W**	**Actual kg-CO$_2$/m^3**	**Relative to P30S70W**	**Relative to target 250 kg-CO$_2$/m^3**	**Actual**	**Relative to P30S70W**	**Actual**	**Relative to P30S70W**
P30S70	Washed sand, control	78	100%	186.1	100%	134%	0.42	100%	15	100%
	Unwashed sand	87	112%	186.3	100%	134%	0.47	112%	27	183%
	20%RCA, U	87	112%	186.3	100%	134%	0.47	111%	28	187%
	5%air, 20%RCA, U	77	99%	186.3	100%	134%	0.42	99%	32	214%
P15S70R15	Washed sand	72	93%	135.7	137%	184%	0.53	126%	19	129%
	Unwashed sand	80	103%	135.7	137%	184%	0.59	141%	31	212%
	20%RCA, U	81	103%	135.4	137%	185%	0.60	143%	32	216%
	5%air, 20%RCA, U	72	93%	135.4	137%	185%	0.53	127%	36	243%
P15S85	Washed sand	60	76%	143.2	130%	175%	0.42	100%	15	103%
	Unwashed sand	66	85%	143.2	130%	175%	0.46	110%	27	186%
	20%RCA, U	66	85%	143.2	130%	175%	0.46	110%	28	190%
	5%air, 20%RCA, U	59	75%	143.2	130%	175%	0.41	98%	32	217%

In terms of the S/eC index, concrete with P15S70R15 and 20% RCA with unwashed sand has the best performance with 143% of P30S70W. It is to note that all concretes except P30S70 and P15S85 with higher air content have exceeded the S/eC index of P30S70W. The 11% reduction assumed for concrete with 5% air entrainment have reduced the S/eC index of P30S70 and P15S85 concrete containing 5% air content. The same P15S85 concrete is the second best in environmental sustainability factor (ESF) category having 217% of the control. The best result of ESF category is from P15S70R15 concrete with 5% air content and 20% RCA with unwashed sand with 243% of P30S70W. Detailed discussions about ESF have been made in Chapter 7.

8.3.3.4 Durability and Permeation properties

The control concrete P30S70W appears to have the best results of rapid chloride permeation resistance as shown in Table 8.6 where none of other concretes have more than 100% performance relative to P30S70W. However most of these results are very low according to ASTM C1202-97 as discussed in Chapter 5 and relative to the target value of 1500 coulombs the results are well within the satisfactory level.

The chloride permeation resistance of concrete with RCA have been found to be higher than 1000 coulomb however it is well within the maximum target of 1500 coulombs and designated as within low category as per ASTM C 1202 as discussed in Chapter 5 and illustrated by Figure 5.9.

Water absorption and water permeation results show a very similar trend of almost matching the performance of P30S70 concretes by P15S70R15 concretes with very low water absorption results and almost zero penetration of water through the concrete cubes subjected under 5 bar water pressures as per BSEN 12390: Part 8 test methods. The water absorption and water permeation results of P15S85 concretes were though higher than the control but well within the accepted range of the target values.

Table 8.6: Validation of P15S70R15 and P15S85 concretes – durability and permeation properties (Highlighted data are equal or above to the control or target values)

		Rapid Chloride Permeability Test, coulomb ASTM C11201			Water Absorption, % BS 1881:122			Water permeation, mm BS EN 12390: Part 8			Chloride Diffusion, 10^{-12} m^2/s CEN TC51/WG12/TG5		
		Actual, coulomb	Relative to P30S70W	Relative to target 1500 coulomb	Actual, %	Relative to P30S70W	Relative to target 2.0 %	Actual, mm	Relative to P30S70W	Relative to target 10mm	Actual, 10^{-12} m^2/s	Relative to P30S70W	Relative to target 5 x 10^{-12} m^2/s
P30S70	Washed sand, control	254	100%	591%	0.7	100%	286%	0	-	-	2.16	100%	231%
	Unwashed sand	375	68%	400%	0.5	140%	400%	0	-	-	1.73	125%	289%
	20%RCA, U	1077	24%	139%	0.6	117%	333%	0	-	-	1.52	142%	329%
	5%air, 20%RCA, U	1077	24%	139%	0.6	117%	333%	0	-	-	1.40	154%	357%
P15S70R15	Washed sand	430	59%	349%	0.7	100%	286%	3	-	333%	1.21	179%	413%
	Unwashed sand	430	59%	349%	0.5	140%	400%	3	-	333%	1.21	179%	413%
	20%RCA, U	1077	24%	139%	0.6	117%	333%	0	-	-	1.52	142%	329%
	5%air, 20%RCA, U	1077	24%	139%	0.6	117%	333%	0	-	-	1.40	154%	357%
P15S85	Washed sand	692	37%	217%	1.4	50%	143%	7	-	143%	1.54	140%	324%
	Unwashed sand	692	37%	217%	1.0	70%	200%	7	-	143%	1.54	140%	324%
	20%RCA, U	1077	24%	139%	1.3	54%	154%	7	-	143%	1.54	140%	324%
	5%air, 20%RCA, U	1077	24%	139%	1.3	54%	154%	7	-	143%	1.42	152%	353%

As expected the chloride diffusion values of all concretes are well within the relative values of the control concrete and the target value of $5x10^{-12}$ m^2/s due to enhanced microstructure of the cement paste contributed by the supplementary cementitious materials and very low w/c ratio. Due to longer testing period and comparatively complicated testing procedure of chloride diffusion test, it is not a popular test method used in the Arabian Peninsula, though it gives a direct result of chloride ion diffusion through the cross section of concrete structure.

8.3.3.5 Summary

It can be summarised from the above discussion and Table 8.5 and Table 8.6, that the compressive strength, environmental performance and the durability & permeation properties of concrete made with P15S70R15 can match the performance of the control concrete made with P30S70. In general, except compressive strengths, all other parameters compared between these three sets of concrete are well within the acceptable targeted limit.

In addition, concrete made with P15S85 with unwashed sand and with or without 20% RCA can match and outperform the different performance criteria of P30S70W concrete, except the compressive strength which is around 86% of P30S70W. Therefore, it can be expected that these two novel concretes made with P15S70R15 and P15S85 cementitious combination with different kind of aggregate and sand type should reach the minimum level of regional acceptance criteria.

8.4 Conclusion

This chapter has been divided into two sections. In the first section the compressive strength, durability and permeation properties of different type of concrete have been analysed together with their corresponding microstructure derived from TG, SEM and MIP techniques to validate the performance of the new concretes compared to the control. In the second section of this chapter the regional implications of the Arabian Peninsula to introduce the novel concretes have been discussed comparing with the control concrete made with P30S70 cementitious material.

The novel concretes were made with P15S70R15 and P15S85 cementitious materials with different combinations of coarse and fine aggregates and air content at 0.32 w/c ratio. The regional implications have been discussed within the parameter of their acceptance criteria by the construction industry, cost competitiveness and their engineering, durability and environmental performances compared with the control concrete.

Factors related to the acceptance by the construction industry such as availability of raw materials, production issues, specification works and conforming to the local environmental standards have been critically analysed between these concretes.

It has been concluded that though the availability of rice husk ash and RCA may be an issue in the earlier stages of the implementation as they are unique and novel materials in the Arabian Peninsula, availability of GGBS is not an issue as GGBS is in use in this region quite extensively to enhance the durability performance of concrete. However, the concrete industry would need to adjust their operation process to handle new cementitious materials and new types of aggregates with potential requirement to increase manpower, equipment and other resources.

Substantial volume of marketing and specification works supported by large scale lab and plant trials would need to convince the clients, engineers and the owners to accept these new novel materials and processes. However, local environmental standards such as PBRS of Estidama of Abu Dhabi, and GSAS of Qatar could provide certain level of legislative frameworks to successfully implement these materials.

Cost competitiveness would be the key to the success as P15S70R15 has relatively higher cost per m^3 of concrete compared to the control and P15S85 concretes due to higher cost of rice husk ash as it is an imported material from India and elsewhere and higher requirement of superplasticizing admixture. It has been reckoned that an additional cost of AED43.8/m^3 for concrete made with P15S70R15 with 20% RCA, unwashed and 5% air compared to the same concrete made with P30S70 would be required. However, this may not be a decisive factor for large infrastructure projects where cost proportion of concrete is not significant compared to the overall cost of the project as environmental benefit would potentially outweigh the additional cost due to the new concrete.

The additional cost due to the additional requirement of concrete volume due to the requirement of larger cross sectional area of the structural element for a given load scenario has also seen to be nominal compared to the total cost of projects. However, at equal compressive strength, the cost per cubic meter of concrete and eCO_2 analysis show that concrete made with P15S85 is more competitive than P15S70R15 compare to the control P30S70.

Finally, an overall discussions comparing the engineering, durability and environmental performance of P15S70R15 and P15S85 concretes comparing with P30S70 suggested that concrete with P15S70R15 with unwashed sand and 20% RCA achieved and outweighed the related performance of the control concrete and targeted values.

Therefore, it could be concluded that these new sets of novel concrete would be able to provide the required environmental sustainability as well as engineering and durability performance required by the local construction industry in the Arabian Peninsula.

Chapter 9

Conclusions and Recommendations

9.1 Introduction

The aim of this research work was to develop new environmentally sustainable concretes with low in eCO_2 with reduced impact on specific environmental factors. The new concretes would need to conform to the mechanical, durability and permeation properties of concretes which currently used and accepted by the construction industry of the Arabian Peninsula.

In order to achieve the above aims the total works were divided into five phases or objectives as described earlier in the Introduction chapter. In the following sections concluding remarks on these phases have been made as the work progressed to meet its final objectives.

9.2 Objective 1: Identifying environmental limitations and control concrete

In order to establish the state of the art of the low carbon concrete in the Arabian Peninsula a comprehensive review of the literature was undertaken. It was concluded that due to very harsh climatic and exposure conditions especially due to very high ionic concentration of chloride and sulfates in the ground, concretes in this region need to be highly durable to withstand these chemical attacks. Use of SCMs specially GGBS and microsilica is a common strategy to design concrete with appropriate durability and permeation properties such as rapid chloride permeability test, water absorption and water permeation generally specified by the local concrete industry. One of the common proportions often used by the industry to address these durability issues is concrete containing 70% GGBS of total cementitious materials by mass.

9.3 Objective 2: Ascertain appropriate forms of new concrete

In order to achieve a low carbon concrete there are two basic strategies can be employed i) reducing eCO_2 of concrete ii) using sustainable practices. As the main contributor of eCO_2 of concrete is Portland cement, reduction or replacement of Portland cement by SCMs is the most common approach. As SCMs are already in use in the Arabian Peninsula to enhance the durability of concrete, the reduction of eCO_2 by the SCMs should be taken into consideration.

The second strategy was to employ a set of sustainable practices to reduce the environmental impact on the production of concrete. It includes the use of unwashed fine limestone aggregates, recycled concrete aggregate, increasing the air content in concrete and recognizing the effect of higher ambient temperature of the Arabian Peninsula on the mechanical and durability properties of concrete.

9.4 Objective 3: Understanding fundamental cement and concrete science

A comprehensive review of the fundamentals of the cement science and concrete technology was undertaken to have a clear understanding of the chemical and physical compositions, hydration mechanisms, hydration products and durability properties of Portland cements, GGBS, fly ash, microsilica and rice husk ash. To understand the effect of the additional finer particles in the unwashed sand, the basic theories of particle packing of concrete ingredients have been reviewed. These reviews were found to be extremely useful to analyse the findings of the analytical techniques used namely TG, SEM and MIP to analyse the hydration products and microstructure of cement pastes and mortars.

9.5 Objective 4: Normalisation of the performance of the new concretes

In order to validate a new sets of concrete for the Arabian Peninsula which are low in carbon footprint and environmentally sustainable, there are two strategies have been considered. The first strategy was to reduce the content of Portland cement by high volume GGBS or other pozzolanic materials.

It has been seen that a cementitious combinations of P15S70R15 have contributed most positive characteristics in terms of plastic and hardened properties of concrete. Among three w/c ratio explored 0.32 w/c ratio appeared to be the best suitable to achieve both plastic and hardened properties. Concrete with P15S85 could also be another viable option to replace Portland cement. The performance of these concretes has been validated with a control concrete made with P30S70 cementitious combination.

Use of excess finer particles of unwashed sand which contains at least 10% finer particles passing 75µm sieve is a novel way to enhance compressive strength, durability and permeation properties of concrete, especially if the compressive strength gain is affected due to lower content of Portland cement. The effect of these excess finer particles of unwashed sand is equally effective for concretes containing natural limestone coarse aggregates or with the combination of RCA.

It has been seen that a 20% replacement of coarse limestone aggregate by the RCA at 0.32 w/c ratio would be a viable option with adequate compressive strength gain and sound durability and permeation properties. The minor reduction in the compressive strength due to the use of RCA can be complemented by using the excess finer particles of the unwashed sand.

One of the practical concerns with low w/c ratio concretes with higher replacement of Portland cement by GGBS and rice husk ash is the development of a sticky and harsh concrete mix during its plastic stage making it difficult to make and place. This problem can be overcome by entraining additional air up to 5% by using air entraining admixture. This additional air would not only save the raw materials to make concrete, but also enhance its durability properties and keeping the permeation properties well within the acceptable range. The reduced compressive strength which is associated with increased air content can be offset by using the unwashed sand.

As the reduction in compressive strength due to the use of low Portland cement and higher air content is a concern, a novel way to design the concrete mix is by recognizing the high ambient temperature of the year of Arabian Peninsula. Tests revealed that P15S70R15 concretes cured at 40°C temperature increased its compressive strength and chloride permeation resistance while maintaining the water permeation properties into an acceptable range.

9.6 Objective 5: Identification of the sustainable concretes

9.6.1 Environmental sustainability factors

Besides eCO_2, one of the main problems to analyze the environmental impact of concrete is to quantify the environmental sustainability factors. Therefore, in order to obtain a quantifiable analysis, total nine types of environmentally sustainable factors (ESF) were identified and quantified by assigning appropriate credit ratings (Table 7.3, Chapter 7) and weightings (Table 7.4, Chapter 7) for each factors. The credit ratings were based on PBRS of Estidama and the weightings were based on the relative impact of each factor on the concrete mixes.

Among different constituent materials of concrete Portland cement has the highest eCO_2 of 930 kg/mt, therefore concrete with high Portland cement content has higher eCO_2. High volume SCMs was used to reduce this eCO_2. However, the associated problem with the replacement of Portland cement is loss of compressive strength. Three concretes namely P30S70, P15S85 and P15S70R15 achieved higher strength with lower eCO_2 content (Figure 7.3 of Chapter 7). In order to identify the optimum relationship between the compressive strength and eCO_2 the concept of S/eC index is introduced in Figure 7.4 where higher S/eC index provided concrete with relatively higher compressive strength with lower eCO_2. As Figure 7.4 shows, concrete with P15S70R15 has the highest S/eC index, followed by P15S85 and the control concrete P30S70.

The effect of unwashed sand, RCA, air content and curing temperature did make certain changes on the S/eC index of respective concrete type mainly due to the change in compressive strength, as the eCO_2 of different type of concrete did not vary substantially.

Based on the above observation concrete with three cementitious combinations of P15S70R15, P15S85 and P30S70 were selected to analyse the effect of the environmental sustainable factors (ESF) on four specific scenarios including concrete with i) washed sand ii) unwashed sand iii) unwashed sand and 20% RCA iv) unwashed sand, 20% RCA and 5% air content. The environmental credit ratings and their respective weightings as discussed earlier are applied on each type of concrete to quantify their impact on the environment.

Based on the analysis as illustrated by Figure 7.8, it is concluded that concrete containing P15S70R15 cementitious combination has the most positive effect on the environment with any given scenarios compared with P15S85 and P30S70.

9.6.2 Discussions and validations of new concretes

Regional implications in terms of acceptance by the local industry, cost competitiveness and finally the validity of these new concretes comparing with the control and a set of target performance in terms of their engineering, durability and environmental properties are critically analysed. The new concretes containing P15S70R15 and P15S85 cementitious combinations in four specific scenarios with different type of sand, RCA and air content are compared with the control P30S70 with corresponding type of scenarios.

The following four specific issues, besides the cost competitiveness, considered to critically analyse prior to validate the new concretes: i) availability of raw materials ii) production and placement of concrete iii) specification works and iv) conformation to local environmental standards. These issues would have direct impact on the successful implementation of these new concrete in the industry.

Cost analysis:

Cost of concrete per m^3 with P15S70R15 is higher than control made with P30S70 mainly due to the requirement of higher dosage of superplasticizer as it is the most expensive ingredients of the concrete mix. Cost of P15S85 is slightly above P30S70 due to the same reason (Figure 8.4, Chapter 8).

Analysis of cost competitiveness in terms of structural element would also need to be taken into account as certain sets of novel concrete would have relatively lower compressive strength than the control P30S70, therefore, for same structural load scenario, the cross sectional area of elements may need to increase. However, this additional cost increment may not be substantial compared to the total cost of projects, especially large infrastructure projects in oil and gas industries in the Arabian Gulf, where low carbon construction approach is a priority.

At equal compressive strength scenario, concrete made with P15S85 appeared to be more cost effective than P15S70R15 concrete with similar eCO_2 values, though the cost of P15S85 would be around 20% higher than concrete made with P30S70 with same compressive strength at 28 days.

Validation of performance:

The compressive strength, durability and environmental properties of P15S70R15 and P15S85 have been validated in Table 8.5 and 8.6 of chapter 8 in two ways. Firstly the performance of these new concretes were compared with the performance of the control P30S70 concrete and secondly they were compared against a specified set of properties as discussed in chapter 3, Table 3.19 as the acceptance limits of durability and permeation properties. Each type of cementitious combinations have been analysed in four specific scenarios based on the sand type, RCA and air content.

It can be concluded that concrete made with P15S70R15 with unwashed sand and with or without RCA replacing 20% of limestone coarse aggregate are the only novel concretes which have superior performance at all categories over the control made with P30S70 cementitious combinations. Therefore, concretes made with P15S70R15 could be considered as the low carbon and sustainable concrete suitable for the Arabian Peninsula.

In summary, a set of novel concretes could be made with reduced Portland cement, reduced natural aggregates using RCA and additional filler of unwashed sand. Higher entrained air can be used to improve the plastic properties and to enhance the ‘greener’ credentials of the concrete. At the same time, the higher ambient temperature of Arabian Peninsula can be considered as one of the design parameters to design and produce environmentally sustainable concretes for the Gulf environment.

9.7 Recommendation for future work

This research work has opened up new possibilities for further works to enhance the plastic and hardened properties as well as cost competitiveness of these novel concretes. Following is a list of work recommended by the author to be undertaken for further improvement of properties of concrete:

1. Introducing fly ash in P15S70R15 mixes to enhance the rheology and to reduce the admixture dosage. The spherical morphology of fly ash particle will enhance the rheology. A quadruple blend may complicate the operation process, but a pre-blended factory made cementitious material will eliminate the handling problem.

2. Reduction of dosage of superplasticizer or alternative admixture to reduce the cost. In this work only one type of superplasticizer was used. Cost optimization is possible by using alternative admixtures.

3. Reduce the water demand of rice husk ash by pretreatment of rice husk ash. Higher water demand of rice husk ash not only increases the dosage of admixture, but also increases the effective w/c ratio compromising the strength and permeation properties. Therefore it is essential to reduce the water demand of rice husk ash. Novel burning technology to reduce the carbon content or chemical treatment perhaps during grinding to reduce the water demand may be the answer.

4. Reduce the water absorption properties of RCA to improve the inconsistency related to RCA. Addition of certain hydrophobic type chemical admixture to provide a hydrophobic lining along the pore wall of the ‘old paste’ of RCA may help to reduce the inconsistency related to RCA concrete and also eliminate the need to pre-soak RCA prior to mixing.

5. Validate the durability performance of the new sustainable concrete in terms of carbonation.

References

ADCO, Abu Dhabi Company for Onshore Oil Operations, 2007. *Engineering Specification, Project No. P 14333 Feed Service for Full Field Development, Document no. 30.99.75.0711, Concrete Works*. Abu Dhabi, ADCO.

ADNOC, Abu Dhabi Oil Company, n.d. *03300 Cast in place concrete, Volume 5, Part A, Civil & Structural Specification*. Abu Dhabi, ADNOC.

Agarwal, A., 2011. An overview of the global cement industry. In: *International cement conference CEMTECH Middle East & Africa: Technology & Markets*. Dubai, 5-8 March 2011.

Ahmed, M.S., et. al., 2009. Evaluation of binary and ternary blends of pozzolanic materials using the rapid chloride permeability test. *Journal of materials in civil engineering*, 21 (2009), pp.446-453.

Al Amoudi, B., 2002. Attack on plain and blended cements exposed to aggressive sulfate environments. *Cement and concrete composites*, 24 (2002), pp.305–316.

Al Amoudi, B., et al., 1994. Influence of chloride ions on sulphate deterioration in plain and blended cements. *Magazine of Concrete Research*, 46(167),pp.113 –123

Alexander, M.G. and Magee, B.J., 1999. Durability performance of concrete containing condensed silica fume. *Cement and Concrete Research*, 29 (1999), pp.917–922.

Al Horr, Y., 2013. GSAS Technical Guide v2.1 – 2013. *Gulf organization for research and development, Qatar*. 2013.

Al-Khaiat, H. and Fattuhi, N.,2002. Carbonation of concrete exposed to hot and arid climate. *Journal of materials in civil engineering*, 14(2), pp. 97-107.

Al Rukaibi, D., 2010. Water resources in GCC countries. University of Texas at Austin. [online] Available at: <http://www.ce.utexas.edu/prof/mckinney/ce397/Topics/Gulf/Gcc_2010.pdf > [Accessed 5 May 2011].

Alonso, C. et. al., 2000. Chloride threshold values to depassivate reinforcing bars embedded in a standardized OPC mortar. *Cement and Concrete Research* 30 (2000) pp.1047- 1055.

Anastasiou, M. et. al., 2006. TG-DTA and FTIR analysis of plasters from Byzantine monuments in Balkan region - Comparative study. Journal of Thermal Analysis and Calorimetry, Vol. 84 (2006) 1, pp.27–32.

Ann, K.Y., et al. 2008. Durability of recycled aggregate concrete using pozzolanic materials. Waste Management, 28, pp.993–999.

ASTM International, 2003. *ASTM C 33 – 03 Standard Specification for Concrete Aggregates.* West Conshohocken, Pennsylvania: ASTM International.

ASTM International, 2003. *C 94/C 94M – 03 Standard Specification for Ready-Mixed Concrete.* West Conshohocken, Pennsylvania: ASTM International.

ASTM International, 2003. *ASTM C 125 – 03 Standard Terminology Relating to Concrete and Concrete Aggregates.* West Conshohocken, Pennsylvania: ASTM International.

ASTM International, 2002. *ASTM C 150 – 02a Standard Specification for Portland Cement.* West Conshohocken, Pennsylvania: ASTM International.

ASTM International, 2002. C192/C192M – 02 *Standard Practice for Making and Curing Concrete Test Specimens in the Laboratory.* West Conshohocken, Pennsylvania: ASTM International.

ASTM International, 1999. *ASTM C 494/C 494M – 99a Standard Specification for Chemical Admixtures for Concrete.* West Conshohocken, Pennsylvania: ASTM International.

ASTM International, 1997. *ASTM C 1202 – 97 Standard Test Method for Electrical Indication of Concrete's Ability to Resist Chloride Ion Penetration1*. West Conshohocken, Pennsylvania: ASTM International.

Atkins. 2010. *Yas Island Water Park Geotechnical interpretative report*. Abu Dhabi: Atkins.

BCA, CSMA, UKQAA Fact sheet 18 (P1), 2009. *Embodied CO2 of UK cement, additions and cementitious materials*. Camberley: BCA, CSMA, UKQAA.

BCA, CSMA, UKQAA Fact sheet 18 (P2), 2009. *Embodied CO2 of factory-made cements and combinations*. Camberley: BCA, CSMA, UKQAA.

Bentz, D. P. 2007. A virtual rapid chloride permeability test. *Cement & Concrete Composites* 29 (2007) pp.723–731.

Beaudoin., J.J. and Marchand., J. 2001. Pore structure. In: Beaudoin., J.J. 2001. *Handbook of analytical techniques in concrete science and technology*. Park Ridge, NJ ; Norwich, NY : William Andrew Pub. 2001 pp.528-628.

Biomass Energy Centre, 2011. *Estimated carbon dioxide emissions for freight transport*. [online] Available at: http://www.biomassenergycentre.org.uk/portal/page?_pageid=75,20043&_dad=portal&_schema=PORTAL [Accessed 24th March 2011]

Black & Veatch in collaboration with the University of Bath, 2001. *Low Carbon Concrete - Guidelines for reducing the carbon footprint of concrete used in flood risk management infrastructure.* Environment Agency UK, August 2011.

Boriboonsomsin, K. and Reza F. 2007, 'Mix Design and Benefit Evaluation of High Solar Reflectance Concrete for Pavements', *Journal of the Transportation Research Board,* No. 2011, Transportation Research Board of the National Academics, Washington D.C., pp.11-20.

BRE. 2001. *BRE Information Paper 11/01:2001 Delayed ettringite formation: In-situ concrete.* London: CRC Ltd.

BRE. 2005. *BRE Special Digest 1:2005 Concrete in aggressive ground*. Watford: BRE Bookshop.

British Standards Institution, 1996. *BS 12:1996 Specification for Portland cement.* London: BSI.

British Standards Institution, 2000. *BS EN 197-1:2000 Cement — Part 1: Composition, specifications and conformity criteria for common cements.* London: BSI.

British Standards Institution, 2000. *BS EN 206-1:2000 Concrete — Part 1: Specification, performance, production and conformity.* London: BSI.

British Standards Institution, 1992. *BS EN 882:1992 Specification for aggregates from natural sources for concrete.* London: BSI.

British Standards Institution, 2009. *BS EN 934-2:2009 Admixtures for concrete, mortar and grout Part 2: Concrete admixtures — Definitions, requirements, conformity, marking and labelling.* London: BSI.

British Standards Institution, 2007. BS EN 450-1, 2007 *Fly ash for concrete — Part 1: Definition, specifications and conformity criteria.* London: BSI.

British Standards Institution, 2002. *BS EN 1008:2002 Mixing water for concrete — Specification for sampling, testing and assessing the suitability of water, including water recovered from processes in the concrete industry, as mixing water for concrete.* London: BSI.

British Standards Institution, 1983. *BS 1881-122:1983 Testing concrete — Part 122: Method for determination of water absorption.* London: BSI.

British Standards Institution, 1980. *BS 3148:1980 Methods of test for Water for making concrete (including notes on the suitability of the water).* London: BSI.

British Standards Institution, 1996. *BS 4027:1996 Specification for Sulfate-resisting Portland Cement.* London: BSI.

British Standards Institution, 1985. *BS 5075-Part 3:1985 Concrete admixtures- Part 3 Specification for superplasticizing admixtures.* London: BSI.

British Standards Institution, 1997. *BS 5328-Part 1:1997 Concrete — Part 1: Guide to specifying concrete.* London: BSI.

British Standards Institution, 1997. *BS 5328-Part 2:1997 Concrete — Part 2: Methods for specifying concrete mixes.* London: BSI

British Standards Institution, 1990. *BS 5328-Part 3:1990 Concrete — Part 3: Specification for the procedures to be used in producing and transporting concrete.* London: BSI.

British Standards Institution, 1990. *BS 5328-Part 4:1990 Concrete Part 4. Specification for the procedures to be used in sampling, testing and assessing compliance of concrete.* London: BSI.

British Standards Institution, 2006. *BS 8500-1:2006 Concrete – Complementary British Standard to BS EN 206-1 – Part 1: Method of specifying and guidance for the specifier.* London: BSI.

British Standards Institution, 2006. *BS 8500-2:2006 Concrete – Complementary British Standard to BS EN 206-1 – Part 2: Specification for constituent materials and concrete.* London: BSI.

British Standards Institution, 2009. *BS EN 12390:2009 Testing hardened concrete Part 8: Depth of penetration of water under pressure.* London: BSI.

British Standards Institution, 2002. *BS EN 12620:2002 Aggregates for concrete.* London: BSI.

Brito, J., and Saikia, N., 2013. *Recycled Aggregate in Concrete Use of Industrial, Construction and Demolition Waste*. London: Springer.

Brouce, G.S., 2001. Durability of silica fume concrete exposed to chloride in hot climate. *Journal of Material in Civil Engineering.* January/February 2001, pp.41-48.

Cemnet GM01, 2006. *Cemnet training course GM 01 – Grinding and milling*. Surrey: International Cement review.

CEN/TC 51 (CEN/TC 104)/JWG12/TG5, 2008. *CEN TC51/WG12/TG5 Draft 4 Version 2 Date: 20 April 2008 Testing Hardened concrete — Part xx: Determination of the chloride resistance of concrete, unidirectional diffusion*. Brussels: CEN

Cheng, A., et. al., 2005. Influence of GGBS on durability and corrosion behavior of reinforced concrete. *Materials Chemistry and Physics*, 93 (2005) pp.404–411.

Chang, J.J. et. al., 2004. Suitability of several current used concrete durability indices on evaluating the corrosion hazard for carbonated concrete. *Materials Chemistry and Physics* 84 (2004) pp.71–78

Chindaprasirt, P. and Rukzon, S., 2008. Strength, porosity and corrosion resistance of ternary blend - Portland cement, rice husk ash and fly ash mortar. *Construction and Building Materials*, 22 (2008), pp.1601–1606.

CIRIA and The Concrete Society, 2002. *CIRIA C577, Concrete Society CS 136 Guide to the construction of reinforced concrete in the Arabian Peninsula.* London: CIRIA / Berkshire: Concrete Society.

Concrete Centre, 2008. *Sheet C1. Embodied CO2 of Concrete and Reinforced Concrete*. Surrey: Concrete Centre.

Concrete Centre, 2009. *Concrete structures 09*. Surrey: Concrete Centre.

Concrete Centre, 2011. *Specifying sustainable concrete – understanding the role of constituent materials*. Surrey: Concrete Centre.

Concrete Society, 2008. *CS 163 Guide to the design of concrete structures in the Arabian Peninsula.* Surrey: Concrete Society.

Concrete Society, 2002. *CS 137 Guide to evaluation and repair of concrete structures in the Arabian Peninsula.* Berkshire: Concrete Society.

Concrete Society, 1988. *CSTR 31 Permeability testing of site concrete – A review of methods and experience*. London: Concrete Society.

Cordon, W. A., 1946. Entrained Air—A Factor in the Design of Concrete Mixes. *Materials Laboratories Report No. C-310*, Research and Geology Division, Bureau of Reclamation, Denver, March 15, 1946

de Larrard, F. and Sedran, T., 2002. Mixture-proportioning of high-performance concrete. *Cement and Concrete Research*, 32, pp.1699–1704.

de Larrard, F. 2009. Concrete optimisation with regard to packing density and rheology. In: *3rd RILEM international symposium on rheology of cement suspensions such as fresh concrete*. Reykjavik, 19-20 August, 2009. Bagneux : RILEM.

Department of Trade and Industry, 2003. Rice husk ash market study. London: Department of Trade and Industry.

Deshinia, A. and Ioannides, A. M., 2012. Undispersed agglomerates and the strength of microsilica concrete. *International Journal of Pavement Engineering*, Vol. 13, No. 3, June 2012, pp.226–234.

Dhinakaran, G. et. al., 2012. Compressive Strength and Chloride Resistance of Metakaolin Concrete. *KSCE Journal of Civil Engineering*, 16(7) 2012, pp.1209-1217.

Dhir, R.K., 2004. Corrosion of embedded steel reinforcement, *CE 51004 Concrete design for durability.* University of Dundee, Unpublished.

Dhir, R.K., et al. 1997. Developing chloride resisting concrete using PFA. *Cement and Concrete Research*, 27(11), pp.1633-1639.

Dhir, R.K., et al. 1988. Contribution of PFA to concrete workability and strength development. Cement and Concrete Research, 18, pp.277-289.

Dhir, R.K. and Byars, E. A. 1993. PFA concrete: Permeation properties of cover to steel reinforcement. *Cement and Concrete Research*, 23, pp.554-566.

Dickie, P., 2007, WWF's Global Freshwater Programme. *Making water - Desalination: option or distraction for a thirsty world?* Gland: WWF International.

DIN Deutsche Institut, 1991, *DIN 1048-5:1991 Testing concrete – Testing of hardened concrete.* Berlin: DIN Deutsche Institut.

Economic Times, 2013. Dubai now home to world's most sustainable building. [online] Available at: <http://articles.economictimes.indiatimes.com/2013-06-18/news/40049440_1_dubai-us-green-building-council-dewa> [Accessed 28 December 2013].

Elchalakani, M. et. al., 2014. Sustainable concrete with high volume GGBFS to build Masdar City in the UAE. *Case Studies in Construction Materials* 1 (2014) pp.10–24.

Elkem, n.d. In house technical presentation. Elkem silicon materials. Kristiansand.

Emirates Wildlife Society in association with WWF. [online] Available at http://uae.panda.org/what_we_do/projects2/2f/ [Accessed 8th February 2011].

Escalante, J.I., et al., 2001. Reactivity of blast-furnace slag in Portland cement blends hydrated under different conditions. *Cement and Concrete Research*, 31 (10), pp.1403-1409.

Estidama, 2011. *Pearl rating system for Estidama – Concrete GHG calculator*. Abu Dhabi: Estidama.

Estidama, 2010. *Pearl Building Rating System: Design & Construction, Version 1.0*. April 2010 Abu Dhabi: Estidama.

European Federation of Concrete Admixture Associations, 2006. *EFCA environmental declaration - Superplasticising admixtures*. EFCA.

European Federation of Concrete Admixture Associations, 2005. *EFCA environmental declaration - Retarding admixtures*. EFCA.

European Federation of Concrete Admixture Associations, 2005. *EFCA environmental declaration – Air entraining admixtures*. EFCA.

Fagerlund, G., 1982. The capillarity of concrete. *Nordic Concrete Research*, 1 (1982).

Fidjestol, P., and Frearson, J., 1994. High-performance concrete using blended and triple blended binders. Malhotra VM ed. In: Proceedings of the ACI International Conference on High Performance Concrete, Singapore, 1994. American Concrete Institute; SP-149.

Fidjestol, P. and Lewis, R., 2003. Microsilica as an addition. In: P.C. Hewlett, ed. 2003. Lea's chemistry of cement and concrete. 4th edition. Butterworth-Heinemann. Ch. 12.

Ganesan, K. et. al., 2008. Rice husk ash blended cement: Assessment of optimal level of replacement for strength and permeability properties of concrete. *Construction and Building Materials*, 22 (2008), pp.1675–1683.

GASCO, Abu Dhabi Gas Industries Limited, 2007. *Design General Specification, Specification for Concrete Supply, DGS 1783-001.* Abu Dhabi, GASCO.

GASCO, Abu Dhabi Gas Industries Limited, 2010. Shah Gas Development Programme *Addendum to DGS specification DGS 1783-001 – Concrete Supply.* Abu Dhabi, GASCO.

Government of Dubai, n.d. *Green Building Regulations and Specifications*. [Online] Dubai : Government of Dubai. Available at <http://www.dewa.gov.ae/images/greenbuilding_eng.pdf> [Accessed 14 June 2014]

Guneyisi, E. and Gesoglu, M., 2008. A study on durability properties of high-performance concretes incorporating high replacement levels of slag. *Materials and Structures*, 41 (2008) pp.479–493

Hamed. O.A., 2004. Evolutionary developments of thermal desalination plants in the Arab Gulf region. *Research &Development Center, SWCC, KSA* (presented in Buirut conference, 2004).

Haque, M.N. and Al Khaiat, H., 1997. Carbonation in concrete structures in hot and dry coastal region. *Cement and concrete composites*, 19 (1997), pp.123-129.

Hewlett, P.C.ed., 2003. *Lea's chemistry of cement and concrete*. 4th edition. Butterworth-Heinemann.

Holland, T.C., 2005. Silica fume user's manual. Springfield: National Technical Information Services.

Ismael, N.F., 1997. Properties and Behavior of Arid Climate Soil Deposits in Kuwait. *Symposium on Civil Engineering and The Environment.* KFUPM, Dhahran, pp. 345-384.

Jones, M.R., et al., 1997. Concrete containing ternary blended binders: Resistance to chloride ingress and carbonation. *Cement and Concrete Research*, 27 (6), pp. 825-831.
Kamoonpuri, H., 2010. Oman emerging as Gulf's mining powerhouse. *Oman Daily Observer*, [online] 15th June 2010. Available at: http://main.omanobserver.om/node/13094 [Accessed 8 February 2011].

Karmani, HK., 2011. GCC Cement sector – Overview and Outlook. In: *International cement conference CEMTECH Middle East & Africa: Technology & Markets*. Dubai, 5-8 March 2011.

Katz, A., 2003. Properties of concrete made with recycled aggregate from partially hydrated old concrete. *Cement and Concrete Research*, 33, pp.703– 711.

Kolani, B., et. al., 2012. Hydration of slag-blended cements. *Cement & Concrete Composites*, 34 (2012), pp.1009–1018.

Kou, SC and Poon, CS, 2013. Long-term mechanical and durability properties of recycled aggregate concrete prepared with the incorporation of fly ash. *Cement & Concrete Composites*, 37 (2013) pp.12–19

Kou, S.C. et al., 2008. Influence of fly ash as a cement addition on the hardened properties of recycled aggregate concrete. *Materials and Structures*, 41, pp.1191–1201.

Lawrence, C.D., 2003. The constitution and specification of Portland cements. In: P.C. Hewlett, ed. 2003. Lea's chemistry of cement and concrete. 4th edition. Butterworth-Heinemann. Ch. 4.

Lawrence, R.M.H., et. al. 2006. The use of TG to measure different concentrations of lime in non-hydraulic lime mortars. *Journals of Thermal Analysis and Calorimetry* (2006) pp.1-6.

Leung, P.W.C and Wong, H.D., 2011. *Final Report on Durability and Strength Development of Ground Granulated Blastfurnace Slag Concrete – Geo report no 258*. Geotechnical Engineering Office, Civil Engineering and Development Department, The Government of the Hong Kong Special Administrative Region.

Liu Z. et. al., 2010. Micro-analysis of the role of interfacial transition zone in salt weathering on concrete. *Construction and Building Materials* 24 (2010) pp.2052–2059.

Macphee, D.E and Lachowski, E.E., 2003. Cement Components and Their Phase Relations. In: Hewlett, P.C. ed. 2003. *Lea's chemistry of cement and concrete*. 4th edition. Butterworth-Heinemann. Ch.3.

Masdar, 2014. About Masdar City. [Online] Available at: http://www.masdar.ae/en/city/detail/one-of-the-worlds-most-sustainable-communities-masdar-city-is-an-emerging-g [Accessed 14 June 2014]

Masdar, 2011. Masdar concrete mix design calculator. [Excel worksheet] (Personal communication, 2011).

Maslehuddin, M. et al., n.d. *King Fahd University of Petroleum and Minerals, & Saudi Aramco, Dhahran, Saudi Arabia*. Characteristics of aggregates in Eastern Saudi Arabia and their influence on concrete properties. [online] Available at <http://www.kfupm.edu.sa/library/ISI/2006/Ajseaggregatepaperfinalmodifiedrevised.pdf> [Accessed 8 February 2011].

Massazza, F., 2003. Pozzolana and Pozzolanic Cements. In: P.C. Hewlett, ed. 2003. Lea's chemistry of cement and concrete. 4th edition. Butterworth-Heinemann. Ch. 10.

Mehta, P.K., 2001. Reducing the environmental impact of concrete – Concrete can be durable and environmentally friendly. *Concrete International*, Oct 2001, pp.61-66.

Moranville-Regourd, M., 2003. Cements made from blastfurnace slag. In: P.C. Hewlett, ed. 2003. Lea's chemistry of cement and concrete. 4th edition. Butterworth-Heinemann. Ch. 11.

Nath, P. and Sarker, P. 2011. Effect of Fly Ash on the Durability Properties of High Strength Concrete. In: The Twelfth East Asia-Pacific Conference on Structural Engineering and Construction. *Procedia Engineering*, 14 (2011) pp.1149–1156

Neville, A.M. 2006. Properties of concrete. 4th ed. Harlow: Pearson Education Limited.

Nikam, V.S. and Tambvekar, V.Y., 2003. Effect of different supplementary cementitious material on the microstructure and its resistance against chloride penetration of concrete. In: Engineering Conferences International, *Advanced Materials for Construction of Bridges, Buildings, and Other Structures III*. 2003

Noguchi, T., 2010. Life-cycle perspective of technologies and properties of recycled aggregate concrete. 2010 International Concrete Sustainability conference. Dubai

O'Connell, M. et. al., 2012. Performance of concrete incorporating GGBS in aggressive waste water environments. *Construction and Building Materials*, 27 (2012) pp.368–374.

Odler, I., 2003. Hydration, setting and hardening of Portland cements. In: P.C. Hewlett, ed. 2003. Lea's chemistry of cement and concrete. 4th edition. Butterworth-Heinemann. Ch. 6.

Osborne, J.G., 1999. Durability of Portland blastfurnace slag cement concrete. *Cement and Concrete Composite*, 21, pp. 11-21

Page, C. L. and Vennesland, O., 1983. Pore solution composition and chloride binding capacity of silica-fume cement pastes. *Materials and structures*, 16 (1), pp.19-25.

Paine, K.A., et al., 2005. Experimental study and modelling of heat evolution of blended cements. *Advances in Cement Research*, 17(3), pp.121–132.

Paine, K.A. and Dhir, R.K., 2010. Recycled aggregates in concrete: a performance-related approach. *Magazine of Concrete Research*, 62(7), pp.519–530.

Pinto, R.C.A., and Hover, K.C., 2001. Frost and Scaling Resistance of High-Strength Concrete. *Research and Development Bulletin RD122, Portland Cement Association*, 2001.

Pocock, D. and Corrans, J. Concrete durability testing in Middle East construction, *Concrete Engineering International*, Summer 2007, pp.52-54.

Ramachandran, V.S. and James J. Beaudoin, J.J., 2001. *Handbook of analytical techniques in concrete science and technology - Principles, Techniques, and Applications.* Noyes Publications Park Ridge, New Jersey, U.S.A.

Ramezanianpour, A. A., et. al., 2009. The effect of rice husk ash on mechanical properties and durability of sustainable concretes. *International Journal of Civil Engineering*. Vol. 7, No. 2, June 2009, pp.83-91.

Rice Husk Ash, 2008. [online] Available at:<http://www.ricehuskash.com> [Accessed 3rd May 2011].

RILEM 1982, 1982. *CPC11.1:1982 Absorption of water by concrete by immersion.* Bagneux: RILEM.

RILEM 1982, 1984. *CPC11.3:1984 Absorption of water by concrete by immersion under vacuum.* Bagneux: RILEM.

Siddique, R. 2011. Properties of self-compacting concrete containing class F fly ash. *Materials and Design*, 32 (2011) pp.1501–1507

Silica fume association, 2003. *Making silica fume concrete in the laboratory.* Lovettsville: Silica fume association.

Sika UAE L.L.C, 2011. *Sikaplast 1400 Eco, Letter to Xtramix Concrete Solutions*. Sika, 2011.

Sivakumar, G. and Ravibaskar, R., 2009. Investigation on the Hydration Properties of the Rice Husk Ash Cement Using Ftir and SEM. Applied Physics Research. Vol 1, No.2 http://ccsenet.org/apr.

Tanaka H, et.al., 1983. Structure of hydrated glassy blastfurnace in concrete. In: Proceedings of the 1st International Congress on Fly Ash, Silica Fume, Slag and other Mineral By-Products in Concrete, Montebello, Canada, 1983. American Concrete Institute Special Publication, 79, pp.963-977.

Tangchirapat, W. et. al., 2008. Influence of rice husk–bark ash on mechanical properties of concrete containing high amount of recycled aggregates. *Construction and Building Materials*, 22 (2008), pp.1812–1819.

Techeco Pty. Ltd., 2013. The Importance of Particle Packing for Strength (Tec-Cements) or Carbonation (Eco-Cements). [online] Available at: <http://www.tececo.com/technical.particle_packing.php> [Accessed 23rd December 2013].

Ukrainczyk, N. et. al. 2006. XRD and TGA investigation of hardened cement paste degradation. Conference on *Materials, Processes, Friction and Wear* MATRIB'06, Vela Luka, pp.22-24.

Understanding cement 2011. *Clinker and Cement hydration*. [online] Available at: <http://www.understanding-cement.com/index.html>[Accessed 8 May 2011].

U.S.GBC, 2009. LEED 2009 for New Construction and Major Renovations Rating System. Washington D.C. USGBC.

WBC SD (World Business Council for Sustainable Development) and IEA (International Energy Agency), 2009. *Cement technology roadmap 2009 – Carbon emissions reductions up to 2050*. Geneva: WBCSD and Paris: IEA.

WeatherSpark, 2014. *Average Weather for Dubai, United Arab Emirates*. [Online] Available at < http://weatherspark.com/averages/32855/Dubai-United-Arab-Emirates> [Accessed 18 June 2014]

Wee, T.H., et.al., 1999. Influence of aggregate fraction in the mix on the reliability of the rapid chloride permeability test. *Cement and Concrete Composites,* 21 (1999), pp.59-72

Wilson, A., 1993. Cement and Concrete: Environmental Considerations. *Environmental Building News*, Volume 2, Number 2, March/April 1993

Xu, Aimin., 1997. Fly ash in concrete. In: Chandra, S., 1997. Waste materials used in concrete manufacturing. New Jersey: Noyes Publications. Ch.3.

Yanagibashi. K et.al., 2002. A new concrete recycling technique for coarse aggregate regeneration process. *Sustainable concrete construction:* Proceedings of the International Conference held at the University of Dundee, Scotland, UK, 9-11 September 2002. London: Thomas Telford Publishing.

Yeau, K. Y. and Kim, E.K., 2005. An experimental study on corrosion resistance of concrete with ground granulate blast-furnace slag. *Cement and Concrete Research,* 35, pp.1391– 1399

Zein A1-Abidien, H. M., 1987. Aggregates in Saudi Arabia: a survey of their properties and suitability for concrete. *Materials and Structures*, 20(4), pp.260-264.

Zhang, X., Zhao, Y., and Lu, Z., 2011. Probabilistic assessment of reinforcing steel depassivation in concrete under aggressive chloride environments based on natural exposure data. *Journal of Wuhan University of Technology--Materials Science Edition,* 26(2011), pp.126-131.

Annex A: RCA 10mm - Classification test for the constituents of coarse recycled aggregate

BS EN 933-1:2009 Test Data Sheet
Tests for Geometrical Properties of Aggregates:
Part 11: Classification test for the constituents of coarse recycled aggregate

ID of the sample	10mm
Laboratory	Mafraq
Operator	

Date sample received	29/09/2010
Date of test	01/12/2010

Drying temperature, T		^{0}C
Mass of the initial sample, M_0	3400	g
Mass of retained at 63mm, M_{63}	0	g
Mass of passing at 4mm, M_4	20	g
Test portion mass, $M_1=M_0-(M_{63}+M_4)$	3380	g
Mass of constituent X, M_X	0	g
Mass of remaining non-floating particles, $M_2=M_1-M_X$	3380	g
Mass of reduced remaining non floating particles, M_3	3380	g

Constituent	Volume, cm^3	Proportion, cm^3/kg	
FL	V_{FL}= 0	1000 x V_{FL}/M_1 =	0

Constituent		Masses, g		Proportions, %	
X		M_X=	0	100 x M_X/M_1=	
Rc		M_{Rc}=	3380	100 x (M_2/M_1) x (M_{Rc}/M_3)=	100
Ru		M_{Ru}=		100 x (M_2/M_1) x (M_{Ru}/M_3)=	0
Rb		M_{Rb}=		100 x (M_2/M_1) x (M_{Rb}/M_3)=	0
Ra		M_{Ra}=		100 x (M_2/M_1) x (M_{Ra}/M_3)=	0
Rg		M_{Rg}=		100 x (M_2/M_1) x (M_{Rg}/M_3)=	0
				ΣP=	100

Constituent	Description
Rc	Concrete, concrete products, mortar Concrete masonry units
Ru	Unbound aggregate, natural stone Hydraulically bound aggregate
Rb	Clay masonry units (i.e. bricks & tiles), Calcium silicate masonry units, Aerated nonfloating concrete
Ra	Bituminous materials
Rg	Glass
X	Other: Cohesive (i.e. clay and soil), Miscellaneous: metals (ferrous and non-ferrous), Non-floating wood, plastic and rubber, Gypsum plaster

Annex B: RCA 20mm - Classification test for the constituents of coarse recycled aggregate

BS EN 933-1:2009 Test Data Sheet
Tests for Geometrical Properties of Aggregates:
Part 11: Classification test for the constituents of coarse recycled aggregate

ID of the sample	20mm
Laboratory	Mafraq
Operator	

Date sample received	29/09/2010
Date of test	01/12/2010

Drying temperature, T		^{0}C
Mass of the initial sample, M_0	3500	g
Mass of retained at 63mm, M_{63}	0	g
Mass of passing at 4mm, M_4	1	g
Test portion mass, $M_1=M_0-(M_{63}+M_4)$	3499	g
Mass of constituent X, M_X	0	g
Mass of remaining non-floating particles, $M_2=M_1-M_X$	3499	g
Mass of reduced remaining non floating particles, M_3	3499	g

Constituent	Volume, cm^3	Proportion, cm^3/kg	
FL	V_{FL}= 0	1000 x V_{FL}/M_1 =	0

Constituent	Masses, g	Proportions, %	
X	M_X= 0	100 x M_X/M_1=	0
Rc	M_{Rc}= 3499	100 x (M_2/M_1) x (M_{Rc}/M_3)=	100
Ru	M_{Ru}=	100 x (M_2/M_1) x (M_{Ru}/M_3)=	0
Rb	M_{Rb}=	100 x (M_2/M_1) x (M_{Rb}/M_3)=	0
Ra	M_{Ra}=	100 x (M_2/M_1) x (M_{Ra}/M_3)=	0
Rg	M_{Rg}=	100 x (M_2/M_1) x (M_{Rg}/M_3)=	0
		ΣP=	100

Constituent	Description
Rc	Concrete, concrete products, mortar Concrete masonry units
Ru	Unbound aggregate, natural stone Hydraulically bound aggregate
Rb	Clay masonry units (i.e. bricks & tiles), Calcium silicate masonry units, Aerated nonfloating concrete
Ra	Bituminous materials
Rg	Glass
X	Other: Cohesive (i.e. clay and soil), Miscellaneous: metals (ferrous and non-ferrous), Non-floating wood, plastic and rubber, Gypsum plaster

Annex C: Calculation of the emission of CO_2 of sand washing:

Water consumption		
Water requirement:	295,000 ltr/2 weeks	24,500 ltr/day
Sand wash output /day: 1 truck = 75 tonnes	12.5 Trucks / day	940 Tonne /day
Water consumption per tonne of sand:	26 ltr	
eCO_2 for water:	1.0	kg-CO_2/tonne
eCO_2 for 26 ltr washing water:	0.026	kg-CO_2/tonne

Waste of materials		
At least 5% of materials is being removed from the sand with having original dust content of 10% For using 10% dust content sand, it saves 5% of materials So, it saves equivalent to 5% eCO_2 of washed sand		
eCO_2 of washed sand	7	kg-CO_2/tonne
Saving	0.35	kg-CO_2/tonne

Transport to disposal		
Waste amount		
Water consumption	24.5	tonne
Daily evaporation:	7.7	tonne
Waste water with sand sludge	16.8	tonne
At least 5% of materials is being removed from the sand with having original dust content of 10%		
So, for 940 tonne daily wash sand production, the approximate quantity of dust to become sludge = 49.5 tonne		
Total sludge weight:	49.5 + 16.8	66.3 tonne
940 tonne washed sand produce 66.3 tonne sludge So, 1 tonne produced 0.07 tonne sludge		
Heavy duty vehicle CO_2 emission	0.092	kg CO_2/tonne - km
Travelling distance to the nearest dump	50	km
eCO_2	4.6	kg CO_2/tonne of sludge
eCO_2 for 0.068 tonne sludge transportation:	0.32	kg CO_2/tonne of sand

Total CO_2 emission for sand washing =	0.026+0.35+0.32 = 0.696 kg CO_2/tonne
eCO_2 for unwashed sand with 10% dust:	7 - 0.7 = 6.30 kg CO_2/tonne which is about 10% less than eCO_2 of washed sand
Electric energy consumption by the washing wheel and conveyor belts are not considered here.	

Annex D: Technical data sheet of Chryso Fluid Optima 245 EMx – Superplasticizing admixture

Concrete admixture

CHRYSO®Fluid Optima 245 EMx

CHRYSO®Fluid Optima 245 EMx

Technical Datasheet

New Generation Admixture For high volume Fly ash and Slag concrete

■ Features

CHRYSO®Fluid Optima 245 EMx is enhanced by EnviroMix® technology whitch combines CHRYSO's latest proprietary polymers along with most advanced developments in terms of hydration rate enhancement.
CHRYSO®Fluid Optima 245 EMx is especially recommended for concrete requiring high early age and long term strengths, whilst maintaining the workability which include High volume fly ash and Slag.

CHRYSO®Fluid Optima 245 EMx enables the production of concrete with very low W/C ratios.

CHRYSO®Fluid Optima 245 EMx enables the production of self-leveling concrete.

■ Benefits

• **CHRYSO®Fluid Optima 245 EMx** provides a cost effective means to produce user friendly high volume fly ash (HVFA) and slag concrete offering normal setting characteristics, controlled heat of hydration, improved Workability & finish ability, enhanced strength development and superior hardened concrete properties. .

• Improves the efficiency of cement in concrete, effectively reducing the quantity of cement required to achieve specified concrete properties. Better cement efficiency means **less CO2. Pollution**.

■ Areas of Application

CHRYSO®Fluid Optima 245 EMx is recommended for all concrete mixes where the usage of high volume fly ash and slag, without effecting the setting time and early strength and match the normal concrete properties.

1. High volume Fly Ash Concrete(HVFAC)
2. High volume Slag Concrete (HVSC)
3. All types of cement
4. Heavy prefabrication
5. High performance concrete
6. Pre-stressed concrete
7. Ready-mix concrete
8. Concrete of humid, plastic or fluid consistency
9. Self-levelling concrete
10. Compatible with Micro silica and other cementitious materials.

M C T CORROTECH® Construction Chemicals

CHRYSO CHEMICAL SOLUTIONS FOR THE CONSTRUCTION MATERIALS INDUSTRY

www.chryso.com

Concrete admixture

Technical Datasheet

■ Description:

Characteristics:
CHRYSO®Fluid Optima 245 EMx is a chemically stable liquid.

1.Nature : liquid
2.Colour : Brownish yellow
3.Density : 1.100 ± 0.020
4.pH : 6 ± 2
5.Cl^- ion content : nil to EN 934 and BS 5075
6.Na_2O equiv. : ≤ 1.0 %

CHRYSO®Fluid Optima 245 EMx does not contain any purposely added calcium chloride or other chloride based components. It will not promote or contribute to corrosion of reinforcing steel in concrete.

Packaging:
– Bulk
– Cubitainers: 1000 L
– Plastic barrels : 215 L
– Drums: 60 L

Standard specifications:
Conforms to ASTM C 494 Type E and F.

■ Directions for use:

Dosage

between 0.3 and 3.0 kg per 100 kg of cement.
A 0.8 % dosage of the product to the weight of cement is Commonly used.
CHRYSO®Fluid Optima 245 EMx can be added to the water before mixing the concrete. However, it can be added to the concrete after mixing.

Dosage rates of **CHRYSO®Fluid Optima 245 EMx** are dependent upon desired concrete performance characteristics and variables including cement quantity and chemistry, concrete temperature and curing conditions.

Because local job conditions vary, please contact your local Chryso sales representative for further assistance if using outside recommended dosage ranges.

Compatibility
CHRYSO®Fluid Optima 245 EMx is compatible with all types of Portland cement, class C and F fly ash, slag, microsilica, calcium chloride, fibers and approved air entraining admixtures.

Precaution:
• Store away from frost. Use **CHRYSO®Fluid Optima 245 EMx** at a temperature superior to 0°C.
• Should the product freeze, its properties can be recovered after thawing and agitating thoroughly.
• This product must be stored in plastic containers, but not in PVC.
• Shelf life: 12 months.

■ Safety:

CHRYSO®Fluid Optima 245 EMx is not considered dangerous to handle. Please refer to the material safety data sheet for additional information.

About CHRYSO:
CHRYSO is a subsidiary of the multi-billion dollar specialty construction chemicals Group, Materis.
Worldwide leader for Concrete and Cement additives, **CHRYSO** has been servicing the construction Industry for over half a century with outstanding innovation and service.
As a result, **CHRYSO**'s name and products have been associated with the most prestigious and demanding construction projects worldwide.

Manufactured under License by,

CORROTECH® M C T
Construction Chemicals

Tel: +971 (04) 811 2100 Fax: +971 (04) 811 2101
P. O. Box: 8344, Dubai, U.A.E. Website: mctuae.com

Annex E: Technical data sheet of Admix CR152 – Retarding admixture

ACP
ADMIXTURES & CONCRETE RELATED PRODUCTS

ADMIX CR 152

HIGH PERFORMANCE RETARDING/PLASTICIZING ADMIXTURE

PRODUCT

ADMIX CR 152 is a high performance retarding admixture developed to maintain high workability retention and to increase the initial and final setting times of concrete especially in high ambient temperature (hot weather concrete).

PROPERTIES

ADMIX CR 152:

- Allows extra time for concrete casting in mass structures and densely reinforced structural elements, thus reducing the risk of cold joint development.
- Improves surface finish and minimizes early development of plastic shrinkage cracking.
- Increases the ultimate strength of the concrete.

SCOPE OF USE

ADMIX CR 152 is ideal to use in hot weather conditions where slump retention over time is important for transport and placement of concrete.

- Transported concrete
- General reinforced concrete
- Ready-mix concrete
- Heavy prefabrication
- Pumped concrete
- Concrete piling

CHARACTERISTICS

Appearance	Liquid
Color	Light yellowish
Specific gravity at 20°C	1.103 - 1.108
Chloride content	Zero to BS 5075
Air entrainment	Up to 1% depending on the dosage and mix design

APPLICABLE STANDARDS

ADMIX CR 152 complies with:
ASTM C 494 Type B
BS 5075 Part – 1, BS EN 934, Part 2.

INSTRUCTION FOR USE

ADMIX CR 152 is totally miscible in water. It is to be added to the concrete mix during the mixing cycle at the same time as the water. No extension to normal mixing time is required.

DOSAGE

Trials should be conducted to determine the optimum dosage of ADMIX CR 152 for a particular mix. A dosage of 150 to 350 ml per 100 kg of cementitious materials is recommended. This may be changed to higher dosage in high ambient and mix temperature conditions.

EFFECTS OF OVER DOSING

A severe over dose of ADMIX CR 152 will result in the following:

- Delay of the initial and final set
- Increase in workability

Providing it is properly cured, the ultimate strength of the concrete will not be adversely affected and will generally be higher than of the normal concrete without ADMIX CR 152.

COMPATIBILITY

ADMIX CR 152 can be used in all types of portland and sulfate-resisting cements and concrete with cementitious materials used as cement replacement. ADMIX CR 152 should be dispensed directly into the mixer and should not be pre-mixed with other admixtures. If other admixtures are to be used in concrete containing ADMIX CR 152, they must be dispensed separately. Consult the company's technical dept. for advice.

SPECIFICATION CLAUSE

ADMIX CR 152, a retarding concrete admixture manufactured to the following specification:
ADMIX CR 152 can be used in all concrete mixes as mentioned, at dosage between 150 and 350 ml per 100 kg of cementitious materials in accordance with the manufacturer's instructions.

DISPENSING

It is preferable that liquid admixtures for concrete should be introduced into a mixer by means of automatic dispensing equipment. Such equipment can be supplied by the company

PACKAGING

ADMIX CR 152 is supplied in:
Bulk, barrels.
Storage tanks can be provided for bulk use.

SODAMCO

ADMIX CR 152

STORAGE
ADMIX CR 152 can be stored up to 1 year from manufacturing date under cover, out of direct sunlight and protected from extreme temperatures.

HEALTH & SAFETY
In case of frost, the product recovers its properties after progressive thawing and homogenizing by agitation. In case of contact with skin or eyes, rinse thoroughly with water. If irritation persists, seek medical attention. If swallowed, do not induce vomiting and seek medical attention.

QUALITY STATEMENT
All our products are manufactured to comply with our internal QA/QC program and quality management system to ensure consistency and quality.

DISCLAIMER

NOTE

Edition: 06/07-A
*Available only in UAE

SODAMCO Holding Tayar Center Bloc B 1st flr. De Gaulle str. P.O.Box 55-654 Sin el Fil Beirut Lebanon
T +961 1 510863/4 M +961 3 380748 F +961 1 510862 sodamco@sodamco.com www.sodamco.com

Lebanon . UAE . Syria . Qatar . KSA . Jordan . kuwait

Annex F: Technical data sheet of Micro-air 100 – Air entraining admixture

BASF
The Chemical Company

MICRO-AIR® 100

Air-entraining admixture for concrete

Description
MICRO-AIR® 100 is an air-entraining admixture, which creates ultra-stable air bubbles that are strong, small and closely spaced.

Applications
Entraining a controlled air content in a wide range of concrete types :

- Normal mix designs.
- Low slump concrete.
- Concrete containing high carbon content fly ash.
- Concrete containing large amounts of fine materials.
- Concrete using high-alkali cements.
- High temperature concrete.
- Concrete with extended mixing times.

Advantages
MICRO-AIR® 100 is especially useful in the types of concrete known for their difficulty to entrain and maintain the air content desired. Entrainment of the optimum air content in concrete results in the following improvements to quality:

- Increased freeze / thaw resistance.
- Reduced permeability - increased watertightness.
- Reduced segregation and bleeding.
- Improved plasticity and workability.
- Increased resistance to scaling.
- Greatly improved stability of air entrainment.
- Ready to use - solution is at optimum strength for accurate dispensing.

MICRO-AIR® 100 is compatible with concrete containing other admixtures or admixture systems - water-reducers, high-range water reducers, accelerators, retarders, densifiers and water repellents. It also increases the entrained air content of concrete made with air-entraining Portland Cement.
The use of MICRO-AIR® 100 with BASF admixtures forms a desirable combination for producing the highest quality, normal or lightweight concrete.

Packaging
MICRO-AIR® 100 is supplied in 210 litre drums and bulk delivery as appropriate.

Typical properties
Properties listed are only for guidance and are not a guarantee of performance

Specific gravity:	0.986 - 1.036
pH:	10.5 - 12.5
Colour:	Amber - brown
Dry extract (%):	11.6 - 13.5
Chloride content:	Nil to BS 5075: 1982
Flash point:	Not applicable
Freeze point:	-1°C

Standards
MICRO-AIR® 100 meets the requirements of:
ASTM C-260-86
AASHTO M-154
CRD-C 13-77
BS 5075: 1982 Part 2
DIN 1048 Part 1

Figure 1 Air content vs mixing time

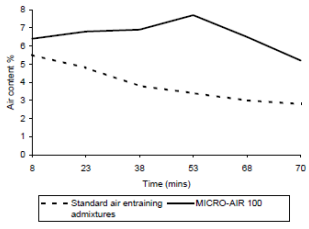

Adding Value to Concrete

BASF
The Chemical Company

MICRO-AIR® 100

1. In accordance with ASTM C-182: 3 minutes mix, 3 minutes rest followed by 2 minutes final mixing.
2. 13 minutes agitation and 2 minutes mixing.
3. Retempered and 2 minutes mixing time.

The graph represents the average of a number of laboratory and field evaluations data. The tests were conducted on concrete mixes known for their difficulty to entrain and maintain the desired air content. These mixtures contained large amounts of fine materials, high carbon content fly ash, high alkali cements, high concrete temperatures and low slumps.

Application procedure

As stated in ACI 212 and other publications, when two or more admixtures are used, they must be added to the mix separately (through dispensers or manually) and must not be mixed with each other prior to adding to the concrete mix.

For optimum, consistent performance, the air-entraining admixture should be dispensed on damp, fine aggregate.

Add MICRO-AIR® 100 admixture to the concrete mix using a dispenser designed for air-entraining admixtures; or add manually using a suitable measuring device that ensures accuracy within ±3% of the required amount.

Dosage

There is no standard dosage rate for MICRO-AIR® 100 admixture. The exact quantity of air-entraining admixtures needed should be determined by trial mixes. Factors are: temperature, cement, sand grading, sand-aggregate ratio, slump, means of conveying and placement, use of extra fine materials such as fly ash and micro silica.

The amount of MICRO-AIR® 100 admixture used will depend upon the amount of entrained air required under actual job conditions. In a trial mix, use 100ml / 100kg of cement and adjust in the light of results obtained. In mixes containing water-reducing, set-controlling admixtures, the amount of MICRO-AIR® 100 needed is somewhat less than the amount required in plain concrete.

Storage

MICRO-AIR® 100 admixture should be stored and dispensed at 2°C or higher. Although freezing does not harm this product, precautions should be taken to protect it from freezing. If it freezes, thaw and reconstitute by mild mechanical agitation. Do not use pressurised air for agitation. Shelf life is 12 months when stored as above.

Safety precautions

MICRO-AIR® 100 is a caustic solution. In case of contact with skin, eyes or clothing, immediately flush the exposed area with water for at least 15 minutes. Remove contaminated clothing and shoes. Call a doctor - especially if contact is with eyes. Wash clothing before re-use and discard shoes. Always keep the product out of the reach of children.

Quality and care

All products originating from BASF's Dubai, UAE facility are manufactured under a management system independently certified to conform to the requirements of the quality, environmental and occupational health & safety standards ISO 9001, ISO 14001 and OHSAS 18001.

01/95 BASF_CC-UAE revised 04/2004

BASF Construction Chemicals UAE LLC
P.O. Box 37127, Dubai, UAE
Tel: +971 4 8090800 Fax: +971 4 8851002
www.basf-cc.ae e-mail: marketingcc.mideast@basf.com

Certificate No. 963680
Certificate No. 945787
Certificate No. 772556

Annex G: Mix design of the cement type series

No	Reference	w/c	Cementitious Materials											Aggregates					Admixture	
			Total	PC		GGBS		FA		MS		RHA		20mm	10mm	5mm Washed	Dune Sand	Water	Superplasticizer	Retarder
			kg	%	kg	%	kg	%	kg	%	kg	%	kg	kg	kg	kg	kg	kg	% by wt of total cement content	
1	1P30S70W	0.25	400	30	120	70	280	-	-	-	-	-	-	647	438	678	303	100	1.75	0.25
2	2P30S70W	0.32	400	30	120	70	280	-	-	-	-	-	-	632	422	642	291	128	0.56	0.25
3	3P30S70W	0.4	400	30	120	70	280	-	-	-	-	-	-	633	384	614	269	160	0.54	0.21
4	1P0S100W	0.25	400	0	0	100	400	-	-	-	-	-	-	642	435	673	300	100	2.00	0.25
5	1P2.5S97.5W	0.25	400	2.5	10	97.5	390	-	-	-	-	-	-	643	435	674	301	100	2.00	0.25
6	1P5S95W	0.25	400	5	20	95	380	-	-	-	-	-	-	643	436	674	301	100	1.87	0.25
7	1P15S85W	0.25	400	15	60	85	340	-	-	-	-	-	-	642	435	673	301	100	1.87	0.25
8	2P0S100W	0.32	400	0	0	100	400	-	-	-	-	-	-	638	418	638	280	128	1.25	0.25
9	2P2.5S97.5W	0.32	400	2.5	10	97.5	390	-	-	-	-	-	-	638	419	638	280	128	0.87	0.25
10	2P5S95W	0.32	400	5	20	95	380	-	-	-	-	-	-	638	419	638	280	128	0.50	0
11	2P15S85W	0.32	400	15	60	85	340	-	-	-	-	-	-	638	419	638	280	128	0.62	0.25
12	3P0S100W	0.4	400	0	0	100	400	-	-	-	-	-	-	609	400	609	267	160	0.62	0.25
13	3P2.5S97.5W	0.4	400	2.5	10	97.5	390	-	-	-	-	-	-	609	400	609	267	160	0.62	0
14	3P5S95W	0.4	400	5	20	95	380	-	-	-	-	-	-	610	400	610	267	160	0.50	0
15	3P15S85W	0.4	400	15	60	85	340	-	-	-	-	-	-	610	400	610	267	160	0.42	0.25
16	1P20F80W	0.25	400	20	80	-	-	80	320	-	-	-	-	644	422	644	282	100	1.50	0.25
17	2P20F80W	0.32	400	20	80	-	-	80	320	-	-	-	-	619	406	619	271	128	0.40	01.2
18	3P20F80W	0.4	400	20	80	-	-	80	320	-	-	-	-	590	387	590	259	160	0.30	0.12
19	1P90M10W	0.25	400	90	360	-	-	-	-	10	40	-	-	674	442	674	296	100	1.75	0.25
20	2P90M10W	0.32	400	90	360	-	-	-	-	10	40	-	-	649	426	649	285	128	1.62	0.25
21	3P90M10W	0.4	400	90	360	-	-	-	-	10	40	-	-	620	407	620	272	160	1.25	0.25
22	1P80R20W	0.25	400	80	320	-	-	-	-	-	-	20	80	673	441	673	295	100	4.37	0.25
23	2P80R20W	0.32	400	80	320	-	-	-	-	-	-	20	80	647	425	647	284	128	2.37	0.25
24	3P80R20W	0.4	400	80	320	-	-	-	-	-	-	20	80	619	406	619	271	160	1.00	0.12

Annex H: Mix designs of the sand type series

No	Reference	w/c	Cementitious Materials											Aggregates				Water	Admixture	
			Total	PC		GGBS		FA		MS		RHA		20mm	10mm	5mm Unwashed	Dune Sand		Superplasticizer	Retarder
			kg	%	kg	%	kg	%	kg	%	kg	%	kg	kg	kg	kg	kg	kg	% by wt of total cement content	
1	1P30S70U	0.25	400	30	120	70	280	-	-	-	-	-	-	647	438	673	303	100	2.25	0.25
2	2P30S70U	0.32	400	30	120	70	280	-	-	-	-	-	-	632	422	638	291	128	0.87	0.25
3	3P30S70U	0.4	400	30	120	70	280	-	-	-	-	-	-	633	384	609	269	160	0.50	0.12
4	1P0S100U	0.25	400	0	0	100	400	-	-	-	-	-	-	642	435	668	300	100	1.62	0
5	2P0S100U	0.32	400	2.5	10	97.5	390	-	-	-	-	-	-	638	418	633	280	128	0.62	0
6	3P0S100U	0.4	400	5	20	95	380	-	-	-	-	-	-	609	400	605	267	160	0.42	0
7	1P20F80U	0.25	400	20	80	-	-	80	320	-	-	-	-	644	422	639	282	100	1.25	0.12
8	2P20F80U	0.32	400	20	80	-	-	80	320	-	-	-	-	619	406	614	271	128	0.50	0.12
9	3P20F80U	0.4	400	20	80	-	-	80	320	-	-	-	-	590	387	586	259	160	0.45	0.12
10	1P90M10U	0.25	400	90	360	-	-	-	-	10	40	-	-	674	442	669	296	100	2.12	0.25
11	2P90M10U	0.32	400	90	360	-	-	-	-	10	40	-	-	649	426	644	285	128	1.75	0.25
12	3P90M10U	0.4	400	90	360	-	-	-	-	10	40	-	-	620	407	615	272	160	1.25	0.25
13	1P80R20U	0.25	400	80	320	-	-	-	-	-	-	20	80	673	441	668	295	100	5.00	0.25
14	2P80R20U	0.32	400	80	320	-	-	-	-	-	-	20	80	647	425	643	284	128	2.50	0.25
15	3P80R20U	0.4	400	80	320	-	-	-	-	-	-	20	80	619	406	614	271	160	1.12	0.12

Annex I: Mix designs of the Recycled concrete aggregate (100% GGBS) series

No	Reference	RCA proportions	w/c	Cementitious materials		Aggregates						Water	Admixture	
				PC	GGBS	20mm R*	10mm R	20mm N*	10mm N	5mm Washed	Dune Sand		Superplasticizer	Retarder
				kg	kg	kg	kg	kg	kg	kg	kg	kg	% by wt of total cement content	
1	1R100N0W	100R	0.25	0	100	601	396	-	-	663	291	100	1.50	-
2	2R100N0W	100R	0.32	0	100	569	372	-	-	648	289	128	0.62	-
3	3R100N0W	100R	0.4	0	100	544	356	-	-	618	276	160	0.50	-
4	1R80N20W	80R+20N	0.25	0	100	492	327	119	78	663	291	100	1.75	-
5	2R80N20W	80R+20N	0.32	0	100	470	312	118	78	638	280	128	0.62	-
6	3R80N20W	80R+20N	0.4	0	100	449	297	112	75	609	267	160	0.45	-
7	1R50N50W	50R+50N	0.25	0	100	313	209	313	210	663	291	100	1.62	-
8	2R50N50W	50R+50N	0.32	0	100	301	201	301	202	638	280	128	0.62	-
9	3R50N50W	50R+50N	0.4	0	100	288	192	287	193	609	267	160	0.27	-
10	1R100N0U	100R	0.25	0	100	601	396	-	-	658	291	100	1.8	-
11	2R100N0U	100R	0.32	0	100	569	372	-	-	643	289	128	0.75	-
12	3R100N0U	100R	0.4	0	100	544	356	-	-	614	276	160	0.60	-
13	1R80N20U	80R+20N	0.25	0	100	492	327	119	78	658	291	100	1.8	-
14	2R80N20U	80R+20N	0.32	0	100	470	312	118	78	633	280	128	0.62	-
15	3R80N20U	80R+20N	0.4	0	100	449	297	112	75	605	267	160	0.52	-
16	1R50N50U	50R+50N	0.25	0	100	313	209	313	210	658	291	100	1.75	-
17	2R50N50U	50R+50N	0.32	0	100	301	201	301	202	633	280	128	0.50	-
18	3R50N50U	50R+50N	0.4	0	100	288	192	287	193	605	267	160	0.42	-

* R = Recycled concrete aggregate N = Natural crushed limestone aggregate

Annex J: Mix designs of Recycled concrete aggregate (triple blend) series

No	Reference	RCA proportions	w/c	Cementitious materials						Aggregates						Water	Admixture	
				PC		GGBS		RHA		20mm R	10mm R	20mm N	10mm N	5mm Washed	Dune Sand		Superplasticizer	Retarder
				%	kg	%	kg	%	kg	kg	kg	kg	kg	kg	kg	kg	% by wt of total cement content	
1	1R0N100TB	100N	0.25	15	60	70	280	15	60	-	-	642	435	673	301	100	4.5	0.12
2	2R0N100TB	100N	0.32	15	60	70	280	15	60	-	-	618	419	648	289	128	1.87	0.12
3	3R0N100TB	100N	0.40	15	60	70	280	15	60	-	-	590	400	618	276	160	0.95	0.12
4	1R100N0TB	100R	0.25	15	60	70	280	15	60	601	396	-	-	663	291	100	4.27	0.25
5	2R100N0TB	100R	0.32	15	60	70	280	15	60	569	372	-	-	648	289	128	1.75	0.25
6	3R100N0TB	100R	0.40	15	60	70	280	15	60	544	356	-	-	618	276	160	0.92	0.12
7	1R50N50TB	50R+50N	0.25	15	60	70	280	15	60	313	209	313	210	663	291	100	-	-
8	2R50N50TB	50R+50N	0.32	15	60	70	280	15	60	301	201	301	202	638	280	128	1.75	0.25
9	3R50N50TB	50R+50N	0.40	15	60	70	280	15	60	288	192	287	193	609	267	160	0.87	0.25
10	1R20N80TB	20R+80N	0.25	15	60	70	280	15	60	119	78	492	327	663	291	100	-	-
11	2R20N80TB	20R+80N	0.32	15	60	70	280	15	60	118	78	470	312	638	280	128	-	-
12	3R20N80TB	20R+80N	0.40	15	60	70	280	15	60	112	75	449	297	609	267	160	-	-

Annex K: Mix design of the Air entrained concrete series

No	Reference	Air		w/c	Cementitious materials					Aggregate				Water	Admixture		
		Design	Actual		Total	PC		MS		20mm	10mm	5mm Unwashed	Dune Sand		Superplasticizer	Retarder	Air entrainer
		%	%		kg	%	kg	%	kg	kg	kg	kg	kg	kg	kg	% by wt of total cement content	
1	1P90M10A2	2	1.1	0.25	400	90	360	10	40	674	442	674	296	100	1.75	0.25	0
2	2P90M10A2	2	1.2	0.32	400	90	360	10	40	649	426	649	285	128	1.62	0.25	0
3	3P90M10A2	2	1.0	0.4	400	90	360	10	40	620	407	620	272	160	1.25	0.25	0
4	1P90M10A5	5	4.8	0.25	400	90	360	10	40	647	424	647	284	100	1.87	0.25	0.17
5	2P90M10A5	5	5.1	0.32	400	90	360	10	40	622	408	622	273	128	1.50	0.25	0.12
6	3P90M10A5	5	5.3	0.4	400	90	360	10	40	593	389	593	260	160	0.25	0.25	0.10
7	1P90M10A10	10	9.8	0.25	400	90	360	10	40	602	395	602	264	100	1.87	0.25	0.45
8	2P90M10A10	10	9.5	0.32	400	90	360	10	40	577	378	577	253	128	1.50	0.25	0.37
9	3P90M10A10	10	9.5	0.4	400	90	360	10	40	548	360	548	240	160	0.82	0.25	0.30
10	1P90M10A15	15	12	0.25	400	90	360	10	40	557	365	557	244	100	1.87	0.25	1.12
11	2P90M10A15	15	12	0.32	400	90	360	10	40	532	349	532	233	128	1.25	0.25	1.00
12	3P90M10A15	15	11.8	0.4	400	90	360	10	40	503	330	503	221	160	0.52	0.25	1.00

Annex L: Mix designs of the higher curing temperatures series

No	Reference	w/c	Cementitious materials							Aggregates				Water	Admixture	
			Total	PC		GGBS		RHA		20mm	10mm	5mm Washed	Dune Sand		Superplasticizer	Retarder
			kg	%	kg	%	kg	%	kg	kg	kg	kg	kg	kg	% by wt of total cement content	
1	1P5S70R25W	0.25	400	5	20	70	280	25	100	639	433	670	299	100	5.50	0.12
2	2P5S70R25W	0.32	400	5	20	70	280	25	100	615	416	645	288	128	2.50	0.12
3	3P5S70R25W	0.4	400	5	20	70	280	25	100	587	398	615	275	160	1.25	0.12
4	1P15S70R15W	0.25	400	15	60	70	280	15	60	642	435	673	301	100	4.50	0.12
5	2P15S70R15W	0.32	400	15	60	70	280	15	60	618	419	648	289	128	1.87	0.12
6	3P15S70R15W	0.4	400	15	60	70	280	15	60	590	400	618	276	160	0.95	0.12

Annex M: Cement Test certificate: National Cement Co, UAE

شركة الأسمنت الوطنية.ش.م.ع
National Cement Co p.s.c.

CEMENT TEST CERTIFICATE

CEMENT TYPE : PORTLAND CEMENT
COMPLYING WITH BS:12/1996 -STRENGTH CLASS 42.5N
WEEKLY PRODUCTION :(09.04.2011 - 15.04.2011)

I. CHEMICAL COMPOSITION

CHARACTERISTICS	UNIT	REQUIREMENTS LOWER LIMIT	REQUIREMENTS UPPER LIMIT	VALUE OBTAINED
LOSS ON IGNITION (LOI)	%	N.S.	3.00	2.90
INSOLUBLE RESIDUE	%	N.S.	1.50	0.29
TOTAL SULPHUR(EXPRESSED AS SO3)	%	N.S.	3.50	2.68
CHLORIDE CONTENT	%	N.S.	0.10	0.01
TOTAL ALKALI(Na2O + 0.658K2O)	%	N.S.	N.S.	0.50
TRICALCIUM ALUMINATE(C3A)	%	N.S.	N.S.	7.28
CLINKER ANALYSIS:				
SILICON DIOXIDE(SIO2)	%	N.S	N.S	21.67
ALUMINIUM TRIOXIDE(AL2O3)	%	N.S	N.S	5.41
FERRIC OXIDE(FE2O3)	%	N.S	N.S	3.94
CALCIUM OXIDE (CaO)	%	N.S	N.S	65.98
MAGNESIUM OXIDE (MgO)	%	N.S	5.00	1.24

II. PHYSICAL TESTS

FINENESS:				
SPECFIC SURFACE AIR PERMEABILITY TEST (BLAINE TEST)	M2/KG	N.S.	N.S.	330.00
SOLNDNESS:				
LE-CHATELIER EXPANSION TEST	mm	N.S.	10.00	1.00
SETTING TIME:				
VICAT TEST				
INITIAL SETTING TIME	Mint.	60.00	N.S.	160.00
FINAL SETTING TIME	Mint.	N.S.	N.S.	255.00
STRENGTH:(MORTAR PRISMS)				
COMPRESSIVE STRENGTH				
7DAYS	N/mm2	N.S.	N.S.	41.80
28DAYS ON DATE(12.03.11 - 18.03.11)	N/MM2	42.50	62.50	55.00

We certify that the cement is from fresh stock, newly manufactured and complies from the chemical and physical points of view with **BS:12/1996**.

(MOHAMED MAJED NOUH)
CHIEF OF WORKS LABORATORY

Date: 25.04.2011

Form: WLP 10F DT 1.1.96 Rev.0
Distribution : SM/CUSTOMER
File : CVL/SM

Commercial Registration No. 41150
Authorised and paid up Share Capital
A E D 3 5 8 , 8 0 0 , 0 0 0
P.O. Box 4041 Dubai - United Arab Emirates
Tel.: +971-4-3388885, Fax: +971-4-3388886
E-mail: cement@nationalcement.ae

Annex N: Cement Test certificate: UK Cement

مختبر علوم التربة لفحص المواد

GEOSCIENCE TESTING LABORATORY

ANALYSIS REPORT ON OPC

LABORATORY RESULTS

Report No. : R2DX14-7957/1 Date : 26/06/2014

Request No. : Q2DX14-7957 Sample No. : S2DX14-7957

Client Name	Abu Saleh
Client Address	Dubai, UAE
Project Name	Not Given
Project No.	Not Given
Consultant	No Specific Consultant
Contractor	No Specific Contractor
Sampled on / Received on	Not Given / 15.06.2014
Sampled by	Client's Representative
Sample brought in by	Client's Representative
Sample Description	**Ordinary Portland Cement (OPC)**
Source of Sample	UK
Sampled from (Location)	UK
Sender Reference	Not Given
Sampling Method	Not Given
Sampling Report No.	Not Given
Appearance	Not Applicable
Lot No / Lot Size / Local Supplier	Not Given / Not Given / Not Given
Sample Container / Size	Plastic Bag / Not Given

RESULTS OF CHEMICAL ANALYSIS : **Date of Analysis : 15/06/2014 - 25/06/2014**

PARAMETER		TEST METHOD (REFERENCE NO.)	UNIT	SPECIFICATION LIMITS BS EN 197-1 : 2000 - CEM I 42.5 N (MAX)	RESULT
Insoluble Residue	(IR)	BS EN 196 Part 2 : 2005	%	5.0	0.51
Silicon Dioxide	as SiO_2		%	-	20.36
Aluminum Oxide	as Al_2O_3		%	-	5.10
Calcium Oxide	as CaO		%	-	64.56
Magnesium Oxide	as MgO		%	-	1.95
Chloride	as Cl		%	0.10	0.01
Sulfate	as SO_3		%	3.5	3.09
Loss On Ignition	(LOI)		%	5.0	2.68
Tricalcium Aluminate	(C_3A)		%	-	7.42
Ferric Oxide	as Fe_2O_3	ASTM C 114 : 2000	%	-	3.60
Sodium Oxide	as Na_2O	APHA / AWWA - 3120 B	%	-	0.20
Potassium Oxide	as K_2O		%	-	0.51
Equivalent Alkalies			%	-	0.54

Test Method Variation : None Tested by : AJS / KA

References : BS EN & APHA - AWWA Standards.

Remarks : The tested specimen complies with the requirements of BS EN 197-1:2000 Class CEM I 42.5 N for the above parameters.

GEOSCIENCE TESTING LABORATORY
Plot No.531-519
Dubai Industrial City
Tel.: 04-431 4690
Fax: 04-431 4570
P.O.Box:61670, Dubai, UAE.

• Results relates only to the items tested.
• Report shall not be reproduced (except in full) without written approval of the Laboratory.

Form : CH - 35 Issue : 01 / 01.08.2001 Rev : 05 / 21.04.2011
Page 1 of 1

Rosana M. Oquendo
Department In Charge
(Chemical)

For GEOSCIENCE TESTING LABORATORY

Dubai : P.O.Box 61670, Tel : +971-4-431 4690, Fax : +971-4-431 4570
Sharjah (Khorfakhan) : P.O. Box: 64800, Tel : +971-9-238 9824, Fax : +971-9-238 9826
Website : www.geoscience.ae E-mail : info@gtl.ae

Annex O: GGBS test certificate

شركة سوبر سمنت الصناعية ذ.م.م.
Super Cement Manufacturing Company L.L.C.

TEST CERTIFICATE

Test report for Ground Granulated Blast Furnace Slag in compliance with BS 6699:1992

Week No.:13/2011 Date:09.04.2011.

Period : 26.03.2011. – 01.04.2011.

Physical Tests			Chemical Tests		
Characteristics	Requirement	Result	Composition (%)	Requirement	Result
Moisture %	1.0 max	0.32	Loss on ignition -LOI	3.00 max	0.34
			Insoluble residue -IR	1.5 max	0.66
Fineness-			Silicon dioxide -SiO2	No limit	34.50
Sp. Surface Area -M2/Kg	275 min	437	Alumina – Al2O3	No limit	13.80
Residue 45 micron -%	No limit	1.68	Iron oxide – Fe2O3	No limit	1.12
			Calcium oxide – CaO	No limit	42.40
Setting time –			Magnesium oxide – MgO	14.0 max	6.20
Initial –minutes	60 min	205	Sulphur trioxide – SO3	2.5 max	0.24
Final – minutes	No limit	310	Sulphide sulphur – 'S'	1.5 max	0.62
			Sodium oxide – Na2O	No limit	0.24
Soundness –			Potassium oxide – K2O	No limit	0.30
Le-Chat. Expn. –mm	10 max	0.50	Chloride – Cl	0.10 max	0.008
			Manganese oxide – MnO	2.0 max	0.52
Compressive strength –					
(Mortar prism)					
Portland Cement (PC)					
2 days – N/mm2	10.0 min	32.80	Chemical modules –		
7 days – N/mm2	No limit	45.50			
28 days –N/mm2*	42.5 min	57.90	(CaO+MgO+SiO2)	66.67 min	83.10
	62.5 max				
70% GGBS+30% PC			(CaO+MgO)/SiO2	1.0 min	1.41
2 days – N/mm2	No limit	11.50			
7 days – N/mm2	12.0 min	30.30	CaO/SiO2	1.4 max	1.23
28 days –N/mm2*	32.5 min	45.10			
*28 days strength of Week No. 10/2011			The testing was carried out at 22 (+/-) degree centigrade and results meet the BS 6699:1992 limits.		

We certify that quality of GGBS conforms to the specification as stated above.

Chief Chemist

Manager Quality Control

TUV NORD ISO 9001
TUV NORD ISO 14001
TUV NORD OHSAS 18001

Plot No.33 & 34 FR6, Sector M-41, ICAD-I - Musaffah Industrial Area
Phone: +971-25502458 Fax: +971-25502203 P.O. Box No. 35119 Abu Dhabi, U.A.E

Annex P: Fly ash test certificate

AL HOTY - STANGER LABORATORIES

مختبرات الحوطي ستانجر

TEST REPORT

CLIENT **XTRAMIX CONCRETE SOLUTIONS L.L.C.**

ANALYSIS OF FLY ASH SAMPLE

Report date : 03.06.11

Report number	**: A11 – 167986 – 1**	**Source**	**: India**
		Sample location	**: Xtramix Batching Plant**
Project number	**: Various**	**Sampled by**	**: Xtramix Technician**
Project name	**: Various**	**Sampling date/time**	**: 05.05.11/1030 Hrs**
Project location	**: Various**	**Sampling method**	**: Random**
Consultant	**: Various**	**Sample delivered by**	**: Client's Rep.**
Contractor	**: Various**	**Sample receiving date/time**	**: 21.05.11/1400 Hrs.**
Client ref./req. no	**: Not specified**	**Date tested**	**: 28.05.11 ~ 02.06.11**
Sample description as identified by the client	**: Fly Ash**	**Tested by**	**: SF – AUH**
		Test Method	i) BS EN 196 – P:2:2005 ii) ICP – OES

Results :

Parameters	Units	Results	Specification limits BS 3892-1984
Moisture content at 100 ± 3°C	% by weight	**0.07**	**0.5 (max.)**
Loss on Ignition at 950°C (LOI)	% by weight	**2.64**	**7 (max.**
Silicon Dioxide (SiO_2)	% by weight	**61.3**	--
Aluminium Oxide (Al_2O_3)	% by weight	**26.8**	--
Ferric Oxide (Fe_2O_3)	% by weight	**3.13**	--
Calcium Oxide (CaO)	% by weight	**1.1**	--
Magnesium Oxide (MgO)	% by weight	**0.8**	**4 (max.)**
Manganese Trioxide (Mn_2O_3)	% by weight	**0.07**	--
Sulphur Trioxide (SO_3)	% by weight	**0.23**	**2.5 (max.)**
Sodium Oxide (Na_2O)	% by weight	**0.43**	--
Potassium Oxide (K_2O)	% by weight	**2.16**	--
Free Calcium Oxide (F.CaO)	% by weight	**0.81**	--
Chloride (Cl)	% by weight	**0.01**	--

Remarks : None
Test method variation : None

AHSL certifies that the above tests were carried out in accordance with BS EN 196 – P:2:2005 & ICP - OES
This report relates only to the sample tested and shall only be reproduced in full and with the written approval of AHS Laboratories.

Jayakumar K.A.
Head of Analytical Section
/vu

AL HOTY-STANGER LABORATORIES

Mohammed Mansoor
Laboratory Manager
For Al Hoty Stanger Laboratories

ISO 9001 CERTIFIED BY BUREAU VERITAS

DU[illegible] U.A.E.,
P.O. BOX 16756
TEL.: (04) 3472201
FAX : (04) 3472727

ABU DHABI, U.A.E.,
P.O. BOX 31039
TEL. : (02) 5542234
FAX. : (02) 5547015

JABEL ALI, U.A.E.,
P.O. BOX 16756
TEL. : (04) 8818461
FAX : (04) 8818461

KALBA SHARJAH,
U.A.E.,
P.O. BOX 145133
TEL. : (09) 2779543
FAX : (09) 2779545

E-mail :
alhoty@emirates.net.ae

Annex Q: Microsilica test certificate

Elkem

CERTIFICATE OF CONFORMITY

Product	:	Elkem Microsilica
Grade	:	920 D, Densified
Standard	:	ASTM C 1240-05
Reference	:	809007406

This is to certify that the material shipped from under the above mentioned reference has been sampled and analysed for mandatory parameters of ASTM C 1240-05.
The material is part of a production, which is in conformity with this standard.

PARAMETER	UNIT	SPECIFICATION	ANALYSIS
Chemical Requirements			
SiO_2	%	Min 85.0	92.2
Loss on Ignition 975° C	%	Max 6.0	1.35
Moisture content	%	Max 3.0	0.18
Physical Requirements			
Specific Surface	m^2/g	Min 15	24.6
Pozz. Activity Index (7d)	%	Min 105	125
Bulk Density	Kg/dm^3	-	0.61

Norway, 2010-02-01

P.O Box 1782

Arne Skagen
Quality Manager

Annex R: Rice husk ash test certificate: Chemical tests

Arab Center المركز العربي
For Engineering Studies للدراسات الهندسية

REPORT ON CHEMICAL TESTING OF RICE HUSK ASH

Client	SEVEN STARS GEN. TRADING CO. LTD.	Report No.	ARM06-23123
Contractor	SEVEN STARS GEN. TRADING CO. LTD.	Date Reported	30 Nov 2006
Consultant	N.P.	Sample No.	ASM06-07725
Project No.	N.P.	Request No.	AQM06-07725
Project Name	Internal Testing	Client Reference	Letter dated 15/11/06
Sample Desc.	RICE HUSK ASH	Sampled By	Client
Source	SEVEN STARS GEN. TRADING CO. LTD.	Sampling Date	N.P.
Sample Location	N.P.	Sampl. Cert. Ref.	N.P.
Lot No.	N.P.	Sampling Method	N.P.
Lot Size	N.P.	Sample Size	5 Kg
Sample Prep.	N.P.	Sample Brt in by.	Client
Test Method	ASTM C 114 / ASTM C 1240	Date Received	15 Nov 2006
Test Method Var.	Nil	Date Tested	18-30 Nov 2006
Remarks	-	Tested by	SINDHU

No.	Constituents		Percent weight of material	
			Sample	Specification ASTM C 1240 : 00
1	Silicon Dioxide	SiO_2	90.10	Min 85.0
2	Ferric Oxide	Fe_2O_3	1.14	-
3	Aluminum Oxide	Al_2O_3	1.72	-
4	Calcium Oxide	CaO	0.41	-
5	Magnesium Oxide	MgO	0.94	-
6	Sodium Oxide	Na_2O	0.59	-
7	Potassium Oxide	K_2O	1.42	-
8	Sulphate	SO_3	0.03	-
9	Chloride	Cl	0.01	-
10	Loss on Ignition @ 1000°C	LOI	1.55	Max 3.0
11	Moisture Content (Dried @ 105°C)		0.88	Max 6.0

Arab Center for Engineering Studies
Dubai, U.A.E.

Annex S: Rice husk ash test certificate: Physical tests

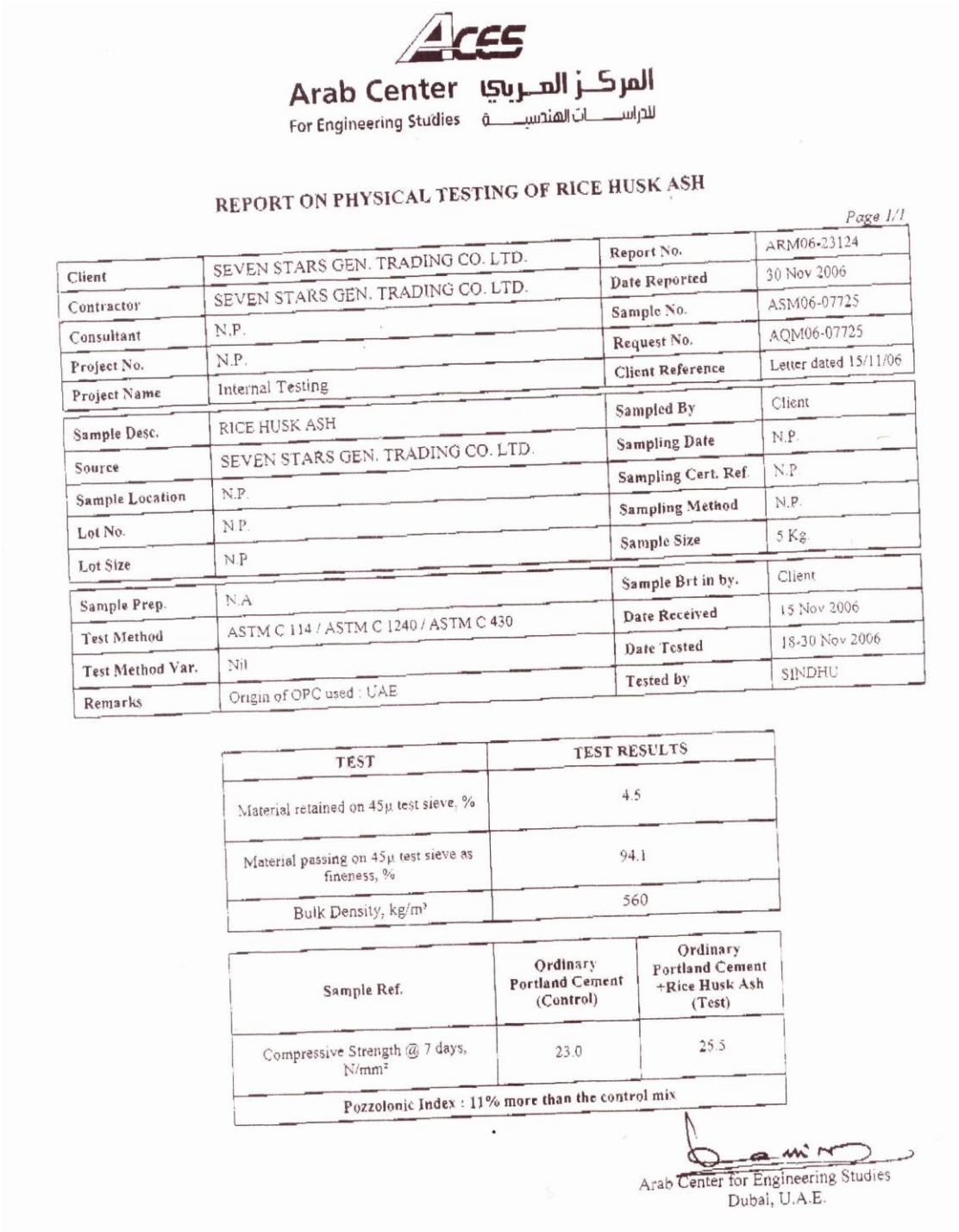

Arab Center المركز العربي
For Engineering Studies للدراسات الهندسية

REPORT ON PHYSICAL TESTING OF RICE HUSK ASH

Page 1/1

Client	SEVEN STARS GEN. TRADING CO. LTD.	Report No.	ARM06-23124
Contractor	SEVEN STARS GEN. TRADING CO. LTD.	Date Reported	30 Nov 2006
Consultant	N.P.	Sample No.	ASM06-07725
Project No.	N.P.	Request No.	AQM06-07725
Project Name	Internal Testing	Client Reference	Letter dated 15/11/06
Sample Desc.	RICE HUSK ASH	Sampled By	Client
Source	SEVEN STARS GEN. TRADING CO. LTD.	Sampling Date	N.P.
Sample Location	N.P.	Sampling Cert. Ref.	N.P.
Lot No.	N.P.	Sampling Method	N.P.
Lot Size	N.P.	Sample Size	5 Kg.
Sample Prep.	N.A	Sample Brt in by.	Client
Test Method	ASTM C 114 / ASTM C 1240 / ASTM C 430	Date Received	15 Nov 2006
Test Method Var.	Nil	Date Tested	18-30 Nov 2006
Remarks	Origin of OPC used : UAE	Tested by	SINDHU

TEST	TEST RESULTS
Material retained on 45μ test sieve, %	4.5
Material passing on 45μ test sieve as fineness, %	94.1
Bulk Density, kg/m³	560

Sample Ref.	Ordinary Portland Cement (Control)	Ordinary Portland Cement +Rice Husk Ash (Test)
Compressive Strength @ 7 days, N/mm²	23.0	25.5
Pozzolonic Index : 11% more than the control mix		

Arab Center for Engineering Studies
Dubai, U.A.E.

Annex T: Durability results – Cement type series

No	REF	RCPT, Coulomb			Absorption, %			Water Penetration, mm		
		Mean	Max	Min	Mean	Max	Min	Mean	Max	Min
1	1P0S100W	450.0	550.0	400.0	0.6	0.7	0.5	3.0	4.0	2.0
2	1P2.5S97.5W	735.0	805.0	600.0	0.5	0.6	0.5	0.0	0.0	0.0
3	1P5S95W	478.0	485.0	449.0	0.6	0.7	0.5	0.0	0.0	0.0
4	1P15S85W	648.9	787.7	559.0	1.2	1.4	1.0	6.0	8.0	4.0
5	1P30S70W	380.0	451.0	339.0	0.8	0.9	0.7	0.0	0.0	0.0
6	2P0S100W	535.0	586.0	500.0	0.6	0.7	0.6	3.0	4.0	1.0
7	2P2.5S97.5W	360.0	415.0	315.0	1.4	1.5	1.4	4.0	6.0	3.0
8	2P5S95W	389.0	442.0	325.0	1.5	1.6	1.5	5.3	6.0	4.0
9	2P15S85W	692.1	726.3	650.0	1.4	1.5	1.3	7.0	8.0	6.0
10	2P30S70W	254.0	271.0	241.0	0.7	0.8	0.6	0.0	0.0	0.0
11	3P0S100W	585.0	695.0	525.0	1.8	1.9	1.8	0.0	0.0	0.0
12	3P2.5S97.5W	538.0	613.0	500.0	1.9	1.9	1.9	5.0	5.0	5.0
13	3P5S95W	181.0	211.0	157.0	0.7	0.8	0.7	0.0	0.0	0.0
14	3P15S85W	744.3	843.9	689.0	1.2	1.3	1.0	7.0	8.0	6.0
15	3P30S70W	306.0	323.0	295.0	1.6	1.7	1.6	0.0	0.0	0.0
16	1P20F80W	253.0	261.0	247.0	0.5	0.6	0.5	2.8	3.9	1.5
17	2P20F80W	162.3	174.9	152.0	1.2	1.3	1.1	0.0	0.0	0.0
18	3P20F80W	274.8	295.4	254.0	1.4	1.5	1.3	0.0	0.0	0.0
19	1P90M10W	231.6	251.0	216.0	1.2	1.3	1.1	0.0	0.0	0.0
20	2P90M10W	185.1	191.3	179.0	1.2	1.4	1.1	0.0	0.0	0.0
21	3P90M10W	253.8	266.4	245.0	1.2	1.3	1.0	0.0	0.0	0.0
22	1P80R20W	287.1	303.3	277.0	0.7	0.9	0.6	0.0	0.0	0.0
23	2P80R20W	175.5	176.5	175.0	0.9	1.1	0.8	0.0	0.0	0.0
24	3P80R20W	198.9	211.0	185.7	1.3	1.5	1.2	0.0	0.0	0.0
25	1P15S70R15W	638.1	653.3	621.0	0.9	1.0	0.9	0.0	0.0	0.0
26	2P15S70R15W	647.1	659.3	632.0	0.7	0.8	0.7	3.0	3.5	2.5
27	3P15S70R15W	701.1	753.3	650.0	0.6	0.7	0.6	5.0	6.0	4.0

Annex U: Durability results – Sand type series

No	REF	RCPT, Coulomb			Absorption, %			Water Penetration, mm		
		Mean	Max	Min	Mean	Max	Min	Mean	Max	Min
1	1P0S100U	491.1	523.3	450.0	1.4	1.9	1.0	0.0	0.0	0.0
2	2P0S100U	508.4	515.2	500.0	1.8	2.0	1.5	0.0	0.0	0.0
3	3P0S100U	701.1	713.3	690.0	1.8	1.9	1.6	1.0	2.0	0.0
4	1P30S70U	475.2	500.0	455.6	0.7	1.0	0.6	0.0	0.0	0.0
5	2P30S70U	375.3	401.0	350.0	0.5	0.5	0.5	0.0	0.0	0.0
6	3P30S70U	342.0	355.0	326.0	0.7	0.9	0.5	0.0	0.0	0.0
7	1P20F80U	318.6	325.8	310.0	0.8	0.9	0.7	5.0	6.0	4.0
8	2P20F80U	612.0	698.0	536.0	0.9	1.0	0.8	5.0	6.0	4.0
9	3P20F80U	675.4	780.0	600.0	0.8	0.9	0.7	3.0	6.0	0.0
10	1P90M10U	324.0	352.0	299.0	0.7	1.0	0.5	2.0	3.0	1.0
11	2P90M10U	339.2	400.0	267.6	0.6	0.7	0.5	0.0	0.0	0.0
12	3P90M10U	541.8	600.0	500.0	0.8	1.0	0.5	0.0	0.0	0.0
13	1P80R20U	195.3	207.9	180.0	0.5	0.6	0.4	0.0	0.0	0.0
14	2P80R20U	272.7	298.0	250.0	0.6	0.7	0.5	0.0	0.0	0.0
15	3P80R20U	379.8	400.0	351.4	1.6	1.9	1.1	0.0	0.0	0.0

Annex V: Durability results – Recycled concrete aggregate series

Washed sand, 100% GGBS:

No	REF	RCPT, Coulomb			Absorption, %			Water Penetration, mm		
		Mean	Max	Min	Mean	Max	Min	Mean	Max	Min
1	1R100N0W	1400.0	1600.0	1200.0	1.2	1.3	1.0	W/L	W/L	W/L
2	2R100N0W	1243.0	1439.0	1000.0	0.9	1.0	0.8	W/L	W/L	W/L
3	3R100N0W	1993.0	2100.0	1850.0	1.3	1.7	1.1	W/L	W/L	W/L
4	1R80N20W	1549.0	1797.0	1325.0	1.0	1.1	0.9	W/L	W/L	W/L
5	2R80N20W	1562.0	1760.0	1400.0	0.9	1.0	0.8	W/L	W/L	W/L
6	3R80N20W	1179.0	1389.0	985.0	1.3	1.4	1.2	W/L	W/L	W/L
7	1R50N50W	1593.0	1839.0	1455.0	2.2	2.5	2.0	25.0	27.0	22.0
8	2R50N50W	1583.0	1797.0	1300.0	1.8	2.0	1.6	22.0	25.0	20.0
9	3R50N50W	1655.0	1717.0	1550.0	1.7	1.8	1.5	17.0	20.0	15.0
10	1R0N100W	450.0	500.0	350.0	0.6	0.6	0.6	3.0	3.0	2.0
11	2R0N100W	535.0	568.0	512.0	0.6	0.8	0.5	3.0	4.0	2.0
12	3R0N100W	585.0	731.0	488.0	1.8	2.0	1.5	0.0	0.0	0.0

Unwashed sand, 100% GGBS:

No	REF	RCPT, Coulomb			Absorption, %			Water Penetration, mm		
		Mean	Max	Min	Mean	Max	Min	Mean	Max	Min
1	1R100N0U	531.0	651.0	382.0	0.5	0.6	0.4	7.0	9.0	5.0
2	2R100N0U	511.0	543.5	498.0	1.5	1.6	1.3	8.0	9.0	7.0
3	3R100N0U	517.5	701.0	550.1	0.8	0.9	0.6	5.0	6.0	4.0
4	1R80N20U	623.7	602.0	518.0	0.8	1.0	0.5	7.0	8.0	6.0
5	2R80N20U	566.1	769.3	499.0	0.6	0.7	0.5	5.0	8.0	2.0
6	3R80N20U	602.1	700.0	613.0	0.5	0.5	0.5	5.0	6.0	4.0
7	1R50N50U	651.6	1325.0	997.0	0.6	0.7	0.5	2.0	5.0	0.0
8	2R50N50U	1118.7	921.0	627.7	0.8	1.0	0.5	16.0	18.0	12.0
9	3R50N50U	801.9	576.0	411.0	1.1	1.2	1.0	20.0	21.0	19.0
10	1R0N100U	491.1	660.0	324.2	1.4	1.5	1.3	0.0	0.0	0.0
11	2R0N100U	508.4	782.0	547.3	1.8	2.0	1.5	0.0	0.0	0.0
12	3R0N100U	701.1	774.0	782.0	1.8	1.9	1.6	1.0	2.0	0.0

Annex W: Durability results – RCA (triple blend) series

No	REF	RCPT, Coulomb			Absorption, %			Water Penetration, mm		
		Mean	Max	Min	Mean	Max	Min	Mean	Max	Min
1	1R100N0TB	1895.4	2000.0	1736.2	0.8	0.9	0.8	12.0	13.0	11.0
2	2R100N0TB	1906.2	1955.0	1850.0	1.0	1.1	0.9	7.0	9.0	5.0
3	3R100N0TB	2145.6	2251.0	1987.0	0.6	0.7	0.5	5.0	6.0	4.0
4	1R50N50TB	1344.6	1462.0	1253.0	1.0	1.1	0.9	3.0	6.0	0.0
5	2R50N50TB	552.6	613.0	489.8	0.7	0.9	0.5	0.0	0.0	0.0
6	3R50N50TB	1512.9	1689.0	1397.7	0.6	0.7	0.5	5.0	7.0	3.0
7	1R20N80TB	778.5	825.5	700.0	0.7	0.8	0.7	2.0	5.0	0.0
8	2R20N80TB	1077.3	1149.9	982.0	0.9	1.1	0.8	0.0	0.0	0.0
9	3R20N80TB	1094.4	1240.2	995.0	1.0	1.2	0.9	0.0	0.0	0.0
10	1R0N100TB	638.1	751.0	574.3	0.9	1.1	0.7	0.0	0.0	0.0
11	2R0N100TB	647.1	723.3	597.0	0.7	0.8	0.6	3.0	4.0	2.0
12	3R0N100TB	701.1	769.0	665.3	0.6	0.7	0.5	5.0	7.0	3.0

Annex X: Durability results – Higher curing temperature series

No	REF	RCPT, Coulomb			Absorption, %			Water Penetration, mm		
		Mean	Max	Min	Mean	Max	Min	Mean	Max	Min
1	1P5S70R25W	326.7	396.0	284.1	1.3	1.6	1.1	4.0	6.0	1.0
2	2P5S70R25W	450.9	511.0	376.7	1.5	1.6	1.4	0.0	0.0	0.0
3	3P5S70R25W	592.2	631.6	552.0	1.3	1.5	1.1	4.0	6.0	2.0
4	1P15S70R15W	326.7	369.0	299.1	0.9	1.0	0.8	6.0	8.0	4.0
5	2P15S70R15W	430.2	454.6	410.0	0.9	1.0	0.7	3.0	4.0	2.0
6	3P15S70R15W	488.7	525.1	452.0	1.3	1.4	1.2	8.0	9.0	7.0

Annex Y: Durability results – Air entrained series

No	REF	RCPT, Coulomb			Absorption, %			Water Penetration, mm		
		Mean	Max	Min	Mean	Max	Min	Mean	Max	Min
1	1P90M10A2	231.6	280.8	203.0	1.2	1.5	1.0	0.0	0.0	0.0
2	2P90M10A2	185.1	213.0	150.3	1.2	1.3	1.1	0.0	0.0	0.0
3	3P90M10A2	253.8	271.0	226.4	1.2	1.4	0.9	0.0	0.0	0.0
4	1P90M10A5	32.4	35.0	30.0	1.3	1.4	1.2	0.0	0.0	0.0
5	2P90M10A5	27.3	30.0	25.0	1.3	1.4	1.1	0.0	0.0	0.0
6	3P90M10A5	27.3	31.0	25.0	1.1	1.2	1.0	0.0	0.0	0.0
7	1P90M10A10	245.7	251.0	243.0	1.2	1.4	1.0	12.0	14.0	10.0
8	2P90M10A10	141.0	152.0	131.0	1.5	1.6	1.4	9.0	10.0	8.0
9	3P90M10A10	55.8	60.4	51.0	1.6	1.7	1.5	11.0	12.0	10.0
10	1P90M10A15	46.8	49.0	45.0	1.3	1.5	1.2	11.0	12.0	10.0
11	2P90M10A15	237.6	250.0	230.0	1.3	1.4	1.2	11.0	13.0	10.0
12	3P90M10A15	293.4	313.2	278.0	1.3	1.5	1.1	8.0	9.0	7.0

Annex Z: Typical calculations of chloride diffusion coefficient of 2P30S70W using Solver data analysis pack of Microsoft Excel

Cx (mm)	Cx(m)	Chloride content %by mass of concrete	Predicted	Error	Sq.error
0	0	0.217	0.217	0.000	0.00000000
1	0.001	0.174	0.189	-0.015	0.00022151
2	0.002	0.162	0.162	0.000	0.00000010
3	0.003	0.147	0.136	0.011	0.00012015
4	0.004	0.125	0.113	0.012	0.00015412
5	0.005	0.11	0.092	0.018	0.00033274
6	0.006	0.061	0.074	-0.013	0.00016398
8	0.008	0.034	0.047	-0.013	0.00015819
10	0.01	0.015	0.030	-0.015	0.00021275

Dnss 2.160

Cs 0.217

Ci 0.012 % by mass of concrete

SUM	0.001363537

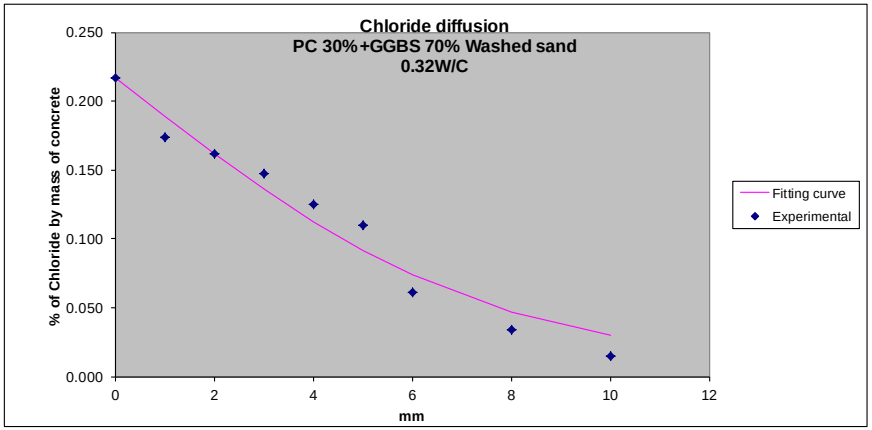

Annex AA: Compressive strength results – Cement type series

No	REF	7 day, N/mm^2				28 day, N/mm^2				56 day, N/mm^2			
		C1	C2	C3	Average	C1	C2	C3	Average	C1	C2	C3	Average
1	1P30S70W	79.0	85.0	79.0	81.0	98.0	105.0	97.0	100.0	113.0	107.0	110.0	110.0
2	2P30S70W	65.0	67.0	69.0	67.0	79.5	82.0	72.5	78.0	87.0	93.0	90.0	90.0
3	3P30S70W	50.0	52.0	54.0	52.0	65.0	68.0	65.0	66.0	70.0	75.0	71.0	72.0
4	1P0S100W	37.0	34.0	35.5	35.5	43.0	45.0	43.1	43.7	45.0	48.0	46.5	46.5
5	1P2.5S97.5W	40.0	43.0	40.0	41.0	56.0	58.0	51.0	55.0	62.0	58.0	57.6	59.2
6	1P5S95W	62.0	62.0	57.5	60.5	72.0	69.0	70.5	70.5	73.0	78.0	75.5	75.5
7	1P15S85W	75.0	77.0	76.0	76.0	83.0	82.0	85.5	83.5	90.0	85.0	92.0	89.0
8	2P0S100W	24.0	25.5	22.5	24.0	35.0	36.0	32.5	34.5	35.0	38.0	35.0	36.0
9	2P2.5S97.5W	20.0	23.0	23.0	22.0	31.0	28.0	31.0	30.0	32.0	39.0	38.5	36.5
10	2P5S95W	35.0	36.0	31.0	34.0	40.0	45.0	41.0	42.0	44.0	45.0	51.1	46.7
11	2P15S85W	50.0	51.0	55.0	52.0	62.0	59.0	57.5	59.5	62.0	66.0	67.0	65.0
12	3P0S100W	3.0	3.0	3.0	3.0	19.0	22.0	22.0	21.0	29.0	35.0	29.0	31.0
13	3P2.5S97.5W	19.0	21.0	20.0	20.0	25.0	23.0	24.0	24.0	36.0	37.0	32.0	35.0
14	3P5S95W	28.0	27.0	32.0	29.0	31.0	29.0	33.0	31.0	41.0	46.0	39.0	42.0
15	3P15S85W	35.0	40.0	37.2	37.4	45.0	40.0	41.3	42.1	45.0	52.0	44.0	47.0
16	1P20F80W	25.0	28.0	28.0	27.0	45.0	43.0	42.2	43.4	60.0	55.0	56.9	57.3
17	2P20F80W	14.0	15.0	14.5	14.5	33.0	30.0	27.9	30.3	35.0	42.0	38.8	38.6
18	3P20F80W	12.0	10.0	10.1	10.7	15.0	19.0	18.2	17.4	25.0	25.0	28.0	26.0
19	1P90M10W	85.0	82.0	83.2	83.4	95.0	99.0	95.2	96.4	105.0	110.0	106.3	107.1
20	2P90M10W	78.0	77.0	83.5	79.5	90.0	95.0	92.2	92.4	105.0	100.0	105.5	103.5
21	3P90M10W	71.0	70.0	67.5	69.5	85.0	90.0	90.5	88.5	95.0	96.0	91.6	94.2
22	1P80R20W	65.0	69.0	70.9	68.3	83.0	85.0	77.4	81.8	105.0	107.0	102.7	104.9
23	2P80R20W	65.0	70.0	66.6	67.2	85.0	78.0	78.2	80.4	100.0	105.0	100.1	101.7
24	3P80R20W	55.0	60.0	58.4	57.8	65.0	69.0	69.4	67.8	80.0	78.0	86.2	81.4
25	1P15S70R15W	70.0	75.0	70.1	71.7	80.0	82.0	78.6	80.2	89.0	94.5	87.1	90.2
26	2P15S70R15W	60.0	58.0	62.6	60.2	70.0	75.0	71.6	72.2	74.0	76.5	77.5	76.0
27	3P15S70R15W	40.0	35.0	41.7	38.9	43.0	47.0	48.0	46.0	51.0	48.5	50.8	50.1

Annex AB: Compressive strength results – Sand type series

No	REF	7 day, N/mm^2				28 day, N/mm^2				56 day, N/mm^2			
		C1	C2	C3	Average	C1	C2	C3	Average	C1	C2	C3	Average
1	1P30S70U	85.0	80.0	84.9	83.3	110.0	105.0	109.0	108.0	115.0	105.0	113.0	111.0
2	2P30S70U	70.5	74.0	67.6	70.7	85.0	90.0	86.3	87.1	100.0	99.0	95.0	98.0
3	3P30S70U	52.0	55.9	58.0	55.3	65.0	70.0	67.8	67.6	75.0	70.0	77.0	74.0
4	1P0S100U	30.0	33.0	28.8	30.6	38.0	44.0	37.7	39.9	50.0	49.0	54.0	51.0
5	2P0S100U	17.0	18.0	19.0	18.0	30.0	28.0	33.5	30.5	38.5	42.0	39.5	40.0
6	3P0S100U	8.0	7.9	8.4	8.1	17.0	15.5	17.0	16.5	24.5	23.0	27.5	25.0
7	1P20F80U	32.0	29.5	28.5	30.0	60.0	63.5	61.9	61.8	70.0	75.0	74.0	73.0
8	2P20F80U	13.0	14.5	16.0	14.5	30.0	35.0	29.5	31.5	42.0	45.0	49.5	45.5
9	3P20F80U	10.0	11.5	10.6	10.7	20.0	19.3	20.7	20.0	31.0	26.0	30.0	29.0
10	1P90M10U	93.0	88.0	90.5	90.5	110.0	105.0	113.5	109.5	120.0	115.0	123.5	119.5
11	2P90M10U	75.0	77.0	72.4	74.8	100.0	98.0	94.5	97.5	100.0	109.0	106.0	105.0
12	3P90M10U	70.0	68.0	76.8	71.6	85.0	92.0	88.5	88.5	101.0	100.0	96.0	99.0
13	1P80R20U	75.0	80.0	78.4	77.8	100.0	105.0	98.0	101.0	110.0	105.0	110.5	108.5
14	2P80R20U	75.0	79.0	74.3	76.1	85.0	92.0	87.0	88.0	99.0	105.0	105.0	103.0
15	3P80R20U	60.0	65.0	63.1	62.7	70.0	75.0	72.5	72.5	85.0	87.0	81.5	84.5

Annex AC: Compressive strength results – RCA (100% GGBS) series

No	REF	7 day, N/mm^2				28 day, N/mm^2				56 day, N/mm^2			
		C1	C2	C3	Average	C1	C2	C3	Average	C1	C2	C3	Average
1	1R100N0W	5.0	4.9	5.7	5.2	20.0	24.0	20.5	21.5	28.0	33.0	26.0	29.0
2	2R100N0W	2.0	3.5	2.3	2.6	15.0	13.0	11.0	13.0	25.0	20.0	21.0	22.0
3	3R100N0W	0.0	0.0	0.0	0.0	12.0	15.0	12.0	13.0	25.0	21.0	17.0	21.0
4	1R80N20W	3.0	4.5	3.0	3.5	25.0	27.0	21.5	24.5	35.0	32.0	28.1	31.7
5	2R80N20W	3.0	4.0	2.0	3.0	15.0	19.0	17.0	17.0	25.0	26.0	24.0	25.0
6	3R80N20W	2.5	2.5	1.0	2.0	19.0	15.0	17.0	17.0	22.0	24.0	20.0	22.0
7	1R50N50W	2.5	2.9	2.4	2.6	10.0	12.0	8.0	10.0	17.0	18.0	16.0	17.0
8	2R50N50W	0.0	0.0	0.0	0.0	8.0	9.0	4.0	7.0	17.0	19.0	15.0	17.0
9	3R50N50W	0.0	0.0	0.0	0.0	5.0	6.0	4.0	5.0	15.0	17.0	13.0	15.0
10	1R0N100W	33.0	39.0	34.5	35.5	44.0	47.0	40.1	43.7	50.0	45.0	44.5	46.5
11	2R0N100W	25.0	27.0	20.0	24.0	38.0	35.0	30.5	34.5	40.0	35.0	33.0	36.0
12	3R0N100W	3.0	4.0	2.0	3.0	22.0	23.0	18.0	21.0	29.0	35.0	29.0	31.0
13	1R100N0U	36.0	32.0	36.7	34.9	40.0	45.0	47.0	44.0	50.0	49.0	55.5	51.5
14	2R100N0U	18.0	20.0	16.3	18.1	25.0	26.0	27.0	26.0	30.0	37.0	32.0	33.0
15	3R100N0U	14.0	15.0	11.8	13.6	20.0	18.5	21.5	20.0	30.0	29.0	35.5	31.5
16	1R80N20U	22.0	25.0	20.5	22.5	32.5	35.0	30.0	32.5	41.0	42.0	35.5	39.5
17	2R80N20U	14.0	17.0	14.0	15.0	26.0	25.0	22.5	24.5	30.0	28.0	35.0	31.0
18	3R80N20U	3.0	2.7	3.3	3.0	10.0	9.0	11.0	10.0	15.0	24.0	18.0	19.0
19	1R50N50U	4.0	5.0	3.0	4.0	17.0	14.0	11.6	14.2	25.0	30.0	26.0	27.0
20	2R50N50U	2.0	2.0	2.0	2.0	13.0	15.9	13.4	14.1	26.0	22.0	24.0	24.0
21	3R50N50U	0.0	0.0	0.0	0.0	4.0	3.8	4.8	4.2	20.0	17.0	17.9	18.3
22	1R0N100U	30.0	29.0	32.8	30.6	41.0	36.2	42.5	39.9	45.0	52.0	56.0	51.0
23	2R0N100U	18.0	17.0	19.0	18.0	31.0	35.0	25.5	30.5	38.0	42.0	40.0	40.0
24	3R0N100U	8.0	9.0	7.3	8.1	14.0	20.0	15.5	16.5	27.0	22.0	26.0	25.0

Annex AD: Compressive strength results - RCA (triple blend) series

No	REF	7 day, N/mm^2				28 day, N/mm^2				56 day, N/mm^2			
		C1	C2	C3	Average	C1	C2	C3	Average	C1	C2	C3	Average
1	1R100N0TB	65.0	59.0	53.3	59.1	75.0	80.0	74.8	76.6	80.0	75.0	81.4	78.8
2	2R100N0TB	55.0	59.0	54.3	56.1	73.0	66.0	64.4	67.8	70.0	65.0	73.5	69.5
3	3R100N0TB	33.0	39.0	33.6	35.2	40.0	45.0	47.6	44.2	50.0	48.0	43.6	47.2
4	1R50N50TB	62.0	58.0	63.0	61.0	72.0	77.0	79.9	76.3	78.0	85.0	77.0	80.0
5	2R50N50TB	58.0	62.0	54.0	58.0	70.0	65.0	72.6	69.2	75.0	70.0	72.5	72.5
6	3R50N50TB	35.0	40.0	39.3	38.1	45.0	52.0	47.6	48.2	50.0	56.0	52.4	52.8
7	1R20N80TB	65.0	59.0	66.2	63.4	75.0	80.0	77.5	77.5	75.0	81.0	78.9	78.3
8	2R20N80TB	58.0	65.0	62.1	61.7	70.0	75.0	74.3	73.1	76.0	70.0	77.5	74.5
9	3R20N80TB	40.0	35.0	42.9	39.3	50.0	55.0	50.7	51.9	55.0	49.5	53.9	52.8
10	1R0N100TB	70.0	77.0	68.1	71.7	85.0	79.0	76.6	80.2	95.0	91.5	84.1	90.2
11	2R0N100TB	60.0	57.0	63.6	60.2	70.0	75.0	71.6	72.2	77.0	71.0	80.0	76.0
12	3R0N100TB	35.0	43.0	38.7	38.9	45.0	48.0	45.0	46.0	50.0	48.0	52.3	50.1

Annex AE: Compressive strength results – Air entrained concrete series

No	REF	7 day, N/mm^2				28 day, N/mm^2				56 day, N/mm^2			
		C1	C2	C3	Average	C1	C2	C3	Average	C1	C2	C3	Average
1	1P90M10A2	85.0	82.0	83.2	83.4	95.0	99.0	95.2	96.4	105.0	110.0	106.3	107.1
2	2P90M10A2	78.0	77.0	83.5	79.5	90.0	95.0	92.2	92.4	105.0	100.0	105.5	103.5
3	3P90M10A2	71.0	70.0	67.5	69.5	85.0	90.0	90.5	88.5	95.0	96.0	91.6	94.2
4	1P90M10A5	60.0	65.0	61.0	62.0	80.0	85.0	87.0	84.0	90.0	91.0	86.0	89.0
5	2P90M10A5	59.0	65.0	56.0	60.0	80.0	85.0	81.3	82.1	90.0	85.0	91.7	88.9
6	3P90M10A5	50.0	47.0	50.0	49.0	55.0	58.0	55.0	56.0	60.0	58.0	60.2	59.4
7	1P90M10A10	55.0	60.0	53.0	56.0	75.0	80.0	79.0	78.0	80.0	85.0	81.9	82.3
8	2P90M10A10	40.0	36.0	47.0	41.0	55.0	51.0	59.0	55.0	60.0	64.0	59.9	61.3
9	3P90M10A10	30.0	35.0	28.0	31.0	38.0	40.0	34.5	37.5	40.0	46.0	40.0	42.0
10	1P90M10A15	30.0	35.0	37.0	34.0	40.0	45.0	46.1	43.7	45.0	43.0	45.8	44.6
11	2P90M10A15	29.5	32.0	31.5	31.0	40.0	39.0	38.3	39.1	40.0	43.0	42.4	41.8
12	3P90M10A15	25.0	22.0	28.0	25.0	30.0	35.0	34.0	33.0	40.0	35.0	36.6	37.2

Annex AF: Compressive strength results – Higher curing temperatures series

No	REF	7 day, N/mm^2								28 day, N/mm^2								56 day, N/mm^2							
		$ct_{20°C}$				$ct_{40°C}$				$ct_{20°C}$				$ct_{40°C}$				$ct_{20°C}$				$ct_{40°C}$			
		C1	C2	C3	Avg	C1	C2	C3	Avg	C1	C2	C3	Avg	C1	C2	C3	Avg	C1	C2	C3	Avg	C1	C2	C3	Avg
1	1P5S70R25W	35.0	37.0	30.0	34.0	40.0	36.0	41.0	39.0	50.0	45.0	49.3	48.1	55.0	58.0	54.7	55.9	55.0	58.0	57.4	56.8	60.0	64.5	59.7	61.4
2	2P5S70R25W	35.0	30.0	33.7	32.9	38.0	40.0	36.9	38.3	42.0	46.0	47.9	45.3	50.0	55.0	51.0	52.0	50.0	55.0	52.8	52.6	55.1	60.0	59.2	58.1
3	3P5S70R25W	18.0	23.0	19.0	20.0	25.0	24.0	20.9	23.3	30.0	25.0	29.0	28.0	30.0	35.0	30.7	31.9	30.0	35.0	28.9	31.3	35.0	30.5	38.6	34.7
4	1P15S70R15W	70.0	75.0	70.1	71.7	70.0	75.0	74.0	73.0	80.0	82.0	78.6	80.2	81.0	87.0	87.0	85.0	89.0	94.5	87.1	90.2	90.0	98.2	95.6	94.6
5	2P15S70R15W	60.0	58.0	62.6	60.2	60.0	65.0	63.7	62.9	70.0	75.0	71.6	72.2	75.0	78.0	73.5	75.5	74.0	76.5	77.5	76.0	78.5	82.0	77.4	79.3
6	3P15S70R15W	40.0	35.0	41.7	38.9	40.0	45.0	44.3	43.1	43.0	47.0	48.0	46.0	50.0	45.0	52.0	49.0	51.0	48.5	50.8	50.1	50.0	55.0	50.1	51.7

Annex AG: Calculation of the decomposition of $Ca(OH)_2$ at TG analysis

Cement combination	Age	Mass of evaporated water mg	Mass of Ca(OH)2, mg	Initial mass, mg	Proportion of Ca(OH)2 as % of initial mass
UKPC	1D	0.24	0.9864	15.15	6.51
	7D	0.4	1.644	14.72	11.17
	365D	0.61	2.5071	18.08	13.87
P30S70	1D	0	0	15.66	0.00
	7D	0.05	0.2055	13.22	1.55
	365D	0.15	0.6165	18.77	3.28
P15S85	1D	0	0	18.44	0.00
	7D	0.05	0.2055	17.62	1.17
	365D	0.05	0.2055	19.7	1.04
P20F80	1D	0	0	0	0.00
	7D	0.07	0.2877	17.8	1.62
	365D	0	0	18.9	0.00
P90M10	1D	0.1	0.411	16.12	2.55
	7D	0.29	1.1919	15	7.95
	365D	0.45	1.8495	18.91	9.78
P80R20	1D	0.14	0.5754	18.55	3.10
	7D	0.39	1.6029	18.53	8.65
	365D	0.35	1.4385	18.96	7.59
P15S70R15	1D	0	0	15.05	0.00
	7D	0.02	0.0822	15.3	0.54
	365D	0.05	0.2055	19.44	1.06

Calculation of the mass of $Ca(OH)_2$

Heat (400 - 500 deg C)

	$Ca(OH)_2$	→	CaO	H_2O
Atomic mass	74		56	18

∴ Mass of $Ca(OH)_2$ = (Mass of evaporated water / 18) x 74

Annex AH: Typical calculation of eCO_2 of concrete

Materials	kg/m^3	Embodied CO_2/kg	Total eCO_2
Total cementitious	400		
OPC	120	0.93	112
GGBS	280	0.212	59
Fly Ash		0.033	0
MS		0.155	0
Rice Husk Ash		0.029	0
20 mm crushed Limestone	647	0.007	5
10 mm crushed Limestone	438	0.007	3
5 mm crushed Limestone	678	0.007	5
Dune sand	303	0.005	2
Water	100	0.001	0
W/C			
Air, 2%			
Total	2566		
Admixture 1, Chryso Fluid Optima 245 Emx	7	0.72	5.0
Admixture 2, Sodamco CR152	1	0.076	0.1
		kg CO_2/m^3	190